

A Study of Drug–Carrier Interactions in Dry Powder Inhaler Formulations Using the Andersen Cascade Impactor, X-Ray Microanalysis and Time of Flight Aerosol Beam Spectrometry (TOFABS)

Teerapol SRICHANA,^{*,a} Anthony BRAIN,^b Christopher MARRIOTT,^c and Gary Peter MARTIN^c

Department of Pharmaceutical Technology, Faculty of Pharmacy, Prince of Songkla University,^a Hat Yai, Songkhla 90112, Thailand, Electron Microscope Unit, King's College London,^b Camden Hill, London W8 7AH, UK, and Department of Pharmacy, King's College London,^c Manresa Road, London SW3 6LX, UK.

Received May 12, 1999; accepted October 21, 1999

The purpose of this study was to determine the *in vitro* deposition of both drug (albuterol sulfate) and carrier (lactose) particles in relation to each other from a dry powder inhaler formulation using an Andersen cascade impactor (ACI) and time of flight aerosol beam spectrometry (TOFABS). In addition, scanning electron microscopy (SEM) combined with X-ray microanalysis was employed to distinguish albuterol sulfate from lactose. Drug particles apparently penetrated deeper into the impactor than lactose particles contained in the formulation. In some certain stages of impactor, drug particles were separated from lactose particles. Although the TOFABS cannot distinguish between albuterol sulfate and lactose, the TOF spectra obtained from the Aerosizer would appear to be partly indicative of the interactions which exist between drug and carrier. One symmetrical TOF peak was obtained from drug or lactose alone. The TOF peak of the drug was always lower than the TOF of lactose. The times obtained for each powder between experiments were highly reproducible and typical of material and particle size. The use of SEM–X-ray microanalysis also allowed some qualitative characterization of shape and state of association of the two components.

Key words albuterol sulfate; lactose; Andersen cascade impactor; X-ray microanalysis; time of flight aerosol beam spectrometry; dry powder aerosol

Dry powder inhaler formulations generally comprise micronized drug particles with a mean aerodynamic diameter (D_a) of 2–5 μm blended with an inert carrier (30–60 μm), usually lactose, to form an interactive mixture of the two components. A carrier is included in the formulation to act as a bulking agent and to aid aerosolization of the drug,¹⁾ and it should be deposited in the upper airways with only the drug particles being liberated into the inspired air, ideally reaching the lower airways.²⁾ Despite the use of impactor data to assess the effect of formulation variables on aerosol cloud characteristics,^{3,4)} there is limited knowledge of drug-carrier interactions and drug release from the carrier during aerosolization. French *et al.*⁵⁾ proposed that the active drug in carrier formulations can exist in a variety of possible states following aerosolization, and these include: a) individual active drug particles, b) active-active drug particle aggregates, c) active drug bound to individual carrier particles in mono- or multi-layers, and d) combined active drug and carrier aggregates. Few previous studies have focused on the characteristics of the carrier counterpart during drug deposition *in vitro* or considered the relative depositions of the drug and carrier. A relatively recent technique, based on the aerodynamic time of flight (TOF), has been used to analyze the particle size distribution in pharmaceutical powders.⁶⁾ In this method, particles are accelerated by the drag forces generated by an accelerating air stream, and while very small particles almost attain sonic velocity, larger particles experience a lower acceleration because of their greater mass. As particles pass through two laser beams in the measuring region spaced at a set distance, the light interception is detected and converted into electronic signals by two photomultiplier tubes. The time required for individual particles to pass between the beams is measured to a precision of 25 nanosec-

onds and is termed the TOF. Since TOF is dependent upon particle size it is possible to obtain a particle size distribution for any powder, including, for example, the lactose and drug deposition on individual plates of an ACI after a dry powder formulation has been aerosolized into the impactor. The size distribution produced by the software of any instrument which measures TOF assumes, as with most particle sizing techniques, sphericity of shape. This, of course, is seldom the case for pharmaceutical powders, and hence the use of scanning electron microscopy (SEM) together with X-ray microanalysis, can be employed to determine the appearance and to distinguish the drug from carrier particles. X-rays are produced whenever an electron beam interacts with matter, as in the use of SEM⁷⁾ for example, and these can be used very effectively to provide information about the chemical composition of the specimens examined. X-ray microanalysis can be regarded as a qualitative non-destructive technique that provides a means of detecting most elements *in situ*, sometimes at levels as low as 10^{-19} g.⁸⁾ The nature of the interaction between lactose and drugs has not been completely characterized. Hence, it was the purpose of this study to determine the interaction between drug and carrier in relation to each other after aerosolization using the ACI. TOF was used to further characterize the samples deposited on each stage of the ACI, and SEM combined with X-ray microanalysis was employed to distinguish albuterol from lactose.

Materials and Methods

Micronized albuterol sulfate (median diameter 2.8 μm) was supplied by Glaxo Wellcome, Ware, UK. Lactochem lactose (medium grade) was obtained from Borculo Whey, Ltd., Chester, UK. Micronized lactose was obtained from Meggle, Wasserburg, Germany. The ISF[®] (Cyclohaler[®]) device was obtained from Pharbita BV, Zaandam, the Netherlands. Capsules (size 3) were obtained from Farillon Limited, Essex, UK. The formulation was

* To whom correspondence should be addressed.

prepared by mixing albuterol sulfate (0.2 g) with lactose (13.5 g) in a Turbula® mixer (Basel, Switzerland) for 2 h. Two size ranges of lactose, medium grade Lactochem® (with a multimodal particle size distribution and a volume median diameter (VMD) of 20.10 μm and geometric standard deviation (GSD) of 1.86) and micronized lactose (with a monomodal distribution and VMD of 8.60 and GSD of 1.71, measured by laser diffraction (Malvern Mastersizer, Worcester, UK)), were used as carriers in the powder blend. 27.4 mg of each blend, equivalent to 400 μg drug, was weighed into each capsule. The uniformity of both blends was 102.2 ± 1.4 and $102.8 \pm 2.4\%$, respectively. Other capsules were prepared containing either 27 mg albuterol sulfate alone or 27 mg of either Lactochem lactose or micronized lactose alone.

Deposition Studies Using the ACI A cascade impactor comprising a pre-separator, eight stages and collection plates (Andersen Sampler, Inc., Atlanta, U.S.A.) was prepared for use by rinsing the cleaned component parts with deionized water. The stages and plates were dried in a hot air oven before being employed in deposition studies, conducted at 28.3 l/min and 60 l/min for 21 and 10 s, respectively. Two formulations, one containing Lactochem lactose and the other micronized lactose as a carrier, were aerosolized into the ACI using a Cyclohaler® device.⁹⁾ After actuating a single dose into the ACI, the glass throat,¹⁰⁾ pre-separator and each stage were rinsed with 50 ml of mobile phase containing the internal standards before determining drug and lactose, as previously described.¹¹⁾ Detection limits of drug and lactose were 0.1 and 2 $\mu\text{g}/\text{ml}$, respectively. The drug and lactose deposition were expressed as a percentage of the nominal dose. The mass median aerodynamic diameter (MMAD) and GSD of drug and lactose was calculated based on the mass distribution of the respective particles deposited on stages 0 to 7 of the ACI,^{12,13)} excluding those particles deposited on the pre-separator and throat part. The drug fine particle fraction (FPF) and the amount of fine particle lactose (FPL) of a formulation were defined by the amounts deposited on stages 2 to 7 after aerosolization at a flow rate of 28.3 l/min, and when the flow rate is changed to 60 l/min, the FPF and FPL was defined by the amounts deposited on stages 1 to 7. The data were analyzed for statistical significance using an analysis of variance, and $p < 0.05$ was considered to be significant.

SEM-X-Ray Microanalysis of Deposited Samples on Each Stage of the ACI The localization of drug relative to carrier particles on each stage of the ACI was assessed qualitatively using SEM and energy dispersive X-ray microanalysis. Recovered particles were mounted on an aluminium stub before coating them with carbon (Polaron E-500, Watford, UK). The coated samples were viewed by a Philips EM501B (Philips Analytical, Eindhoven, The Netherlands) scanning electron microscope. X-ray microanalysis was used to identify the presence of the sulfur atom in albuterol sulfate, enabling a distinction to be made between drug and carrier particles on the basis of X-ray spectra. Such spectra in combination with the electron micrographs, allowed the determination of drug-carrier and carrier-carrier interactions in the powders deposited on each stage of the ACI.

Time of Flight Determination of Dry Powders Deposited on Each Stage of the ACI The ACI was operated as described above except that three doses of each formulation were aerosolized sequentially into the impactor at two flow rates (28.3 or 60 l/min). The empty capsule was removed from the device after aerosolization of each dose, to be replaced by a full capsule, and the device was not washed between doses. The particles retained on each stage of the ACI were carefully removed by scraping each plate with a thin sheet of paper, and were then loaded into the sample cup of the Aerodisperser connected to the Aerosizer Mach 2 (Amherst Process Instruments, Amherst, MA, U.S.A.). The optimum sample run time was 200–500 s, depending upon the sample count rate, and when the feed rate reached 100%, the run was considered complete. In particular, it is essential that no selective sampling of the smaller particles occurs due to larger particles being unsampled. The amount of powder recovered from the lower impaction plates (*i.e.* stages 4 and 5) provided sufficient data for statistical analysis (>100000 particles). Powder build up and electrostatic charge effects within the Aerodisperser were not found to occur using run times ≤ 500 s.¹⁴⁾ The shear force was set at 3 psi, as specified by the manufacturer, because the particle size was known to be lower than 10 μm (the powder having been recovered from stages 0–7 on the ACI). The deagglomeration was set at 14 l/min to prevent excessive impaction energy on the particles, and the feed rate was set at 5000 particles/s. Although this flow rate is lower than that employed in the ACI (28.3 l/min). It has to be appreciated that the air flow of the Aerosizer represents linear velocity rather than flow rate. All parameters set were kept constant in each experiment, and the results are displayed as TOF. The photomultiplier tube (PMT) voltage was set at 1100 V in order not only to provide maximum sensitivity but also to allow the detec-

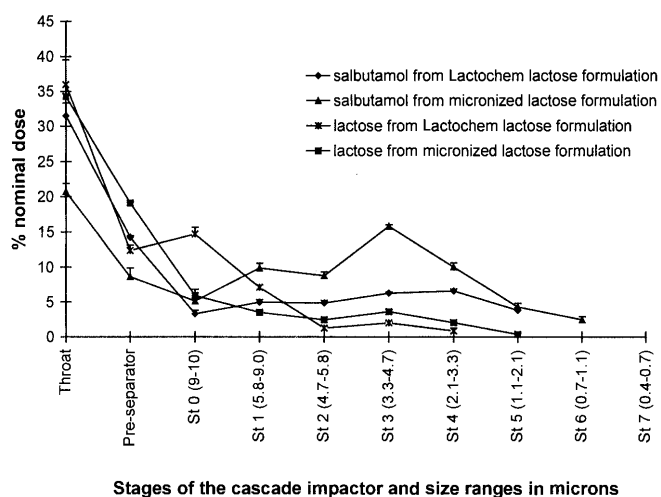


Fig. 1. The Deposition of Albuterol Sulfate and Lactose from Two Formulations of Albuterol Sulfate Containing Either Lactochem or Micronized Lactose as Diluent after Aerosolization into an ACI at 28.3 l/min (mean \pm S.D., $n=5$)

tion of particles with a size greater than 0.5 μm . A higher PMT voltage setting resulted in increased noise pulses and required a longer run time (>300 s). Both the Aerosizer and the Aerodisperser have been comprehensively described by both Niven⁶⁾ and Hindle and Byron.¹⁴⁾ The TOF of pure albuterol sulfate and pure carriers were determined as a marker for drug and carrier TOF spectra. The TOF results were gained as a normalized frequency distribution by number.¹⁵⁾ Each experiment was carried out in triplicate.

Results

Deposition Studies Using the ACI The stage cut-off diameters of each stage of the ACI, based on calibration of uncoated plates at 28.3 l/min, are 9, 5.8, 4.7, 3.3, 2.1, 1.1, 0.7, 0.4 μm , for stage 0, 1, 2, 3, 4, 5, 6 and 7, respectively.¹²⁾ The cut-off diameters at 60 l/min have not been previously reported, however, according to Eqs. 1 and 2, these values can be calculated.¹⁶⁾

$$d_{50} = \sqrt{\frac{9Stk_{50}\eta\pi D_j^3 N}{4\rho FC}} \quad (1)$$

where F =total flow rate through the jets, N =total number of jets, d_{50} =effective cut-off diameter, ρ = density of particle (g cm^{-3}), C =Cunningham slip correction factor, Stk_{50} =Stokes number for 50% collection efficiency, η =fluid viscosity ($\text{dyne} \cdot \text{s cm}^{-2}$), D_j =jet width (cm).

All parameters are constant if the same impactor and operating conditions are used, therefore, the simplified Eq. 2 is obtained.

$$d_{50} \propto \left(\frac{1}{F}\right)^{1/2} \quad (2)$$

From the known d_{50} at 28.3 l/min, the cut-off diameter at 60 l/min is calculated based on Eq. 2, and the values are 6.2, 4.0, 3.2, 2.3, 1.4, 0.8, 0.5, 0.3 μm for stage 0, 1, 2, 3, 4, 5, 6 and 7, respectively. The size distributions of the fine lactose and drug delivered from the two formulations at 28.3 and 60 l/min, are presented in Figs. 1 and 2. Drug particles were detected as low as stage 5 of the ACI when the Lactochem lactose formulation was aerosolized at 28.3 l/min, but with the same formulation at 60 l/min, some drug penetrated as far as stage 6 (Figs. 1, 2). After aerosolization of the Lactochem

lactose formulation at 28.3 l/min lactose could also be detected as having been deposited as far as stage 4 of the ACI (Fig. 1), whereas at the higher flow rate, carrier particles could only be determined as reaching stage 3 (Fig. 2). Drug particles were found to be deposited as far as stage 6 when the micronized lactose formulation was aerosolized at 28.3 l/min, and since no lactose was detected on stage 6 from this formulation, it can be assumed that the drug on this stage was separated from carrier particles (Fig. 1). When the flow rate was increased to 60 l/min, drug particles penetrated to stage 7, whereas carrier particles reached only stage 4. Drug particles were entrained into the airstream in higher quantities at the higher flow rate (the percent fine particle fraction of drug increasing ($p < 0.01$) from 21.6 to 29.7% for the Lactochem lactose formulation and 41.3 to 44.3% for the micronized lactose formulation). However, at a flow rate of 60 l/min, the amount of drug which completely detached from the lactose particles was 8.8% (particles deposited on stages 4, 5 and 6) for the Lactochem lactose formulation whereas the comparable value for the micronized lactose formulation was only 2.3% (particles depositing on stages 5, 6 and 7) (Fig. 2). When the micronized lactose formulation was aerosolized at 28.3 l/min, it would appear that the FPL was much higher than that derived from the Lactochem lactose formulation at the same flow rate (8.5% and 4.2%), respectively. At the higher flow rate, the amount of FPL increased to a greater extent from the micronized lactose formulation (8.5% at 28.3 l/min to 15.0% at 60 l/min) than from the Lactochem lactose formulation (4.2 to 4.3%). When the particle size was plotted as a log-probability distribution, as described in the USP XXIII,¹³ it was found that the MMAD of

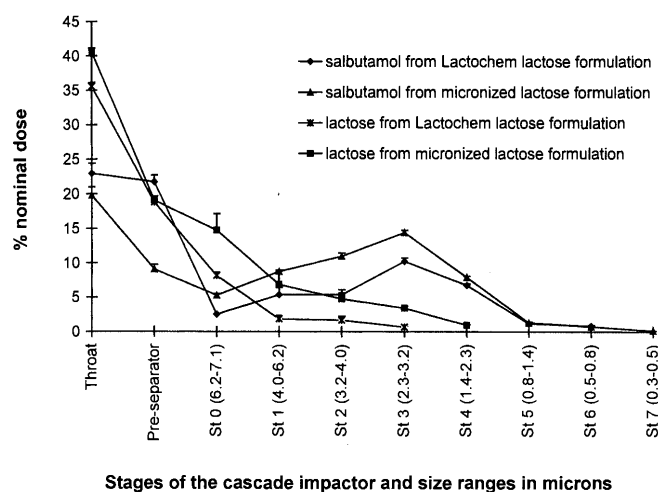
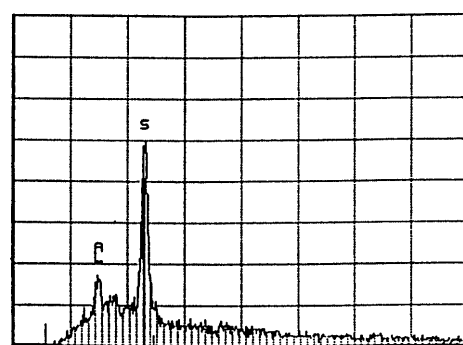


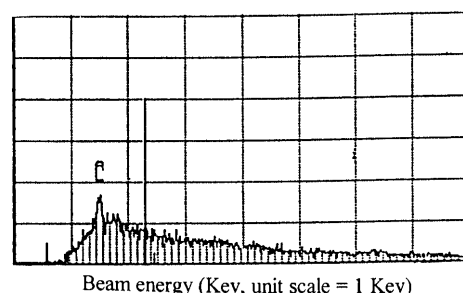
Fig. 2. The Deposition of Albuterol Sulfate and Lactose from Two Formulations of Albuterol Sulfate Containing Either Lactochem or Micronized Lactose as Diluent after Aerosolization into an ACI at 60 l/min (mean \pm S.D., $n=5$)

albuterol sulfate in the Lactochem lactose formulation at 28.3 l/min was $4.89 \mu\text{m}$, while in the micronized lactose formulation it was $4.07 \mu\text{m}$ (Table 1), although these two values were not statistically different ($p > 0.05$). Aerosolization of the drug at the higher flow rate (60 l/min) resulted in a lower MMAD of the drug, a value of $2.8 \mu\text{m}$ being obtained irrespective of formulation (Table 1). The MMAD of lactose deposited within the impactor from the Lactochem lactose containing formulation was not surprisingly higher than that of the drug particles, although the MMAD did not change significantly ($p > 0.05$) when the flow rate was increased. Despite the MMAD of lactose from the formulation containing the micronized excipient being smaller ($5.10 \mu\text{m}$ at 28.3 l/min) than that in the formulation containing Lactochem lactose, it again did not change significantly as a function of flow rate. The GSD of both drug and carrier particle size was approximately 2 in all experiments.

SEM-X-Ray Microanalysis of Samples Deposited on Each Stage of the ACI X-ray microanalysis enabled drug particles to be distinguished from lactose, as shown in Fig. 3. Sulfur atoms present in albuterol are capable of being de-



(a) Albuterol sulfate



(b) Lactose

Fig. 3. The X-Ray Spectrum of a) Albuterol Sulfate (S) and b) Lactose

The peak (s) is indicative of the sulfur atom present in albuterol sulfate, which is absent from the X-ray spectrum of a lactose particle. (Al=aluminium, unit scale of x-axis=1 KeV)

Table 1. MMAD of Albuterol Sulfate and Lactose Carrier Obtained from ACI Data (mean \pm S.D., $n=5$)

Formulation	Flow rate (l/min)	MMAD (μm) of drug	GSD of drug	MMAD (μm) of lactose	GSD of lactose
Lactochem lactose	28.3	4.89 ± 0.11	1.74 ± 0.03	6.94 ± 0.05	1.95 ± 0.01
	60	2.81 ± 0.04	2.00 ± 0.02	4.48 ± 0.11	1.65 ± 0.10
Micronized lactose	28.3	4.07 ± 0.09	2.01 ± 0.10	5.10 ± 0.11	2.02 ± 0.03
	60	2.80 ± 0.02	1.86 ± 0.04	4.42 ± 0.22	2.30 ± 0.04

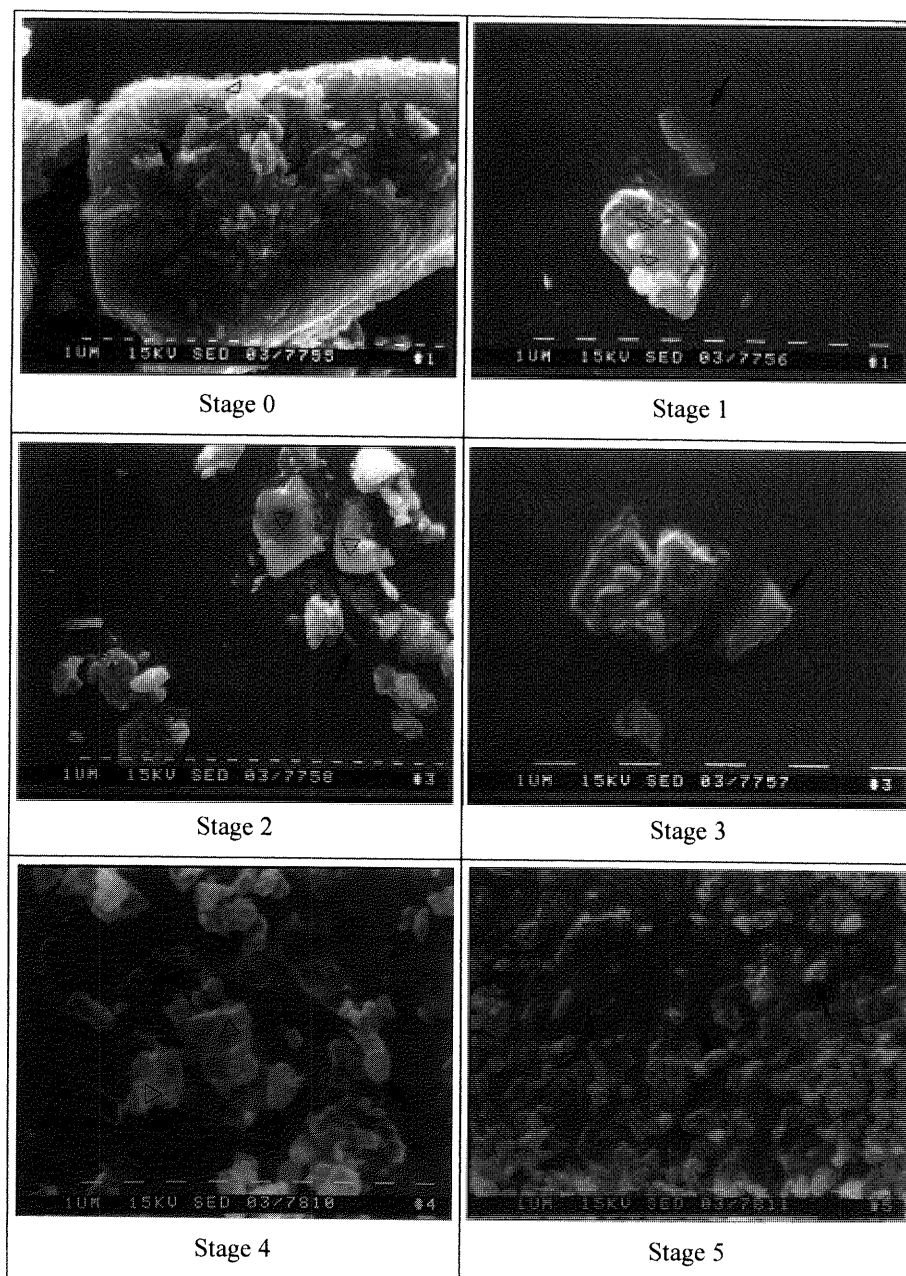


Fig. 4. Electron Micrographs of Albuterol Sulfate (Black Arrows) and Lactose (Empty Deltas) on Each Stage of the ACI after Aerosolization of the Lactochem Lactose Formulation at 28.3 l/min (Bars Correspond to a Distance of 1 μ m)

tected as an X-ray peak, even in a single crystal. The electron micrographs, together with X-ray microanalysis, show how drug and lactose orientate on each stage of the ACI. In addition, as the electron beam from the microscope tracked across the surface of the particles, it was found that while the lactose crystals changed visibly, possibly as a result of localized heating, this did not occur for albuterol. Such *in situ* observations enabled an accurate and reproducible identification of the two materials. Figure 4 shows an electron micrograph of particles derived from stages 0 to 5 of the ACI for the Lactochem lactose formulation aerosolized at 28.3 l/min. Stage 0 indicated clearly that both fine drug and lactose particles adhered on the surface of coarse lactose particles. The numbers of adhered drug particles were found to be markedly lower than the fine lactose particles, being present in an approximate ratio of 1 : 4. The same trends were appar-

ent for powder deposited from the micronized lactose formulation, although the number of drug particles was even lower in comparison to the fine lactose particles. The electron micrographs obtained for powder depositing on stage 1 showed the presence of drug particles which did not adhere to the surface of lactose. Not surprisingly, the size of lactose particles on stage 1 were smaller than those seen on stage 0. Powder derived from stages 2 and 3 showed that free drug particles were found in combination with aggregates of drug particles, and sometimes these aggregates were found in association with lactose particles. However, on stages 4 and 5 of the ACI, with the Lactochem lactose formulation aerosolized at 28.3 l/min, free drug particles were seen more frequently (in the ratio of approximately 4 : 1) than lactose particles. The higher the stage number of the ACI (stages 3—6), the easier it was to find drug particles either in the aggregated or

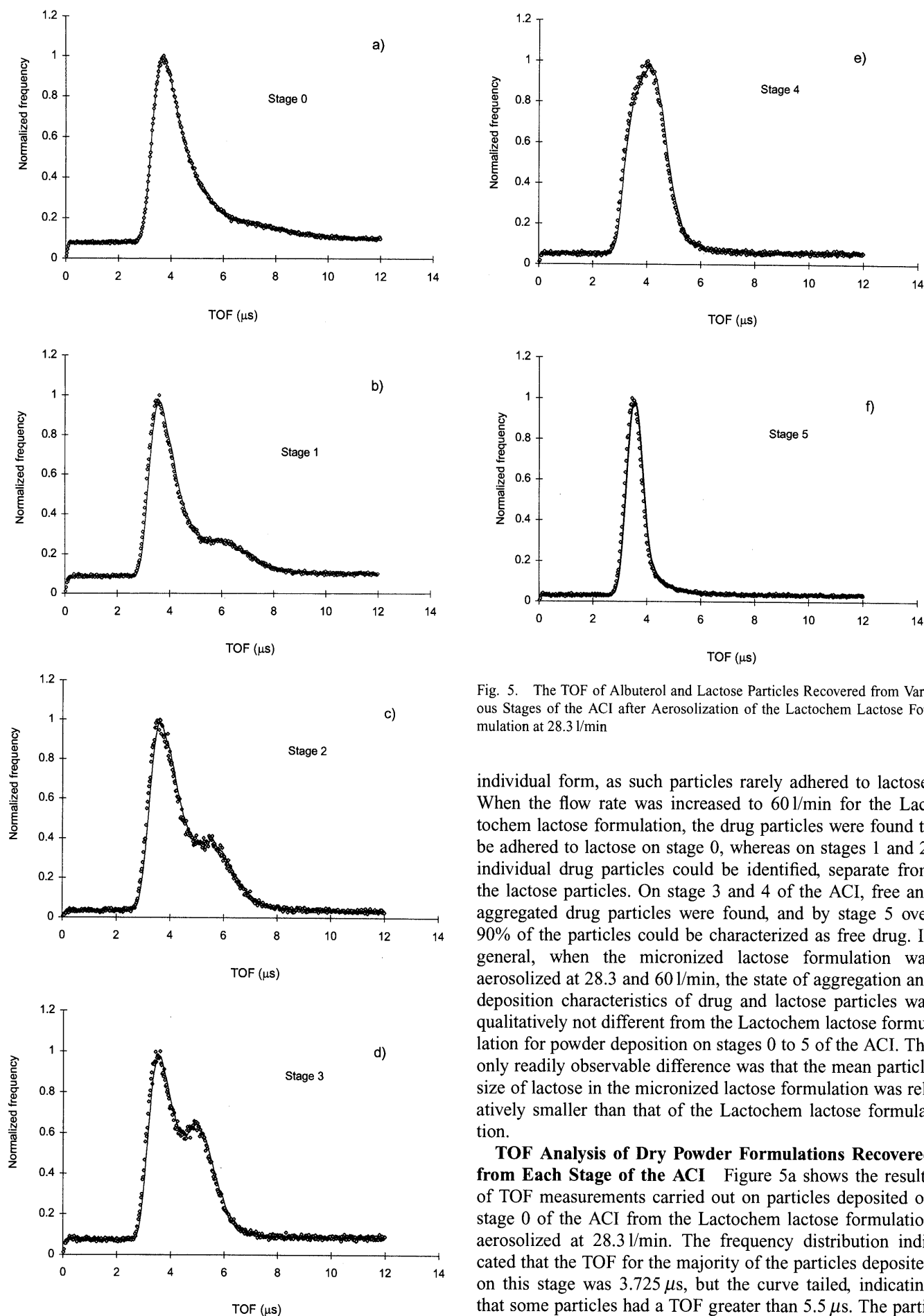


Fig. 5. The TOF of Albuterol and Lactose Particles Recovered from Various Stages of the ACI after Aerosolization of the Lactochem Lactose Formulation at 28.3 l/min

individual form, as such particles rarely adhered to lactose. When the flow rate was increased to 60 l/min for the Lactochem lactose formulation, the drug particles were found to be adhered to lactose on stage 0, whereas on stages 1 and 2, individual drug particles could be identified, separate from the lactose particles. On stage 3 and 4 of the ACI, free and aggregated drug particles were found, and by stage 5 over 90% of the particles could be characterized as free drug. In general, when the micronized lactose formulation was aerosolized at 28.3 and 60 l/min, the state of aggregation and deposition characteristics of drug and lactose particles was qualitatively not different from the Lactochem lactose formulation for powder deposition on stages 0 to 5 of the ACI. The only readily observable difference was that the mean particle size of lactose in the micronized lactose formulation was relatively smaller than that of the Lactochem lactose formulation.

TOF Analysis of Dry Powder Formulations Recovered from Each Stage of the ACI Figure 5a shows the results of TOF measurements carried out on particles deposited on stage 0 of the ACI from the Lactochem lactose formulation aerosolized at 28.3 l/min. The frequency distribution indicated that the TOF for the majority of the particles deposited on this stage was $3.725 \mu\text{s}$, but the curve tailed, indicating that some particles had a TOF greater than $5.5 \mu\text{s}$. The particles deposited on stage 1 (Fig. 5b) of the ACI from the same

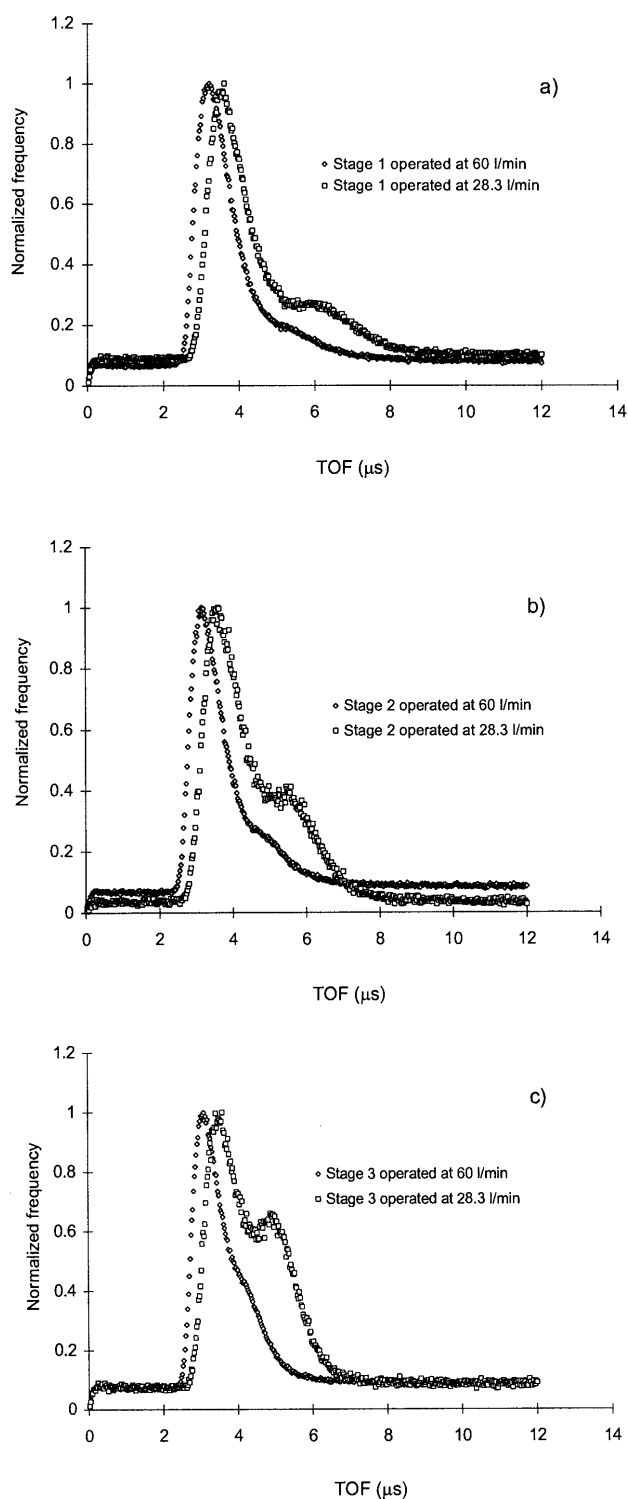


Fig. 6. The TOF of Albuterol and Lactose Particles Recovered from Various Stages of the ACI after Aerosolization of the Lactochem Lactose Formulation at 28.3 and 60 l/min

formulation, when re-aerosolized into the Aerosizer, produced two peaks in the TOF spectra, one corresponding to $3.600\ \mu\text{s}$ but also a second indicating a proportion of the particles with a TOF of about $6.2\ \mu\text{s}$. Powder collected from stages 2 and 3 (Figs. 5c, 5d) also exhibited split peaks at 5.5 and $5.0\ \mu\text{s}$, respectively, the second peak not being fully separated from the common first peak found at $3.600\ \mu\text{s}$. However, when the powder deposited on stage 4 (Fig. 5e) was analyzed, the second peak was no longer apparent, leaving only

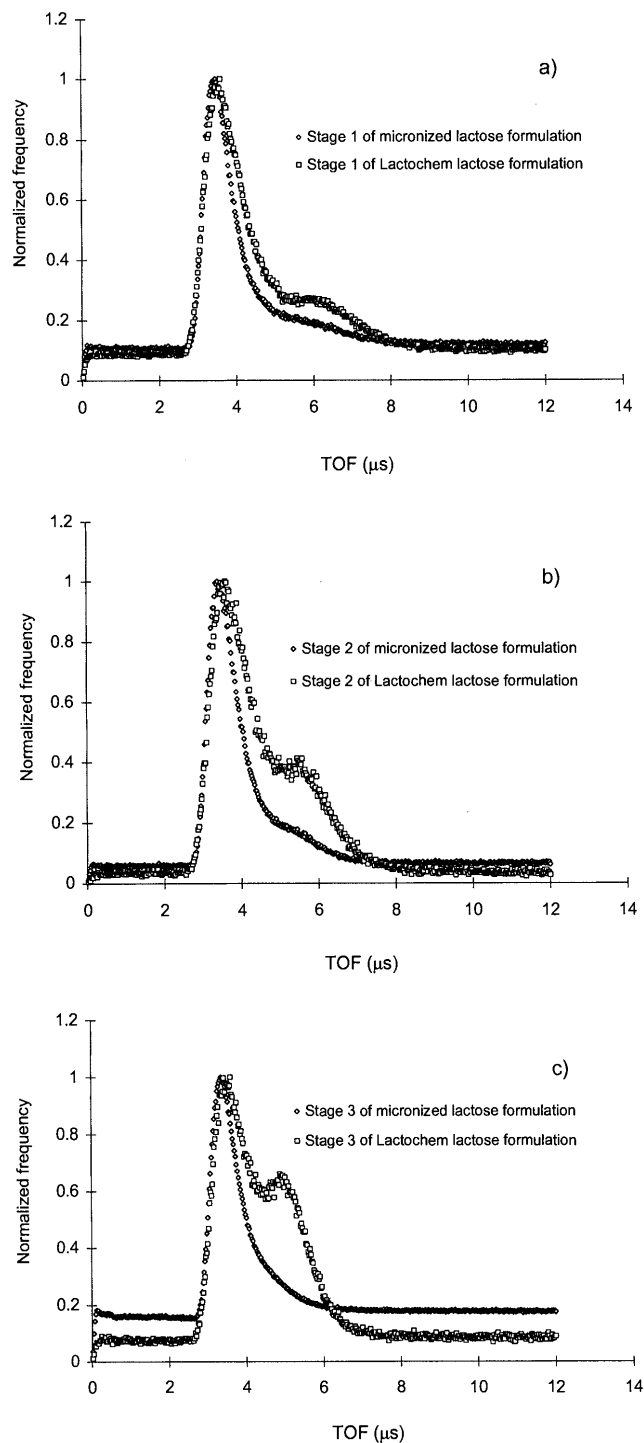


Fig. 7. The TOF of Albuterol and Lactose Particles from Two Formulations of Albuterol Sulfate Containing Either Lactochem or Micronized Lactose as Diluent Recovered from Different Stages of the ACI after Aerosolization at 28.3 l/min

a broad single peak with a TOF for the particles of $4.025\ \mu\text{s}$. Meanwhile, for particles deposited on stage 5 (Fig. 5f), a sharp single peak in the TOF spectrum was obtained at $3.425\ \mu\text{s}$. When the flow rate was increased to $60\ \text{l/min}$, the TOF spectrum for particles from the Lactochem lactose formulation, which was deposited on stages 1, 2 and 3, showed less tailing of the principal peak compared to those obtained at $28.3\ \text{l/min}$ (Fig. 6), and the peak in the TOF spectra appeared at a shorter time. For example, the maximum in the TOF profile for particles collected from stage 1 of the ACI after

aerosolization at 60 l/min was after 3.2 μ s, compared to after 3.5 μ s when the same formulation was aerosolized at 28.3 l/min. In addition, for the powder collected from stages 2 and 3 after aerosolization at 60 l/min, although a slight shoulder appeared in the TOF profile after 4.5 and 4.0 μ s, respectively, a distinct split peak was not obtained (Figs. 6b, 6c), as was the case when the powder collected from the same plates after aerosolization at 28.3 l/min was analyzed. The particles from the micronized lactose formulation, collected from plates 1, 2 and 3 of the ACI operated at 28.3 l/min, showed tailing of the sole peak in the TOF spectrum of the re-aerosolized powder, in contrast to the distinct shoulders and split peaks found for particles from the Lactochem formulation deposited on the same plates (Fig. 7). The TOF spectra obtained for pure drug or lactose was found to produce a single symmetrical peak. Shorter TOF peaks were obtained for albuterol (3.425–3.475 μ s) compared with those for lactose particles (>4 μ s). Different size ranges of lactose (Lactochem and micronized) also gave different TOF peaks ($p < 0.01$). The relevant densities of lactose and albuterol sulfate are 1.54 g/ml¹⁷) and 1.32 g/ml,¹⁸) respectively. Therefore, the TOF obtained depended on the type and size of materials analyzed.

Discussion

There was a clear indication that the interactions (which existed) between the particles of lactose and drug were different in the Lactochem and micronized lactose formulations from data derived using the ACI operated at 28.3 and 60 l/min. At higher flow rates more drug particles were separated from the lactose carrier, irrespective of the formulation. The separation of drug particles from lactose particles was not complete for powder deposited on stage 0 when the Lactochem lactose formulation was aerosolized at 28.3 l/min. The electron micrographs confirmed that large numbers of fine drug particles had adhered to the coarse lactose particles present on this stage. Also, the TOF spectra of particles collected from stage 0 showed tailing because the drug had not been separated from the lactose carrier on this impactor plate. If the shear force from the aerosolization process was sufficient to overcome the adhesive forces between the drug and lactose, the spectra would be predicted to split into a doublet peak. Individual drug particles, aggregates of drug and some aggregates of drug with lactose were apparent from electron micrographs taken of powder deposited on stages 1–4, which showed peak splitting in their TOF spectra. The TOF spectrum for powder from the Lactochem lactose formulation recovered from stage 4, after aerosolization at 28.3 l/min (Fig. 5e), contained a single but broader peak than that found on stage 5 (Fig. 5f), and this was due to the contribution of small lactose particles present together with drug particles. The sharp TOF peak on stage 5 appeared to be due to only drug particles being present, and this was supported by HPLC analysis as well as electron microscopy studies. The surface of lactose particles was damaged by the X-ray beam, while this phenomenon was not apparent when the beam passed over the drug particles. It is possible that the change in appearance of the lactose was due to the loss of water, which occurs due to localized heating.

This study employed an ACI without the plates being coated, usually carried out to reduce the possibility of parti-

cle bounce and re-entrainment in the airstream. If the plates were coated, then difficulties would have arisen when attempting to recover powder from the plates due to adherence of the powder to the plate. It was also thought that the coating material might interfere with HPLC analysis and X-ray microanalysis. In addition, it was considered that the aerosolized powders (lactose and albuterol sulfate) employed in this study, which are both plastic materials,^{17,18}) were not likely to bounce which would have a marked influence on the results obtained.

Conclusions

Deposition studies carried out using an ACI required a large number of chemical analyzes to be carried out by HPLC, for both drug and lactose, and thus proved to be a very time consuming exercise. Nevertheless, the results obtained by this technique were quantitative in nature and certain conclusions could be derived in relation to the strength of the interaction between the drug and carrier. However, the results of this study show that TOFABS can be employed in conjunction with the ACI to validate the deposition profiles obtained by HPLC analysis if the components of the formulation possess different physical properties (*i.e.* density and size). In the case of a binary mixture, after aerosolization of powder into the ACI, the TOF will give only a single symmetrical peak if a single component (either drug or carrier) is present on an individual plate. When split peaks are obtained, then both components are present. Use of TOFABS does not require a prolonged analytical procedure, therefore, once set up, the influence of subtle changes in formulation on the detachment of drug from carrier can be investigated relatively rapidly. SEM–X-ray microanalysis, which is also a time consuming method to carry out, is useful to view the shape and orientation of particles. In the case of albuterol sulfate and lactose, the X-ray spectra can clearly distinguish between drug and lactose particles. On the basis of the results from study it is concluded that TOFABS studies carried out on powder deposition on individual plates within an impactor can provide useful information on particle–particle interaction. If a difference in particle size and density exists between drug and excipient, then it is apparent that the particles, upon re-aerosolization with sufficient force to disrupt particulate interactions, exhibit measurable differences in their TOF. During formulation development, determining the TOF of the particles after deposition on impactor plates would provide an indication of whether a drug remains associated with lactose, is deposited as an aggregate or is primarily in individual particles. Should a drug remain extensively associated with a lactose of large particle size, then large amount of drug that would be detected in samples taken from low numbered stages. Such a drug is unlikely to be respirable. Obviously, the TOFABS data are strengthened by the analysis of the relative amounts of drug and lactose deposited on each plate, as carried out in this study. However, TOFABS studies alone would allow some prediction to be made as to whether the interactions between particles might change as a function of air flow or change in the nature (*e.g.* particle size, shape, crystallinity, processing, *etc.*) of drug and/or vehicle. X-ray microanalysis provides excellent supporting qualitative data of adherence between particles, providing that one of the particles contains an atom with an appropriate absorbing

spectrum. In conclusion, TOF, SEM-X-ray microanalysis and drug-carrier analysis from the ACI all proved to be useful tools in studying the interaction of drug and carrier in dry powder inhalers. It may be possible to relate those results to the possible states of interaction which exist between drug and carrier particles during passage through the airways after aerosolization.

References and Notes

- 1) Ganderton D., Kassem N. M., "Dry powder inhalers," Vol. 6, ed. by Ganderton D., Jones T., *Advances in Pharmaceutical Sciences*, Academic Press, London, 1992, pp. 165—191.
- 2) Hickey A. J., Concession N. M., Van Oort N. M., Platz R. M., *Pharm. Technol.*, **18**, 58—82 (1994).
- 3) Atkins P. J., *Pharm. Technol.*, **16**, 26—32 (1992).
- 4) Milosovich S. M., *Pharm. Technol.*, **16**, 82—86 (1992).
- 5) French D. L., Edwards D. A., Niven R. W., *J. Aerosol Sci.*, **27**, 769—783 (1996).
- 6) Niven R. W., *Pharm. Technol.*, **17**, 72—78 (1993).
- 7) Goldstein P. J., Newbury D. E., Echlin P., Joy D. C., Fiori C., Lifsin E., "Scanning Electron Microscopy and X-ray Microanalysis," Plenum Press, New York, 1981, pp. 1—10.
- 8) Lawes G., "Scanning Electron Microscopy and X-ray Microanalysis," John Wiley & Sons, Chichester, 1987, pp. 100—103.
- 9) Srichana T., Martin G. P., Marriott C., *Int. J. Pharm.*, **167**, 13—23 (1998).
- 10) British Pharmacopoeia 1993 (BP1993), Appendix XVII, A193—A196.
- 11) Srichana T., Martin G. P., Marriott C., *Eur. J. Pharm. Sci.*, **7**, 73—80 (1998).
- 12) Andersen Sampler, Operating Manual for 1 ACFM Non-viable Ambient Particle Sizing Sampler, Georgia (1985).
- 13) United States Pharmacopeia 1995 (USP XXIII), 3584—3591.
- 14) Hindle M., Byron P. R., *Pharm. Technol.*, **19**, 64—78 (1995).
- 15) Amherst Process Instruments, Aerosizer Technical Manual, Massachusetts (1995).
- 16) Stein S. W., Olson B. A., *Pharm. Res.*, **14**, 1718—1725 (1997).
- 17) Wade A., Weller P. J., *Handbook of Pharmaceutical Excipients*, 2nd edition, London, 1994, The Pharmaceutical Press.
- 18) Marple V. A., Olson B. A., Miller, N. C., *Aerosol Sci. Technol.*, **22**, 124—134 (1995).

Multiple Solubility Maxima of Oxolinic Acid in Mixed Solvents and a New Extension of Hildebrand Solubility Approach

Abolghasem JOUYBAN-GHARAMALEKI,^{*,a} Susana ROMERO,^b Pilar BUSTAMANTE,^b Brian J. CLARK^a

Drug Design Group, School of Pharmacy, University of Bradford,^a Bradford BD7 1DP, UK and Department of Farmacia y Tecnología Farmacéutica, Facultad de Farmacia, Universidad de Alcalá,^b Alcalá de Henares, 28871 Madrid, Spain.

Received June 25, 1999; accepted September 30, 1999

A new extension of the Hildebrand solubility approach which describes drug solubility in solvent mixtures showing multiple solubility peaks, the chameleonic effect, is proposed. The experimental solubilities of oxolinic acid were measured at 25 °C in solvent mixtures of ethanol–water and ethanol–ethyl acetate. A plot of the mole fraction of the drug against the solubility parameter (δ) of the solvent mixtures displays two peaks at $\delta=30.78$ MPa^{1/2} (80% v/v of ethanol in water) and at $\delta=20.90$ MPa^{1/2} (30% v/v of ethanol in ethyl acetate). The new extension proposed reproduces two solubility peaks. The thermograms of the solid phase before and after equilibration with the solvent mixtures did not show significant changes. The new extension was also tested with experimental data previously reported for drugs showing two solubility peaks of different height. The accuracy of other published models for describing two solubility maxima is also compared.

Key words multiple solubility maxima; hildebrand solubility approach; oxolinic acid; chameleonic effect; mixed solvent

Oxolinic acid possesses antibacterial effects against Gram-negative organisms. Its bactericidal action is similar to that of nalidixic acid. Oxolinic acid is used in the treatment of urinary tract infections due to Gram-negative organisms other than *Pseudomonas* species.¹⁾ Very low solubility of oxolinic acid restricts its therapeutic use. Its aqueous solubility at 20 °C is 10 ± 0.5 mg l⁻¹ and the solubility of its salt form is 20.5 ± 0.5 mg l⁻¹ at 20 °C.²⁾

Solubility determination of drugs in water–cosolvent mixtures provides useful data for better understanding of the solubility phenomenon in these media. In addition to the theoretical applications of the results of these determinations, the data can be employed for building the mathematical models and optimising the appropriate concentration of the pharmaceutical cosolvents for preparing liquid pharmaceutical preparations. In this study we focused on the theoretical applications of the cosolvency phenomenon.

The main aim of solubility data modelling is to provide a mathematical equation to represent the experimental results. By using these equations, it is possible 1) to report the data as a few model parameter values rather than presenting in a tabular form, 2) to screen the experimental data to detect the possible outliers, 3) to explore basic mechanisms of the solubility phenomenon and, finally, 4) to predict future results by the model parameters calculated based on training data set. In the pharmaceutical area, there has been considerable interest in forming a mathematical representation of solubility data in mixed solvents and several models have been presented over the past two decades.^{3–6)} One of the most popular models for this purpose is the extended Hildebrand solubility approach (EHSA), which was proposed by Martin and

co-workers. This model is able to calculate solubility data of drugs in water–cosolvent mixtures showing no peaks or a single maximum.^{3,7)} However, EHSA cannot predict drug solubility in solvent mixtures displaying multiple solubility peaks.^{8,9)}

The aim of this paper is to propose a new extension of the Hildebrand solubility approach for calculating solubility in mixed solvents showing multiple peaks and to compare the accuracy of the proposed model with that of previously published models.

Theoretical Treatment The EHSA introduced an interaction term W to replace the product $\delta_1\delta_2$ of the Hildebrand equation^{3,7)}:

$$-\ln X_2 = -\ln X_2^i + \frac{V_2\phi_1^2(\delta_1^2 + \delta_2^2 - 2W)}{RT} \quad (1)$$

where X_2 represents the mole fraction solubility of a drug in mixed solvent, X_2^i stands for the ideal solubility of the solute, V_2 is the molar volume of the solute, ϕ_1 denotes the volume fraction of the solvent, R is the molar gas constant, T is the absolute temperature, and δ_1 and δ_2 are the solubility parameters of the solvent and the solute. The term W is an adhesion parameter which represents solute–solvent interactions and is correlated by a power series of solubility parameters of the mixed solvent³⁾:

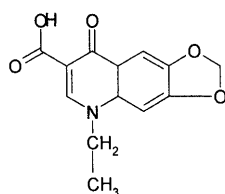
$$W = P_0 + P_1\delta_1 + P_2\delta_1^2 + \dots + P_n\delta_1^n \quad (2)$$

The solubility parameters of the mixed solvent (δ_1) are calculated from:

$$\delta_1 = \sum f_i \delta_i \quad (3)$$

where δ_i is the solubility parameter of the pure solvents and f_i is their volume fraction in the mixture.

Rearranging Eq. 1, $\ln \alpha_2/A$ can be also regressed against a polynomial in δ_1 , where α is the activity coefficient defined as the ratio of the ideal to the experimental solubility (X_2^i/X_2), and A is $\frac{V_2\phi_1^2}{RT}$. Martin *et al.*³⁾ also showed that $\ln X_2$ can be regressed on a polynomial in the volume fraction of the cosolvent. This was discussed in more detail by Barzegar-



Chemical structure of oxolinic acid

* To whom correspondence should be addressed.

Jalali and Jouyban-Gharamaleki.⁶⁾

The extended Hildebrand method (Eqs. 1 and 2) is not able to reproduce two solubility peaks, the so-called chameleonic effect. Bustamante and co-workers^{8,9)} described this effect for the first time in a quantitative way using partial solubility parameters related to Lewis acid–base interactions:

$$\ln X_2 = C_0 + C_1 \delta_1 + C_2 \delta_1^2 + C_3 \delta_{1a} + C_4 \delta_{1b} + C_5 \delta_{1a} \delta_{1b} \quad (4)$$

where C_0 – C_5 are the model constants, and δ_{1a} and δ_{1b} are the acidic and basic partial solubility parameters which are calculated from the volume fraction of the cosolvent as shown in Eq. 3. Equation 4 predicts two solubility peaks as found experimentally and explains the chameleonic effect in terms of differences of Lewis acid–base interactions of the solvent mixtures. Jouyban-Gharamaleki and Barzegar-Jalali¹⁰⁾ then proposed a computer optimised model to calculate the solubility of solutes with two solubility peaks, using ratios of partial solubility parameters.

With the EHSA, one can predict the solubility of compounds showing multiple solubility maxima provided that some modifications are made. For two binary systems with a common solvent or for actual ternary systems, the δ_1 values in Eq. 2 are calculated by Eq. 5:

$$\delta_1 = f_a \delta_{1(\text{solvent a})} + f_b \delta_{1(\text{solvent b})} + f_c \delta_{1(\text{solvent c})} \quad (5)$$

where $f_a + f_b + f_c = 1$. By substitution of f_b with $1 - f_a - f_c$ in Eq. 5:

$$\delta_1 = f_a \delta_{1(\text{solvent a})} + (1 - f_a - f_c) \delta_{1(\text{solvent b})} + f_c \delta_{1(\text{solvent c})} \quad (6)$$

Rearrangements in this equation yield:

$$\delta_1 = f_a \delta_{1(\text{solvent a})} + \delta_{1(\text{solvent b})} - f_a \delta_{1(\text{solvent b})} - f_c \delta_{1(\text{solvent b})} + f_c \delta_{1(\text{solvent c})} \quad (7)$$

$$\delta_1 = \delta_{1(\text{solvent b})} + f_a (\delta_{1(\text{solvent a})} - \delta_{1(\text{solvent b})}) + f_c (\delta_{1(\text{solvent c})} - \delta_{1(\text{solvent b})}) \quad (8)$$

Substitution of δ_1 values from Eq. 8 into Eq. 2 yields:

$$W' = P_0 + P_1 \{ \delta_{1(\text{solvent b})} + f_a (\delta_{1(\text{solvent a})} - \delta_{1(\text{solvent b})}) + f_c (\delta_{1(\text{solvent c})} - \delta_{1(\text{solvent b})}) \} + P_2 \{ [\delta_{1(\text{solvent b})} + f_a (\delta_{1(\text{solvent a})} - \delta_{1(\text{solvent b})}) + f_c (\delta_{1(\text{solvent c})} - \delta_{1(\text{solvent b})})]^2 \} + \dots \quad (9)$$

Appropriate rearrangements in this equation, considering δ_1 values for pure solvents as constant figures and deleting $f_a f_c$ terms yield:

$$W' = L_0 + L_1 f_a + L_2 f_c + L_3 f_a^2 + L_4 f_c^2 + \dots \quad (10)$$

in which W' stands for the interaction term and L_0 – L_4 are the model constants. In all solvent mixtures which exhibited multiple solubility peaks, the value of f_a or f_c is zero, thus all terms containing $f_a f_c$ are omitted from the equation. It should be noted that for 4 component solvent mixtures, e.g. water–ethanol, ethanol–ethyl acetate and ethyl acetate–hexane, the corresponding W' equation includes the additional terms f_d (volume fraction of hexane) and f_d^2 .

The δ_2 value is a characteristic of the solute, therefore omitting δ_2^2 from Eq. 1 and assuming the values of ϕ_1 to be equal to 1,¹¹⁾ the experimental values of W' can be calculated by Eq. 11. It should be noted that the solute solubility parameter is considered in the constant term of Eq. 10, i.e. L_0 term.

$$W' = \left[\frac{(\ln X_2 - \ln X_2^1) RT}{2V_2} \right] + \left[\frac{\delta_1^2}{2} \right] \quad (11)$$

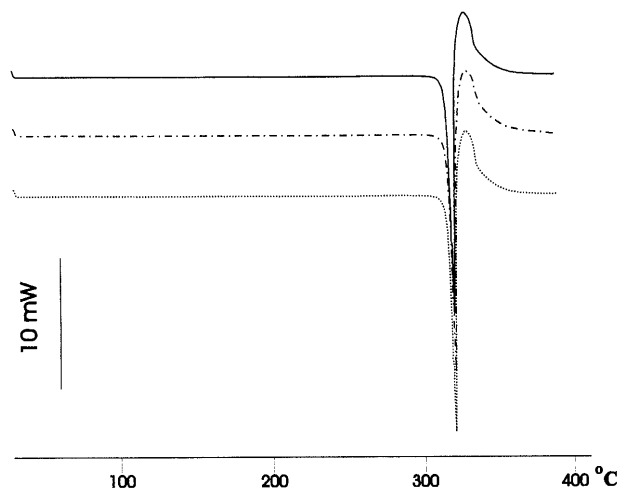


Fig. 1. DSC Profile of Oxolinic Acid, (—) Original Powder, Solid Phase after Equilibration with 50% v/v Ethanol in Water (-----) and 50% v/v Ethyl Acetate in Ethanol (.....)

The term W' should not be confused with W . In the original EHSA, W is an adhesion term for the solute–solvent interaction whereas W' includes the adhesion term plus a cohesion term, the square of the solubility parameter of the solute, δ_2^2 .

To compare the accuracy of the models, percent mean error, PME, was calculated using Eq. 12:

$$\text{PME} = \left(\frac{100}{N} \right) \sum_{i=1}^N \left(\frac{|X_m^{\text{calculated}} - X_m^{\text{observed}}|}{X_m^{\text{observed}}} \right) \quad (12)$$

where N denotes the number of experimental data points in each set. The average percent mean error (APME) was considered as an overall judgement criterion to compare the accuracy of the models.

Materials and Methods

Oxolinic acid was purchased from Sigma. The solvents used were ethyl acetate, ethanol (spectrophotometric grade, Panreac, Monplet and Esteban, Barcelona, Spain) and double distilled water.

Solubility Measurements Sealed flasks containing an excess of powder in the pure solvents and solvent mixtures were shaken at $25 \pm 0.1^\circ\text{C}$ in a temperature-controlled bath (Heto SH 02/100). The dissolution curves of drug dissolved *versus* time were studied. When the saturation concentration was attained, the solid phase was removed by filtration (Durapore membranes, $0.2 \mu\text{m}$ pore size). The drug did not significantly adsorb onto the membranes. Separate experiments (sedimentation, centrifugation) gave similar results to those obtained from filtration. The clear solutions were diluted with ethanol 96% v/v and assayed in a double beam spectrophotometer (Bausch Lomb 2000). The densities of the solutions were determined at $25 \pm 0.1^\circ\text{C}$ in a 10 ml pycnometer. All the experimental results are the average of at least three replicated experiments. The coefficient of variation ($\text{CV} = \text{S.D./mean} \times 100$) is within 2% among replicated samples.

Differential Scanning Calorimetry The thermograms of oxolinic acid were obtained with a differential scanning calorimeter (Mettler TA 4000). The melting point and the heat of fusion were measured in triplicate. Samples of 5–6 mg in perforated aluminium pans were heated at a rate of 5°C/min under nitrogen purge. The temperature range studied was 30 – 350 degrees.

Thermograms of the solid phase after equilibration with the pure solvents and several solvent mixture ratios were also obtained to detect possible changes in the solid phase. The solvent excess was evaporated at room temperature until it reached a constant weight.

Results and Discussion

The molar enthalpy of fusion of oxolinic acid was $\Delta H^F = 166.7 \text{ J/g}$, and the temperature of fusion is $T^F = 319.3^\circ\text{C}$.

Neither decomposition nor polymorphic changes was observed at the experimental temperature range. The thermograms did not vary after equilibration of the solid phase with the solvent systems (Fig. 1). Therefore, the presence of two solubility peaks could not be related to thermal changes of the solid phase and it can be attributed to the different hydrogen bonding ability of the two solvent mixtures.

The mole fraction solubilities of oxolinic acid at 25 °C in the two solvent mixtures which cover a large range of the solubility parameter scale, from 18 to 48 (MPa)^{1/2}, are listed in Table 1. Figure 2 displays the experimental solubility (mole fraction units) against the solubility parameter of the solvent mixtures. Oxolinic acid shows chameleonic behavior, *i.e.* two solubility peaks. The solubility of the drug increases from 100% water ($\delta_1=47.97$ MPa^{1/2}) to reach a maximum at 80% v/v ethanol in water. Larger ethanol concentrations decrease the solubility. Addition of ethyl acetate to ethanol lowers the polarity of the solvent enhancing the solubility of oxolinic acid to reach a second maximum at 30% v/v ethanol in ethyl acetate ($\delta_1=20.9$ MPa^{1/2}) which is higher than that found in ethanol–water ($\delta_1=29.73$ MPa^{1/2}). A possible explanation for the two solubility peaks is that the possibility of dimerisation of the solute increases in less polar solvents. Therefore, we have two different solubility parameters for the solute. The

Table 1. Experimental Solubility (Mole Fraction) of Oxolinic Acid in Ethanol–Water and Ethyl Acetate–Ethanol at 25 °C^{a)}

	δ_1	δ_{1a}	δ_{1b}	X_2
% v/v Ethanol				
0	47.86	13.71	65.46	10785×10^{-6}
10	45.73	14.03	60.04	29211×10^{-6}
20	43.59	14.36	54.62	53991×10^{-6}
30	41.46	14.69	49.19	74102×10^{-6}
40	39.32	15.01	43.77	99686×10^{-6}
50	37.19	15.34	38.35	12658×10^{-5}
60	35.05	15.67	32.93	16336×10^{-5}
70	32.92	16.00	27.51	20166×10^{-5}
80	30.78	16.32	22.09	20990×10^{-5}
90	28.64	16.65	16.67	16879×10^{-5}
100	26.51	16.98	11.25	82357×10^{-6}
% v/v Ethyl acetate				
10	25.71	16.36	10.51	11781×10^{-5}
20	24.91	15.75	9.78	16534×10^{-5}
30	24.10	15.14	9.04	22560×10^{-5}
50	22.50	13.91	7.57	34887×10^{-5}
60	21.70	13.30	6.83	38134×10^{-5}
70	20.90	12.68	6.10	41588×10^{-5}
90	19.29	11.46	4.62	34276×10^{-5}
100	18.49	10.84	3.89	24502×10^{-5}

a) δ_1 : total solubility parameter of the solvent mixtures, δ_{1a} and δ_{1b} : acidic and basic partial solubility parameters, X_2 : the mole fraction solubility of the drug.

Table 2. The Model Constants and Statistical Parameters for Eqs. 10 and 11

No. ^{a)}	$L_0^{b)}$	$L_1^{b)}$	$L_2^{b)}$	$L_3^{b)}$	$L_4^{b)}$	$r^{2c)}$	F ^{d)}	PME ^{e)}	N ^{f)}
1	341.896	595.283	-170.467	169.773	-7.540	1.000	344383	7.75	21
2	345.674	605.847	-174.145	142.195	-g)	1.000	331830	9.23	24
3	336.890	590.174	-177.820	175.494	-g)	1.000	276070	13.69	26
4	359.4063	581.178	-183.731	168.665	-17.780	1.000	105238	12.73	25
5	332.454	596.615	-181.959	182.067	9.649	1.000	304421	11.87	19

a) Numbers 1–5 represent sulphanilamide,⁹⁾ sulphamethazine,⁹⁾ sulphamethoxypyridazine,⁸⁾ paracetamol¹⁷⁾ and oxolinic acid dissolved in water–ethanol and ethanol–ethyl acetate mixtures. b) The numerical values of the curve-fit parameters (L_0 – L_4) were computed by fitting the experimental values of W' using Eq. 10. c) r^2 is the coefficient of determination and $r^2=1.000$ means $r^2>0.999$. d) F is the calculated value of F-test which was used to assess the significance of the correlation. e) PME is the percent mean error which is calculated by Eq. 12. f) N is the number of data points in each data set. g) These parameters are not significant ($p>0.05$).

solubility parameter comes from the Hildebrand solubility approach, *i.e.* Eq. 1 with $W=\delta_2\delta_1$, and originally was developed for simple non-associated liquid mixtures. This approach has been applied for non-polar solids by assuming these chemicals as supercooled liquids. The solute's solubility parameters can be calculated using different methods including solubility data.¹²⁾ Although different methods for determining the solute's solubility parameter give slightly different results, this parameter has been applied in various fields of pharmaceutical sciences such as solubility,¹³⁾ drug binding to plasma proteins¹⁴⁾ and tablet technology.¹⁵⁾ More details of pharmaceutical applications of the solubility parameter were recently reviewed by Hancock *et al.*¹⁶⁾

As for sulfonamides,^{8,9)} the solubility curve is asymmetrical, the solvent power of the less polar mixture being larger. In contrast, the solubility peaks of paracetamol¹⁷⁾ are of similar height in both mixtures. The location and height of the peaks could be related to the polarity of the solute. The highest ratio at the solubility maximum in ethanol–water to ethanol–ethyl acetate corresponds to paracetamol, which shows a solubility parameter larger than that for sulfonamides.

The extended Hildebrand method is applied to the experimental data of oxolinic acid (Eq. 2) and $\ln X_2$ is back calculated by Eq. 11. This method was not able to calculate the two solubility peaks, as shown in Fig. 2. In contrast, the modification proposed in this work (Eqs. 10 and 11) reproduces these two peaks (Fig. 2). The statistical significance of the curve-fit parameters (the L terms) was evaluated by using t -test and all parameters were significant ($p<0.05$).

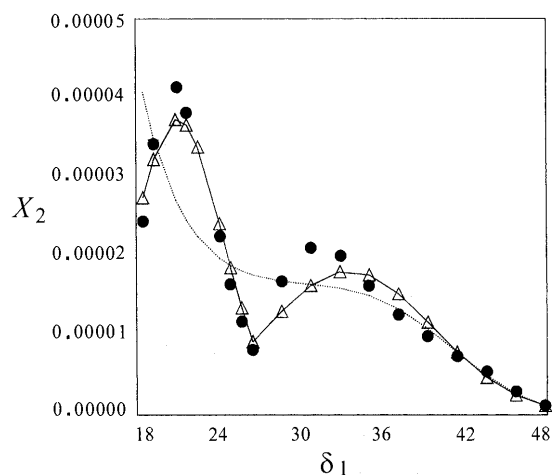


Fig. 2. Experimental Solubility (Mole Fraction) of Oxolinic Acid in Ethanol–Water and Ethyl Acetate–Ethanol Mixtures at 25 °C

(●) Experimental solubility values. Calculated solubility values: (.....) with Eq. 2, (---) with Eq. 4 and (—) with Eq. 10.

Table 3. The Percent Mean Error (PME) and Average Percent Mean Error (APME) Values for Different Models

No. ^{a)}	Eq. 4	Eq. 10	EFE	CNIBS/R-K
1	8.39 ^{b)}	7.75	2.65 ^{c)}	2.56 ^{c)}
2	11.29 ^{b)}	9.23	7.30 ^{c)}	4.53 ^{c)}
3	18.19 ^{b)}	13.69	2.42 ^{c)}	2.47 ^{c)}
4	12.31 ^{b)}	12.73	8.92 ^{c)}	5.32 ^{c)}
5	11.81	11.87	8.05	1.03
APME	12.40	11.05	5.87	3.18
No. of constant terms	6	6	7	9

a) The key to the drugs is the same as Table 2. b) PME values are calculated by employing the model constants taken from the references.^{8,9,17)} c) PME values are taken from the references.^{18,19)}

In addition to the data of oxolinic acid, four solubility data sets showing two maxima of different heights cited in the literature^{8,9,17)} are fitted to Eqs. 10 and 11. The coefficients and PME values obtained are shown in Table 2. In all cases, these equations reproduce the two solubility peaks. As mentioned in the theoretical section, one can use another version of the proposed extension, *i.e.* Eq. 10, for correlating solute solubility in higher order multicomponent mixed solvents. In an earlier paper, Escalera *et al.*⁸⁾ reported a wider solvent polarity range using water–ethanol, ethanol–ethyl acetate and ethyl acetate–hexane mixtures. This mixture provides a solvent media covering the solubility parameter ranging from 14.9 to 47.8 MPa^{1/2}. The corresponding equation for expressing the W' term for the solubility of sulphamethoxypyridazine in the solvent mixture is:

$$W' = 336.879 + 590.229f_a - 177.772f_c - 283.945f_d + 175.452f_a^2 - 16.411f_d^2 \quad (13)$$

$$r^2 = 1.000, F = 189949, p < 0.0005, \text{PME} = 13.79, N = 29$$

All the model constants in Eq. 13 are statistically significant at $p < 0.004$.

Two theoretical cosolvency models for reproducing multiple solubility maxima have been shown in recent papers.^{18,19)} Williams and Amidon⁴⁾ proposed an excess free energy (EFE) approach to estimate solute solubility in ternary solvent mixtures. This model was applied with modifications for reproducing multiple solubility peaks in mixed solvents.¹⁸⁾ An extension of the combined nearly ideal binary solvent/Redlich-Kister (CNIBS/R-K) was also employed to describe the solubility profile of solvent mixtures showing two solubility peaks.¹⁹⁾ Table 3 summarises the PME values and the number of constant terms of the models describing two solubility maxima in solvent mixtures. The CNIBS/R-K model produced the most accurate results. Our recent study showed that this is also the most accurate model for calculating solute solubility data in binary mixtures.²⁰⁾

Whilst considering the number of constant terms, as shown in Table 3, the more constant the terms the more accurate the predictions. However, in terms of Eqs. 4 and 10 containing an equal number of constant terms, the order of accuracy is Eq. 10 > Eq. 4.

Although the original EHSA equation cannot reproduce the solute solubility data in mixed solvents showing two maxima (Fig. 1), the results show that the modified EHSA is able to produce two solubility peaks. Of the theoretical models, EFE and CNIBS/R-K, produced the most accurate results, although the intercept is not significant statistically in the case of oxolinic acid.

Acknowledgements A. Jouyban-Gharamaleki thanks the Iranian Ministry of Health and Medical Education for providing financial support and the ORS committee for providing him with an Overseas Research Scholarship to study at the University of Bradford. The experimental data were obtained with the financial support of the University of Alcalá (project E007/99). S. Romero acknowledges a grant provided by Comunidad de Madrid (683/96).

References

- 1) Martindale the Extra Pharmacopoeia 28th ed. by Reynolds E. F., Prasad A.B., The Pharmaceutical Press, London, 1982, pp. 1052–1053.
- 2) Brazier M., Julien R., Ceolin R., Robert H., Khodadad P., *Pharm. Acta Helv.*, **66**, 226–229 (1991).
- 3) Martin A., Wu P. L., Adjei A., Lindstrom R. E., Elworthy P. H., *J. Pharm. Sci.*, **71**, 849–856 (1982).
- 4) Williams N. A., Amidon G. L., *J. Pharm. Sci.*, **73**, 9–13 (1984).
- 5) Acree W. E., Jr., *Thermochim. Acta*, **198**, 71–79 (1992).
- 6) Barzegar-Jalali M., Jouyban-Gharamaleki A., *Int. J. Pharm.*, **152**, 247–250 (1997).
- 7) Martin A., Wu P. L., Velasquez T., *J. Pharm. Sci.*, **74**, 277–282 (1985).
- 8) Escalera J. B., Bustamante P., Martin A., *J. Pharm. Pharmacol.*, **46**, 172–176 (1994).
- 9) Bustamante P., Ochoa R., Reillo A., Escalera J. B., *Chem. Pharm. Bull.*, **42**, 1129–1133 (1994).
- 10) Jouyban-Gharamaleki A., Barzegar-Jalali M., *Pharm. Sci.*, **2**, 559–560 (1996).
- 11) Yalkowsky S. H., Amidon G. L., Zografi G., Flynn G. L., *J. Pharm. Sci.*, **64**, 48–52 (1975).
- 12) Cave G., Kothari R., Poisieux G., Martin A. N., Carstensen J. T., *Int. J. Pharm.*, **5**, 267–272 (1980).
- 13) Bustamante P., Escalera B., Martin A., Selles E., *J. Pharm. Sci.*, **78**, 567–573 (1989).
- 14) Bustamante P., Selles E., *J. Pharm. Sci.*, **75**, 639–643 (1986).
- 15) Rowe C. E., *Int. J. Pharm.*, **41**, 219–222 (1988).
- 16) Hancock B. C., York P., Rowe R. C., *Int. J. Pharm.*, **148**, 1–21 (1997).
- 17) Romero S., Reillo A., Escalera B., Bustamante P., *Chem. Pharm. Bull.*, **44**, 1061–1064 (1996).
- 18) Jouyban-Gharamaleki A., *Chem. Pharm. Bull.*, **45**, 1383–1384 (1997).
- 19) Jouyban-Gharamaleki A., Acree W. E., Jr., *Int. J. Pharm.*, **167**, 177–182 (1998).
- 20) Jouyban-Gharamaleki A., Valaee L., Barzegar-Jalali M., Clark B. J., Acree W. E., Jr., *Int. J. Pharm.*, **177**, 92–101 (1999).

Partial Solubility Parameters of Lactose, Mannitol and Saccharose Using the Modified Extended Hansen Method and Evaporation Light Scattering Detection

M. Angeles PEÑA,^a Youssef DAALI,^b Jerome BARRA,^c and Pilar BUSTAMANTE^a

Department of Farmacia y Tecnología Farmacéutica, Facultad de Farmacia, Universidad de Alcalá,^a Alcalá de Henares, 28871 Madrid, Spain, School of Pharmacy, Laboratory of Pharmaceutical Analytical Chemistry, University of Geneva,^b Bd. d'Yvoy 20, 1211 Geneva 4, Switzerland, and School of Pharmacy, Department of Pharmaceutical Technology, University of Geneva,^c Quai Ernest-Ansermet 30, 1211 Geneva 4, Switzerland.

Received July 5, 1999; accepted September 29, 1999

The modified extended Hansen method was tested for the first time to determine partial solubility parameters of non-polymeric pharmaceutical excipients. The method was formerly tested with drug molecules, and is based upon a regression analysis of the logarithm of the mole fraction solubility of the solute against the partial solubility parameters of a series of solvents of different chemical classes. Two monosaccharides and one disaccharide (lactose monohydrate, saccharose and mannitol) were chosen. The solubility of these compounds was determined in a series of solvents ranging from nonpolar to polar and covering a wide range of the solubility parameter scale. Sugars do not absorb at the UV-vis region, and the saturated solutions were assayed with a recent chromatographic technique coupled to an evaporative light scattering detector. This technique was suitable to determine the concentration dissolved in most solvents. The modified extended Hansen method provided better results than the original approach. The best model was the four parameter equation, which includes the dispersion δ_d , dipolar δ_p , acidic δ_a and basic δ_b partial solubility parameters. The partial solubility parameters obtained, expressed as $\text{MPa}^{1/2}$, were $\delta_d=17.6$, $\delta_p=28.7$, $\delta_h=19$, $\delta_a=14.5$, $\delta_b=12.4$, $\delta_T=32.8$ for lactose, $\delta_d=16.2$, $\delta_p=24.5$, $\delta_h=14.6$, $\delta_a=8.7$, $\delta_b=12.2$, $\delta_T=32.8$ for mannitol and $\delta_d=17.1$, $\delta_p=18.5$, $\delta_h=13$, $\delta_a=11.3$, $\delta_b=7.6$, $\delta_T=28.4$ for saccharose. The high total solubility parameters δ_T obtained agree with the polar nature of the sugars. The dispersion parameters δ_d are quite similar for the three sugars indicating that the polar δ_p and hydrogen bonding parameters (δ_h , δ_a , δ_b) are responsible for the variation in the total solubility parameters δ_T obtained, as also found for drugs. The results suggest that the method could be extended to determine the partial solubility parameters of other non-polymeric pharmaceutical excipients.

Key words lactose monohydrate; saccharose; mannitol; light scattering; partial solubility parameter

Solubility parameters and other cohesion parameters provide a means to correlate and predict cohesive and adhesive properties of materials from a knowledge of the properties of their components.¹⁾ Hansen determined the partial solubility parameters of polymers, resins and plasticizers to predict paint component affinities²⁾ but these parameters are unknown for most pharmaceutical excipients. The knowledge of cohesion parameters would help to predict drug-excipient interactions and to allow selection of the most suitable excipients for a drug. Hansen divided the Hildebrand solubility parameter³⁾ δ_T into partial solubility parameters δ_d , δ_p , and δ_h , related to van der Waals dispersion forces, Keesom dipole interactions and hydrogen bonding, respectively.^{2,4)} The partial solubility parameters of solvents are found in the literature¹⁾ and the extended Hansen method was proposed for solid drug molecules.⁵⁾ Hansen determined the cohesion parameters of polymers and resins from semiquantitative solubility measurements.²⁾ The usual procedure is to contact the polymer or resin with a given amount of solvent and to examine the solubility behavior using a qualitative scale (clear solution, almost soluble, strongly swollen, slight solubility, swollen, little swelling and no visible effect). These data are then plotted in a suitable manner and a region of solubility is defined including the solvents dissolving the polymer. The use of techniques based on quantitative solubility measurements would provide more accurate values for the cohesion parameters. The partial solubility parameters of sugars have not been determined; only the values for lactose are

reported.⁶⁾ In earlier work, we modified the extended Hansen method of Beerbower⁵⁾ to determine the partial solubility parameters of drugs.^{7–9)} The modified method relates the logarithm of the experimental mole fraction solubility of the drug to the solubility parameters of the solvents, using the three- and four-partial solubility parameter models. The modified method improved the significance of the partial parameters obtained in relation to those determined with the original extended Hansen method.

With the three parameter model, the logarithm of the experimental mole fraction solubility X_2 is regressed against the partial solubility parameters of the solvents:

$$\ln X_2 = C_0 + C_1\delta_{1d}^2 + C_2\delta_{1d} + C_3\delta_{1p}^2 + C_4\delta_{1p} + C_5\delta_{1h}^2 + C_6\delta_{1h} \quad (1)$$

In a similar fashion, the four parameter model is written:

$$\ln X_2 = C_0 + C_1\delta_{1d}^2 + C_2\delta_{1d} + C_3\delta_{1p}^2 + C_4\delta_{1p} + C_5\delta_{1a} + C_6\delta_{1b} + C_7\delta_{1a}\delta_{1b} \quad (2)$$

In Eqs. 1 and 2, $\ln X_2$ replaces the original variable of the extended Hansen method, $\ln \alpha_2/U$, where α_2 is the activity coefficient defined as the ratio of the ideal to the experimental mole fraction solubility, and U is related to the molar volume of the drug and the volume fraction of the solute. In Eq. 2, the hydrogen bonding parameter is divided into the acidic and basic partial solubility parameters related to the proton donor and proton acceptor capability.

The partial solubility parameters of solid drugs were calculated from the regression coefficients of Eqs. 1 and 2. From Eq. 1:

* To whom correspondence should be addressed.

$$\delta_{2d} = -(C_2/2C_1); \delta_{2p} = -(C_4/2C_3) \text{ and } \delta_{2h} = -(C_6/2C_5) \quad (3)$$

and from Eq. 2:

$$\delta_{2d} = -(C_2/2C_1); \delta_{2p} = -(C_4/2C_3); \delta_{2a} = -(C_6/C_7) \text{ and } \delta_{2b} = -(C_5/C_7) \quad (4)$$

The modified extended Hansen method (Eqs. 1—4) is applied here for the first time to three pharmaceutical excipients, lactose, saccharose and mannitol. These saccharides are widely used in pharmaceutical industry and drug formulation. The partial solubility parameters of mannitol and saccharose are reported in this work for the first time. Since the dispersion, dipolar and hydrogen bonding parameters of lactose were obtained from a different experimental method⁶⁾ these values serve to test the validity of the method used here. In addition, the acidic and basic partial solubility parameters of lactose are obtained in this work for the first time. The UV-vis spectrophotometric technique cannot be applied to accurately determine the solubility of sugars because these compounds do not present absorption peaks. An evaporative light scattering detector (ELSD) was proposed for the analysis of compounds that do not absorb UV radiation or do so at inconvenient wavelengths where sensitivity is low.^{10—12)} This is a quite recent technique and was used in this work.

Experimental

Materials Lactose monohydrate, mannitol and saccharose were kindly provided by UPSA (France). D-Fructose (Fluka Biochemika) was used as internal standard for the assay. The solvents employed (spectrophotometric or analytical grade, Table 1) include several chemical classes from nonpolar to highly polar to cover a wide range of the solubility parameter scale.

Methods The water content of lactose, mannitol and saccharose was determined in triplicate using the Karl Fischer rapid test as previously reported.⁸⁾ The molar heats and temperatures of fusion were determined by differential scanning calorimetry (Mettler TA 4000). The solubility experiments were performed as follows. An excess of the sugar powders was placed in contact with the solvents. The suspensions were shaken at $25 \pm 0.2^\circ\text{C}$ in a temperature-controlled bath (Heto SH 02/100, Germany) during 5—6 days. After equilibrium solubility was achieved, the nondissolved solid phase was removed by filtration (0.2 μm pore size membranes Nylaflo, Durapore or Fluoropore). The saturation concentrations were determined by a liquid chromatographic procedure associated with an evaporative light scattering detector (see below). The densities of the solutions were measured in 10 ml-pycnometers. All the results are the average of at least three replicated experiments. Weighted multiple regression analysis was performed with a number cruncher statistical system (NCSS Software, Kayesville, UT, U.S.A.). Residual analysis and the Cook distance were used to detect deviations of individual cases from the overall regression. A smaller weight (0.001) was assigned to the solvents that least fitted the models.

Liquid Chromatographic Procedure The liquid chromatograph (LC) consisted of Waters 600E multisolvent delivery system and a Waters 717 plus autosampler (both from Milford, MA, U.S.A.). The measurements were carried out on a gel column packed with a micro-particulate resin in the calcium form (300 \times 6.5 mm) from Waters and thermostated at 80°C . The flow rate of the mobile phase (distilled water) was 0.5 ml/min and the injection volume 20 μl . The LC column was coupled to a Sedex 55 evaporative light scattering detector (Sedere, Alfortville, France). Nebulization of the eluent in the ELSD was provided by a stream of pressurized air at 2.5 bar with a flow rate of approximately 4 l/min. The nebulization was performed at room temperature, and the nebulized solvent was evaporated at 40°C . The detection output was interfaced to a computer using a Chrom-Card software (Fisons Instruments, Milan, Italy) for data handling and chromatogram generation. Samples of water-miscible saturated solutions of lactose monohydrate, mannitol and saccharose were either diluted with distilled water or evaporated to concentrate the solute. Samples of non-water-miscible saturated solutions were directly evaporated and the residues were then diluted in water. To avoid variations in the ELSD response over time, fructose was used as an internal standard for all the sugars studied. The experimental error of the solubility measurements of lactose, mannitol and saccharose ranges between 0.2—7%, except for the solutions of lactose in propionic

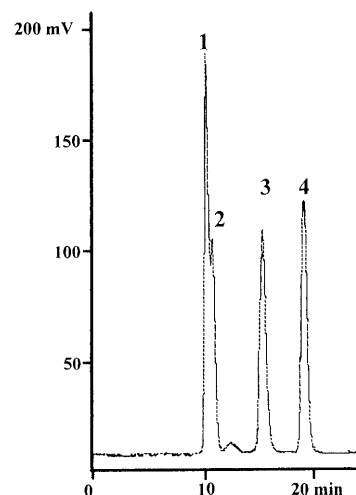


Fig. 1. Separation by Liquid Chromatography of Different Sugars Detected by Evaporative Light Scattering

1: saccharose, 2: lactose monohydrate, 3: fructose, 4: mannitol.

acid (23%) and in acetone (21.7%).

Results and Discussion

Evaporative Light Scattering Technique The detection principle of ELSD is based on column effluent nebulization into droplets which are carried by a nebulizing gas in an evaporator tube and then directed towards a light beam.^{13,14)} Light is scattered by residual particles of non-volatile material and measured by a photomultiplier. Then, the signal intensity is related to the mass of the analyte in the eluent.

Detector response linearity was determined by preparing five calibration samples covering a 0.05—0.50 mg/ml concentration range. Each sample was injected in triplicate. Because ELSD gives a nonlinear response, a plot of the ratio between the peak areas of the solute and the internal standard *versus* the sample concentration in double logarithmic coordinates was used,¹⁴⁾

$$\log A = \log a + b \log C \quad (5)$$

where A is the peak area ratio, C the concentration, and a and b constants determined principally by the nature of the mobile phase. Separation of the different sugars with the internal standard (fructose) was quite efficient as illustrated in Fig. 1.

Solubility of Lactose, Mannitol and Saccharose as Related to the Total Solubility Parameter of the Solvents The water content was 6.12%, 0.41% and 2.6% for lactose monohydrate, mannitol and saccharose, respectively. The ideal solubility was obtained from the molar heat and temperature of fusion.⁷⁾ At a heating rate of $5^\circ\text{C}/\text{min}$, lactose shows a dehydration peak at 141°C and then melts at 214.2°C . The heat of fusion is 98.48 kJ/mol. Chidavaenzi *et al.*¹⁵⁾ reported endothermic peaks for dehydration (152°C) and fusion (204°C) at a heating rate of $20^\circ\text{C}/\text{min}$. The temperatures and heats of fusion are 166.6°C and 50.5 kJ/mol for mannitol and 189.8°C and 44.53 kJ/mol for saccharose. The ideal solubilities X_2^i of mannitol ($X_2^i = 1.6 \times 10^{-3}$) and saccharose ($X_2^i = 1.7 \times 10^{-3}$) are very similar. The lowest value corresponds to lactose ($X_2^i = 2 \times 10^{-4}$). This means that the energy needed to liquefy the crystal to enter into the solution is larger for lactose than for the other two saccharides.

Figures 2–4 show the logarithm of the solubility mole fraction against the total solubility parameter δ_T which serves as a measure of the overall polarity of the solvents. The plots illustrate in a qualitative way the polarity region and the kind of solvents providing maximum solubility. Lactose is much more soluble in strongly dipolar solvents of high dielectric constant values (formamide and water) than in alcohols and nonpolar solvents. The region of maximum solubility corresponds to large solubility parameter values (from 36 to 50 MPa^{1/2}), the highest solubility being observed in formamide. Alcohols of low solubility parameter values are poor solvents whereas lactose is quite soluble in glycols. The solubility in basic solvents such as dioxane is similar to that observed in acidic solvents and increases as the solubility parameter of the solvent becomes larger.

As for lactose, the maximum solubility of mannitol occurs in the region corresponding to the highest solubility parameter values (from 36 to 50 MPa^{1/2}). The solubilities are larger than for lactose in most of the solvents owing to the higher ideal solubility of mannitol. Strongly dipolar solvents (formamide, *N,N*-dimethylformamide and water) with large solubility parameter values are the best solvents for mannitol, and the experimental solubilities are similar to those found for lactose in these solvents.

The solubility of saccharose in propionic acid, diethyl ether and in most of the nonpolar solvents was too low to be detected by the method of assay. The structure of saccharose which contains two closed rings is similar to that of lactose and both sugars differ from the open structure of mannitol. However, the solubility in formamide and in strongly dipolar solvents is less than for the other two sugars. Among the solvents tested, formamide, *N,N*-dimethylformamide and water provide the maximum solubility. Glycols are better solvents than alcohols, and the region of maximum solubility is located at large polarity values (δ_T above 35 MPa^{1/2}). The solubility plots against the total solubility parameter are scattered (Figs. 2–4) because this single parameter does not differentiate the several kinds of interactions (dispersion, polar, hydrogen bonding). Using a polynomial in the second degree (theoretical curves of Figs. 2–4) the correlation of $\ln X_2$ against the total solubility parameter (δ_T) is poor ($r^2=0.73$ for lactose and mannitol and $r^2=0.68$ for saccharose). This justifies the use of partial solubility parameters in the models used in this work (Eqs. 1 and 2).

Partial Solubility Parameters of Lactose, Mannitol and Saccharose The experimental logarithm of the mole fraction solubility (Table 1) was fitted to Eqs. 1 and 2. The values of the partial solubility parameters used in the regression analysis were previously published.⁸⁾ The original variable of the extended Hansen approach was also tested using $\ln \alpha_2/U$ instead of $\ln X_2$ in Eqs. 1 and 2. The activity coefficient α_2 was obtained from the ratio of the ideal to the experimental solubility mole fraction $\alpha_2 = X_2^i/X_2$. The term U was calculated from the volume fraction of the solvent ϕ_1 and the molar volume of the solute V_2 , $U = V_2\phi_1^2/RT$ where R is the gas constant and T the absolute temperature. For lactose, $\ln \alpha_2/U$ did not give good results; the signs of some of the regression coefficients were not correct with either the three- or the four parameter model; therefore, this variable is not included in Table 1. The best results were obtained with the dependent variable of the modified method, $\ln X_2$, and the four

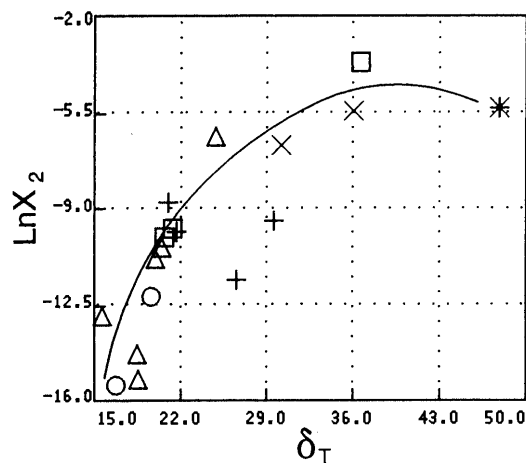


Fig. 2. Experimental Log Mol Fraction Solubility of Lactose against the Solubility Parameter of the Solvents

○, nonpolar; △, bases; □, acids; +, alcohols; ×, glycols; *, water.

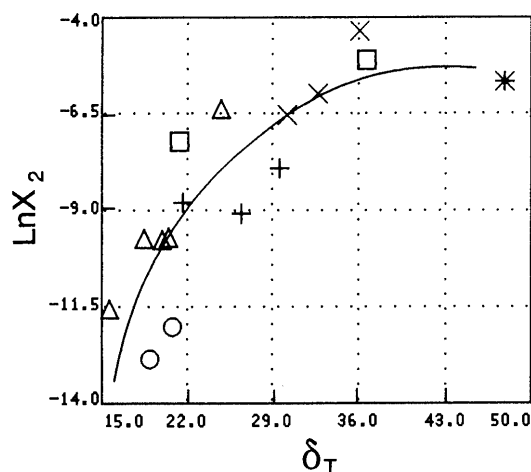


Fig. 3. Experimental Log Mol Fraction Solubility of Mannitol against the Solubility Parameter of the Solvents

○, nonpolar; △, bases; □, acids; +, alcohols; ×, glycols; *, water.

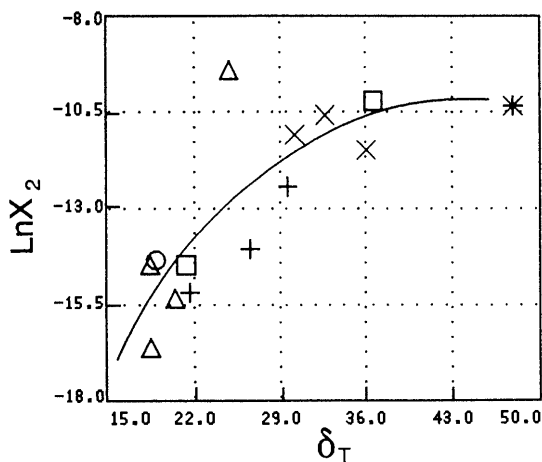


Fig. 4. Experimental Log Mol Fraction Solubility of Saccharose against the Solubility Parameter of the Solvents

○, nonpolar; △, bases; □, acids; +, alcohols; ×, glycols; *, water.

parameter model (Eq. 2). The solvents that least fitted the model were ethanol, methanol, 1,2 propanediol and ethyl acetate. Water was included in the regression analysis because

Table 1. Dependent Variables for Lactose, Mannitol and Saccharose

Solvents	Lactose $\ln X_2$	Mannitol $\ln X_2$	Saccharose $\ln X_2$
Ethanol	-11.6131	-9.0891	-16.4608
Chloroform	^{b)}	^{b)}	-168667
Methanol	-9.4781	-7.9205	-14.2283
Benzene	-15.2384	^{b)}	-20.0631
Dioxane	-10.4385	-9.6962	-18.2647
Acetic acid	-9.7587	-7.2356	-17.0504
Pentanol	-9.8703	-8.80489	-18.0534
Cyclohexane	-15.4443	^{b)}	^{b)}
Ethylene dichloride	^{b)}	^{b)}	^{b)}
1,2-Propanediol	-6.7154	-6.5430	-12.3425
Formamide	-3.6711	-5.1104	-11.1010
Ethylene glycol	^{c)}	-5.9881	-11.6191
Glycerol	-5.4614	^{c)}	-12.8991
Octanol	-8.8128	^{c)}	^{b)}
Ethyl acetate	-14.2996	-9.73011	-17.0410
Heptane	^{b)}	^{b)}	^{b)}
Chlorobenzene	-12.2240	^{b)}	^{b)}
Propionic acid	-10.0713	^{b)}	^{b)}
Diethyl ether	-12.9426	-11.5626	^{b)}
Water	-5.3507	-5.6732	-11.2876
Acetone	-10.8519	^{b)}	^{b)}
Acetophenone	^{c)}	^{c)}	^{b)}
N,N-Dimethyl formamide	-6.3961	-6.3834	-9.9817

a) $\ln \alpha_2 = \ln X_2 / \ln X_1$ and $U = V_2 \Phi_2^2 / RT$. See Barra *et al.*⁷⁾ b) The concentration dissolved was not detectable by evaporative light scattering detection. c) A problem appeared during the measurement, probably because of degradation of the sugar during the drying of the saturated phase.

this solvent is located at the region of maximum solubility of lactose and was compatible with the model. Water is usually very influent for less polar solutes showing a high Cook distance and should not be included in these cases.⁸⁾ The three parameter model also provided significant partial parameters for lactose, but the number of incompatible solvents with the model was larger, and the polar partial solubility parameter obtained was too high ($\delta_p = 37.25 \text{ MPa}^{1/2}$) to be realistic.

The parameters listed in Table 2 for lactose were obtained with the four parameter model and are quite close to those reported by Huu-Phuoc *et al.*⁶⁾ ($\delta_{2d} = 19.6$, $\delta_{2p} = 26.2$, $\delta_{2h} = 23.1$, $\delta_{2T} = 39.9 \text{ MPa}^{1/2}$) using a completely different method. Instead of solubility measurements, these authors employed chromatographic parameters obtained from gas-solid chromatography. The set of solvents was different from the one used here. Highly polar solvents (glycols and water) were not employed, and the acidic and basic partial solubility parameters of lactose were not determined. Examination of the parameters obtained in the present study shows that lactose is very polar (high δ_{2p} value) which agrees with the large number of polar groups of the molecule. The Lewis acid ability is somewhat larger than the Lewis base properties (δ_{2a} is about two units higher than δ_{2b}). The dispersion partial solubility parameter is like the values determined for drug molecules. Therefore, the large values of the dipolar and hydrogen bonding parameters are responsible for the high total solubility parameter obtained.

As for lactose, the four parameter model associated with the dependent variable $\ln X_2$ (Eq. 2) provided the best results for mannitol. The solvents that least fitted the model were pentanol, ethylene glycol and ethylene dichloride. The partial solubility parameters obtained are listed in Table 2. Water

Table 2. Partial Solubility Parameters ($\text{MPa}^{1/2}$) of Lactose, Mannitol and Saccharose with $\ln X_2$ as the Dependent Variable.^{a)}

Dependent variable, $\ln X_2$	δ_d	δ_p	$\delta_h^{b)}$	δ_a	δ_b	δ_T	r^2
Lactose	17.57	28.67	18.99	14.50	12.43	38.61	0.96
Mannitol	16.15	24.53	14.56	8.71	12.18	32.78	0.99
Saccharose	17.09	18.52	13.05	11.26	7.57	28.38	0.99

a) The total and partial solubility parameters of the solvents used in the regression analysis are found in Bustamante *et al.* (1998a).⁸⁾ The parameters were obtained with Eqs. 2 and 4. The standard errors of the regression are: lactose, S.D.=0.77, mannitol, S.D.=0.25 and saccharose, S.D.=0.21. b) Calculated from $\delta_h^2 = 2\delta_a\delta_b$.

was compatible with the overall regression. Mannitol has high δ_{2p} , δ_{2h} and δ_{2T} values although they are lower than for lactose. The dispersion partial parameters of lactose and mannitol are very similar, as expected.

The variable $\ln \alpha_2 / U$ was not calculated for saccharose. This compound decomposed near fusion and accurate heats of fusion could not be determined. As for lactose and mannitol, the four parameter model associated with the dependent variable $\ln X_2$ provided the best results, with significant regression coefficients. Ethanol and 1-pentanol were the solvents that least fitted the model.

As observed in Table 2, the dispersion partial solubility parameter is similar for the three compounds studied. Lactose, mannitol and saccharose are quite polar showing high dipolar and total solubility parameters. The two cyclic sugars, lactose and saccharose are better Lewis acids ($\delta_{2a} > \delta_{2b}$) whereas mannitol, with an open structure, is a better Lewis base ($\delta_{2a} < \delta_{2b}$) against the solvents used. The ratio δ_a / δ_b of the three sugars increases from mannitol (0.72) to lactose (1.17) and saccharose (1.49). The three compounds have a high overall hydrogen bonding capability, showing δ_h values above $13 \text{ MPa}^{1/2}$.

The results show that the modified extended Hansen method can be applied to obtain partial solubility parameters of sugars. The parameters determined for lactose are close to those obtained by Huu-Phuoc⁶⁾ using another technique and a different set of solvents. The modified extended Hansen method has been applied for the first time to pharmaceutical excipients and the most suitable model was the four parameter equation, as earlier found for drug molecules.⁷⁻⁹⁾ The partial solubility parameters obtained for lactose, mannitol and saccharose provide a quantitative measure of their ability to interact through dispersion, dipolar and hydrogen bonding with other excipients and drugs. The large values of the dipolar and hydrogen bonding parameters agree with the highly polar nature of these excipients, being larger than those previously found for semipolar drugs. The values of δ_a and δ_b are also large, indicating the ability of the sugars to interact through both Lewis acid and Lewis base interactions. Therefore, the interaction of the excipients studied will be larger either with acidic or basic drugs showing high δ_p values. The partial solubility parameters very much improve the fit of solubility when compared with the results obtained with a single parameter (δ_T). According to the r^2 values shown in Table 2, more than 96% of the solubility change is accounted for by the model (Eq. 4). With a single parameter, only 68—70% of the variance is explained, resulting in scattered plots (Figs. 2—4). The evaporative light scattering technique of assay provided good results with most solvents and was suit-

able to accurately measure the solubility of sugars in individual solvents. The results suggest that the modified extended Hansen method could be applied to determine partial solubility parameters of other non-polymeric pharmaceutical excipients, provided that an accurate method to measure the experimental solubility is available.

Acknowledgments This research was supported by the University of Alcalá, Spain (Project No. E007/99).

References

- 1) Barton A. F. M., Handbook of Solubility Parameters and Other Cohesion Parameters. CRC Press, Boca Raton, Florida, 1991.
- 2) Hansen C. M., *J. Paint Tech.*, **39**, 511—514 (1967).
- 3) Hildebrand J. H., Prausnitz J. M., Scott R. L., "Regular and Related Solutions," Van Nostrand Reinhold, New York, 1970.
- 4) Hansen C., Beerbower A., Encyclopedia of Chemical Technology, Suppl. 2nd ed., Wiley, 1971.
- 5) Beerbower A., Wu P. L., Martin A., *J. Pharm. Sci.*, **73**, 179—188 (1984).
- 6) Huu-Phuoc N., Phan Tan Luu R., Munafo A., Ruelle P., Nam-Tran H., Buchmann M., Kesselring U. W., *J. Pharm. Sci.*, **75**, 68—72 (1986).
- 7) Barra J., Lescure F., Doelker E., Bustamante P., *J. Pharm. Pharmacol.*, **49**, 644—651 (1997).
- 8) Bustamante P., Peña M. A., Barra J., *J. Pharm. Pharmacol.*, **50**, 975—982 (1998a).
- 9) Bustamante P., Peña M. A., Barra J., *Int. J. Pharmaceutics*, **174**, 141—150 (1998b).
- 10) Lafosse M., Elfakir C., Morin-Allory L., Dreux M., *J. High Resolution Chromatography*, **15**, 312—318 (1992).
- 11) Herbreteau B., Lafosse M., Morin-Allory L., Dreux M., *Chromatographia*, **33**, 325—330 (1992).
- 12) Dreux M., Lafosse M., Morin-Allory L., *LG-GC International*, **9**, 148—156 (1996).
- 13) Honda S., Suzuki S., Nose A., Yamamoto K., Kakehi K., *Carbohydr. Res.*, **215**, 193—198 (1996).
- 14) Charlesworth J. M., *Anal. Chem.*, **50**, 1414—1420 (1978).
- 15) Chidavaenzi O. W., Buckton G., Koosha F., Pathack R., *Int. J. Pharmaceutics*, **159**, 67—74 (1997).

Development of Plasmin-Selective Inhibitors and Studies of Their Structure–Activity Relationship¹⁾

Yoshio OKADA,^{*,a} Yoshikazu MATSUMOTO,^a Yuko TSUDA,^a Mayako TADA,^{a,b} Keiko WANAKA,^b Akiko HIJIKATA-OKUNOMIYA,^c and Shosuke OKAMOTO^b

Faculty of Pharmaceutical Sciences, Kobe Gakuin University,^a Nishi-ku, Kobe 651–2180, Japan, Kobe Research Projects on Thrombosis and Haemostasis,^b 3–15–18, Asahigaoka, Tarumi-ku, Kobe 655–0033, Japan, and Faculty of Health Sciences, Kobe University School of Medicine,^c Suma-ku, Kobe 654–0142, Japan.

Received July 5, 1999; accepted October 9, 1999

Various compounds were synthesized by combining three components at positions P₁, P_{1'} and P₂. Of these, *N*-(*trans*-4-aminomethylcyclohexanecarbonyl)-Tyr(*O*-2-bromobenzyloxycarbonyl)-octylamide inhibited plasmin selectively with IC₅₀ values of 0.80 and 0.23 μM towards S-2251 and fibrin, respectively. This compound also inhibited plasma kallikrein, urokinase, thrombin and trypsin with IC₅₀ values of 10, >50, >50 and 1.6 μM, respectively.

Key words plasmin inhibitor; selectivity; structure–activity relationship; *N*-(*trans*-4-aminomethylcyclohexanecarbonyl)-Tyr(*O*-2-BrZ)-octylamide

It is well known that proteinases and their natural inhibitors regulate biological functions cooperatively to maintain homeostasis, while any imbalance between proteinases and their natural inhibitors can cause serious disorders.^{2,3)} With regard to plasmin (PL), α₂-macroglobulin (α₂-M)⁴⁾ and α₂-plasmin inhibitor (α₂-PI)⁵⁾ are known as endogenous inhibitors. It is also well known that α₂-PI consists of two parts: one part binds to the active site (catalytic site) of PL and another to the lysine binding site (LBS) of PL. An imbalance between PL and its natural inhibitors causes a serious syndrome, such as hyperfibrinolysis.^{6–8)} At present, ε-aminocaproic acid⁹⁾ and *trans*-4-aminomethylcyclohexanecarboxylic acid (*trans*-AMCHA)¹⁰⁾ are used clinically as PL inhibitors. These inhibitors show fairly potent inhibition of fibrinolysis by PL with an IC₅₀ value of 60 μM, but poor inhibition of the amidolysis of small peptide substrates and fibrinogenolysis by PL. This is because these inhibitors act on PL by blocking the LBS of an enzyme, which is not the catalytic site.¹¹⁾

With the objectives of obtaining a powerful new tool to study the role of PL and developing novel types of clinical therapy, we focused our attention on the synthesis of potent active center-directed PL inhibitors. Previously, we reported the development of active center-directed inhibitors of PL^{12,13)} and studies of their structure–inhibitory activity relationship.¹⁴⁾ Our inhibitors consist of three parts, P₁, P_{1'} and P₂,¹⁵⁾ and their structure–activity relationship is summarized

in Table 1.

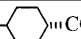
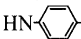
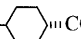
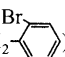
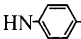
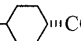
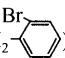
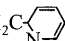
As shown in Table 1, compound **I** inhibits plasma kallikrein (PK) specifically, compound **II** inhibits both PL and PK, and compound **III** inhibits PL specifically. These results, showed that we could design enzyme-selective inhibitors by combining various kinds of substituents at positions P₁, P_{1'} and P₂.

Bearing in mind the above results, we designed and synthesized a series of plasmin-selective inhibitors and this report deals with these PL inhibitors and their structure–activity relationship.

Tyr(*O*-2-BrZ) was selected as the P_{1'} substituent, since it is known that this residue can increase the affinity for some part of the active center of trypsin-like proteinases.¹⁴⁾ As the P₁ substituent, we chose 6-aminohexanoic acid or *trans*-4-aminomethylcyclohexanecarboxylic acid.

First of all, alkyl amines with various chain lengths were used as the P₂ substituent. As illustrated in Chart 1, Boc-Tyr(*O*-2-BrZ)-OH was coupled with alkylamine to give Boc-Tyr(*O*-2-BrZ)-NH-R (R: *n*-pentyl, *n*-hexyl, *n*-heptyl, *n*-octyl, *n*-nonyl, 3-methylbutyl, 1,1-dimethylpropyl). After removal of Boc with HCl–dioxane, the resulting amine was coupled with Boc-EACA-OH or Boc-Tra-OH to give Boc-EACA- or Boc-Tra-Tyr(*O*-2-BrZ)-NH-R, which were treated with 6N HCl–dioxane to give compounds **1–14**. Their inhibitory activities against a series of enzymes are summarized in Table 2. As the P₁ substituent, the Tra group is more suitable than

Table 1. IC₅₀ Values (μM) of Compounds **I–III** for PL and PK

Compound	P ₁	P _{1'}	P ₂	PL	PK
				S-2251	S-2302
I	H ₂ NH ₂ C–  –CO	Phe	HN–  –CH ₂ COOH	630	1.3
II	H ₂ NH ₂ C–  –CO	Tyr(<i>O</i> -CO ₂ CH ₂ – )	HN–  –COCH ₃	0.23	0.37
III	H ₂ NH ₂ C–  –CO	Tyr(<i>O</i> -CO ₂ CH ₂ – )	OH ₂ C– 	4.2	>100 (30%) ^{a)}

a) Value in parenthesis are % inhibition at the concentration described (μM).

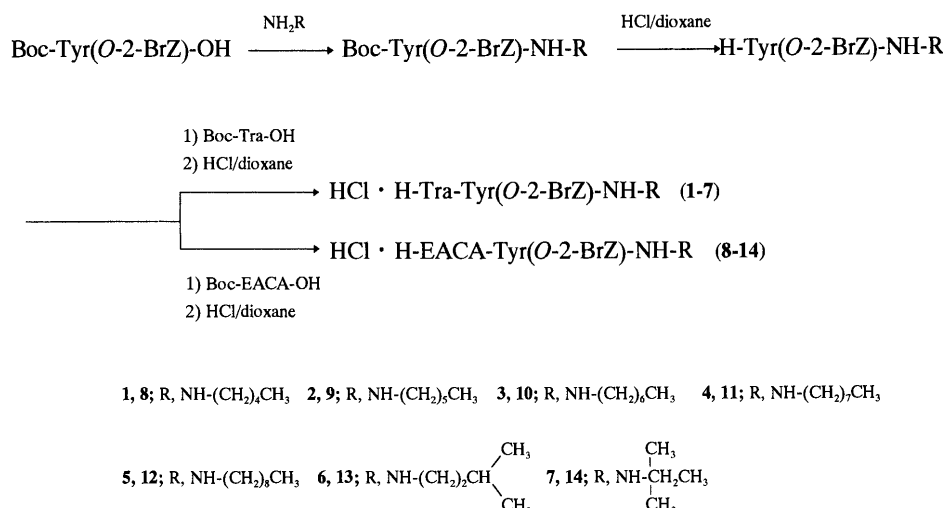
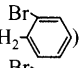
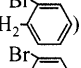
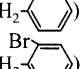
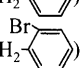
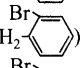
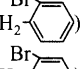
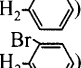
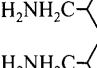
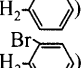
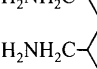
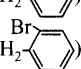
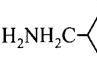
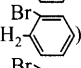
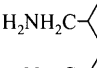
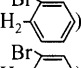
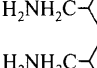
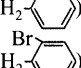
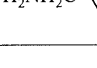
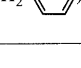
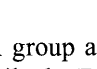
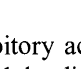


Chart 1. Synthetic Scheme for Compounds 1—14

Table 2. IC₅₀ Values (μM) of Compounds 1—14 for Various Enzymes

Peptide ID	P ₁	P _{1'}	P _{2'}	PL		PK	UK	TH		TRY
				S-2251	Fn	S-2302	S-2444	S-2238	Fg	S-2238
1	NH ₂ -(CH ₂) ₅ -CO	Tyr(O-CO ₂ CH ₂ - )	NH-(CH ₂) ₄ -CH ₃	10	1.3	110	>250	140	>100	85
2	NH ₂ -(CH ₂) ₅ -CO	Tyr(O-CO ₂ CH ₂ - )	NH-(CH ₂) ₅ -CH ₃	13	2.7	58	>250	>50	>50	80
3	NH ₂ -(CH ₂) ₅ -CO	Tyr(O-CO ₂ CH ₂ - )	NH-(CH ₂) ₆ -CH ₃	11	3.3	60	>500	>50	>50	>75
4	NH ₂ -(CH ₂) ₅ -CO	Tyr(O-CO ₂ CH ₂ - )	NH-(CH ₂) ₇ -CH ₃	7.0	1.8	75	>250	>50	>25	>150
5	NH ₂ -(CH ₂) ₅ -CO	Tyr(O-CO ₂ CH ₂ - )	NH-(CH ₂) ₈ -CH ₃	8.3	1.3	200	>10	100	>10	>150
6	NH ₂ -(CH ₂) ₅ -CO	Tyr(O-CO ₂ CH ₂ - )	NH-(CH ₂) ₂ -CH(CH ₃) ₂	6.2	1.2	91	>250	200	>100	68
7	NH ₂ -(CH ₂) ₅ -CO	Tyr(O-CO ₂ CH ₂ - )	NH-CH(CH ₃) ₂ -CH ₂ -CH ₃	85	19	170	>250	230	>250	>150
8	H ₂ NH ₂ C-  -CO	Tyr(O-CO ₂ CH ₂ - )	NH-(CH ₂) ₄ -CH ₃	1.1	0.1	8.8	>300	150	>100	3.3
9	H ₂ NH ₂ C-  -CO	Tyr(O-CO ₂ CH ₂ - )	NH-(CH ₂) ₅ -CH ₃	1.2	0.38	9.0	>50	>50	>25	1.4
10	H ₂ NH ₂ C-  -CO	Tyr(O-CO ₂ CH ₂ - )	NH-(CH ₂) ₆ -CH ₃	1.1	0.43	10	>50	>50	>25	5.9
11	H ₂ NH ₂ C-  -CO	Tyr(O-CO ₂ CH ₂ - )	NH-(CH ₂) ₇ -CH ₃	0.8	0.23	16	>50	>50	>25	1.6
12	H ₂ NH ₂ C-  -CO	Tyr(O-CO ₂ CH ₂ - )	NH-(CH ₂) ₈ -CH ₃	0.5	0.10	22	>10	100	>10	1.9
13	H ₂ NH ₂ C-  -CO	Tyr(O-CO ₂ CH ₂ - )	NH-(CH ₂) ₂ -CH(CH ₃) ₂	0.46	0.056	2.1	260	70	>100	1.4
14	H ₂ NH ₂ C-  -CO	Tyr(O-CO ₂ CH ₂ - )	NH-CH(CH ₃) ₂ -CH ₂ -CH ₃	13	1.7	69	>200	160	>100	23

the EACA group as far as potent inhibitory activity is concerned, while the EACA group increased the difference in inhibitory activity between PL and the other enzymes examined so far. As far as the P_{2'} substituent is concerned, increasing the chain length resulted in increased inhibitory activity against PL and reduced inhibitory activity against PK. Compounds 11, 12 inhibited PL potently and selectively. Previously, it was reported that 6-amidino-2-naphthyl *p*-guanidinobenzoate dimethanesulfonate (FUT-175) inhibited PL, PK and thrombin (TH) with IC₅₀ values of 0.12, 1.9 and 3.9 μM

(substrate: *N*^α-tosylarginine methyl ester, TAME), respectively.¹⁶⁾ Our compounds contain an amide bond, while FUT-175 contains an ester structure and our compounds exhibited much weaker inhibition of TH compared with FUT-175.

Since compound II in Table 1 inhibited both PL and PK potently, the 4-acetyl group at the P_{2'} position was exchanged for alkyl groups of various chain lengths. As summarized in Table 3, the inhibitory activity of compounds 15—18 was less than that of compounds 19—22. Compound 19—22 exhibited similar inhibitory activity against PL and trypsin

Table 3. IC₅₀ Values (μM) of Compounds **15**—**22** for Various Enzymes

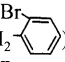
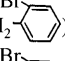
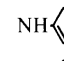
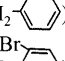
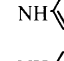
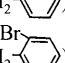
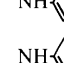
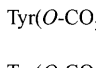
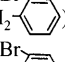
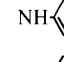
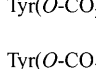
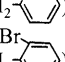
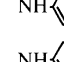
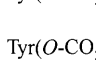
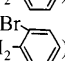
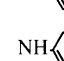
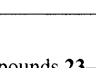
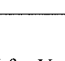

Peptide ID	P ₁	P _{1'}	P _{2'}	PL		PK		UK		TH		TRY	
				S-2251	Fn	S-2302	S-2444	S-2238	Fg	S-2238		S-2238	
15	NH ₂ -(CH ₂) ₅ -CO	Tyr(<i>O</i> -CO ₂ CH ₂ - )	NH-(CH ₂) ₂ -CH ₃	9.2	2.0	19	>50	96	>20	1.9			
16	NH ₂ -(CH ₂) ₅ -CO	Tyr(<i>O</i> -CO ₂ CH ₂ - )	NH-  -(CH ₂) ₃ -CH ₃	9.0	2.3	39	>20	>25	>10	>10			
17	NH ₂ -(CH ₂) ₅ -CO	Tyr(<i>O</i> -CO ₂ CH ₂ - )	NH-  -(CH ₂) ₄ -CH ₃	9.0	4.7	58	>25	60	>10	>75			
18	NH ₂ -(CH ₂) ₅ -CO	Tyr(<i>O</i> -CO ₂ CH ₂ - )	NH-  -(CH ₂) ₅ -CH ₃	6.0	3.5	52	>40	>20	>10	>150			
19	H ₂ NH ₂ C-  -CO	Tyr(<i>O</i> -CO ₂ CH ₂ - )	NH-  -CH ₂ -CH ₃	0.63	0.098	0.71	>50	89	>10	0.52			
20	H ₂ NH ₂ C-  -CO	Tyr(<i>O</i> -CO ₂ CH ₂ - )	NH-  -(CH ₂) ₃ -CH ₃	0.79	0.090	1.0	>25	>25	>10	0.27			
21	H ₂ NH ₂ C-  -CO	Tyr(<i>O</i> -CO ₂ CH ₂ - )	NH-  -(CH ₂) ₄ -CH ₃	0.57	0.070	1.7	>50	>50	>20	0.33			
22	H ₂ NH ₂ C-  -CO	Tyr(<i>O</i> -CO ₂ CH ₂ - )	NH-  -(CH ₂) ₅ -CH ₃	0.49	0.24	7.9	>40	>20	>10	1.4			

Table 4. IC₅₀ Values (μM) of Compounds **23**—**26** for Various Enzymes

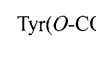
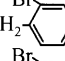
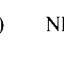
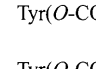
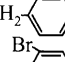
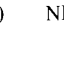
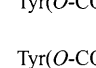
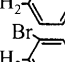
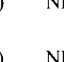
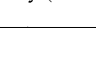
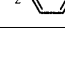
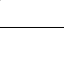
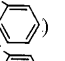
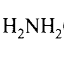
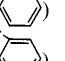
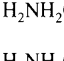
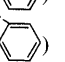
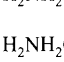
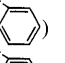
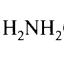
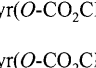
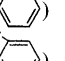
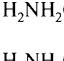
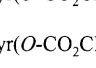
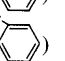
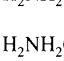
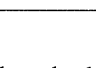
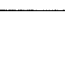
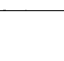
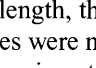
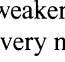
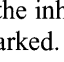
Peptide ID	P ₁	P _{1'}	P _{2'}	PL		PK		UK		TH		TRY	
				S-2251	Fn	S-2302	S-2444	S-2238	Fg	S-2238		S-2238	
23	H ₂ NH ₂ C-  -CO	Tyr(<i>O</i> -CO ₂ CH ₂ - )	NH- 	0.98	0.17	0.29	19	91	>100	0.74			
24	H ₂ NH ₂ C-  -CO	Tyr(<i>O</i> -CO ₂ CH ₂ - )	NH-CH ₂ - 	5.3	1.4	14	72	240	>200	4.9			
25	H ₂ NH ₂ C-  -CO	Tyr(<i>O</i> -CO ₂ CH ₂ - )	NH-(CH ₂) ₂ - 	1.5	0.52	12	78	310	>200	4.3			
26	H ₂ NH ₂ C-  -CO	Tyr(<i>O</i> -CO ₂ CH ₂ - )	NH-(CH ₂) ₂ - 	1.1	0.30	7.0	>50	>50	>50	3.0			

Table 5. IC₅₀ Values (μM) of Compounds **27**—**34** for Various Enzymes

Peptide ID	P ₁	P _{1'}	P _{2'}	PL		PK		UK		TH		TRY	
				S-2251	Fn	S-2302	S-2444	S-2238	Fg	S-2238		S-2238	
27	NH ₂ -(CH ₂) ₅ -CO	Tyr(<i>O</i> -CO ₂ CH ₂ - )	H ₂ NH ₂ C-  -COOCH ₃	9.0	6.1	56	>50	>100	>100	90			
28	NH ₂ -(CH ₂) ₅ -CO	Tyr(<i>O</i> -CO ₂ CH ₂ - )	H ₂ NH ₂ C-  -COO(CH ₂) ₃ CH ₃	18	4.3	>200	>100	>200	>10	>150			
29	NH ₂ -(CH ₂) ₅ -CO	Tyr(<i>O</i> -CO ₂ CH ₂ - )	H ₂ NH ₂ C-  -COO(CH ₂) ₆ CH ₃	24	3.9	>200	>100	>50	>10	>150			
30	NH ₂ -(CH ₂) ₅ -CO	Tyr(<i>O</i> -CO ₂ CH ₂ - )	H ₂ NH ₂ C-  -COO(CH ₂) ₇ CH ₃	>100	5.0	>400	>100	>100	>10	>150			
31	H ₂ NH ₂ C-  -CO	Tyr(<i>O</i> -CO ₂ CH ₂ - )	H ₂ NH ₂ C-  -COOCH ₃	1.0	0.78	15	>10	>10	>20	0.80			
32	H ₂ NH ₂ C-  -CO	Tyr(<i>O</i> -CO ₂ CH ₂ - )	H ₂ NH ₂ C-  -COO(CH ₂) ₅ CH ₃	1.5	0.40	40	>50	>50	>10	4.5			
33	H ₂ NH ₂ C-  -CO	Tyr(<i>O</i> -CO ₂ CH ₂ - )	H ₂ NH ₂ C-  -COO(CH ₂) ₆ CH ₃	1.4	0.42	37	>50	>50	>10	10			
34	H ₂ NH ₂ C-  -CO	Tyr(<i>O</i> -CO ₂ CH ₂ - )	H ₂ NH ₂ C-  -COO(CH ₂) ₇ CH ₃	2.5	0.56	45	>50	>50	>10	27			

(TRY). The longer the chain length, the weaker the inhibition of PK, although the differences were not very marked.

Next, methylene groups were inserted between NH and the aromatic ring of the P_{2'} moiety. As summarized in Table 4, compound **23** inhibited both PL and PK potently, while insertion of methylene groups reduced the inhibition of PK more

than that of PL.

Finally, as the P_{2'} moiety, *trans*-4-aminomethylcyclohexanecarboxylic acid alkyl esters of various chain lengths were used because we believed that the bulkiness of the cleft and stereogeometry of the active site of PL and PK were quite different. Compounds **27**—**34** were prepared and their in-

hibitory activities are summarized in Table 5. The inhibitory activity against PL is more potent than against PK, presumably due to the bulkiness of the P₂ moiety.

In conclusion, it was found that the cleft of the active center of PL is larger than that of PK and other enzymes and that the compound **11** interacts with the active center of PL, as shown in Fig. 1. For the further study of PL selective inhibitors, the compound **11** was selected as the lead compound.

Experimental

Melting points were determined on a Yanagimoto micro-melting point apparatus without correction. Optical rotations were measured with an automatic polarimeter, model DIP-360 (Japan Spectroscopic Co.). On TLC (Kieselgel G, Merck), *R_f*¹, *R_f*², *R_f*³, *R_f*⁴ and *R_f*⁵ values refer to the systems of CHCl₃, MeOH and AcOH (90:8:2); CHCl₃, MeOH and H₂O (89:10:1); CHCl₃, MeOH and H₂O (8:3:1, lower phase); *n*-BuOH, AcOH and H₂O (4:1:5, upper phase) and *n*-BuOH, AcOH, pyridine and H₂O (4:1:1:2), respectively.

General Procedure for Synthesis of Boc-Tyr(O-2-BrZ)-NH-X [X: *n*-pentyl, *n*-hexyl, *n*-heptyl, *n*-octyl, *n*-nonyl, 3-methylbutyl, 1,1-dimethylpropyl] A mixed anhydride of Boc-Tyr(O-2-BrZ)-OH [prepared routinely from Boc-Tyr(O-2-BrZ)-OH (1.5 g, 3.0 mmol), isobutyl chloroformate (0.45 ml, 3.0 mmol) and Et₃N (0.45 ml, 3.0 mmol)] in tetrahydrofuran (THF, 15 ml) was added to a solution of NH₂X (X: *n*-pentyl, *n*-hexyl, *n*-heptyl, *n*-octyl, *n*-nonyl, 3-methylbutyl, 1,1-dimethylpropyl) (3.3 mmol) in THF (10 ml). The reaction mixture was stirred at 4 °C overnight. After removal of

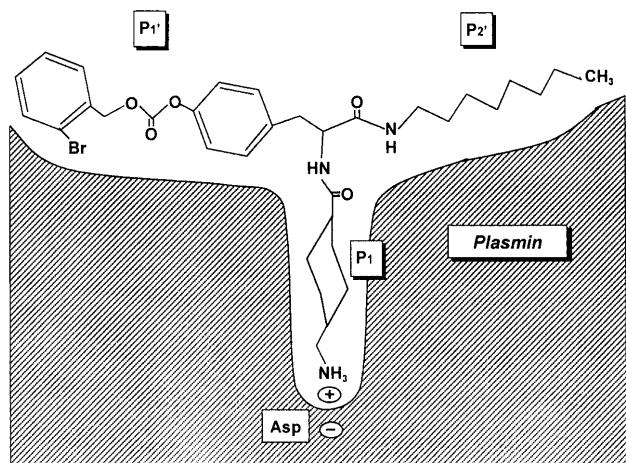


Fig. 1. Schematic Representation of Interaction of Tra-Tyr(O-2-BrZ)-octylamide (**11**) with Plasmin

the solvent, the residue was extracted with AcOEt. The extract was washed with 10% citric acid, 5% Na₂CO₃ and water, dried over Na₂SO₄ and evaporated to dryness. Ether was added to the residue to afford crystals, which were collected by filtration. The yield, mp, [α]_D²⁵ values, elemental analysis and *R_f* values are summarized in Table 6.

General Procedure for Synthesis of Boc-EACA-Tyr(O-2-BrZ)-NH-X [X: *n*-pentyl, *n*-hexyl, *n*-heptyl, *n*-octyl, *n*-nonyl, 3-methylbutyl, 1,1-dimethylpropyl] A mixed anhydride of Boc-EACA-OH [prepared routinely from Boc-EACA-OH (221 mg, 0.89 mmol), isobutyl chloroformate (0.13 ml, 0.89 mmol) and Et₃N (0.12 ml, 0.89 mmol)] in THF (15 ml) was added to a solution of H-Tyr(O-2-BrZ)-NH-X·HCl [X: *n*-pentyl, *n*-hexyl, *n*-heptyl, *n*-octyl, *n*-nonyl, 3-methylbutyl, 1,1-dimethylpropyl; prepared routinely from Boc-Tyr(O-2-BrZ)-NH-X (0.89 mmol) and 7.2*N* HCl-dioxane (2.0 ml, 14.4 mmol)] in DMF (30 ml) containing Et₃N (0.15 ml, 1.1 mmol) at 0 °C. The reaction mixture was stirred at 4 °C overnight. After removal of the solvent, ether was added to the residue to afford crystals, which were collected by filtration and washed with water. The yield, mp, [α]_D²⁵ values, elemental analysis and *R_f* values are summarized in Table 7.

General Procedure for Synthesis of H-EACA-Tyr(O-2-BrZ)-NH-X·HCl (1—7) [X: *n*-pentyl, *n*-hexyl, *n*-heptyl, *n*-octyl, *n*-nonyl, 3-methylbutyl, 1,1-dimethylpropyl] Boc-EACA-Tyr(O-2-BrZ)-NH-X [X: *n*-pentyl, *n*-hexyl, *n*-heptyl, *n*-octyl, *n*-nonyl, 3-methylbutyl, 1,1-dimethylpropyl; (0.2 mmol)] was dissolved in 5.4*N* HCl-dioxane (0.5 ml, 2.7 mmol) at 0 °C and the reaction mixture was stirred at the same temperature for 5 min. After addition of dioxane (0.2 ml), the reaction mixture was stirred at room temperature for 90 min. After removal of the solvent, dry ether was added to the residue to afford a precipitate. The yield, mp, [α]_D²⁵ values, elemental analysis and *R_f* values are summarized in Table 8.

General Procedure for Synthesis of Boc-Tra-Tyr(O-2-BrZ)-NH-X [X: *n*-pentyl, *n*-hexyl, *n*-heptyl, *n*-octyl, *n*-nonyl, 3-methylbutyl, 1,1-dimethylpropyl] A mixed anhydride of Boc-Tra-OH [prepared routinely from Boc-Tra-OH (245 mg, 0.89 mmol), isobutyl chloroformate (0.13 ml, 0.89 mmol) and Et₃N (0.12 ml, 0.89 mmol)] in THF (15 ml) was added to a solution of H-Tyr(O-2-BrZ)-NH-X·HCl [X: *n*-pentyl, *n*-hexyl, *n*-heptyl, *n*-octyl, *n*-nonyl, 3-methylbutyl, 1,1-dimethylpropyl; prepared routinely from Boc-Tyr(O-2-BrZ)-NH-X (0.89 mmol) and 7.2*N* HCl-dioxane (2.0 ml, 14.4 mmol)] in DMF (20 ml) containing Et₃N (0.15 ml, 1.1 mmol) at 0 °C and the reaction mixture was stirred at 4 °C overnight. After removal of the solvent, ether was added to the residue to afford crystals, which were collected by filtration and washed with water. The yield, mp, [α]_D²⁵ values, elemental analysis and *R_f* values are summarized in Table 9.

General Procedure for Synthesis of H-Tra-Tyr(O-2-BrZ)-NH-X·HCl (8—14) [X: *n*-pentyl, *n*-hexyl, *n*-heptyl, *n*-octyl, *n*-nonyl, 3-methylbutyl, 1,1-dimethylpropyl] Boc-Tra-Tyr(O-2-BrZ)-NH-X [X: *n*-pentyl, *n*-hexyl, *n*-heptyl, *n*-octyl, *n*-nonyl, 3-methylbutyl, 1,1-dimethylpropyl; (0.14 mmol)] was dissolved in 5.4*N* HCl-dioxane (0.5 ml, 2.7 mmol) at 0 °C and the reaction mixture was stirred at the same temperature for 5 min. After addition of dioxane (0.2 ml), the reaction mixture was stirred at room temperature for 90 min. After removal of the solvent, dry ether was added to the residue to afford a precipitate. The yield, mp, [α]_D²⁵ values, elemental analysis and *R_f*

Table 6. Yield, Melting Point, Optical Rotation, Elemental Analysis and *R_f* Value of Boc-Tyr(O-2-BrZ)-NH-X

X	Yield (%)	mp (°C)	[α] _D ²⁵ (CHCl ₃)	Formula	Elemental analysis Calcd (Found)			TLC <i>R_f</i> ¹
					C	H	N	
<i>n</i> -Pentyl	83	117—118	+2.4 (<i>c</i> =1.0)	C ₂₇ H ₃₅ BrN ₂ O ₆	57.54 (57.45)	6.27 6.32	4.97 (4.98)	0.80
<i>n</i> -Hexyl	82	117—119	+2.9 (<i>c</i> =1.0)	C ₂₈ H ₃₇ BrN ₂ O ₆	58.23 (58.17)	6.47 6.30	4.85 (4.83)	0.78
<i>n</i> -Heptyl	77	118—121	+3.2 (<i>c</i> =1.0)	C ₂₉ H ₃₉ BrN ₂ O ₅	58.87 (58.83)	6.66 6.64	4.73 (4.76)	0.78
<i>n</i> -Octyl	78	113—118	+3.05 (<i>c</i> =1.0)	C ₃₀ H ₄₁ BrN ₂ O ₆	59.30 (59.39)	6.82 6.99	4.61 (4.70)	0.88
<i>n</i> -Nonyl	72	103—105	+4.0 (<i>c</i> =1.0)	C ₃₁ H ₄₃ BrN ₂ O ₆	60.09 (59.89)	6.99 7.10	4.52 (4.50)	0.69
3-Methylbutyl	88	134—136	+2.3 (<i>c</i> =1.0)	C ₂₇ H ₃₅ BrN ₂ O ₆	57.54 (57.81)	6.27 6.21	4.97 (5.02)	0.81
1,1-Dimethylpropyl	83	74—76	+2.1 (<i>c</i> =1.0)	C ₂₇ H ₃₅ BrN ₂ O ₆	57.54 (57.26)	6.27 6.12	4.97 (4.96)	0.80

Table 7. Yield, Melting Point, Optical Rotation, Elemental Analysis and *R_f* Value of Boc-EACA-Tyr(*O*-2-BrZ)-NH-X

X	Yield (%)	mp (°C)	[α] _D ²⁵ (CHCl ₃)	Formula	Elemental analysis Calcd (Found)			TLC	
					C	H	N	<i>R_f</i> ¹	
<i>n</i> -Pentyl	87	113—115	+1.5 (<i>c</i> =1.0) ^{a)}	C ₃₃ H ₄₆ BrN ₃ O ₇	58.57 (58.33)	6.87 (6.85)	6.21 (6.14)	0.65	
<i>n</i> -Hexyl	84	105—107	−0.5 (<i>c</i> =1.0)	C ₃₄ H ₄₈ BrN ₃ O ₇	59.12 (59.04)	7.02 (7.01)	6.08 (5.92)	0.70	
<i>n</i> -Heptyl	80	120—122	−1.0 (<i>c</i> =1.0)	C ₃₅ H ₅₀ BrN ₃ O ₇	59.65 (59.53)	7.17 (7.21)	5.96 (5.84)	0.71	
<i>n</i> -Octyl	84	128—131	−0.6 (<i>c</i> =1.0)	C ₃₆ H ₅₂ BrN ₃ O ₇	60.15 (59.91)	7.31 (7.34)	5.84 (5.73)	0.80	
<i>n</i> -Nonyl	67	124—126	−5.1 (<i>c</i> =1.0) ^{b)}	C ₃₇ H ₅₄ BrN ₃ O ₇	60.64 (60.38)	7.42 (7.50)	5.73 (5.74)	0.85	
3-Methylbutyl	92	97—99	+1.5 (<i>c</i> =1.0) ^{a)}	C ₃₃ H ₄₆ BrN ₃ O ₇	58.57 (58.36)	6.87 (6.85)	6.21 (6.08)	0.72	
1,1-Dimethylpropyl	65	Amorphous	−1.7 (<i>c</i> =1.0) ^{a)}	C ₃₃ H ₄₆ BrN ₃ O ₇	58.57 (58.68)	6.87 (7.15)	6.21 (6.13)	0.75	

a) MeOH, b) DMF.

Table 8. Yield, Melting Point, Optical Rotation, Elemental Analysis and *R_f* Values of H-EACA-Tyr(*O*-2-BrZ)-NH-X · HCl (1—7)

X	Peptide ID	Yield (%)	mp (°C)	[α] _D ²⁵ (MeOH)	Formula	Elemental analysis Calcd (Found)			TLC	
						C	H	N	<i>R_f</i> ¹	<i>R_f</i> ³
<i>n</i> -Pentyl	1	96	139—143	+8.3 (<i>c</i> =1.0)	C ₂₈ H ₃₈ BrN ₃ O ₅ · HCl · 0.5H ₂ O	54.07 (54.25)	6.48 (6.92)	6.75 (7.48)	0.20	0.67
<i>n</i> -Hexyl	2	87	175—177	+5.2 (<i>c</i> =1.0)	C ₂₉ H ₄₀ BrN ₃ O ₅ · HCl · 0.5H ₂ O	54.76 (54.86)	6.66 (6.68)	6.61 (6.79)		0.35
<i>n</i> -Heptyl	3	93	178—181	+6.2 (<i>c</i> =1.0)	C ₃₀ H ₄₂ BrN ₃ O ₅ · HCl · 0.5H ₂ O	55.43 (55.53)	6.67 (6.87)	6.46 (6.49)		0.32
<i>n</i> -Octyl	4	88	162—165	+7.9 (<i>c</i> =1.0)	C ₃₁ H ₄₄ BrN ₃ O ₅ · HCl	56.83 (57.07)	6.92 (7.19)	6.41 (6.49)		0.35
<i>n</i> -Nonyl	5	87	174—176	+6.9 (<i>c</i> =1.0)	C ₃₂ H ₄₆ BrN ₃ O ₅ · HCl · 0.5H ₂ O	56.67 (56.60)	7.13 (7.21)	6.19 (6.38)		0.40
3-Methylbutyl	6	74	123—127	+8.3 (<i>c</i> =1.0)	C ₂₈ H ₃₈ BrN ₃ O ₅ · HCl · 0.5H ₂ O	54.07 (53.53)	6.48 (6.83)	6.75 (7.28)		0.32
1,1-Dimethylpropyl	7	56	Amorphous	+7.5 (<i>c</i> =1.0)	C ₂₈ H ₃₈ BrN ₃ O ₅ · HCl · 2H ₂ O	51.81 (52.13)	6.67 (7.13)	6.47 (7.08)		0.32

Table 9. Yield, Melting Point, Optical Rotation, Elemental Analysis and *R_f* Values of Boc-Tra-Tyr(*O*-2-BrZ)-NH-X

X	Yield (%)	mp (°C)	[α] _D ²⁵ (DMF)	Formula	Elemental analysis Calcd (Found)			TLC	
					C	H	N	<i>R_f</i> ¹	<i>R_f</i> ²
<i>n</i> -Pentyl	58	202.5—205	−9.4 (<i>c</i> =1.0)	C ₃₅ H ₄₈ BrN ₃ O ₇	59.82 (59.52)	6.88 (7.03)	5.98 (5.89)	0.60	0.70
<i>n</i> -Hexyl	81	199—200	−8.3 (<i>c</i> =1.0)	C ₃₆ H ₅₀ BrN ₃ O ₇	60.32 (60.14)	7.05 (7.01)	5.86 (5.75)	0.71	
<i>n</i> -Heptyl	62	180—182	−2.3 (<i>c</i> =1.0) ^{a)}	C ₃₇ H ₅₂ BrN ₃ O ₇	60.81 (60.65)	7.19 (7.22)	5.75 (5.70)	0.78	
<i>n</i> -Octyl	65	177—181	−8.4 (<i>c</i> =1.0)	C ₃₈ H ₅₄ BrN ₃ O ₇	61.27 (61.28)	7.32 (7.47)	5.64 (5.61)	0.70	
<i>n</i> -Nonyl	77	189—191	−8.9 (<i>c</i> =1.0)	C ₃₉ H ₅₆ BrN ₃ O ₇	61.73 (61.66)	7.43 (7.77)	5.53 (5.51)	0.87	
3-Methylbutyl	84	186—188	−8.8 (<i>c</i> =1.0)	C ₃₅ H ₃₉ BrN ₃ O ₇	59.81 (59.83)	6.90 (7.06)	5.98 (5.97)	0.76	
1,1-Dimethylpropyl	84	89—92	−8.2 (<i>c</i> =1.0) ^{b)}	C ₃₅ H ₃₉ BrN ₃ O ₇	59.81 (59.74)	6.90 (6.74)	5.98 (5.87)	0.72	

a) CHCl₃, b) MeOH.

Table 10. Yield, Melting Point, Optical Rotation, Elemental Analysis and R_f Values of H-Tyr(O-2-BrZ)-NH-X·HCl (**8**—**14**)

X	Peptide ID	Yield (%)	mp (°C)	$[\alpha]_D^{25}$ (MeOH)	Formula	Elemental analysis Calcd (Found)			TLC		
						C	H	N	R_f^3	R_f^4	R_f^5
<i>n</i> -Pentyl	8	98	200—204	+0.4 ($c=0.9$)	$C_{30}H_{40}BrN_3O_5 \cdot HCl \cdot H_2O$	54.84 (54.67)	6.59 (6.28)	6.39 (6.41)		0.30	0.27
<i>n</i> -Hexyl	9	95	207—209	+1.8 ($c=1.0$)	$C_{31}H_{42}BrN_3O_5 \cdot HCl \cdot 0.5H_2O$	56.23 (56.19)	6.70 (6.58)	6.35 (6.29)	0.42		
<i>n</i> -Heptyl	10	87	218—220	+6.4 ($c=1.0$)	$C_{32}H_{44}BrN_3O_5 \cdot HCl \cdot 0.5H_2O$	56.85 (56.90)	6.71 (6.87)	6.22 (6.25)	0.38		
<i>n</i> -Octyl	11	90	210—212	+0.7 ($c=1.0$)	$C_{33}H_{46}BrN_3O_5 \cdot HCl \cdot 0.5H_2O$	57.43 (57.25)	7.01 (6.91)	6.09 (6.21)	0.33		
<i>n</i> -Nonyl	12	93	208—210	+3.0 ($c=1.0$)	$C_{34}H_{48}BrN_3O_5 \cdot HCl \cdot 0.5H_2O$	57.99 (57.85)	7.15 (7.05)	5.96 (5.95)	0.43		
3-Methylbutyl	13	92	203—208	+1.3 ($c=1.0$)	$C_{30}H_{40}BrN_3O_5 \cdot HCl \cdot 0.5H_2O$	55.60 (55.30)	6.53 (6.54)	6.51 (6.56)	0.32		
1,1-Dimethylpropyl	14	92	126—130	-2.7 ($c=1.0$)	$C_{30}H_{40}BrN_3O_5 \cdot HCl \cdot 1.5H_2O$	54.10 (53.77)	6.66 (6.49)	6.31 (6.38)	0.26		

Table 11. Yield, Melting Point, Optical Rotation, Elemental Analysis and R_f Value of Boc-Tyr(O-2-BrZ)-NH- ϕ -X

X	Yield (%)	mp (°C)	$[\alpha]_D^{25}$ (CHCl ₃)	Formula	Elemental analysis Calcd (Found)			TLC
					C	H	N	R_f^1
Ethyl	92	162—164	-2.8 ($c=1.0$)	$C_{30}H_{33}BrN_2O_5$	60.30 (60.13)	5.58 (5.62)	4.69 (4.74)	0.95
<i>n</i> -Butyl	74	160—163	-1.2 ($c=1.0$)	$C_{32}H_{37}BrN_2O_6$	61.43 (61.57)	5.97 (5.96)	4.48 (4.47)	0.78
<i>n</i> -Pentyl	82	164—168	-3.2 ($c=1.0$)	$C_{33}H_{39}BrN_2O_6$	61.97 (61.87)	6.16 (6.09)	4.38 (4.32)	0.92
<i>n</i> -Hexyl	79	137—141	-3.3 ($c=1.0$)	$C_{34}H_{41}BrN_2O_6$	62.47 (62.33)	6.32 (6.44)	4.28 (4.34)	

Table 12. Yield, Melting Point, Optical Rotation, Elemental Analysis and R_f Value of Boc-EACA-Tyr(O-2-BrZ)-NH- ϕ -X

X	Yield (%)	mp (°C)	$[\alpha]_D^{25}$ (CHCl ₃)	Formula	Elemental analysis Calcd (Found)			TLC
					C	H	N	R_f^1
Ethyl	95	137—139	+23.1 ($c=1.0$) ^{a)}	$C_{36}H_{44}BrN_3O_7$	60.84 (60.72)	6.25 (6.34)	5.91 (5.74)	0.90
<i>n</i> -Butyl	90	120—123	+22.5 ($c=1.0$) ^{a)}	$C_{38}H_{48}BrN_3O_7$	61.78 (61.91)	6.56 (6.54)	5.69 (5.60)	0.70
<i>n</i> -Pentyl	76	134—137	+2.9 ($c=1.0$)	$C_{39}H_{50}BrN_3O_7$	62.22 (62.08)	6.71 (6.64)	5.58 (5.51)	0.70
<i>n</i> -Hexyl	65	134—137	+2.5 ($c=1.0$)	$C_{40}H_{52}BrN_3O_7$	62.65 (62.54)	6.85 (6.86)	5.48 (5.45)	0.68

a) DMF.

values are summarized in Table 10.

General Procedure for Synthesis of Boc-Tyr(O-2-BrZ)-NH- ϕ -X [X: ethyl, *n*-butyl, *n*-pentyl, *n*-hexyl] A mixed anhydride of Boc-Tyr(O-2-BrZ)-OH [prepared routinely from Boc-Tyr(O-2-BrZ)-OH (1.5 g, 3.0 mmol), isobutyl chloroformate (0.45 ml, 3.0 mmol) and Et₃N (0.45 ml, 3.0 mmol)] in THF (15 ml) was added to a solution of NH₂- ϕ -X (X: ethyl, *n*-butyl, *n*-pentyl, *n*-hexyl) (3.3 mmol) in THF (10 ml). The reaction mixture was stirred at 4 °C overnight. After removal of the solvent, the residue was extracted with AcOEt. The extract was washed with 10% citric acid, 5% Na₂CO₃ and water, dried over Na₂SO₄ and evaporated to dryness. Ether was added to the residue to afford crystals, which were collected by filtration. The yield, mp, $[\alpha]_D^{25}$ values, elemental analysis and R_f values are summarized in Table 11.

General Procedure for Synthesis of Boc-EACA-Tyr(O-2-BrZ)-NH- ϕ -X

X [X: ethyl, *n*-butyl, *n*-pentyl, *n*-hexyl] A mixed anhydride of Boc-EACA-OH [prepared routinely from Boc-EACA-OH (221 mg, 0.89 mmol), isobutyl chloroformate (0.13 ml, 0.89 mmol) and Et₃N (0.12 ml, 0.89 mmol)] in THF (15 ml) was added to a solution of H-Tyr(O-2-BrZ)-NH- ϕ -X·HCl [X: ethyl, *n*-butyl, *n*-pentyl, *n*-hexyl; prepared routinely from Boc-Tyr(O-2-BrZ)-NH- ϕ -X (0.89 mmol) and 7.2 N HCl-dioxane (2.0 ml, 14.4 mmol)] in DMF (30 ml) containing Et₃N (0.15 ml, 1.1 mmol) at 0 °C. The reaction mixture was stirred at 4 °C overnight. After removal of the solvent, ether was added to the residue to afford crystals, which were collected by filtration and washed with water. The yield, mp, $[\alpha]_D^{25}$ values, elemental analysis and R_f values are summarized in Table 12.

General Procedure for Synthesis of H-EACA-Tyr(O-2-BrZ)-NH- ϕ -X·HCl (15**—**18**) [X: ethyl, *n*-butyl, *n*-pentyl, *n*-hexyl]** Boc-EACA-Tyr(O-2-BrZ)-NH- ϕ -X [X: ethyl, *n*-butyl, *n*-pentyl, *n*-hexyl (0.2 mmol)]

Table 13. Yield, Melting Point, Optical Rotation, Elemental Analysis and R_f Value of H-EACA-Tyr(*O*-2-BrZ)-NH- C_6H_4 -X \cdot HCl (**15**—**18**)

X	Peptide ID	Yield (%)	mp (°C)	$[\alpha]_D^{25}$ (MeOH)	Formula	Elemental analysis Calcd (Found)			TLC
						C	H	N	R_f^3
Ethyl	15	75	Amorphous	+31.2 ($c=1.0$)	$\text{C}_{31}\text{H}_{36}\text{BrN}_3\text{O}_5 \cdot \text{HCl} \cdot \text{H}_2\text{O}$	55.98 (55.90)	5.91 (5.70)	6.31 (6.32)	0.56
<i>n</i> -Butyl	16	92	148—152	+27.3 ($c=1.0$)	$\text{C}_{33}\text{H}_{40}\text{BrN}_3\text{O}_5 \cdot \text{HCl} \cdot 0.5\text{H}_2\text{O}$	57.94 (57.56)	6.19 (6.01)	6.14 (6.28)	0.57
<i>n</i> -Pentyl	17	90	Amorphous	+23.7 ($c=1.0$)	$\text{C}_{34}\text{H}_{42}\text{BrN}_3\text{O}_5 \cdot \text{HCl} \cdot 0.5\text{H}_2\text{O}$	58.50 (58.28)	6.35 (6.17)	6.02 (5.81)	0.45
<i>n</i> -Hexyl	18	77	Amorphous	+25.7 ($c=1.0$)	$\text{C}_{35}\text{H}_{44}\text{BrN}_3\text{O}_5 \cdot \text{HCl} \cdot \text{H}_2\text{O}$	58.29 (58.14)	6.56 (6.46)	5.82 (5.59)	0.76

Table 14. Yield, Melting Point, Optical Rotation, Elemental Analysis and R_f Value of Boc-Tra-Tyr(*O*-2-BrZ)-NH- C_6H_4 -X

X	Yield (%)	mp (°C)	$[\alpha]_D^{25}$ (DMF)	Formula	Elemental analysis Calcd (Found)			TLC
					C	H	N	R_f^1
Ethyl	95	219—222	+18.0 ($c=1.0$)	$\text{C}_{38}\text{H}_{46}\text{BrN}_3\text{O}_7$	61.95 (61.72)	6.31 (6.39)	5.70 (5.63)	0.90
<i>n</i> -Butyl	90	196—199	+17.2 ($c=1.0$)	$\text{C}_{40}\text{H}_{50}\text{BrN}_3\text{O}_7$	62.81 (62.82)	6.60 (6.55)	5.49 (5.51)	0.74
<i>n</i> -Pentyl	77	199—202	+18.7 ($c=1.0$)	$\text{C}_{41}\text{H}_{52}\text{BrN}_3\text{O}_7$	63.22 (64.14)	6.74 (6.78)	5.39 (5.28)	0.63
<i>n</i> -Hexyl	65	181—183	+18.3 ($c=1.0$)	$\text{C}_{42}\text{H}_{54}\text{BrN}_3\text{O}_7$	63.62 (63.74)	6.88 (7.03)	5.30 (5.32)	0.78

Table 15. Yield, Melting Point, Optical Rotation, Elemental Analysis and R_f Value of H-Tra-Tyr(*O*-2-BrZ)-NH- C_6H_4 -X \cdot HCl (**19**—**22**)

X	Peptide ID	Yield (%)	mp (°C)	$[\alpha]_D^{25}$ (MeOH)	Formula	Elemental analysis Calcd (Found)			TLC
						C	H	N	R_f^3
Ethyl	19	95	200—203	+18.3 ($c=1.0$)	$\text{C}_{33}\text{H}_{38}\text{BrN}_3\text{O}_5 \cdot \text{HCl} \cdot 1.5\text{H}_2\text{O}$	56.61 (56.45)	6.04 (5.68)	6.00 (6.23)	0.58
<i>n</i> -Butyl	20	81	Amorphous	+19.4 ($c=1.0$)	$\text{C}_{35}\text{H}_{42}\text{BrN}_3\text{O}_5 \cdot \text{HCl} \cdot 1.5\text{H}_2\text{O}$	57.74 (58.00)	6.37 (6.07)	5.77 (5.80)	0.62
<i>n</i> -Pentyl	21	101	175—178	+17.6 ($c=1.0$)	$\text{C}_{36}\text{H}_{44}\text{BrN}_3\text{O}_5 \cdot \text{HCl} \cdot \text{H}_2\text{O}$	58.99 (58.73)	6.46 (6.32)	5.73 (5.70)	0.43
<i>n</i> -Hexyl	22	84	188—190	+17.1 ($c=1.0$)	$\text{C}_{37}\text{H}_{46}\text{BrN}_3\text{O}_5 \cdot \text{HCl} \cdot 0.75\text{H}_2\text{O}$	59.84 (59.79)	6.58 (6.42)	5.65 (5.63)	0.55

was dissolved in 5.4 *N* HCl–dioxane (0.5 ml, 2.7 mmol) at 0 °C and the reaction mixture was stirred at the same temperature for 5 min. After addition of dioxane (0.2 ml), the reaction mixture was stirred at room temperature for 90 min. After removal of the solvent, dry ether was added to the residue to afford a precipitate. The yield, mp, $[\alpha]_D^{25}$ values, elemental analysis and R_f values are summarized in Table 13.

General Procedure for Synthesis of Boc-Tra-Tyr(*O*-2-BrZ)-NH- C_6H_4 -X [X: ethyl, *n*-butyl, *n*-pentyl, *n*-hexyl] A mixed anhydride of Boc-Tra-OH [prepared routinely from Boc-Tra-OH (245 mg, 0.89 mmol), isobutyl chloroformate (0.13 ml, 0.89 mmol) and Et₃N (0.12 ml, 0.89 mmol)] in THF (15 ml) was added to a solution of H-Tyr(*O*-2-BrZ)-NH- C_6H_4 -X \cdot HCl [X: ethyl, *n*-butyl, *n*-pentyl, *n*-hexyl; prepared routinely from Boc-Tyr(*O*-2-BrZ)-NH- C_6H_4 -X (0.89 mmol) and 7.2 *N* HCl–dioxane (2.0 ml, 14.4 mmol)] in DMF (20 ml) containing Et₃N (0.15 ml, 1.1 mmol) at 0 °C and the reaction mixture was stirred at 4 °C overnight. After removal of the solvent, ether was added to the residue to afford crystals, which were collected by filtration and washed with water. The yield, mp, $[\alpha]_D^{25}$ values, elemental analysis and R_f values are summarized in Table 14.

General Procedure for Synthesis of H-Tra-Tyr(*O*-2-BrZ)-NH- C_6H_4 -X \cdot HCl (19**—**22**) [X: ethyl, *n*-butyl, *n*-pentyl, *n*-hexyl]** Boc-Tra-Tyr(*O*-2-BrZ)-NH- C_6H_4 -X [X: ethyl, *n*-butyl, *n*-pentyl, *n*-hexyl; (0.14 mmol)] was dis-

solved in 5.4 *N* HCl–dioxane (0.5 ml, 2.7 mmol) at 0 °C and the reaction mixture was stirred at the same temperature for 5 min. After addition of dioxane (0.2 ml), the reaction mixture was stirred at room temperature for 90 min. After removal of the solvent, dry ether was added to the residue to afford a precipitate. The yield, mp, $[\alpha]_D^{25}$ values, elemental analysis and R_f values are summarized in Table 15.

General Procedure for Synthesis of Boc-Tyr(*O*-2-BrZ)-NH-X [X: 4-pyridyl, 4-picolyl, 2-(2-pyridyl)ethyl, β -phenethyl] A mixed anhydride of Boc-Tyr(*O*-2-BrZ)-OH [prepared routinely from Boc-Tyr(*O*-2-BrZ)-OH (1.5 g, 3.0 mmol), isobutyl chloroformate (0.45 ml, 3.0 mmol) and Et₃N (0.45 ml, 3.0 mmol)] in THF (15 ml) was added to a solution of NH₂-X (X: 4-pyridyl, 4-picolyl, 2-(2-pyridyl)ethyl, β -phenethyl) (3.3 mmol) in THF (10 ml). The reaction mixture was stirred at 4 °C overnight. After removal of the solvent, the residue was extracted with AcOEt. The extract was washed with 10% citric acid, 5% Na₂CO₃ and water, dried over Na₂SO₄ and evaporated to dryness. Ether was added to the residue to afford crystals, which were collected by filtration. The yield, mp, $[\alpha]_D^{25}$ values, elemental analysis and R_f values are summarized in Table 16.

General Procedure for Synthesis of Boc-Tra-Tyr(*O*-2-BrZ)-NH-X [X: 4-pyridyl, 4-picolyl, 2-(2-pyridyl)ethyl, β -phenethyl] A mixed anhydride of Boc-Tra-OH [prepared routinely from Boc-Tra-OH (245 mg, 0.89 mmol),

Table 16. Yield, Melting Point, Optical Rotation, Elemental Analysis and *R_f* Values of Boc-Tyr(*O*-2-BrZ)-NH-X

X	Yield (%)	mp (°C)	[α] _D ²⁵ (MeOH)	Formula	Elemental analysis Calcd (Found)			TLC	
					C	H	N	<i>R_f</i> ¹	<i>R_f</i> ²
4-Pyridyl	27	126—128	+36.6 (<i>c</i> =0.9)	C ₂₇ H ₂₈ BrN ₃ O ₆	56.84 (56.57)	4.94 (4.94)	7.36 (7.44)	0.25	0.54
4-Picolyl	59	156.5—158	+1.5 (<i>c</i> =1.0)	C ₂₈ H ₃₀ BrN ₃ O ₆	57.54 (57.57)	5.17 (5.17)	7.18 (7.20)	0.49	0.53
2-(2-Pyridyl)ethyl	75	114—122	−0.11 (<i>c</i> =0.9)	C ₂₉ H ₃₂ BrN ₃ O ₆	58.19 (57.76)	5.38 (5.25)	7.02 (6.87)	0.65	0.62
β-Phenethyl	75	152—155	−1.6 (<i>c</i> =1.0) ^{a)}	C ₃₀ H ₃₃ BrN ₂ O ₆	60.30 (60.46)	5.58 (5.57)	4.69 (4.63)	0.83	

a) CHCl₃.Table 17. Yield, Melting Point, Optical Rotation, Elemental Analysis and *R_f* Values of Boc-Tra-Tyr(*O*-2-BrZ)-NH-X

X	Yield (%)	mp (°C)	[α] _D ²⁵ (MeOH)	Formula	Elemental analysis Calcd (Found)			TLC	
					C	H	N	<i>R_f</i> ¹	<i>R_f</i> ²
4-Pyridyl	66	178—180	+19.4 (<i>c</i> =1.0)	C ₃₅ H ₄₁ BrN ₄ O ₇	58.50 (58.72)	5.89 (5.86)	7.80 (7.71)	0.40	0.57
4-Picolyl	59	189—192	−13.2 (<i>c</i> =1.0)	C ₃₆ H ₄₃ BrN ₄ O ₇	59.75 (59.48)	5.98 (5.86)	7.74 (7.71)	0.46	0.48
2-(2-Pyridyl)ethyl	65	195—195.5	−14.6 (<i>c</i> =0.9)	C ₃₇ H ₄₅ BrN ₄ O ₇	59.51 (59.55)	6.14 (6.13)	7.50 (7.48)	0.57	0.42
β-Phenethyl	81	198—200	−7.8 (<i>c</i> =1.0)	C ₃₈ H ₄₆ BrN ₃ O ₇	61.95 (61.77)	6.31 (6.31)	5.70 (5.72)	0.76	

Table 18. Yield, Melting Point, Optical Rotation, Elemental Analysis and *R_f* Value of H-Tra-Tyr(*O*-2-BrZ)-NH-X · HCl (**23**—**26**)

X	Peptide ID	Yield (%)	mp (°C)	[α] _D ²⁵ (MeOH)	Formula	Elemental analysis Calcd (Found)			TLC
						C	H	N	<i>R_f</i> ³
4-Pyridyl	23	83	Amorphous	+40.3 (<i>c</i> =0.9)	C ₃₀ H ₃₃ BrN ₄ O ₅ · 2HCl · 2.5H ₂ O	49.48 (49.53)	5.16 (5.54)	7.42 (7.70)	0.39
4-Picolyl	24	72	Amorphous	−0.35 (<i>c</i> =0.9) ^{a)}	C ₃₁ H ₃₅ BrN ₄ O ₅ · 2HCl · 2.5H ₂ O	50.21 (49.93)	5.71 (5.40)	7.56 (7.28)	0.39
2-(2-Pyridyl)ethyl	25	80	Amorphous	−4.4 (<i>c</i> =0.6) ^{a)}	C ₃₂ H ₃₇ BrN ₄ O ₅ · 2HCl · 3H ₂ O	50.27 (50.10)	5.93 (5.30)	7.32 (7.20)	0.52
β-Phenethyl	26	74	204—206	−3.5 (<i>c</i> =1.0)	C ₃₃ H ₃₈ BrN ₃ O ₅ · HCl · 0.5H ₂ O	58.11 (57.81)	5.91 (5.84)	6.16 (6.17)	0.30

a) 0.1 N HCl.

isobutyl chloroformate (0.13 ml, 0.89 mmol) and Et₃N (0.12 ml, 0.89 mmol)] in THF (15 ml) was added to a solution of H-Tyr(*O*-2-BrZ)-NH-X · HCl [X: 4-pyridyl, 4-picolyl, 2-(2-pyridyl)ethyl, β-phenethyl; prepared routinely from Boc-Tyr(*O*-2-BrZ)-NH-X (0.89 mmol) and 7.2 N HCl-dioxane (2.0 ml, 14.4 mmol) as usual] in DMF (20 ml) containing Et₃N (0.15 ml, 1.1 mmol) at 0 °C and the reaction mixture was stirred at 4 °C overnight. After removal of the solvent, ether was added to the residue to afford crystals, which were collected by filtration and washed with water. The yield, mp, [α]_D²⁵ values, elemental analysis and *R_f* values are summarized in Table 17.

General Procedure for Synthesis of H-Tra-Tyr(*O*-2-BrZ)-NH-X · HCl (23**—**26**) [X: 4-pyridyl, 4-picolyl, 2-(2-pyridyl)ethyl, β-phenethyl]** Boc-Tra-Tyr(*O*-2-BrZ)-NH-X [X: 4-pyridyl, 4-picolyl, 2-(2-pyridyl)ethyl, β-phenethyl; (0.14 mmol)] was dissolved in 5.4 N HCl-dioxane (0.5 ml, 2.7 mmol) at 0 °C and the reaction mixture was stirred at the same temperature for 5 min. After addition of dioxane (0.2 ml), the reaction mixture was stirred at room temperature for 90 min. After removal of the solvent, dry ether was added to the residue to afford a precipitate. The yield, mp, [α]_D²⁵ values, elemental analysis and *R_f* values are summarized in Table 18.

General Procedure for Synthesis of Boc-Tyr(*O*-2-BrZ)-Tra-O-X [X:

methyl, *n*-hexyl, *n*-heptyl, *n*-octyl] A mixed anhydride of Boc-Tyr(*O*-2-BrZ)-OH [prepared routinely from Boc-Tyr(*O*-2-BrZ)-OH (1.5 g, 3.0 mmol), isobutyl chloroformate (0.45 ml, 3.0 mmol) and Et₃N (0.45 ml, 3.0 mmol)] in THF (15 ml) was added to a solution of NH₂-X (X: methyl, *n*-hexyl, *n*-heptyl, *n*-octyl) (3.3 mmol) in THF (10 ml). The reaction mixture was stirred at 4 °C overnight. After removal of the solvent, the residue was extracted with AcOEt. The extract was washed with 10% citric acid, 5% Na₂CO₃ and water, dried over Na₂SO₄ and evaporated to dryness. Ether was added to the residue to afford crystals, which were collected by filtration. The yield, mp, [α]_D²⁵ values, elemental analysis and *R_f* values are summarized in Table 19.

General Procedure for Synthesis of Boc-EACA-Tyr(*O*-2-BrZ)-Tra-O-X [X: methyl, *n*-hexyl, *n*-heptyl, *n*-octyl] A mixed anhydride of Boc-EACA-OH [prepared routinely from Boc-EACA-OH (221 mg, 0.89 mmol), isobutyl chloroformate (0.13 ml, 0.89 mmol) and Et₃N (0.12 ml, 0.89 mmol)] in THF (15 ml) was added to a solution of H-Tyr(*O*-2-BrZ)-Tra-O-X · HCl [X: methyl, *n*-hexyl, *n*-heptyl, *n*-octyl; prepared routinely from Boc-Tyr(*O*-2-BrZ)-Tra-O-X (0.89 mmol) and 7.2 N HCl-dioxane (2.0 ml, 14.4 mmol)] in DMF (30 ml) containing Et₃N (0.15 ml, 1.1 mmol) at 0 °C. The reaction mixture was stirred at 4 °C overnight. After removal of the solvent, ether was

Table 19. Yield, Melting Point, Optical Rotation, Elemental Analysis and *R_f* Value of Boc-Tyr(*O*-2-BrZ)-Tra-O-X

X	Yield (%)	mp (°C)	[α] _D ²⁵ (CHCl ₃)	Formula	Elemental analysis Calcd (Found)			TLC
					C	H	N	<i>R_f</i> ¹
Methyl	70	144—147	−0.1 (<i>c</i> =1.0)	C ₃₁ H ₃₉ BrN ₂ O ₈	57.50 (57.37)	6.08 5.92	4.32 4.29	0.70
<i>n</i> -Hexyl	87	98—101	+1.2 (<i>c</i> =1.0)	C ₃₆ H ₄₉ BrN ₂ O ₈	60.24 (60.05)	6.90 6.95	3.90 3.87	0.81
<i>n</i> -Heptyl	89	109—112	+1.8 (<i>c</i> =1.0)	C ₃₇ H ₅₁ BrN ₂ O ₈	60.72 (60.67)	7.04 7.08	3.83 3.82	0.75
<i>n</i> -Octyl	89	95—99	−0.5 (<i>c</i> =1.0)	C ₃₈ H ₅₃ BrN ₂ O ₈	61.20 (61.17)	7.18 6.91	3.75 3.72	0.95

Table 20. Yield, Melting Point, Optical Rotation, Elemental Analysis and *R_f* Value of Boc-EACA-Tyr(*O*-2-BrZ)-Tra-O-X

X	Yield (%)	mp (°C)	[α] _D ²⁵ (DMF)	Formula	Elemental analysis Calcd (Found)			TLC
					C	H	N	<i>R_f</i> ¹
Methyl	84	103—106	−2.5 (<i>c</i> =1.0) ^{a)}	C ₃₇ H ₄₈ BrN ₃ O ₉	58.41 (58.28)	6.37 6.56	5.52 5.44	0.70
<i>n</i> -Hexyl	86	94—97	−4.3 (<i>c</i> =1.0)	C ₄₂ H ₆₀ BrN ₃ O ₉	60.71 (60.49)	7.29 7.31	5.05 5.02	0.69
<i>n</i> -Heptyl	80	101—103	−5.35 (<i>c</i> =1.0)	C ₄₃ H ₆₂ BrN ₃ O ₉	61.12 (60.97)	7.41 7.33	4.97 4.86	0.72
<i>n</i> -Octyl	73	118—120	−4.15 (<i>c</i> =1.0)	C ₄₄ H ₆₄ BrN ₃ O ₉	61.52 (61.30)	7.53 7.56	4.89 4.80	0.71

a) CHCl₃.Table 21. Yield, Melting Point, Optical Rotation, Elemental Analysis and *R_f* Value of H-EACA-Tyr(*O*-2-BrZ)-Tra-O-X·HCl (27—30)

X	Peptide ID	Yield (%)	mp (°C)	[α] _D ²⁵ (MeOH)	Formula	Elemental analysis Calcd (Found)			TLC
						C	H	N	<i>R_f</i> ³
Methyl	27	82	168—178	+7.2 (<i>c</i> =1.0)	C ₃₂ H ₄₂ BrN ₃ O ₇ · HCl·H ₂ O	53.74 (53.70)	6.34 6.19	5.88 6.12	0.21
<i>n</i> -Hexyl	28	90	155—157	+6.7 (<i>c</i> =1.0)	C ₃₇ H ₅₂ BrN ₃ O ₇ · HCl·H ₂ O	56.60 (56.45)	7.06 6.83	5.35 5.29	0.38
<i>n</i> -Heptyl	29	92	156—159	+6.6 (<i>c</i> =1.0)	C ₃₈ H ₅₄ BrN ₃ O ₇ · HCl·H ₂ O	57.11 (56.82)	7.19 6.96	5.26 5.17	0.69
<i>n</i> -Octyl	30	91	159—161	+7.0 (<i>c</i> =1.0)	C ₃₉ H ₅₆ BrN ₃ O ₇ · HCl·1.5H ₂ O	56.97 (56.95)	7.35 7.15	5.11 5.09	0.61

added to the residue to afford crystals, which were collected by filtration and washed with water. The yield, mp, [α]_D²⁵ values, elemental analysis and *R_f* values are summarized in Table 20.

General Procedure for Synthesis of H-EACA-Tyr(*O*-2-BrZ)-Tra-O-X·HCl (27—30) [X: methyl, *n*-hexyl, *n*-heptyl, *n*-octyl] Boc-EACA-Tyr(*O*-2-BrZ)-Tra-O-X [X: methyl, *n*-hexyl, *n*-heptyl, *n*-octyl (0.2 mmol)] was dissolved in 5.4*N* HCl-dioxane (0.5 ml, 2.7 mmol) at 0 °C and the reaction mixture was stirred at the same temperature for 5 min. After addition of dioxane (0.2 ml), the reaction mixture was stirred at room temperature for 90 min. After removal of the solvent, dry ether was added to the residue to afford a precipitate. The yield, mp, [α]_D²⁵ values, elemental analysis and *R_f* values are summarized in Table 21.

General Procedure for Synthesis of Boc-Tra-Tyr(*O*-2-BrZ)-Tra-O-X [X: methyl, *n*-hexyl, *n*-heptyl, *n*-octyl] A mixed anhydride of Boc-Tra-OH [prepared routinely from Boc-Tra-OH (245 mg, 0.89 mmol), isobutyl chloroformate (0.13 ml, 0.89 mmol) and Et₃N (0.12 ml, 0.89 mmol)] in THF (15 ml) was added to a solution of H-Tyr(*O*-2-BrZ)-Tra-O-X·HCl [X: methyl, *n*-hexyl, *n*-heptyl, *n*-octyl; prepared routinely from Boc-Tyr(*O*-2-BrZ)-Tra-O-X (0.89 mmol) and 7.2*N* HCl-dioxane (2.0 ml, 14.4 mmol)] in

DMF (20 ml) containing Et₃N (0.15 ml, 1.1 mmol) at 0 °C and the reaction mixture was stirred at 4 °C overnight. After removal of the solvent, ether was added to the residue to afford crystals, which were collected by filtration and washed with water. The yield, mp, [α]_D²⁵ values, elemental analysis and *R_f* values are summarized in Table 22.

General Procedure for Synthesis of H-Tra-Tyr(*O*-2-BrZ)-Tra-O-X·HCl (31—34) [X: methyl, *n*-hexyl, *n*-heptyl, *n*-octyl] Boc-Tra-Tyr(*O*-2-BrZ)-Tra-O-X [X: methyl, *n*-hexyl, *n*-heptyl, *n*-octyl (0.14 mmol)] was dissolved in 5.4*N* HCl-dioxane (0.5 ml, 2.7 mmol) at 0 °C and the reaction mixture was stirred at the same temperature for 5 min. After addition of dioxane (0.2 ml), the reaction mixture was stirred at room temperature for 90 min. After removal of the solvent, dry ether was added to the residue to afford a precipitate. The yield, mp, [α]_D²⁵ values, elemental analysis and *R_f* values are summarized in Table 23.

Assay Procedure The enzymes used were as follows: human PL and PK (KABI Co.), bovine TH (Mochida Seiyaku Co.), porcine glandular kallikrein (GK) (Sigma Chemical Co.), human urokinase (UK) (Green Cross) and TRY (Sigma Chemical Co.). Enzymatic activities of PL, PK, TH, GK, UK and TRY were determined by the method described previously,¹⁷⁾

Table 22. Yield, Melting Point, Optical Rotation, Elemental Analysis and *R_f* Value of Boc-Tra-Tyr(*O*-2-BrZ)-Tra-O-X

X	Yield (%)	mp (°C)	[α] _D ²⁵ (DMF)	Formula	Elemental analysis Calcd (Found)			TLC
					C	H	N	<i>R_f</i> ¹
Methyl	82	219—222	−4.5 (<i>c</i> =1.0) ^{a)}	C ₃₉ H ₅₀ BrN ₃ O ₉	59.53 (59.46)	6.66 6.65	5.34 5.31)	0.64
<i>n</i> -Hexyl	67	189—191	−8.5 (<i>c</i> =1.0)	C ₄₄ H ₆₂ BrN ₃ O ₉	61.66 (61.64)	7.31 7.44	4.90 4.89)	0.81
<i>n</i> -Heptyl	68	185—187	−7.9 (<i>c</i> =1.0)	C ₄₅ H ₆₄ BrN ₃ O ₉	62.05 (62.06)	7.42 7.41	4.82 4.73)	0.72
<i>n</i> -Octyl	88	184—187	−7.8 (<i>c</i> =1.0)	C ₄₆ H ₆₆ BrN ₃ O ₉	62.42 (62.52)	7.53 7.63	4.75 4.69)	0.73

a) CHCl₃.Table 23. Yield, Melting Point, Optical Rotation, Elemental Analysis and *R_f* Value of H-Tra-Tyr(*O*-2-BrZ)-Tra-O-X·HCl (31—34)

X	Peptide ID	Yield (%)	mp (°C)	[α] _D ²⁵ (MeOH)	Formula	Elemental analysis Calcd (Found)			TLC
						C	H	N	<i>R_f</i> ³
Methyl	31	95	213—216	−1.1 (<i>c</i> =1.0)	C ₃₄ H ₄₄ BrN ₃ O ₇ · HCl·1.5H ₂ O	54.45 (54.79)	6.45 6.53	5.60 5.66)	0.17
<i>n</i> -Hexyl	32	86	200—203	+1.0 (<i>c</i> =1.0)	C ₃₉ H ₅₄ BrN ₃ O ₇ · HCl·1.5H ₂ O	58.38 (58.34)	7.03 7.11	5.23 5.22)	0.66
<i>n</i> -Heptyl	33	75	212—214	−0.4 (<i>c</i> =1.0)	C ₄₀ H ₅₆ BrN ₃ O ₇ · HCl·0.5H ₂ O	58.85 (58.93)	7.16 7.22	5.14 5.18)	0.71
<i>n</i> -Octyl	34	82	198—202	+1.0 (<i>c</i> =1.0)	C ₄₁ H ₅₈ BrN ₃ O ₇ · HCl·1.5H ₂ O	58.05 (58.16)	7.38 7.07	4.95 4.94)	0.83

using D-Val-Leu-Lys-*p*NA (S-2251), D-Pro-Phe-Arg-*p*NA (S-2302), D-Phe-Pip-Arg-*p*NA (S-2238), D-Val-Leu-Arg-*p*NA (S-2266), <Glu-Gly-Arg-*p*NA (S-2444) and D-Phe-Pip-Arg-*p*NA (S-2238), respectively. Fibrin and fibrinogen were used as substrates for PL and TH, respectively. IC₅₀ values were determined as follows: 1) Antiamidolytic assay¹⁸⁾; the IC₅₀ value was taken as the concentration of inhibitor which reduced the absorbance at 405 nm by 50% compared with the absorbance measured under the same conditions without inhibitor. 2) Antifibrinolytic assay¹⁸⁾; the IC₅₀ value was taken as the concentration of inhibitor which prolonged the complete lysis time two-fold compared with that without inhibitor. 3) Antifibrinogenolytic assay: to a borate saline buffer (pH 7.4) was added solutions containing various concentrations of the inhibitor to be tested (0.5 ml), 0.2% bovine fibrinogen in the above buffer (0.4 ml), and bovine TH 4 U/ml (0.1 ml). The assay was carried out at 37 °C and the clotting time was measured. The IC₅₀ value was taken as the concentration of inhibitor which prolonged the clotting time two-fold compared with that without inhibitor.

Acknowledgement The authors are grateful for the assistance of Drs. L. H. Lazarus and S. D. Bryant of the National Institute of Environmental Health Sciences (NIEHS) for their kind help during the preparation of this manuscript.

References and Notes

- 1) The customary L-configuration for amino acid residues is omitted. Abbreviations used in this report for amino acids, peptides and their derivatives are those recommended by the IUPAC-IUB Commission on Biochemical Nomenclature: *Biochemistry*, **5**, 2485—2489 (1966); **6**, 362—364 (1967); **11**, 1726—1732 (1972). The following additional abbreviations are used: AcOEt, ethyl acetate; DMF, *N,N*-dimethylformamide; TFA, trifluoroacetic acid; Boc, *tert*-butoxycarbonyl; TEA, triethylamine; (Boc)₂O, di-*tert*-butyldicarbonate; 2-BrZ, 2-bromobenzyloxycarbonyl; Tra, 4-aminomethylcyclohexanecarbonyl; EACA, 6-aminohexanoic acid; PK, plasma kallikrein; PL, plasmin; TH, thrombin; GK, glandular kallikrein; UK, urokinase; TRY, trypsin; Fg, fibrinogen; Fn, fibrin.
- 2) Katsunuma N., Kominami E., *Rev. Physiol. Biochem. Pharmacol.*, **108**, 1—20 (1987).
- 3) Senior R. M., Tegner H., Kuhn K., Ohlsson K., Starcher B. C., Pierce J. A., *Am. Rev. Respir. Dis.*, **116**, 469—475 (1977).
- 4) Iwamoto M., Abiko Y., *Biochim. Biophys. Acta*, **214**, 402—410 (1970).
- 5) Moroi M., Aoki N., *J. Biol. Chem.*, **251**, 5956—4965 (1976).
- 6) Aoki N., *Semin. Thromb. Hemostasis*, **10**, 42—50 (1984).
- 7) Romisch J., Dickneite G., Paques E.-P., Heimburg N., *Jpn. J. Thromb. Hemostasis*, **3**, 73—94 (1992).
- 8) Markus G., *Semin. Thromb. Hemostasis*, **10**, 61—70 (1984).
- 9) Okamoto S., *Keio J. Med.*, **8**, 211—247 (1959).
- 10) Okamoto S., Sato S., Tanaka Y., Okamoto U., *Keio J. Med.*, **13**, 177—185 (1964).
- 11) Iwamoto M., *Thrombos. Diathes. Haemorrh.*, **33**, 573—585 (1975).
- 12) Okada Y., Tsuda Y., Teno N., Wanaka K., Bohgaki M., Hijikata-Okunomiya A., Naito T., Okamoto S., *Chem. Pharm. Bull.*, **36**, 1289—1297 (1988).
- 13) Teno N., Wanaka K., Okada Y., Tsuda Y., Okamoto U., Hijikata-Okunomiya A., Naito T., Okamoto S., *Chem. Pharm. Bull.*, **39**, 2340—2346 (1991).
- 14) Teno N., Wanaka K., Okada Y., Taguchi H., Okamoto U., Hijikata-Okunomiya A., Okamoto S., *Chem. Pharm. Bull.*, **41**, 1079—1090 (1993).
- 15) Schechter I., Berger A., *Biochem. Biophys. Res. Commun.*, **27**, 157—162 (1967).
- 16) Yamamoto T., Ino Y., Ozeki M., Oda M., Sato T., Koshiyama Y., Suzuki S., Fujita M., *Jpn. J. Pharmacol.*, **35**, 203—227 (1984).
- 17) Tsuda Y., Teno N., Okada Y., Wanaka K., Bohgaki A., Hijikata-Okunomiya A., Okamoto U., Naito T., Okamoto S., *Chem. Pharm. Bull.*, **37**, 3108—3111 (1989).
- 18) Okada Y., Tsuda Y., Teno N., Wanaka K., Bohgaki N., Hijikata-Okunomiya A., Naito T., Okamoto S., *Chem. Pharm. Bull.*, **36**, 1289—1297 (1988).

Inhibition of Human Immunodeficiency Virus Type 1 Reverse Transcriptase and Ribonuclease H Activities by Constituents of *Juglans mandshurica*

Byung-Sun MIN,^{a,b} Norio NAKAMURA,^a Hirotosugu MIYASHIRO,^a Young-Ho KIM,^b and Masao HATTORI^{*,a}

Institute of Natural Medicine, Toyama Medical and Pharmaceutical University,^a 2630 Sugitani, Toyama, 930-0194, Japan, and College of Pharmacy, Chungnam National University,^b Taejeon 305-764, Korea.

Received July 7, 1999; accepted October 20, 1999.

From the stem-bark of *Juglans mandshurica*, two new naphthalenyl glucopyranosides, 1,4,8-trihydroxy-naphthalene 1-*O*-[α -L-arabinofuranosyl-(1 \rightarrow 6)- β -D-glucopyranoside] (1) and 1,4,8-trihydroxynaphthalene 1-*O*- β -D-[6'-*O*-(3'',5''-dihydroxy-4''-methoxybenzoyl)]glucopyranoside (4), and two new α -tetralonyl glucopyranosides, 4 α ,5,8-trihydroxy- α -tetralone 5-*O*- β -D-[6'-*O*-(3'',5''-dihydroxy-4''-methoxybenzoyl)]glucopyranoside (7) and 4 α ,5,8-trihydroxy- α -tetralone 5-*O*- β -D-[6'-*O*-(3'',4'',5''-trihydroxybenzoyl)]glucopyranoside (8), were isolated together with three known naphthalenyl glucopyranosides (2, 3 and 5), one α -tetralonyl glucopyranoside (6), four flavonoids (9–12), and two galloyl glucopyranosides (13, 14).

Amongst the isolated compounds, 1,2,6-trigalloylglucopyranose (13) and 1,2,3,6-tertagalloylglucopyranose (14) exhibited the most potent inhibition of reverse transcriptase (RT) activity with IC₅₀ values of 0.067 and 0.040 μ M, respectively, while the latter compound also inhibited ribonuclease H (RNase H) activity with an IC₅₀ of 39 μ M, comparable in potency to illimaquinone used as a positive control. 1,4,8-Trihydroxy-naphthalene 1-*O*- β -D-glucopyranoside (2), 1,4,8-trihydroxynaphthalene 1-*O*- β -D-[6'-*O*-(4''-hydroxy-3'',5''-dimethoxybenzoyl)]glucopyranoside (3) and 8 showed moderate inhibition against both enzyme activities, and inhibitory potency of 2 against RNase H activity (IC₅₀=156 μ M) was slightly greater than that against the RT activity (IC₅₀=290 μ M). The inhibitory potencies of 4 α ,5,8-trihydroxy- α -tetralone 5-*O*- β -D-[6'-*O*-(4''-hydroxy-3'',5''-dimethoxybenzoyl)]glucopyranoside (6), 7 and 8 against RT activity increased accompanied by an increase in the number of free hydroxyls on the galloyl residues, as represented by the IC₅₀ values of >500, 330 and 5.8 μ M, respectively.

Key words human immunodeficiency virus; *Juglans mandshurica*; naphthalenyl glucopyranoside; reverse transcriptase; ribonuclease H; α -tetralonyl glucopyranoside

Reverse transcriptase (RT) of human immunodeficiency virus type 1 (HIV-1) has been demonstrated to be important for viral replication.^{1,2)} The crucial role of RT in the early stages of the HIV-1 life cycle has made it one of the most reliable targets for potential anti-AIDS chemotherapy.³⁾ The enzyme possesses not only RT activity but also DNA-dependent DNA polymerase and ribonuclease H (RNase H) activities. The single-stranded RNA genome of HIV is reverse-transcribed by the RNA-dependent DNA polymerase activity (RT activity) into the minus DNA strand to form an RNA–DNA hybrid. Then, RNase H catalyzes hydrolysis of the RNA component of the hybrid leaving small RNA primers for the subsequent synthesis of complementary plus DNA strand by the DNA-dependent DNA polymerase activity.^{4,5)} The enzyme from HIV-1 consists of a pair of polypeptides, in which the DNA polymerase activity resides in the N-terminal domain, whereas the RNase H activity is located in the C-terminal domain.⁶⁾

Inhibition of each catalytic function of RT interferes with virus production. Two classes of inhibitors of RT have been developed up to the present; nucleoside analogues and non-nucleoside compounds, which are distinguished by their different inhibitory mechanisms. The nucleoside analogues 3'-azido-2',3'-dideoxythymidine (AZT), 2',3'-dideoxycytidine (DDC) and 2',3'-dideoxyinosine (DDI) act by chain termination and are known to inhibit competitively with respect to substrates, deoxynucleoside triphosphates. Unfortunately, their use for treatment of patients with AIDS is limited due to emergence of resistant virus and their cellular toxicity. On

the other hand, non-nucleoside inhibitors act at sites other than the substrate binding sites of the polymerase.⁷⁾ These include compounds, such as nevirapine,⁷⁾ calanoides,⁸⁾ coumarin derivatives,⁹⁾ benzodiazepine derivatives,¹⁰⁾ pyridinone,¹¹⁾ catechin derivatives¹²⁾ and psychotrine.¹³⁾ These inhibitors have been reported to exert low levels of toxicity. However, these compounds also lead to rapid drug cross-resistance. The need for development of an effective and selective inhibitor of HIV-1 with a new mechanism of action still remains. A relatively large volume of research has been conducted on the inhibition of RT activity, but there are only a few reports on the selective inhibition of RNase H activity, such as herparin,¹⁴⁾ illimaquinone,¹⁵⁾ novenamides (U-34445, U-35122 and U-35401)¹⁶⁾ and a degradation product of cephalosporin (HP 0.35).¹⁷⁾

Therefore, we examined a conventional assay method for RNase H activity associated with HIV-1 RT to find new inhibitory substances from natural sources. During *in vitro* screening, we found that naphthoquinone derivatives and naphthalene derivatives from *Lithospermum erythrorhizon* SIEBOLD *et* ZUCCARINI (Borraginaceae), *Limonium tetragonum* A. A. BULLOCK (Plumbaginaceae), and *Juglans (J.) mandshurica* MAXIMOWICZ (Juglandaceae) inhibited RNase H activity. Of the tested plants, the extract of *J. mandshurica* (stem-bark) appreciably inhibited RNase H activity with a 50% inhibitory concentration (IC₅₀) of 22 μ g/ml, while it more potently inhibited RT activity (IC₅₀, 0.047 μ g/ml).

J. mandshurica has been used as a folk medicine for treatment of cancer in Korea.¹⁸⁾ Several naphthoquinones, naph-

* To whom correspondence should be addressed.

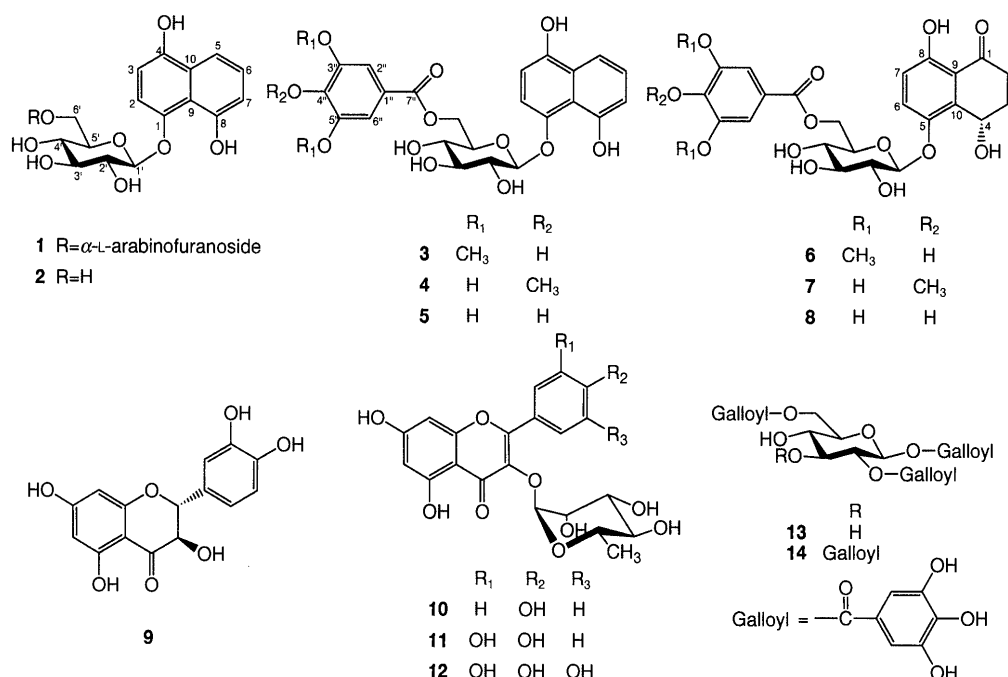


Chart 1. Structures of Isolated Compounds

thalenyl glucopyranosides, α-tetralonyl glucopyranosides and diarylheptanoyl glucopyranosides have been isolated from this plant^{18–20} and these compounds have been shown to display cytotoxicity to human colon and lung carcinoma.²⁰ In this paper, we describe the characterization of compounds isolated from the stem-bark of this plant and their inhibitory potencies against HIV-1 RT and RNase H activities.

Results and Discussion

Isolation and Structure Determination Repeated column chromatography of an EtOAc-soluble fraction of the MeOH extract of *J. mandshurica* (stem-bark) on silica gel followed by gel filtration on Sephadex LH-20 and reversed phase medium pressure liquid chromatography (MPLC) led to the isolation of five naphthalenyl glucopyranosides (1–5), three α-tetralonyl glucopyranosides (6–8), four flavonoids (9–12) and two galloyl glucopyranosides (13–14). The known compounds were identified as 1,4,8-trihydroxynaphthalene 1-O-β-D-glucopyranoside (2),²¹ 1,4,8-trihydroxynaphthalene 1-O-β-D-[6'-O-(4"-hydroxy-3",5"-dimethoxybenzoyl)]glucopyranoside (3),¹⁹ 1,4,8-trihydroxynaphthalene 1-O-β-D-[6'-O-(3",4",5"-trihydroxybenzoyl)]glucopyranoside (5),¹⁹ 4,5,8-trihydroxy-α-tetralone 5-O-β-D-[6'-O-(4"-hydroxy-3",5"-dimethoxybenzoyl)]glucopyranoside (6),²⁰ taxifolin (9),²² afzelin (10),²³ quercitrin (11),²⁴ myricitrin (12),²⁴ 1,2,6-trigalloylglucopyranose (13)²⁵ and 1,2,3,6-tetragalloylglucopyranose (14)²⁶ by comparing their spectral data with those previously reported.

Compound 1 was obtained as a light brown amorphous powder, $[\alpha]_D -94^\circ$. Its positive FAB-MS spectrum gave a quasi-molecular ion peak at m/z 471 $[M+H]^+$. The ¹H-NMR spectrum showed signals for five aromatic protons at δ 6.70, 6.81, 7.21, 7.26 and 7.65, eleven sugar protons between δ 3.42 to 4.10, and two anomeric protons at δ 4.95 and 4.97 (Table 1). The ¹³C-NMR spectrum, in combination with distortionless enhancement by polarization transfer (DEPT) and ¹H-detected multiple quantum coherence (HMQC) experi-

Table 1. ¹H-NMR Spectral Data of Compounds 1 and 4 in CD₃OD

Position	1 ^{a)}	4 ^{b)}
1		
2	6.70 d (8.4)	6.44 d (8.2)
3	7.21 d (8.4)	7.06 d (8.2)
4		
5	7.65 dd (8.4, 1.1)	7.55 dd (8.3, 1.1)
6	7.26 dd (8.4, 7.5)	7.16 dd (8.3, 7.6)
7	6.81 dd (7.5, 1.1)	6.71 dd (7.6, 1.1)
8		
9		
10		
1'	4.95 d (7.7)	4.87 d (7.5)
2'	3.53 m	3.49 m
3'	3.47 m	3.43 m
4'	3.42 dd (17.8, 8.6)	3.41 m
5'	3.64 m	3.71 m
6'	3.68 m	4.42 dd (11.8, 7.0)
	4.10 m	4.58 dd (11.8, 2.2)
1''	4.97 d (1.3)	
2''	4.04 dd (3.4, 1.3)	7.05 s
3''	3.86 dd (5.9, 3.4)	
4''	3.99 m	
5''	3.63 dd (11.8, 5.1)	
	3.73 dd (11.8, 3.2)	
6''		7.05 s
7''		
3'',5''-OCH ₃		
4''-OCH ₃		3.82 s

a) 500 MHz. b) 400 MHz.

δ values in ppm and coupling constants (in parentheses) in Hz.

ments, showed signals for five aromatic methine carbons at δ 108.3, 112.1, 113.0, 114.6 and 127.1, seven aliphatic methine carbons in a region at δ 71.8 to 85.6, two anomeric carbons at δ 105.2 and 110.0, two aliphatic methylenes at δ 62.9 and 68.3, and five quaternary carbons (Table 2). On the basis of spectroscopic evidence obtained by ¹H-¹H correlation spectroscopy (COSY) and HMQC experiments, all protons and carbons of sugars were assigned as shown in Tables 1 and 2,

Table 2. ^{13}C -NMR Spectral Data of Compounds **1**, **4** and **6–8** in CD_3OD

Position	1 ^{a)}	4 ^{b)}	6 ^{a)}	7 ^{b)}	8 ^{b)}
1	148.5	148.6	206.3	206.4	206.4
2	108.3	108.4	33.5	33.5	33.5
3	113.0	113.3	30.2	30.2	30.2
4	150.5	150.5	61.3	61.3	61.3
5	114.6	114.6	148.3	148.5	148.5
6	127.1	127.1	128.7	128.8	128.8
7	112.1	112.2	118.8	119.1	119.2
8	154.7	154.6	159.2	159.3	159.3
9	117.8	117.8	116.1	116.4	116.1
10	128.8	128.9	135.4	135.2	135.1
1'	105.2	105.3	104.2	104.6	104.6
2'	75.1	75.1	75.2	75.3	75.3
3'	78.1	78.1	77.8	78.0	77.9
4'	71.8	71.8	71.9	71.9	71.7
5'	77.2	76.0	75.8	75.7	75.8
6'	68.3	65.1	65.0	64.9	64.6
1''	110.0	126.5	121.1	126.4	121.0
2''	83.4	110.4	108.3	110.2	110.1
3''	78.8	151.8	148.9	151.9	146.7
4''	85.6	141.4	142.3	141.5	140.4
5''	62.9	151.8	148.9	151.9	146.7
6''		110.4	108.3	110.2	110.1
7''		167.7	167.7	167.7	168.2
3'',5''-OCH ₃			56.9		
4''-OCH ₃	148.5	60.8		60.8	

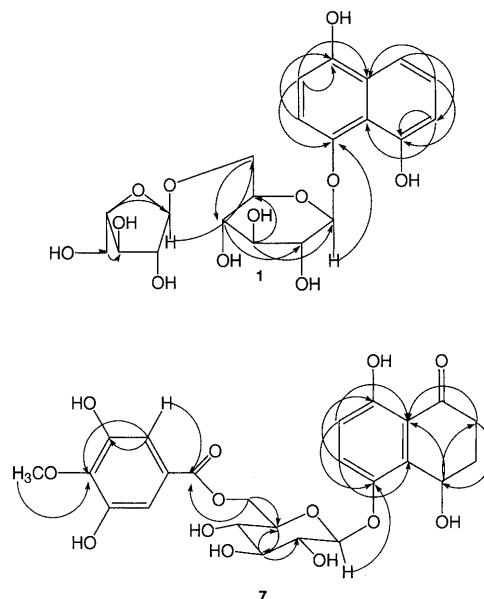
a) 125 MHz. b) 100 MHz.

respectively.^{27,28)}

The sugar linkages were determined by heteronuclear multiple-bond correlations (HMBC, Fig. 1), which showed correlations between signals at δ_{H} 4.95 (Glc-H-1') and at δ_{C} 148.5 (C-1 of the aglycone), and at δ_{H} 4.97 (Ara-H-1'') and δ_{C} 68.3 (Glc-C-6'), indicating glycosylation at C-1 with an Ara (1 \rightarrow 6)Glc moiety. The positions of the hydroxy groups on the naphthalene ring were deduced from the coupling pattern in the ^1H -NMR spectrum and the correlations between signals at δ_{H} 6.70 (H-2) and 7.21 (H-3), and among signals at δ_{H} 7.65 (H-5), 7.26 (H-6) and 6.81 (H-7) in the ^1H - ^1H COSY spectrum. This was further confirmed by an HMBC experiment, where long-range correlations were observed between signals at δ_{H} 6.70 (or 7.21) and δ_{C} 150.5 (C-4), and at δ_{H} 7.26 (or 6.81) and δ_{C} 154.7 (C-8) (Fig. 1).

Acid hydrolysis of **1** afforded glucose and arabinose as monosaccharide units, which were identified on TLC by comparison with authentic samples. Furthermore, these sugars were determined to be D-glucose and L-arabinose, respectively, by GLC of their pertrimethylsilylated L-cysteine methyl ester derivatives.²⁹⁾ The configuration of the glycosidic linkage of the glucopyranose moiety in **1** was determined to be β on the basis of the $J_{1',2'}$ value (7.7 Hz) of the anomeric proton, while that of the arabinofuranose moiety was α from the $J_{1'',2''}$ value (1.3 Hz) and the chemical shifts of C-1 (δ_{C} 110.0) and C-2 (δ_{C} 83.4) in the ^{13}C -NMR spectrum.^{27,28)} Consequently, the structure of **1** was determined as 1,4,8-trihydroxynaphthalene 1-O-[α -L-arabinofuranosyl-(1 \rightarrow 6)- β -D-glucopyranoside].

Compound **4**, a light brown amorphous powder, gave a quasi-molecular ion peak $[\text{M}+\text{H}]^+$ at m/z 505 in the positive FAB-MS spectrum. The ^1H - and ^{13}C -NMR spectra of **4** were similar to those of **1**, except for signals due to a methylated galloyl moiety instead of the arabinose signals. It showed a

Fig. 1. HMBC Correlation of **1** and **7**

methoxy proton at δ 3.82 and an aromatic proton at δ 7.05 in the ^1H -NMR spectrum (Table 1). The methylated galloyl moiety was deduced from the chemical shift of the methoxy carbon at δ 60.8, two chemically equivalent aromatic carbons at δ 110.4 (C-2'', 6'') and 151.8 (C-3'', 5''), two substituted aromatic carbons, and one carbonyl carbon at δ 167.7 in the ^{13}C -NMR spectrum (Table 2). The chemical shift values and coupling constants of the glucosynaphthalene moiety were essentially identical to those of **1**. The glycone part was identified as glucose on TLC after acid hydrolysis. The position linked with the galloyl group was determined by HMBC, which showed correlations between signals at δ_{H} 4.42 (H-6') and δ_{C} 167.7 (C-7''), as well as between signals at 7.05 (H-2'', 6'') and δ_{C} 167.7 (C-7''). The position of a methoxy group on the galloyl moiety was assigned at C-4'' by observation of an equivalent signal in the ^1H -NMR spectra (δ 7.05; H-2'', 6'') and the ^{13}C -NMR (δ 110.4; C-2'', 6'' and 151.8; C-3'', 5''). Furthermore, it was confirmed by the presence of correlations of ^1H -signals at δ_{H} 7.05 (H-2'', 6'') and 3.82 (OCH₃) with a ^{13}C -signal at δ_{C} 141.4 (C-4'') in the HMBC spectrum. The configuration of the glucosidic linkage was assigned as β on the basis of the coupling constant, which was similar to that in **1**. The structure of **4** was thus determined to be 1,4,8-trihydroxynaphthalene 1-O- β -D-[6'-O-(3'',5''-dihydroxy-4''-methoxybenzoyl)]glucopyranoside.

Compound **7**, a light yellow amorphous powder, showed a quasi-molecular ion peak $[\text{M}+\text{Na}]^+$ at m/z 545 in the positive FAB-MS spectrum. The ^1H - and ^{13}C -NMR spectra of **7** were similar to those of **4**. However, it had signals assignable to two methylenes at δ 2.16 (2H), 2.48 (1H) and 3.01 (1H), and an oxymethylene at δ 5.32 (t, $J=3.3$ Hz) in the ^1H -NMR spectrum (Table 3), and signals for a carbonyl carbon at δ 206.4, two methylene carbons at δ 30.2 and 33.5, and a carbinol carbon at δ 61.3 in the ^{13}C -NMR spectrum (Table 2), indicating an oxygenated α -tetralone moiety in **7**. The presence of this aglycone was further confirmed by the positive FAB-MS spectrum, which showed a prominent fragment ion peak at m/z 329 $[\text{M}-\text{tetralone moiety}]^+$.²⁰⁾ The sugar linkages and the methylated galloyl group were determined

Table 3. ^1H -NMR Spectral Data of Compounds **6**–**8** in CD_3OD

Position	6 ^{a)}	7 ^{b)}	8 ^{b)}
1			
2 β	2.44 dt (17.7, 3.4)	2.48 dt (17.7, 3.4)	2.48 dd (17.6, 3.4)
2 α	3.00 ddd (17.7, 12.6, 5.6)	3.01 ddd (17.7, 11.8, 6.8)	3.01 ddd (17.6, 11.9, 6.5)
3	2.13 m	2.16 m	2.16 m
4	5.30 t (3.2)	5.32 t (3.3)	5.32 t (3.2)
5			
6	7.36 d (9.1)	7.40 d (9.2)	7.41 d (9.2)
7	6.60 d (9.1)	6.74 d (9.2)	6.75 d (9.2)
8			
9			
10			
1'	4.81 d (7.5)	4.78 d (7.7)	4.78 d (7.7)
2'	3.54 m	3.54 m	3.55 t (8.2)
3'	3.50 m	3.48 m	3.49 m
4'	3.43 m	3.44 m	3.45 m
5'	3.70 ddd (9.5, 7.3, 2.2)	3.67 ddd (9.3, 7.2, 2.2)	3.67 td (7.8, 1.9)
6'	4.47 dd (11.8, 7.3)	4.45 dd (11.8, 7.0)	4.44 dd (11.8, 6.8)
	4.63 dd (11.8, 2.1)	4.56 dd (11.8, 2.2)	4.55 dd (11.8, 2.1)
1''			
2''	7.25 s	7.02 s	7.06 s
3''			
4''			
5''			
6''	7.25 s	7.02 s	7.06 s
7''			
3'',5''-OCH ₃	3.83 s		
4''-OCH ₃		3.87 s	

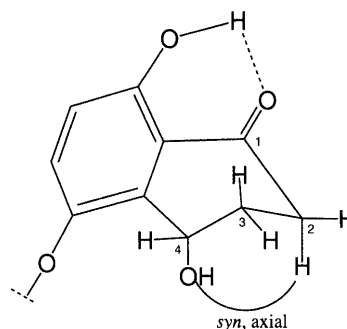
a) 500 MHz. b) 400 MHz. δ values in ppm and coupling constants (in parentheses) in Hz.

by HMBC correlations observed between signals at δ_{H} 4.78 (Glc-H-1') and δ_{C} 148.5 (C-5), and at δ_{H} 4.45 (H-6') and δ_{C} 167.7 (C-7'') (Fig. 1). The anomeric configuration of the sugar was determined to be β ($J_{1',2'}=7.7$ Hz).

To determine the absolute configuration of the chiral center at C-4 in **6**–**8**, these compounds were hydrolyzed with naingenase to give the same product 4,5,8-trihydroxy- α -tetralone (**6a**, $[\alpha]_{\text{D}} +13^\circ$ in EtOH), which afforded a tribenzoate (**6b**, $[\alpha]_{\text{D}} -17^\circ$ in EtOH) on benzylation. The circular dichroic (CD) spectrum of **6a** exhibited a negative Cotton effect at 265 nm ($\Delta\epsilon=-16.8$), indicating *S*-configuration at C-4 in comparison with the reported data of natural tetralones, such as (4*R*)-shinanolone ($\Delta\epsilon=+3.0$ at 272 nm),³⁰⁾ (4*R*)-isoshinanolone ($\Delta\epsilon=+33.0$ at 240 nm)³¹⁾ and (4*S*)-regiolone ($\Delta\epsilon=-44.3$ at 238 nm).³²⁾

In compound **7**, a hydroxy group at C-4 was subsequently arranged at an α -oriented axial position on the basis of the ^1H -NMR spectrum, where the coupling constant of H-4 (t) was $J_{4\beta,3\alpha}=J_{4\beta,3\beta}=3.3$ Hz. This was further supported by the conformation of the cyclohexanone ring possessing a half-chair form (Fig. 2), which was deduced from the multiplicities of H α -2 (axial) at δ 3.01 (ddd, $J_{2\alpha,2\beta}=17.7$ Hz, $J_{2\alpha,3\beta}=11.8$ Hz, $J_{2\alpha,3\alpha}=6.8$ Hz) and H β -2 (equatorial) at δ 2.48 (dt, $J_{2\beta,2\alpha}=17.7$ Hz, $J_{2\beta,3\alpha}=J_{2\beta,3\beta}=3.4$ Hz). The appreciable difference in chemical shifts of the above protons might be caused by environmental differences around the protons: *i.e.*, H α -2 experiences the deshielding effects of the C=O and axial C₄-OH, whereas H β -2 only feels the effect of C=O. Thus, H α -2 was more deshielded compared to H β -2.³²⁾ The structure of **7** was consequently determined as 4 α ,5,8-trihydroxy- α -tetralone 5-*O*- β -D-[6'-*O*-(3'',5''-dihydroxy-4''-methoxybenzoyl)] glucopyranoside.

Compound **8**, a light yellow amorphous powder, showed a

Fig. 2. Partial Structure of **7**

quasi-molecular ion peak $[\text{M}+\text{Na}]^+$ at m/z 531 in the positive FAB-MS spectrum. Inspection of the NMR data (Tables 2 and 3) of **8** suggested a similar structure with **7**, except the absence of a methyl group in the galloyl moiety. This was supported by the difference of 14 mass units between quasi-molecular ion peaks of **7** and **8** in the positive FAB-MS, as well as the presence of a [galloyl group] $^+$ ion peak at m/z 153 in **8**. The connectivities of the sugar and galloyl groups were established by the HMBC experiment, where glucose and the galloyl group were linked at C-5 and C-6', respectively. The anomeric configuration was determined to be β ($J_{1',2'}=7.7$ Hz). The configuration of the hydroxy group at C-4 was the same as that of **7**. From these findings, the structure of **8** was established as 4 α ,5,8-trihydroxy- α -tetralone 5-*O*- β -D-[6'-*O*-(3'',4'',5''-trihydroxybenzoyl)] glucopyranoside.

Inhibitory Effects of Compounds on RT and RNase H Activities In an effort to develop anti-AIDS agents, we have so far isolated several inhibitory substances against enzymes essential for proliferation of HIV, from medicinal plants, *i.e.*, putranjivan A from *Phyllanthus emblica*,³³⁾ corilagin and 1,3,4,6-tetragalloylglucose from *Chamaesyce hysopifolia*,³⁴⁾ and magnesium lithospermate, calcium and magnesium rosmarinat from *Cordia spinescens*,³⁵⁾ on RT (RNA-dependent DNA polymerase). However, they were not sufficiently potent for further development as anti-HIV drugs. In the course of screening for novel natural products with anti-HIV-1 RT and RNase H activities, we found that the methanol extract of *J. mandshurica* (stem-bark) appreciably inhibited both enzyme activities. The extract was further fractionated with various solvents into hexane-, ethyl acetate- and butanol-soluble fractions. Of these, the ethyl acetate-soluble fraction inhibited the HIV-RT and RNase H activities most potently with IC_{50} values of 0.047 and 22 $\mu\text{g}/\text{ml}$. From the ethyl acetate-soluble fraction, 14 compounds (**1**–**14**) were isolated as mentioned above and their inhibitory potencies were examined against both enzyme activities.

Substances that inhibit *in vitro* HIV RT are likely to fall into one of three categories; i) substances potently blocking both RT and RNase H activities; ii) those inhibiting preferably the RT activity; and iii) those selectively inhibiting the RNase H activity without any significant effect on the RT function.³⁶⁾ Of the compounds isolated in this experiment, **8**, **13** and **14** belonged to the second category; they showed potent inhibition against HIV-1 RT activity with IC_{50} values of 5.8, 0.067, and 0.040 μM , respectively, but showed moderate inhibition against RNase H activity with IC_{50} values of 330, 310 and 39 μM (Fig. 3, Table 4). The inhibitory potencies of **13** and **14** against HIV-1 RT were stronger than those of cori-

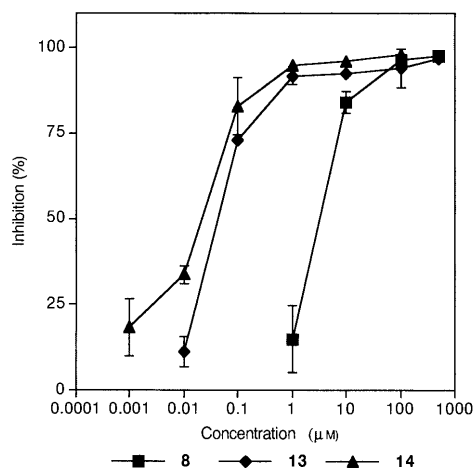


Fig. 3. Effect of **8**, **13** and **14** on RT Activity (Mean \pm S.D., $n=3$)

Table 4. Effects of Compounds Isolated from *J. mandshurica* on RT and RNase H Activities of HIV-1 RT

Compound	IC ₅₀ (μM)	
	RT	RNase H
1	>500	490
2	290	156
3	323	460
4	>500	>500
5	>500	>500
6	>500	>500
7	330	>500
8	5.8	330
9	>500	>500
10	>500	>500
11	>500	>500
12	>500	>500
13	0.067	310
14	0.040	39
Adriamycin ^{a)}	45	
Illimaquinone ^{b)}		50

a) Inhibitor of HIV-1 RT. b) Inhibitor of RNase H.

lugin and 1,3,4,6-tetragalloylglucose, which lack a galloyl group at C-2 and showed IC₅₀ values of 20 and 86 μM, respectively, in our previous experiment,³⁴⁾ a galloyl group attached at C-2 of glucopyranose seems to enhance significantly the inhibitory potency of galloylglucoses against HIV-1 RT. Compound **14** was comparable in inhibitory potency to illimaquinone with an IC₅₀ of 50 μM and used as a positive control (Fig. 4, Table 4). Of the characteristic ingredients such as naphthalenyl and α-tetralonyl glycosides present in this plant, **2**, **3** and **8** showed moderate inhibition against both enzyme activities, and the inhibitory potency of **2** against RNase H activity (IC₅₀=156 μM) was stronger than that against RT activity (IC₅₀=290 μM). The inhibitory potencies of **6**, **7** and **8** against RT activity increased in this order, as represented by IC₅₀ values of >500, 330 and 5.8 μM, being proportional to the number of free hydroxyls on the galloyl residue in the molecule. It has been reported that naphthalene derivatives such as naphthalenesulfonic acid³⁷⁾ and *N*-(4-*tert*-butylbenzoyl)-2-hydroxy-1-naphthaldehyde hydrazone (BBNH),³⁸⁾ have anti-HIV-1 RT activity. Flavonoids, **9**–**12**, were inactive against HIV-1 RT and RNase H activities.

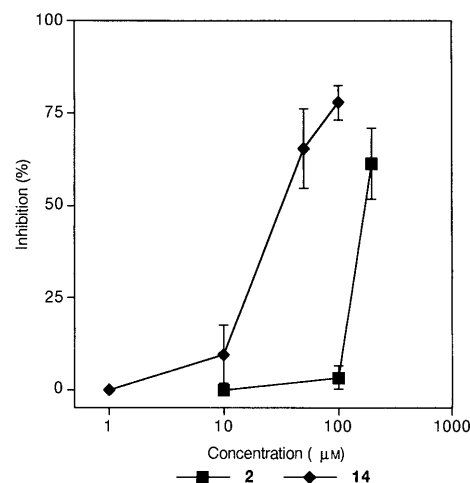


Fig. 4. Effect of **2** and **14** on RNase H Activity (Mean \pm S.D., $n=3$)

Experimental

Optical rotations were measured with a DIP-360 automatic polarimeter (JASCO Co., Tokyo, Japan). UV spectra were measured with a UV-2200 UV-VIS recording spectrophotometer (Shimadzu Co., Kyoto, Japan). CD spectra were recorded in EtOH on a JASCO J-715 CD dispersion spectrometer (JASCO Co.). IR spectra were measured with an FT/IR-230 infrared spectrometer (JASCO Co.). ¹H- and ¹³C-NMR spectra were measured with UNITY 500 (¹H, 500 MHz; ¹³C, 125 MHz; Varian Co., Palo Alto, U.S.A.) or JEOL JNA-LAA 400 WB-FT (¹H, 400 MHz; ¹³C, 100 MHz; JEOL Co., Tokyo, Japan) spectrophotometers. The chemical shifts are presented as ppm with tetramethylsilane as an internal standard. FAB-MS was measured with a JEOL JMX-AX 300L spectrometer (JEOL Co.) using glycerol as a matrix. Column chromatography was carried out on silica gel (Kieselgel 60, 70–230 mesh, Merck Co., Darmstadt, Germany), Sephadex LH-20 (Pharmacia, Upsala, Sweden), Amberlite MB-3 (Rohm and Haas Co., Philadelphia U.S.A.), and ODS (Chromatorex, 100–200 mesh, Fuji Silysia Chemical Ltd., Aichi, Japan). MPLC was carried out on LiChroprep RP-18 (size A, Merck Co.). TLC was carried out on pre-coated silica gel 60 F₂₅₄ plates (0.25 mm, Merck Co.), and spots were detected under UV light and by 10% H₂SO₄ followed by heating.

Plant Materials The stem-bark of *J. mandshurica* was collected during September 1998 at a mountain area of Kimchun, Kyungbook, Korea, and dried at room temperature for 3 weeks. A voucher specimen is deposited at the herbarium of the College of Pharmacy, Chungnam National University, Taejeon, Korea.

Isolation Procedure The stem-bark of *J. mandshurica* (3.0 kg) was extracted with MeOH (6000 ml \times 3) at room temperature for 24 h to give an extract (390 g). A part of the MeOH extract (300 g) was suspended in H₂O (2500 ml) and extracted with hexane (2500 ml \times 3) to give a hexane-soluble fraction (48 g). The resulting H₂O layer was extracted with CH₂Cl₂ (3000 ml \times 3), EtOAc (3000 ml \times 3) and BuOH (3000 ml \times 3), successively. The EtOAc-soluble fraction (90 g) was chromatographed on a column of silica gel (1 kg). The column was eluted using a stepwise gradient of CHCl₃, MeOH and H₂O to give 6 fractions (Fr. A–F; 2.7, 15.9, 23.9, 7.5, 5.4 and 10.2 g, respectively). Repeated column chromatography of Fr. B on silica gel (CHCl₃–MeOH, 9:1), Sephadex LH-20 (CHCl₃–MeOH, 1:9) and reversed phase ODS (50% aq. MeOH), followed by MPLC on RP-18 (50% aq. MeOH and 70% aq. CH₃CN) afforded **3** (60 mg), **4** (15 mg), **6** (335 mg), **7** (3.3 mg), **9** (165 mg) and **10** (189 mg). Repeated column chromatography of Fr. C on Sephadex LH-20 (MeOH and CHCl₃–MeOH, 1:9), silica gel (CHCl₃–MeOH, 8:2) and reversed phase ODS (40% aq. MeOH), followed by MPLC on RP-18 (40% aq. MeOH and 80% aq. CH₃CN) furnished **1** (18 mg), **2** (5 mg), **5** (164 mg), **8** (11 mg), **11** (168 mg), **12** (345 mg), **13** (340 mg) and **14** (294 mg).

1,4,8-Trihydroxynaphthalene 1-O-[α-L-Arabinofuranosyl-(1→6)-β-D-glucopyranoside] (1) Light brown amorphous powder, [α]_D²⁰ –94° (*c*=0.1, MeOH). IR ν_{max} cm^{–1}: 3400, 1610, 1520, 1405, 1375, 1255, 1165. UV λ_{max} nm (log ε): 224 (4.6), 306 (3.8), 326 (3.7), 342 (3.7). Positive FAB-MS *m/z*: 493 [M+Na]⁺, 471 [M+H]⁺. ¹H- and ¹³C-NMR data: see Tables 1 and 2.

1,4,8-Trihydroxynaphthalene 1-O-β-D-Glucopyranoside (2) Brown amorphous powder, [α]_D²⁰ –85° (*c*=0.1, MeOH). IR ν_{max} cm^{–1}: 3400, 1615, 1520, 1405, 1375, 1260, 1070. UV λ_{max} nm (log ε): 224 (4.6), 306 (4.2), 326

(4.1), 342 (4.1).

1,4,8-Trihydroxynaphthalene 1-O- β -D-[6'-O-(4"-Hydroxy-3",5"-dimethoxybenzoyl)]glucopyranoside (3)¹⁹ Light brown amorphous powder, $[\alpha]_D -49^\circ$ ($c=0.1$, MeOH). IR ν_{\max} cm^{-1} : 3400, 1680, 1610, 1520, 1460, 1420, 1340, 1215, 1120. UV λ_{\max} nm (log ϵ): 224 (4.8), 288 (4.1), 326 (4.1), 342 (3.8).

1,4,8-Trihydroxynaphthalene 1-O- β -D-[6'-O-(3",5"-Dihydroxy-4"-methoxybenzoyl)]glucopyranoside (4) Light brown amorphous powder, $[\alpha]_D -49^\circ$ ($c=0.1$, MeOH). IR ν_{\max} cm^{-1} : 3400, 1700, 1610, 1520, 1360, 1240, 1160. UV λ_{\max} nm (log ϵ): 224 (4.7), 265 (3.9), 305 (3.9), 326 (3.8), 342 (3.8). Positive FAB-MS m/z : 527 $[M+Na]^+$, 505 $[M+H]^+$. ¹H- and ¹³C-NMR data: see Tables 1 and 2.

1,4,8-Trihydroxynaphthalene 1-O- β -D-[6'-O-(3",4",5"-Trihydroxybenzoyl)]glucopyranoside (5)¹⁹ Brown needles (MeOH-H₂O), $[\alpha]_D -53^\circ$ ($c=0.1$, MeOH). IR ν_{\max} cm^{-1} : 3400, 1690, 1610, 1520, 1445, 1350, 1070, 1030. UV λ_{\max} nm (log ϵ): 224 (4.8), 282 (4.1), 326 (3.9), 342 (3.9).

4 α ,5,8-Trihydroxy- α -tetralone 5-O- β -D-[6'-O-(4"-Hydroxy-3",5"-dimethoxybenzoyl)]glucopyranoside (6)²⁰ Light yellow amorphous powder, $[\alpha]_D -53^\circ$ ($c=0.1$, MeOH). IR ν_{\max} cm^{-1} : 3400, 1705, 1645, 1610, 1515, 1465, 1410, 1335, 1225, 1115, 1070. UV λ_{\max} nm (log ϵ): 216 (4.5), 262 (4.1), 348 (3.5).

4 α ,5,8-Trihydroxy- α -tetralone 5-O- β -D-[6'-O-(3",5"-Dihydroxy-4"-methoxybenzoyl)]glucopyranoside (7) Light yellow amorphous powder, $[\alpha]_D -18^\circ$ ($c=0.1$, MeOH). IR ν_{\max} cm^{-1} : 3400, 1700, 1640, 1600, 1470, 1440, 1360, 1250, 1160. UV λ_{\max} nm (log ϵ): 214 (4.5), 260 (4.1), 348 (3.3). Positive FAB-MS m/z : 545 $[M+Na]^+$, 523 $[M+H]^+$. ¹H- and ¹³C-NMR data: see Tables 3 and 2.

4 α ,5,8-Trihydroxy- α -tetralone 5-O- β -D-[6'-O-(3",4",5"-Trihydroxybenzoyl)]glucopyranoside (8) Light yellow amorphous powder, $[\alpha]_D -34^\circ$ ($c=0.1$, MeOH). IR ν_{\max} cm^{-1} : 3400, 1700, 1640, 1610, 1470, 1350, 1340, 1230, 1070. UV λ_{\max} nm (log ϵ): 216 (4.6), 262 (4.1), 350 (3.5). Positive FAB-MS m/z : 531 $[M+Na]^+$, 509 $[M+H]^+$. ¹H- and ¹³C-NMR data: see Tables 3 and 2.

Taxifolin (5,7,3',4'-Tetrahydroxyflavanol, 9)²² White amorphous powder, $[\alpha]_D +20^\circ$ ($c=0.1$, MeOH). IR ν_{\max} cm^{-1} : 3420, 1620, 1520, 1470, 1360, 1265, 1165. UV λ_{\max} nm (log ϵ): 288 (4.2), 328 (sh).

Afzelin (Kaempferol 3-O- α -L-Rhamnopyranoside, 10)²³ Yellow amorphous powder, $[\alpha]_D -184^\circ$ ($c=0.1$, MeOH). IR ν_{\max} cm^{-1} : 3280, 1655, 1615, 1500, 1450, 1365, 1070, 1060. UV λ_{\max} nm (log ϵ): 264 (4.3), 342 (4.1).

Quercitrin (Quercetin 3-O- α -L-Rhamnopyranoside, 11)²⁴ Yellow amorphous powder, $[\alpha]_D -178^\circ$ ($c=0.1$, MeOH). IR ν_{\max} cm^{-1} : 3320, 1660, 1610, 1500, 1450, 1360, 1300, 1200. UV λ_{\max} nm (log ϵ): 254 (4.2), 314 (sh), 350 (4.1).

Myricitrin (Myricetin 3-O- α -L-Rhamnopyranoside, 12)²⁴ Yellow amorphous powder, $[\alpha]_D -141^\circ$ ($c=0.1$, MeOH). IR ν_{\max} cm^{-1} : 3270, 1655, 1610, 1500, 1455, 1340, 1290. UV λ_{\max} nm (log ϵ): 254 (4.2), 312 (sh), 354 (4.1).

1,2,6-Trigalloylglucopyranose (13)²⁵ White amorphous powder, $[\alpha]_D -94^\circ$ ($c=0.1$, MeOH). IR ν_{\max} cm^{-1} : 3420, 1710, 1610, 1540, 1525, 1450, 1355, 1310, 1240, 1210. UV λ_{\max} nm (log ϵ): 216 (4.6), 278 (4.4).

1,2,3,6-Tetragalloylglucopyranose (14)²⁶ White amorphous powder, $[\alpha]_D +39^\circ$ ($c=0.1$, MeOH). 3400, 1700, 1610, 1540, 1455, 1355, 1200. UV λ_{\max} nm (log ϵ): 216 (4.9), 278 (4.5).

Determination of Sugars in 1, 4, 7 and 8 Each sample (2 mg) was refluxed with 4 N HCl-dioxane (1 : 1, 2 ml) for 2 h. The mixture was extracted with EtOAc (5 ml \times 3). The residual water layer was neutralized with Amberlite MB-3 and dried to give a residue. The residue was dissolved in pyridine (1 ml), to which 0.1 M L-cysteine methyl ester hydrochloride in pyridine (2 ml) was added. The mixture was kept at 60 °C for 1.5 h. After the reaction mixture was dried *in vacuo*, the residue was trimethylsilylated with hexamethyldisilazane-trimethylchlorosilane (0.1 ml) at 60 °C for 1 h. The mixture was partitioned between hexane and H₂O (0.3 ml each) and the hexane extract was analyzed by gas-liquid chromatography (GLC). In the acid hydrolysate of 1, D-glucose and L-arabinose were confirmed by comparison of the retention times of their derivatives with those of D-glucose, L-glucose, D-arabinose and L-arabinose derivatives prepared in a similar way, which showed retention times of 21.34, 22.00, 17.37 and 16.34 min, respectively.

The sugars from acid hydrolysis of 4, 7 and 8 were identified by TLC on silica gel with a solvent system of EtOAc-MeOH-H₂O-AcOH (65 : 20 : 15 : 15). The spots on the plate were visualized by spraying an anisaldehyde-H₂SO₄ solution.

Enzymatic Hydrolysis of 6–8 Naringinase (50 mg, Sigma Co.) was added to a suspension of 6, 7 or 8 (5–10 mg) in 50 mM acetate buffer (pH

5.5) and the mixture was stirred at 37 °C for 5 h. The reaction mixture was extracted with EtOAc (10 ml \times 3) and evaporated to dryness. The residue was chromatographed on silica gel eluting with hexane-acetone (2 : 1) to give 4,5,8-trihydroxy- α -tetralone (6a) in 50–60% yields. Compound 6a, yellow amorphous powder, $[\alpha]_D^{26} +13^\circ$ ($c=0.1$, EtOH). UV λ_{\max} nm (log ϵ): 235 (4.0), 265 (3.7), 372 (3.5). CD ($c=1.55\times 10^{-2}$) $\Delta\epsilon$ (nm): -16.79 (265), -5.79 (319). ¹H-NMR (CDCl₃+CD₃OD) δ : 2.60 (ddd, $J=17.3$, 10.3, 4.7 Hz, H β -2), 2.90 (ddd, $J=17.3$, 7.1, 4.5 Hz, H α -2), 2.33 (m, H β -3), 2.20 (m, H α -3), 5.21 (dd, $J=8.1$, 4.5 Hz, H-4), 7.07 (d, $J=9.3$ Hz, H-6), 6.81 (d, $J=9.3$ Hz, H-7). ¹³C-NMR (CDCl₃+CD₃OD) δ : 204.4 (C-1), 35.2 (C-2), 30.8 (C-3), 65.5 (C-4), 147.4 (C-5), 126.3 (C-6), 118.0 (C-7), 156.0 (C-8), 115.2 (C-9), 128.0 (C-10).

Benzoylation of 6a Benzoyl chloride (100 mg) was added to a solution of 6a (2.5 mg) in pyridine (0.1 ml) and the reaction mixture was kept overnight at room temperature. The mixture was evaporated to give a residue, which was purified by preparative thin layer chromatography on silica gel with hexane-acetone (3 : 1) to give 4,5,8-tribenzoyloxy- α -tetralone (2.6 mg, 6b); white amorphous powder, $[\alpha]_D^{26} -17^\circ$ ($c=0.1$, EtOH). UV λ_{\max} nm (log ϵ): 235 (4.0). CD ($c=0.59\times 10^{-2}$) $\Delta\epsilon$ (nm): -2.35 (254), -3.24 (280). ¹H-NMR (CDCl₃) δ : 2.61 (dt, $J=16.8$, 3.6 Hz, H β -2), 2.98 (ddd, $J=16.8$, 13.1, 5.6 Hz, H α -2), 2.48 (2H, m), 6.61 (t, $J=3.3$ Hz, H-4), 7.37 (5H, m), 7.57 (5H, m), 7.66 (1H, m), 7.86 (2H, m), 7.99 (2H, m), 8.26 (2H, m). ¹³C-NMR (CDCl₃) δ : 195.5 (C-1), 34.5 (C-2), 27.1 (C-3), 64.5 (C-4), 146.9 (C-5), 164.9, 165.7, 169.2 (3 \times benzoyl group C=O).

RNase H Activity Assay For the assay of HIV-1 RT-associated RNase H,⁴ HIV-1 RT was adjusted to 2.5 U/ μ l with a solution of 50 mM Tris-HCl (pH 8.0), 50 mM KCl, 8 mM MgCl₂ and 2.5 mM dithiothreitol (DTT). A mixture (20 μ l) containing of 50 mM Tris-HCl (pH 8.0), 50 mM KCl, 8 mM MgCl₂, 2.5 mM DTT, 7.2 nM of [³H]poly(rA)·poly(dT) (370 kBq/ml), and a test sample in dimethyl sulfoxide (DMSO; final concentration of 5%) was preincubated at 37 °C for 5 min. The reaction mixture was kept for 2 h at 37 °C. A blank reaction was carried out under the same conditions without adding enzyme, and a control reaction was done in the absence of a test sample. The reaction was terminated by addition of 20 μ l of 0.02 M EDTA. The mixture was applied onto a Whatman DE81 paper disc, which was washed batchwise with 3 ml of 5% Na₂HPO₄, distilled water three times, ethanol once and ether once. The paper disc was then dried and immersed in 3 ml of scintillation fluid. The RNase H activity was measured as the inhibition of the degradation of RNA in a hybrid in the presence of a test sample as follows:

$$\text{inhibition (\%)} = [1 - (\text{dpm}_{\text{blank}} - \text{dpm}_{\text{sample}}) / (\text{dpm}_{\text{blank}} - \text{dpm}_{\text{control}})] \times 100$$

Illimaquinone was used as a positive control and inhibited RNase H activity with an IC₅₀ of 50 μ M under the above conditions.

DNA-RNA Hybrid Preparation 0.57 nM poly(dT) was annealed to 0.32 nM poly(rA) and 5 pM [³H]poly(rA) in 50 μ l of H₂O. The mixture was heated to 90 °C for 5 min, allowed to cool gradually to 37 °C, incubated for 30 min, kept at room temperature for 30 min and finally stored at -20 °C.³⁹

RT Activity Assay For the assay of RT,^{40,41} HIV-1 RT was adjusted to 0.01 U/ μ l with a solution of 0.2 M phosphate buffer (pH 7.2), 50% glycerol, 2 mM DTT and 0.02% of Triton X-100. The reaction mixture (20 μ l) containing 50 mM Tris-HCl (pH 8.3), 30 mM NaCl, 10 mM MgCl₂, 5 mM DTT, 1.25 μ g/ml (ca. 16 nM) poly(rA)·oligo(dT)_{12–18} as a template-primer, 250 nM dTTP, 100 nM [³methyl-³H]dTTP (18.5 MBq/ml) and 0.01 U/ μ l of RT, and 1.0 μ l of a test sample dissolved in DMSO (final concentration of 5%) was incubated at 37 °C for 1 h. A control reaction was done under the same conditions without adding a test sample. The reaction was terminated by addition of 20 μ l of 0.02 M EDTA. The resulting mixture was applied onto Whatman DE81 paper disc and washed in a similar manner as described above. The paper disc was then dried and immersed in 3 ml of scintillation fluid. The amount of a polymer fraction was determined by counting the radioactivity on the paper disc according to the incorporation of ³H-labeled substrate into the DNA polymer. The calculation of the inhibitory potency for the test sample was done as follows:

$$\text{inhibition (\%)} = [1 - (\text{dpm}_{\text{comp.}} / \text{dpm}_{\text{control}})] \times 100$$

Adriamycin was employed as a positive control and inhibited the RT with an IC₅₀ of 46 μ M under the above conditions.

Acknowledgment Part of this study was financially supported by a Grant-in-Aid for Scientific Research from the Ministry of Education, Science, Sports and Culture of Japan.

References and Notes

- 1) Goff S. P., *J. Acquired Immune Defic. Syndr.*, **3**, 817—831 (1990).
- 2) Fauci A. S., *Science*, **239**, 617—622 (1988).
- 3) De Clercq E., *Med. Res. Rev.*, **13**, 229—258 (1993).
- 4) Loya S., Hizi A., *J. Biol. Chem.*, **268**, 9323—9328 (1993).
- 5) Starnes M. C., Cheng Y. C., *J. Biol. Chem.*, **264**, 7073—7077 (1989).
- 6) Tan C. K., Zhang J., Li Z. Y., Tarpley W. G., Downey K. M., So A. G., *Biochemistry*, **30**, 2651—2655 (1991).
- 7) Palaniappan C., Fay P. J., Bambara R. A., *J. Biol. Chem.*, **270**, 4861—4869 (1995).
- 8) Kashman Y., Gustafson K. R., Fuller R. W., Cardellina J. H., McMahon J. B., Currens M. J., Buckheit R. W., Hughes S. H., Cragg G. M., Boyd M. R., *J. Med. Chem.*, **35**, 2735—2743 (1992).
- 9) Tayer P. B., Culp J. S., Debouck C., Johnson R. K., Patil A. D., Woolf D. J., Brooks I., Hertzberg R. P., *J. Biol. Chem.*, **269**, 6325—6331 (1994).
- 10) Gopalakrishnan V., Benkovic S. J., *J. Biol. Chem.*, **269**, 4110—4115 (1994).
- 11) Carroll S. S., Olsen D. B., Bennett C. D., Gotlib L., Graham D. J., Condra J. H., Stern A. M., Shafer J. A., Kuo L. C., *J. Biol. Chem.*, **268**, 276—281 (1993).
- 12) Nakane H., Ono K., *Biochemistry*, **29**, 2841—2845 (1990).
- 13) Tan G. T., Kinghorn A. D., Hughes S. H., Pezzuto J. M., *J. Biol. Chem.*, **266**, 23529—23536 (1991).
- 14) Moelling K., Schulze T., Diringier H., *J. Virol.*, **63**, 5489—5491 (1989).
- 15) Loya S., Tal R., Kashman Y., Hizi A., *Antimicrob. Agents Chemother.*, **34**, 2009—2012 (1990).
- 16) Althaus I. W., Franks K. M., Langley K. B., Kézdy F. J., Peterson T., Buxser S. E., Decker D. E., Dolak L. A., Ulrich R. G., Reusser F., *Experientia*, **52**, 329—335 (1996).
- 17) Hafkemeyer P., Neftel K., Hobi R., Pfaltz A., Lutz H., Lüthi K., Focher F., Spadari S., Hübscher U., *Nucleic Acids Res.*, **19**, 4059—4065 (1991).
- 18) Son J. K., *Arch. Pharm. Res.*, **18**, 203—205 (1995).
- 19) Joe Y. K., Son J. K., Park S. H., Lee I. J., Moon D. C., *J. Nat. Prod.*, **59**, 159—160 (1996).
- 20) Kim S. H., Lee K. S., Son J. K., Je G. H., Lee J. S., Lee C. H., Cheong C. J., *J. Nat. Prod.*, **61**, 643—645 (1998).
- 21) Gupta S. R., Ravindranath B., Seshadri T. R., *Phytochemistry*, **11**, 2634—2636 (1972).
- 22) Agrawal P. K., Agrawal S. K., Rastogi R. P., Osterdahal B. G., *Planta Med.*, **43**, 82—85 (1981).
- 23) Matthes H. W. D., Luu B., Ourisson G., *Phytochemistry*, **19**, 2643—2650 (1980).
- 24) Markhan K. R., Ternai B., Stanley R., Geiger H., Mabry T. J., *Tetrahedron*, **34**, 1389—1397 (1978).
- 25) Nonaka G., Nishioka I., Nagasawa T., Oura H., *Chem. Pharm. Bull.*, **29**, 2862—2870 (1981).
- 26) Nishioka I., *Yakugaku Zasshi*, **103**, 125—142 (1983).
- 27) Agrawal P. K., Bansal M. C., “Carbon-13 NMR of Flavonoids,” ed. by Agrawal P. K., Elsevier, Amsterdam, 1989, p. 283.
- 28) Usui T., Tsushima S., Yamaoka N., Matsuda K., Tsuzimura K., Sugiyama H., Seto S., Fujieda K., Miyajima G., *Agric. Biol. Chem.*, **38**, 1409—1410 (1974).
- 29) Ma C., Nakamura N., Hattori M., *Chem. Pharm. Bull.*, **46**, 982—987 (1998).
- 30) Kuroyanagi M., Yoshihira K., Natori S., *Chem. Pharm. Bull.*, **19**, 2314—2317 (1971).
- 31) Tezuka M., Takahashi C., Kuroyanagi M., Satake M., Yoshihira K., Natori S., *Phytochemistry*, **12**, 175—183 (1973).
- 32) Talapatra S. K., Karmacharya B., De S. C., Talapatra B., *Phytochemistry*, **27**, 3929—3932 (1988).
- 33) El-Mekkawy S., Meselhy M. R., Kusumoto I. T., Kadoda S., Hattori M., Namba T., *Chem. Pharm. Bull.*, **43**, 641—648 (1995).
- 34) Lim Y. A., Ma C. M., Kusumoto I. T., Miyashiro H., Hattori M., Gupta M. P., Correa M., *Phytother. Res.*, **11**, 22—27 (1997).
- 35) Lim Y. A., Kojima S., Nakamura N., Miyashiro H., Fushimi H., Komatsu K., Hattori M., Shimotohno K., Gupta M. P., Correa M., *Phytother. Res.*, **11**, 490—495 (1997).
- 36) Loya S., Reshef V., Mizrahi E., Silberstein C., Rachamim Y., Carmeli S., Hizi A., *J. Nat. Prod.*, **61**, 891—895 (1998).
- 37) Mohan P., Loya S., Avidan O., Verma S., Dhindsa G. S., Wong M. F., Huang P. P., Yashiro M., Baba M., Hizi A., *J. Med. Chem.*, **37**, 2513—2519 (1994).
- 38) Borkow G., Fletcher R. S., Barnard J., Arion D., Motakis D., Dmitrienko G. I., Parniak M. A., *Biochemistry*, **36**, 3179—3185 (1997).
- 39) DeStefano J. J., Buiser R. G., Mallaber L. M., Bambara R. A., Fay P. J., *J. Biol. Chem.*, **266**, 24295—24301 (1991).
- 40) Grandgenett D. P., Gerard G. F., Green M., *Proc. Natl. Acad. Sci. U.S.A.*, **70**, 230—234 (1973).
- 41) Kakiuchi N., Hattori M., Namba T., Nishizawa M., Yamagishi T., Okuda T., *J. Nat. Prod.*, **48**, 614—621 (1985).

New Monoterpene Glycoside Esters and Phenolic Constituents of *Paeoniae Radix*, and Increase of Water Solubility of Proanthocyanidins in the Presence of Paeoniflorin

Takashi TANAKA, Maki KATAOKA, Nagisa TSUBOI, and Isao KOUNO*

School of Pharmaceutical Sciences, Nagasaki University, 1-14 Bunkyo-machi, Nagasaki 852-8521, Japan.

Received July 14, 1999; accepted October 15, 1999

Seven new monoterpene glycoside esters related to paeoniflorin were isolated from *Paeoniae Radix*, together with polymeric proanthocyanidins, polygalloylglucoses and 48 known compounds (a benzoylsucrose, seven aromatic acids, adenosine, nine monoterpene glycosides, eight flavan-3-ols, a catechin dimer formed by oxidation, seven proanthocyanidins, three galloylsucroses, five galloylglucoses, and six ellagitannins). The structures of the new compounds were determined by spectral investigation including two-dimensional NMR techniques. In addition, increased water solubility of polymeric proanthocyanidin in the presence of paeoniflorin was examined by *n*-octanol–water partition and ¹H-NMR spectral experiments.

Key words *Paeonia obovata*; monoterpene glycoside; tannin; *Paeoniae Radix*; proanthocyanidin; hydrophobic association

Paeoniae Radix (Shaoyao) is an important crude drug in Japanese and Chinese traditional medicine. Although the roots of *Paeoniae lactiflora* PALLAS and related species are usually used after removal of cortex, the root with cortex is also used medicinally for different purposes, for example improvement of blood flow. It was inferred from this that a difference in the constituents of these two crude drugs was responsible for the difference in the medicinal usage. Hence, we compared these two types of *Paeoniae Radix* by reversed phase HPLC and chemically investigated in detail the constituents of commercial *Paeoniae Radix* with cortex originating from *Paeoniae obovata* MAXIM. In addition, the change in water solubility of polymeric proanthocyanidin in the presence of paeoniflorin, the major monoterpene glycoside of the crude drug, was also examined.

Results and Discussion

Figure 1 shows reversed phase HPLC chromatograms (Fig. 1) of hot water extracts of two typical commercial *Paeoniae Radix* samples (A, commercial *Paeoniae Radix* without the cortex part originating from *P. lactiflora* cultivated in Japan; B, commercial *Paeoniae Radix* with the cortex part originating from *P. obovata* imported from China). A rise of baseline in chromatogram B (crude drug with cortex) suggested the presence of polymeric proanthocyanidins. This was also supported by thin-layer chromatography showing a reddish-orange coloration at the origin with the *p*-anisaldehyde–H₂SO₄ reagent. In addition, many peaks arising from minor constituents appeared in chromatogram B. It was not clear whether the difference between the two chromatograms arose from the difference in the plant species, or from the presence of the cortex part.

Commercial *Paeoniae Radix* with cortex (dried root of *P. obovata*) was extracted with a mixture of acetone and water, and the extract was partitioned successively with ethyl ether and ethyl acetate. The ethyl acetate extract and water layer were separately subjected to a combination of column chromatography on Sephadex LH-20, MCI gel CHP20P, Chromatorex ODS, TSK-gel Toyopearl HW40F, and silica gel to yield a total of 55 compounds, together with polygalloylglucoses¹⁾ and polymeric proanthocyanidins. Among these com-

pounds, eight (1–7) were found to be new compounds and one (8) was isolated for the first time from natural source. The remaining compounds were identified as seven aromatic carboxylic acids (gallic acid, benzoic acid, vanillic acid, syringic acid, *p*-hydroxybenzoic acid, 4,5-dihydroxy-3-methoxybenzoic acid, and an equilibrium mixture of *m*- and *p*-digallate²⁾), adenosine, nine monoterpene glycosides [paeoniflorin (9),³⁾ oxypaeoniflorin (10),³⁾ benzoylpaeoniflorin (11),³⁾ benzoyloxypaeoniflorin (12),⁴⁾ galloylpaeoniflorin (13),⁴⁾ galloyloxypaeoniflorin (14),⁴⁾ mudanpiosides E (15),⁵⁾ and F (17),^{5,6)} and desbenzoylpaeoniflorin (16)³⁾], 6-*O*- (18), 1'-*O*- (19), and 6'-*O*- (20) galloylsucroses,⁷⁾ (+)-catechin, catechin 5-*O*-, 7-*O*-, 3'-*O*-, and 4'-*O*-glucosides,⁸⁾ catechin 7-*O*-gallate,⁹⁾ catechin 3'(4')-*O*-gallate (an equilibrium mixture),¹⁰⁾ epicatechin 3-*O*-gallate,¹¹⁾ catechin dimer formed by oxidation (21),¹²⁾ seven proanthocyanidins [procyanidins B-3 (22),¹³⁾ B-1 (23),¹⁴⁾ B-1 3-*O*-gallate (24),¹⁴⁾ B-2 3'-*O*-gallate (25),¹¹⁾ and B-7 (26),¹⁵⁾ AC-trimer (27),¹⁵⁾ and arecatannin A-1 (28)¹⁵⁾], 1,2,3-tri-,¹⁶⁾ 1,2,6-tri-,¹³⁾ 1,2,3,4-tetra-,¹³⁾ and 1,2,3,4,6-penta-*O*-galloyl-β-D-glucoses,²⁾ 2,3,4,6-tetra-*O*-galloyl-D-glucose,¹³⁾ and six ellagitannins [2,3-(*S*)-hexahydroxydiphenyl-D-glucose (29),¹⁷⁾ eugenin (30),¹⁸⁾

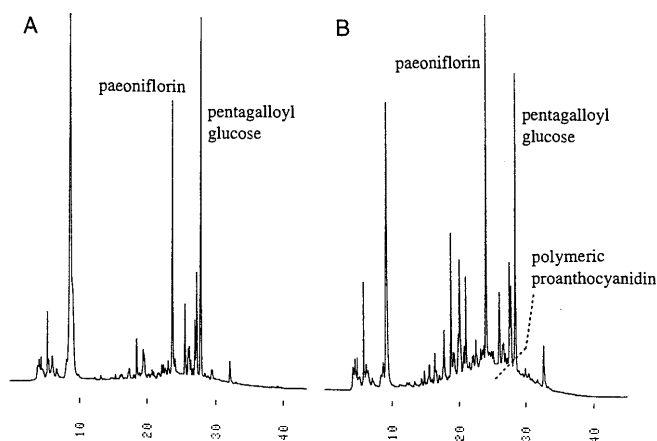
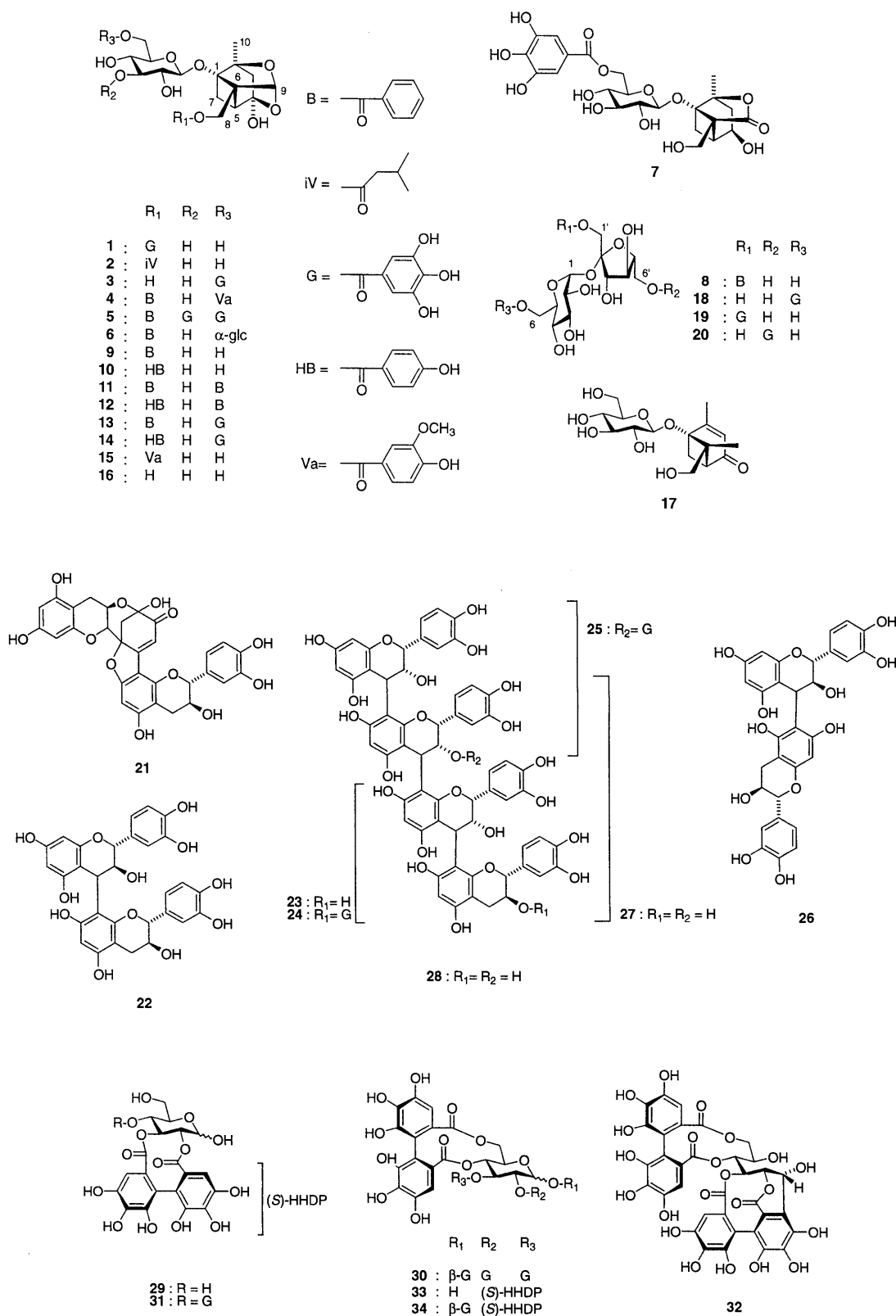


Fig. 1. HPLC Chromatograms of Hot-Water Extract of *Paeoniae Radix*

A, crude drug from the root of *P. lactiflora* without the cortex part; B, crude drug from the root of *P. obovata* with the cortex part. Conditions: Cosmosil 5C₁₈-AR, 5%→35% (30 min)→75% (20 min) CH₃CN in 50 mM H₃PO₄, 0.8 ml/min, 280 nm.

* To whom correspondence should be addressed.



pterocaryanin B (31),¹⁹⁾ casuarii (32),²⁰⁾ pedunculagin (33),¹⁷⁾ and 1(β)-O-galloylpedunculagin (34)¹⁷⁾. These known compounds were identified by comparison of physical and ¹H-NMR data with those of authentic samples or described in literature. The mixture of polymeric proanthocyanidins (Fig. 2) was characterized by the thiol degradation method²¹⁾ and ¹³C-NMR spectral analysis (see Experimental). The extension units were suggested to be (–)-epicate-

chin (65%, estimated by HPLC analysis of thiol degradation products), (±)-catechin (21%), and (–)-epicatechin 3-O-gallate (14%), and the terminal units were (+)-catechin (69%) and (–)-epicatechin 3-O-gallate (31%). Furthermore, the ratio of extension/terminal units was estimated to be about 7.6. The structural characteristics seemed to be an extension of those of procyanidin dimer–tetramers (22–28).

Compound 1 was obtained as a tan amorphous powder and

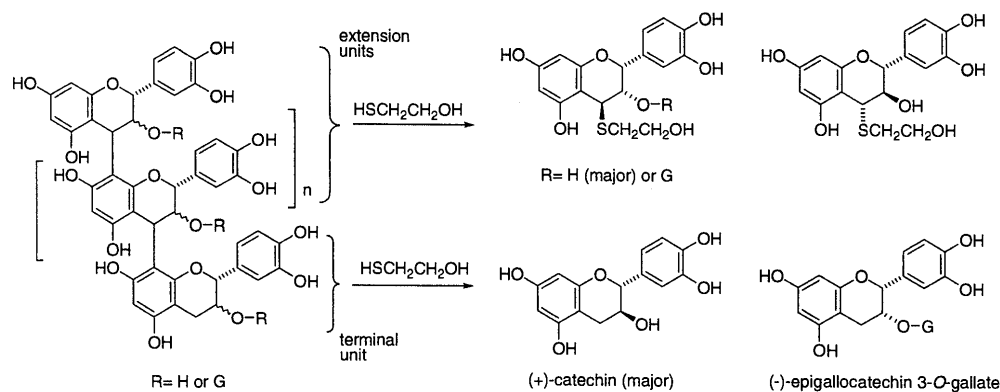


Fig. 2. Thiol Degradation of Polymeric Proanthocyanidin

Table 1. ^1H -NMR Spectral Data for Compounds 1–7 (in $\text{MeOH}-d_4$)

	1 ^{a)}	2 ^{a)}	3 ^{a)}	4 ^{b)}	5 ^{a)}	6 ^{b)}	7 ^{b)}
H-3	2.19 (d, 13) 1.80 (dd, 1, 13)	2.16 (d, 12) 1.78 (dd, 1, 12)	1.90 (d, 12) 1.65–1.69 (m)	1.88 (d, 13) 1.71 (d, 13)	1.94 (d, 13) 1.71 (d, 13)	2.32 (d, 13) 1.78 (dd, 1, 13)	1.92 (dd, 6, 15) 1.80 (d, 15)
H-4							3.97 (dd, 5, 6)
H-5	2.57 (dd, 1, 6)	2.46 (dd, 1, 7)	2.30–2.37 (m)	2.51 (d, 7)	2.55 (d, 6)	2.58 (dd, 1, 7)	2.54 (dd, 5, 8)
H-7	2.50 (dd, 6, 11) 1.95 (d, 11)	2.41 (dd, 7, 11) 1.90 (d, 11)	2.30–2.37 (m) 1.65–1.69 (m)	2.47 (dd, 7, 11) 1.77 (d, 11)	2.48 (dd, 6, 11) 1.79 (d, 11)	2.52 (dd, 7, 11) 2.02 (d, 11)	2.64 (dd, 8, 11) 1.62 (d, 11)
H-8	4.69 (d, 12) 4.61 (d, 12)	4.50 (d, 12) 4.47 (d, 12)	3.95 (d, 12) 3.87 (d, 12)	4.71 (2H, s) —	4.70 (2H, s) —	4.77 (d, 12) 4.73 (d, 12)	3.92 (2H, s) —
H-9	5.38 (s)	5.27 (s)	5.23 (s)	5.38 (s)	5.39 (s)	5.41 (s)	
H-10	1.36 (s)	1.33 (s)	1.22 (s)	1.26 (s)	1.28 (s)	1.35 (s)	1.34 (s)
Glc-1	4.53 (d, 7.5)	4.48 (d, 8)	4.55 (d, 8)	4.57 (d, 8)	4.69 (d, 8)	4.56 (d, 8)	4.59 (d, 8)
Glc-2	3.17–3.31	3.19 (dd, 8, 9)	3.22–3.32 (m)	3.26 (dd, 8, 9)	3.51 (dd, 8, 9)	3.22 (dd, 8, 9)	3.40 (dd, 4, 9)
Glc-3	3.17–3.31	3.24 (m)	3.22–3.32 (m)	3.38 (t, 9)	5.15 (t, 9)	3.32 (t, 9)	3.67 (t, 9)
Glc-4	3.17–3.31	3.24 (m)	3.22–3.32 (m)	3.32 (t, 9)	3.61 (t, 9)	3.25 (t, 9)	3.34 (t, 9)
Glc-5	3.17–3.31	3.35 (m)	3.22–3.32 (m)	3.58 (m)	3.68 (m)	3.49 (ddd, 2, 7, 9)	3.65 (ddd, 2, 5, 9)
Glc-6	3.86 (dd, 2, 12) 3.60 (dd, 5, 12)	3.85 (dd, 2, 12) 3.60 (dd, 6, 12)	4.50 (dd, 3, 12) 4.44 (dd, 6, 12)	4.59 (dd, 2, 12) 4.44 (dd, 8, 12)	4.48 (dd, 6, 13) 4.54 (dd, 3, 13)	3.82 (dd, 7, 11) 3.71 (dd, 2, 11)	3.78 (dd, 2, 12) 3.69 (dd, 5, 12)
Benzoyl-2, 6				8.02 (br d, 7)	8.03 (br, d, 8)	8.05 (br d, 8)	
Benzoyl-3, 5				7.47 (br t, 7)	7.48 (br, t, 8)	7.49 (br t, 8)	
Benzoyl-4				7.61 (br t, 7)	7.61 (br t, 8)	7.62 (br t, 8)	
Galloyl	7.08 (s)		7.07 (s)		7.09 (s)		7.08 (s)
Isovaleryl-2		2.25 (d, 7)		7.13 (s)			
Isovaleryl-3		2.09 (m)					
Isovaleryl-4, 5		0.97 (d, 7)					
Vanillyl-2				7.55 (d, 2)			
Vanillyl-5				6.84 (d, 8)			
Vanillyl-6				7.58 (dd, 2, 8)			
OMe				3.87 (s)			

δ in ppm from TMS. Coupling constants in Hz are given in parentheses. a) 300 MHz. b) 500 MHz.

showed a dark blue coloration with the FeCl_3 reagent. The ^1H -NMR spectrum (Table 1) was closely related to that of **9**, except for the appearance of an aromatic two-proton singlet at δ 7.08 instead of benzoyl signals. This observation indicated the presence of a galloyl group at C-8 of the monoterpene moiety and the ^{13}C -NMR spectrum also confirmed the presence of a galloyl group in place of the benzoyl group of **9**. This was further supported by the $[\text{M}+\text{Na}]^+$ peak at m/z 551 in the FAB-MS. Therefore, the structure of this compound was determined as shown in formula **1**, and named 8-*O*-galloyl desbenzoylpaeoniflorin.

The ^1H -NMR spectrum of compound **2** (Table 1) was also related to that of **1** and **9**, showing similar signals due to monoterpene and glucopyranosyl moieties. The distinctive features of the spectrum were the appearance of two methyls

(δ 0.97, 6H, d, $J=7$ Hz), methine (δ 2.09, 1H, m), and methylene (δ 2.25, 2H, d, $J=7$ Hz) signals, instead of the aromatic signals of **1** and **9**. These aliphatic signals indicated the presence of an isovaleryl group at the C-8 of monoterpene moiety. Furthermore, the ^{13}C -NMR spectrum [isovaleryl: δ 174.68 (C-1), 44.16 (C-2), 26.84 (C-3), and 22.76 (C-4, 5)] and FAB-MS (m/z 483, $[\text{M}+\text{Na}]^+$) of **2** verified the structure. This compound was named 8-*O*-isovaleryl desbenzoylpaeoniflorin.

Compound **3** showed a dark blue coloration with the FeCl_3 reagent, and the negative ion FAB-MS (m/z 527, $[\text{M}-\text{H}]^-$) indicated that the molecular weight of **3** was the same as that of **1**. ^1H -NMR spectral comparison of **3** and **1** (Table 1) indicated that these two were positional isomers differing in the location of the galloyl group (**3**: δ 7.07, 2H, s). In the spec-

trum of **3**, the glucose H-6 signals appeared at lower field (δ 4.44, dd, $J=6$, 12 Hz; 4.50, dd, $J=3$, 12 Hz) and the H-8 signals of the monoterpene moiety were shifted upfield (δ 3.87 and 3.95, each d, $J=12$ Hz) compared with those of **1**. From this spectral analysis, compound **3** was determined to be 6'-*O*-galloyl desbenzoylpaeoniflorin (**3**).

The ^1H -NMR spectrum of compound **4** (Table 1) was similar to that of **9** and showed signals due to benzoyl, glucosyl and monoterpene moieties. However, the glucose H-6 signals (δ 4.44, dd, $J=8$, 12 Hz; 4.59, dd, $J=2$, 12 Hz) were observed at lower field, and additional ABX-type aromatic proton signals (δ 7.55, d, $J=2$ Hz; 6.84, d, $J=8$ Hz; 7.58, dd, $J=2$, 8 Hz), along with a methoxyl signal (δ 3.87, 3H, s) appeared. The ^{13}C -NMR spectrum exhibited two carboxyl carbon signals at δ 168.08 and 167.69 together with two oxygen bearing aromatic carbon signals at δ 148.76 and 152.99, suggesting the presence of a vanillyl group. This was supported by the $[\text{M}+\text{Na}]^+$ peak at m/z 653 in the FAB-MS. The locations of the benzoyl and vanillyl groups were unequivocally confirmed by the heteronuclear multiple bond correlation (HMBC) spectrum, in which both glucose H-6 signals were correlated with the carboxyl signal at δ 167.7, which also correlated with an aromatic doublet at δ 7.55 (d, $J=2$ Hz), indicating that the vanillyl group was attached to the C-6 position of glucose. Thus, compound **4** was characterized as 6'-*O*-vanillylpaeoniflorin (**4**).

Compound **5** showed a dark blue coloration with the FeCl_3 reagent and a $[\text{M}-\text{H}]^-$ peak in the negative FAB-MS at m/z 783, which is 152 mass units larger than galloylpaeoniflorin. This difference coincided with the mass of a galloyl group. The ^1H -NMR spectrum (Table 1), which was closely related to that of **9**, indicated the presence of two galloyl groups (δ 7.09 and 7.13) in the molecule of **5**. On hydrolysis with tannase, **5** yielded **9** and gallic acid, confirming that **5** is a digalloyl ester of **9**. The locations of the galloyl groups were determined to be the C-3 and C-6 positions of the glucosyl moiety, since the proton signals at these positions resonated at lower field compared to those for **1** and **2** (Table 1). On the basis of these observations, compound **5** was established as 3',6'-di-*O*-galloylpaeoniflorin.

The ^1H -NMR spectrum of compound **6** (Table 1) also resembled that of paeoniflorin (**9**), except for the appearance of extra sugar proton signals. The $[\text{M}+\text{Na}]^+$ peak at m/z 665 in the FAB-MS revealed that this compound contains an additional hexose in the molecule, and this was also supported by ^{13}C -NMR spectral analysis. The coupling constants for the sugar proton signals (Table 1) suggested the presence of α - and β -glucopyranoses. In addition, a large low field shift for C-6 (δ 68.1) of the β -glucose in the ^{13}C -NMR spectrum indicated glycosidation at this position. The connection of the two sugars and the aglycone was confirmed by the HMBC experiment. The anomeric proton of α -glucose correlated with the C-6 of the β -glucose, and the anomeric proton of the β -glucose was coupled with the C-1 of the monoterpene moiety. Other HMBC correlations were consistent with the structure shown in formula **6**. Thus, this compound was characterized as 6'-*O*- α -glucopyranosylpaeoniflorin, and named isomaltopaeoniflorin (**6**).

Compound **7** showed a $[\text{M}-\text{H}]^-$ peak at m/z 527 in the FAB-MS, and indicated that this compound is an isomer of **1** and **3**. Appearance of a two-proton singlet signal at δ 7.08 in

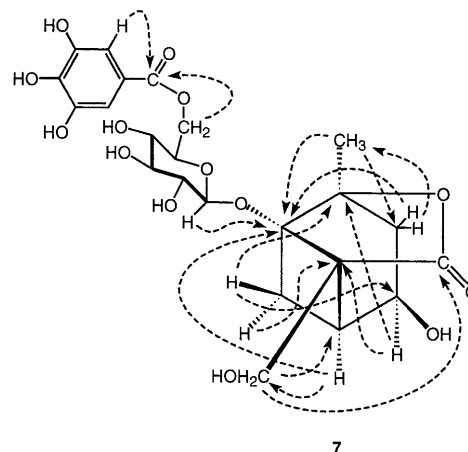


Fig. 3. Selected HMBC Correlations ($\text{H} \rightarrow \text{C}$, 3J) for Compound **7**

the ^1H -NMR spectrum, in addition to a dark blue coloration with the FeCl_3 reagent, indicated the presence of a galloyl group in the molecule. In the ^{13}C -NMR spectrum, the chemical shifts of ten carbon signals including one methyl group, three methylenes, two methines, three quaternary carbons, and a single carboxyl carbon, were similar to those of the aglycone part of albiflorin,²² except for the absence of benzoyl signals. In comparison with the spectrum of **3**, signals due to a carboxyl carbon (δ 178.7, C-9) and a secondary alcohol (δ 68.3, C-4) were observed in place of two acetal carbons (δ 106.34, C-4; 102.09, C-9) for **3**. These spectral observations strongly suggested that **7** is a galloyl ester of desbenzoylalbiflorin. The location of the galloyl group was determined to be at the glucose C-6 position because the glucose H-6 signals (δ 4.52, dd, $J=8$, 12 Hz; 4.47, dd, $J=3$, 12 Hz) appeared at lower field compared with those of **1** and **2**. Final confirmation of the structure was achieved by analysis of the HMBC spectrum, as shown in Fig. 3, and hence, this compound was characterized as 6'-*O*-galloyl desbenzoylalbiflorin (**7**). In this investigation of the constituents of *Paeoniae Radix*, albiflorin was not isolated.

The ^1H -NMR spectrum of compound **8** was closely related to that of 1'-*O*-galloylsucrose (**19**),⁷ except for the appearance of signals due to a benzoyl group instead of a galloyl group. The sugar carbon signals of **8** in the ^{13}C -NMR were also superimposable to those of **19**. From this spectral data, compound **8** was deduced to be 1'-*O*-benzoylsucrose. Although **8** has been synthesized,²³ this is the first report of isolation from plants.

As shown by HPLC analysis, the presence of polymeric proanthocyanidin is one of the distinctive features of *Paeoniae Radix* with cortex, compared to that without cortex. In addition, a considerable number of the minor peaks observed in the HPLC chromatogram of the sample with cortex (Fig. 1, B) were probably attributable to proanthocyanidins with lower molecular weight (**19**–**25**), catechin and its derivatives, sucrose esters, galloyl esters of monoterpene glycoside, and ellagitannins. Hence, the difference in medicinal applications may be related to the presence of these phenolic substances. Proanthocyanidins and the related flavan-3-ol are known to be excellent antioxidants and radical scavengers and increase the resistance of blood plasma towards oxidative stress.²⁴ It was also reported that proanthocyanidins inhibit oxidation of low-density lipoprotein and show antiatheroscle-

Table 2. Solubility of Polymeric Proanthocyanidins in the Presence of Paeoniflorin (9), Amygdalin, Apiosyl liquiritin, Glycyrrhizin, and Sucrose (Proanthocyanidin 2 mg in 1 ml of Water, 28 °C)

	Conc. (M)	Solubility (%, relative value ^{a)})
50% MeOH		100
None		75
Paeoniflorin	0.01	81
	0.02	84
Amygdalin	0.01	82
	0.02	87
Apiosyl liquiritin	0.01	87
	0.02	98
Glycyrrhizin	0.01	106
	0.02	104
Sucrose	0.01	79
	0.02	79

a) Relative solubility was estimated by comparison of the HPLC peak area with that of 50% MeOH solution (100%).

Table 3. Change of the Chemical Shifts of Paeoniflorin (9) in the Presence of Polymeric Proanthocyanidin (9, 0.013 M; Proanthocyanidin <7.5 mg/ml in D₂O,^{a)} at 20 °C)

	Paeoniflorin	+ Polymer	+ Tannase (30 min)	+ Tannase (3 h)
B-2, 6	8.058	8.040	8.043	8.044
B-4	7.699	7.684	7.687	7.688
B-3, 5	7.553	7.532	7.536	7.537
H-9	5.625	5.621	5.620	5.619

a) After dissolution in D₂O by heating, the solution was cooled to 20 °C, and the resulting precipitate was removed by filtration.

rotic activity.²⁵⁾ These beneficial properties seem to be consistent with those of *Paeoniae Radix* with cortex, and are different to those from plant without cortex containing lesser amounts of proanthocyanidins, which are mainly used for restoration of blood flow circulation.

In addition to the above structural investigation, we are interested in the water solubility of polymeric proanthocyanidin, which showed poor water solubility in a purified form. Previously, we have demonstrated the increase in water solubility of rhubarb polymeric proanthocyanidins in the presence of an anthraquinone glycoside.²⁶⁾ Since large amounts of paeoniflorin coexist with proanthocyanidin in the extract of *Paeoniae Radix*, the change in water solubility of polymeric proanthocyanidin from *Paeoniae Radix* in the presence of 9 was examined. After dissolution in water at 80 °C, 25% of the polymeric proanthocyanidin precipitated from solution as the temperature was cooled down to 28 °C, and 75% remained in solution. When 9 (0.02 M) was present, the amount of precipitate was decreased and 84% of the proanthocyanidin remained in solution (Table 2). On the other hand, the presence of sucrose did not affect the water solubility. The increase in water solubility was attributable to the hydrophobic association between 9 and polymeric proanthocyanidins. This was deduced from the ¹H-NMR chemical shift change of 9 in the presence of polymeric proanthocyanidin (Table 3). When polymeric proanthocyanidin coexists in aqueous solution, the aromatic proton signals shifted upfield. This phenomenon was similar to that observed for association between anthraquinone glycoside and polymeric proantho-

cyanidin from rhubarb. In addition, treatment with tannase partially restored the chemical shift to lower field. This observation suggested that the presence of galloyl groups in the polymeric proanthocyanidins was important for the association with 9. Other glycosides contained in major Japanese traditional crude drugs having amphipathic structure also increased the water solubility (Table 2). Water solubility is an important factor for bioavailability and affects the biological activities especially with orally administered drugs. Hence, the increased water solubility of polymeric proanthocyanidins by coexisting compounds may be important in oriental medicine.

Experimental

Column chromatography was performed with Sephadex LH-20 (25–100 mm, Pharmacia Fine Chemical Co. Ltd.), Diaion HP-20 and MCI-gel CHP 20P (75–150 mm, Mitsubishi Chemical Industries, Ltd.), Bondapak ODS (Waters), TSK-gel Toyopearl HW40F (TOSOH Co.), Chromatorex ODS (Fuji Silysia), and Silica gel 60 (Merck). Thin layer chromatography was performed on precoated Silica gel 60 F₂₅₄ plates (0.2 mm thick, Merck) with CHCl₃–MeOH–H₂O (70:30:5, v/v) or benzene–HCO₂Et–HCO₂H (1:7:1 or 1:7:2, v/v), and spots were detected by ultraviolet (UV) illumination, by spraying with 5% H₂SO₄ followed by heating, by spraying with 2% ethanolic FeCl₃ reagent, and by *p*-anisaldehyde–H₂SO₄ reagent. Analytical HPLC was performed on a Cosmosil 5C₁₈-AR (Nacalai Tesque Inc.) column (4.6 i.d. × 250 mm) (mobile phase, CH₃CN–50 mM H₃PO₄, gradient elution; flow rate, 0.8 ml/min, detection, UV absorption at 280 nm). Negative FAB-MS were recorded on a JEOL JMX DX-303 spectrometer with glycerol as a matrix. ¹H- and ¹³C-NMR spectra were obtained with Varian Unity plus 500 and Varian Gemini 300 spectrometers operating at 500 and 300 MHz for ¹H, and 125 and 75 MHz for ¹³C, respectively; chemical shifts are reported in parts per million on the δ scale with tetramethylsilane (TMS) as the internal standard, and coupling constants are in Hertz.

Extraction and Isolation From H₂O Layer: Commercial *Paeoniae Radix* with the cortex part (2.0 kg, imported from China) originating from the root of *P. obovata* was extracted with a mixture of acetone–water (7:3, v/v) three times and then with MeOH two times. The extracts were combined and defatted by partition between water and Et₂O (Et₂O extract, 24.6 g). The aqueous layer was extracted with AcOEt five times (AcOEt extract, 47.5 g), and the water layer was subjected to Diaion HP-20 column chromatography with water containing increasing amounts of MeOH to give four fractions: frs. 1–4. The first fraction was fractionated once again by Diaion HP-20 chromatography to five fractions. Fraction 1-1 was mainly comprised of sugars. Fraction 1-5 contained paeoniflorin as the major compound and was combined together with fr. 3. Fractions 1-2–1-4 were separately subjected to a combination of column chromatography over Sephadex LH-20, MCI-gel CHP 20P, Chromatorex ODS, Toyopearl HW-40 and Bondapak ODS with water–methanol to yield adenosine (47.2 mg), mudanpiosides E (15, 6.7 mg) and F (17, 81.1 mg), desbenzoylpaeoniflorin (16, 26.0 mg), oxypaeoniflorin (10, 1.28 g), paeoniflorin (9, 3.66 g), 6-*O*-galloylsucrose (18, 22.1 mg), 1'-*O*-galloylsucrose (19, 29.4 mg), 6'-*O*-galloylsucrose (20, 92.1 mg), catechin 7-*O*-glucoside (47.3 mg), catechin 5-*O*-glucoside (37.8 mg), catechin 3'-*O*-glucoside (34.6 mg), catechin 4'-*O*-glucoside (32.7 mg), 2,3-(*S*)-hexahydroxydiphenoyl-*D*-glucose (29, 24.5 mg), pterocaryanin B (31, 36.3 mg), casuarinin (32, 59.7 mg), pedunculagin (33, 346 mg), procyanidin B-3 (22, 265 mg), 8-*O*-galloyl desbenzoylpaeoniflorin (1, 11.9 mg), 8-*O*-isovaleryl desbenzoylpaeoniflorin (2, 25.3 mg), 6'-*O*-galloyl desbenzoylpaeoniflorin (3, 129.9 mg), and 6'-*O*-galloyl desbenzoylalbiflorin (7, 35.7 mg). Fraction 2 was fractionated by Diaion HP-20 (H₂O–MeOH) to give two fractions: frs. 2-1 (19.9 g) and 2-2 (39.9 g). The latter fraction contained mainly 9 and was combined with fr. 3. Fraction 2-1 was separated by Sephadex LH-20, MCI-gel CHP 20P, and Chromatorex ODS to give AC-trimer A (27, 454 mg) and arecatannin A-1 (28, 76.5 mg), and polymeric proanthocyanidin (2.3 g). Fraction 3 (81.6 g in total) was applied to a column of Sephadex LH-20 with water containing increasing amounts of MeOH and then water–acetone (1:1, v/v) to give two fractions: frs. 3-1 and 3-2. Fraction 3-1 was subjected to a combination of chromatography over MCI-gel CHP 20P, Sephadex LH-20, Chromatorex ODS and silica gel 60 to give 10 (0.5 g) and 9 (ca. 40 g), isomaltopaeoniflorin (6, 30.8 mg), and 1'-*O*-benzoylsucrose (8, 51.0 mg). Fraction 3-2 was mainly composed of proanthocyanidins and gallotannins. Fraction 4 (17.5 g) was

separated by Sephadex LH-20 chromatography into two fractions: frs. 4-1 and 4-2. Fraction 4-1 was chromatographed over MCI-gel CHP 20P followed by Chromatorex ODS to yield galloylpaeoniflorin (**13**, 1.05 g), the structure of which was confirmed by spectral comparison and tannase hydrolysis affording **9** and gallic acid. Fraction 4-2, mainly comprised of proanthocyanidins, was combined with fr. 3-2 and applied to a column of Sephadex LH-20 with water–acetone (1 : 1, v/v). The fraction positive to *p*-anisaldehyde–H₂SO₄ reagent was concentrated, and the residue was precipitated from H₂O–MeOH to give a mixture of polymeric proanthocyanidins (10.1 g).

Isolation from AcOEt Layer: The AcOEt layer (47.5 g) was subjected to Sephadex LH-20 column chromatography with water containing increasing amounts of MeOH and then water–acetone (1 : 1, v/v) to give seven fractions: frs. 1' (5.8 g), 2' (5.1 g), 3' (4.7 g), 4' (1.5 g), 5' (4.8 g), 6' (7.4 g), and 7' (6.23 g). The first fraction contained sugars and **9** as the major components and was not examined further. Fractions 2'–6' were separately subjected to a combination of column chromatography similar to those described for the aqueous layer to yield gallic acid (759 mg), benzoic acid (78.6 mg), *p*-hydroxybenzoic acid (16.9 mg), 4,5-dihydroxy-3-methoxybenzoic acid (13.6 mg), vanillic acid (29.3 mg), syringic acid (19.0 mg), galloylpaeoniflorin (**13**, 950 mg), galloyloxypaeoniflorin (**14**, 65.6 mg), benzoylpaeoniflorin (**11**, 693 mg), benzoyloxypaeoniflorin (**12**, 141 mg), and 6'-*O*-vanillylpaeoniflorin (**4**, 58.6 mg) from fr. 2'; (+)-catechin (531 mg), procyanidins B-1 (**23**, 63.5 mg) and B-3 (**22**, 34.9 mg) from fr. 3'; a mixture of *m*- and *p*-digallate (8.8 mg), procyanidin B-7 (**26**, 59.4 mg), AC-trimer (**27**, 81.7 mg), 1,2,3-tri-*O*-galloyl- β -glucose (33.8 mg), and pedunculagin (**33**, 55.0 mg) from fr. 4'; catechin 3-*O*-gallate (76.2 mg), 7-*O*-gallate (37.8 mg), and 3'-(4')-*O*-gallate (equilibrium mixture, 14.3 mg), epicatechin 3-*O*-gallate (76.2 mg), catechin oxidation product (**21**, 18.5 mg), procyanidins B-3 (**22**, 14.6 mg), B-1 3-*O*-gallate (**24**, 47.5 mg), B-7 (**26**, 95.8 mg), B-2 3'-*O*-gallate (**25**, 19.7 mg), 1,2,3,4-tetra-*O*-galloyl- β -D-glucose (50.1 mg), and 3',6'-di-*O*-galloylpaeoniflorin (**5**, 10.9 mg) from fr. 5; 1(β)-*O*-galloylpedunculagin (**34**, 111 mg), eugenin (327 mg), 2,3,4 6-tetra-*O*-galloylglucose (315 mg), and 1,2,3,4,6-penta-*O*-galloyl- β -D-glucose (2.33 g) from fr. 6. The structure of **14** was confirmed by tannase hydrolysis yielding **10**. The last fraction (fr. 7') was characterized as a mixture of polygalloylglucoses by ¹H-NMR spectral analysis which showed complex aromatic multiplet signals around 6.7–7.5 ppm along with signals due to an acylated sugar core related to that of pentagalloyl- β -D-glucose.

8-*O*-Galloyl Desbenzoylpaeoniflorin (1) A tan amorphous powder, [α]_D –4.9° (*c*=0.35, MeOH). *Anal.* Calcd for C₂₃H₂₈O₁₄·2H₂O: C, 48.92; H, 5.72. Found: C, 48.60; H, 5.43. FAB-MS *m/z*: 551 [M+Na]⁺. ¹H-NMR (MeOH-*d*₄, 300 MHz): Table 1. ¹³C-NMR (MeOH-*d*₄, 75.5 MHz) δ : monoterpene moiety: 89.28 (C-1), 87.32 (C-2), 44.58 (C-3), 106.40 (C-4), 44.09 (C-5), 72.31 (C-6), 23.72 (C-7), 61.26 (C-8), 102.33 (C-9), 19.56 (C-10); glucose moiety: 100.17 (C-1'), 75.04 (C-2'), 78.01, 77.90 (C-3', 5'), 71.78 (C-4'), 62.90 (C-6'); galloyl group: 121.22 (C-1''), 110.20 (C-2'', 6''), 147.55 (C-3'', 5''), 139.98 (C-4''), 168.25 (C-7'').

8-*O*-Isovaleryl Desbenzoylpaeoniflorin (2) A tan amorphous powder, [α]_D –19.6° (*c*=0.33, MeOH). *Anal.* Calcd for C₂₁H₃₂O₁₁·3/4H₂O: C, 53.20; H, 7.12. Found: C, 53.17; H, 6.88. FAB-MS *m/z*: 483 [M+Na]⁺. ¹H-NMR (MeOH-*d*₄, 300 MHz): Table 1. ¹³C-NMR (MeOH-*d*₄, 75.5 MHz) δ : monoterpene moiety: 89.19 (C-1), 87.21 (C-2), 44.55 (C-3), 106.31 (C-4), 43.95 (C-5), 72.02 (C-6), 23.30 (C-7), 60.93 (C-8), 102.20 (C-9), 19.57 (C-10); glucose moiety: 100.14 (C-1'), 74.98 (C-2'), 78.06, 77.92 (C-3' and 5'), 72.02 (C-4'), 62.88 (C-6'); isovaleryl group: 174.68 (C-1''), 44.16 (C-2''), 26.84 (C-3''), 22.76 (C-4''), 5'').

6'-*O*-Galloyl Desbenzoylpaeoniflorin (3) A tan amorphous powder, [α]_D –12.8° (*c*=0.46, MeOH). *Anal.* Calcd for C₂₃H₂₈O₁₄·3/2H₂O: C, 49.92; H, 5.23. Found: C, 49.91; H, 5.49. Negative ion FAB-MS *m/z*: 527 [M–H][–]. ¹H-NMR (MeOH-*d*₄, 300 MHz): Table 1. ¹³C-NMR (MeOH-*d*₄, 75.5 MHz) δ : monoterpene moiety: 89.34 (C-1), 87.22 (C-2), 44.54 (C-3), 106.34 (C-4), 43.46 (C-5), 73.44 (C-6), 22.95 (C-7), 59.00 (C-8), 102.09 (C-9), 19.53 (C-10); glucose moiety: 99.76 (C-1'), 74.90 (C-2'), 77.91 (C-3'), 72.04 (C-4'), 75.19 (C-5'), 64.69 (C-6'); galloyl group: 121.38 (C-1''), 110.16 (C-2'', 6''), 146.53 (C-3'', 5''), 139.89 (C-4''), 168.08 (C-7'').

6'-*O*-Vanillylpaeoniflorin (4) A white amorphous powder, [α]_D –12.6° (*c*=0.53, MeOH). *Anal.* Calcd for C₃₁H₃₄O₁₄·3/2H₂O: C, 56.62; H, 5.67. Found: C, 56.77; H, 5.57. FAB-MS *m/z*: 653 [M+Na]⁺. ¹H-NMR (MeOH-*d*₄, 300 MHz): Table 1. ¹³C-NMR (MeOH-*d*₄, 125 MHz) δ : monoterpene moiety: 89.15 (C-1), 87.08 (C-2), 44.41 (C-3), 106.20 (C-4), 43.78 (C-5), 71.93 (C-6), 23.10 (C-7), 61.57 (C-8), 102.17 (C-9), 19.56 (C-10); glucose moiety: 99.95 (C-1'), 74.90 (C-2'), 77.78 (C-3'), 72.06 (C-4'), 75.26 (C-5'), 64.97 (C-6'); benzoyl group: 131.10 (C-1''), 130.62 (C-2'', 6''), 129.60 (C-3'',

5''), 134.39 (C-4''), 167.69 (C-7''); vanillyl group: 122.36 (C-1''), 113.49 (C-2''), 148.76 (C-3''), 152.99 (C-4''), 116.00 (C-5''), 125.14 (C-6''), 168.08 (C-7'').

3',6'-Di-*O*-galloylpaeoniflorin (5) A brown amorphous powder, [α]_D –5.7° (*c*=0.77, MeOH). *Anal.* Calcd for C₃₇H₃₆O₁₉·2H₂O: C, 54.15; H, 4.42. Found: C, 54.13; H, 4.70. Negative ion FAB-MS *m/z*: 783 [M–H][–]. ¹H-NMR (MeOH-*d*₄, 300 MHz): Table 1. ¹³C-NMR (MeOH-*d*₄, 75.5 MHz) δ : monoterpene moiety: 90.05 (C-1), 87.61 (C-2), 44.93 (C-3), 106.76 (C-4), 44.26 (C-5), 72.48 (C-6), 23.40 (C-7), 62.04 (C-8), 102.68 (C-9), 20.12 (C-10); glucose moiety: 100.57 (C-1'), 73.98 (C-2'), 79.44 (C-3'), 71.05 (C-4'), 75.71 (C-5'), 64.96 (C-6'); benzoyl group: 131.66 (C-1''), 131.07 (C-2'', 6''), 130.11 (C-3'', 5''), 134.89 (C-4''), 168.53 (C-7''); galloyl group: 121.89, 122.22 (C-1''), 110.72, 110.72 (C-2'', 6'', 2''), 146.89, 147.08 (C-3'', 5'', 3''), 140.23, 140.47 (C-4'', 4''), 168.71, 168.08 (C-7'', 7''). Tannase hydrolysis of **5** (1 mg) yielded gallic acid and **9**, which were identified by TLC and HPLC comparison.

Isomaltopaeoniflorin (6) A white amorphous powder, [α]_D 30.9° (*c*=0.39, MeOH). *Anal.* Calcd for C₂₉H₃₈O₁₆·5/2H₂O: C, 50.65; H, 6.30. Found: C, 50.92; H, 5.98. FAB-MS *m/z*: 665 [M+Na]⁺. ¹H-NMR (MeOH-*d*₄, 500 MHz): Table 1. ¹³C-NMR (MeOH-*d*₄, 125 MHz) δ : monoterpene moiety: 89.38 (C-1), 87.32 (C-2), 44.57 (C-3), 106.47 (C-4), 44.05 (C-5), 72.32 (C-6), 23.60 (C-7), 61.72 (C-8), 102.34 (C-9), 19.80 (C-10); β -glucose moiety: 100.07 (C-1'), 74.95 (C-2'), 78.00 (C-3'), 71.96 (C-4'), 76.07 (C-5'), 68.09 (C-6'); α -glucose moiety: 99.86 (C-1''), 73.48 (C-2''), 71.24 (C-3''), 71.62 (C-4''), 73.38 (C-5''), 62.58 (C-6''); benzoyl group: 131.20 (C-1''), 130.66 (C-2'', 6''), 129.64 (C-3'', 5''), 134.41 (C-4''), 167.98 (C-7'').

6'-*O*-Galloyl Desbenzoylalbiflorin (7) A tan amorphous powder, [α]_D –4.9° (*c*=0.41, MeOH). *Anal.* Calcd for C₂₃H₂₈O₁₄·3/2H₂O: C, 49.92; H, 5.23. Found: C, 49.67; H, 5.41. Negative ion FAB-MS *m/z*: 527 [M–H][–]. ¹H-NMR (MeOH-*d*₄, 300 MHz): Table 1. ¹³C-NMR (MeOH-*d*₄, 125 MHz) δ : monoterpene moiety: 86.96 (C-1), 93.06 (C-2), 41.43 (C-3), 68.25 (C-4), 40.83 (C-5), 57.84 (C-6), 27.08 (C-7), 59.95 (C-8), 178.74 (C-9), 20.33 (C-10); glucose moiety: 99.27 (C-1'), 74.55 (C-2'), 77.99 (C-3'), 72.27 (C-4'), 75.19 (C-5'), 64.67 (C-6'); galloyl group: 121.37 (C-1''), 110.17 (C-2'', 6''), 146.58 (C-3'', 5''), 139.91 (C-4''), 167.90 (C-7'').

1'-*O*-Benzoylsucrose (8) A tan amorphous powder, [α]_D 43.2° (*c*=0.48, MeOH). *Anal.* Calcd for C₁₉H₂₆O₁₂·5/4H₂O: C, 48.67; H, 6.13. Found: C, 48.71; H, 5.76. FAB-MS *m/z*: 469 [M+H]⁺. ¹H-NMR (MeOH-*d*₄, 300 MHz): δ : 3.30–4.05 (m), 4.22 (1H, dd, *J*=2, 9 Hz, H-3), 4.59, 4.39 (each 1H, d, *J*=12 Hz, H-1), 5.48 (1H, d, *J*=4 Hz, H-1'), 7.49 (2H, br t, *J*=8 Hz, H-3'', 5''), 7.63 (1H, br t, *J*=8 Hz, H-4''), 8.06 (2H, br t, *J*=8 Hz, H-2'', 6''). ¹³C-NMR (MeOH-*d*₄, 125 MHz) δ : 64.42 (C-1), 104.13 (C-2), 78.91 (C-3), 74.98 (C-4), 83.83 (C-5), 63.25 (C-6), 94.18 (C-1'), 73.03 (C-2'), 74.43, 74.60 (C-3'', 5''), 71.38 (C-4''), 62.21 (C-6''); benzoyl group: 131.08 (C-1''), 130.66 (C-2'', 6''), 129.64 (C-3'', 5''), 134.43 (C-4''), 167.33 (C-7'').

Polymeric Proanthocyanidin A brown powder from H₂O. ¹³C-NMR (acetone-*d*₆, 75.5 MHz) δ : 28.4 (C-4 of terminal unit), 36.7 (C-4 of extension unit), 67.5 (C-3 of terminal catechin unit), 71.9 (C-3 of extension units), 76.8 (C-2 of extension units), 81.9 (C-2 of terminal catechin unit), 96.7 (A-ring C-6 and/or 8), 101.2 (A-ring C-4a), 107.8 (A-ring C-8 or 6), 109.8 (galloyl C-2, 6), 114.7, 115.6, 118.9 (B-ring C-2', 5', 6'), 120.5 (galloyl C-1), 129.2, 129.8, 131.8 (B-ring C-1'), 139.4 (galloyl C-4), 144.9, 145.7 (B-ring C-3', 4'), galloyl C-3, 5), 154.1, 155.9, 157.2 (A-ring C-5, 7, 8a), 166–168 (C-7, galloyl C-7).

Thiol Degradation of Polymeric Proanthocyanidin Isolation of the Products: Polymeric proanthocyanidin (500 mg) was treated with a mixture of mercaptoethanol (4 ml), 0.5 M HCl (16 ml) and MeOH (10 ml) at 50 °C for 7 h. After concentration to about half volume, the solution was applied to a column of MCI-gel CHP 20P with water containing increasing amounts of MeOH to give (+)-catechin (12.3 mg), [α]_D +4.1° (*c*=0.8, acetone) and epicatechin 3-*O*-gallate (4 mg), [α]_D –50.0° (*c*=0.3, acetone) from terminal units; (±)-catechin 4-(2-hydroxyethyl)thio ether (12.8 mg), [α]_D 0° (*c*=0.2, acetone), epicatechin 4-(2-hydroxyethyl)thio ether (101.0 mg), [α]_D –53.5° (*c*=0.3, acetone), and epicatechin 3-*O*-gallate 4-(2-hydroxyethyl)thio ether (55.6 mg), [α]_D –91.0° (*c*=0.4, acetone) from extension units.²¹⁾

HPLC Analysis of Thiol Degradation Products: Polymeric proanthocyanidin (10 mg) was treated with a mixture of mercaptoethanol (0.3 ml), acetic acid (0.3 ml) and ethanol (2.4 ml) in N₂ gas at 50 °C for two days. The mixture was diluted with water, passed through Sepak ODS (60% MeOH), and analyzed by reversed phase HPLC [10%→30% (40 min) CH₃CN in 50 mM H₃PO₄]. Retention time (min): (+)-catechin (12.63), epicatechin 3-*O*-gallate (26.36), (±)-catechin 4-(2-hydroxyethyl)thio ether (18.16), (–)-epicatechin 4-(2-hydroxyethyl)thio ether (22.76), (–)-epicatechin 3-*O*-gallate 4-(2-hydroxyethyl)thio ether (30.62). The molar ratio of the products was estimated

by comparison of peak area with those of standard solutions: (–)-epicatechin (65%), (±)-catechin (21%), and (–)-epicatechin 3-*O*-gallate (14%) for extension units, (+)-catechin (69%) and (–)-epicatechin 3-*O*-gallate (31%) for terminal units (average value obtained from four samples with four injections for each sample).

Water Solubility of Polymeric Proanthocyanidin Polymeric proanthocyanidin (2 mg) was dissolved in water (1 ml) containing 0, 0.01 or 0.02 M of test compounds at 80 °C. The solution was cooled to 28 °C and left to stand for 15 h. The resulting precipitates were removed by centrifugation (3000 rpm, 20 min), and the supernatant was analyzed by reversed-phase HPLC (Cosmosil 5C₁₈-AR, 15–45% (20 min) CH₃CN–50 mM H₃PO₄, 0.8 ml/min).

Acknowledgements The authors are grateful to Mr. K. Inada for NMR measurements, Mr. N. Yamaguchi for MS measurements, and Miss H. Ohta for microanalysis.

References and Notes

- 1) Nishizawa M., Yamagishi T., Nonaka G., Nishioka I., *Chem. Pharm. Bull.*, **28**, 2850–2852 (1980).
- 2) Nishizawa M., Yamagishi T., Nonaka G., Nishioka I., *J. Chem. Soc., Perkin Trans. 1*, **1982**, 2963–2968.
- 3) Kaneda M., Iitaka Y., Shibata S., *Tetrahedron*, **28**, 4309–4317 (1972).
- 4) Yoshikawa M., Uchida E., Kawaguchi A., Kitagawa I., Yamahara J., *Chem. Pharm. Bull.*, **40**, 2248–2250 (1992), and references cited therein.
- 5) Lin H.-C., Ding H.-Y., Wu T.-S., Wu P.-L., *Phytochemistry*, **41**, 237–242 (1996).
- 6) Lemmich J., *Phytochemistry*, **41**, 1337–1340 (1996).
- 7) Kashiwada Y., Nonaka G., Nishioka I., *Phytochemistry*, **27**, 1469–1472 (1988).
- 8) Kashiwada Y., Nonaka G., Nishioka I., *Chem. Pharm. Bull.*, **34**, 3208–3222 (1988).
- 9) Malan E., *Phytochemistry*, **30**, 2737–2739 (1991).
- 10) Lee M.-E., Morimoto S., Nonaka G., Nishioka I., *Phytochemistry*, **31**, 2117–2120 (1992).
- 11) Nonaka G., Kawahara O., Nishioka I., *Chem. Pharm. Bull.*, **31**, 3906–3914 (1983).
- 12) Guyot S., Vercauteren J., Cheynier V., *Phytochemistry*, **42**, 1279–1288 (1996).
- 13) Tanaka T., Nonaka G., Nishioka I., *Phytochemistry*, **22**, 2575–2678 (1983).
- 14) Nonaka G., Nishioka I., Nagasawa T., Oura H., *Chem. Pharm. Bull.*, **29**, 2862–2870 (1981).
- 15) Nonaka G., Hsu F.-L., Nishioka I., *J. Chem. Soc., Chem. Comm.*, **1981**, 781–783.
- 16) Nonaka G., Nakayama S., Nishioka I., *Chem. Pharm. Bull.*, **37**, 2030–2036 (1989).
- 17) Tanaka T., Nonaka G., Nishioka I., *J. Chem. Research (S)*, **1985**, 176–177; *idem*, *J. Chem. Research (M)*, **1985**, 2001–2029.
- 18) Nonaka G., Harada M., Nishioka I., *Chem. Pharm. Bull.*, **28**, 685–687 (1980).
- 19) Saijo R., Nonaka G., Nishioka I., *Chem. Pharm. Bull.*, **37**, 2063–2070 (1989).
- 20) Nonaka G., Sakai T., Tanaka T., Mihashi K., Nishioka I., *Chem. Pharm. Bull.*, **38**, 2151–2156 (1990).
- 21) Tanaka T., Takahashi R., Kouno I., Nonaka G., *J. Chem. Soc., Perkin Trans. 1*, **1994**, 3013–3022.
- 22) Yamasaki K., Kaneda M., Tanaka Y., *Tetrahedron Lett.*, **44**, 3965–3968 (1976).
- 23) Carrea G., Riva S., Secundo F., *J. Chem. Soc., Perkin Trans. 1*, **1989**, 1057–1061.
- 24) Koga T., Moro K., Nakamori K., Yamakoshi J., Hosoyama H., Kataoka S., Ariga T., *J. Agric. Food Chem.*, **47**, 1892–1897 (1999).
- 25) Yamakoshi J., Kataoka S., Koga T., Ariga T., *Atherosclerosis*, **1999**, 139–149.
- 26) Tanaka T., Zhang H., Jiang Z., Kouno I., *Chem. Pharm. Bull.*, **45**, 1891–1897 (1997).

Determination of Hydration Kinetics of Sulfaguanidine Anhydrate in Aqueous Solution by Calorimetry¹⁾

Yasuo YOSHIHASHI,* Etsuo YONEMOCHI, Midori MAKITA, Shigeo YAMAMURA, Eihei FUKUOKA, and Katsuhide TERADA

School of Pharmaceutical Sciences, Toho University, 2-2-1 Miyama, Funabashi, Chiba 274-8510, Japan.

Received July 16, 1999; accepted October 9, 1999

A heat conduction microcalorimeter was used to evaluate the isothermal transition in water from anhydrate to monohydrate at 298 K. Sulfaguanidine (SGN) anhydrate was used as a model compound for the measurement of hydration kinetics in water. It is the well-known that SGN is very slightly soluble in water and capable of existing as the anhydrate or monohydrate form in the solid state. The transition rates of SGN anhydrate to monohydrate in tablets and granules were investigated. The hydration kinetics of tablets with controlled surface areas, obtained by coating the side with paraffin in aqueous solution, followed an apparent zero-order mechanism. On the other hand, the transition mechanism of the granules involved a phase boundary-controlled contracting interface reaction.

Key words hydration kinetics; calorimetry; sulfaguanidine; tablets; granules

In the development of solid dosage forms, the phase transition of the active ingredient from the metastable form to the stable form can be a problem. When solid preparations are administered orally, the phase transition may influence the release or dissolution of the active agents from the solid dosage forms. For this reason it is important to measure the transition rate of anhydrate to hydrate in water. The phase transition of drug in the solid state can be determined by many methods,^{2,3,4a)} however, measurement of the transition kinetics in water is none, because it is difficult to determine the rate under such conditions. Although the transition behavior in water has already been investigated by measuring the dissolution profile,²⁾ is the transition of drug inside solid dosage forms can't be determined by this method. Hence, it is desirable to develop a method for investigating the phase transition rates inside solid dosage forms in water.

In the present study, sulfaguanidine (SGN) was selected as a model compound for the measurement of the hydration kinetics in water because SGN is very slightly soluble in water and capable of existing as the anhydrate and monohydrate forms in the solid state. The hydration rates in water for solid dosage forms, *i.e.*, tablets and granules, were determined continuously by the calorimetric method.^{4a)} Using this method, it is possible to investigate the phase transition kinetics and the transition mechanism of solid dosage forms in liquids.

Experimental

Materials SGN monohydrate was recrystallized from distilled water and then allowed to dry on filter paper at room temperature. The material was then ground gently in an agate mortar. The fraction passed through a 100 mesh sieve was used. This fraction was heated at 90 °C for 3 h under vacuum with P₂O₅ and then stored in a desiccator containing P₂O₅. This material was used as the test sample.

Preparations of Tablets and Granules The compression equip and tablet preparation were as described in the previous paper.^{4b)} Sample powder, 250 mg, was compressed under a pressure of 5000 kg/cm² with flat-faced punches in a die of 7.0 mm internal diameter at a speed of 50 mm/min. The tablets were used in this form or the side was coated with paraffin. The tablets were crushed in the agate mortar and the 12–22 mesh fraction was used as granules. The sample weight was 250 mg.

Calorimetry A twin-type heat conduction microcalorimeter CM-204D1 (Electronic Laboratory, Ltd.) was used throughout the studies. The proce-

dures for the calorimetric measurements was as described in the previous paper.^{4a)} All measurements were carried out at 25 °C.

Determination of Hydration Rate by Microcalorimetry The hydration rates of SGN were determined as follows. Fifty milliliters of saturated SGN aqueous solution with its fine crystals was transferred to the reaction vessel and the thermogram measured without stirring. The hydration rate (dw/dt), *i.e.*, dQ/dt , was analyzed by the deconvolution method described in the previous paper.⁴⁾ To obtain the thermogram of the heat generated instantaneously in the reaction vessel, *i.e.*, the weight function in the deconvolution equation, a Nichrome wire was used. The Nichrome wire was immersed in the solvent in the reaction vessel on the sample side. The heat were generated by passing an electric current for 0.1 s through the Nichrome wire, change transforming the voltage from 130 to 80 V.

Measurement of Moisture Content The moisture content of SGN monohydrate and anhydrate was determined by the Karl Fisher method as described in the previous paper.^{4c)} This showed that SGN monohydrate and anhydrate contained 1 and 0 mol moisture, respectively.

X-Ray Diffraction Powder X-ray diffractometry was performed as described in the previous paper.^{4c)}

Results and Discussion

Confirmation of Change from SGN Anhydrate to Monohydrate in Water Figure 1 shows the powder X-ray diffraction patterns of SGN anhydrate before and after immersion in water.

From the X-ray powder diffraction profiles, it was found that SGN anhydrate was completely transformed into monohydrate in water.⁵⁾

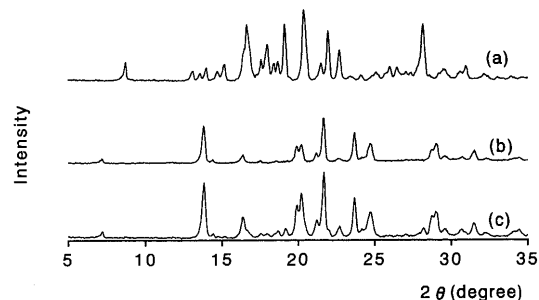


Fig. 1. X-Ray Powder Diffraction Patterns of SGN Anhydrate, before and after Immersion in Water, and Monohydrate

(a) anhydrate before immersion in water, (b) anhydrate after immersion in water, (c) monohydrate.

* To whom correspondence should be addressed.

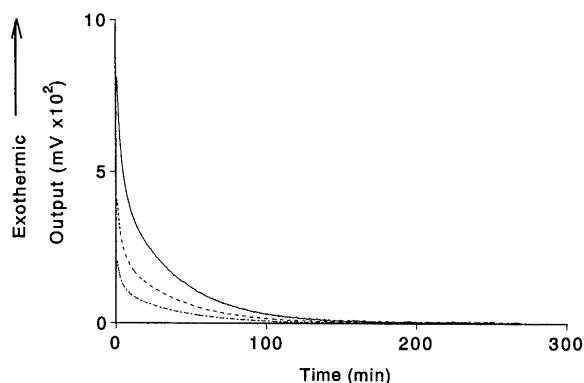


Fig. 2. Thermograms Obtained by Passing an Electric Current through Nichrome Wire

—, 2.80 J; ---, 1.38 J; ···, 0.71 J.

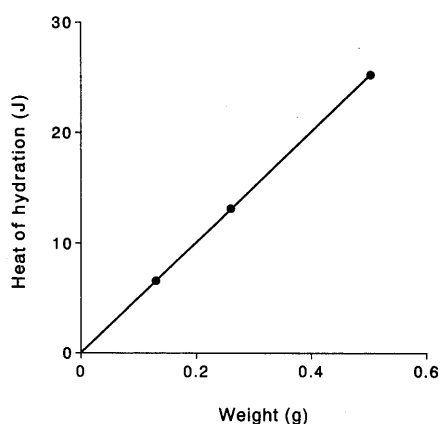


Fig. 3. Relationship between Weight and Heat of Hydration of SGN Anhydrate

Analysis of Hydration Rates by the Deconvolution Method The thermograms obtained by passing different amounts of electric current through the Nichrome wire placed in SGN saturated solution are shown in Fig. 2. From Fig. 2, the heat conduction behavior was considered to behave as a linear system. In addition, it was confirmed that the relationship between the heat of hydration and weight of SGN anhydrate was also linear. The relationship between the weight and heat of hydration of SGN anhydrate is shown in Fig. 3. A linear relationship was observed over the region from 0 to 0.5 g sample weight. This result indicates that the weight of SGN anhydrate is directly proportional to the heat of hydration for the transformation in water from SGN anhydrate to monohydrate. Furthermore, the weight of SGN anhydrate is directly proportional to the weight of transformed SGN monohydrate. Consequently, the heat evolved at time t (dQ/dt) and the hydration rate (dw/dt) can be expressed by the following formula:

$$dw/dt \text{ (g/min)} = k \cdot dQ/dt \text{ (J/min)}$$

Where k (g/J) is a constant with a value of 0.020. Therefore, the thermograms obtained upon passing an electric current through the Nichrome wire correspond to an input function and the thermograms for the hydration of SGN tablets and granules can be considered as a response to an arbitrary input. From these thermograms, the hydration rates of SGN anhydrate in water could be obtained by the deconvolution

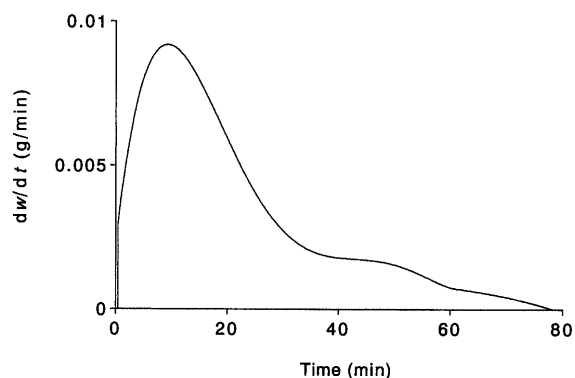


Fig. 4. Hydration Rate of Sulfaguanidine Tablets in Water

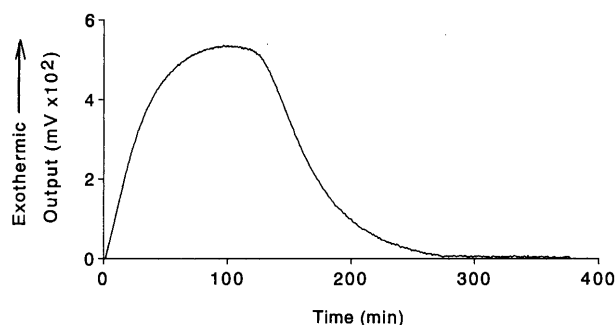


Fig. 5. Thermogram of Hydration of SGN Anhydrate Tablets with Controlled Surface Areas, Obtained by Coating the Side with Paraffin

method. This method makes it possible to measure the transition in water of a drug inside solid dosage forms, something that was so far been considered difficult to do.

Measurements of Hydration Rate of Tablets The hydration rate (dw/dt) of SGN tablets in water determined by the deconvolution method is shown in Fig. 4. When a tablet was immersed in water, dw/dt increased rapidly after a *ca.* 30 s time-lag and the maximum dw/dt was attained about 10 min after immersion. Furthermore, if the SGN tablet was placed in a flask filled with water, lamination of the side of tablet occurred rapidly. This result suggested that, as the water penetrated into the tablet, hydration took place readily and then lamination the side of tablet occurred. After about 40 min, the hydration rate decreased gradually. This result indicated that hydration of the mass of disintegrated tablet was a slow process.

Measurement of Hydration Rate for Tablets with Controlled Surface Areas by Coating the Side with Paraffin The hydration kinetics of SGN anhydrate tablets with controlled surface areas, obtained by coating the side with paraffin, in water was determined. The thermogram is shown in Fig. 5. Following a *ca.* 75 s time-lag, the heat curve rose linearly for about 30 min, increased for up to about 60 min, and then remained approximately constant for a period of about 60 min before decreasing rapidly. This result suggested that nucleation and nuclear growth occurred during the time-lag and heat was generated during the period of hydration and then the heat curve decreased rapidly in the neighborhood of the end-point of hydration. Using the data in Figs. 2 and 5, the isothermal transition curve was determined by the deconvolution method. The result is shown in Fig. 6. As shown in Fig. 6, the hydration rate can be expressed by apparent zero-

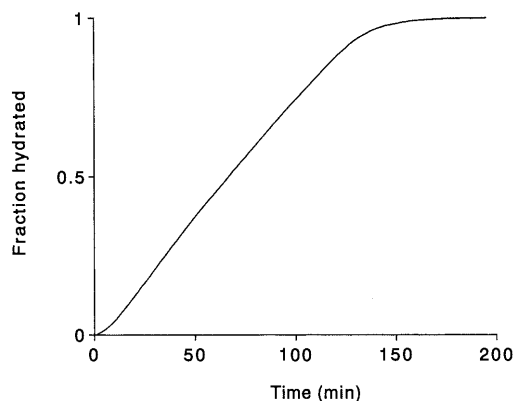


Fig. 6. Hydration Profile of SGN Anhydrate Tablets with Controlled Surface Areas, Obtained by Coating the Side with Paraffin

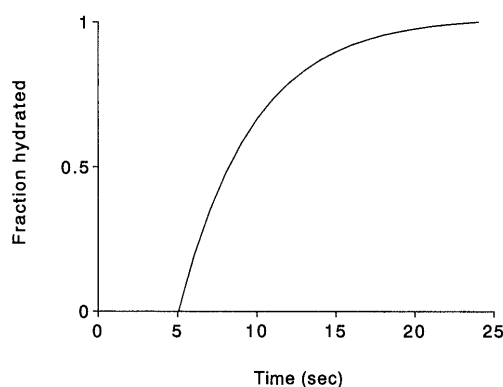


Fig. 7. Hydration Profile of SGN Granules in Water

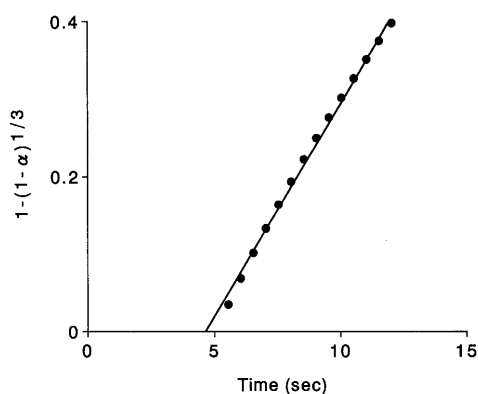


Fig. 8. Plot of $1-(1-\alpha)^{1/3}$ versus t for the Isothermal Transition of Anhydrate to Monohydrate in Water at 25 °C

order kinetics for the time-lag. From these results, it was considered that the area of the hydrating interface was constant.

Measurement of Hydration Rate of Granules The hydration profile of SGN granules in water is shown in Fig. 7. The hydration of granules was achieved almost instantly with a *ca.* 5 s time-lag. The hydration behavior was determined from a theoretical equation for solid-state decomposition.⁶⁾ Assuming the granules are spherical and the hydration rate

can be expressed by an apparent zero-order mechanism, the hydration rate of granules can be represented by the following equation:

$$1-(1-\alpha)^{1/3}=kt$$

where α is the fractional hydration at time t and k is a constant. A range of 0.1–0.8 for the fractional hydration was used in the analysis of the hydration mechanism. Figure 8 shows a plot of $1-(1-\alpha)^{1/3}$ versus t for the isothermal transition of anhydrate to monohydrate in water at 25 °C. A linear relationship between $1-(1-\alpha)^{1/3}$ and time was observed. However, the straight line did not pass through the origin. This can be explained by the time-lag. As a *ca.* 5 s time-lag was present, the origin was shifted by about 5 s and the straight line crossed the time axis at about 5 s. This result suggested that the hydration reaction is a phase boundary-controlled contracting interface reaction.

Conclusion

The hydration kinetics of solid dosage forms in water was determined by a calorimetric method. The hydration reaction was analyzed by a theoretical equation for solid-state decomposition. The kinetics of hydration in water for tablets with controlled surface areas, obtained by coating the side with paraffin, was found to be the apparent zero-order. The hydration reaction of the granules was a phase boundary-controlled contracting interface reaction. This method may be useful for the measurement of phase transition behavior within solid dosage forms in liquids.

References and Notes

- 1) The present work was presented at the 114th Annual Meeting of the Pharmaceutical Society of Japan, Tokyo, March 1994.
- 2) Nogami H., Nagai T., Yotsuyanagi T., *Chem. Pharm. Bull.*, **17**, 499–509 (1969); Aguiar A. J., Zelmer J. E., *J. Pharm. Sci.*, **58**, 983–987 (1969).
- 3) Shefter E., Kmack G., *J. Pharm. Sci.*, **56**, 1028–1029 (1967); Shefter E., Fung H., Mok O., *ibid.*, **62**, 791–794 (1973); Nakamachi H., Wada Y., Aoki I., Kodama Y., Kuroda K., *Chem. Pharm. Bull.*, **29**, 2956–2965 (1981); Matsuda Y., Kawaguchi S., *ibid.*, **34**, 1289–1298 (1986); Otsuka M., Kaneniwa N., *ibid.*, **36**, 4914–4920 (1988); Suzuki E., Shimomura K., Sekiguchi K., *ibid.*, **37**, 493–497 (1989); Otsuka M., Kaneniwa N., Kawakami K., Umezawa O., *J. Pharm. Sci.*, **42**, 606–610 (1990); *idem*, *ibid.*, **43**, 226–231 (1991); Angberg M., Nystrom C., Castensson S., *Int. J. Pharm.*, **73**, 209–220 (1991); *idem*, *ibid.*, **77**, 269–277 (1991); *idem*, *ibid.*, **81**, 153–167 (1992); *idem*, *ibid.*, **83**, 11–23 (1992); Imamura K., Oishi N., Ishida Y., Ogawa K., Araki K., *Yakugaku Zasshi*, **112**, 750–756 (1992); Otsuka M., Kaneniwa N., Otsuka K., Kawakami K., Umezawa O., Matsuda Y., *J. Pharm. Sci.*, **81**, 1189–1193 (1992); Bringgner L.-E., Buckton G., Bystrom K., Darcy P., *Int. J. Pharm.*, **105**, 125–135 (1994); Agbada C. O., York P., *ibid.*, **106**, 33–40 (1994).
- 4) a) Fukuoka E., Makita M., Yamamura S., Yoshihashi Y., *Chem. Pharm. Bull.*, **42**, 2139–2142 (1994); b) Yoshihashi Y., Makita M., Yamamura S., Fukuoka E., Terada K., *ibid.*, **46**, 473–477 (1998); c) *Idem*, *ibid.*, **46**, 1148–1152 (1998).
- 5) Sekiguchi K., Shirotani K., Sakata O., Suzuki E., *Chem. Pharm. Bull.*, **32**, 1558–1567 (1984).
- 6) Mampel K. L., *Z. Phys. Chem.*, **43**, 235–249 (1940); Acheson R. J., Jacobs P. W. M., *J. Phys. Chem.*, **74**, 281–288 (1970); Dollimore D., Tinsley D., *J. Chem. Soc. (A)*, 3043–3047 (1971); Hancock J. E., Sharp K. H., *J. Am. Ceram. Soc.*, **55**, 74–77 (1972).

Reactions of *N*-Hydroxysuccinimide Esters of Anthranilic Acids with Anions of β -Keto Esters. A New Route to 4-Oxo-3-quinolinecarboxylic Acid Derivatives

Christos MITSOS, Alexandros ZOGRAFOS, and Olga IGGLESSI-MARKOPOULOU*

Chemical Engineering Department, National Technical University of Athens, Zografou 157–73, Athens, Greece.

Received July 26, 1999; accepted October 12, 1999

A new approach for the synthesis of 4-oxo-3-quinolinecarboxylic acid derivatives is described. This methodology involves the *C*-acylation of the anions of appropriate β -keto esters with novel *N*-hydroxysuccinimide esters of anthranilic acids. The intermediate *C*-acylation products **3** are spontaneously cyclized to afford 3-ethoxycarbonyl-4-oxoquinoline derivatives **4**. The introduction of a variety of substituents at positions 1 and 2 of the quinoline ring is feasible with the selection of suitable anthranilic acids and β -keto esters. The structure of the obtained 2-substituted 3-ethoxycarbonyl-4-oxoquinolines was confirmed by IR and NMR spectral data.

Key words quinolones; *N*-hydroxysuccinimide esters; *C*-acylation reaction

4-Oxo-3-quinolinecarboxylic acid derivatives constitute a class of heterocyclic compounds of great importance in pharmaceutical science. The group of antibacterial agents collectively known as 'quinolones,' comprises quinoline and 1,8-naphthyridine derivatives containing the 4-oxo-3-carboxylic acid moiety. The synthesis and evaluation of antibacterial activity of related compounds is a field of continuing research in medicinal chemistry.¹⁾ Apart from their antimicrobial activity, 4-oxo-3-quinolinecarboxylic acid derivatives have shown anticoccidial²⁾ and antitumor³⁾ activity. The inhibition of cell respiration by a series of 4-oxo-3-quinolinecarboxylic acids has been studied as a measure of their membrane-transport properties.⁴⁾ Moreover, several reports have appeared concerning the biological properties of 4-oxo-3-quinolinecarboxamides. Recently, the inhibition of human erythrocyte calpain I by quinolinecarboxamides has been reported.⁵⁾ The antihypertensive activity of related carboxamides, with or without a substituent at position 2, has also been examined.⁶⁾ The antibacterial activity of tricyclic derivatives containing an N-1 to C-2 bridge has been studied in the past few years.⁷⁾ 2-Substituted 4-hydroxy-3-quinolinecarboxamides have shown antiarthritic and analgesic activities⁸⁾ and it was stated that the nature of the substituent at position 2 specifies the actual activity of these derivatives. A series of 3-quinolinecarboxamides has been designed as serotonin 5-HT₃ receptors antagonists.⁹⁾

Recently, we have established a convenient methodology for the construction of quinoline-2,4-dione derivatives, which involves the *C*-acylation of active methylene compounds with 3,1-benzoxazin-4-ones.¹⁰⁾ A variety of 3-substituted 4-hydroxyquinolin-2-ones, which have found attention lately as *N*-methyl-D-aspartate (NMDA) receptors antagonists,¹¹⁾ can be prepared according to this method. However, this approach is limited to *N*-unsubstituted analogues and we have failed to extend its applicability to the synthesis of 2-substituted 3-quinolinecarboxylic acid derivatives. In the literature, there have been relatively few investigations concerning the preparation of 2-substituted 3-quinolinecarboxylic acids.¹²⁾ The most widely used method involves the reaction of isoic anhydrides with β -keto esters and the cyclization of the intermediate *C*-acylation compounds.¹³⁾ Although, this approach appears to be general, the use of polar solvents with high

boiling points and elevated reaction temperatures are required. Nevertheless, the yields reported are low in many cases. Alternative active derivatives of anthranilic acids, capable of reacting with nucleophiles under mild conditions, would be very useful for the preparation of various heterocyclic compounds possessing interesting biological properties.

Results and Discussion

In the course of our studies concerning the synthesis of quinoline derivatives, we elected to prepare the *N*-hydroxysuccinimide (HOSu) esters of anthranilic acids **1a–c** as starting materials in reactions with anions of β -keto esters to produce the 2-substituted 3-ethoxycarbonylquinolin-4-ones **4a–i**, as outlined in Chart 1.

The HOSu esters of many *N*-protected α -amino acids have been prepared¹⁴⁾ and found wide application in peptide synthesis. Especially, the HOSu ester of anthranilic acid (**2a**) has been found to be an efficient agent for 2-aminobenzoylation of amines.¹⁵⁾ According to the literature preparation, condensation of anthranilic acid with HOSu in the presence of *N,N'*-dicyclohexylcarbodiimide (DCC) and a catalytic quantity of 4-dimethylaminopyridine resulted the HOSu ester **2a** in 52% yield.¹⁵⁾ Recrystallization from propanol-1 was necessary to obtain the product in acceptable purity. Several attempts made to optimise this procedure gave no satisfactory results. The low yield may be attributed to the formation of

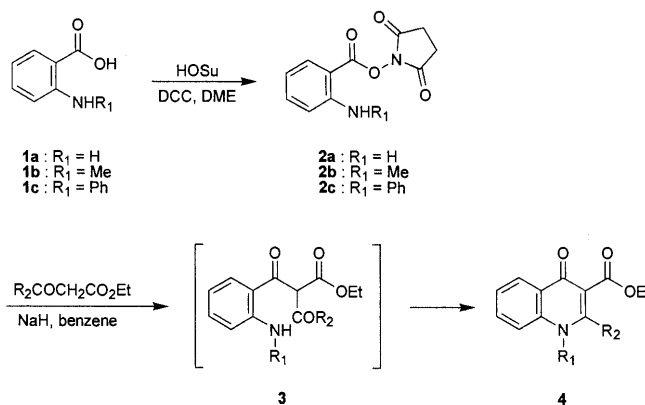
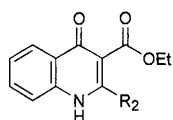


Chart 1

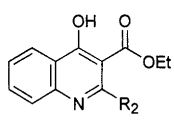
* To whom correspondence should be addressed.

Table 1. 3-Ethoxycarbonyl-4-oxoquinolines Obtained with the New Methodology

Product	R ¹	R ²	Method	Yield (%)	Product	R ¹	R ²	Method	Yield (%)
4a	H	Me	A	34	4g	Ph	Me	A	65
4b	H	Pr ⁿ	A	28	4g	Ph	Me	B	72
4c	H	Ph	A	13	4h	Ph	Pr ⁿ	A	55
4d	M	Me	A	26	4h	Ph	Pr ⁿ	B	64
4e	Me	Pr ⁿ	A	40	4i	Ph	Ph	A	60
4f	Me	Ph	A	51	4i	Ph	Ph	B	74



4-Oxoquinoline



4-Hydroxyquinoline

Fig. 1

polyamide products due to partial intermolecular condensation of the active aminoester. In the case of the *N*-substituted anthranilic acids we expected that the secondary amino group would display low nucleophilicity and further protection prior the active ester formation would be unnecessary. Actually, application of a standard protocol involving the condensation of equimolar amounts of **1b** (or **1c**) and HOSu in the presence of 1 eq of DCC afforded the active ester **2b** (or **2c**) in high yield (88 and 76% for **2b** and **2c** respectively). The HOSu esters **2b** and **2c** produced with this procedure were pure solids and could be used without further purification. These products proved to be stable for a long period, even under storage at room temperature.

The reactions of active esters **2a–c** with anions of β -keto esters were performed using a three-fold excess of the β -keto ester and sodium hydride (method A). At least one eq excess of the anion is required to react with the highly acidic methine proton of the tricarbonyl compounds **3**. Under these conditions the *C*-acylation products **3** undergo spontaneous cyclization to the desired quinolones **4**. This cyclization clearly involves attack of the amine nucleophile to the ketonic group of the intermediate **3** and subsequent dehydration produces 3-ethoxycarbonyl-4-oxoquinolines **4**. The alternative reaction path involving attack at the ester carbonyl of the intermediate **3** would afford 3-acyl-4-hydroxyquinolin-2-ones. However, formation of quinolin-2-ones was not observed. The *N*-substituted 4-oxoquinolines **4d–i** were isolated by evaporation of the solvent *in vacuo* after washing the reaction mixture with water to remove the water-soluble byproduct HOSu and the excess of the β -keto ester. Quinolones **4a–c** possessing an acidic proton were extracted in water and precipitated after acidification of the aqueous extract. Attempts to isolate intermediates **3** were unsuccessful. These compounds may be water-soluble or unstable to the work-up procedure.

Under the conditions mentioned above, reasonable yields of quinolin-4-ones **4** were obtained only after prolonged reaction times. Modification of the reaction conditions in the case of the *N*-phenyl active ester **2c** resulted in the formation of quinolones **4g–i** in shorter reaction times (method B). Thus, ester **2c** was stirred with 2.2 eq of the anion of ethyl acetoacetate at room temperature for 2 h, then the tempera-

ture was raised slowly to 80 °C and the mixture refluxed for 1 h. Work-up afforded compound **4g** in good yield. The obtained yields are summarized in Table 1.

Although compounds **4d–i**, bearing a substituent on N-1, clearly possess a 4-oxoquinoline structure, compounds **4a–c** may also adopt the tautomeric 4-hydroxyquinoline structure as shown in Fig. 1.

The structure of compounds **4a–i** was established based on IR and NMR spectral data. The IR spectra of compounds **4d–i** in Nujol show absorptions at 1710–1730 cm⁻¹ for the ester carbonyl and 1620 cm⁻¹ for the ring carbonyl, as expected for their 3-ethoxycarbonyl-4-oxoquinoline structure. The presence of similar absorptions at 1710–1720 cm⁻¹ and 1630–1640 cm⁻¹ for compounds **4a–c**, indicates a 4-quinolone structure for these derivatives, as well. This assignment is in agreement with previously published¹⁶⁾ structural studies of related *N*-unsubstituted derivatives.

The structure of quinolones **4a–i** in solution was studied by ¹H- and ¹³C-NMR spectroscopy. The proton NMR spectra of compounds **4a–c** exhibit a broad signal approximately at 12 ppm which can be assigned either as a NH or an enolic OH proton of the 4-oxo- or 4-hydroxyquinoline form, respectively. Although, proton NMR spectral data do not serve to discriminate the two possible tautomeric forms, ¹³C-NMR data (see Table 2) indicate the existence of compounds **4a–c** in the 4-oxoquinoline form in solution. The ¹³C chemical shifts of **4a–c** have no significant difference from the corresponding *N*-substituted compounds indicating a similar structure for all these compounds. Furthermore, the C-4a signals of compounds **4a–c** appear approximately at 125 ppm, a value representative of 4-oxoquinoline derivatives.¹⁷⁾

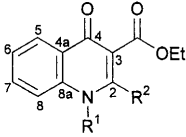
Conclusion

In summary, the synthetically and biologically interesting title compounds can be prepared in one step under mild conditions and in good yields. The proposed methodology provides useful intermediates for the synthesis of more complex substrates in the “quinolone” series.

Experimental

Melting points were determined on a Gallenkamp MFB-595 melting point apparatus and are uncorrected. The IR spectra were recorded on a Perkin-Elmer 267 spectrometer. The NMR spectra were recorded on a Gemini-2000 300 MHz spectrometer. Chemical shifts are quoted in ppm (s=singlet, d=doublet, t=triplet, q=quartet, dd=doublet of doublets, m=multiplet).

2-Aminobenzoic Acid 2,5-Dioxopyrrolidin-1-yl Ester 2a Following the literature procedure¹⁵⁾ the title compound was obtained in 42% yield as a yellow solid, mp 158–162 °C (from 1-propanol) (lit.¹⁵⁾ mp 161.5–163 °C). IR (Nujol) cm⁻¹: 3480 (ν_{as} NH₂), 3430 (ν_s NH₂), 1730 (C=O, ester and imide). ¹H-NMR (CDCl₃) δ : 2.89 [4H, s, (CH₂)₂], 5.65 (2H, s, NH₂), 6.64–6.70 (2H, m, 5-H, 3-H), 7.35 (1H, pseudotriplet, 4-H), 7.97 (1H, dd, *J*_{5,6}=8.8 Hz, *J*_{4,6}=1.5 Hz, 6-H). ¹³C-NMR (CDCl₃) δ : 25.5 [(CH₂)₂], 105.1 (C-1), 116.7, 116.8 (C-3, C-5), 131.2 (C-6), 136.3 (C-4), 151.9 (C-2), 162.8 (ArCO), 169.8 (CON).

Table 2. ^{13}C NMR Spectral Data for 3-Ethoxycarbonyl-4-oxoquinolines **4a–i**


	C-2	C-3	C-4	C-4a	C-5	C-6	C-7	C-8	C-8a	CO ₂ Et	CH ₂	CH ₃	R ¹ and R ²
4a	149.0	114.9	173.6	124.7	125.2	123.8	132.3	118.1	139.3	167.0	60.3	14.0	18.0 (2-CH ₃)
4b	154.8	115.3	176.1	125.4	125.8	124.6	132.6	119.4	140.1	167.8	61.2	14.2	35.0—23.0—13.9 (2-Pr ⁿ)
4c	149.6	115.7	173.9	124.8	125.1	124.2	132.6	118.9	139.7	166.4	60.2	13.6	133.9—130.4—128.8—128.4 (2-Ph)
4d	149.3	118.5	174.3	126.4	126.8	123.9	132.6	115.4	141.2	168.0	61.3	14.1	34.5 (N-CH ₃), 19.1 (2-CH ₃)
4e	152.6	118.7	174.7	126.6	127.1	124.0	132.7	115.5	141.5	168.0	61.4	14.1	34.5 (N-CH ₃), 34.1—22.3—14.0 (2-Pr ⁿ)
4f	152.3	119.2	174.1	126.9	127.2	124.3	132.9	116.0	141.2	166.4	60.8	13.6	37.0 (N-CH ₃), 133.6—129.9—128.8 (2-Ph)
4g	149.3	118.0	174.6	125.7	126.4	124.0	132.1	117.7	142.2	167.7	61.4	14.1	19.6 (2-CH ₃), 138.7—130.7—130.0—129.0 (N-Ph)
4h	153.2	117.8	174.9	125.8	126.4	124.1	132.1	118.1	142.4	167.8	61.4	14.1	33.8—22.9—14.1 (2-Pr ⁿ), 138.4—130.5—130.1—129.5 (N-Ph)
4i	151.8	119.1	124.6	126.2	126.7	124.4	132.4	118.2	142.1	166.3	60.9	13.5	138.7—133.3—130.1—129.7—129.6—129.2—129.0—127.7 (N-, 2-Ph)

2-Methylaminobenzoic Acid 2,5-Dioxopyrrolidin-1-yl Ester 2b A solution of DCC (2.5 mmol, 5.16 g) in 1,2-dimethoxyethane (DME) (15 ml) was added dropwise over a period of 20 min to a solution of *N*-methylanthranilic acid (2.5 mmol, 3.78 g) and HOSu (2.5 mmol, 2.88 g) in DME (50 ml) under cooling in an ice-water bath. The mixture was stirred at room temperature for 48 h and the precipitated solid was filtered off and washed with DME. The filtrate was evaporated *in vacuo* and the solid residue treated with diethyl ether, filtered off and washed with diethyl ether to afford compound **2b** as a yellow solid (5.46 g, 88%), mp 142—146 °C. *Anal.* Calcd for C₁₂H₁₂N₂O₄: C, 58.06; H, 4.87; N, 11.29. Found: C, 57.97; H, 4.87; N, 11.29. IR (Nujol) cm⁻¹: 3430 (NH), 1720 (C=O, ester and imide). ¹H-NMR (CDCl₃) δ: 2.87 [4H, s, (CH₂)₂], 2.90 (3H, d, *J*=4.4 Hz, NCH₃), 6.63 (1H, pseudotriplet, 5-H), 6.69 (1H, d, *J*_{3,4}=8.3 Hz, 3-H), 7.19 (1H, s, NH), 7.46 (1H, pseudotriplet, 4-H), 8.02 (1H, dd, *J*_{5,6}=8.3 Hz, *J*_{4,6}=1.5 Hz, 6-H). ¹³C-NMR (CDCl₃) δ: 25.5 [(CH₂)₂], 29.4 (NCH₃), 104.2 (C-1), 111.1 (C-3), 114.9 (C-5), 131.7 (C-6), 136.8 (C-4), 153.1 (C-2), 163.3 (ArCO), 169.9 (CON).

2-Phenylaminobenzoic Acid 2,5-Dioxopyrrolidin-1-yl Ester 2c A solution of DCC (2.5 mmol, 5.16 g) in DME (15 ml) was added dropwise over a period of 20 min to a solution of *N*-phenylanthranilic acid (2.5 mmol, 5.34 g) and HOSu (2.5 mmol, 2.88 g) in DME (80 ml) under cooling in an ice-water bath. The mixture was stirred at room temperature for 24 h and the precipitated solid was filtered off and washed with DME. The filtrate was evaporated *in vacuo*, the oily residue was treated with diethyl ether and the formed solid was filtered off and washed with diethyl ether to afford compound **2c** as a green solid (5.92 g, 76%), mp 126—128 °C (from 2-propanol). *Anal.* Calcd for C₁₇H₁₄N₂O₄: C, 65.80; H, 4.55; N, 9.03. Found: C, 65.59; H, 4.64; N, 9.19. IR (Nujol) cm⁻¹: 3350 (NH), 1720 (C=O, ester and imide). ¹H-NMR (CDCl₃) δ: 2.91 [4H, s, (CH₂)₂], 6.76 (1H, pseudotriplet, 5-H), 7.12—7.42 (7H, m, 3-H, 4-H, NPh), 8.11 (1H, dd, *J*_{5,6}=8.3, *J*_{4,6}=1.5 Hz, 6-H), 8.86 (1H, s, NH). ¹³C-NMR (CDCl₃) δ: 25.6 [(CH₂)₂], 106.0 (C-1), 114.0 (C-3), 117.4 (C-5), 123.7 (C-2'), 124.8 (C-4'), 129.6 (C-3'), 131.7 (C-6), 136.8 (C-4), 139.7 (C-1'), 149.7 (C-2), 163.3 (ArCO), 169.7 (CON).

General Procedures for the Preparation of 2-Substituted 4-Oxoquinoline-3-carboxylic Acid Ethyl Esters **4a–i**.

Method A: The appropriate β-keto ester (7.5 mmol) was added dropwise to a dispersion of sodium hydride (55—60% sodium hydride in oil; 7.5 mmol) in anhydrous benzene (30 ml) and the thick slurry thus formed was stirred at room temperature for 1 h. The active ester **2** (2.5 mmol) was added and the mixture stirred at room temperature for 3—5 d. a) Compounds **4a–c**: The reaction mixture was extracted twice with water and the combined aqueous extracts acidified with 10% hydrochloric acid under cooling in an ice-water bath. The precipitated product was collected by filtration and washed with ice-cold water. b) Compounds **4d–i**: The reaction mixture was extracted once with a small amount of water (*ca.* 5 ml), the organic phase was dried over sodium sulfate and evaporated *in vacuo* to afford an oily residue which crystallized after standing at room temperature for 2—3 d.

Method B: The appropriate β-keto ester (2.2 mmol) was added dropwise to a dispersion of sodium hydride (60% sodium hydride in oil; 2.2 mmol) in anhydrous benzene (15 ml) and the thick slurry thus formed was stirred at

room temperature for 1 h. The active ester **2c** (1.0 mmol) was added, the mixture was stirred at room temperature for 2 h, then the temperature was raised slowly to 80 °C and the mixture was refluxed for 1 h. After cooling to room temperature the reaction mixture was extracted with a small amount of water (*ca.* 5 ml), the organic phase was dried over sodium sulfate and evaporated *in vacuo* to afford an oily residue which crystallized after standing at room temperature for 2—3 d.

1,4-Dihydro-2-methyl-4-oxoquinoline-3-carboxylic Acid Ethyl Ester

4a The reaction mixture [compound **2a** (0.78 g, 3.3 mmol), ethyl acetoacetate (1.30 g, 10 mmol) and sodium hydride (55—60% sodium hydride in oil; 0.44 g, 10 mmol) in anhydrous benzene (40 ml)] was stirred for 3 d and worked-up according to procedure (a) to afford the title compound as a beige solid (0.26 g, 34%), mp 233—234 °C (from methanol) (lit.¹⁶) mp 231—232 °C. IR (Nujol) cm⁻¹: 3280 (NH), 1710 (C=O, ester), 1640 (C=O, ketone), 1610 (C=C). ¹H-NMR (DMSO-*d*₆) δ: 1.24 (3H, t, *J*=7.0 Hz, CH₂CH₃), 2.37 (3H, s, CH₃), 4.21 (2H, q, *J*=7.0 Hz, CH₂CH₃), 7.32 (1H, pseudotriplet, 6-H), 7.51 (1H, d, *J*_{7,8}=8.2 Hz, 8-H), 7.65 (1H, pseudotriplet, 7-H), 8.04 (1H, dd, *J*_{5,6}=7.9 Hz, *J*_{5,7}=1.3 Hz, 5-H), 11.85 (1H, s, NH).

1,4-Dihydro-4-oxo-2-propylquinoline-3-carboxylic Acid Ethyl Ester

4b The reaction mixture [compound **2a** (1.18 g, 5.0 mmol), ethyl butyrylacetate (2.38 g, 15 mmol) and sodium hydride (55—60% sodium hydride in oil; 0.65 g, 15 mmol) in anhydrous benzene (45 ml)] was stirred for 2 d and worked-up according to procedure (a) to afford compound **4b** as a white solid (0.36 g, 28%), mp 215—216 °C (from dichloromethane-light petroleum). *Anal.* Calcd for C₁₅H₁₇NO₃: C, 69.48; H, 6.61; N, 5.40. Found: C, 69.40; H, 6.61; N, 5.36. IR (Nujol) cm⁻¹: 1720 (C=O, ester), 1630 (C=O, ketone), 1610 (C=C). ¹H-NMR (CDCl₃) δ: 0.87 (3H, t, *J*=7.3 Hz, CH₂CH₂CH₃), 1.23 (3H, t, *J*=7.0 Hz, OCH₂CH₃), 1.78 (2H, m, CH₂CH₂CH₃), 2.82 (2H, m, CH₂CH₂CH₃), 4.21 (2H, q, *J*=7.0 Hz, OCH₂CH₃), 7.34 (1H, pseudotriplet, 6-H), 7.60 (1H, pseudotriplet, 7-H), 7.78 (1H, d, *J*_{7,8}=8.5 Hz, 8-H), 8.34 (1H, dd, *J*_{5,6}=8.2 Hz, *J*_{5,7}=1.3 Hz, 5-H), 12.06 (1H, s, NH).

1,4-Dihydro-4-oxo-2-phenylquinoline-3-carboxylic Acid Ethyl Ester

4c The reaction mixture [compound **2a** (0.94 g, 4.0 mmol), ethyl benzoylacetate (2.31 g, 12 mmol) and sodium hydride (60% sodium hydride in oil; 0.48 g, 12 mmol) in anhydrous benzene (40 ml)] was stirred for 3 d and worked-up according to procedure (a) to afford the title compound as a yellow solid (0.24 g, 20%), mp 265—267 °C (from methanol). *Anal.* Calcd for C₁₈H₁₅NO₃: C, 73.71; H, 5.15; N, 4.78. Found: C, 73.64; H, 5.12; N, 4.80. IR (Nujol) cm⁻¹: 3100 (NH), 1710 (C=O, ester), 1610 (C=C, C=O, ketone). ¹H-NMR (DMSO-*d*₆) δ: 0.88 (3H, t, *J*=7.0 Hz, CH₂CH₃), 3.94 (2H, q, *J*=7.0 Hz, CH₂CH₃), 7.39 (1H, pseudotriplet, 6-H), 7.52—7.78 (7H, m, 7-H, 8-H, Ph), 8.04 (1H, dd, *J*_{5,6}=7.9 Hz, *J*_{5,7}=1.0 Hz, 5-H), 12.06 (1H, s, NH).

1,4-Dihydro-1,2-dimethyl-4-oxoquinoline-3-carboxylic Acid Ethyl Ester

4d The reaction mixture [compound **2b** (0.62 g, 2.5 mmol), ethyl acetoacetate (0.99 g, 7.6 mmol) and sodium hydride (55—60% sodium hydride in oil; 0.33 g, 7.6 mmol) in anhydrous benzene (30 ml)] was stirred for 3 d and worked-up according to procedure (b) to afford the title compound as a white solid (0.16 g, 26%), mp 143—144 °C (from dichloromethane-light petroleum) (lit.¹³) mp 142—144 °C. IR (Nujol) cm⁻¹: 1720 (C=O, ester),

1620 (C=O, ketone), 1600 (C=C). ¹H-NMR (CDCl₃) δ: 1.37 (3H, t, *J*=7.1 Hz, CH₂CH₃), 2.46 (3H, s, CH₃), 3.69 (3H, s, NCH₃), 4.39 (2H, q, *J*=7.1 Hz, CH₂CH₃), 7.30 (1H, pseudotriplet, 6-H), 7.41 (1H, d, *J*_{7,8}=8.8 Hz, 8-H), 7.59 (1H, pseudotriplet, 7-H), 8.35 (1H, dd, *J*_{5,6}=7.8 Hz, *J*_{5,7}=1.5 Hz, 5-H).

1,4-Dihydro-1-methyl-4-oxo-2-propylquinoline-3-carboxylic Acid Ethyl Ester 4e The reaction mixture [compound **2b** (0.62 g, 2.5 mmol), ethyl butyrylacetate (1.20 g, 7.6 mmol) and sodium hydride (55–60% sodium hydride in oil; 0.33 g, 7.6 mmol) in anhydrous benzene (30 ml)] was stirred for 3 d and worked-up according to procedure (b) to afford compound **4e** as a white solid (0.27 g, 40%), mp 103–105 °C (from diethyl ether) (lit.¹³) mp 102–104 °C. IR (Nujol) cm⁻¹: 1720 (C=O, ester), 1630 (C=O, ketone), 1600 (C=C). ¹H-NMR (CDCl₃) δ: 1.06 (3H, t, *J*=7.3 Hz, CH₂CH₂CH₃), 1.39 (3H, t, *J*=7.1 Hz, OCH₂CH₃), 1.76 (2H, m, CH₂CH₂CH₃), 2.75 (2H, m, CH₂CH₂CH₃), 3.76 (3H, s, NCH₃), 4.42 (2H, q, *J*=7.1 Hz, OCH₂CH₃), 7.38 (1H, pseudotriplet, 6-H), 7.51 (1H, d, *J*_{7,8}=8.8 Hz, 8-H), 7.67 (1H, pseudotriplet, 7-H), 8.45 (1H, dd, *J*_{5,6}=7.8 Hz, *J*_{5,7}=1.5 Hz, 5-H).

1,4-Dihydro-1-methyl-4-oxo-2-phenylquinoline-3-carboxylic Acid Ethyl Ester 4f The reaction mixture [compound **2b** (0.62 g, 2.5 mmol), ethyl benzoylacetate (1.46 g, 7.6 mmol) and sodium hydride (55–60% sodium hydride in oil; 0.33 g, 7.6 mmol) in anhydrous benzene (30 ml)] was stirred for 3.5 d and worked-up according to procedure (b) to afford the title compound as a beige solid (0.39 g, 51%), mp 164–169 °C (from dichloromethane-light petroleum) (lit.¹³) mp 167–168 °C. IR (Nujol) cm⁻¹: 1730 (C=O, ester), 1620 (C=O, ketone), 1600 (C=C). ¹H-NMR (CDCl₃) δ: 0.89 (3H, t, *J*=7.1 Hz, CH₂CH₃), 3.51 (3H, s, NCH₃), 3.96 (2H, q, *J*=7.1 Hz, CH₂CH₃), 7.36–7.51 (6H, m, 6-H, Ph), 7.53 (1H, d, *J*_{7,8}=8.3 Hz, 8-H), 7.70 (1H, pseudotriplet, 7-H), 8.50 (1H, dd, *J*_{5,6}=7.8 Hz, *J*_{5,7}=1.5 Hz, 5-H).

1,4-Dihydro-2-methyl-4-oxo-1-phenylquinoline-3-carboxylic Acid Ethyl Ester 4g

(i) Following Method A: The reaction mixture [compound **2c** (0.78 g, 2.5 mmol), ethyl acetoacetate (0.98 g, 7.5 mmol) and sodium hydride (60% sodium hydride in oil; 0.30 g, 7.5 mmol) in anhydrous benzene (30 ml)] was stirred for 5 d and worked-up according to procedure (b) to afford the title compound as a beige solid (0.50 g, 65%).

(ii) Following Method B: The reaction mixture [compound **2c** (0.59 g, 1.9 mmol), ethyl acetoacetate (0.55 g, 4.2 mmol) and sodium hydride (60% sodium hydride in oil; 0.17 g, 4.2 mmol) in anhydrous benzene (20 ml)] was stirred at room temperature for 2 h and under reflux for 1 h. Work-up according to procedure (b) afforded the title compound as a beige solid (0.42 g, 72%), mp 132–137 °C (from diethylether). *Anal.* Calcd for C₁₉H₁₇NO₃: C, 74.25; H, 5.58; N, 4.56. Found: C, 74.39; H, 5.65; N, 4.46. IR (Nujol) cm⁻¹: 1710 (C=O, ester), 1620 (C=O, ketone), 1600 (C=C). ¹H-NMR (CDCl₃) δ: 1.41 (3H, t, *J*=7.3 Hz, CH₂CH₃), 2.12 (3H, s, CH₃), 4.44 (2H, q, *J*=7.3 Hz, CH₂CH₃), 6.62 (1H, d, *J*=7.8 Hz, 8-H), 7.24–7.46 (4H, m, 6-H, NPh), 7.57–7.69 (3H, m, 7-H, NPh), 8.45 (1H, dd, *J*_{5,6}=7.8 Hz, *J*_{5,7}=1.5 Hz, 5-H).

1,4-Dihydro-4-oxo-1-phenyl-2-propylquinoline-3-carboxylic Acid Ethyl Ester 4h

(i) Following Method A: The reaction mixture [compound **2c** (0.78 g, 2.5 mmol), ethyl butyrylacetate (1.19 g, 7.5 mmol) and sodium hydride (60% sodium hydride in oil; 0.30 g, 7.5 mmol) in anhydrous benzene (30 ml)] was stirred for 7 d and worked-up according to procedure (b) to afford the title compound as a white solid (0.46 g, 55%).

(ii) Following Method B: The reaction mixture [compound **2c** (0.31 g, 1.0 mmol), ethyl butyrylacetate (0.35 g, 2.2 mmol) and sodium hydride (60% sodium hydride in oil; 0.09 g, 2.2 mmol) in anhydrous benzene (15 ml)] was stirred at room temperature for 2 h and under reflux for 1 h. Work-up according to procedure (b) afforded the title compound as a white solid (0.33 g, 64%), mp 157–159 °C (from diethyl ether). *Anal.* Calcd for C₂₁H₂₁NO₃: C, 75.20; H, 6.31; N, 4.18. Found: C, 75.26; H, 6.34; N, 4.14. IR (Nujol) cm⁻¹: 1730 (C=O, ester), 1620 (C=O, ketone), 1600 (C=C). ¹H-NMR (CDCl₃) δ: 0.71 (3H, t, *J*=7.3 Hz, CH₂CH₂CH₃), 1.40 (3H, t, *J*=7.1 Hz, OCH₂CH₃), 1.54 (2H, m, CH₂CH₂CH₃), 2.40 (2H, m, CH₂CH₂CH₃), 4.43 (2H, q, *J*=7.1 Hz, OCH₂CH₃), 6.57 (1H, d, *J*=8.3 Hz, 8-H), 7.27–7.44 (4H, m, 6-H, NPh), 7.58–7.69 (3H, m, 7-H, NPh), 8.44 (1H, dd, *J*_{5,6}=7.8 Hz, *J*_{5,7}=2.0 Hz, 5-H).

1,4-Dihydro-1,2-diphenyl-4-oxoquinoline-3-carboxylic Acid Ethyl Ester 4i

(i) Following Method A: The reaction mixture [compound **2c** (0.78 g, 2.5 mmol), ethyl benzoylacetate (1.45 g, 7.5 mmol) and sodium hydride (60% sodium hydride in oil; 0.30 g, 7.5 mmol) in anhydrous benzene (30 ml)] was

stirred for 7 d and worked-up according to procedure (b) to afford compound **4i** as a white solid (0.56 g, 60%).

(ii) Following Method B: The reaction mixture [compound **2c** (0.31 g, 1.0 mmol), ethyl benzoylacetate (0.43 g, 2.2 mmol) and sodium hydride (60% sodium hydride in oil; 0.09 g, 2.2 mmol) in anhydrous benzene (15 ml)] was stirred at room temperature for 2 h and under reflux for 1 h. Work-up according to procedure (b) afforded the title compound as a white solid (0.27 g, 74%), mp 222–223 °C (from diethyl ether). *Anal.* Calcd for C₂₄H₁₉NO₃: C, 78.03; H, 5.18; N, 3.79. Found: C, 78.16; H, 5.19; N, 3.91. IR (Nujol) cm⁻¹: 1730 (C=O, ester), 1620 (C=O, ketone), 1600 (C=C). ¹H-NMR (CDCl₃) δ: 0.89 (3H, t, *J*=7.1 Hz, CH₂CH₃), 4.00 (2H, q, *J*=7.1 Hz, CH₂CH₃), 6.79 (1H, d, *J*=8.3 Hz, 8-H), 7.08–7.51 (12H, m, 6-H, 7-H, 2-Ph, NPh), 8.53 (1H, dd, *J*_{5,6}=7.8 Hz, *J*_{5,7}=1.5 Hz, 5-H).

Acknowledgements We wish to thank the Committee of Research of the National Technical University of Athens for a doctoral assistantship (C. M.).

References

- Recent publications: a) Hong C. Y., Kim S. H., Kim Y. K., *Bioorg. Med. Chem. Lett.*, **7**, 1875–1878 (1997); b) MacDonald A. A., DeWitt S. H., Hogan E. M., Ramage R., *Tetrahedron Lett.*, **37**, 4815–4818 (1996); c) Todo Y., Nitta J., Miyajima M., Fukuoka Y., Yamashiro Y., Nishida N., Saikawa I., Narita H., *Chem. Pharm. Bull.*, **42**, 2063–2070 (1994).
- Mizzoni R. H., Goble F., Szanto J., Maplesden D. C., Brown J. E., Boxer J., De Stevens G., *Experientia*, **24**, 1188–1199 (1968).
- Sukhova N. M., Lapina T. V., Lidak M. Yu., *Chem. Heterocycl. Comp.*, **19**, 1207–1210 (1984).
- Coats E. A., Shah K. J., Milstein S. R., Genther C. S., Nene D. M., Roesener J., Schmidt J., Pleiss M., Wagner E., Baker J. K., *J. Med. Chem.*, **25**, 57–63 (1982).
- Graybill T. L., Dolle R. E., Osifo I. K., Schmidt S. J., Gregory J. S., Harris A. L., Miller M. S., *Bioorg. Med. Chem. Lett.*, **5**, 387–392 (1995).
- a) Wentland M. P., Perni R. B., Dorff P. H., Brundage R. P., Castaldi M. J., Bailey T. R., Carabateas P. M., Bacon E. R., Young D. C., Woods M. G., Rosi D., Drozd M. L., Kullnig R. K., Dutko F. J., *J. Med. Chem.*, **36**, 1580–1596 (1993); b) Wentland M. P., Carlson J. A., Dorff P. H., Aldous S. C., Perni R. B., Young D. C., Woods M. G., Kingsley S. D., Ryan K. A., Rosi D., Drozd M. L., Dutko F. J., *ibid.*, **38**, 2541–2545 (1995).
- a) Schroeder M. C., Kiely J. S., *J. Heterocycl. Chem.*, **25**, 1769–1772 (1988); b) Matsuoka M., Segawa J., Makita Y., Ohmachi S., Kashima T., Nakamura K., Hattori M., Kitano M., Kise M., *ibid.*, **34**, 1773–1779 (1997).
- Clemence F., Le Martret O., Delevallee F., Benzoni J., Jouanen A., Jouquey S., Mouren M., Deraedt R., *J. Med. Chem.*, **31**, 1453–1462 (1988).
- Hayashi H., Miwa Y., Ichikawa S., Yoda N., Miki I., Ishii A., Kono M., Yasuzawa T., Suzuki F., *J. Med. Chem.*, **36**, 617–626 (1993).
- a) Mitsos C., Zografos A., Igglessi-Markopoulou O., *Heterocycles*, **51**, 1543–1562 (1999); b) Zografos A., Mitsos C., Igglessi-Markopoulou O., *ibid.*, **51**, 1609–1623 (1999).
- Rowley M., Leeson P. D., Stevenson G. I., Moseley A. M., Stansfield I., Sanderson I., Robinson L., Baker R., Kemp J. A., Marshall G. R., Foster A. C., Grimwood S., Tricklebank M. D., Saywell K. L., *J. Med. Chem.*, **36**, 3386–3396 (1993).
- a) Kiely J. S., Huang S., Lesheski L. E., *J. Heterocycl. Chem.*, **26**, 1675–1681 (1989); b) Clemence F., Le Martret O., Collard J., *ibid.*, **21**, 1345–1353 (1984).
- Coppola G. M., Hardtmann G. E., *J. Heterocycl. Chem.*, **16**, 1605–1610 (1979).
- Anderson G. W., Zimmerman J. E., Callahan F. M., *J. Am. Chem. Soc.*, **86**, 1839–1842 (1964).
- Hinman C., Vaughan K., *Synthesis*, **1980**, 719–721.
- Kononov L. I., Veinberg G. A., Liepin'sh E. E., Dipan I. V., Sukhova N. M., Lukevits E., *Chem. Heterocycl. Comp.*, **24**, 765–771 (1989).
- Coppola G. M., Kahle A. D., Shapiro M. J., *Org. Magn. Res.*, **17**, 242–245 (1981).

Synthesis and Pharmacokinetics of 1α -Hydroxyvitamin D₃ Tritiated at 22 and 23 Positions Showing High Specific Radioactivity

Akira KAWASE,^a Fumihiko ICHIKAWA,^a Nobuo KOIKE,^a Shinichi KAMACHI,^a Walter E. STUMPF,^b Yasuho NISHII,^a and Noboru KUBODERA^{*,a}

Chugai Pharmaceutical Co., Ltd.,^a 2-1-9, Kyobashi, Chuo-ku Tokyo 104-8301, Japan and International Institute of Drug Distribution, Cytopharmacology and Cytotoxicology,^b 2612 Damascus Church Rd. Chapel Hill, NC 27516, U.S.A.

Received July 28, 1999; accepted October 28, 1999

A novel synthesis of a radioactive compound of 1α -hydroxyvitamin D₃ ($1\alpha\text{OHD}_3$) (1) and its pharmacokinetics are described. Radioactive $1\alpha\text{OHD}_3$ tritiated at 22 and 23 positions ($[22,23\text{-}^3\text{H}_4]1\alpha\text{OHD}_3$) (5) was prepared via key reactions of the reduction of acetylenic side chain in the ketone (12) with tritium gas in the presence of palladium-charcoal and the subsequent Wittig reaction with the A-ring synthon (16). $[22,23\text{-}^3\text{H}_4]1\alpha\text{OHD}_3$ (5) showed high specific radioactivity (111.5 Ci/mmol) and was used successfully in pharmacokinetics studies with rats. In the pharmacokinetics studies, the plasma concentration level of the active form of vitamin D₃, $1\alpha,25$ -dihydroxyvitamin D₃ [$1\alpha,25(\text{OH})_2\text{D}_3$] (2), after oral or intravenous administration of $[22,23\text{-}^3\text{H}_4]1\alpha\text{OHD}_3$ (5), showed longer half-life, lower maximum concentration, and lower area under the curve than those after treatment of $1\alpha,25(\text{OH})_2\text{D}_3$ tritiated at 26 and 27 positions (4). These results might suggest a beneficial therapeutic utility of $1\alpha\text{OHD}_3$ (1) over the treatment of $1\alpha,25(\text{OH})_2\text{D}_3$ (2).

Key words $1\alpha,25$ -dihydroxyvitamin D₃; 1α -hydroxyvitamin D₃; pharmacokinetics; tritiated compound; tritium gas; specific radioactivity

Background 1α -Hydroxyvitamin D₃ ($1\alpha\text{OHD}_3$) (1) is now well known as a synthetic prodrug of $1\alpha,25$ -dihydroxyvitamin D₃ [$1\alpha,25(\text{OH})_2\text{D}_3$] (2), a hormonally active form of vitamin D₃,¹⁾ and has been used clinically for the treatment of rickets, hypovitaminosis, hypocalcemia, chronic renal failure, and osteoporosis.²⁾ Regarding pharmacokinetics and distribution studies of $1\alpha\text{OHD}_3$ (1),³⁾ administered radioactivity was simply traced using $1\alpha\text{OHD}_3$ tritiated at 2 position ($[2\text{-}^3\text{H}]1\alpha\text{OHD}_3$) (3) in which specific radioactivity was shown to be very low (4.2 Ci/mmol).⁴⁾ Detailed plasma concentration level of bioconverted $1\alpha,25(\text{OH})_2\text{D}_3$ (2) by the hydroxylation at 25 position of dosed $1\alpha\text{OHD}_3$ (1) has not been compared with $1\alpha,25(\text{OH})_2\text{D}_3$ level after administration of $1\alpha,25(\text{OH})_2\text{D}_3$ (2) itself. The non-availability of such important information about the bioconversion from a prodrug, $1\alpha\text{OHD}_3$ (1), to an active form, $1\alpha,25(\text{OH})_2\text{D}_3$ (2), has been due to lack of tritiated $1\alpha\text{OHD}_3$ possessing high specific radioactivity. We have also been interested in the relevance of tissue distribution studies and cytopharmacology with cellular autoradiography of $1\alpha\text{OHD}_3$ (1) to determine its mode-of-action in bone.⁵⁾ In microautoradiography experiments, $[2\text{-}^3\text{H}]1\alpha\text{OHD}_3$ (3) is, however, far from satisfactory due to quite low specific radioactivity.

Although the synthesis of $1\alpha,25(\text{OH})_2\text{D}_3$ tritiated at 26 and 27 positions ($[26,27\text{-}^3\text{H}_6]1\alpha,25(\text{OH})_2\text{D}_3$) (4) possessing high specific radioactivity is known, the preparative method for tritiated $1\alpha\text{OHD}_3$ with high specific radioactivity has never, to our knowledge, been reported. In this paper we describe: 1) a novel procedure for the preparation of $1\alpha\text{OHD}_3$ tritiated at 22 and 23 positions ($[22,23\text{-}^3\text{H}_4]1\alpha\text{OHD}_3$) (5) showing high specific radioactivity and 2) pharmacokinetics results of $1\alpha,25(\text{OH})_2\text{D}_3$ levels after administration of $[22,23\text{-}^3\text{H}_4]1\alpha\text{OHD}_3$ (5) to rats in comparison with after administration of $[26,27\text{-}^3\text{H}_6]1\alpha,25(\text{OH})_2\text{D}_3$ (4) (Chart 1).

Synthetic Results After many unsuccessful trials to convert commercially available $[26,27\text{-}^3\text{H}_6]1\alpha,25(\text{OH})_2\text{D}_3$ (4) to $1\alpha\text{OHD}_3$ tritiated at 26 and 27 positions by removal of the

hydroxy group at 25 position, we focused our synthetic strategy on the tritiation of the acetylenic side chain by the catalytic reduction using tritium gas. The key intermediate for the tritiation reaction should be the acetylenic derivative 12, which would be transformed to $[22,23\text{-}^3\text{H}_4]1\alpha\text{OHD}_3$ (5) via the Wittig reaction with the A-ring synthon (16) of active vitamin D₃ after tritiation (Chart 2).

The Inhoffen-Lythgoe diol (6),⁶⁾ prepared from vitamin D₂ by ozonolysis, was converted to the known aldehyde (7)⁶⁾ by acetylation of the primary hydroxy moiety in 6, silylation of the secondary hydroxy group, deacetylation by the reduction with lithium aluminum hydride (LiAlH_4), and oxidation of the resulting primary hydroxy group with pyridinium chlorochromate (PCC). The formyl group in 7 was transformed to the ketene dibromide (8) in 96% yield by Corey's method⁷⁾ using carbon tetrabromide (CBr_4) and triphenyl phosphine (PPh_3) in dichloromethane (CH_2Cl_2). The ketene dibromide (8) was treated with *n*-butyllithium (*n*-BuLi) at -78°C , followed by a reaction with isobutylaldehyde to yield the acetylenic alcohol (9), quantitatively.⁷⁾ Removal of the secondary hydroxy group in 9 by the Barton method,⁸⁾ *i.e.* initial formation of thioester by treatment with phenyl chlorothionoformate (PhOCSCl) and the subsequent reduction of the resulting thioester with tri-*n*-butyltin hydride (*n*-Bu₃SnH), was accomplished clearly to give a 98% yield of the acetylene (10). Desilylation of the protecting group in 10 by aqueous hydrochloric acid (HCl) in tetrahydrofuran (THF) gave the alcohol 11 in 68% yield, which was oxidized by PCC to afford the acetylenic ketone (12) in 56% yield.

Having obtained the key intermediate 12, catalytic hydrogenation was first carried out as a model experiment for tritiation reaction using tritium gas. Thus, hydrogenolysis of 12 in the presence of palladium-charcoal (Pd-C) in ethyl acetate (AcOEt) afforded the ketone (13), quantitatively. The ketone (13) was allowed to react with the A-ring synthon (16), prepared by Hatakeyama's method,⁹⁾ followed by desilylation with tetra-*n*-butylammonium fluoride (TBAF) to give

* To whom correspondence should be addressed.

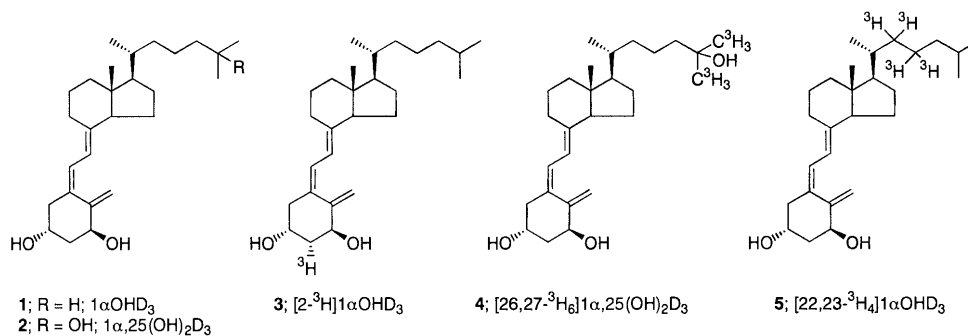
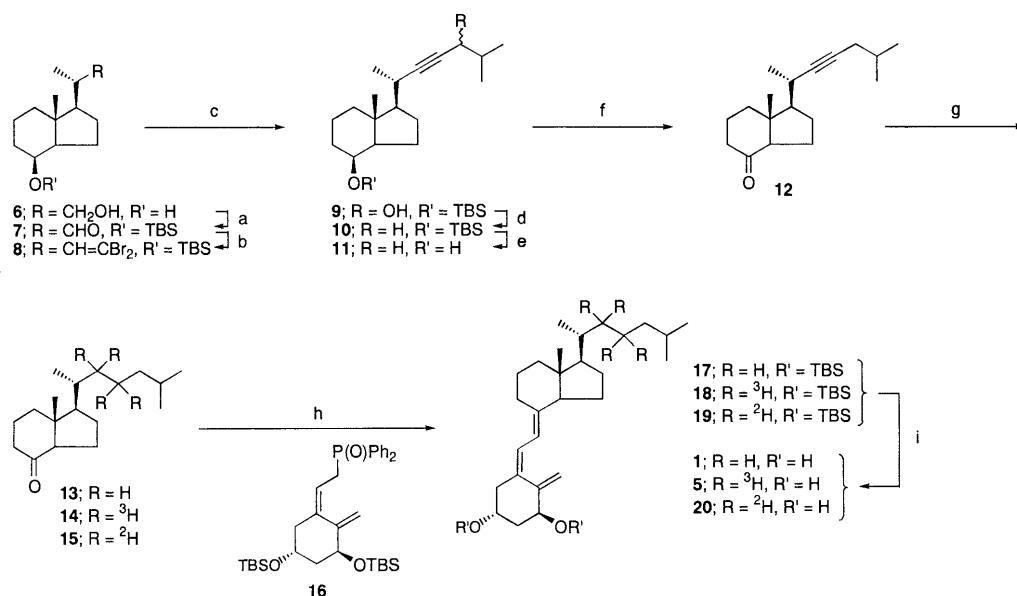


Chart 1



TBS = *tert*-butyldimethylsilyl. a) 1) Ac₂O/pyridine, 2) TBSCl, 3) LiAlH₄, 4) PCC; b) CBr₄/PPh₃; c) *n*-BuLi/isobutylaldehyde; d) 1) PhOCSCl/pyridine, 2) *n*-Bu₃SnH; e) aqueous HCl; f) PCC/Celite; g) H₂, ²H₂ or ³H₂/Pd-C/AcOEt; h) *n*-BuLi; i) TBAF

Chart 2

1 α OHD₃ (**1**), which was completely identical with authentic material.¹⁰⁾ The described thirteen-step synthesis from the Inhoffen-Lythgoe diol (**6**) to 1 α OHD₃ (**1**) provides a novel convergent method for the preparation of clinically important **1**.

The same reaction conditions as used in the hydrogenolysis of **12** were applied to prepare the tritiated ketone (**14**). The tritiation of the acetylenic part in **12** with tritium gas in the presence of Pd-C afforded the tritiated ketone (**14**) in 95% radiochemical purity with 116 Ci/mmol specific radioactivity. [22,23-³H₄]1 α OHD₃ (**5**) was obtained with 111.5 Ci/mmol (4125.5 GBq/mmol) specific radioactivity and 98% radiochemical purity by the Wittig reaction (17% yield) with the A-ring synthon (**16**) and the subsequent desilylation (48% yield) with TBAF. When deuterium gas was used instead of tritium gas, 1 α OHD₃ deuterated at 22 and 23 positions ([22,23-²H₄]1 α OHD₃) (**20**) was also obtained in a comparable yield (Chart 2). Since [22,23-³H₄]1 α OHD₃ (**5**) has high specific radioactivity, microautoradiography experiments of 1 α OHD₃ were carried out successfully using **5** and the results have been reported recently.¹¹⁾

Pharmacokinetics Results [22,23-³H₄]1 α OHD₃ (**5**) or [26,27-³H₆]1 α ,25(OH)₂D₃ (**4**) were given to Sprague-Dawley male rats (6-week-old) orally or intravenously at a dose of 5

nmol (*ca.* 2 μ g)/kg/50 μ Ci, respectively. The plasma levels of total radioactivity, 1 α ,25(OH)₂D₃ fraction and 1 α OHD₃ fraction (in case of [22,23-³H₄]1 α OHD₃ (**5**) administration) were determined at 5 min, 0.5, 1, 2, 3, 4, 6, 8, 10, 12, 24, 48 and 72 h after fractionation by HPLC. The results are shown in Fig. 1 for the administration of [22,23-³H₄]1 α OHD₃ (**5**) and Fig. 2 for [26,27-³H₆]1 α ,25(OH)₂D₃ (**4**). Calculated pharmacokinetics parameters, plasma half-life (*T*_{1/2}), maximum concentration (*C*_{max}), time at *C*_{max} (*T*_{max}) and area under the curve (*AUC*) are also summarized in Table 1.

Plasma concentration of 1 α ,25(OH)₂D₃ after oral or intravenous administration of [22,23-³H₄]1 α OHD₃ (**5**) showed longer *T*_{1/2}, lower *C*_{max}, and lower *AUC* than those after treatment of [26,27-³H₆]1 α ,25(OH)₂D₃ (**4**). In our radioassay experiments which were carried out separately from the present pharmacokinetics studies, 1 α ,25(OH)₂D₃ fraction in rat bone after 1 α OHD₃ treatment was sustained for longer than that after 1 α ,25(OH)₂D₃ treatment.¹¹⁾ We also confirmed in the microautoradiography studies that localization of radioactivity in bone after treatment with 1 α OHD₃ or 1 α ,25(OH)₂D₃ is observed in osteoblast nuclei.¹¹⁾ Radioactivity in the nuclei after 1 α OHD₃ treatment was also sustained longer than that after 1 α ,25(OH)₂D₃ treatment. Taking the results obtained in

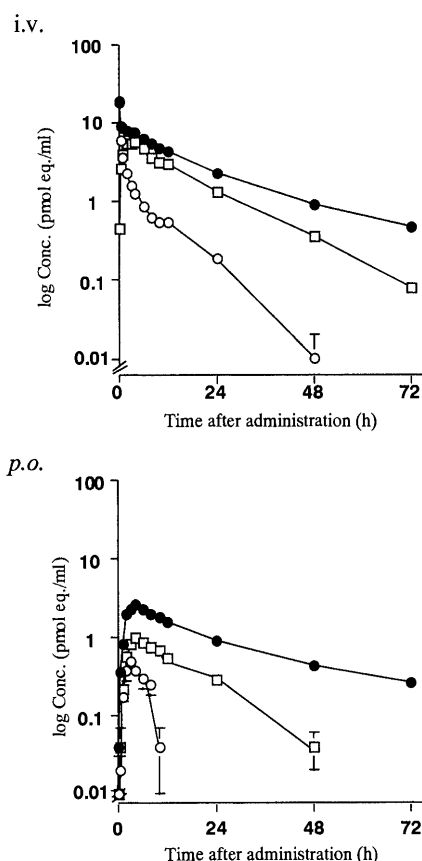


Fig. 1. Plasma Concentration of Radioactivity after Oral (*p.o.*) or Intravenous (*i.v.*) Administration of [22,23- $^3\text{H}_4$]1 α OHD $_3$ (5)

—●—: total radioactivity, —○—: 1 α OHD $_3$ fraction, —□—: 1 α ,25(OH) $_2$ D $_3$ fraction.

the present pharmacokinetics studies and the above-mentioned radioassay in bone and microautoradiography in osteoblast nuclei into consideration, treatment of a prodrug [1 α OHD $_3$ (1)] supplies bone with an active form of drug [1 α ,25(OH) $_2$ D $_3$ (2)] more steadily and stably than those of 1 α ,25(OH) $_2$ D $_3$ (2) treatment. Although these results might suggest a beneficial therapeutic utility of a prodrug [1 α OHD $_3$ (1)] over treatment of an active form of vitamin D $_3$ [1 α ,25(OH) $_2$ D $_3$ (2)], further basic and clinical trials are necessary to clarify the disparate characters of 1 α OHD $_3$ (1) on bone from 1 α ,25(OH) $_2$ D $_3$ (2).

Experimental

General Methods for Synthetic Studies Infrared (IR) spectra were recorded with a Hitachi 270-30 spectrometer, proton nuclear magnetic resonance (NMR) spectra with a JEOL FX-200 or JEOL FX-270, mass (MS) spectra with a Shimadzu GCMS-QP 1000, and ultraviolet (UV) spectra with a Shimadzu UV-240. Gas chromatography was performed with a Shimadzu GC-17A (Capillary GC, FID) using column DB-17 (J & W Scientific 0.53 mm 15 m). Flash column chromatography was carried out with Merck Kieselgel 60 (Art 9385), and preparative TLC was performed on 20×20 cm plates coated with 0.25 mm thickness of Merck Kieselgel 60 coating F254. Reverse phase high-performance liquid chromatography (HPLC) was carried out on YMC ODS A-312 at a flow rate of 1 ml/min with EtOH/H $_2$ O (85:15). Radioactivity was measured with an Aloka LSC-900.

(8 β)-De-A,B-23,23-dibromo-8-(*tert*-butyldimethylsilyloxy)-24-norchole-22-ene (8) To a stirred solution of the aldehyde (7)⁶⁾ (4.69 g, 14.4 mmol) in CH $_2$ Cl $_2$ (25 ml) was rapidly added CBr $_4$ (9.55 g, 28.8 mmol) and PPh $_3$ (15.1 g, 57.6 mmol) in CH $_2$ Cl $_2$ (25 ml). The mixture was then stirred at room temperature for 3 min and diluted with *n*-hexane. The insoluble material was filtered out. The filtrate was washed with saturated aqueous NaHCO $_3$ and saturated aqueous NaCl, dried over MgSO $_4$, and evaporated. The residue was

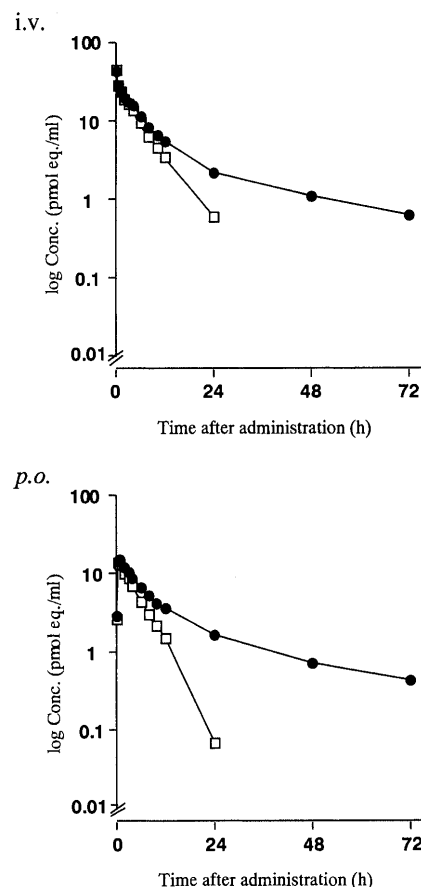


Fig. 2. Plasma Concentration of Radioactivity after Oral (*p.o.*) or Intravenous (*i.v.*) Administration of [26,27- $^3\text{H}_6$]1 α ,25(OH) $_2$ D $_3$ (4)

—●—: total radioactivity, —□—: 1 α ,25(OH) $_2$ D $_3$ fraction.

Table 1. Pharmacokinetics Parameters of Plasma 1 α ,25(OH) $_2$ D $_3$ Fraction after Oral (*p.o.*) or Intravenous (*i.v.*) Administration of [22,23- $^3\text{H}_4$]1 α OHD $_3$ (5) or [26,27- $^3\text{H}_6$]1 α ,25(OH) $_2$ D $_3$ (4)

	Route	$T_{1/2}$ (h)	C_{\max} (pmol/ml)	T_{\max} (h)	AUC (pmol·h/ml)
[22,23- $^3\text{H}_4$]1 α OHD $_3$ (5)	<i>p.o.</i>	10.2	0.88	6.00	18.0
	<i>i.v.</i>	11.4	5.99	3.25	102
[26,27- $^3\text{H}_6$]1 α ,25(OH) $_2$ D $_3$ (4)	<i>p.o.</i>	3.17	14.9	0.75	75.8
	<i>i.v.</i>	4.31	46.4	—	175

taken up with *n*-hexane. The insoluble material was removed by filtration, and the filtrate was evaporated. The crude product was purified by flash column chromatography with *n*-hexane as the eluant to give the ketene dibromide (8) (6.63 g, 96%) as a colorless oil. NMR (CDCl $_3$) δ : 6.17 (1H, d, J =9.8 Hz), 4.00 (1H, br s), 2.48 (1H, m), 1.00 (3H, d, J =6.8 Hz), 0.96 (3H, s), 0.89 (9H, s), 0.01 (6H, s).

(8 β)-De-A,B-8-(*tert*-butyldimethylsilyloxy)-22-cholestyne-24-ol (9) To a stirred solution of the ketene dibromide (8) (1.00 g, 2.08 mmol) in THF (15 ml) was added *n*-BuLi (1.61 M solution in hexane, 2.71 ml, 4.37 mmol) dropwise at -78°C under argon. The mixture was stirred at -78°C for 1 h and at room temperature for 30 min. Isobutylaldehyde (0.62 ml, 6.86 mmol) was added dropwise to the mixture at -78°C . The resulting mixture was stirred at -78°C for 20 min, poured into H $_2$ O at room temperature and extracted with AcOEt. The extract was washed with saturated aqueous NaCl, dried over MgSO $_4$ and evaporated. The crude product was purified by flash column chromatography with *n*-hexane/AcOEt (15:1) as the eluant to give the acetylene (9) (838 mg, quantitatively) as a colorless oil. NMR (CDCl $_3$) δ : 4.14 (1H, br s), 4.00 (1H, br s), 2.46 (1H, m), 1.18 (3H, d, J =6.8 Hz), 0.99 (6H, d, J =6.8 Hz), 0.96 (6H, d, J =6.8 Hz), 0.93 (3H, s), 0.89 (9H, s), 0.01 (6H, s). IR (neat): 3430, 2950, 2860, 1470, 1375, 1250, 1160, 1080, 1025 cm $^{-1}$.

(8 β)-De-A,B-8-(*tert*-butyldimethylsilyloxy)-22-cholestyne (10) To a stirred solution of the acetylene (9) (810 mg, 2.06 mmol) in CH_2Cl_2 (15 ml) were added pyridine (0.58 ml, 7.21 mmol) and PhOCSiCl (0.43 ml, 3.09 mmol) under argon. The resulting mixture was stirred at room temperature for 2 h and extracted with AcOEt. The extract was washed with cold 0.5 M HCl, saturated aqueous NaHCO_3 and saturated aqueous NaCl, dried over MgSO_4 and evaporated to give a yellow oil which was dissolved in toluene (30 ml). To the resulting solution was added *n*-Bu $_3$ SnH (0.83 ml, 3.09 mmol) and 2,2-azobisisobutyronitrile (67.7 mg, 0.41 mmol). The mixture was refluxed for 3 h and evaporated. The residue was purified by flash column chromatography with *n*-hexane as the eluant to give the acetylene (10) (760 mg, 98%) as a colorless oil. NMR (CDCl_3) δ : 4.00 (1H, br s), 2.66 (1H, m), 1.15 (3H, d, $J=6.8$ Hz), 0.95 (6H, dd, $J=6.8, 1.5$ Hz), 0.93 (3H, s), 0.89 (9H, s), 0.01 (6H, s).

(8 β)-De-A,B-22-cholestyne-8-ol (11) A solution of the acetylene (10) (740 mg, 1.96 mmol) and 6 N HCl (10 ml) in THF (20 ml) was refluxed for 7 h. The mixture was then diluted with AcOEt, washed with saturated aqueous NaHCO_3 and saturated aqueous NaCl, dried over MgSO_4 and evaporated. The crude product was purified by flash column chromatography with *n*-hexane/AcOEt (10:1) as the eluant to give the alcohol (11) (351 mg, 68%) as a colorless oil. NMR (CDCl_3) δ : 4.09 (1H, br s), 2.68 (1H, m), 2.42 (1H, m), 1.16 (3H, d, $J=6.8$ Hz), 0.95 (6H, d, $J=6.3$ Hz), 0.95 (3H, s). IR (neat): 3450, 2950, 2860, 1460, 1375, 1280, 1165, 1065 cm^{-1} .

De-A,B-22-cholestyne-8-one (12) A mixture of the alcohol (11) (340 mg, 1.30 mmol), Celite (1.0 g) and PCC (356 mg, 1.95 mmol) in CH_2Cl_2 (5 ml) was stirred at room temperature for 1.5 h. The mixture was diluted with Et_2O , treated with Florisil column chromatography and evaporated. The crude product was purified by flash column chromatography with *n*-hexane/AcOEt (15:1) as the eluant to give the ketone (12) (189 mg, 56%) as a colorless oil. NMR (CDCl_3) δ : 2.47 (1H, m), 2.26 (1H, m), 1.21 (3H, d, $J=6.9$ Hz), 0.95 (6H, d, $J=6.6$ Hz), 0.68 (3H, s). IR (neat): 2950, 2875, 1715, 1460, 1380, 1305, 1220 cm^{-1} . MS m/z : 260 (M^+), 133 (100%).

De-A,B-8-oxocholestane (13) A mixture of the ketone (12) (12.5 mg, 48.0 μmol) and 5% Pd-C (10.5 mg) in AcOEt (1 ml) was stirred at room temperature for 30 min under hydrogen. The mixture was treated with Celite/silica gel column chromatography using AcOEt as a solvent to give the ketone (13) (12.5 mg, quantitatively) as a colorless oil. NMR (CDCl_3) δ : 0.95 (3H, d, $J=5.8$ Hz), 0.86 (6H, d, $J=6.3$ Hz), 0.64 (3H, s). IR (neat): 2950, 2875, 1715, 1470, 1380, 1310, 1240, 1055 cm^{-1} . MS m/z : 264 (M^+), 125 (100%).

1 $\alpha,3\beta$ -Bis(*tert*-butyldimethylsilyloxy)-9,10-secocholesta-5,7,10(19)-triene (17) To a stirred solution of the A-ring synthon (16) (58 mg, 99.7 μmol) in THF (0.75 ml) was added *n*-BuLi (1.63 M solution in THF, 130 μmol) dropwise at -75°C under argon. The mixture was stirred at -75°C for 5 min. The ketone (13) (4.6 mg, 17.4 μmol) in THF (0.3 ml) was added dropwise to the mixture at -75°C . The resulting mixture was stirred at -75°C for 105 min and at room temperature for 15 min, poured into NaCl and extracted with AcOEt. The extract was washed with saturated aqueous NaCl, dried over MgSO_4 and evaporated. The crude product was purified by preparative TLC developed with *n*-hexane/AcOEt (24:1) to give 17 (5.0 mg, 46%) as a colorless oil, whose TLC, NMR, IR, UV and MS were completely identical with those of authentic material.¹²⁾

1 α -Hydroxyvitamin D $_3$ (1) A solution of 17 (29.3 mg, 46.6 μmol) and TBAF (1 M solution in THF, 500 μl , 500 μmol) in THF (1 ml) was refluxed mildly for 2 h. The mixture was diluted with AcOEt, washed with 0.5 M HCl, saturated aqueous NaHCO_3 and saturated aqueous NaCl, dried over MgSO_4 and evaporated. The crude product was purified by preparative TLC developed with *n*-hexane/AcOEt/EtOH (20:10:1) to give 1 αOHD_3 (1) (18.4 mg, 98%) as a colorless foam, whose HPLC, TLC, NMR and UV were completely identical with those of authentic material.¹⁰⁾

De-A,B-[22,22,23,23- $^3\text{H}_4$]-8-oxocholestane (14) A mixture of the ketone (12) (12.5 mg, 48.0 μmol) and 10% Pd-C (10.5 mg) in AcOEt (1 ml) was stirred at room temperature under tritium gas (10 Ci) in a tritiation vessel for 3 h. The insoluble material was filtered out and the filtrate was evaporated with EtOH (10 ml \times 4) to give the crude ketone (14) (3 Ci). The crude 14 (3 Ci) was purified by preparative TLC developed with *n*-hexane/AcOEt (9:1) to give the analytically pure 14 (2.1 Ci). This was dissolved in EtOH (50 ml) and analyzed. Specific radioactivity: 116 Ci/mmol. Radiochemical purity: 95%. The behavior of 14 on TLC and HPLC was identical with cold authentic 13.

1 $\alpha,3\beta$ -Bis(*tert*-butyldimethylsilyloxy)-[22,22,23,23- $^3\text{H}_4$]-9,10-secocholesta-5,7,10(19)-triene (18) To a stirred solution of the A-ring synthon (16) (45 mg, 77.3 μmol) in THF (0.4 ml) was added *n*-BuLi (1.69 M solution in THF, 92 μl , 155 μmol) dropwise at -75°C under argon. The mixture was

stirred at -75°C for 5 min. The ketone (14) (900 mCi) in THF (0.25 ml) was added dropwise to the mixture at -75°C , and the resulting mixture was stirred at -75°C for 1 h and at room temperature for 10 min, poured into aqueous NaCl and extracted with AcOEt. The extract was washed with saturated aqueous NaCl, dried over MgSO_4 and evaporated. The crude product was purified by preparative TLC developed with *n*-hexane/AcOEt (24:1) to give 18 (149 mCi, 17%), which was identical with cold authentic 17 on TLC and HPLC.

1 α -Hydroxy-[22,22,23,23- $^3\text{H}_4$]-vitamin D $_3$ (5) A solution of 18 (201 mCi) and TBAF (1 M solution in THF, 100 μl , 100 μmol) in THF (0.5 ml) was refluxed mildly for 2.5 h. The mixture was diluted with AcOEt, washed with 0.5 M HCl, saturated aqueous NaHCO_3 and saturated aqueous NaCl, dried over MgSO_4 and evaporated. The crude product was purified by preparative TLC developed with CH_2Cl_2 /EtOH (50:3) to give [22,22,23,23- $^3\text{H}_4$]-1 αOHD_3 (5) (95.7 mCi, 48%), which was identical with cold authentic 1 on TLC and HPLC. Specific radioactivity: 111.5 Ci/mmol (4125.5 GBq/mmol). Radiochemical purity: 98%.

De-A,B-[22,22,23,23- $^2\text{H}_4$]-8-oxocholestane (15) A mixture of the ketone (12) (10.4 mg, 39.9 μmol) and 5% Pd-C (10.5 mg) in AcOEt (1 ml) was stirred at room temperature for 30 min under deuterium gas. The mixture was treated with Celite/silica gel column chromatography to give the ketone (15) (10.7 mg, quantitatively) as a colorless oil. NMR (CDCl_3) δ : 0.94 (3H, d, $J=6.3$ Hz), 0.87 (6H, d, $J=6.8$ Hz), 0.64 (3H, s). IR (neat): 2950, 2875, 1710, 1460, 1380, 1310, 1220, 1050 cm^{-1} . MS m/z : 268 (M^+), 125 (100%).

1 $\alpha,3\beta$ -Bis(*tert*-butyldimethylsilyloxy)-[22,22,23,23- $^2\text{H}_4$]-9,10-secocholesta-5,7,10(19)-triene (19) To a stirred solution of the A-ring synthon (16) (56 mg, 95.6 μmol) in THF (0.75 ml) was added *n*-BuLi (1.63 M solution in THF, 88 μl , 143 μmol) dropwise at -78°C under argon. The mixture was stirred at -78°C for 5 min. The ketone (15) (5.6 mg, 21.2 μmol) in THF (0.3 ml) was added dropwise to the mixture at -78°C . The resulting mixture was stirred at -78°C for 1.75 h and at room temperature for 15 min, poured into aqueous NaCl and extracted with AcOEt. The extract was washed with saturated aqueous NaCl, dried over MgSO_4 and evaporated. The crude product was purified by preparative TLC developed with *n*-hexane/AcOEt (24:1) to give 19 (11.2 mg, 84%) as a colorless oil. NMR (CDCl_3) δ : 6.24 (1H, d, $J=11.5$ Hz), 6.02 (1H, d, $J=11.5$ Hz), 5.18 (1H, d, $J=2.2$ Hz), 4.87 (1H, d, $J=2.2$ Hz), 4.44—4.32 (1H, m), 4.27—4.12 (1H, m), 0.96—0.82 (24H, m), 0.53 (3H, s), 0.06 (12H, s). IR (neat): 2940, 2850, 1465, 1375, 1360, 1245, 1080 cm^{-1} . MS m/z : 632 (M^+), 249 (100%). UV λ_{max} nm 265.

1 α -Hydroxy-[22,22,23,23- $^2\text{H}_4$]-vitamin D $_3$ (20) A solution of 19 (6.1 mg, 9.6 μmol) and TBAF (1 M solution in THF, 200 μl , 200 μmol) in THF (1.5 ml) was refluxed mildly for 2 h. The mixture was diluted with AcOEt, washed with 0.5 M HCl, saturated aqueous NaHCO_3 and saturated aqueous NaCl, dried over MgSO_4 and evaporated. The crude product was purified by preparative TLC developed with *n*-hexane/AcOEt/EtOH (20:10:1) to give [22,22,23,23- $^2\text{H}_4$]-1 αOHD_3 (20) (3.3 mg, 84%) as a colorless oil. NMR (CDCl_3) δ : 6.39 (1H, d, $J=11.2$ Hz), 6.02 (1H, d, $J=11.2$ Hz), 5.33 (1H, br s), 4.51—4.37 (1H, m), 4.31—4.13 (1H, m), 2.90—2.76 (1H, m), 2.68—2.52 (1H, m), 2.40—2.24 (1H, m), 0.91 (3H, d, $J=5.9$ Hz), 0.87 (6H, d, $J=6.3$ Hz), 0.54 (3H, s). IR (neat): 3350, 2950, 2850, 1460, 1375, 1210, 1050 cm^{-1} . MS m/z : 404 (M^+), 134 (100%). UV λ_{max} nm 264.

Pharmacokinetics Studies Six-week-old male Sprague-Dawley rats were purchased from S.L.C. Japan Co., Ltd., (Shizuoka, Japan). After an acclimation period of one week with standard rodent chow containing 1.25% calcium and 1.06% phosphate (CE-2, Clea Japan Inc.), rats were starved overnight prior to administration. [22,22,23,23- $^3\text{H}_4$]-1 αOHD_3 (5) or [26,26,26,27,27- $^3\text{H}_6$]-1 $\alpha,25(\text{OH})_2\text{D}_3$ (4) (purchased from Amersham International plc.), was administered orally or intravenously in saline or intravenously in saline containing 1% EtOH and 1% Tween 20 as a solvent at a dose of 5 nmol (*ca.* 2 μg)/kg/50 μCi . Blood was taken periodically at 5 min, 0.5, 1, 2, 3, 4, 6, 8, 10, 12, 24, 48 and 72 h from the tail vein. Total radioactivity was determined by liquid scintillation counter (Tri-Carb 2500TR, Packard). Radioactive fractions were separated by HPLC (SCL-10A, Shimadzu) and detected by liquid scintillation counter. The radioactivity of 1 $\alpha,25(\text{OH})_2\text{D}_3$ fraction was fitted to the least squares method to calculate elimination rate constant (*ke*). Plasma $T_{1/2}$ was calculated as $\ln 2/\text{ke}$ and AUC was determined by the trapezoidal rule with extrapolation using the *ke*.

Acknowledgments We are grateful to Amersham International plc. for the tritiation reaction. Thanks are also due to Drs. M. Nanjo, T. Kawanishi, and H. Watanabe, Fuji-Gotemba Research Laboratories, Chugai Pharmaceutical Co., Ltd., for their assistance.

References

- 1) Bouillon R., Okamura W. H., Norman A. W., *Endocrine Rev.*, **16**, 200—257 (1995).
- 2) Higuchi Y., Sato K., Nanjo M., Isogai T., Takeda S., Kumaki K., Nishii Y., *Vitamins*, **68**, 87—93 (1994).
- 3) Tohira Y., Ochi K., Matsunaga I., Fukushima M., Takanashi S., Hata K., Kaneko C., Suda T., *Anal. Biochem.*, **77**, 495—502 (1977).
- 4) Tohira Y., Nakano Y., Ogawa M., Kamiyama H., Nakano H., Takanashi S., Suda T., *Vitamins*, **52**, 341—352 (1978).
- 5) Stumpf W. E., *Drug Metab. Dispos.*, **23**, 885—886 (1995).
- 6) Wovkulich P. M., Barcelos F., Batcho A. D., Sereno J. F., Baggiolini E. G., Hennessy B. M., Uskokovic M. R., *Tetrahedron*, **40**, 2283—2296 (1984).
- 7) Corey E. J., Fuchs P. L., *Tetrahedron Lett.*, **36**, 3769—3772 (1972).
- 8) Robins M. J., Wilson J. S., Hausske F., *J. Am. Chem. Soc.*, **105**, 4059—4065 (1983).
- 9) Hatakeyama S., Numata H., Osanai K., Takano S., *J. Org. Chem.*, **54**, 3515—3517 (1989).
- 10) Kaneko C., Yamada S., Sugimoto A., Eguchi Y., Ishikawa M., Suda T., Suzuki M., Kakuta S., Sasaki S., *Steroids*, **23**, 75—92 (1974).
- 11) Koike N., Ichikawa F., Nishii Y., Stumpf W. E., *Calcif. Tissue Int.*, **63**, 391—395 (1998).
- 12) Matsuura F., Kato M., Shimizu H., Michishita T., Japan. Patent 62-29875, Dec. 25 (1987) [*Chem. Abstr.*, **109**, 93445 (1988)].

Fluorinative Beckmann Fragmentation: Fluorinative α -Cleavage of Cyclic Ketoximes by Diethylaminosulfur Trifluoride

Masayuki KIRIHARA,* Kanako NIIMI, Maiko OKUMURA, and Takefumi MOMOSE

Faculty of Pharmaceutical Sciences, Toyama Medical and Pharmaceutical University, Sugitani 2630, Toyama 930-0194, Japan. Received July 28, 1999; accepted October 20, 1999

Diethylaminosulfur trifluoride reacted with cyclic ketoximes bearing substituent(s) that can stabilize a carbocation to cause fluorinative fragmentation, affording fluorinated carbonitrile. Ketoximes lacking such substituents afforded complex mixtures. However, the introduction of a sulfur functionality, which can stabilize a carbocation and can be easily removed from the reaction products, into the ketoxime was effective for producing the fluorinative fragmentation.

Key words fluorinative Beckmann fragmentation; fluorination; diethylaminosulfur trifluoride

Beckmann rearrangement, the acid-mediated isomerization of oximes to amides, is one of the most famous and useful reactions in organic synthesis.¹⁾ However, a fragmentation reaction occurs if one of the oxime substituents can produce a relatively stable carbocation. This type of reaction is also known as Beckmann fragmentation (abnormal Beckmann rearrangement), and is widely utilized to synthesize ω -nitriles.¹⁾ Because the carbocation intermediates in this fragmentation are very active electrophiles, carbon nucleophiles react with these intermediates to provide a new carbon–carbon bond formation (Chart 1).²⁾

We assumed that Beckmann fragmentation in the presence of fluoride ion would afford fluorinated carbonitriles, and found that the treatment of cyclic ketoximes with diethylaminosulfur trifluoride (DAST)^{3,4)} caused a ring fragmentation resulting in the formation of the desired compounds. We reported this result in a preliminary communication.⁵⁾ We now report the full details of this reaction.

Results and Discussion

We first examined the reaction of camphor oxime (**1a**), which is a typical substrate for the Beckmann fragmentation, with several nucleophilic fluorinating agents. These results are summarized in Table 1. Hydrogen fluoride–pyridine, tetrabutylammonium fluoride, and tetrabutylammonium dihydrogentrifluoride were inert toward **1a** (runs 1–7). The reaction of **1a** (R=H) with Ishikawa's reagent (*N,N*-diethyl-1,1,2,3,3,3-hexafluoropropylamine)⁶⁾ afforded the desired fluorinated carbonitrile (**2a**) in low yield (run 8) along with the olefin (**2a'**) as the major product. For the reaction with DAST, **2a** could be obtained in high yield (run 9).

These results correspond to the fluorination of a hydroxy group using the above fluorinating reagents. DAST is a more powerful reagent than other reagents used for the replace-

ment of the hydroxy group with fluorine, and dehydration (elimination) appears to be less of a problem with DAST than with others.³⁾ Middleton reported that cyclooctanol reacts with DAST to give a 70:30 ratio of cyclooctyl fluoride to cyclooctene, whereas Ishikawa's reagent reacts to give only cyclooctene.³⁾

We then examined the reaction of DAST toward several cyclic ketoximes (**1**). These results are summarized in Table 2. The presence of a substituent(s) capable of strongly stabilizing a carbocation at position α to the oximino carbon is essential for obtaining the fluorinated carbonitriles. Oximes lacking such substituents (**1f**, **1g**) afforded complex mixtures. In the case of **1e**, the product was a 1:1 mixture of stereoisomers.

The reaction mechanism is depicted in Chart 2. The first step is nucleophilic displacement of a fluorine in DAST by the oxygen of the oximino substrate **1** with the subsequent elimination of hydrogen fluoride. Next, the elimination of diethylaminosulfinyl fluoride from intermediate A causes bond cleavage and produces the carbocation intermediate B. Finally, the fluoride ion attacks B to afford the fluorinated carbonitrile **2** (path a). In the case of compounds lacking substituents to stabilize the α -carbocation, the reaction proceeds through a mechanism similar to that of the "normal" Beckmann rearrangement. The carbon–carbon bond *anti* to the oximino leaving group in intermediate A migrates to the nitro-

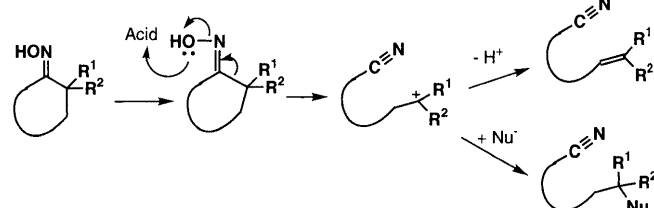


Chart 1. Beckmann Fragmentation

* To whom correspondence should be addressed.

Table 1

Run	1a	Reaction conditions	2a	2a'
1	R=H	<i>n</i> -Bu ₄ NF, THF, reflux		N.R.
2	R=H	70% HF/pyridine, THF, r.t.		N.R.
3	R=Ts	<i>n</i> -Bu ₄ NF, THF, reflux		N.R.
4	R=Ts	<i>n</i> -Bu ₄ NH ₂ F ₃ , THF, reflux		N.R.
5	R=Tf	<i>n</i> -Bu ₄ NF, THF, reflux		N.R.
6	R=Tf	<i>n</i> -Bu ₄ NH ₂ F ₃ , THF, reflux		N.R.
7	R=Tf	70% HF/pyridine, THF, r.t.		N.R.
8	R=H	CF ₃ CHFCF ₃ NEt ₂ (Ishikawa's reagent), THF, reflux	11%	48%
9	R=H	Et ₂ NSF ₃ , CH ₂ Cl ₂ , -78 °C	69%	31%

THF=tetrahydrofuran. N.R.=no reaction.

Table 2

Entry	Starting material	Product	Yield (%)
1			77
2			91
3			75
4			63 ^{a)}
5		Complex mixture	—
6		Complex mixture	—

a) A 1 : 1 mixture of stereoisomers.

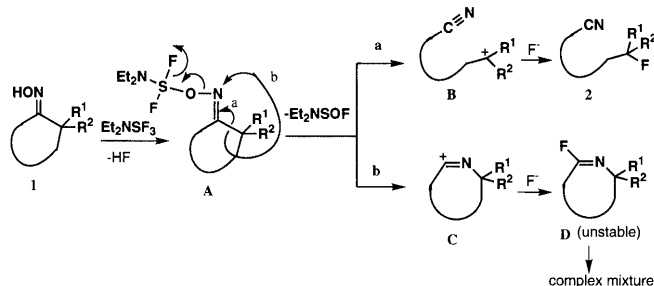


Chart 2

gen atom to afford the carbocation C. The fluoride ion attacks C to give an unstable compound D, which leads to a complex mixture (path b).

As described above, the starting cyclic ketoximes (**1**) must have substituent(s) that can strongly stabilize a carbocation at position α to the oximino carbon in order to cause the fluorinative fragmentation. Next, we introduced a sulfur functionality, which can stabilize a carbocation and can be easily removed from the reaction products, into the cyclic ketoximes to overcome this limitation. Ketoximes bearing a phenylthio-group at position α to the oximino carbon (**3**) efficiently reacted with DAST to cause the fluorinative fragmentation leading to the desired α -fluoro sulfides (**4**). Since the α -fluoro sulfides (**4**) were not stable, they were subjected, without

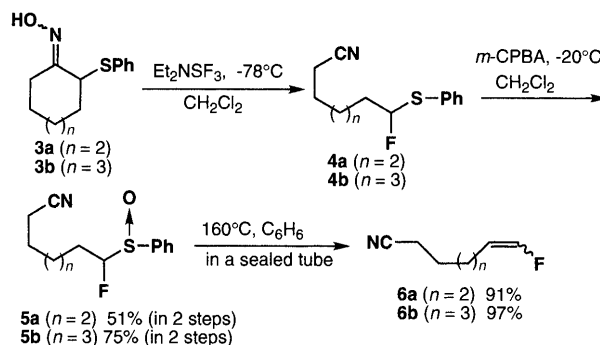


Chart 3

purification, to oxidation with *m*-chloroperbenzoic acid (*m*-CPBA). The resulting sulfoxides (**5**) were heated in a sealed tube at 160 °C to afford fluoroalkenes (**6**) in high yields (Chart 3).

Experimental

Infrared spectra (IR) were measured using a Perkin-Elmer 1600 series FT-IR spectrophotometer. ¹H- and ¹⁹F-NMR spectra were performed on a JEOL GX270, Varian Gemini 300 or Varian UNITY plus 500 instrument with tetramethylsilane (for ¹H) and chlorotrifluoromethane (for ¹⁹F) as the internal standards. Mass spectra (MS) and high-resolution mass spectra (HR-MS) were measured on a JEOL JMS D-200 spectrometer. Column chromatography was performed on silica gel (Merck Kieselgel 60).

General Procedure for the Fluorinative Fragmentation of Cyclic Ketoximes To a solution of the oxime (**1**) (1.0 mmol) in dichloromethane (3 ml) was added DAST (1.0 mmol) at -78 °C under an inert atmosphere, and the reaction mixture was then stirred for 30 min. A saturated sodium bicarbonate solution was added to the reaction mixture, and the resulting mixture was extracted with dichloromethane. The extract was dried over anhydrous sodium sulfate, filtered, and evaporated to afford the crude product. Purification by chromatography (silica gel/ hexane dichloromethane) gave the pure sample.

2-(3-Fluoro-2,2,3-trimethylcyclopentyl)ethanenitrile (2a): A 1 : 1 mixture of stereoisomers. A part of the mixture was separated into two stereoisomers by chromatography. A less polar isomer; A colorless oil; IR (neat) cm^{-1} : 2246. ¹H-NMR (CDCl_3) δ : 0.91 (3H, s), 0.97 (3H, d, $J=1.9$ Hz), 1.28 (3H, d, $J=22.6$ Hz), 1.60–1.67 (1H, m), 1.78–1.92 (1H, m), 1.99–2.16 (3H, m), 2.33–2.46 (2H, m). ¹⁹F-NMR (CDCl_3) δ : -142.4–-142.8 (m). Anal. Calcd for $\text{C}_{10}\text{H}_{16}\text{FN}$: C, 70.97; H, 9.53; N, 8.28. Found: C, 71.18; H, 9.39; N, 8.17. A more polar isomer; A colorless oil; IR (neat) cm^{-1} : 2304. ¹H-NMR (CDCl_3) δ : 0.69 (3H, s), 1.00 (3H, d, $J=1.5$ Hz), 1.29 (3H, d, $J=22.2$ Hz), 1.36–1.44 (1H, m), 1.78–2.04 (2H, m), 2.09–2.23 (2H, m), 2.34–2.39 (2H, m). ¹⁹F-NMR (CDCl_3) δ : -143.3–-143.8 (m). Anal. Calcd for $\text{C}_{10}\text{H}_{16}\text{FN}$: C, 70.97; H, 9.53; N, 8.28. Found: C, 70.79; H, 9.60; N, 8.33.

2-(2,2,3-Trimethylcyclopent-3-enyl)ethanenitrile (2a'): The spectral data for this sample were identical with those in the literature.⁷⁾

3-[2-(1-Fluoro-1-methylethyl)phenyl]propanenitrile (2b): A colorless oil; IR (neat) cm^{-1} : 2245; ¹H-NMR (CDCl_3) δ : 1.76 (6H, d, $J=22.0$ Hz), 2.46 (2H, t, $J=7.5$ Hz), 3.17 (2H, td, $J=7.5, 3.0$ Hz), 7.21–7.29 (4H, m); ¹⁹F-NMR (CDCl_3) δ : -134.6 (septet, $J=22.0$ Hz). MS m/z 191 (M^+), 172 (M^+-F). HR-MS Calcd for $\text{C}_{12}\text{H}_{14}\text{FN}$: 191.1110. Found: 191.1137.

3-[2-(1-Fluorocyclohexyl)phenyl]propanenitrile (2c): A colorless oil; IR (neat) cm^{-1} : 2245. ¹H-NMR (CDCl_3) δ : 1.70–1.85 (10H, m), 2.64 (2H, t, $J=3.5$ Hz), 3.15–3.18 (2H, m), 7.21–7.27 (4H, m). ¹⁹F-NMR (CDCl_3) δ : -158.2 (t, $J=40.6$ Hz). MS m/z 231 (M^+), 211 (M^+-HF). HR-MS Calcd for $\text{C}_{15}\text{H}_{18}\text{FN}$: 231.1424. Found: 231.1418.

6-Fluoro-6,6-diphenylhexanenitrile (2d): A colorless oil; IR (neat) cm^{-1} : 2246. ¹H-NMR (CDCl_3) δ : 1.50–1.55 (2H, m), 1.70 (2H, quintet, $J=7.6$ Hz), 2.31 (2H, t, $J=7.6$ Hz), 2.36–2.44 (2H, m), 7.27–7.38 (10H, m); ¹⁹F-NMR (CDCl_3) δ : -150.6 (t, $J=23.4$ Hz). MS m/z 267 (M^+), 247 (M^+-HF). HR-MS Calcd for $\text{C}_{18}\text{H}_{18}\text{FN}$: 267.1423. Found: 267.1409.

(14*R*)-3-Acetoxy-13-fluoro-13,17-secoestra-1,3,5(10)-trienonitrile (2e): An inseparable 1 : 1 mixture of stereoisomers. A colorless oil; IR (neat) cm^{-1} : 2245, 1761. ¹H-NMR (CDCl_3) δ : 1.22–2.18 (14H, m), 2.29 (3H, s), 2.31–2.64 (4H, m), 6.80–7.30 (3H, m). ¹⁹F-NMR (CDCl_3) δ : -130.5–-130.9 (1/2F, m), -160.0–-160.2 (1/2F, m). MS m/z 329 (M^+), 309

($M^+ - HF$). HR-MS Calcd for $C_{20}H_{24}FNO_2$: 329.1791. Found: 329.1786.

Representative Procedure for the Fluorinative Fragmentation of 2-Phenylthiocycloalkanone Oxime and the Successive Oxidation To a solution of 2-phenylthiocycloheptanone oxime (**3a**) (513 mg, 2.18 mmol) in dichloromethane (6 ml) was added DAST (346 μ l, 2.62 mmol) at -78°C under an inert atmosphere, then the reaction mixture was stirred for 15 min. A saturated sodium bicarbonate solution was added to the reaction mixture, and the resulting mixture was extracted with dichloromethane (50 ml \times 2). The extract was dried over anhydrous sodium sulfate, filtered, and evaporated to afford the crude α -fluorosulfide (**4a**). The crude product was dissolved in dichloromethane (15 ml) and cooled to -20°C under an inert atmosphere. A dichloromethane (15 ml) solution of *m*-CPBA (376 mg, 2.18 mmol) was added dropwise to the mixture and stirred for 5 min. Saturated sodium bicarbonate (15 ml) was added and the resulting mixture was extracted with chloroform (50 ml \times 2). The extract was dried over anhydrous magnesium sulfate, filtered, and evaporated to afford the crude product. Purification by chromatography (silica gel/hexane: ethyl acetate=3:1) gave **5a** (281 mg, 51%) as a 1:1 mixture of diastereoisomers.

7-Fluoro-7-(phenylsulfinyl)heptanenitrile (5a): A part of the mixture was separated into the two stereoisomers. Less polar isomer; A colorless oil: IR (neat) cm^{-1} : 2245, 1048. $^1\text{H-NMR}$ (CDCl_3) δ : 1.50—1.59 (4H, m), 1.60—1.72 (4H, m), 2.35 (2H, t, $J=7.0$ Hz), 4.93 (1H, ddd, $J=49.2$, 8.5, 3.3 Hz), 7.40—7.60 (3H, m), 7.61—7.70 (2H, m). $^{19}\text{F-NMR}$ (CDCl_3) δ : -179.7 — -180.1 (m). MS m/z 253 (M^+). HR-MS Calcd for $C_{13}H_{16}FNOS$: 253.0858. Found: 253.0863. More polar isomer; A colorless oil: IR (neat) cm^{-1} : 2245, 1049. $^1\text{H-NMR}$ (CDCl_3) δ : 1.53—2.25 (8H, m), 2.34 (2H, t, $J=6.9$ Hz), 5.10 (1H, ddd, $J=48.1$, 9.2, 3.9 Hz), 7.53—7.60 (3H, m), 7.61—7.70 (2H, m). $^{19}\text{F-NMR}$ (CDCl_3) δ : -185.7 (ddd, $J=48.1$, 34.5, 14.7 Hz). MS m/z 253 (M^+). HR-MS Calcd for $C_{13}H_{16}FNOS$: 253.0858. Found: 253.0901.

8-Fluoro-8-(phenylsulfinyl)octanenitrile (5b): A part of the mixture was separated into the two stereoisomers. Less polar isomer; A colorless oil: IR (neat) cm^{-1} : 2245, 1049. $^1\text{H-NMR}$ (CDCl_3) δ : 1.35—1.52 (4H, m), 1.59—1.68 (4H, m), 1.99—2.12 (2H, m), 2.34 (2H, t, $J=7.1$ Hz), 4.91 (1H, ddd, $J=49.3$, 8.7, 2.8 Hz), 7.56—7.58 (3H, m), 7.66—7.68 (2H, m). $^{19}\text{F-NMR}$ (CDCl_3) δ : -179.8 (ddd, $J=49.3$, 32.0, 19.7 Hz). MS m/z 267 (M^+). HR-MS Calcd for $C_{14}H_{18}FNOS$: 267.1078. Found: 267.1099. More polar isomer; A colorless oil: IR (neat) cm^{-1} : 2244, 1049. $^1\text{H-NMR}$ (CDCl_3) δ : 1.25—1.58 (4H, m), 1.62—1.78 (4H, m), 1.89—2.05 (2H, m), 2.33 (2H, t, $J=7.1$ Hz), 5.08 (1H, ddd, $J=49.2$, 9.1, 3.6 Hz), 7.56—7.58 (3H, m), 7.64—7.67 (2H, m). $^{19}\text{F-NMR}$ (CDCl_3) δ : -185.7 (ddd, $J=49.2$, 34.5, 14.8 Hz). MS m/z 267 (M^+). HR-MS Calcd for $C_{14}H_{18}FNOS$: 267.1078. Found: 267.1089.

Representative Procedure for the Desulfurization of α -Fluorosulfoxides A benzene (3 ml) solution of **5a** (100 mg, 0.422 mmol) was heated in a sealed tube at 160°C for 10 h. The reaction mixture was evaporated, and the resulting residue was subjected to chromatography (silica gel/hexane: ethyl acetate=20:1) to give **6a** (49 mg, 91%) as a 1:1 mixture of stereoisomers.

7-Fluorohept-6-enenitrile (6a): A colorless oil: IR (neat) cm^{-1} : 2246. $^1\text{H-}$

NMR (CDCl_3) δ : 1.51—1.58 (2H, m), 1.65—1.72 (2H, m), 1.95—2.00 (1H, m), 2.14—2.20 (1H, m), 2.35 (2H, t, $J=7.1$ Hz), 2.37 (2H, t, $J=7.1$ Hz), 4.72 (0.5H, dtd, $J=41.7$, 7.7, 4.7 Hz), 5.28—5.37 (0.5H, m), 6.49 (0.5H, dtd, $J=85.5$, 4.8, 1.4 Hz), 6.52 (0.5H, dtd, $J=85.5$, 11.1, 1.3 Hz). $^{19}\text{F-NMR}$ (CDCl_3) δ : -129.7 (0.5F, dd, $J=85.5$, 18.5 Hz), -130.57 (0.5F, dd, $J=85.5$, 41.7 Hz). MS m/z 128 ($M^+ + H$). HR-MS Calcd for $C_7H_{11}FN$ ($M^+ + H$): 128.0936. Found: 128.0867.

8-Fluorohept-7-enenitrile (6b): A 1:1 mixture of stereoisomers; a colorless oil: IR (neat) cm^{-1} : 2246. $^1\text{H-NMR}$ (CDCl_3) δ : 1.36—1.51 (4H, m), 1.64—1.71 (2H, m), 1.91—1.96 (1H, m), 2.12—2.18 (1H, m), 2.35 (2H, t, $J=7.1$ Hz), 4.72 (0.5H, dtd, $J=43.2$, 7.7, 4.7 Hz), 5.28—5.37 (0.5H, m), 6.47 (0.5H, dtd, $J=85.5$, 4.7, 1.5 Hz), 6.51 (0.5H, dtd, $J=85.7$, 11.1, 1.4 Hz). $^{19}\text{F-NMR}$ (CDCl_3) δ : -130.5 (0.5F, dd, $J=86.1$, 19.7 Hz), -130.14 (0.5F, dd, $J=86.1$, 44.3 Hz). MS m/z 142 ($M^+ + H$). HR-MS Calcd for $C_8H_{13}FN$ ($M^+ + H$): 142.0973. Found: 142.1042.

Acknowledgements This work was sponsored in part by the Foundation for the Promotion of Higher Education in Toyama Prefecture and by a Grant-in-Aid (No. 09771900) for Scientific Research from the Ministry of Education, Science, Sports and Culture, Japan.

References and Notes

- 1) Gawley R. E., *Org. React.* (N. Y.), **35**, 1—420, (1988) and references cited therein.
- 2) Fujioka H., Miyazaki M., Yamanaka T., Yamamoto H., Kita Y., *Tetrahedron Lett.*, **31**, 5951—5954 (1990); Fujioka H., Yamamoto H., Miyazaki M., Yamanaka T., Takuma K., Kita Y., *ibid.*, **32**, 5367—5368 (1991); Fujioka H., Yamanaka T., Takuma K., Miyazaki M., Kita Y., *J. Chem. Soc., Chem. Commun.*, **1991**, 533—534; Fujioka H., Kitagawa H., Yamanaka T., Kita Y., *Chem. Pharm. Bull.*, **40**, 3118—3120 (1992); Fujioka H., Miyazaki M., Kitagawa H., Yamanaka T., Yamamoto H., Takuma K., Kita Y., *J. Chem. Soc., Chem. Commun.*, **1993**, 1634—1636.
- 3) Middleton W. J., *J. Org. Chem.*, **40**, 574—578 (1975).
- 4) Hudlicky M., *Org. React.* (N. Y.), **35**, 513—637, (1988); Wnuk S. F., Robins M. J., *J. Org. Chem.*, **55**, 4757—4760 (1990); Kikugawa Y., Matsumoto K., Mitsui K., Sakamoto T., *J. Chem. Soc., Chem. Commun.*, **1992**, 921—922; Neef G., Ast G., Michl G., Schwede W., Vierhufe H., *Tetrahedron Lett.*, **35**, 8587—8590 (1994); Ratcliffe A. J., Warner I., *ibid.*, **36**, 3881—3884 (1995); Kuroboshi M., Furuta S., Hiyama T., *ibid.*, **36**, 6121—6122 (1995); Bildstein S., Ducep J., Jacobi D., Zimmermann P., *ibid.*, **37**, 4941—4944 (1996); Bildstein S., Ducep J., Jacobi D., *ibid.*, **37**, 8759—8762 (1996); Kiriha M., Kambayashi T., Momose T., *Chem. Commun.*, **1996**, 1103—1104.
- 5) Kiriha M., Niimi K., Momose T., *Chem. Commun.*, **1997**, 599—600.
- 6) Takaoka A., Iwakiri H., Ishikawa N., *Bull. Chem. Soc. Jpn.*, **52**, 3377—3380 (1979).
- 7) Sato T., Obase H., *Tetrahedron Lett.*, **1967**, 1633—1636.

Mechanism of Superoxide Dismutase-Like Activity of Fe(II) and Fe(III) Complexes of Tetrakis-*N,N,N',N'*-(2-pyridylmethyl)ethylenediamine

Tomohisa HIRANO,^a Masaaki HIROBE,^a Kazuo KOBAYASHI,^b Akira ODANI,^c Osamu YAMAUCHI,^c Masanori OHSAWA,^a Yoshinori SATOW,^a and Tetsuo NAGANO*,^a

Graduate School of Pharmaceutical Sciences, The University of Tokyo,^a 7-3-1 Hongo, Bunkyo-ku, Tokyo 113-0033, Japan, Institute of Scientific and Industrial Research, Osaka University,^b 8-1 Mihogaoka, Ibaraki, Osaka 567-0047, Japan, and Department of Chemistry, Faculty of Science,^c Nagoya University, Chikusa-ku, Nagoya 464-0814, Japan.

Received July 29, 1999; accepted November 7, 1999

The superoxide dismutase (SOD) activity of iron(II) tetrakis-*N,N,N',N'*-(2-pyridylmethyl)ethylenediamine complex (Fe-TPEN) was reexamined using a pulse radiolysis method. In our previous study (*J. Biol. Chem.*, 264, 9243–9249 (1989)), we reported that this complex has a potent SOD activity in a cyt. c (cytochrome c)-based system ($IC_{50}=0.8\ \mu\text{M}$) and protects *E. coli* cells against paraquat toxicity. The present pulse radiolysis experiment revealed that Fe(II)TPEN reacts stoichiometrically with superoxide to form Fe(III)TPEN with a second-order rate constant of $3.9\times 10^6\ \text{M}^{-1}\text{s}^{-1}$ at pH 7.1, but superoxide did not reduce Fe(III)TPEN to Fe(II)TPEN. The reaction of Fe(III)TPEN and superoxide was biphasic. In the fast reaction, an adduct (Fe(III)TPEN-superoxide complex) was formed at the second-order rate constant of $8.5\times 10^5\ \text{M}^{-1}\text{s}^{-1}$ at pH 7.4. In the slow one, the adduct reacted with another molecule of the adduct, regenerating Fe(III)TPEN. In the cyt. c method with catalase, this Fe(III)TPEN-superoxide complex showed cyt. c oxidation activity, which had led to overestimation of its SOD activity. Based on the titration data, the main species of complex in aqueous media at neutral pH was indicated to be Fe(III)TPEN(OH⁻). A spectral change after the reduction with hydrated electron indicates that the OH⁻ ion coordinates directly to Fe(III) by displacing one of the pyridine rings. The X-ray analysis of [Fe(II)TPEN]SO₄ supported this structure. From the above results we propose a novel reaction mechanism of FeTPEN and superoxide which resembles a proton catalyzed dismuting process, involving Fe(III)TPEN-superoxide complex.

Key words superoxide dismutase mimics; Tetrakis-*N,N,N',N'*-(2-pyridylmethyl)ethylenediamine; free radical; pulse radiolysis; X-ray analysis; pH-titration

Since superoxide generated *in vivo* is involved in the pathology of many diseases, superoxide dismutases (SODs)^{1,2)} are useful not only as biological tools, but also potentially as pharmaceuticals.^{3–6)} For these reasons, many low-molecular SOD mimics, mainly copper and manganese complexes, have been synthesized and examined for activity *in vitro* and partially *in vivo*, as functional models of the native enzymes.^{7–18)} Some compounds have been identified as candidate pharmaceuticals.^{19–23)} We are therefore interested in studying SOD model compounds to learn how the structural and physical properties of the metal complexes are related to the chemical function of superoxide dismuting activity.

Although the reaction mechanisms of some mimetics have been investigated in detail,^{24,25)} they remain unclear in most cases. Generally, metal-catalyzed superoxide dismutation is described by the following two equations:



Most low-molecular metal complexes that have been studied in the past were believed to catalyze the superoxide dismutation reaction *via* the above scheme. We previously reported the novel SOD mimic, Fe(II)-tetrakis-*N,N,N',N'*-(2-pyridylmethyl)ethylenediamine (Fe(II)TPEN).^{26–28)} This complex had high SOD activity measured by the cyt. c assay and protected *Escherichia coli* against paraquat toxicity. However, Iuliano and co-workers investigated the interaction of Fe-TPEN with reactive oxygen species under *in vitro* conditions.²⁹⁾ They reported that Fe(II)TPEN acts as a Fenton catalyst and generates hydroxyl radical from hydrogen peroxide, and suggested that this is the reason for the much lower efficacy of the complex in *E. coli* cells than expected from its

in vitro activity. Weiss and co-workers also demonstrated that Fe-TPEN did not enhance the dismutation reaction of superoxide and suggested that our overestimation of the SOD activity of Fe-TPEN was due to its cyt. c peroxidase activity.³⁰⁾ We agree with them in respect to the Fenton reactivity and the cyt. c peroxidase activity of Fe(II)TPEN, as we previously obtained almost the same results. But their proposed reaction mechanisms are incomplete as regards the interaction of Fe(III)TPEN with superoxide and do not account fully for the entire superoxide dismuting reactions of Fe-TPEN.

In this paper, we propose a different mechanism of SOD activity of Fe-TPEN, based on an examination of each step using a pulse radiolysis method. The mechanism is also supported by data obtained using pH titration techniques and X-ray crystallographic analysis.

Experimental

Materials Catalase, cyt. c (type III), and xanthine sodium salt were obtained from Sigma. Xanthine oxidase was from Boehringer Mannheim GmbH. The other chemicals were all reagent-grade products from Aldrich or Tokyo Kasei Kogyo, Ltd.

Methods Pulse Radiolysis Method³¹⁾: Pulse radiolysis experiments were performed with the electron linear accelerator at the Institute of Scientific and Industrial Research, Osaka University. The pulse width and energy were 8–10 ns and 20–35 MeV, respectively. The light source was a 1-kilowatt xenon lamp. The light intensities transmitted through the optical path were analyzed and monitored by a fast spectrophotometric system composed of a Nikon monochromator, a 1-P-28 photomultiplier with a short response time, and a Tektronix 7834 memorizing oscilloscope fitted with a Polaroid camera. For each wavelength, transmittance changes were recorded by photographing the oscilloscope traces. Photolysis by the analyzing light was minimized by means of an optical shutter and selected filters. Samples of iron complexes for pulse radiolysis were prepared by bubbling oxygen gas through a solution of complexes containing 10 mM acetate buffer (pH 4–6), or 10 mM phosphate buffer (pH 6–8), or 10 mM borate buffer (pH 8–10),

* To whom correspondence should be addressed.

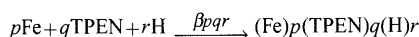
and 100 mM *tert*-BuOH to scavenge $\cdot\text{OH}$. A quartz cell with a 1 cm light path containing approximately 1 ml of reaction solution was placed in front of the accelerator. Fresh solution was used for each irradiation. The concentration of superoxide generated by pulse radiolysis was estimated from the absorption change at 280 nm ($\epsilon_{280}=950\text{ M}^{-1}\text{ cm}^{-1}$) in the absence of complexes. Optical absorption spectra were measured using a Shimadzu UV-265 spectrophotometer. Absorption changes (ΔA) were calculated according to the following equation from the transmittance changes (ΔT) after the pulse.

$$\Delta A = \log 100/100 - \Delta T$$

pH Titration:

1) Apparatus and procedure.³²⁾ Measurements of pH were made with an Orion Research 901 ion meter equipped with an Orion 90-10-00 glass electrode and a 91-12-00 double junction reference electrode. The meter was calibrated with NBS (*N*-bromosuccinimide) standard buffer solutions (4.008, 7.413, and 9.180 at 25 °C). Conversion of the pH meter reading (pHM) to $-\log [\text{H}^+]$, where $[\text{H}^+]$ refers to proton concentration, was made by correcting the difference (0.060) between pHM and $-\log [\text{H}^+]$ obtained by titrating 0.01 M HNO_3 with 1.0 M KOH at the ionic strength (*I*) of 1.0 M (KNO_3). The hydroxide ion concentration $[\text{OH}^-]$ was calculated from the apparent ion product of water $\text{p}K_w' = 13.91$ ($=\text{pHM} - \log [\text{OH}^-]$) determined by titrating 0.1 M KNO_3 with 0.1 M KOH. Titrations were performed at 25 ± 0.05 °C under N_2 for solutions containing a ligand only and those containing a ligand and Fe(II) or Fe(III) in the molar ratio of 1 : 1, 1 : 2, and 1 : 4.

2) Calculation of equilibrium constants and species distributions. The equilibria in the present system and the relevant equilibrium constants, β_{pqr} , are defined by the following equations (charges are omitted for simplicity):



$$\beta_{pqr} = [\text{Fe}_p\text{L}_q\text{H}_r] / [\text{Fe}]^p[\text{L}]^q[\text{H}]^r \quad (\text{L} = \text{TPEN})$$

where *p*, *q*, and *r* are the numbers of moles of metal (M), ligand (L), and proton (H) in the complex, respectively, and a negative value of *r* denotes the hydroxyl ion. Calculation of β_{pqr} was done using the program MINIQAD where the function minimized is the sums of the squares of the residuals in the mass balance equations for total hydrogen ion, total metal, and total ligand. Calculation of species distribution was done with the program SUPERQUAD, developed by Gans *et al.*³³⁾

Syntheses of TPEN and Iron Complexes: All chemicals were commercial products of reagent-grade quality, and were used without further purification.

1) Synthesis of TPEN. TPEN was prepared from 2-picoly chloride hydrochloride by reaction with ethylenediamine in H_2O at pH < 9.5 at room temperature under an Ar atmosphere. Full details of the procedure can be found in refs. 34 and 35. mp 110 °C (lit. 110–111.5 °C); $^1\text{H-NMR}$ (CDCl_3/TMS) δ 2.76 (s, 4H), 3.78 (s, 8H), 7.11 (dd, 4H, *J* = 4.0, 7.7 Hz), 7.45 (d, 4H, *J* = 7.7 Hz), 7.57 (ddd, 4H, *J* = 1.8, 7.7, 7.7 Hz), 8.49 (dd, 4H, *J* = 1.8, 4.0 Hz); Mass, 424 (M^+), 332 ($\text{M}^+ - \text{CH}_2\text{C}_5\text{H}_4\text{N}$), 212 ($\text{M}^+ - \text{CH}_2\text{N}(\text{CH}_2\text{C}_5\text{H}_4\text{N})_2$). Anal. Calcd for: $\text{C}_{26}\text{H}_{28}\text{N}_6$: C, 73.55; H, 6.65; N, 19.80. Found: C, 73.81; H, 6.66; N, 19.77.

2) Preparation of Fe(II)TPEN(SO_4) for X-ray analysis. FeSO_4 (27.8 mg) in MeOH was added to an MeOH solution of TPEN (42.4 mg), and the reaction mixture was left standing at room temperature for 5 min. The solvent was thoroughly removed, leaving a yellow powder. Recrystallization from CH_3CN afforded yellow plates. To obtain a sample for X-ray analysis, this recrystallization was repeated three times.

X-Ray Structure Determinations: The single-crystal structure determinations were carried out at the Graduate School of Pharmaceutical Sciences, The University of Tokyo. Diffraction data were collected on an Enraf-Nonius CAD-4turbo automated *k*-axis diffractometer equipped with a graphite-crystal monochromator. The $w/2\theta$ scan technique was used to record the intensities for all nonequivalent reflections.

Data were collected at 278 K for both crystals. Pertinent details regarding the structure determinations are listed in Table 1.

Results

The Reaction of Fe(II)TPEN and Superoxide The pulse radiolysis technique is very useful for measurement of rate constants and identification of unstable intermediates in the reactions of superoxide and various compounds.^{24,31,36)} This technique was used to obtain the reaction rate constant of Fe(II)TPEN and superoxide. An aqueous solution of

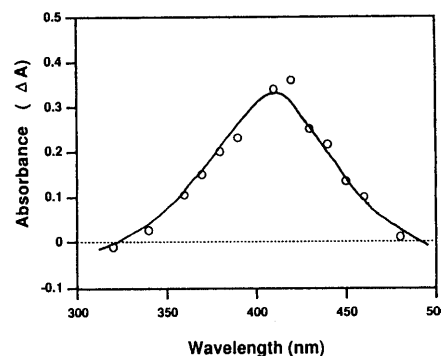


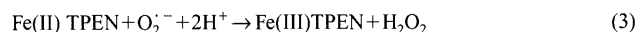
Fig. 1. The Difference Spectrum of Absorption Changes at 10 ms after Pulse Irradiation

The quartz reaction cell contained 10 mM phosphate buffer (pH 7.4), 100 mM *tert*-butyl alcohol, and 50 μM Fe(II)TPEN under oxygen saturation. The traces were started just after pulse irradiation. The transmittance changes were recorded by photographing the oscilloscope traces. The absorption changes (ΔA) were calculated from the transmittance changes (ΔT) using the following equation, $\Delta A = \log 100/100 - \Delta T$. Open circles represent calculated absorption changes at 10 ms after pulse irradiation. Solid line represents the difference spectrum (Fe(II)TPEN)–(Fe(III)TPEN) in phosphate buffer (pH 7.4) at the same concentrations. Under these experimental conditions, 43.4 μM superoxide was generated by pulse irradiation. Irradiation conditions are given in the Experimental section.

Fe(II)TPEN has absorption at 416 nm (λ_{max} , $\epsilon = 10,800$) due to charge transfer from the ligand to ferrous iron, while an aqueous solution of Fe(III)TPEN has little absorption in the visible region. Formation of a 1 : 1 Fe(II) complex of TPEN in aqueous or polar organic solvents was previously revealed by means of a continuous plotting technique.²⁶⁾ We monitored the decay of this characteristic absorption of Fe(II)TPEN and tried to examine the direct reaction of Fe(II)TPEN and superoxide.

The reaction solution contained Fe(II)TPEN (50–300 μM) in 10 mM phosphate buffer with *tert*-butanol (100 mM) and catalase under the condition of oxygen saturation. When exposed to pulse irradiation, Fe(II)TPEN was rapidly bleached to Fe(III)TPEN with a reduction of the absorption at around 420 nm. We obtained the difference absorption spectrum between before and after irradiation by measuring the transmittance change at various wavelengths (Fig. 1). The open circles show the experimental values (ΔA) measured at 13 wavelengths and the solid line indicates the difference spectrum between Fe(II)TPEN and Fe(III)TPEN.

Since the open circles were well fitted to the difference spectra, Fe(III)TPEN was confirmed to be the product in the reaction of Fe(II)TPEN and superoxide generated by the pulse irradiation. The concentration of superoxide generated under these conditions was 43.4 μM . This shows that superoxide reacts stoichiometrically with Fe(II)TPEN, based on the value of ΔA .



To determine the second-order rate constant of this reaction, we examined the absorption decay (430 nm) at several concentrations of the ferrous complex (100, 200, and 300 μM) under *pseudo* first-order conditions $[\text{Fe(II)TPEN}] \gg [\text{superoxide}]$. Under these conditions, $[\text{superoxide}]$ was 6–10 μM . The observed first-order rate constants (*k*_{app}) were determined from a plot of the absorbance changes of Fe(II)TPEN as a function of time. The second-order rate constant ($3.9 \times 10^6 \text{ M}^{-1} \text{ s}^{-1}$ at pH 7.1) was determined by plotting the observed first-order rate constants as a function of

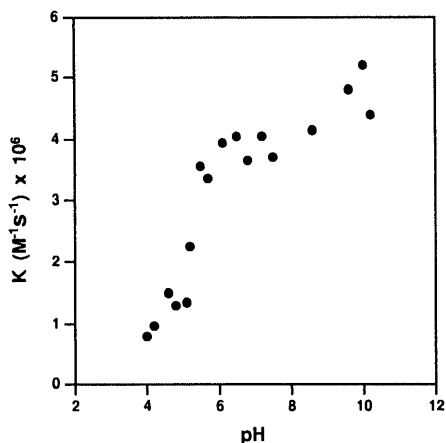


Fig. 2. pH Profile of the Second-Order Rate Constant of the Reaction of Fe(II)TPEN and Superoxide

The second-order rate constants were calculated from the time of half-elimination of Fe(II)TPEN ($\tau_{1/2} = \ln 2 / k_{app}$, $k = k_{app} / [\text{Fe(II)TPEN}]_0$) under pseudo first-order conditions. In this pulse experiment, the initial concentration of Fe(II)TPEN was $95 \mu\text{M}$ and the concentration of generated superoxide was $3.1\text{--}5.8 \mu\text{M}$. The buffers were 10 mM acetate buffer at pH 4–5, 10 mM phosphate buffer at pH 5–9 and 10 mM borate buffer at pH 9–11, respectively. Other conditions are the same as in the legend to Fig. 1.

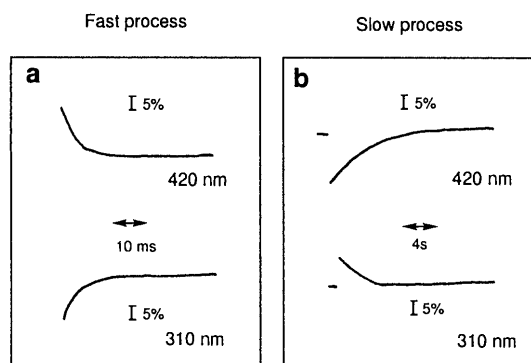


Fig. 3. The Oscilloscope Traces of Transmittance Changes after Pulse Radiolysis of Fe(III)TPEN

Fe(III)TPEN was prepared by oxidation of Fe(II)TPEN with equimolar hydrogen peroxide followed by the addition of enough catalase to extinguish residual hydrogen peroxide. The transmittance changes were monitored on for 20 s from the first pulse at 420 and 310 nm. The reaction mixture contained $96 \mu\text{M}$ Fe(III)TPEN, $43\text{--}60 \mu\text{M}$ superoxide, 100 mM *tert*-butyl alcohol and 10 mM phosphate buffer at pH 7.4 under oxygen saturation. Irradiation conditions are given in the Experimental section. It should be noted that the transmittance changes are illustrated on different time scales for the fast process (a) and the slow one (b).

$[\text{Fe(II)TPEN}]_0$.

Figure 2 shows a plot of the second-order rate constants as a function of pH. The value of the second-order rate constant decreased drastically at pH under 6. Since the pK_a value of superoxide is 4.88, the ratio of protonated superoxide, HO_2 radical, in the reaction mixture increased as the pH was lowered. This pH profile demonstrates that Fe(II)TPEN has very low reactivity, if any, with the HO_2 radical. This suggests that the reaction includes charge transfer from Fe(II)TPEN to superoxide and that the negative charge of superoxide is essential for the interaction with Fe(II)TPEN.

The Reaction of Fe(III)TPEN and Superoxide The reaction of Fe(III)TPEN and superoxide was also examined using pulse radiolysis. Figures 3a and b show typical transmittance changes at 420 and 310 nm after irradiation of an aqueous Fe(III)TPEN solution saturated with dioxygen at pH 7.4. The reaction was biphasic. The fast reaction was completed within 10 ms, and caused the absorbance changes (the

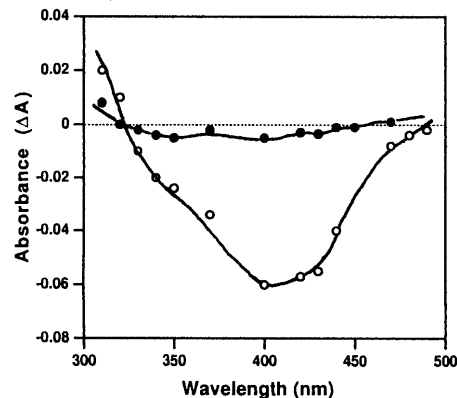
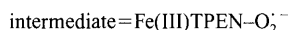


Fig. 4. Kinetic Difference Spectra at 20 ms and 10 s after Pulse Radiolysis of Fe(III)TPEN

Fe(III)TPEN was prepared as described in the legend to Fig. 3. Both the absorption difference between Fe(III)TPEN and the species at 20 ms (open circles) and 10 s (closed circles) after pulse irradiation are illustrated. Reaction mixtures contained $96 \mu\text{M}$ Fe(III)TPEN and $42 \mu\text{M}$ superoxide in each reaction, in 100 mM *tert*-butyl alcohol in 10 mM phosphate buffer at pH 7.5 under oxygen saturation.

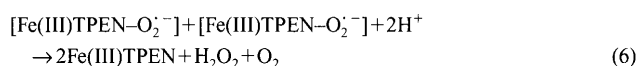
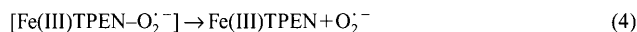
decrease at 420 nm and the increase at 310 nm). On the other hand, the slow reaction took several seconds to reach completion, and the absorbance changes were opposite to those in the fast process both at 420 nm and 310 nm. Figure 4 illustrates the difference spectra from Fe(III)TPEN at 20 ms (open circles) and 10 s (closed circles) after the first irradiation. This indicates that Fe(III)TPEN was regenerated in 20 s via an "intermediate" formed within 20 ms in the reaction of Fe(III)TPEN and superoxide. This intermediate was different from Fe(II)TPEN, based on the characteristic absorption around 400 nm. In addition, since this reaction could be repeated within the reaction cell by successive pulse irradiations, Fe(III)TPEN acts as a catalyst in the reaction with superoxide, without formation of Fe(II)TPEN.

This intermediate is proposed to be Fe(III)TPEN-superoxide complex, the superoxide adduct³⁷⁾ of Fe(III)TPEN or an equivalent species, based on the fact that it is not Fe(II)TPEN, as indicated by its difference spectrum at 20 ms after pulse irradiation.



The above results suggest that there are two processes in the catalytic reaction of superoxide with Fe(III)TPEN; the first one forms Fe(III)TPEN-superoxide complex, and the second regenerates Fe(III)TPEN with the formation of hydrogen peroxide and dioxygen. The observed rate constants of the fast process were plotted against the concentration of Fe(III)TPEN under pseudo first-order conditions, and the second-order rate constant was determined as $8.5 \times 10^5 \text{ M}^{-1} \text{ s}^{-1}$ at pH 7.4. Figure 5 shows the second-order rate constant of the fast process as a function of pH.

There are three possibilities for the slow process in which Fe(III)TPEN was reproduced:



Since this slow reaction is a second-order reaction (data

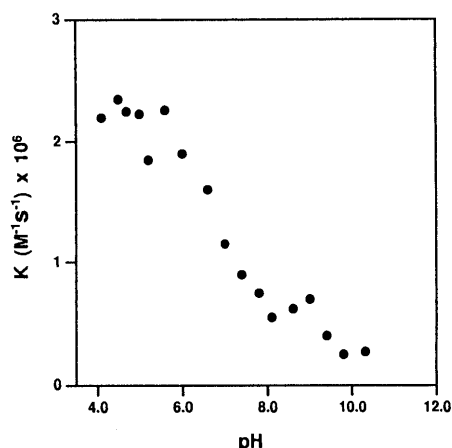


Fig. 5. pH Profile of the Second-Order Rate Constant of the Reaction of Fe(III)TPEN and Superoxide (in the Fast Process)

The second-order rate constants of the fast process were calculated from the half life time of elimination of Fe(III)TPEN under pseudo first-order conditions. The employed buffers and irradiation conditions are the same as described in the legend to Fig. 2.

not shown), Eq. (4), simple release of superoxide from the intermediate complex, can be ruled out. The second possibility, Eq. (5), can also be rejected because the superoxide had completely disappeared within 20 ms after pulse irradiation in the reaction cell. Thus, we consider that two Fe(III)TPEN-superoxide complexes react as shown in Eq. (6) under these experimental conditions. We estimated the rate constant of reaction (6) to be $10^3 \text{ M}^{-1} \text{ s}^{-1}$ from the time taken to regenerate the unadducted form.

The reaction mechanism proposed above may be applicable only under pulse radiolysis conditions. In the presence of an excess amount of superoxide or when superoxide is continuously being generated, reaction (5) would rather be favored.

The Reaction of FeTPEN in the Cyt. c Assay As mentioned above, superoxide does not reduce Fe(III)TPEN to Fe(II)TPEN, while it oxidized the latter to the former in the pulse radiolysis experiments. This cannot explain the catalytic SOD activity of Fe-TPEN. Iuliano *et al.*²⁹⁾ and Weiss *et al.*³⁰⁾ suggested that our overestimation of the SOD activity of Fe-TPEN was due to Fenton reactivity. However, our experimental system based on the cyt. c method contained a sufficient concentration of catalase to decompose hydrogen peroxide generated by the xanthine/xanthine oxidase system; therefore the hydrogen peroxide-dependent reaction of Fe-TPEN cannot account for the inhibition of cyt. c reduction. We therefore examined cyt. c (red) reoxidation in the presence of both Fe(III)TPEN and superoxide. The reaction mixture contained equal concentrations of cyt. c (red) and cyt. c (ox) (total concentration was 10 mM), catalase, and xanthine in phosphate buffer (line A in Fig. 6). When Fe(III)TPEN was added to this solution, no absorption change was observed, but when xanthine oxidase was added, cyt. c (red) began to be reoxidized. This indicates that both Fe(III)TPEN and superoxide are required to reoxidize cyt. c (red). This reaction reached a steady state. For line B, the reaction mixture contained cyt. c (ox), catalase, xanthine and Fe(III)TPEN in phosphate buffer. When xanthine oxidase was added to this reaction system, the reduction started immediately. However, the reduction was not complete, but reached the same equilibrium state as in the former experiment. The above results

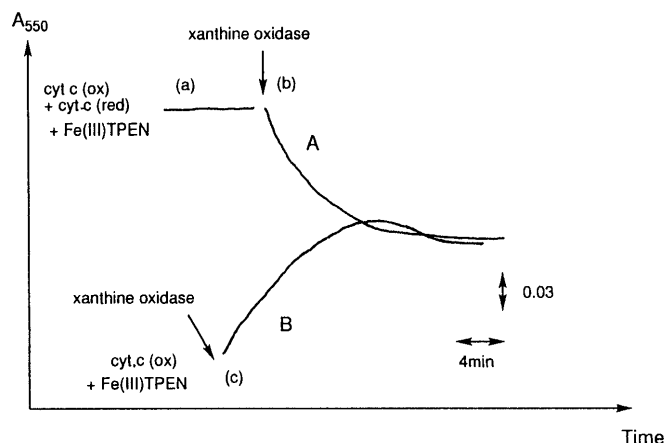


Fig. 6. The Superoxidase Activity of Fe(III)TPEN

In experiment A (line A), the reaction mixture contained half-reduced 10 μM cyt. c (by $\text{Na}_2\text{S}_2\text{O}_4$), 50 mM xanthine, and 2500 units/ml catalase. At point a, 1.0 mM Fe(III)TPEN was added and at point b, 4.0 units/ml of xanthine oxidase. In experiment B (line B) the reaction mixture contained 10 μM oxidized cyt. c, 50 mM xanthine, 2500 unit/ml of catalase and 1.0 μM Fe(III)TPEN in 50 mM phosphate buffer (pH 7.4). At point c, 4.0 units/ml of xanthine oxidase was added. The reduction and oxidation of cyt. c were monitored at 550 nm.

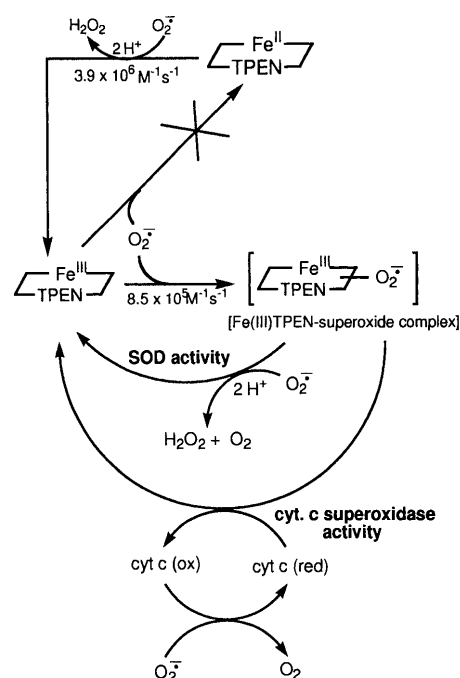


Chart 1. Mechanism of SOD Activity and Cyt. c-Superoxidase Activity of Fe-TPEN

are summarized in Chart 1. We propose that the Fe(III)TPEN-superoxide complex, which was produced in the pulse radiolysis experiment, has cyt. c "superoxidase" activity. Because all experiments were conducted in the presence of an adequate concentration of catalase, "peroxidase" activity of Fe(III)TPEN can be excluded.

Solution Equilibrium Chemistry of Fe-TPEN pH Titration^{32,33)}: The coordination chemistry of Fe(III)TPEN in aqueous solution has a major influence on the reactivities. We therefore studied the coordination states and species distribution in aqueous media, and carried out pH titration³⁸⁾ to analyze the solution equilibria.

Based on the titration curves, the overall proton-ligand stability constant was calculated with the MINQUAD program

to be $7.6 \times 10^{13} \text{ M}^{-1}$. Calculated stepwise dissociation constants (stepwise $\text{p}K_a$) are 6.96, 4.29, 3.20, 2.71, 2.50, and below 2.0. According to these values, the protonation of the least basic pyridine ring of TPEN occurs only below pH 2. Therefore, this pyridine is assumed to have low coordination activity.

The calculated species distribution curves for Fe(III)TPEN were obtained by simulating the results with the SUPERQUAD program. Figure 7 shows that the main species at about neutral pH is Fe(III)TPEN(OH⁻). At lower pH, Fe(III)TPEN is dominant. The higher the pH value becomes, the lower the ratio of Fe(III)TPEN(OH⁻) species is. In the pulse radiolysis study, the second-rate constant of the fast reaction of Fe(III)TPEN and superoxide showed pH dependency (Fig. 5). If Fe(III)TPEN(OH⁻) is the reacting species under that condition, it is reasonable that the rate constant decreases with decrease of the ratio of this species as the pH value becomes higher.

Pulse Radiolysis Study We next examined the reduction of Fe(III)TPEN(OH⁻) by hydrated electrons generated by irradiation in the absence of oxygen. Figure 8c shows the difference spectra from Fe(III)TPEN at 5 and 500 μs after irradiation. Hydrated electrons reacted with Fe(III) and were eliminated within 3 μs , but, by 5 ms after irradiation, no absorption of Fe(II)TPEN had appeared. Thus, as soon as a hydrated electron reacts with Fe(III), Fe(III) is reduced to Fe(II), but there is a lag time until the appearance of the reduced complex. Insets of Fig. 8a and b show the elimina-

tion of the hydrated electron (600 nm) and the appearance of Fe(II)TPEN (420 nm). The weak basicity of one of the four pyridine rings suggests that the configuration of Fe(III)TPEN(OH⁻) may be as shown in Chart 2. One pyridine ring is assumed to have been displaced by a hydroxyl ion. In contrast, TPEN ligates to Fe(II) with all six nitrogen

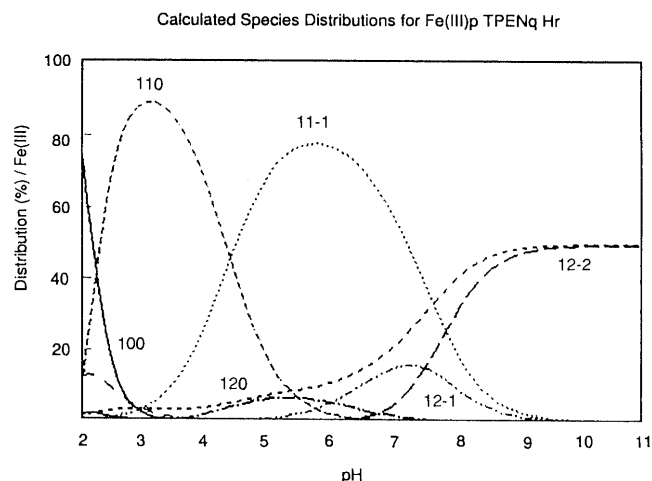


Fig. 7. Calculated Species Distribution for Fe(III)TPEN

Species distributions were calculated for Fe(III)*p*(TPEN)*q*Hr by SUPERQUAD. [Fe(III)]=[TPEN]=1.0 mM. The negative value of *r* indicates that hydroxyl ion takes part in the formation of the complex instead of a proton. 100; Fe(III)aq, 110; Fe(III)TPEN, 11-1; Fe(III)TPEN(OH⁻), 120; Fe(III)(TPEN)₂, 12-1; Fe(III)(TPEN)₂(OH⁻), 12-2; Fe(III)(TPEN)₂(OH⁻)₂.

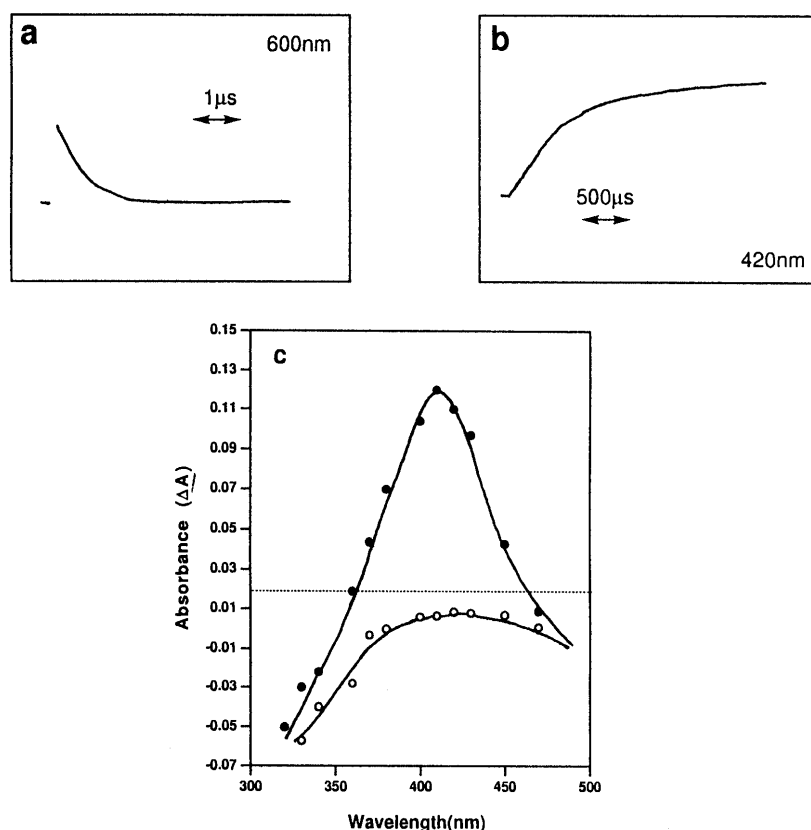


Fig. 8. The Reduction of Fe(III)TPEN by Hydrated Electrons under Deoxygenated Condition

(a) and (b); The transmittance changes of hydrated electrons (a) and of Fe(III)TPEN on reduction with hydrated electrons (b). Deoxygenation was performed by bubbling each cell with nitrogen gas for more than 30 min and the absolute deoxygenation was confirmed by the absence of superoxide production. Irradiation was carried out in 10 mM phosphate buffer (pH 7.4). The concentration of generated hydrated electrons was 12 μM and that of Fe(III)TPEN was 96 μM under this experimental condition. Monitored wavelengths were 600 and 420 nm for (a) and (b), respectively. (c); The difference spectrum of the reduced form of the complex and Fe(III)TPEN *per se* after pulse irradiation. Open circles represent the difference absorbance at the respective wavelengths at 5 μs after pulse irradiation. After 5 μs , hydrated electrons were no longer detectable. Closed circles represent the difference absorbance at 500 μs after pulse irradiation. ΔA was calculated from the changes of transmittance.

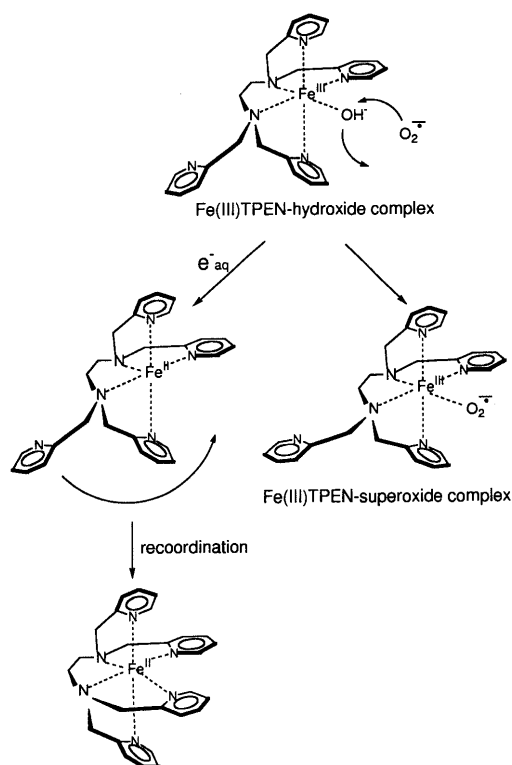


Chart 2. Conformation Change after Reduction by Hydrated Electron and Proposed Structure of Fe(III)TPEN-Superoxide Complex

atoms. The absorption around 420 nm of Fe(II)TPEN is due to this coordinating configuration. Thus, the time at which the absorption of Fe(II)TPEN appears is believed to represent the time at which the free pyridine arm recoordinates to Fe(II).

The proposed structure of Fe(III)TPEN(OH⁻) is strongly supported by these data. The adduct of superoxide may be produced by substitution at the OH⁻ coordination site (Chart 2).

X-Ray Crystallographic Analysis We conducted an X-ray crystallographic study on Fe(II)TPEN(SO₄). A previous study³⁹⁾ on Fe(II)TPEN[(ClO₄)₂] recrystallized from MeOH/H₂O demonstrated that all six nitrogens of TPEN coordinated to Fe(II) to create an octagonal structure. Because the counter anions ClO₄⁻ have no coordination ability due to their bulkiness, they lie outside the complex. This structure is distorted by the two pyridine rings ligated from the equatorial direction. The structures of metal-EDTA have also been reported. According to the literature, H₂O coordinates to the complex as the 7th ligand.⁴⁰⁾ In the case of Fe(II)TPEN[(ClO₄)₂], there is no ligand other than the six nitrogens of TPEN.^{41,42)}

The structure of Fe(II)TPEN(SO₄) obtained in an organic solvent is shown in Fig. 9 and the crystallographic data are listed in Table 1. One of the pyridine rings coordinating from the equatorial direction is substituted by one of the oxygen atoms of the sulfate ion. In the crystal lattice there are 8 molecules, consisting of 4 pairs of asymmetric complexes.

The low basicity of one pyridine ring is consistent with its displacement by sulfate. The mass spectrum showed the molecular ion concomitantly with the sulfate ion (data not shown), again supporting the coordination of sulfate ion as the 6th ligand. The affinity of oxygen for Fe(II)TPEN and the

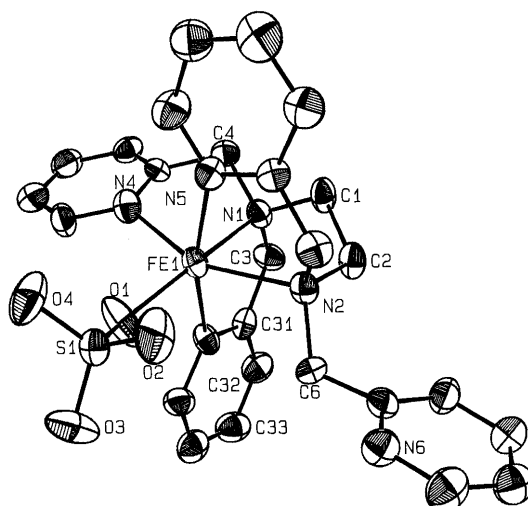


Fig. 9. Crystal Structure of Fe(II)TPENSO₄

Table 1. Crystallographic Parameters

Fe(II)TPEN(SO ₄)	
Cell dimensions	
<i>a</i> (Å)	9.9088
<i>b</i> (Å)	16.3676
<i>c</i> (Å)	39.6851
β (degree)	115.5600
<i>V</i> (Å ³)	5806.3683
Space group	P21 / c
<i>Z</i>	8
Formula	FeC ₂₆ H ₂₈ N ₆ SO ₄ xH ₂ O (x=4)
<i>M</i>	648.523
<i>d</i> _{calc} (g/cm ³)	1.3774
Data collection	
Crystal size (mm)	0.28×0.23×0.23
Diffractometer	Enraf-Nonius CAD-4 turbo
Radiation	Graphite monochromated MoK α 0.7107 Å
Scan mode	$\omega/2\theta$
Sin θ / λ range	< 0.6289
<i>h k l</i> range	-5 < <i>h</i> < 12 -8 < <i>k</i> < 23 -50 < <i>l</i> < 50
Temperature (K)	297 ± 2
Resolution (Å)	0.7950
Rmerge ^{a)}	0.016
R factor	0.0621
weighted R factor	0.0862
No. of reflections	11971
No. of unique reflections	9132
No. of reflections With <i>I</i> > 3 σ (<i>I</i>)	8963

a) Rmerge = $\sum |I_{\text{ave}}(h) - I(h)| / \sum I_{\text{ave}}(h)$.

existence of a direct reaction site on the metal center for activated oxygen species are noteworthy findings.

Discussion

Initially, we employed TPEN as a membrane-permeable metal chelator to inhibit the Fe-driven Haber-Weiss reaction. TPEN, as an iron chelator, completely inhibited *in vitro* aromatic hydroxylation by OH radical secondarily produced from superoxide and hydrogen peroxide by Haber-Weiss reaction in the xanthine/xanthine oxidase system (our unpub-

lished data). TPEN also inhibited aromatic hydroxylation in the presence of EDTA, which is known to enhance the Fe-catalyzed Haber–Weiss reaction.⁴³⁾ This suggested that TPEN should influence the xanthine/xanthine oxidase system. However, Fe(II)TPEN had no influence on the consumption of xanthine or the production of urate. We then examined the reactivity of the Fe complex of TPEN. Fe(II)TPEN reacted with hydrogen peroxide with the rate constant of $7.8 \times 10^1 \text{ M}^{-1} \text{ s}^{-1}$ at pH 7.0 (data not shown), forming the potent oxidant hydroxyl radical or its equivalent species, while Fe(III)TPEN was inactive. So, the Haber–Weiss reaction inhibiting activity of Fe-TPEN can be explained in terms of superoxide quenching activity.

Iuliano and co-workers reported that Fe-TPEN has no SOD activity.²⁹⁾ They suggested that our overestimation was caused by the reaction of Fe(II)TPEN and hydrogen peroxide. Weiss and co-workers have recently shown that Fe-TPEN has no SOD activity by means of a stopped-flow technique, and they also referred to the reaction of Fe(II)TPEN and hydrogen peroxide.³⁰⁾ However, we had known of the reactivity of Fe(II)TPEN and hydrogen peroxide, and our experimental system contained catalase in order to diminish its effect. Therefore, the apparent SOD activity of Fe-TPEN cannot be explained by the reaction with hydrogen peroxide.

As mentioned above, Fe(II)TPEN is oxidized by superoxide generated by irradiation with the second-order rate constant of $3.9 \times 10^6 \text{ M}^{-1} \text{ s}^{-1}$. The redox potentials of superoxide/hydrogenperoxide and Fe(II)TPEN/Fe(III)TPEN are +940 and +545 mV vs. S.C.E. in H_2O (our unpublished data), respectively. This indicates that the reaction (3) can occur in H_2O . However, contrary to our expectation, Fe(III)TPEN was not reduced by superoxide to Fe(II)TPEN; but this does not imply that Fe(III)TPEN is inactive towards superoxide. We obtained optical data suggesting the production of the Fe(III)TPEN–superoxide adduct (Fig. 4). This is a key complex to understand the whole reaction. Next, we observed the regeneration of Fe(III)TPEN from this adduct. This reaction is not a simple separation reaction of Fe(III)TPEN and superoxide because it was second-order (rate constant is $10^3 \text{ M}^{-1} \text{ s}^{-1}$). In this pulse experiment, it seemed to proceed according to reaction (6), because 20 μs after the pulse, superoxide had been completely eliminated. But if the Fe(III)TPEN were exposed to a flux of superoxide, reaction (5) would occur predominantly. The apparent SOD activity of Fe-TPEN in cyt. c assay can thus be explained in terms of superoxidase activity (summarized in Chart 1).

Superoxide dismutation requires the protonation process. This process brings about a potential difference between two superoxide molecules and enables charge transfer. The Fe(III)TPEN-catalyzed reaction can also be considered as well as the proton-catalyzed process. Superoxide would coordinate to the site of Fe(III)TPEN where one pyridine ring is substituted by hydroxylate ion. In this process, a potential difference would be generated between the adduct and superoxide, and the dismutation reaction would be induced by this potential difference. This complex would receive one electron from superoxide through the outer sphere, regenerating free Fe(III)TPEN with the release of O_2^{2-} or a protonated form, HO_2^- or H_2O_2 (Eq. 5).

Here we propose a mechanism for the inhibition of PQ toxicity in *E. coli* by Fe-TPEN. PQ toxicity involves the Fe-

driven Haber–Weiss reaction,⁴⁴⁾ and some chelators such as EDTA can enhance this toxicity. In this reaction, superoxide plays a role in reducing the catalyzing metal to its reduced form, which is reactive with hydrogen peroxide. Our experiments show that once Fe(II)TPEN is oxidized to Fe(III)TPEN, reduction by superoxide does not occur, and Fe(II)TPEN cannot be regenerated. But we have found that Fe(III)TPEN is reduced by other biological reductants such as NADH. This means that in *E. coli* cells Fe(III)TPEN may be reduced to regenerate Fe(II)TPEN by biological reducing systems. However, even if Fe(II)TPEN were produced, OH^\cdot would not be generated, because the reaction rate of H_2O_2 is 10^4 times slower than that of superoxide. We propose that superoxide *per se* inhibits the Fe-driven Haber–Weiss reaction by forming a reaction cycle between Fe(III)TPEN and its superoxide adduct.

It was reported that Fe(II)TPEN $[(\text{ClO}_4)_2]$ is a spin cross-over complex between high spin state and low spin state during measurement of the Mossbauer spectrum, depending on the temperature in the solid state.³⁹⁾ The distance between Fe and nitrogen becomes longer than that in the low spin state. This “relaxed state of coordination” is necessary for Fe(II) to be in a high spin state. In H_2O , Fe(II)TPEN (SO_4) shows almost the same UV-vis. absorption, redox potential and NMR features as Fe(II)TPEN $[(\text{PF}_6)_2]$ or Fe(II)TPEN $[(\text{ClO}_4)_2]$, indicating that they have the same conformation and are in a low spin state in H_2O . On the other hand, in an organic solvent, Fe(II)TPEN (SO_4) shows quite different spectra. This suggests the direct coordination of oxygen of sulfate ion as the 6th ligand. These circumstances make the complex very relaxed in comparison with that in H_2O , favoring the high spin state.

In summary, when Fe(II)TPEN reacts with superoxide, it donates one electron to superoxide to generate peroxide and Fe(III)TPEN. Once oxidized, Fe(III)TPEN (OH^-) becomes the major species in H_2O . In this complex, Fe(III) is assumed to be coordinated by five nitrogen atoms and one oxygen derived from hydroxyl ion. This substitution generates a relaxed complex in the high spin state. In the dismutation reaction, the 6th ligand, OH^- , is displaced by superoxide, forming the Fe(III)TPEN–superoxide complex.

Superoxide dismutation reactions catalyzed by metal complexes are often described by Eq. (1) and (2); however, the mechanism of Fe-TPEN is quite distinct from that, somewhat resembling a proton-catalyzed process. Reexamination of the reaction mechanisms of other SOD mimics reported so far might be desirable.

Acknowledgment This work was supported by a research grant from the Ministry of Education, Science, Sports and Culture of Japan.

References

- 1) McCord J. M., Fridovich I., *J. Biol. Chem.*, **244**, 6049–6055 (1969).
- 2) Fridovich I., *J. Biol. Chem.*, **264**, 7761–7764 (1989).
- 3) Igarashi R., Hoshino J., Takenaga M., Kawai S., Morizawa Y., Yasuda A., Otani M., Mizushima Y., *J. Pharmacol. Exp. Ther.*, **262**, 1214–1219 (1992).
- 4) Tan S., McAdams M., Royall J., Freeman B. A., Parks D. A., *Free Radic. Biol. Med.*, **24**, 427–434 (1998).
- 5) Yao T., Esposti S. D., Huang L., Arnon R., Spangenberg A., Zern M. A., *Am. J. Physiol.*, **267**, 476–484 (1994).
- 6) Leuthauser S. W. C., Oberley L. W., Oberley T. D., Sorenson J. R. J., Ramakrishna K., *J. Natl. Cancer Inst.*, **66**, 1077–1081 (1981).
- 7) Pasternack R. F., Halliwell B., *J. Am. Chem. Soc.*, **101**, 1026–1031

- (1979).
- 8) Lengfelder E., Fuchs C., Younes M., Weser U., *Biochim. Biophys. Acta*, **567**, 492—502 (1979).
- 9) Kimura E., Yatsunami A., Watanabe A., Machida R., Koike T., Fujioka H., Kuramoto Y., Sumomogi M., Kunimizu K., Yamashita A., *Biochim. Biophys. Acta*, **745**, 37—43 (1983).
- 10) Liu Z. X., Robinson G. B., Gregory E. M., *Arch. Biochem. Biophys.*, **315**, 74—81 (1994).
- 11) Kitajima N., Osawa M., Tamura N., Moro-oka Y., Hirano T., Hirobe M., Nagano T., *Inorg. Chem.*, **32**, 1879—1880 (1993).
- 12) Faulkner K. M., Stevens R. D., Fridovich I., *Arch. Biochem. Biophys.*, **310**, 341—346 (1994).
- 13) Riley D. P., Weiss R. H., *J. Am. Chem. Soc.*, **116**, 387—388 (1994).
- 14) Riley D. P., Lennon P. J., Neumann W. L., Weiss R. H., *J. Am. Chem. Soc.*, **119**, 6522—6528 (1997).
- 15) Batinic-Haberle I., Benov L., Spasojevic I., Fridovich I., *J. Biol. Chem.*, **273**, 24521—24528 (1998).
- 16) Baudry M., Etienne S., Bruce A., Palucki M., Jacobsen E., Malfroy B., *Biochem. Biophys. Res. Commun.*, **192**, 964—968 (1993).
- 17) Xiang D. F., Duan C. Y., Than X. S., Hang Q. W., Tang W. X., *J. Chem. Soc., Dalton Trans.*, **1998**, 1201—1204.
- 18) Yamato K., Miyahara I., Ichimura A., Hirotsu K., Kojima Y., Sakurai H., Shiomi D., Sato K., Takui T., *Chem. Lett.*, **1999**, 295—296.
- 19) Day B. J., Fridovich I., Crapo J. D., *Arch. Biochem. Biophys.*, **347**, 256—262 (1997).
- 20) Baker K., Marcus C. B., Huffman K., Kurk H., Malfroy B., Doctrw S. R., *J. Pharm. Exp. Thera.*, **284**, 215—221 (1998).
- 21) Weiss R. H., Fretland D. J., Baron D. A., Ryan U. S., Riley D. P., *J. Biol. Chem.*, **271**, 26149—26156 (1996).
- 22) Lowe D., Pagel P. S., McGough M. F., Hetttrick D. A., Warltier D. C., *Eur. J. Pharmacol.*, **304**, 81—86 (1996).
- 23) Hardy M. M., Flickinger A. G., Riley D. P., Weiss R. H., Ryan U. S., *J. Biol. Chem.*, **269**, 18535—18540 (1994).
- 24) Goldstein S., Czapski G., Meyerstein D., *J. Am. Chem. Soc.*, **112**, 6489—6492 (1990).
- 25) Bull C., McClune G. J., Fee J. A., *J. Am. Chem. Soc.*, **105**, 5290—5300 (1983).
- 26) Nagano T., Hirano T., Hirobe M., *J. Biol. Chem.*, **264**, 9243—9249 (1989).
- 27) Nagano T., Hirano T., Hirobe M., *Free Rad. Res. Commun.*, **12—13**, 221—227 (1991).
- 28) Moon J. O., Park S.-K., Nagano T., *Biol. Pharm. Bull.*, **21**, 284—288 (1998).
- 29) Iuliano L., Pedersen J. Z., Ghiselli A., Pratico D., Rotilio G., Violi F., *Arch. Biochem. Biophys.*, **293**, 153—157 (1992).
- 30) Weiss R. H., Flickinger A. G., River W. J., Hardy M. M., Aston K. W., Ryan U. S., Riley D. P., *J. Biol. Chem.*, **268**, 23049—23054 (1993).
- 31) Kobayashi K., Hayashi K., Sono M., *J. Biol. Chem.*, **264**, 15280—15283 (1989).
- 32) Odani A., Masuda H., Inukai K., Yamauchi O., *J. Am. Chem. Soc.*, **114**, 6294—6300 (1992).
- 33) Gans P., Sabatini A., Vacca A., *J. Chem. Soc., Dalton Trans.*, **1985**, 1195—1200.
- 34) Anderegg G., Wenk F., *Helv. Chim. Acta*, **50**, 2330—2332 (1967).
- 35) Anderegg G., Hubmann E., Podder N. G., Wenk F., *Helv. Chim. Acta*, **60**, 123—140 (1977).
- 36) Hsu J. L., Hsieh Y., Tu C., O'Connor D., Nick H. S., Silverman D. N., *J. Biol. Chem.*, **271**, 17687—17691 (1996).
- 37) Tsang P. K. S., Sawyer D. T., *Inorg. Chem.*, **29**, 2848—2855 (1990).
- 38) Flynn C. M., Jr., *Chem. Rev.*, **84**, 31—41 (1984).
- 39) Chang H. R., McCusker J. K., Toftlund H., Wilson S. R., Trautwein A. X., Winkler H., Hendrickson D. N., *J. Am. Chem. Soc.*, **112**, 6814—6827 (1990).
- 40) Lind M. D., Hamor M. J., Hamor T. A., Hoard J. L., *Inorg. Chem.*, **3**, 34—43 (1964).
- 41) Mandel J. B., Maricondi C., Douglas B. E., *Inorg. Chem.*, **27**, 2990—2996 (1988).
- 42) Mandel J. B., Douglas B. E., *Inorganica Chimica Acta*, **155**, 55—69 (1989).
- 43) Rush J. D., Koppenol W. H., *J. Biol. Chem.*, **261**, 6730—6733 (1986).
- 44) Korbashi P., Kohen R., Katzhendler J., Chevion M., *J. Biol. Chem.*, **261**, 12472—12476 (1986).

Molecular State of Chlorpheniramine in Resinates

Prasert AKKARAMONGKOLPORN,^{*,a} Etsuo YONEMOCHI,^b and Katsuhide TERADA^b

Department of Pharmaceutical Technology, Faculty of Pharmacy, Silpakorn University,^a Nakorn Pathom, Thailand and

Department of Pharmaceutics, School of Pharmaceutical Sciences, Toho University,^b Japan.

Received August 9, 1999; accepted October 9, 1999

Chlorpheniramine (CPM) maleate was prepared as a series of resinates by the batch method. The several resinates were investigated by differential scanning calorimetry (DSC), X-ray powder diffraction (XRPD) and infrared (IR) spectrometry. The results from DSC and XRPD showed that the molecular state of the entrapped drug changed from the crystalline to amorphous state. IR spectra indicated that only CPM species was entrapped in the resinates. Moreover, it also showed that the positively charged amine group of the drug interacted with the sulfonate groups of the resin by ionic association. The dissolution of the drug and resinates was also studied where it was found that the dissolution of the resinates was retarded by their crosslinked structure and markedly affected by the quantity of resin.

Key words chlorpheniramine maleate; ion exchange; X-ray diffraction; differential scanning calorimetry; infrared spectrometry

It has been recognized that the physicochemical properties of a drug can be changed in a number of ways. For example, a significant decrease in crystallinity and improvement in the dissolution rates of glibenclamide and oxazepam were observed with inclusion complexes of cyclodextrins.^{1,2)} The use of a vacuum or microwave energy to prepare felodipine surface solid dispersions led to a significant improvement in drug dissolution, which was caused partly by the amorphous state of the drug.³⁾ The ground drug and mixture, depending on the grinding time, were less crystalline and dissolved to greater extent in organic solvents than the intact drug.^{4,5)} A resinate is a complex of a drug and resin⁶⁾ and it can be used to formulate sustained-release products, some of which have been marketed. A large number of drugs have been extensively studied as resinates such as propranolol HCl, some NSAIDs and dextromethorphan HBr.^{7–9)} Furthermore, encapsulated resinates with some polymers have been prepared, and it has been claimed that a more controllable release was obtained.¹⁰⁾ However, information about the molecular state of a drug in the resinate is rare.

Therefore, this work was carried out to investigate the molecular state of a drug manipulated as a series of resinates. Chlorpheniramine (CPM) maleate and Amberlite® IRP 69 (in powder form) were used as the model drug and resin, respectively. This resin is an insoluble, strongly cationic exchanger with 8% cross-linkage derived from a sulfonated copolymer of styrene and divinylbenzene (Fig. 1). The molecular state of the resinates as well as the drug was investigated by differential scanning calorimetry (DSC), X-ray powder diffraction (XRPD) and IR. In addition, the dissolution of samples was also determined and discussed.

Experimental

Materials Amberlite® IRP 69 (Sigma, U.S.A.), CPM maleate (Sigma, U.S.A.), monobasic potassium phosphate (Wako, Japan) and sodium hydroxide (Jensei, Japan) were used.

Purification of Resin The resin (20 g) was placed in a 250 ml beaker and 200 ml distilled water was added. The slurry was stirred with a magnetic bar for 5 min, and allowed to settle for 15 min; then, the supernatant was removed by decantation. The resin was washed another two times according to the above procedure. The washed resin was collected by filtration and dried overnight in a hot air oven at 50 °C. The dried resin was kept in a tight vial until preparation of the resinates.

Preparation of Resinates The resin (1 g) was weighed and added to

100 ml of 0.15, 0.5 or 1.0% w/v CPM maleate solution. The mixtures were left in the dark at room temperature (25 °C) for 48 h and periodically shaken. The resinates were isolated by filtration and washed with an excess of distilled water which was then collected and added to the previous filtrate. The resinates were dried overnight in a hot air oven at 50 °C, and stored in a tight vial. The drug content in each final filtrate, which consisted of the filtrate and the washing water, was analyzed by UV spectroscopy (UV-160, Shimadzu, Japan) at 261 nm. The amount of drug loaded on the resinates was obtained by subtracting the amount of drug remaining in the final filtrate from the initial amount.

Preparation of CPM Base CPM base was prepared by making CPM maleate solution alkaline with 1.0N sodium hydroxide. Then, ether was added and the mixture was shaken gently. The ether phase was removed and evaporated on a water bath until only CPM base remained. Finally, the CPM base was kept in a vacuum chamber until investigation.

DSC A differential scanning calorimeter (DSC 7, Perkin Elmer, U.S.A.) was used and each sample was placed in an aluminum pan and crimped with its cover (Perkin Elmer, U.S.A.). The heating and cooling rates were 20 and 200 °C/min, respectively. All measurements were obtained over 25–250 °C under nitrogen.

XRPD A Rigaku X-ray powder diffractometer was used and measuring conditions were as follows: CuK α radiation, Ni filtered, graphite monochromator, voltage 35 kV and current 10 mA. All samples were run at 1° (2 θ) min⁻¹ from 5 to 35° (2 θ).

IR Spectrometry IR spectra were obtained using a Fourier transform infrared spectrometer (FT/IR-7300, Jasco, Japan) and measurements were carried out on KBr disks.

Dissolution Study The dissolution of the drug and resinates was studied using the USP paddle apparatus.¹¹⁾ The sample was accurately weighed to obtain the equivalent of 15 mg of drug and added to vessels containing 450 ml phosphate buffer, pH 7.0 \pm 0.2.¹¹⁾ The temperature and paddle speed were set at 37 \pm 0.1 °C and 50 \pm 1 rpm, respectively. At suitable times, the amount of drug released was analyzed by UV spectroscopy.

Water Content Determination Karl Fisher titration with an Aquacounter® (AQU-6, Hiranuma, Japan) was used.

Results and Discussion

No water was detected in the CPM maleate. On the other

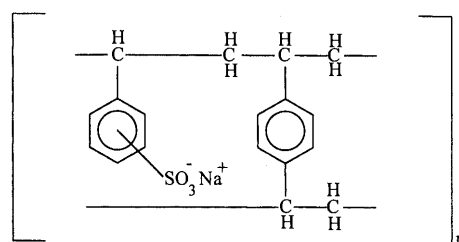


Fig. 1. Structure of Amberlite® IRP 69

* To whom correspondence should be addressed.

Table 1. Obtained Resinates

Resinate	CPM content (% w/w)	Water content (% w/w)	CPM content on a dry basis ^a (% w/w)
Resinate I (RS I)	12.31	10.63	14.67
Resinate II (RS II)	30.59	10.49	35.06
Resinate III (RS III)	43.21	7.99	48.23

a) Water content of dried resin=18.34% w/w.

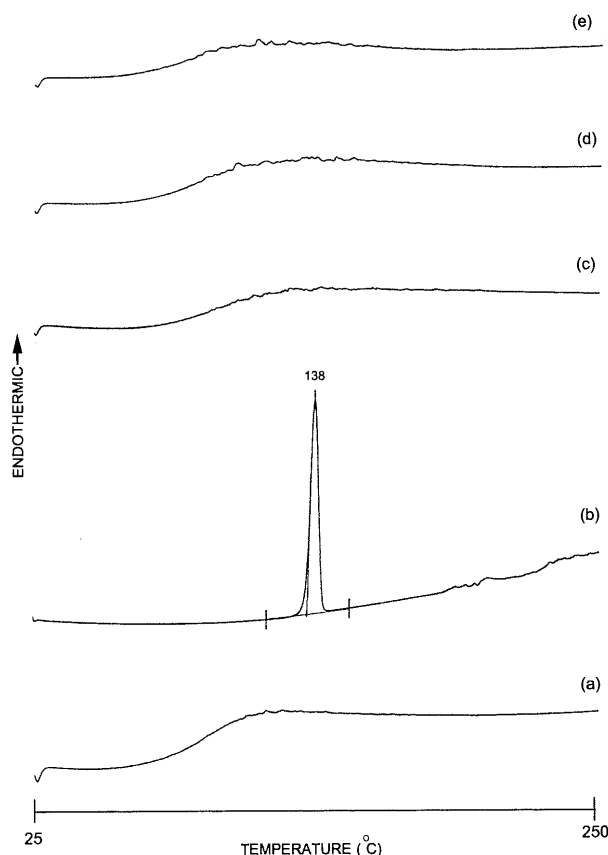


Fig. 2. DSC Curves of Resin (a), CPM Maleate (b), RS I (c), RS II (d), and RS III (e)

hand, the resin and the resinates contained high and varying amounts of water, even when dried overnight at 50 °C. The drug content without and with (on a dry basis) water subtraction is shown in Table 1. In a certain quantity of resinate, it was found that the amount of drug calculated from the drug content without water subtraction underestimated the actual drug content calculated from the drug content on a dry basis (6.11, 2.52 and 2.63% w/w in RS I, RS II and RS III, respectively). To obtain the actual drug content as required, the drug content on a dry basis was used to calculate each quantity of resinate, which contained the equivalent drug content, for the dissolution study.

Molecular State of Drug in Resinates Figure 2 shows the DSC curves of the resin, CPM maleate and resinates. CPM maleate has an endothermic peak at 138 °C, indicating the temperature of drug melting, whereas no peak over the range 25–250 °C was observed in the DSC curves of the resin and all resinates. The XRPD patterns of the samples are shown in Fig. 3. It appears that the molecular state of CPM maleate is crystalline, but the resin is amorphous. The resinates also showed a halo' pattern. DSC and XRPD

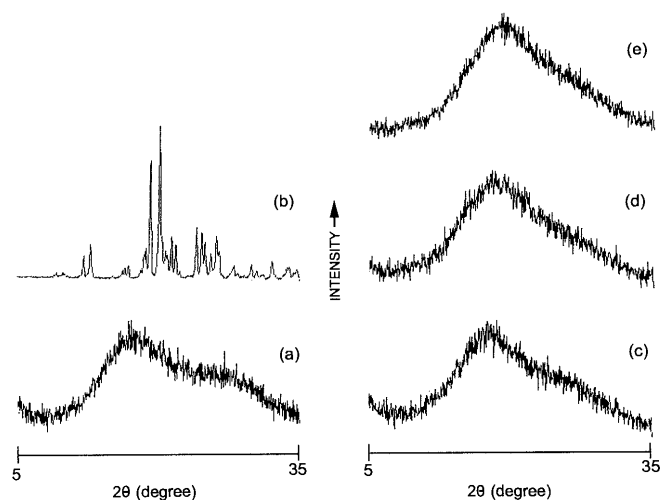


Fig. 3. X-Ray Patterns of Resin (a), CPM Maleate (b), RS I (c), RS II (d), and RS III (e)

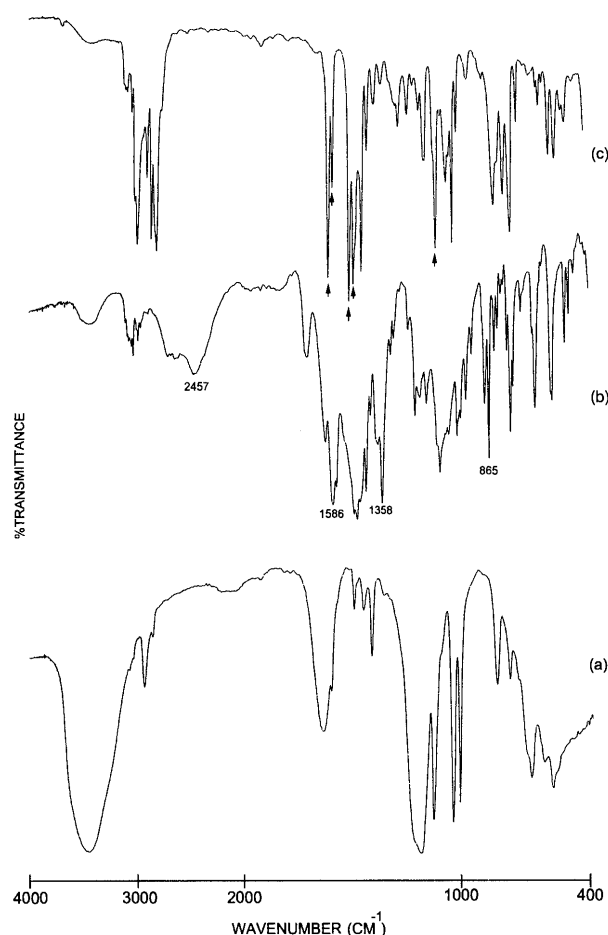


Fig. 4. IR Spectra of Resin (a), CPM Maleate (b), and CPM Base (c)

showed that the molecular state of the entrapped drug in the resinates changed from the crystalline to the amorphous state. From this it appears that the drug is dispersed monomolecularly in the resinates.¹²⁾

Interaction in Resinates IR spectra of the resin, CPM maleate and resinates are shown in Figs. 4–5. The three peaks at 1586, 1358 and 865 cm⁻¹, corresponding to the stretching of the carbonyl group (C=O), carbon-oxygen group (C–O) and ethylene group (C=C) of the maleate

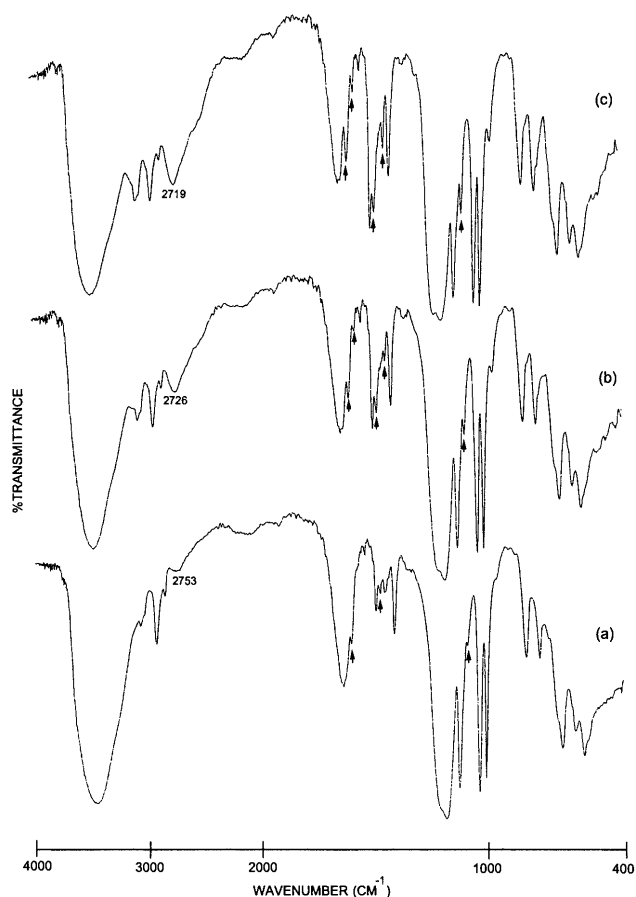


Fig. 5. IR Spectra of RS I (a), RS II (b), and RS III (c)

species, disappeared in IR spectra of the resins. This confirmed the absence of maleate species in the resins, in accordance with the theory that only a positively charged species can exchange on a cationic exchanger.¹³⁾

The IR spectrum of the CPM base was also measured and this is shown in Fig. 4. Comparing the IR spectra for CPM maleate, CPM base, resin and resins, the IR spectra of the resins could be divided into two different regions. One around the region of 800 to 2000 cm^{-1} showed the existence of major characteristic peaks of CPM base (indicated with arrows), whose intensities increased on increasing the amount of drug entrapped in the resins. This indicated that the CPM species was entrapped in the resins. The other, from 2000 to 4000 cm^{-1} , was more similar to the CPM maleate (salt form) and resin spectra, at the same region, than to that of the CPM base and resin spectra. This confirmed the stretching of the positively charged amine group (NH^+) in the IR spectra of the resins. Furthermore, the NH^+ peak of the drug was shifted from 2457 cm^{-1} to around 2719–2753 cm^{-1} in the resins. The above evidence shows that the CPM species in the resins exists in the positively charged form which interacts with the sulfonate groups in the resin. This kind of ionic association is referred as a “salt bridge” (Fig. 6).¹⁴⁾ Like the hydrogen-bonding effect, the degree of this ionic association, which closely relates to the H-donating and accepting ability of an ion pair, significantly affects the NH^+ stretching. As the ionic association increases, the NH^+ stretching decreases and subsequently shifts to a lower frequency, and *vice versa*. Therefore, the shifting of the NH^+ stretching in the drug to a

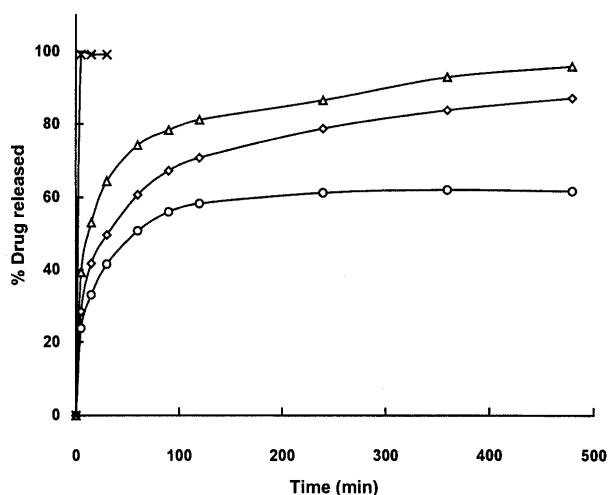
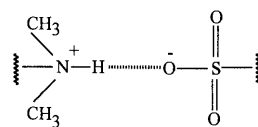
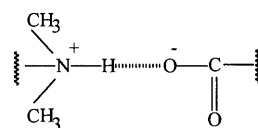


Fig. 7. Dissolution Profiles of CPM Maleate (X), RS I (O), RS II (◇), and RS III (△)



(b)



(a)

Fig. 6. Depiction of the Ionic Association in CPM Maleate (a), and in Resins (b)

higher frequency in the resins suggests that the ionic association in the resins is weaker than in the drug. One explanation might be that the H-accepting ability, corresponding to the basicity, of the sulfonate group is weaker than that of the carboxylate group.¹⁵⁾ Moreover, a related text attributing the interaction in the resinate to a weak ionic association in which no chemical bond was formed, supports this hypothesis.¹³⁾ In conclusion, CPM was dispersed monomolecularly in the resins and an ionic association was formed between the sulfonate groups of the resin and the NH^+ group of CPM.

Release Study The dissolution of the drug and resins is presented in Fig. 7. The dissolution rate of the drug was faster than that of the resins. The retard release in the resins, in spite of the amorphous molecular state of the drug, was attributed to their crosslinked structure which resists drug diffusion through the resin beads.^{8,9)} The amount of CPM released increased from 61.93 to 87.54 and 96.36% w/w in RS I, RS II and RS III, respectively, indicating that drug distribution in the resins greatly affected the amount of drug released. This was due to the decreasing quantity of resin in RS I, RS II, RS III, respectively. A detailed explanation was proposed in a recently published study showing that increasing the quantity of the resin reduced the effectiveness

Table 2. Retained Fraction in Resinates

Resinate ^{a)}	Quantity of resin ($\times 10^{-3}$ g)	Exchange capacity ^{b)} (meq)	CPM retained ^{c)} (meq)	Retained fraction ^{d)}
RS I	87.2	0.3750	0.0146	0.0389
RS II	27.8	0.1195	0.0048	0.0402
RS III	16.1	0.0692	0.0014	0.0202

a) All resinates contain the equivalent of 15 mg CPM maleate. b) Quantity of resin multiplied by total exchange capacity of resin (4.3 meq/g). c) MW of CPM maleate=390.8. d) CPM retained divided by exchange capacity.

of the vehicle; unfortunately, no experimental evidence was provided.¹⁶⁾ The relationship determining the fraction of drug retained is presented in Table 2. It was found that the fraction of drug retained in the resinates reached an equilibrium value. This behavior suggests that the quantity of the resin in resinates directly affects the amount of drug released. At an equivalent drug content, the proportion of the quantity of drug required for that retained fraction (Table 2) to the quantity of drug released increases on increasing the quantity of resin in the resinates, which consequently leads to less drug release.

Acknowledgments This work was supported by a grant from the Japan Society for the Promotion of Science and National Research Council of Thailand (JSPS-NRCT).

References

- 1) Sanghavi N. M., Venkatesh H., Tandel V., *Drug. Dev. Ind. Pharm.*, **20**, 1275—1283 (1994).
- 2) Moyano J. R., Gines J. M., Arias M. J., Rabasco A. M., *Int. J. Pharm.*, **114**, 95—102 (1995).
- 3) Kerc J., Srcic S., Kofler B., *Drug. Dev. Ind. Pharm.*, **24**, 359—363 (1998).
- 4) Yonemochi E., Oda K., Saeki S., Oguchi T., Nakai Y., Yamamoto K., *Chem. Pharm. Bull.*, **42**, 1948—1950 (1994).
- 5) Oguchi T., Matsumoto K., Yonemochi E., Nakai Y., Yamamoto K., *Int. J. Pharm.*, **113**, 97—102 (1995).
- 6) Bhaskar R., Murthy R. S. R., Miglani B. D., Visawanthan K., *Int. J. Pharm.*, **28**, 59—66 (1986).
- 7) Burke G. M., Mendes R. W., Jambhekar S. S., *Drug Dev. Ind. Pharm.*, **12**, 713—732 (1986).
- 8) Irwin W. J., Machale R., Watts P. J., *Drug Dev. Ind. Pharm.*, **16**, 883—898 (1990).
- 9) Pongpaibul Y., Sayed H., Whitworth C. W., *Drug Dev. Ind. Pharm.*, **16**, 935—943 (1990).
- 10) Ranghunatan Y., Amsel L., Hinsvark O., Bryant W., *J. Pharm. Sci.*, **70**, 379—384 (1981).
- 11) United States Pharmacopeia, Vol. 23, The United States Pharmacopeial Convention, Inc., Rockville, MD, 1995.
- 12) Oguchi T., Terada K., Yamamoto K., Nakai Y., *Chem. Pharm. Bull.*, **37**, 1881—1885 (1989).
- 13) Russel P. (ed), "An Introduction to Ion-Exchange Resins," Laydon and Son, Ltd., UK, 1970.
- 14) Isaacs N. S. (ed), "Physical Organic Chemistry," Vol. 2., Longman Singapore Publisher, Ltd., Singapore, 1995.
- 15) Hand C. W., Blewitt H. L. (ed), "Acid-Base Chemistry," Macmillan Publishing Co., New York, 1986.
- 16) Conaghey O. M., Corish J., Corrigan O. I., *Int. J. Pharm.*, **170**, 215—224 (1998).

Mechanism of Antioxidative Activity of Fluvastatin–Determination of the Active Position

Takashi NAKAMURA,^{*,a} Hiroyuki NISHI,^a Yoshio KOKUSENYA,^a Kenichi HIROTA,^b and Yozo MIURA^{*,b}

Analytical Chemistry Department, Product and Technology Development Laboratory, Tanabe Seiyaku Co., Ltd.,^a Yodogawa-ku, Osaka 532–8505, Japan and Department of Applied Chemistry, Faculty of Engineering, Osaka City University,^b Sumiyoshi-ku, Osaka 558–8585, Japan. Received August 9, 1999; accepted October 15, 1999

In order to clarify the mechanism of action for the antioxidative activity of fluvastatin sodium (FLV, (±)-sodium (3*RS*, 5*RS*, 6*E*)-7-[3-(4-fluorophenyl)-1-(1-methylethyl)-1*H*-indol-2-yl]-3,5-dihydroxy-6-heptanoate) and its derivatives, reaction of the corresponding methyl ester of FLV with di-*tert*-butyl diperoxyoxalate was examined, and the corresponding keto derivative was isolated from the reaction mixture. On the basis of this result, it was concluded that the active site is the allylic carbon conjugated with the indole ring.

Key words fluvastatin; 3-hydroxy-3-methylglutaryl coenzyme A reductase inhibitor; antioxidative activity; spin trapping; hydrogen-atom abstraction

Hypercholesterolemia drugs such as 3-hydroxy-3-methylglutaryl coenzyme A (HMG-CoA) reductase inhibitors lower the level of plasma cholesterol by inhibiting the key enzyme in the biosynthetic pathway from HGM-CoA to mevalonic acid, a precursor of cholesterol.^{1,2)} Recently, it was reported that this type of medicine is effective for prevention of arteriosclerosis and myocardial infarction.^{3,4)} The medical effectiveness of medicines for these diseases is considered to be due to their antioxidative activity. Accordingly, other antioxidative compounds such as probucol have also received much attention.^{5,6)}

Recently, it was shown that fluvastatin sodium (FLV, (±)-sodium (3*RS*, 5*RS*, 6*E*)-7-[3-(4-fluorophenyl)-1-(1-methylethyl)-1*H*-indol-2-yl]-3,5-dihydroxy-6-heptanoate), one of the HMGCoA reductase inhibitors, has *in vivo* and *in vitro* antioxidative activity.^{7–13)} For example, FLV scavenged hydroxyl radical and superoxide anion,^{11–13)} inhibited microsomal lipid peroxidation,^{11,12)} reduced the susceptibility of low density lipoprotein (LDL) to lipid peroxidation,^{7–10)} and suppressed progression of arteriosclerosis.⁹⁾ However, in spite of many studies on the antioxidative activity of FLV, the mechanism for the antioxidative behavior of FLV remains unresolved, and we considered that it is very important to determine the active position. In the present study, we performed hydrogen-atom abstraction from the corresponding methyl ester of FLV (FLV-Me) using *tert*-butoxyl radicals generated by thermolysis of di-*tert*-butyl diperoxyoxalate (DBDP) and isolated a keto form of FLV-Me (FLV-K-Me) from the reaction mixture. On the basis of this result, we could unambiguously determine that the active site for the antioxidative ability of FLV is the allylic carbon conjugated with the indole ring.

Experimental

Materials and Reagents FLV-Me was prepared by Tanabe R and D Service Co., Ltd (Tokyo, Japan). FLV-R-Me was prepared by Tanabe Seiyaku Co., Ltd. (Osaka, Japan). DBDP was prepared by the reported method.¹⁴⁾ Phenyl-*N-tert*-butyl nitron (PBN) and 2,2,6,6-tetramethylpiperidinyl-*N*-oxyl (TEMPO) were purchased from Sigma Aldrich. Column chromatography was carried out on silica gel (BW127ZH, Fuji Silysia Chemical Co., Ltd., Aichi, Japan), and TLC plates (Kieselgel 60F₂₅₄) were purchased from Merck.

Measurements ¹H- and ¹³C-NMR spectra were recorded with a Bruker DRX-500 spectrometer with tetramethylsilane as an internal standard; chemical shifts are given in ppm (δ). Liquid chromatography (LC)-MS

spectra were taken on a Hitachi M-1000 LC-API mass spectrometer. ESR spectra were measured with a Bruker ESP300 spectrometer equipped with 100 kHz field modulation. HPLC was carried out on a Shimadzu LC-6A equipped with a SPD-6A UV detector, a CTO-6A column oven, and a C-R5A computer system. The column was a Shiseido Capcellpak C₁₈, and the mobile phase was phosphate buffer saline (50 mmol/L, pH 6.5):CH₃CN (11:9).

Reaction of FLV-Me with DBDP A solution of FLV-Me (50 mg, 0.117 mmol) and DBDP (117 mg, 0.50 mmol) in benzene (10 ml) was stirred at 40 °C for 1 h under a nitrogen stream. The reaction mixture was evaporated under reduced pressure, and the residue was chromatographed on silica gel with benzene:ethyl acetate (3:1). The light yellow zone was collected and concentrated to give FLV-K-Me in 23% yield (11.4 mg, 0.0269 mmol). Recrystallization from hexane gave pale yellow prisms with mp 99–100 °C. IR (KBr): 1744 (C=O) cm⁻¹. ¹H-NMR (CDCl₃): 7.75 (1H, d, *J*=16 Hz, –CO–CH=CH–), 7.57 (1H, d, *J*=8 Hz, aromatic), 7.50 (1H, d, *J*=8 Hz, aromatic), 7.38 (2H, m, aromatic), 7.28 (1H, t, *J*=8 Hz, aromatic), 7.17 (2H, m, aromatic), 7.10 (1H, t, *J*=8 Hz, aromatic), 6.29 (1H, d, *J*=16 Hz, –CO–CH=CH–), 4.95 (1H, septet, *J*=7 Hz, –CHMe₂), 4.50 (1H, m, –CH₂–CH(OH)–CH₂–), 3.71 (3H, s, –COOCH₃), 3.54 (1H, d, *J*=4 Hz, –CH(OH)–), 2.72 (2H, d, *J*=6 Hz, –CH(OH)–CH₂–CO–), 2.55 (2H, d, *J*=6 Hz, –OCOCH₂–), 1.70 (6H, d, *J*=7 Hz, –CH(CH₃)₂). ¹³C-NMR (CDCl₃): 198.8 (s), 172.7 (s), 162.5 (*J*_{C-F}=238 Hz), 137.5 (s), 132.4 (d), 132.4 (overlapped), 132.3 (d, *J*_{C-F}=8 Hz), 131.0 (s), 128.8 (s), 128.0 (d), 124.5 (d), 121.7 (s), 121.1 (d), 120.9 (d), 116.3 (d, *J*_{C-F}=21 Hz), 112.7 (d), 65.1 (d), 52.2 (q), 48.5 (d), 47.4 (t), 41.0 (t), 22.3 (q). LC-MS (APCI) (rel. int. %) *m/z*: 424 (M+H)⁺ (100), 322 (32). Anal. Calcd for C₂₅H₂₆FNO₄: C, 70.91; H, 6.19; N, 3.31. Found: C, 70.67; H, 6.22; N, 3.25.

Reaction of FLV-Me with DBDP in the Presence of TEMPO The reaction of FLV-Me with DBDP in benzene was carried out in the presence of TEMPO in the same manner as above. Thus, a solution of FLV-Me (50 mg, 0.117 mmol), DBDP (117 mg, 0.50 mmol), and TEMPO (39 mg, 0.25 mmol)

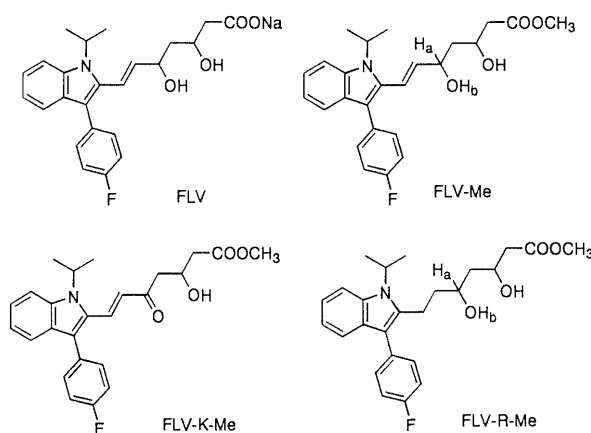


Chart 1

* To whom correspondence should be addressed.

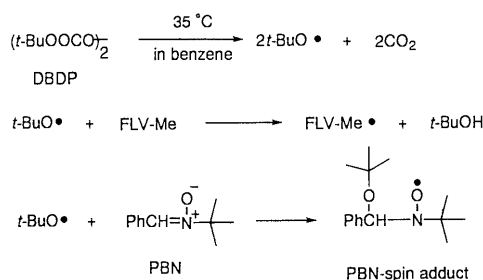


Chart 2

in benzene (10 ml) was stirred at 40 °C for 1 h under a nitrogen stream, and the mixture was evaporated under reduced pressure. The residue was then chromatographed on silica gel with benzene:ethyl acetate (3:1), and the light yellow zone was collected and concentrated to give FLV-K-Me in 52% yield (25.8 mg, 0.061 mmol). Melting point, IR and ¹H- and ¹³C-NMR spectra agreed completely with those of the above sample.

Spin Trapping of *tert*-Butoxyl Radical by PBN in the Presence of FLV-Me Benzene solutions (1.0 ml) containing PBN (10 mmol/l), DBDP (5.0 mmol/l), FLV-Me (0–10.0 mmol/l) in ESR tubes were degassed with three freeze-pump-thaw cycles, and the tubes were sealed. After standing at 35 °C for 30 min, ESR measurements were carried out. The results are shown in Fig. 1.

Competitive Reaction of FLV-Me and FLV-R-Me with *tert*-Butoxyl Radical A solution of FLV-Me (50.0 mg, 0.118 mmol), FLV-R-Me (50.4 mg, 0.118 mmol), DBDP (55 mg, 0.236 mmol), and TEMPO (36.9 g, 0.236 mmol) in benzene (10 ml) was stirred at 35 °C under a nitrogen stream. Every 30 min, 0.1 ml of the reaction mixture was taken and diluted to 10 ml with the mobile phase. Twenty μl of the sample solution was used for HPLC measurements. The results are shown in Fig. 2.

Results and Discussion

Activity of FLV-Me as a Scavenger for *tert*-Butoxyl Radicals Since oxygen-centered free radicals such as ·OH or ·OOH play an important role for oxidation *in vivo*, it is desirable that ·OH or ·OOH radicals be used for hydrogen-atom abstraction from FLV. However, it is very difficult to generate these radicals effectively. We therefore chose *tert*-butoxyl radical as an oxygen-centered radical instead of ·OH or ·OOH radical. Since *tert*-butoxyl radical can be effectively generated by thermolysis of DBDP in hydrocarbons such as benzene and hexane.¹⁴⁾ However, FLV is insoluble in benzene and hexane. We therefore used FLV-Me instead of FLV because of its good solubility in benzene.¹⁵⁾ At first, the antioxidative activity of FLV-Me was evaluated using the spin trapping method.¹⁶⁾ A solution of FLV-Me, PBN and DBDP in benzene was placed in an ESR tube and, after the solution was degassed and allowed to stand at 35 °C for 30 min, ESR spectra were measured. DBDP is decomposed in a homolytic mechanism in hydrocarbon solvents at room temperature to give two *tert*-butoxyl radicals and two CO₂ molecules in quantitative yields.¹⁷⁾ The generated *tert*-butoxyl radicals react with PBN to give PBN-spin adducts or abstract a hydrogen atom from FLV-Me, as shown in Chart 2. If FLV-Me has no active hydrogen, *tert*-butoxyl radicals are trapped by PBN or decompose to nonradical compounds. In this case, the intensity of the ESR signal due to the PBN-spin adduct would be constant regardless of the concentration of FLV-Me. As found in Fig. 1, the intensity of ESR signal due to the PBN-spin adduct is drastically decreased with an increase in the concentration of FLV-Me, and when the concentrations of FLV-Me are higher than 1.25 mmol/l, the ESR signal intensity is less than 10% of the case of the absence of FLV-Me. This indicates that most *tert*-butoxyl radicals generated are

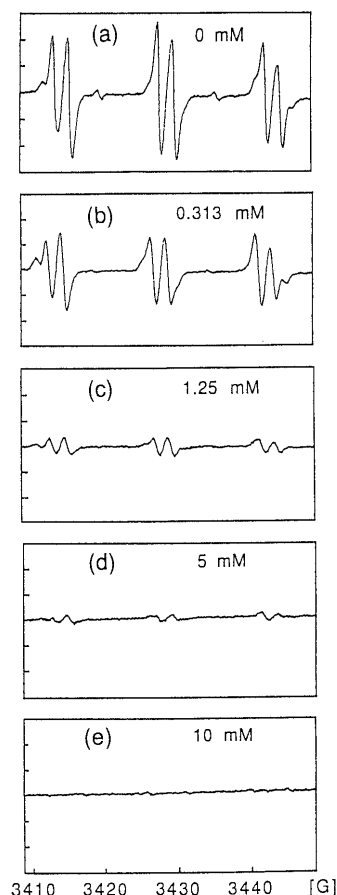


Fig. 1. ESR Spectra from Solutions of FLV-Me (0–10), DBDP (5.0), and PBN (10 mmol/l) in Benzene

FLV-Me: (a) 0, (b) 0.313, (c) 1.25, (d) 5.00, (e) 10.0 mmol/l.

consumed by hydrogen-atom abstraction from FLV-Me, indicating that FLV-Me has high radical scavenging ability.

Determination of the Active Position for FLV-Me To determine the active site for the antioxidative activity of FLV-Me the reaction of FLV-Me with DBDP was carried out in benzene in the presence of TEMPO. TEMPO is a very stable free radical which has the ability to trap a wide variety of intermediate radicals. We therefore expected that TEMPO might capture an intermediate radical generated by hydrogen-atom abstraction from FLV-Me by *tert*-butoxyl radicals to give a stable coupled product. The reaction was carried out at 40 °C for 1 h under a nitrogen atmosphere. TLC inspection showed three spots. Two of them were due to FLV-Me and TEMPO, and the third spot (light yellow) was due to the product. ESR measurements of the reaction mixture showed that the concentration of TEMPO was constant within experimental error during the reaction. Isolation of the product was performed by column chromatography with benzene:ethyl acetate (3:1), and FLV-K-Me was obtained in 52% yield (see, Chart 3). Crystallization from hexane gave pale yellow prisms with mp 99–100 °C.

The reaction of FLV-Me with DBDP was also carried out in the absence of TEMPO. In this case, TLC analysis showed formation of many minor products other than FLV-K-Me, and FLV-K-Me was obtained in a lower yield (23%).

The structure of FLV-K-Me was determined by flow injection LC-MS and ¹H- and ¹³C-NMR spectroscopy. The flow injection LC-MS gave *m/z* 424 as a (M+H)⁺ ion. The ¹H-

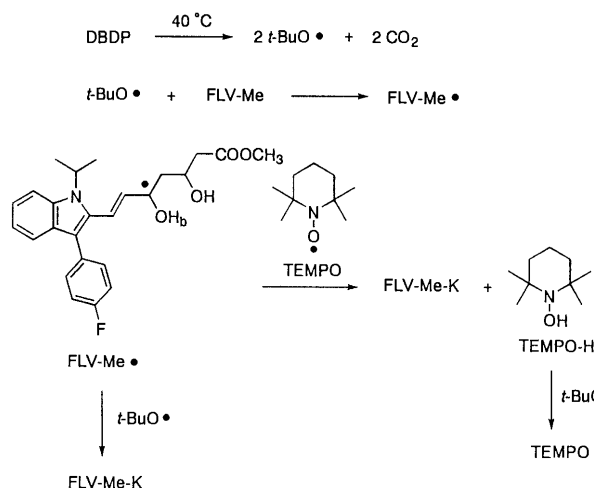


Chart 3

NMR spectrum showed that the *N*-isopropyl-3-(4-fluorophenyl)indole group remained unchanged. On the other hand, disappearance of the peak at 4.13 ppm due to the allylic hydrogen (H_a) and that at 3.32 ppm due to the hydroxy proton (H_b) of FLV-Me was observed. The ^{13}C -NMR spectrum showed the appearance of a new peak due to a carbonyl carbon at 198.8 ppm. The formation of the carbonyl group was also confirmed by IR. Elemental analysis was in satisfactory agreement with the calculated values.

A plausible mechanism for formation of FLV-K-Me is shown in Chart 3. *tert*-Butoxyl radical generated by thermolysis of DBDP abstracts the allylic hydrogen-atom (H_a) from FLV-Me to give intermediate FLV-Me• radical. In the presence of TEMPO, the FLV-Me• radical is subject to immediate hydrogen-atom abstraction by TEMPO to give FLV-K-Me and TEMPO-H. Since TEMPO-H is known to be highly reactive for hydrogen-atom abstraction,¹⁸⁾ this compound must be immediately converted to TEMPO by reaction with *tert*-butoxyl radical. The constant concentration of TEMPO can be explained by this mechanism. In the absence of TEMPO, other reactions are anticipated for the FLV-Me• radical. Since the main product is FLV-K-Me, the main reaction is hydrogen-atom abstraction from the FLV-Me• radical by *tert*-butoxyl radical. As other possible reactions, coupling reaction between the FLV-Me• radicals or hydrogen-atom abstraction by FLV-Me• from nonradical compounds or coexisting radicals are expected. However, since the byproducts were not isolated, the detailed mechanism for the decomposition of FLV-Me• radicals is unclear.

Competitive Hydrogen-atom Abstraction from FLV-Me and FLV-R-Me by *tert*-Butoxyl Radical Competitive hydrogen abstraction from FLV-Me and FLV-R-Me by *tert*-butoxyl radical was carried out to clarify whether the double bond conjugated with the indole ring plays an important role or not in the antioxidative activity of FLV-Me. A solution of an equimolar amount of FLV-Me and FLV-R-Me (0.118 mmol), DBDP (0.236 mmol), and TEMPO (0.236 mmol) in benzene (10 ml) was stirred at 35 °C, and the consumption of FLV-Me and FLV-R-Me and formation of FLV-K-Me were followed by HPLC. The relative concentrations of these compounds are plotted as a function of time in Fig. 2.¹⁹⁾ It is obvious that FLV-Me is consumed much more rapidly than FLV-R-Me, indicating that *tert*-butoxyl radical abstracts dominantly a hy-

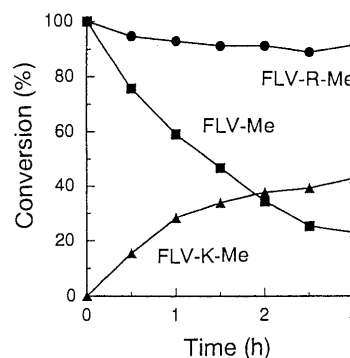


Fig. 2. Plots of the Relative Concentrations of FLV-Me, FLV-R-Me, and FLV-K-Me vs. Time

Reaction conditions: [FLV-Me]=11.8 mmol/l; [FLV-R-Me]=11.8 mmol/l; [DBDP]=23.6 mmol/l; [TEMPO]=23.6 mmol/l; benzene 10 ml; temperature, 35 °C.

drogen-atom from FLV-Me. On the basis of this result, we can conclude that the double bond conjugated with the indole ring plays an important role for the antioxidative activity of FLV-Me. Since the $-\text{CH}(\text{OH})-\text{CH}=\text{CH}$ -indole ring skeleton is common to FLV and FLV-Me, it is most likely that the antioxidative mechanism of FLV is the same as that of FLV-Me.

Conclusions

Hydrogen-atom abstraction from FLV-Me by *tert*-butoxyl radical gave FLV-K-Me. From the formation of FLV-K-Me, it was concluded that the active position in FLV-Me is the allylic carbon having an OH group. Competitive hydrogen-atom abstraction from FLV-Me and FLV-R-Me by *tert*-butoxyl radical showed that the double bond conjugated with the indole ring plays an important role in the high antioxidative activity of FLV-Me.

References and Notes

- 1) Tsujita S., *PROTEIN, NUCLEIC ACID AND ENZYME*, **38**, 1919 (1993).
- 2) Tabe K., *Medicine and Drug Journal*, **29**, 2146 (1993).
- 3) The Pravastatin Multinational Study Group for Cardiac Risk Patients, *Am. J. Cardiol.*, **72**, 1031 (1993).
- 4) Koide M., Kawahara Y., *Medicine and Drug Journal*, **32**, 2965 (1996).
- 5) Gotoh N., Shimizu K., Komuro E., Tsuchiya J., Noguchi N., Niki E., *Biochim. Biophys. Acta*, **1128**, 147 (1992).
- 6) Noguchi N., Gotoh N., Niki E., *Biochim. Biophys. Acta*, **1213**, 176 (1994).
- 7) Mitani H., Bandoh T., Ishikawa J., Kimura M., Totsuka T., Hayashi S., *Br. J. Pharmacol.*, **119**, 1269 (1996).
- 8) Leonhardt W., Kurkschiev T., Meissner D., Lattke P., Abletshauser C., Weidinger G., Jaross W., Hanefeld M., *Eur. J. Clin. Pharmacol.*, **53**, 65 (1997).
- 9) Hussein O., Schlezinger S., Rosenblat M., Keidar S., Aviram M., *Arteriosclerosis*, **128**, 11, (1997).
- 10) Herd J. A., Ballantyne C. M., Farmer J. A., Ferguson J. J., Jones P. H., West M. S., Gould K. L., Gottor A. M., Jr., *Am. J. Cardiol.*, **80**, 278–286 (1997).
- 11) Yamamoto A., Hoshi K., Ichihara K., *Eur. J. Pharm.*, **361**, 143 (1998).
- 12) Nakashima A., Ohtawa M., Masuda N., Morikawa H., Bando T., *Yakugaku Zasshi*, **119**, 93 (1999).
- 13) Suzumura K., Yasuhara M., Tanaka K., Odawara A., Narita H., Suzuki T., *Chem. Pharm. Bull.*, **47**, 1010 (1999).
- 14) Bartlett P. D., Benzing E. P., Pincock R. E., *J. Am. Chem. Soc.*, **82**, 1762 (1960).
- 15) FLV-Me is soluble in benzene, different from FLV.
- 16) Niki E., Yokoi S., Tsuchiya J., Kamiya Y., *J. Am. Chem. Soc.*, **105**, 1498 (1983).
- 17) DBDP is rapidly decomposed by an ionic mechanism in polar solvents such as methanol.¹⁴⁾
- 18) Miura Y., Masuda S., Kinoshita M., *Macromol. Chem.*, **160**, 243 (1972).
- 19) The concentration of TEMPO was constant during the reaction, in agreement with the ESR results mentioned above.

A Facilitated Cyclic Ether Formation and Its Potential Application in Solid-Phase Peptide and Organic Synthesis

Daxian SHAN,^{a,1)} Ailian ZHENG,^{a,1)} C. Eric BALLARD,^a Wei WANG,^a Ronald T. BORCHARDT,^b and Binghe WANG^{*,a}

Department of Chemistry, North Carolina State University,^a Raleigh, NC, 27695–8204, U.S.A. and Department of Pharmaceutical Chemistry, The University of Kansas,^b Lawrence, KS 66047, U.S.A.

Received August 18, 1999; accepted October 25, 1999

A “trimethyl lock” system has been known to facilitate lactonization reactions through what has been termed a stereopopulation control mechanism. We have found that a similar trimethyl lock system can also facilitate cyclic ether formation with the concomitant release of a carboxylic acid in the presence of anhydrous tetrabutylammonium fluoride. To study this base-mediated trimethyl lock-facilitated cyclic ether formation, we synthesized fifteen model compounds. All model compounds underwent base-mediated cyclic ether formation in high yields at 0 °C to room temperature (r.t.) with the concomitant release of the attached carboxylate. Such a system potentially could be used for the development of a two-dimensional linker for solid phase peptide and organic synthesis.

Key words “trimethyl lock”; cyclization; linker; fluoride; quinone; hydroquinone

A “trimethyl lock” system has been known to facilitate lactonization reactions²⁾ and cyclic ether formation in aqueous solutions.³⁾ The mechanism through which such a trimethyl lock facilitates certain cyclization reactions has been thought to be due to the conformational restrictions imposed by the trimethyl lock (Chart 1).²⁾ Such trimethyl lock-facilitated lactonization reactions have been used to develop redox-, esterase-, and phosphatase-sensitive prodrugs⁴⁾ and redox-sensitive protecting groups for amines.^{5,6)} In our studies of such trimethyl lock-facilitated cyclization reactions, we have found that facile base-mediated cyclic ether formation can be also accomplished at room temperature (r.t.) through treatment of the open-chain system **2** (R=CH₃) with tetrabutylammonium fluoride (TBAF) (Chart 1).

Recently, there has been a great deal of interest in developing linkers that are stable during synthetic reactions yet readily cleavable under mild reaction conditions for solid phase synthesis.⁷⁾ Conceivably, this cyclization system could be used for the development of a two-dimensional linker for solid phase peptide and organic synthesis. In such a design, the quinone ester moiety **1** could be attached to an appropriate solid phase material, and the carboxylic acid moiety (R) could be either a protected amino acid for solid phase peptide synthesis or another organic acid, which would be modified through solid phase reactions. Such a linker, if successfully developed, would have the advantages of being cleavable with a mild reducing agent, such as Na₂S₂O₄, and TBAF, and of being more stable under acidic conditions than the commonly used benzyl ester linker.⁸⁾ In addition, many

amino acid side chain protections are expected to be stable under the cleavage conditions. Therefore, this type of resin linker will be particularly suitable for the synthesis of large peptides and small proteins using segment synthesis methods.⁸⁾ The final cleavage is a two-step process: reduction followed by treatment with TBAF. This helps to minimize the stability problems of this linker (**1**) during any single chemical transformation.

To study the feasibility of such a system for the development of a novel two-dimensional linker for solid phase synthesis, we synthesized a series of esters **1** of acids with different structural features. These acids included protected amino acids and simple aliphatic and aromatic carboxylic acids. The cyclic ether formation with the concomitant release of the acid was studied after the reduction of the quinone moiety **1** to the hydroquinone **2** (Chart 1). We have found that such cyclizations could be accomplished with esters of acids with a variety of different structural features, indicating the general applicability of such a system in the development of a novel linker for solid phase synthesis.

Results and Discussion

For **1** to be used as a potential solid phase linker for peptide and organic syntheses, it was necessary to test the cyclization reactions of esters **2** with different structural features. First, we were interested in studying the cyclic ether formation of **2** with protected amino acids attached to the quinone moiety. Among the twenty natural amino acids, we chose nine representative ones (Chart 2). This group in-

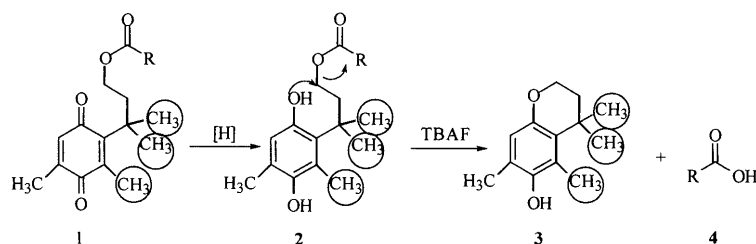


Chart 1. A “Trimethyl Lock”-Facilitated Cyclic Ether Formation

The methyl groups involved in the “trimethyl lock” are circled.

* To whom correspondence should be addressed.

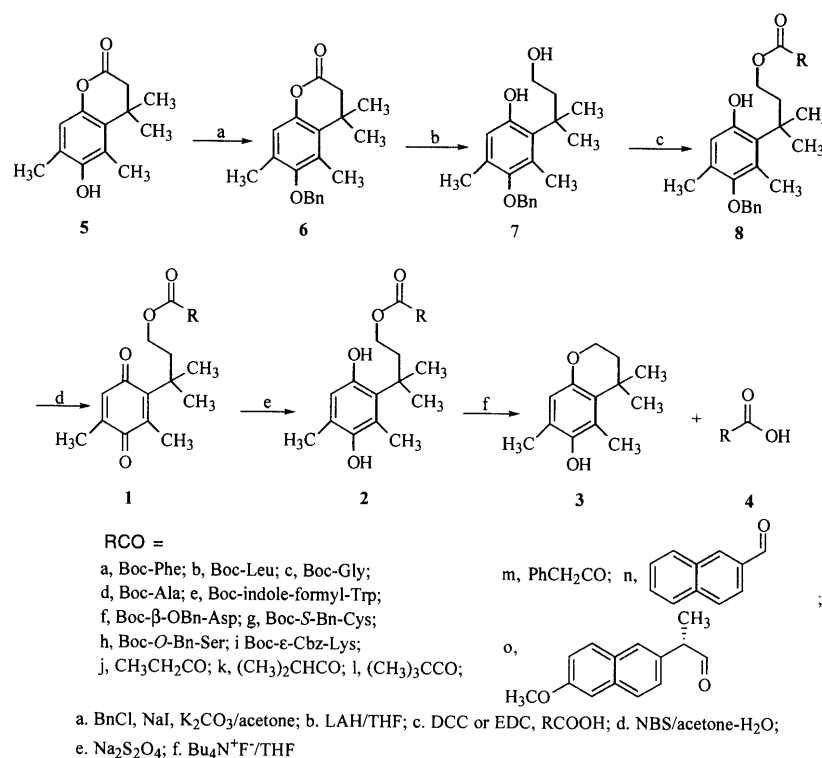


Chart 2. Synthesis and Cyclization Studies of Esters 2

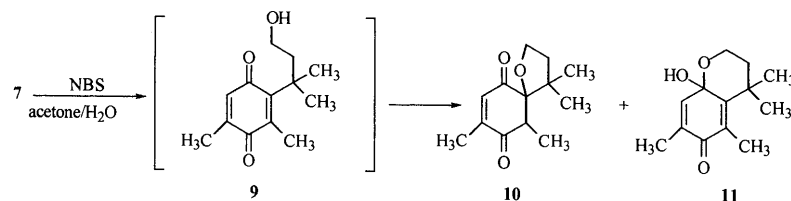


Chart 3. The Formation of Spiroether 10 and Hemiketal 11

cluded amino acids bearing non-polar side chains (**2a–e**), aromatic side chains (**2a, e**), and protected side chain functional groups such as hydroxyl (**2h**), thiol (**2g**), amino (**2i**), and carboxyl groups (**2f**). We also synthesized the esters **2** of several other carboxylic acids with different structural features. Compounds **2j–m**, and **o** are all esters of aliphatic carboxylic acids with different steric hindrances and functional groups, and compound **2n** is an ester of an aromatic carboxylic acid.

Synthesis The synthesis of these esters **2** started with lactone **5**. The hydroxyl group of **5** was first protected as a benzyl ether to give **6**, which was then reduced using LiAlH_4 (LAH) to give the diol **7** (Chart 2).³⁾ It is known that without the benzyl protection of the phenol hydroxyl group, the reduction reaction is very slow due to the negative charge of the phenoxide.³⁾ Our initial plan was to oxidize the phenol **7** to quinone **9** (Chart 3), which would be followed by acylation of the primary hydroxyl group to give the desired products **1**. However, this approach did not lead to the formation of the desired product. Similar quinones in the presence of a trimethyl lock are known to undergo cyclizations to give a mixture of the spiroether **10** and a hemiketal **11** (Chart 3), which makes the acylation of the hydroxyl group of quinone **9** impossible.⁹⁾ Therefore, we studied the feasibility of selective acylation of the primary hydroxyl group of the diol inter-

mediate **7** for the preparation of the desired product **1**. The selective acylation of the primary hydroxyl group of **7** was easily accomplished in high yields (about 90%) when the acids were protected amino acids (**8a–i**) activated with either dicyclohexylcarbodiimide (DCC) or 1-(3-dimethylaminopropyl)-3-ethylcarbodiimide (EDC). Presumably due to the steric hindrance presented by the *gem*-dimethyl groups of **7** and the relative steric bulkiness of protected amino acids, the esterification occurred almost exclusively on the primary hydroxyl group to give the desired products **8** (Table 1).

Other acids bearing α -substituents also gave high yields of the monoester. Such was the case for **8k, o**. However, acids that did not have an α -substituent tended to give the diester as the side product. Such was the case for **8j, m**, and **n**. For 2,2-dimethylpropanoic acid (**8l**), the reaction using DCC as the activating agent was very slow, presumably because of the steric hindrance imposed by the *tert*-butyl group. Therefore, *N,N*-bis(2-oxo-3-oxazolidinyl)phosphinic chloride (Bop-Cl)¹⁰⁾ was used for the preparation of this compound (**8l**) in 67% yield. Oxalyl chloride was used as the activating reagent for the preparation of **8n, o**. The diester side product was found for the preparation of **8n**, which was the reason for the relatively low yield (73%).

For subsequent model studies, the hydroquinone was first

Table 1. Reaction Yields^{a)}

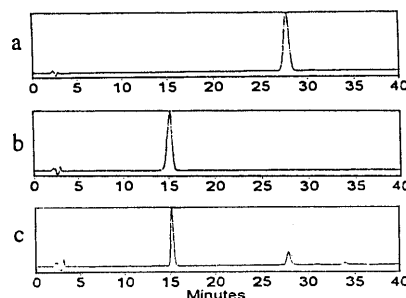
RCO	Formation of 8	Formation of 1	Final release
a Boc-Phe	95	99	92
b Boc-Leu	99	97	93
c Boc-Gly	99	99	93
d Boc-Ala	93	97	94
e Boc- <i>N</i> -formyl-Trp	93	91	100 (80)
f Boc- β -OBn-Asp	100	98	88
g Boc- <i>S</i> -Bn-Cys	93	73	93
h Boc- <i>O</i> -Bn-Ser	95	95	100
i Boc- ϵ -Cbz-Lys	85	99	92
j COCH ₂ CH ₃	72	99	95
k COCH(CH ₃) ₂	89	95	97
l COC(CH ₃) ₃	67	96	99
m COCH ₂ C ₆ H ₅	80	96	95
n CO-C ₁₀ H ₇	73	98	99
o (+)-COCH(CH ₃)-C ₁₀ H ₆ -6-OMe	91	99	93 (93)

a) Yields for the formation of **8** and **1** were isolated yields. Yields for the final release were determined by HPLC, except for the yields in parentheses, which were isolated yields.

converted to the corresponding quinone compound **1** through oxidation with *N*-bromosuccinimide (NBS). The yields for this step of the reaction were generally close to quantitative, except for **8g**, the cysteine ester. It was suspected that the oxidation of the sulfur atom by NBS was the reason for this low yield. However, no detailed study was carried out to characterize the side product(s) from this oxidation reaction.

Final Cleavage The reduction of the quinone **1** to hydroquinone **2** was accomplished by shaking an ether solution of the quinone ester (**1a–o**) and an aqueous solution of Na₂S₂O₄ at r.t. The reaction color quickly changed from yellow to almost colorless, indicating the completion of the reduction. Approximately 20-fold Na₂S₂O₄ was employed. The yields were almost quantitative. The cyclization reaction was carried out by treatment of **2** with 1 M TBAF/tetrahydrofuran (THF) solution. These cyclization reactions were studied using reversed-phase HPLC by monitoring both the formation of the cyclic ether **3** and the disappearance of the starting material **2**. The formation of the acid **4** was also monitored when the acid had a chromophore. Figure 1 shows a typical HPLC reaction profile.

The quantitation of these compounds was carried out using the corresponding standard curves. The yields of these reactions were generally very high (Table 1). For two compounds (**2e, o**), the isolated yields were determined (Table 1). It should be noted that the cyclization was usually accompanied by a color change from yellow to orange and finally to blue/green. For the esters of protected amino acids, the cyclization was carried out at 0 °C under a nitrogen atmosphere with a TBAF/ester ratio of 3/1. However, the same reaction for the esters of the other carboxylic acids (**2j–n**) did not occur at 0 °C; instead the reactions were carried out at r.t. It should also be noted that for these non-amino acid esters, the reactions were carried out with a ratio of TBAF/ester of 8/1. Low reaction temperature (0 °C) and a lower ratio of TBAF/ester (3/1) led to lower yields. This indicated that the carboxylic acid moiety does influence the cyclization reaction. This is particularly relevant for the proper design of the reaction conditions in solid phase organic/peptide synthesis.

Fig. 1. HPLC Studies of the Deprotection of **1n**

Panel A, cycloether **3**; panel B, 2-naphthoic acid; panel C, **1n** after treatment with Na₂S₂O₄ in ether and water followed by Bu₄NF in THF for 1 h at r.t.

It suggests that peptides synthesized on this linker could probably be cleaved at 0 °C, whereas organic compounds could only be released from the solid phase at r.t.

It should be noted that TBAF is a very commonly used reagent, most notably for the cleavage of silyl protecting groups, and is known not to compromise the chiral integrity of protected amino acids, peptides, and other organic compounds.¹¹⁾ However, we did not specifically examine the issue of racemization in this study. In a separate study, we have attached this linker to polystyrene resin beads. This linker was used for the successful synthesis of two short peptides [Boc-Trp-Ala-Gly-Gly-OH and Boc-Asn-Ala-Ser(OBn)-Gly-Glu(OBn)-OH],¹²⁾ further demonstrating the utility of such a linker system. However, because of the potential NBS oxidation problems associated with sulfur-containing amino acids, the application of this linker for the synthesis of peptides with the first amino acid being either protected cysteine or methionine may be problematic.

Conclusion

These model studies indicate that the base-mediated trimethyl lock-facilitated cyclic ether formation with concomitant release of a carboxylic acid generally gives high yields with esters of acids bearing different structural features. This makes it possible to use this trimethyl lock-based system for the development of a stable and readily cleavable linker for solid phase synthesis.

Experimental

General Melting points were determined using an electrothermal melting point apparatus and are uncorrected. NMR spectra were obtained on a 300 MHz Varian instrument. Chemical shifts are reported in parts per million (ppm) relative to Me₄Si as an internal standard. Unless stated otherwise commercial reagents were used without purification. Radial preparative layer chromatography (RPLC) was carried out on a Chromatotron (Harrison Research Co., Palo Alto, CA). Silica gel (200–400 mesh) was used for column chromatography. Solvent mixtures used for chromatography are expressed as v/v. Methylene chloride was distilled from CaH₂ under nitrogen. THF was distilled from sodium/benzophenone under nitrogen. TBAF-THF solution (1 M) was purchased from Aldrich Chemical Co. Sodium hydrosulfite (tech, ca. 85%) was used for the reduction reaction. All deprotection reactions were conducted in flame-dried glassware under a nitrogen atmosphere. HPLC analyses of the deprotection reaction were carried out using a Shimadzu HPLC system consisting of a SCL-10A system controller, two LC-10AS pumps, a SPD-10AV UV-VIS detector, and a SIL-10A auto injector (detection wavelength: 210 nm and 208 nm). The column was a C₁₈ reversed phase analytical column from YMC (length=15 cm, i.d.=4.6 cm, particle size=5 mm). The solvent system was a gradient of 0.1% trifluoroacetic acid in acetonitrile and water. Abbreviations: Boc, *tert*-butoxycarbonyl; Bn, benzyl; Cbz, carbobenzyloxy.

6-Benzylxy-4,4,5,7-tetramethylhydrocoumarin (6) The lactone **5**

(13.17 g, 59.9 mmol), benzyl chloride (15.16 g, 120 mmol), K_2CO_3 (16.52 g, 120 mmol), NaI (0.5 g, 13 mmol) and 120 ml of acetone (dried on molecular sieves, 4 Å) were mixed in a flask. The reaction mixture was refluxed for 20 h. Acetone was evaporated and the residue was mixed with 100 ml of water. This was extracted with methylene chloride (2×100 ml). The combined CH_2Cl_2 layers were washed with 100 ml of water and dried over $MgSO_4$. Solvent removal afforded a residue. Then 50 ml of hexanes was added to give a white precipitate (18.17 g, 98%): mp 95.5–96.5 °C; 1H -NMR ($CDCl_3$) δ 7.50–7.40 (m, 5H), 6.78 (s, 1H), 4.75 (s, 2H), 2.58 (s, 2H), 2.42 (s, 3H), 2.28 (s, 3H), 1.45 (s, 6H); ^{13}C -NMR ($CDCl_3$) δ 168.15, 152.71, 147.31, 137.21, 130.83, 129.60, 128.46, 128.01, 127.99, 117.36, 74.39, 45.81, 35.45, 27.57, 16.24, 14.87; IR (film) 1769, 1611, 1476, 1408, 1369, 1249, 1186, 1121, 981, 746, 699 cm^{-1} ; FAB-MS m/z : 310.2 (M^+). *Anal.* Calcd for $C_{20}H_{22}O_3$: C, 77.39; H, 7.14. Found: C, 77.31; H, 7.16.

3-(5'-Benzyloxy-2'-hydroxy-4',6'-dimethylphenyl)-3-methyl-1-butanol (7) To a $LiAlH_4$ (4.16 g, 109.6 mmol) suspension in 150 ml of dry THF cooled in an ice/water bath was added dropwise a solution of **6** (17.00 g, 54.8 mmol) in 80 ml of THF with stirring. After addition, the icy bath was removed and the reaction mixture was stirred at r.t. for 7 h. The reaction mixture was then slowly added to 300 g of ice containing 50 ml of concentrated HCl with stirring. This was followed by the addition of 50 ml of hexanes to separate the THF layer. The aqueous layer was extracted with ethyl acetate (4×150 ml). The combined organic layers were washed with water (2×100 ml) and dried over $MgSO_4$. After solvent evaporation, 100 ml of hexanes was added and the mixture was stored in a freezer for crystallization. A white solid product **7** (16.69 g, 97%) was obtained: mp 106.5–107.0 °C; 1H -NMR ($CDCl_3$) δ 7.48–7.26 (m, 5H), 6.39 (s, 1H), 4.70 (s, 2H), 3.64 (t, $J=6.8$ Hz, 2H), 2.44 (s, 3H), 2.20 (s, 3H), 2.20 (t, $J=6.8$ Hz, 2H), 1.58 (s, 6H); ^{13}C -NMR ($CDCl_3$) δ 151.31, 150.12, 137.70, 131.57, 130.58, 129.18, 128.44, 127.84, 127.74, 117.42, 74.22, 61.45, 44.96, 39.94, 32.16, 16.27, 16.10; IR (film) 3384, 1601, 1452, 1400, 1368, 1227, 1023, 753, 696 cm^{-1} ; MS m/z 314 (M^+). *Anal.* Calcd for $C_{20}H_{26}O_3$: C, 76.40; H, 8.33. Found: C, 76.51; H, 8.42.

General Procedure for the Preparation of Amino Acid-diols Monoesters 8a–k, m Method A: DCC (1.0 equiv) was added to a solution of the diol **7** (1.0–2.0 eq), amino acid (1.0 equiv) and 4-(dimethylamino) pyridine (DMAP) (0.1–0.2 eq) in methylene chloride in an ice-water bath with stirring. After stirring for 10 min, the ice-water bath was withdrawn and stirring was continued overnight at r.t. The precipitates were filtered off. The filtrates were washed with 5% HCl solution, saturated $NaHCO_3$ solution, and water, and purified on a silica gel column.

Method B: EDC (2 equiv) was added to a solution of the diol **7** (1.0 eq), amino acid (2 eq) and DMAP (0.5 eq) in methylene chloride cooled in an ice-water bath with stirring. After the addition, the ice bath was removed and stirring was continued for 5 h at r.t. The reaction mixture was washed with 5% HCl solution, saturated $NaHCO_3$ solution and water, and dried over $MgSO_4$. Filtration and evaporation gave an oily residue which was purified on a silica gel column to afford the monoester **8**.

Diol-Phe Ester 8a: To a solution of the diol **7** (1.450 g, 4.62 mmol), Boc-Phe-OH (1.224 g, 4.62 mmol) and DMAP (56 mg, 0.46 mmol) in 65 ml of CH_2Cl_2 in an ice-water bath was added DCC (952 mg, 4.62 mmol). After the addition the ice bath was removed. Stirring was continued overnight at r.t. The precipitates were filtered off. The filtrates were washed with 5% HCl solution (3×30 ml), saturated $NaHCO_3$ (3×30 ml) and water (3×40 ml) and dried over $MgSO_4$. Filtration and evaporation gave a residue, which was purified on a silica gel column (ethyl acetate:hexanes=1:5) to afford 2.57 g (99%) (**8a**) as a white foam: 1H -NMR ($CDCl_3$) δ 7.50–7.05 (m, 10H), 6.40 (s, 1H), 4.69 (s, 2H), 4.38 (m, 1H), 4.20 (m, 1H), 4.00 (m, 1H), 3.04–2.90 (m, 2H), 2.44 (s, 3H), 2.20 (s, 3H), 2.15 (m, 2H), 1.55 (2s, 6H), 1.41 (s, 9H); ^{13}C -NMR ($CDCl_3$) δ 172.10, 155.62, 151.62, 150.23, 137.99, 136.33, 131.67, 130.16, 129.45, 129.25, 128.85, 128.64, 128.59, 127.96, 127.88, 127.07, 117.34, 80.30, 74.40, 64.43, 54.64, 41.39, 40.19, 38.31, 32.05, 28.47, 16.26; IR (film) 3377, 1736, 1713, 1689, 1603, 1497, 1400, 1366, 1227 1164 cm^{-1} ; FAB-MS m/z 562 (M^+). *Anal.* Calcd for $C_{34}H_{43}NO_6$: C, 72.70; H, 7.72; N, 2.49. Found: C, 72.56; H, 7.99; N, 2.46.

Diol-Leu Ester 8b: Diol **7** (126 mg, 0.4 mmol), Boc-Leu-OH (199 mg, 0.8 mmol), EDC (154 mg, 0.8 mmol) and DMAP (24 mg, 0.2 mmol) were treated according to the general procedure (Method B). A white foam product (216 mg, 100%) was obtained: 1H -NMR ($CDCl_3$) δ 7.50–7.30 (m, 5H), 6.44 (s, 1H), 4.69 (s, 2H), 4.25 (m, 1H), 4.08 (m, 1H), 3.95 (m, 1H), 2.59 (m, 2H), 2.45 (s, 3H), 2.20 (s, 3H), 2.07 (m, 2H), 1.58, 1.53 (2s, 6H), 1.46 (s, 9H), 1.42 (m, 1H), 0.88 (d, $J=6.6$ Hz, 6H); ^{13}C -NMR ($CDCl_3$) δ 173.80, 156.09, 151.89, 150.03, 137.99, 131.52, 130.22, 129.11, 128.59, 127.90, 117.31, 80.32, 74.39, 64.29, 52.26, 41.62, 41.44, 40.25, 32.23, 31.76, 28.51,

24.91, 22.99, 21.87, 16.30, 16.21; IR (film) 3365, 1713, 1686, 1604, 1400, 1367, 1228, 1163, 733, 697 cm^{-1} ; FAB-MS m/z 528 (M^+). *Anal.* Calcd for $C_{31}H_{45}NO_6$: C, 70.56; H, 8.59; N, 2.65. Found: C, 70.52; H, 8.54; N 2.66.

Diol-Gly Ester 8c: Diol **7** (126 mg, 0.4 mmol), Boc-Gly-OH (140 mg, 0.8 mmol), EDC (154 mg, 0.8 mmol) and DMAP (24 mg, 0.2 mmol) were treated according to the general procedure (Method B) to give a white foam (186 mg, 99%): 1H -NMR ($CDCl_3$) δ 7.51–7.26 (m, 5H), 6.40 (s, 1H), 4.69 (s, 2H), 4.12 (t, $J=6.9$ Hz, 2H), 3.70 (d, $J=5.7$ Hz, 2H), 2.44 (s, 3H), 2.33 (t, $J=6.9$ Hz, 2H), 2.20 (s, 3H), 1.56 (s, 6H), 1.45 (s, 9H); ^{13}C -NMR ($CDCl_3$) δ 170.52, 156.29, 151.46, 150.43, 138.05, 131.85, 130.32, 129.41, 128.67, 128.04, 127.95, 117.39, 80.48, 74.46, 64.33, 42.60, 41.41, 40.27, 32.07, 29.92, 28.57, 16.29; FAB-MS m/z 472 (M^+). *Anal.* Calcd for $C_{27}H_{37}NO_6$: C, 68.77; H, 7.91; N, 2.97. Found: C, 68.63; H, 7.90; N, 2.99.

Diol-Ala Ester 8d: Diol **7** (126 mg, 0.4 mmol), Boc-Ala-OH (151 mg, 0.8 mmol), EDC (154 mg, 0.8 mmol) and DMAP (24 mg, 0.2 mmol) were treated according to the general procedure (Method B). The reaction afforded a white foam (182 mg, 94%): 1H -NMR ($CDCl_3$) δ 7.47–7.32 (m, 5H), 6.41 (s, 1H), 4.68 (s, 2H), 4.14 (t, $J=7.2$ Hz, 2H), 4.05 (m, 1H), 2.44 (s, 3H), 2.21 (m, 2H), 2.18 (s, 3H), 1.57, 1.55 (2s, 6H), 1.45 (s, 9H), 1.27 (d, $J=6.8$ Hz, 3H); ^{13}C -NMR ($CDCl_3$) δ 173.59, 155.62, 151.71, 150.10, 137.96, 131.59, 130.09, 129.22, 128.59, 127.93, 117.29, 80.29, 74.43, 64.51, 49.45, 41.36, 40.23, 32.03, 31.88, 28.52, 18.61, 16.27, 16.22; IR (film) 3377, 1736, 1713, 1689 1604, 1499, 1452, 1400, 1367, 1227, 1184 cm^{-1} ; FAB-MS m/z 485 (M^+). *Anal.* Calcd for $C_{28}H_{39}NO_6$: C, 69.26; H, 8.09; N, 2.88. Found: C, 68.92; H, 8.11; N, 3.14.

Diol-Trp Ester 8e: Diol **7** (126 mg, 0.4 mmol), Boc-Trp(For)-OH (266 mg, 0.8 mmol), EDC (154 mg, 0.8 mmol) and DMAP (24 mg, 0.2 mmol) were treated according to the general procedure (Method B). The reaction afforded a white foam (234 mg, 93%): 1H -NMR ($CDCl_3$) δ 9.38, 9.00 (2s, 1H), 8.39–7.26 (m, 10H), 6.47, 6.38 (2s, 1H), 5.10 (m, 1H), 4.68 (s, 2H), 4.59 (m, 1H), 4.09 (m, 1H), 3.16 (m, 2H), 2.41 (s, 3H), 2.26 (m, 2H), 2.19 (s, 3H), 1.60, 1.53 (2s, 6H), 1.45 (s, 9H); FAB-MS m/z 628 (M^+). *Anal.* Calcd for $C_{37}H_{44}N_2O_7$: C, 70.67; H, 7.05; N, 4.46. Found: C, 70.51; H, 7.22; N, 4.43.

Diol-Asp Ester 8f: Diol **7** (126 mg, 0.4 mmol), Boc-Asp(OBn)-OH (258 mg, 0.8 mmol), EDC (154 mg, 0.8 mmol) and DMAP (24 mg, 0.2 mmol) were treated according to the procedure (Method B). The reaction afforded a white foam (247 mg, 100%): 1H -NMR ($CDCl_3$) δ 7.50–7.30 (m, 10H), 6.37 (s, 1H), 5.10 (s, 2H), 4.69 (s, 2H), 4.41 (m, 1H), 4.13 (m, 2H), 2.79 (m, 2H), 2.42 (s, 3H), 2.19 (s, 3H), 2.15 (m, 2H), 1.55, 1.54 (2s, 6H), 1.44 (s, 9H); FAB-MS m/z 620 (M^+). *Anal.* Calcd for $C_{36}H_{45}NO_8$: C, 69.76; H, 7.32; N, 2.26. Found: C, 69.70; H, 7.53; N, 2.54.

Diol-Cys Ester 8g: Diol **7** (94 mg, 0.3 mmol), S-Bn-Boc-Cys-OH (93 mg, 0.3 mmol), DCC (62 mg, 0.3 mmol) and DMAP (7 mg, 0.06 mmol) were treated according to the general procedure (Method A). The reaction afforded **8g** (169 mg, 93%) as a white solid: 1H -NMR ($CDCl_3$) δ 7.46–7.23 (m, 10H), 6.38 (s, 1H), 4.67 (s, 2H), 4.22 (m, 2H), 4.02 (m, 1H), 3.65 (s, 2H), 2.74 (m, 2H), 2.49 (m, 2H), 2.44 (s, 3H), 2.19 (s, 3H), 1.58, 1.54 (2s, 6H), 1.46 (s, 9H); FAB-MS m/z 608 (M^+). *Anal.* Calcd for $C_{35}H_{45}NO_6S$: C, 69.16; H, 7.46; N, 2.30. Found: C, 69.26; H, 7.56; N, 2.49.

Diol-Ser Ester 8h: Diol **7** (94 mg, 0.3 mmol), O-Bn-Boc-Ser-OH (89 mg, 0.3 mmol), DCC (62 mg, 0.3 mmol) and DMAP (7 mg, 0.06 mmol) were treated according to the general procedure (Method A). The reaction afforded a white foam **8h** (166 mg, 94%): 1H -NMR ($CDCl_3$) δ 7.44–7.30 (m, 10H), 6.34 (s, 1H), 4.68 (s, 2H), 4.49 (m, 2H), 4.24 (m, 2H), 4.01 (m, 1H), 3.73 (m, 2H), 2.55 (m, 2H), 2.43 (s, 3H), 2.18 (s, 3H), 1.56, 1.54 (2s, 6H), 1.46 (s, 9H); FAB-MS m/z 591 (M^+). *Anal.* Calcd for $C_{35}H_{45}NO_7$: C, 71.05; H, 7.67; N, 2.37. Found: C, 71.14; H, 7.78; N, 2.34.

Diol-Lys Ester 8i: Diol **7** (94 mg, 0.3 mmol), Boc- ϵ -Cbz-Lys-OH (114 mg, 0.3 mmol), DCC (62 mg, 0.3 mmol) and DMAP (7 mg, 0.06 mmol) were treated according to the general procedure (Method A). The reaction afforded a white foam **8i** (173 mg, 85%): 1H -NMR ($CDCl_3$) δ 7.47–7.26 (m, 10H), 6.46 (s, 1H), 5.12 (s, 2H), 4.69 (s, 2H), 4.16–4.03 (m, 3H), 3.17 (m, 2H), 2.56 (m, 2H), 2.43 (s, 3H), 2.19 (s, 3H), 1.62 (m, 4H), 1.57 (d, $J=6.1$ Hz, 6H), 1.43 (s, 9H), 1.26 (m, 2H); FAB-MS m/z 677 (M^+). *Anal.* Calcd for $C_{39}H_{52}N_2O_8$: C, 69.21; H, 7.74; N, 4.14. Found: C, 69.08; H, 8.00; N, 4.41.

Diol-Propionic Ester 8j: DCC (104 mg, 0.5 mmol), propionic acid (37.3 ml, 0.5 mmol), diol **7** (314 mg, 1.0 mmol) and DMAP (6 mg, 0.05 mmol) in 12 ml methylene chloride were stirred for 72 h at r.t. The mixture was treated according to the general procedure (Method A) to give **8j** (133 mg, 72%) as a white solid: 1H -NMR ($CDCl_3$) δ 7.44 (m, 5H), 6.34 (s, 1H), 4.68 (s, 2H), 4.01 (t, $J=7.2$ Hz, 2H), 2.44 (s, 3H), 2.29 (t, $J=7.2$ Hz, 2H), 2.24 (q, $J=7.2$ Hz, 2H), 2.20 (s, 3H), 1.58 (s, 6H), 1.08 (t, $J=7.2$ Hz, 3H); FAB-MS m/z

370 (M^+). *Anal.* Calcd for $C_{23}H_{30}O_4$: C, 74.56; H, 8.16. Found: C, 74.39; H, 7.98.

Diol-Isobutyric Ester **8k**: DCC (206 mg, 1.0 mmol), diol **7** (314 mg, 1.0 mmol), isobutyric acid (44 mg, 0.5 mmol) and DMAP (6 mg, 0.05 mmol) in 20 ml of CH_2Cl_2 were treated according to the general procedure (Method A) to afford **8k** (170 mg, 89%) as a white solid: 1H -NMR ($CDCl_3$) δ 7.35 (m, 5H), 6.30 (s, 1H), 4.64 (s, 2H), 3.97 (t, $J=7.2$ Hz, 2H), 2.43 (m, 1H), 2.40 (s, 3H), 2.25 (t, $J=7.2$ Hz, 2H), 2.12 (s, 3H), 1.56 (s, 6H), 1.11 (d, $J=7.2$ Hz, 6H); FAB-MS m/z : 384 (M^+). *Anal.* Calcd for $C_{24}H_{32}O_4$: C, 74.97; H, 8.39. Found: C, 74.84; H, 8.41.

Diol-Trimethylacetic Ester **8l**: To a solution of the diol **7** (235 mg, 0.75 mmol), trimethylacetic acid (44 mg, 0.43 mmol) and TEA (76 mg, 0.75 mmol) in 10 ml of methylene chloride was added Bop-Cl (191 mg, 0.75 mmol). The reaction mixture was stirred for 24 h at r.t. Methylene chloride was evaporated. The residue was separated on a silica gel column (ethyl acetate : hexanes = 1 : 4) to give **8l** (114 mg, 67%) as a white solid: 1H -NMR ($CDCl_3$) δ 7.40 (m, 5H), 6.37 (s, 1H), 4.69 (s, 2H), 4.00 (t, $J=7.2$ Hz, 2H), 2.45 (s, 3H), 2.28 (t, $J=7.2$ Hz, 2H), 2.20 (s, 3H), 1.59 (s, 6H), 1.15 (s, 9H); FAB-MS m/z 398 (M^+). *Anal.* Calcd for $C_{25}H_{34}O_4$: C, 75.34; H, 8.60. Found: C, 75.04; H, 8.40.

Diol-Phenylacetic Ester **8m**: The diol **7** (314 mg, 1.0 mmol), phenylacetic acid (68 mg, 0.5 mmol), DCC (104 mg, 0.5 mmol) and DMAP (6 mg, 0.05 mmol) in 15 ml of methylene chloride were treated according to the general procedure (Method A) to give **8m** (172 mg, 80%) as a white solid: 1H -NMR ($CDCl_3$) δ 7.46–7.17 (m, 10H), 6.27 (s, 1H), 4.63 (s, 2H), 4.00 (t, $J=7.2$ Hz, 2H), 3.48 (s, 2H), 2.37 (s, 3H), 2.25 (t, $J=7.2$ Hz, 2H), 2.13 (s, 3H), 1.51 (s, 6H); ^{13}C -NMR ($CDCl_3$) δ 172.04, 151.04, 150.61, 138.00, 131.99, 130.31, 129.49, 128.67, 128.04, 127.94, 127.20, 117.45, 74.46, 64.00, 41.69, 41.39, 40.28, 31.96, 16.29; FAB-MS m/z 432 (M^+). *Anal.* Calcd for $C_{28}H_{32}O_4$: C, 77.75; H, 7.46. Found: C, 77.51; H, 7.63.

Diol-Naphthoic Ester **8n**: Oxalyl chloride (191 mg, 1.5 mmol) was added to a solution of 2-naphthoic acid (86 mg, 0.5 mmol), and DMF (1 drop) in 20 ml of benzene at 45 °C. The mixture was stirred for 1 h and evaporated to dryness. The residue was then dissolved in 10 ml of methylene chloride. This mixture was added to a solution of the diol **7** (314 mg, 1.0 mmol) and triethylamine (TEA) (101 mg, 1.0 mmol) in 25 ml of methylene chloride. The mixture was stirred at r.t. for 72 h. After solvent evaporation, the product was purified on a silica gel column (ethyl acetate : hexanes = 1 : 9, v/v) to give 170 mg (73%) of white solid product: 1H -NMR ($CDCl_3$) δ 8.40 (s, 1H), 7.96–7.79 (m, 4H), 7.60–7.47 (m, 2H), 7.42–7.30 (m, 5H), 6.35 (s, 1H), 4.57 (s, 2H), 4.37 (t, $J=7.2$ Hz, 2H), 2.51 (t, $J=7.2$ Hz, 2H), 2.47 (s, 3H), 2.11 (s, 3H), 1.66 (s, 6H); FAB-MS m/z 468.3 (M^+). *Anal.* Calcd for $C_{31}H_{32}O_4$: C, 79.46; H, 6.88. Found: C, 78.93; H, 7.02.

Diol-Methoxy- α -methyl-naphthaleneacetic Ester **8o**: (+)-6-Methoxy- α -methyl-2-naphthaleneacetic acid (115 mg, 0.5 mmol), DMF (1 drop), benzene (20 ml), oxalyl chloride (190 mg, 1.5 mmol), the diol **7** (314 mg, 1.0 mmol), and TEA (101 mg, 1.0 mmol) were treated according to the method used for the product **8n** to afford 240 mg (91%) of **8o** as a white solid: 1H -NMR ($CDCl_3$) δ 7.68–7.08 (m, 11H), 6.27 (s, 1H), 4.63 (s, 2H), 4.01 (m, 2H), 3.89 (s, 3H), 3.75 (q, $J=7.2$, 1H), 2.35 (s, 3H), 2.23 (m, 2H), 2.15 (s, 3H), 1.52 (d, $J=7.2$ Hz, 3H), 1.50 (s, 6H); FAB-MS m/z 526 (M^+). *Anal.* Calcd for $C_{34}H_{38}O_5$: C, 77.54; H, 7.27. Found: C, 77.37; H, 7.37.

General Procedure for the Preparation of Quinone-Esters 1a—o Monoester **8** (1 equiv) was dissolved in a mixture of acetone and water (5 : 1, v/v). Then solid NBS (0.98 equiv) was added in one portion. The reaction mixture was stirred for 15 min. After the acetone was evaporated, the aqueous phase was extracted with ether. The product was purified on a silica gel column (hexanes : ethyl acetate = 3 : 1).

Quinone-Phe Ester **1a**: Diol-ester **8a** (2.425 g, 4.37 mmol) and NBS (584 mg, 4.32 mmol) were treated according to the general procedure to give **1a** (2.03 g, 99%) as a yellow oil: 1H -NMR ($CDCl_3$) δ 7.22 (m, 5H), 6.45 (m, 1H), 4.52 (m, 1H), 4.05 (m, 2H), 2.97 (m, 2H), 2.16 (s, 3H), 2.15 (m, 2H), 2.00 (s, 3H), 1.40 (s, 9H), 1.39 (s, 6H); ^{13}C -NMR ($CDCl_3$) δ 189.41, 188.28, 172.01, 155.14, 150.84, 144.06, 142.04, 136.20, 135.15, 129.77, 129.47, 128.70, 127.18, 80.05, 63.11, 54.67, 41.00, 39.43, 38.58, 30.39, 28.48, 15.57, 14.78; IR (film) 1731, 1717, 1648, 1497, 1365, 1168, 700 cm^{-1} ; FAB-MS m/z 469 (M^+). *Anal.* Calcd for $C_{27}H_{35}NO_6$: C, 69.06; H, 7.51; N, 2.98. Found: C, 68.97; H, 7.52; N, 2.95.

Quinone-Leu Ester **1b**: Diol-ester **8b** (170 mg, 0.312 mmol) and NBS (55 mg, 0.312 mmol) were treated according to the general procedure to give **1a** (137 mg, 97%) as a yellow oil: 1H -NMR ($CDCl_3$) δ 6.48 (q, $J=1.35$ Hz, 1H), 4.21 (m, 1H), 4.08 (m, 2H), 2.22 (m, 2H), 2.20 (s, 3H), 2.00 (d, $J=1.35$ Hz, 3H), 1.71 (m, 3H), 1.43 (s, 15), 0.93 (m, 6H); ^{13}C -NMR ($CDCl_3$) δ

189.44, 188.33, 173.63, 155.48, 150.82, 144.06, 142.05, 135.15, 79.92, 63.01, 52.27, 41.94, 41.03, 39.52, 30.48, 28.50, 24.92, 23.04, 22.02, 15.62, 14.78; IR (film) 1742, 1716, 1649, 1507, 1366, 1163 cm^{-1} ; FAB-MS m/z 435 (M^+). *Anal.* Calcd for $C_{24}H_{37}NO_6$: C, 66.18; H, 8.56; N, 3.21. Found: C, 66.37; H, 8.73; N, 3.29.

Quinone-Gly Ester **1c**: Diol-ester **8c** (135 mg, 0.288 mmol) was treated with NBS (51 mg, 0.288 mmol) according to the general procedure to give **1b** (107 mg, 99%) as a yellow oil: 1H -NMR ($CDCl_3$) δ 6.48 (q, $J=1.8$ Hz, 1H), 4.10 (t, $J=7.2$ Hz, 2H), 3.82 (d, $J=5.4$ Hz, 2H), 2.21 (t, $J=7.2$ Hz, 2H), 2.19 (s, 3H), 2.01 (d, $J=1.8$ Hz, 3H), 1.44 (s, 9H), 1.43 (s, 6H); ^{13}C -NMR ($CDCl_3$) δ 189.41, 188.27, 170.35, 155.74, 150.85, 144.02, 141.94, 135.13, 80.11, 63.12, 42.63, 41.07, 39.48, 30.42, 28.47, 15.53, 14.72; IR (film) 1742, 1717, 1649, 1513, 1366, 1166 cm^{-1} ; FAB-MS m/z 379 (M^+). *Anal.* Calcd for $C_{20}H_{29}NO_6$: C, 63.31; H, 7.70; N, 3.69. Found: C, 63.18; H, 7.79; N, 3.58.

Quinone-Ala Ester **1d**: Diol-ester **8d** (124 mg, 0.256 mmol) was treated with NBS (45 mg, 0.256 mmol) according to the general procedure to give **1d** (98 mg, 97%) as a yellow oil: 1H -NMR ($CDCl_3$) δ 6.48 (m, 1H), 4.23 (m, 1H), 4.09 (m, 2H), 2.21 (m, 2H), 2.20 (s, 3H), 2.00 (d, $J=1.2$ Hz, 3H), 1.44 (s, 9H), 1.43 (s, 6H), 1.33 (d, $J=7.2$ Hz, 3H); ^{13}C -NMR ($CDCl_3$) δ 189.48, 188.36, 173.47, 155.17, 150.93, 144.10, 142.07, 135.19, 80.05, 63.22, 49.47, 41.10, 39.58, 30.50, 28.55, 18.83, 15.60, 14.81; IR (film) 1736, 1715, 1648, 1508, 1453, 1366, 1244, 1166 cm^{-1} ; FAB-MS m/z 393 (M^+). *Anal.* Calcd for $C_{21}H_{31}NO_6$: C, 64.10; H, 7.94; N, 3.56. Found: C, 64.24; H, 7.93; N, 3.61.

Quinone-Trp Ester **1e**: Diol-ester **8e** (159 mg, 0.253 mmol) was treated with NBS (45 mg, 0.253 mmol) according to the general procedure to give **1e** (123 mg, 91%) as a yellow oil: 1H -NMR ($CDCl_3$) δ 9.40, 9.11 (2s, 1H), 8.04–7.19 (m, 5H), 6.45 (s, 1H), 4.60 (m, 1H), 4.03 (m, 2H), 3.24–3.12 (m, 2H), 2.30 (m, 2H), 2.20 (s, 3H), 1.98 (s, 3H), 1.43 (s, 6H), 1.37 (s, 9H); ^{13}C -NMR ($CDCl_3$) δ 189.48, 188.28, 171.84, 159.38, 155.21, 150.73, 144.18, 142.15, 135.16, 131.61, 125.65, 124.75, 123.40, 120.35, 119.33, 116.42, 109.91, 80.39, 63.44, 53.77, 41.02, 39.43, 30.39, 28.52, 28.31, 15.59, 14.81; IR (film) 1736, 1712, 1648, 1458, 1366, 1167, 793, 749 cm^{-1} ; FAB-MS m/z 537 (M^+). *Anal.* Calcd for $C_{30}H_{36}N_2O_7$: C, 67.15; H, 6.75; N, 5.22. Found: C, 67.12; H, 6.82; N, 5.10.

Quinone-Asp Ester **1f**: Diol-ester **8f** (47 mg, 0.076 mmol) was treated with NBS (14 mg, 0.076 mmol) according to the general procedure to give **1f** (35 mg, 98%) as a yellow oil: 1H -NMR ($CDCl_3$) δ 7.35 (m, 5H), 6.47 (d, $J=1.3$ Hz, 1H), 5.12 (s, 2H), 4.49 (m, 1H), 4.06 (m, $J=7.0$ Hz, 2H), 2.87 (m, 2H), 2.18 (s, 3H), 2.15 (m, 2H), 1.99 (d, $J=1.2$ Hz, 3H), 1.44 (s, 9H), 1.40 (s, 6H); ^{13}C -NMR ($CDCl_3$) δ 189.23, 188.13, 170.93, 170.62, 155.25, 150.58, 143.89, 141.98, 135.47, 134.97, 128.60, 128.39, 128.27, 80.14, 66.78, 63.47, 50.11, 40.73, 39.36, 36.86, 30.25, 28.32, 15.39, 14.60; IR (film) 1734, 1719, 1648, 1498, 1366, 1166 cm^{-1} ; MS m/z 527 (M^+). *Anal.* Calcd for $C_{29}H_{37}NO_8$: C, 66.02; H, 7.07; N, 2.66. Found: C, 65.97; H, 7.17; N, 2.58.

Quinone-Cys Ester **1g**: Diol-ester **8g** (119 mg, 0.196 mmol) was treated with NBS (35 mg, 0.196 mmol) according to the general procedure to give **1g** (60 mg, 73%) as a yellow oil: 1H -NMR ($CDCl_3$) δ 7.30 (m, 5H), 6.46 (s, 1H), 4.43 (m, 1H), 4.10 (m, 2H), 3.70 (s, 2H), 2.81 (m, 2H), 2.23 (m, 2H), 2.19 (s, 3H), 1.99 (s, 3H), 1.45 (s, 9H), 1.42 (s, 6H); ^{13}C -NMR ($CDCl_3$) δ 189.47, 188.35, 171.26, 155.64, 150.83, 144.16, 142.20, 137.94, 135.20, 129.17, 128.83, 127.47, 80.01, 63.60, 53.53, 41.08, 39.59, 37.03, 33.98, 30.50, 28.58, 15.63, 14.87; IR (film) 1742, 1714, 1649, 1495, 1167, 702 cm^{-1} ; FAB-MS m/z 515 (M^+). *Anal.* Calcd for $C_{28}H_{37}NO_8$: C, 65.22; H, 7.23; N, 2.72. Found: C, 65.28; H, 7.35; N, 2.98.

Quinone-Ser Ester **1h**: Diol-ester **8h** (118 mg, 0.200 mmol) was treated with NBS (36 mg, 0.2 mmol) according to the general procedure to give **1h** (95 mg, 95%) as a yellow oil: 1H -NMR ($CDCl_3$) δ 7.30 (m, 5H), 6.46 (s, 1H), 4.50 (m, 2H), 4.35 (m, 1H), 4.09 (m, 2H), 3.79–3.63 (m, 2H), 2.19 (m, 2H), 2.17 (s, 3H), 1.99 (s, 3H), 1.44 (s, 9H), 1.41 (s, 6H); ^{13}C -NMR ($CDCl_3$) δ 189.47, 188.36, 170.84, 155.64, 150.93, 144.09, 142.15, 137.81, 135.21, 128.65, 128.04, 127.82, 80.19, 73.54, 70.26, 63.41, 54.33, 41.08, 39.58, 30.44, 28.57, 15.61, 14.81; IR (film) 1742, 1714, 1649, 1164 cm^{-1} ; FAB-MS m/z 500 (M^+). *Anal.* Calcd for $C_{28}H_{37}NO_7$: C, 67.32; H, 7.46; N, 2.80. Found: C, 67.26; H, 7.52; N, 2.91.

Quinone-Lys Ester **1i**: Diol-ester **8i** (68 mg, 0.1 mmol) was treated with NBS (18 mg, 0.1 mmol) according to the general procedure to give **1i** (60 mg, 99%) as a yellow oil: 1H -NMR ($CDCl_3$) δ 7.34 (m, 5H), 6.48 (d, $J=1.4$ Hz, 1H), 5.09 (s, 2H), 4.18 (m, 1H), 4.08 (m, 2H), 3.19 (m, 2H), 2.22 (m, 2H), 2.19 (s, 3H), 1.99 (s, 3H), 1.50 (m, 6H), 1.42 (s, 15H); ^{13}C -NMR ($CDCl_3$) δ 189.54, 188.37, 172.87, 156.70, 150.88, 144.14, 142.14, 136.90, 135.22, 128.73, 128.29, 80.15, 66.87, 63.21, 53.48, 41.14, 39.57, 32.62,

30.48, 29.92, 29.66, 28.55, 22.64, 15.61, 14.95; IR (film) 1736, 1713, 1649, 1522, 1455, 1366, 1247, 1169 cm^{-1} ; MS m/z 585 (M+H). *Anal.* Calcd for $\text{C}_{32}\text{H}_{44}\text{N}_2\text{O}_8$: C, 65.73; H, 7.59; N, 4.79. Found: C, 65.85; H, 7.58; N, 4.82.

Quinone-Propionic Ester **1j**: Diol-ester **8j** (133 mg, 0.36 mmol) and NBS (64 mg, 0.36 mmol) were treated according to the general procedure to give **1j** (99 mg, 99%) as a yellow oil: $^1\text{H-NMR}$ (CDCl_3) δ 6.47 (s, 1H), 4.02 (t, $J=7.2$ Hz, 2H), 2.26–2.16 (m, 7H), 2.00 (s, 3H), 1.43 (s, 6H), 1.08 (t, $J=7.5$ Hz, 3H); FAB-MS m/z 278 (M^+). *Anal.* Calcd for $\text{C}_{16}\text{H}_{22}\text{O}_4$: C, 69.05; H, 7.97. Found: C, 69.18; H, 8.03.

Quinone-Isobutyric Ester **1k**: Diol-ester **8k** (166 mg, 0.43 mmol) and NBS (77 mg, 0.43 mmol) were treated according to the general procedure to give **1k** (120 mg, 95%) as a yellow oil: $^1\text{H-NMR}$ (CDCl_3) δ 6.48 (q, $J=1.5$ Hz, 1H), 4.02 (t, $J=7.2$ Hz, 2H), 2.43 (m, $J=6.9$ Hz, 1H), 2.20 (s, 3H), 2.19 (t, $J=7.2$ Hz, 2H), 2.00 (d, $J=1.5$ Hz, 3H), 1.43 (s, 6H), 1.10 (d, $J=6.9$ Hz, 6H); $^{13}\text{C-NMR}$ (CDCl_3) δ 189.53, 188.48, 177.25, 151.30, 143.94, 141.91, 135.29, 62.21, 41.29, 39.69, 34.21, 30.56, 19.13, 15.60, 14.78; IR (film) 1733, 1648, 1576, 1470, 1239, 1190, 1156 cm^{-1} ; FAB-MS m/z 292 (M^+). *Anal.* Calcd for $\text{C}_{17}\text{H}_{24}\text{O}_4$: C, 69.84; H, 8.27. Found: C, 69.90; H, 8.40.

Quinone-Trimethylacetic Ester **1l**: Diol-ester **8l** (60 mg, 0.151 mmol) and NBS (26 mg, 0.148 mmol) were treated according to the general procedure to give **1l** (44 mg, 96%) as a yellow oil: $^1\text{H-NMR}$ (CDCl_3) δ 6.50 (q, $J=1.5$ Hz, 1H), 4.01 (t, $J=7.2$ Hz, 2H), 2.20 (s, 3H), 2.19 (t, $J=7.2$ Hz, 2H), 2.00 (d, $J=1.5$ Hz, 3H), 1.43 (s, 6H), 1.14 (s, 9H); $^{13}\text{C-NMR}$ (CDCl_3) δ 189.55, 188.49, 178.76, 151.24, 143.98, 142.08, 135.31, 62.37, 41.19, 39.75, 38.84, 30.61, 27.39, 15.61, 14.82; IR (film) 1726, 1649, 1576, 1480, 1283, 1238, 1155 cm^{-1} ; FAB-MS m/z 306 (M^+). *Anal.* Calcd for $\text{C}_{18}\text{H}_{26}\text{O}_4$: C, 70.56; H, 8.55. Found: C, 70.77; H, 8.43.

Quinone-Phenylacetic Ester **1m**: Diol-ester **8m** (93 mg, 0.215 mmol) and NBS (38 mg, 0.210 mmol) were treated according to the general procedure to give **1m** (70 mg, 96%) as a yellow oil: $^1\text{H-NMR}$ (CDCl_3) δ 7.31–7.20 (m, 5H), 6.46 (q, $J=1.5$ Hz, 1H), 4.04 (t, $J=7.2$ Hz, 2H), 3.53 (s, 2H), 2.18 (t, $J=7.2$ Hz, 2H), 2.15 (s, 3H), 1.99 (d, $J=1.5$ Hz, 3H), 1.39 (s, 6H); $^{13}\text{C-NMR}$ (CDCl_3) δ 189.41, 188.28, 171.64, 151.14, 143.94, 141.94, 135.25, 134.10, 129.38, 128.89, 128.78, 127.30, 62.83, 41.61, 41.14, 39.65, 30.50, 15.60, 14.74; IR (film) 1735, 1648, 1454, 1239, 1151 cm^{-1} ; FAB-MS m/z 340 (M^+). *Anal.* Calcd for $\text{C}_{21}\text{H}_{24}\text{O}_4$: C, 74.09; H, 7.11. Found: C, 73.97; H, 6.98.

Quinone-Naphthoic Ester **1n**: Diol-ester **8n** (115 mg, 0.245 mmol) and NBS 43 mg, 0.241 mmol) were treated according to the general procedure to give **1n** (90 mg, 98%) as a yellow oil: $^1\text{H-NMR}$ (CDCl_3) δ 8.49 (s, 1H), 7.96–7.82 (m, 4H), 7.62–7.52 (m, 2H), 6.35 (q, $J=1.5$ Hz, 1H), 4.41 (t, $J=6.9$ Hz, 2H), 2.41 (t, $J=6.9$ Hz, 2H), 2.22 (s, 3H), 1.73 (d, $J=1.5$ Hz, 3H), 1.51 (s, 6H); IR (film) 1715, 1647, 1283, 1227, 1195, 779, 762 cm^{-1} ; FAB-MS m/z 376 (M^+). *Anal.* Calcd for $\text{C}_{24}\text{H}_{24}\text{O}_4$: C, 76.57; H, 6.43. Found: C, 76.69; H, 6.60.

Quinone-(+)-methoxy- α -methyl-naphthaleneacetic Ester **1o**: Diol-ester **8o** (254 mg, 0.480 mmol) and NBS (86 mg, 0.480 mmol) were treated according to the general procedure to give **1o** (208 mg, 99%) as a yellow oil: $^1\text{H-NMR}$ (CDCl_3) δ 7.70–7.05 (m, 6H), 6.39 (m, 1H), 4.00 (m, 2H), 3.91 (s, 3H), 3.72 (m, 1H), 2.13 (t, $J=6.9$ Hz, 2H), 2.05 (d, $J=2.1$ Hz, 3H), 1.95 (s, 3H), 1.52, 1.50 (d, $J=6.9$ Hz, 3H), 1.33 (s, 6H); $^{13}\text{C-NMR}$ (CDCl_3) δ 189.48, 188.37, 174.78, 157.91, 151.12, 143.87, 141.96, 135.80, 135.21, 133.94, 129.47, 129.18, 127.37, 126.36, 126.10, 119.19, 105.91, 62.77, 55.53, 45.71, 41.06, 39.65, 30.47, 18.76, 15.58, 14.69; IR (film) 1730, 1647, 1606, 1264, 1172 cm^{-1} ; FAB-MS m/z 434 (M^+). *Anal.* Calcd for $\text{C}_{27}\text{H}_{30}\text{O}_5$: C, 74.63; H, 6.96. Found: C, 74.64; H, 6.94.

Reduction of Quinones 1a–o A solution of quinone **1a–o** in ethyl ether was shaken with 20 eq of aqueous sodium hydrosulfite solution at r.t. in a separatory funnel until the color of the reaction mixture changed from yellow to colorless. The ether layer was separated and the aqueous phase was extracted with ether. The combined ether layers were washed with saturated NaCl and then dried over MgSO_4 . Solvent evaporation afforded the hydroquinone **2a–o**.

Release of the Carboxylic Acid a–i and o To a 7–8 mm solution of the hydroquinone **2a–i, o** (0.04–0.19 mmol) in THF was added dropwise TBAF (1.0 M in THF) (0.16–0.77 mmol) by a syringe with stirring under nitrogen at 0 °C. Five minutes after the addition, the ice-bath was removed and stirring was continued at r.t. The color of the mixture changed from colorless to yellow then to orange then to green, and finally to blue. After the disappearance of the starting material by TLC analysis (hexanes/ethyl acetate = 3/1, v/v), the mixture was diluted with acetonitrile and water (1/3) to 25.00 ml, from which 2.00 ml of solution was taken and diluted to 100.00 ml. This diluted solution was analyzed by HPLC.

Release of the carboxylic acids **j–n** were carried out following similar

procedures with 18 mm solutions of hydroquinone **2j–n** (0.07–0.12 mmol) and 8-fold TBAF at r.t.

N-Boc-indole-formyl-tryptophan A solution of quinone-trp ester **1e** (100 mg, 0.186 mmol) in 40 ml of ether was shaken with a solution of sodium hydrosulfite (2 g, 9.77 mmol) in 10 ml of water until the color of the reaction mixture changed from yellow to colorless. The organic layer was separated and the aqueous layer was extracted with ether (2×40 ml). The combined organic layers were washed with brine (2×10 ml) and dried over MgSO_4 for 3 h. Solvent evaporation afforded 99 mg of the hydroquinone monoester **2e**.

The hydroquinone **2e** was dissolved in freshly distilled THF (25 ml) which was chilled and stirred in an ice/water bath under a nitrogen atmosphere. To this solution 740 μl (0.74 mmol) of 1.0 M TBAF solution in THF was added dropwise. Five minutes after addition, the ice bath was withdrawn and stirring was continued for an additional 1.5 h at r.t. HPLC analysis of the reaction mixture showed 100% conversion to the cyclic ether and N-Boc-indole-formyl-tryptophan.

The reaction mixture was then concentrated and separated by RPLC (silica gel), gradient elution with methylene chloride/methanol (15/1 to 7/1), to give 28 mg (74%) of cyclic ether **3** and 49 mg (80%) of Boc-indole-formyl-tryptophan which was identified by $^1\text{H-NMR}$.

6-Methoxy- α -methyl-2-naphthaleneacetic Acid A solution of compound **1o** (100 mg, 0.23 mmol) in 40 ml of ether was mixed with a solution of sodium hydrosulfite (2 g, 9.77 mmol) in 10 ml of water. The resulting mixture was shaken in a separatory funnel until the color of the reaction mixture changed from yellow to colorless. The organic layer was separated and the aqueous phase was extracted with ether (2×5 ml). The organic fraction was washed with brine (2×10 ml) and dried over MgSO_4 for 3 h. Solvent evaporation afforded the hydroquinone **2o** (97 mg).

To a solution of the hydroquinone **2o** (97 mg, 0.223 mmol) in freshly distilled THF (25 ml) cooled with an ice bath was slowly added dropwise TBAF (1.0 M in THF) (670 μl , 0.67 mmol) by a syringe with stirring under N_2 . Five minutes after addition, the ice bath was removed and stirring was continued for an additional 2 h at r.t. The reaction solution was concentrated under reduced pressure to give the residue, to which 5 ml of 1 N NaOH was added. The aqueous solution was washed with ethyl ether (3×10 ml) and the combined organic layers were dried over MgSO_4 . The residue after solvent removal was purified by column chromatography (hexanes: ethyl acetate = 3:1) to give cyclic ether **3** (38 mg) in 83% yield. The aqueous phase was acidified with 1 N HCl solution (10 ml) and a white precipitate was formed. The precipitate was extracted with ethyl ether (4×20 ml) and the combined organic extracts were dried over MgSO_4 . Filtration and solvent evaporation gave a pale yellow solid (48 mg, 93%) which was identical to (+)-6-methoxy- α -methyl-2-naphthaleneacetic acid according to $^1\text{H-NMR}$.

Acknowledgement Financial support from the National Institutes of Health (GM52515) is gratefully acknowledged. CEB gratefully acknowledges a Burroughs-Wellcome graduate fellowship.

References and Notes

- 1) Ailian Zheng and Daxian Shan made equal contributions to this paper.
- 2) a) Hillery P. S., Cohen L. A., *J. Org. Chem.*, **48**, 3465–3471 (1983); b) Milstein S., Cohen L. A., *J. Am. Chem. Soc.*, **94**, 9158–9165 (1972); c) Wang B., Nicolaou M. G., Liu S., Borchardt R. T., *Bioorg. Chem.*, **24**, 39–49 (1996); d) Caswell M., Schmir G., *J. Am. Chem. Soc.*, **102**, 4815–4821 (1980); e) Danforth C., Nicholson A. W., James J. C., Loudon G. M., *ibid.*, **98**, 4275–4280 (1976); f) Hillery P. S., Cohen L. A., *Bioorg. Chem.*, **20**, 313–322 (1992); g) Winans R. E., Wilcox C. F., *J. Am. Chem. Soc.*, **98**, 4281–4285 (1976).
- 3) Borchardt R. T., Cohen L. A., *J. Am. Chem. Soc.*, **94**, 9166–9174 (1972).
- 4) a) Amsberry K. L., Borchardt R. T., *J. Org. Chem.*, **55**, 5867–5877 (1990); b) *Idem*, *Pharm. Res.*, **8**, 323–330 (1991); c) Amsberry K. L., Gerstenberger A. L., Borchardt R. T., *ibid.*, **8**, 455–461 (1991); d) Carpino L. A., Triolo S. A., Berglund R. A., *J. Org. Chem.*, **54**, 3303–3310 (1989); e) Ueda Y., Mikkilineni A. B., Knip J. O., Rose W. C., Casazza A. M., Vyas D. M., *Bioorg. Med. Chem. Lett.*, **3**, 1761–1766 (1993); f) Nicolaou M. G., Yuan C.-S., Borchardt R. T., *J. Org. Chem.*, **61**, 8636–8641 (1996); g) Wang B., Gangwar S., Pauletti G. M., Siahaan T., Borchardt R. T., *ibid.*, **62**, 1362–1367 (1997).
- 5) Wang B., Liu S., Borchardt R. T., *J. Org. Chem.*, **60**, 539–543 (1995).
- 6) Carpino L. A., Nowshad F., *Tetrahedron Lett.*, **34**, 7009–7012 (1993).
- 7) a) Gayo L. M., Suto M. J., *Tetrahedron Lett.*, **38**, 211–214 (1997); b)

- Routledge A., Abell C., Balasubramanian S., *ibid.*, **38**, 1227—1230 (1997); c) Ngu K., Patel D. V., *ibid.*, **38**, 973—976 (1997); d) Zhao X., Jung K. W., Janda K. D., *ibid.*, **38**, 977—980 (1997); e) Richter L. S., Desai M. C., *ibid.*, **38**, 321—322 (1997); f) Alsina J., Chiva C., Ortiz M., Rabanal F., Giralt E., Albericio F., *ibid.*, **38**, 883—886 (1997); g) Noda M., Yamaguchi M., Ando E., Takeda K., Nokihara K., *J. Org. Chem.*, **59**, 7968—7975 (1994); h) Chao H., Bernatowicz M. S., Reiss P. D., Klimas C. E., Matsueda G. R., *J. Am. Chem. Soc.*, **116**, 1746—1752 (1994).
- 8) Stewart J. M., Young J. D., "Solid Phase Peptide Synthesis," Pierce Chemical Company, Rockford, IL, 1984.
- 9) Borchardt R. T., Cohen L. A., *J. Am. Chem. Soc.*, **95**, 8308—8313 (1973).
- 10) Tung R. D., Rich D. H., *J. Am. Chem. Soc.*, **107**, 4342—4343 (1985).
- 11) a) Sieber P., *Helv. Chimica Acta*, **60**, 2711—2716 (1977); b) Plunkett M. J., Ellman J. A., *J. Org. Chem.*, **60**, 6006—6007 (1995); c) Chen-
era B., Finkelstein J. A., Veber F. D., *J. Am. Chem. Soc.*, **117**, 11999—
12000 (1995); d) Mullen D. G., Barany G., *Tetrahedron Lett.*, **28**,
491—494 (1987); e) Greene T. W., Wuts P. G. M., "Protective Groups
in Organic Synthesis," John-Wiley & Sons: New York, 1991 and refer-
ences cited therein.
- 12) Zheng A., Shan D., Shi X., Wang B., *J. Org. Chem.*, **64**, 7459—7466 (1999).

[2-(ω -Phenylalkyl)phenoxy]alkylamines II: Synthesis and Selective Serotonin-2 Receptor Binding

Naoki TANAKA,^a Riki GOTO,^a Rie ITO,^{a,1)} Miho HAYAKAWA,^a Atsuhiko SUGIDACHI,^b Taketoshi OGAWA,^b Fumitoshi ASAI,^b and Koichi FUJIMOTO*,^a

Medicinal Chemistry Research Laboratories^a and Pharmacology and Molecular Biology Research Laboratories,^b Sankyo Co., Ltd., 1–2–58 Hiromachi, Shinagawa-ku, Tokyo 140–8710, Japan.

Received August 23, 1999; accepted November 2, 1999

A series of [2-(ω -phenylalkyl)phenoxy]alkylamines was synthesized and their receptor binding affinity was examined *in vitro*. These compounds showed an affinity for serotonin-2 (5-HT₂) and dopamine-2 (D₂) receptors. [2-(2-phenylethyl)phenoxy]alkylamine derivatives with a pyrrolidine or piperidine moiety in the structure showed higher affinity for 5-HT₂ receptors but lower affinity for D₂ receptors. Among these compounds, (S)-2-[2-[2-(3-methoxyphenyl)ethyl]phenoxy]ethyl-1-methylpyrrolidine, (S)-27, exhibited the most potent and selective affinity for 5-HT₂ receptors. Furthermore, (S)-27 was effective in inhibiting 5-HT-induced vasoconstriction *in vitro* and platelet aggregation both *in vitro* and *ex vivo*.

Key words serotonin-2 (5-HT₂) receptor; antiplatelet; antagonist; [2-(2-phenylethyl)phenoxy]alkylamines

Serotonin (5-hydroxytryptamine; 5-HT) produces a wide variety of biological activities on many organ systems including the central nervous, gastrointestinal, and cardiovascular systems. These responses to 5-HT are mediated by its receptors on the cell membranes. To date, there are at least 16 identified subtypes of 5-HT receptors, which are now categorized into five main classes (5-HT₁, 5-HT₂, 5-HT₃, 5-HT₄, and 5-HT₇).^{2,3)} The most well-characterized of these receptor subtypes is the 5-HT₂ receptor, due to the availability of reasonably selective agonists and antagonists.^{4–7)} 5-HT₂ receptors are located both centrally and peripherally. Peripheral 5-HT₂ receptors are located on blood vessels and platelets, and are intimately involved in hemostasis and thrombosis.^{8–11)}

Ketanserin, a 5-HT₂ receptor antagonist, shows high affinity for 5-HT₂ receptors on platelets and inhibits 5-HT-induced platelet aggregation and vasoconstriction.¹²⁾ However, this compound shows relatively high affinity for adrenergic (α_1) receptors, in addition to 5-HT₂ receptors.^{13,14)} Sarpogrelate, a more selective 5-HT₂ antagonist, has been developed, and is now clinically available for the treatment of peripheral arterial occlusive diseases.^{15,16)}

We previously reported that [2-(4-phenylbutyl)phenoxy]alkylamine derivatives have high affinity for both 5-HT₂ and dopamine-2 (D₂) receptors.¹⁷⁾ In the course of a study of [2-(ω -phenylalkyl)phenoxy]alkylamine derivatives, [2-(2-phenylethyl)phenoxy]alkylamine derivatives with a pyrrolidine or piperidine moiety in the structure showed relatively potent and selective affinity for 5-HT₂ receptors. Thus, we have attempted to synthesize highly potent and selective antagonists for peripheral 5-HT₂ receptors on blood vessels and platelets. In this paper, we describe the synthesis and structure–activity relationships (SAR) of these compounds. We also report biological activities of (S)-27, the most active compound as a peripheral 5-HT₂ antagonist, in comparison with ketanserin and sarpogrelate.

Chemistry The phenol derivatives 4–8 were synthesized as shown in Chart 1. Aldehydes 1 and phosphonium chloride 2 were subjected to the Wittig reaction to give the corresponding olefins 3, which were then converted to the phenol derivatives 4–8 by catalytic hydrogenation.

The syntheses of the racemic cyclic amino derivatives having an ω -phenyl ring 11–43 are outlined in Chart 2. Piperidine (X=CH₂) and morpholine (X=O) derivatives (11–17, 20–26, 29, 30) were synthesized as described below. Compounds 10 were prepared by the alkylation of 4–8 with tosylates (9: R²=OTs) (method A), or by means of the Mitsunobu reaction¹⁸⁾ between 4–8 and a hydroxy derivative (9: R²=OH) (method B). The resulting compounds 10 were reduced with lithium aluminum hydride to give *N*-methylated (*N*-Me) compounds (11–17, 21, 23, 25, 29, 30). *N*-nonalkylated (*N*-H) compounds (20, 22, 24, 26) were prepared by the treatment of 10 with HCl. *N*-Methylpyrrolidine derivatives (18, 19, 27, 31–43) were prepared by alkylation of 4 or 6 with 2-(2-chloroethyl)-1-methylpyrrolidine hydrochloride (method C), or by means of the Mitsunobu reaction¹⁸⁾ between 4 or 6 and 1-methyl-2-pyrrolidineethanol (method D). *N*-H compound 28 was prepared by alkylation of 4 with 1-*tert*-butoxycarbonyl-2-[2-(*p*-toluenesulfonyloxy)ethyl]-pyrrolidine followed by the treatment with HCl.

The synthesis of the *N*-methylpyrrolidine derivative having an ω -cyclohexane, 48, is shown in Chart 3. 2-Benzyloxybenzylchloride 44 was converted to the corresponding Grignard reagent and the Grignard reagent was treated with cyclohexanecarboxaldehyde to afford 45. The hydroxy group of 45 was replaced with a chlorine atom by thionyl chloride, and the chlorine atom was replaced with a hydrogen atom by tributyltin hydride to provide 46. Removal of the benzyl group by catalytic hydrogenation afforded phenol 47, which was then treated with 2-(2-chloroethyl)-1-methylpyrrolidine hydrochloride in the presence of *tert*-BuOK to give 48.

The syntheses of the optically active pyrrolidine intermediates ((S)-51, (R)-55, (S)-55, and (S)-60) are outlined in Charts 4–6. They were performed as follows: The tosylate (S)-51 was synthesized from the commercially available 2-pyrrolidinemethanol (S)-49 through protection by ethyl chloroformate to give carbamate (S)-50, and tosylation (Chart 4).

The tosylate (R)-55 was prepared in four steps starting from the tosylate (R)-51 (Chart 5). The one carbon elongation of (R)-51 with sodium cyanide provided (R)-52, and the resulting nitrile group was hydrolyzed in an acidic condition

* To whom correspondence should be addressed.

to give an ester (*R*)-**53**. The ester (*R*)-**53** was reduced with lithium aluminum hydride to give an alcohol (*R*)-**54**, which was then converted to the tosylate (*R*)-**55**. The enantiomer of (*R*)-**55**, (*S*)-**55** was prepared in the same manner.

The tosylate (*S*)-**60** was prepared in five steps starting from the alcohol (*S*)-**50** (Chart 6). The Swern oxidation¹⁹⁾ of the alcohol (*S*)-**50** provided an aldehyde (*S*)-**56**, which was then subjected to the Wittig reaction to give an α,β -unsaturated ester (*S*)-**57**. The ester (*S*)-**57** was hydrogenated, and the following reduction of the saturated ester (*S*)-**58** with lithium aluminum hydride gave an alcohol (*S*)-**59**, which was then converted to the tosylate (*S*)-**60**.

The syntheses of the target compounds ((*R*)-**27**, (*S*)-**27**, (*S*)-**62**, and (*S*)-**63**) are shown in Chart 7. The phenol **4a** ($R^1=3\text{-OMe}$) was alkylated with the tosylates ((*S*)-**51**, (*R*)-**55**, (*S*)-**55**, and (*S*)-**60**) to give carbamates, which were then reduced with lithium aluminum hydride to give the desired

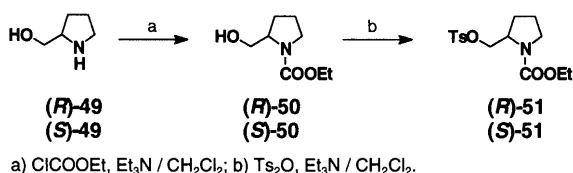


Chart 4

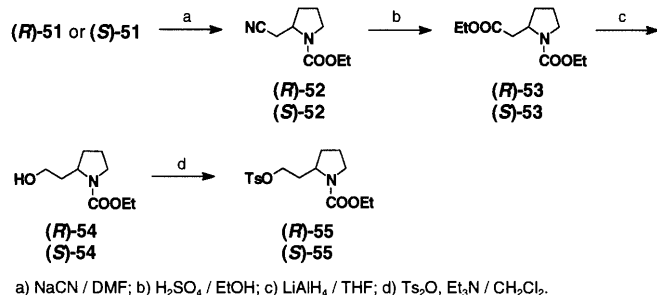


Chart 5

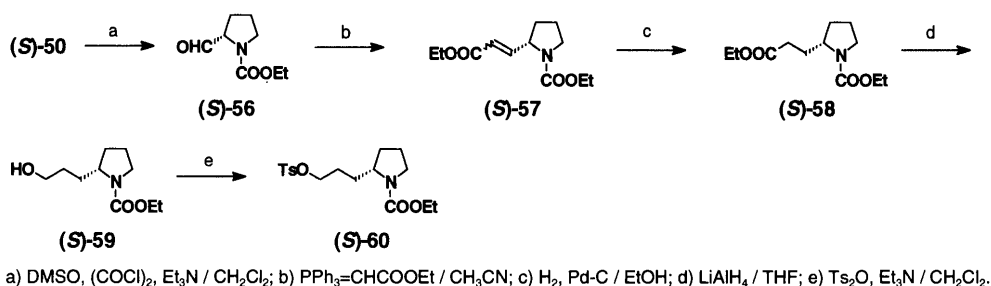


Chart 6

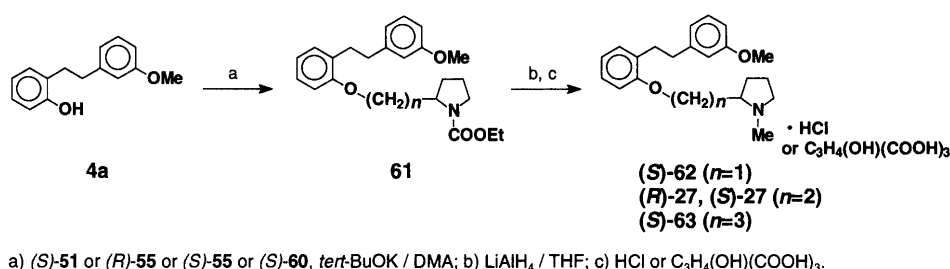


Chart 7

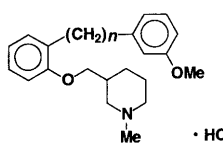
products. This was followed by their corresponding salt formation.

Results and Discussion

All compounds have diphenylalkylene structures connecting two phenyl parts in this series. In the previous paper, we reported the relationship between the alkylene chain length and D_2 receptor binding of 3-dimethylamino-1-(ω -phenylalkylphenoxy)-2-propanol derivatives.¹⁷⁾ Only the tetramethylene derivative showed D_2 receptor affinity, and the tetramethylene derivatives with a piperidine moiety, including compound **13**, exhibited high affinity for 5-HT₂ and D_2 receptors. Thus, we examined the influence of the alkylene chain length in the diphenylalkylene moiety of compound **13** (Table 1). The compounds in Table 1 exhibited high affinity for 5-HT₂ receptors with their IC_{50} values between 1.9 and 31 nM. Among them, the dimethylene derivative **11** and the tetramethylene derivative **13** were highly potent; their IC_{50} values were smaller than that of M-1, the active metabolite of sargogrelate. In the D_2 receptor binding studies, the tetramethylene derivative **13** exhibited high affinity with an IC_{50} of 9.2 nM, while other compounds had markedly reduced activity (IC_{50} s > 150 nM). This is consistent with the results reported for 3-dimethylamino-1-(ω -phenylalkylphenoxy)-2-propanol derivatives.¹⁷⁾

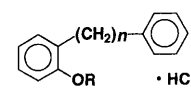
Among the [2-(ω -phenylalkyl)phenoxy]alkylamine derivatives with a piperidine or pyrrolidine moiety, the dimethylene and tetramethylene derivatives (**16**–**19**) were examined in 5-HT₂ and D_2 receptor binding assays (Table 2). The dimethylene derivatives **16** and **18** showed higher 5-HT₂ and lower D_2 receptor affinity compared with the corresponding tetramethylene derivatives, **17** and **19**, respectively. Thus, the dimethylene chain was suitable for selectivity of the 5-HT₂ receptor.

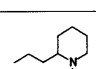
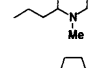
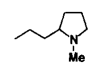
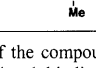
The dimethylene derivatives with a cyclic amino group were examined in 5-HT₂ and D_2 receptor binding assays (Table 3). The introduction of a 3-methoxy group on the ω -phenyl ring increased the affinity for the 5-HT₂ receptor (**16** vs. **21**, **18** vs. **27**), which is consistent with our previous re-

Table 1. Affinity of 3-[2- ω -(3-Methoxyphenyl)alkyl]phenoxyethyl-1-methylpiperidine Derivatives for 5-HT₂ and D₂ Receptors


Compd.	<i>n</i>	IC ₅₀ (nm) ^{a)}		Ratio ^{b)} D ₂ /5-HT ₂
		5-HT ₂	D ₂	
11	2	1.9	150	79
12	3	17	490	29
13^{c)}	4	2.2	9.2	4.2
14	5	31	270	8.7
15	6	28	1800	64
Sarpogrelate		150	>5000	ND ^{d)}
M-1		16	>5000	ND ^{d)}
Ketanserin		5.3	940	180

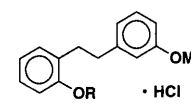
a) Interaction of the compounds with rat brain 5-HT₂ and D₂ receptors was determined by conventional binding assay using [³H]ketanserin and [³H]raclopride. b) Ratio: the IC₅₀ values for D₂ vs. 5-HT₂ receptors. c) Data from reference 17. d) Not determined.

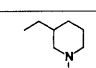
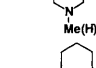
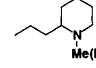
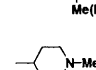
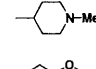
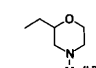
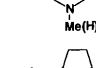
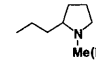
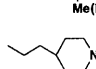
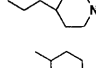
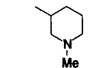
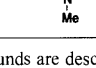
Table 2. Affinity of Dimethylene and Tetramethylene Derivatives with a 2-(ω -phenylalkyl)phenoxy Group for 5-HT₂ and D₂ Receptors


Compd.	R	<i>n</i>	IC ₅₀ (nm) ^{a)}		Ratio ^{b)} D ₂ /5-HT ₂
			5-HT ₂	D ₂	
16		2	4.7	470	100
17^{c)}		4	11	40	3.6
18		2	6.1	760	120
19^{c)}		4	32	28	0.88

a) Interaction of the compounds with rat brain 5-HT₂ and D₂ receptors was determined by conventional binding assay using [³H]ketanserin and [³H]raclopride. b) Ratio: the IC₅₀ values for D₂ vs. 5-HT₂ receptors. c) Data from reference 17.

sults.¹⁷⁾ Among this series of compounds, the 5-HT₂ and D₂ receptor affinity of *N*-Me compounds (**11**, **21**, **23**, **25**, **27**) were higher than those of the corresponding *N*-H compounds (**20**, **22**, **24**, **26**, **28**). Compound **21**, which has a 2-(2-piperidinylethyl) structure, showed high affinity for 5-HT₂ receptors. However, **21** also showed high affinity for D₂ receptors, and its D₂/5-HT₂ ratio was smaller than that of **11**. The D₂ receptor affinity of compound **23** was six-fold lower than that of **11**, and its 5-HT₂ receptor affinity was also slightly lower than **11**. It is interesting to note that these three compounds (**11**, **21**, **23**) with potent affinity (IC₅₀ < 10 nm) for 5-HT₂ receptors, have three carbon atoms between the piperidine nitrogen and the etheral oxygen. In contrast, the other piperidine derivatives such as **29** with five carbon atoms and **30** with two carbon atoms between the piperidine nitrogen and etheral oxygen, respectively, were less active. In the previous paper, we reported that the D₂ receptor affinity depends on the lipophilicity around the amino moiety in a series of compounds.¹⁷⁾ Morpholine derivative **25**, which has an oxygen instead of a methylene group at the 4-position of piperidine, was prepared in an attempt to reduce the D₂ receptor

Table 3. Affinity of Cyclic Amino Derivatives with a 2-[2-(3-Methoxyphenyl)ethyl]phenoxy Group for 5-HT₂ and D₂ Receptors


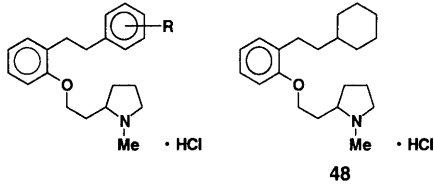
Compd. ^{a)}	R ^{a)}	IC ₅₀ (nm) ^{a,b)}		Ratio ^{c)} D ₂ /5-HT ₂
		5-HT ₂	D ₂	
11		1.9	150	79
(20)		(5.0)	(890)	(180)
21		3.6	120	33
(22)		(55)	(>3000)	(ND ^{d)})
23		7.7	1000	130
(24)		(32)	(>3000)	(ND ^{d)})
25		11	1600	150
(26)		(17)	(>3000)	(ND ^{d)})
27		2.0	670	340
(28)		(39)	(>3000)	(ND ^{d)})
29		46	230	5.0
30		77	>5000	(ND ^{d)})

a) *N*-H compounds are described in parentheses. b) Interaction of the compounds with rat brain 5-HT₂ and D₂ receptors was determined by conventional binding assay using [³H]ketanserin and [³H]raclopride. c) Ratio: the IC₅₀ values for D₂ vs. 5-HT₂ receptors. d) Not determined.

affinity by decreasing the lipophilicity around the amino moiety. As expected, the D₂ receptor affinity of **25** was lower than that of the piperidine derivative, **11**. However, the 5-HT₂ receptor affinity of **25** also decreased in parallel. Compound **27**, which has a pyrrolidine ring instead of a piperidine ring, was as potent as **11** and **21** for its 5-HT₂ receptor affinity, but less potent for its D₂ receptor affinity compared to **11** and **21**. Among these three compounds, **27** exhibited the highest D₂/5-HT₂ ratio (340), suggesting a high selectivity. The pyrrolidine derivatives, therefore, seemed superior to the piperidine derivatives as selective 5-HT₂ antagonists.

The effect of the substituent on the ω -phenyl group was examined (Table 4). Most compounds show high affinity for 5-HT₂ receptors, regardless of the type of the substituent. Compounds substituted at the 3-position (**27**, **34**, **37**) of the ω -phenyl ring showed higher affinity than those substituted at the 2- or 4-position (**31**, **33**, **36** or **32**, **35**, **38**). The methoxy-substituted compounds showed slightly more potent activity than their corresponding ethoxy compounds. Compounds **37** and **39**, having a chlorine and a fluorine atom, respectively, on the ω -phenyl ring also showed more potent activity than the bromo analog **40**. These results show that the introduction of a bulky substituent decreases the affinity for 5-HT₂ receptors. The introduction of a hydrophilic hydroxy group (**43**) instead of the etheral *O*-methyl group of **27** also decreased the 5-HT₂ receptor affinity. The reduction of the ω -phenyl ring, which leads to an ω -cyclohexane in compound **48**, maintained the 5-HT₂ receptor affinity. In the case of 2-(1-methyl-2-pyrrolidinylethyl) derivatives, as indicated in Table 4, all of the compounds showed low activity for D₂ receptors (IC₅₀s > 460 nm). However, compounds with a

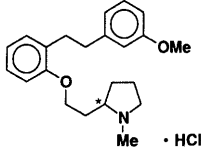
Table 4. Affinity of 1-Methyl-2-[2-(2-phenylethyl)phenoxy]ethylpyrrolidine Derivatives and 2-[2-(2-(2-Cyclohexylethyl)phenoxy)ethyl]-1-methylpyrrolidine Derivative for 5-HT₂ and D₂ Receptors



Compd.	R	IC ₅₀ (nM) ^{a)}		Ratio ^{b)} D ₂ /5-HT ₂
		5-HT ₂	D ₂	
18	H	6.1	760	120
31	2-OMe	3.5	1100	310
27	3-OMe	2.0	670	340
32	4-OMe	6.1	780	130
33	2-OEt	10	1700	170
34	3-OEt	6.7	640	96
35	4-OEt	12	460	38
36	2-Cl	15	1100	73
37	3-Cl	4.5	660	150
38	4-Cl	7.9	1200	150
39	3-F	4.4	600	140
40	3-Br	8.7	960	110
41	3-CN	5.4	610	110
42	3-Me	5.0	700	140
43	3-OH	17	1500	88
48		4.8	530	110

a) Interaction of the compounds with rat brain 5-HT₂ and D₂ receptors was determined by conventional binding assay using [³H]ketanserin and [³H]raclopride. b) Ratio: the IC₅₀ values for D₂ vs. 5-HT₂ receptors.

Table 5. Affinity of (R,S)-27 and Its Optically Active Compounds for 5-HT₂ and D₂ Receptors



Compd.	IC ₅₀ (nM) ^{a)}		Ratio ^{b)} D ₂ /5-HT ₂
	5-HT ₂	D ₂	
(R,S)-27	2.0	670	340
(S)-27	1.8	1100	610
(R)-27	6.4	490	77

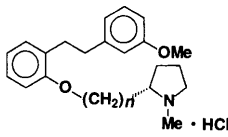
a) Interaction of the compounds with rat brain 5-HT₂ and D₂ receptors was determined by conventional binding assay using [³H]ketanserin and [³H]raclopride. b) Ratio: the IC₅₀ values for D₂ vs. 5-HT₂ receptors.

changed substituent on the ω-phenyl ring were not as potent and selective for 5-HT₂ receptors as 27.

Although 27 had potent and selective affinity for 5-HT₂ receptors, this compound has the asymmetric carbon atom at the 2-position of the pyrrolidine ring. Therefore, each of the enantiomers was prepared to examine its binding affinity for 5-HT₂ and D₂ receptors (Table 5). The compound with (S) configuration, (S)-27, exhibited higher 5-HT₂ receptor affinity and lower D₂ receptor affinity than racemic 27. These results indicate that (S)-27 is the active enantiomer in 5-HT₂ receptor affinity.

Table 6 shows the effect of the alkylene chain attached to

Table 6. Affinity of (S)-27 and Its Analogs for 5-HT₂ and D₂ Receptors



Compd.	n	IC ₅₀ (nM) ^{a)}		Ratio ^{b)} D ₂ /5-HT ₂
		5-HT ₂	D ₂	
(S)-62	1	6.4	>3000	ND ^{c)}
(S)-27	2	1.8	1100	610
(S)-63 ^{d)}	3	20	2500	130

a) Interaction of the compounds with rat brain 5-HT₂ and D₂ receptors was determined by conventional binding assay using [³H]ketanserin and [³H]raclopride. b) Ratio: the IC₅₀ values for D₂ vs. 5-HT₂ receptors. c) Not determined. d) Citrate.

Table 7. 5-HT-Induced Human PRP Aggregation (*in Vitro*)

Compd.	IC ₅₀ (μM) ^{a)}
(S)-27	0.057 (0.049—0.066)
Sarpogrelate	>100
M-1	3.6 (2.8—4.7)
Ketanserin	0.14 (0.083—0.24)

a) Data are expressed as the mean values and 95% confidence limits in parentheses.

the 2-position of pyrrolidine. Among these compounds, (S)-27 (n=2) showed the highest affinity for 5-HT₂ receptors. Compared with (S)-27, (S)-62 (n=1) and (S)-63 (n=3) showed lower affinity. These results show that the 5-HT₂ receptor affinity was the highest for pyrrolidine derivatives with three carbon atoms between the pyrrolidine nitrogen and etheral oxygen. This is consistent with results in the study of the piperidine derivatives.

Table 7 shows the IC₅₀ values (μM) for the test compounds ((S)-27, ketanserin, sarpogrelate, and M-1, the active metabolite of sarpogrelate) against *in vitro* human platelet aggregation. (S)-27 inhibited platelet aggregation in a concentration-dependent manner with an IC₅₀ value of 0.057 μM. Ketanserin and M-1 also inhibited platelet aggregation, but these agents were less potent than (S)-27. Sarpogrelate produced the minimum inhibition on platelet aggregation. These results clearly indicate that (S)-27 has more potent *in vitro* antiaggregatory activity compared to those of sarpogrelate, M-1, and ketanserin.

The *ex vivo* effects of 5-HT₂ antagonists, (S)-27, ketanserin and sarpogrelate on 5-HT-induced platelet aggregation were examined in cats (Fig. 1). Single bolus administration of (S)-27 (100 μg/kg, i.v.) resulted in a marked inhibition (90%) of platelet aggregation at 0.5 h postdose. The inhibition disappeared gradually, but was still evident even at 6 h (29% inhibition). Ketanserin (100 μg/kg, i.v.) also showed an inhibition (61%) at 0.5 h postdose, but the extent of the inhibition was smaller than (S)-27. In addition, the effect of ketanserin disappeared at 4 h postdose. Sarpogrelate even at the highest dose (1000 μg/kg, i.v.) failed to inhibit platelet aggregation, indicating weak efficacy of this agent. These results suggest that (S)-27 is a potent antiplatelet agent with long duration of action *in vivo*.

The addition of (S)-27 alone to platelet-rich plasma (PRP) did not cause any platelet aggregation up to 1 mM. Thus, this

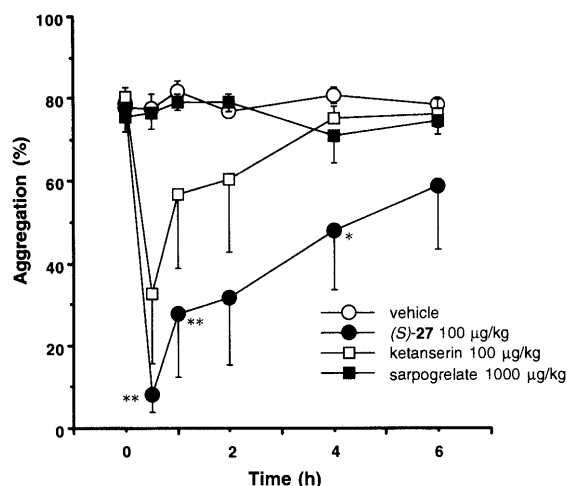


Fig. 1. *Ex Vivo* Antiplatelet Effects of (S)-27, Ketanserin and Sarpogrelate in Cats

Data are represented as the mean \pm S.E.M. ($n=4-6$). * $p<0.05$, ** $p<0.01$ vs. vehicle (Dunnett's test).

compound is unlikely to have any agonistic activity for 5-HT₂ receptors. (S)-27 also did not cause vasoconstriction, but inhibited 5-HT-induced vasoconstriction with an IC₅₀ value of 2.2 nM. These results suggest that (S)-27 is a 5-HT₂ receptor antagonist and not an agonist.

The binding affinity of (S)-27 was further examined for other receptors (α_1 , β , 5-HT₁, and 5-HT₃). (S)-27 exhibited low affinity with IC₅₀s (nM) of 490 for α_1 and over 5000 for β , 5-HT₁, and 5-HT₃, respectively. This clearly indicates that (S)-27 is highly selective for 5-HT₂ receptors.

In conclusion, we found that new [2-(2-phenylethyl)phenoxy]alkylamine derivatives with a pyrrolidine or piperidine moiety in their structure have high affinity for 5-HT₂ receptors but low affinity for D₂ receptors. Among these compounds, (S)-27 exhibited the highest selectivity and potency for 5-HT₂ receptors in the binding assays. This compound was also effective in inhibiting 5-HT-induced vasoconstriction *in vitro* and platelet aggregation both *in vitro* and *ex vivo*.

Experimental

Melting points were determined with a Yanagimoto micro melting point apparatus and were uncorrected. ¹H-NMR spectra were obtained on a JEOL EX270 spectrometer and were reported as δ values relative to Me₄Si as the internal standard. Abbreviations of the ¹H-NMR peak patterns are as follows: br=broad, s=singlet, d=doublet, t=triplet, q=quartet, and m=multiplet. IR spectra were taken on a JASCO FT/IR-8900 spectrometer. Merck Silica gel 60 (230–400 mesh) was used in the column chromatography. Tetrahydrofuran, *N,N*-dimethylacetamide, and dimethylsulfoxide are abbreviated as THF, DMA, and DMSO, respectively.

1-*tert*-Butoxycarbonyl-3-[2-[2-(3-methoxyphenyl)ethyl]phenoxy-methyl]piperidine (10; $m=1$, $n=2$, $R^1=3\text{-OMe}$, $X=\text{CH}_2$) (Method A) To a solution of 2-[2-(3-methoxyphenyl)ethyl]phenol¹⁶⁾ **4a** ($R^1=3\text{-OMe}$) (790 mg, 3.46 mmol) in DMA (8 ml) was added *tert*-BuOK (388 mg, 3.46 mmol) and the mixture was stirred at 0 °C for 10 min. Then a solution of 1-*tert*-butoxycarbonyl-3-(*p*-toluenesulfonyloxymethyl)piperidine **9** ($m=1$, $X=\text{CH}_2$) (1.28 g, 3.46 mmol) in DMA (7 ml) was added and the mixture was stirred overnight at room temperature. The resulting suspension was diluted with EtOAc and washed with H₂O and brine. The organic layer was dried and concentrated. The resulting residue was chromatographed on a silica gel column (hexane/EtOAc=5/1–4/1) to give **10** ($m=1$, $n=2$, $R^1=3\text{-OMe}$, $X=\text{CH}_2$) (1.09 g, 2.56 mmol, 74%) as a colorless oil. ¹H-NMR (CDCl₃) δ : 1.12–1.79 (3H, m), 1.43 (9H, s), 1.85–2.12 (2H, m), 2.71–3.03 (6H, m), 3.79 (3H, s), 3.85 (2H, d, $J=5.9$ Hz), 3.88–4.25 (2H, m),

6.70–6.94 (5H, m), 7.08–7.31 (1H, m).

3-[2-[2-(3-Methoxyphenyl)ethyl]phenoxy]methyl-1-methylpiperidine Hydrochloride (11) A solution of 1-*tert*-butoxycarbonyl-3-[2-[2-(3-methoxyphenyl)ethyl]phenoxy]methylpiperidine **10** ($m=1$, $n=2$, $R^1=3\text{-OMe}$, $X=\text{CH}_2$) (850 mg, 2.00 mmol) in THF (6 ml) was added to a suspension of LiAlH₄ (113 mg, 2.98 mmol) in THF (10 ml) at room temperature. The mixture was stirred at room temperature for 2 h and then refluxed for 2.5 h. The mixture was cooled, and to the mixture Na₂SO₄ decahydrate was added slowly and the slurry was then stirred for 30 min. The insoluble material was filtered away, and the filtrate was concentrated. The resulting residue was chromatographed on a silica gel column (CH₂Cl₂/MeOH=20/1–10/1) to give 3-[2-[2-(3-methoxyphenyl)ethyl]phenoxy]methyl-1-methylpiperidine (520 mg, 1.53 mmol, 77%) as a colorless oil. This oil was dissolved in EtOAc (5 ml) and was treated with 4N HCl in dioxane (1.15 ml, 4.59 mmol). The mixture was stirred at room temperature for 10 min and concentrated. The oily residue was dissolved in a mixture of EtOAc/CH₂Cl₂=9/1, and the solution was allowed to stand at room temperature. The precipitate formed was collected by filtration to give **11** (443 mg, 1.18 mmol, 77%) as colorless crystals.

3-[2-[2-(3-Methoxyphenyl)ethyl]phenoxy]methylpiperidine Hydrochloride (20) A solution of 1-*tert*-butoxycarbonyl-3-[2-[2-(3-methoxyphenyl)ethyl]phenoxy]methylpiperidine **10** ($m=1$, $n=2$, $R^1=3\text{-OMe}$, $X=\text{CH}_2$) (240 mg, 0.564 mmol) in EtOAc (4 ml) was treated with 4N HCl in dioxane (4 ml) and the mixture was stirred at room temperature for 3 h and then concentrated. The oily residue was dissolved in EtOAc, and the solution was allowed to stand at room temperature. The precipitate formed was collected by filtration to give **20** (183 mg, 0.506 mmol, 90%) as colorless crystals.

Similarly, the morpholine derivatives **25** and **26** and other piperidine derivatives **11–16**, **20–22**, and **29** were prepared by alkylation of phenol derivatives **4–8**²⁰⁾ with tosylates, followed by a treatment with lithium aluminum hydride or HCl as described in method A.

1-*tert*-Butoxycarbonyl-4-[2-[2-(3-methoxyphenyl)ethyl]phenoxy]piperidine (10; $m=0$, $n=2$, $R^1=3\text{-OMe}$, $X=\text{CH}_2$) (Method B) Diethyl azodicarboxylate (DEAD) (1.05 ml, 6.67 mmol) was added to a solution of 2-[2-(3-methoxyphenyl)ethyl]phenol **4a** ($R^1=3\text{-OMe}$) (456 mg, 2.00 mmol), 1-*tert*-butoxycarbonyl-4-hydroxypiperidine (1.20 g, 5.96 mmol) and triphenylphosphine (1.73 g, 6.60 mmol) in CH₂Cl₂ (30 ml) and the mixture was stirred at room temperature for 3 h. The solvent was removed and the resulting residue was chromatographed on a silica gel column (hexane/EtOAc=4/1) to give **10** ($m=0$, $n=2$, $R^1=3\text{-OMe}$, $X=\text{CH}_2$) (379 mg, 0.92 mmol, 46%) as a colorless oil. ¹H-NMR (CDCl₃) δ : 1.47 (9H, s), 1.71–2.03 (4H, m), 3.36–3.52 (2H, m), 3.60–3.73 (2H, m), 3.78 (3H, s), 4.46–4.59 (1H, m), 6.70–6.92 (5H, m), 7.10–7.29 (1H, m).

4-[2-[2-(3-Methoxyphenyl)ethyl]phenoxy]-1-methylpiperidine Hydrochloride (23) A solution of 1-*tert*-butoxycarbonyl-4-[2-[2-(3-methoxyphenyl)ethyl]phenoxy]piperidine **10** ($m=0$, $n=2$, $R^1=3\text{-OMe}$, $X=\text{CH}_2$) (482 mg, 1.17 mmol) in THF (5 ml) was treated with a suspension of LiAlH₄ (44.5 mg, 1.17 mmol) in THF (5 ml) under cooling. The resulting mixture was refluxed for 1 h and then cooled. To the resulting suspension was slowly added Na₂SO₄ decahydrate and the mixture was stirred for 30 min. The insoluble material was filtered away and the filtrate was concentrated. The resulting residue was chromatographed on a silica gel column (CH₂Cl₂/MeOH=20/1–10/1) to give 4-[2-[2-(3-methoxyphenyl)ethyl]phenoxy]-1-methylpiperidine (220 mg, 0.68 mmol, 58%) as a light yellow oil. This oil was dissolved in EtOAc (5 ml) and was treated with 4N HCl in dioxane (0.25 ml, 1.00 mmol). The resulting solution was concentrated. The oily residue was dissolved in EtOAc (20 ml), and the solution was allowed to stand at room temperature. The precipitate formed was collected by filtration to give **23** (170 mg, 0.47 mmol, 69%) as colorless crystals.

Similarly, other piperidine derivatives **17**, **24**, and **30** were prepared by means of the Mitsunobu reaction¹⁸⁾ between the phenol derivatives **4–8**²⁰⁾ and a hydroxy derivative (**9**), followed by a treatment with lithium aluminum hydride or HCl as described in method B.

1-Methyl-2-[2-(2-phenylethyl)phenoxy]ethylpyrrolidine Hydrochloride (18) (Method C) To a solution of 2-(2-phenylethyl)phenol **4b** ($R^1=\text{H}$) (1.00 g, 5.04 mmol) in DMA (10 ml) was added *tert*-BuOK (566 mg, 5.04 mmol) and the mixture was stirred at room temperature for 10 min. Then a solution of 2-(2-chloroethyl)-1-methylpyrrolidine hydrochloride (928 mg, 5.04 mmol) in DMA (10 ml) was added, and stirring continued at room temperature for 3 h and at 60 °C for 3 h. The resulting solution was diluted with EtOAc and washed with H₂O and brine. The organic layer was dried and concentrated. The resulting residue was chromatographed on a silica gel column (CH₂Cl₂/MeOH=20/1–10/1) to give 1-methyl-2-[2-(2-phenylethyl)phenoxy]ethylpyrrolidine (480 mg, 1.55 mmol, 31%) as a col-

Table 8. Physical Data for [2-(ω -Phenylalkyl)phenoxy]alkylamines

Compd. ^{a)}	Formula	Yield (%) ^{b)}	mp (°C)	Analysis (%) Calcd (Found)			
				C	H	N	Cl
11	C ₂₂ H ₂₉ NO ₂ ·HCl	59	191—193	70.29 (69.99)	8.04 (8.15)	3.73 (3.74)	9.43 (9.38)
12	C ₂₃ H ₃₁ NO ₂ ·HCl	75	106—107	70.84 (70.84)	8.27 (8.33)	3.59 (3.63)	9.09 (9.02)
14	C ₂₅ H ₃₅ NO ₂ ·HCl	58	90—91	71.83 (71.65)	8.68 (8.61)	3.35 (3.32)	8.48 (8.75)
15	C ₂₆ H ₃₇ NO ₂ ·HCl	63	100	72.28 (72.00)	8.87 (8.84)	3.24 (3.22)	8.32 (8.53)
16	C ₂₂ H ₂₉ NO·HCl	48	128—130	73.41 (73.42)	8.40 (8.54)	3.89 (3.92)	9.85 (9.70)
18	C ₂₁ H ₂₇ NO·HCl	7.5	154—156	72.92 (72.56)	8.16 (8.32)	4.05 (4.01)	10.25 (10.21)
20	C ₂₁ H ₂₇ NO ₂ ·HCl	90	155—157	69.69 (69.35)	7.80 (7.81)	3.87 (3.87)	9.80 (9.67)
21	C ₂₃ H ₃₁ NO ₂ ·HCl	37	115—117	70.84 (70.72)	8.27 (8.31)	3.59 (3.75)	9.09 (9.03)
22	C ₂₂ H ₂₉ NO ₂ ·HCl	33	102—104	70.29 (70.12)	8.04 (7.93)	3.73 (3.75)	9.43 (9.42)
23	C ₂₁ H ₂₇ NO ₂ ·HCl·0.15H ₂ O	40	147—148	69.18 (69.26)	7.82 (7.85)	3.84 (3.95)	9.72 (9.60)
24	C ₂₀ H ₂₅ NO ₂ ·HCl·0.15H ₂ O	91	121—122	68.52 (68.48)	7.56 (7.55)	4.00 (3.99)	10.11 (10.23)
25	C ₂₁ H ₂₇ NO ₃ ·HCl	65	174—176	66.74 (66.43)	7.47 (7.41)	3.71 (3.82)	9.38 (9.30)
26	C ₂₀ H ₂₅ NO ₃ ·HCl·0.15H ₂ O	26	110—112	65.53 (65.58)	7.23 (7.14)	3.82 (3.83)	9.67 (9.70)
27	C ₂₂ H ₂₉ NO ₂ ·HCl	28	109—110	70.29 (69.98)	8.04 (8.06)	3.73 (3.76)	9.43 (9.26)
28	C ₂₁ H ₂₇ NO ₂ ·HCl	61	86—87	69.69 (69.36)	7.80 (7.81)	3.87 (3.98)	9.80 (10.13)
29	C ₂₁ H ₃₁ NO ₂ ·HCl	56	97—99	70.84 (70.46)	8.27 (8.38)	3.59 (3.61)	9.09 (9.12)
30	C ₂₁ H ₂₇ NO ₂ ·HCl	49	158—160	69.69 (69.44)	7.80 (7.73)	3.87 (3.96)	9.80 (9.73)
31	C ₂₂ H ₂₉ NO ₂ ·HCl·0.35H ₂ O	11	143—145	69.13 (69.05)	8.10 (8.13)	3.66 (3.70)	9.27 (9.45)
32	C ₂₂ H ₂₉ NO ₂ ·HCl·0.20H ₂ O	20	136—138	69.62 (69.56)	8.31 (8.09)	3.54 (3.71)	8.97 (9.07)
33	C ₂₃ H ₃₁ NO ₂ ·HCl·0.30H ₂ O	24	148—150	69.87 (70.25)	8.27 (7.93)	3.58 (3.65)	9.09 (8.59)
34	C ₂₃ H ₃₁ NO ₂ ·HCl	18	120—121	70.84 (70.61)	8.27 (7.47)	3.58 (3.60)	9.09 (9.16)
35	C ₂₃ H ₃₁ NO ₂ ·HCl	50	133—134	70.84 (70.65)	8.27 (8.24)	3.58 (3.61)	9.09 (9.15)
36	C ₂₁ H ₂₆ ClNO·HCl	26	187—188	66.31 (66.01)	7.16 (7.09)	3.68 (3.71)	18.64 (18.56)
37	C ₂₁ H ₂₆ ClNO·HCl	32	119—121	66.31 (66.24)	7.16 (7.37)	3.68 (3.65)	18.64 (18.32)
38	C ₂₁ H ₂₆ ClNO·HCl	21	145—146	66.31 (66.34)	7.16 (7.15)	3.68 (3.72)	18.64 (18.42)
39 ^{c)}	C ₂₁ H ₂₆ FNO·HCl	35	135—136	69.31 (69.40)	7.48 (7.44)	3.85 (3.81)	9.74 (9.86)
40 ^{d)}	C ₂₁ H ₂₆ BrNO·HCl	26	127—129	59.38 (59.13)	6.41 (6.32)	3.30 (3.35)	8.35 (8.29)
41	C ₂₂ H ₂₆ N ₂ O·HCl·0.30H ₂ O	24	101	70.22 (70.21)	7.39 (7.52)	7.44 (7.45)	9.42 (9.38)
42	C ₂₂ H ₂₉ NO·HCl·0.15H ₂ O	5.1	128—130	72.87 (72.86)	8.42 (8.25)	3.86 (3.85)	9.78 (9.67)
43	C ₂₁ H ₂₇ NO ₂ ·HCl	38	68—70	69.69 (69.66)	7.80 (7.86)	3.87 (3.91)	9.80 (10.00)
48	C ₂₁ H ₃₃ NO·HCl·0.62H ₂ O	28	101—102	69.46 (69.84)	9.78 (9.96)	3.86 (4.04)	9.76 (9.36)
(S)-27	C ₂₂ H ₂₉ NO ₂ ·HCl	85	133—135	70.29 (70.14)	8.04 (8.24)	3.73 (3.81)	9.43 (9.75)
(R)-27	C ₂₂ H ₂₉ NO ₂ ·HCl	67	133—136	70.29 (70.21)	8.04 (8.07)	3.73 (3.83)	9.43 (9.65)
(S)-62	C ₂₁ H ₂₇ NO ₂ ·HCl	18	124—126	69.69 (69.40)	7.80 (7.83)	3.87 (3.91)	9.80 (9.64)
(S)-63	C ₂₉ H ₃₉ NO ₉ ·0.50H ₂ O	87	Oil	62.80 (62.78)	7.27 (7.44)	2.53 (2.45)	

a) Compounds 13, 17, and 19 were reported in reference 17. b) Yield not optimized. c) Anal. Calcd: F, 5.22. Found: F, 5.09. d) Anal. Calcd: Br, 18.81. Found: Br, 19.18.

Table 9. Physical Data for [2-(ω -Phenylalkyl)phenoxy]alkylamines

Compd. ^{a)}	¹ H-NMR δ (CDCl ₃)
11	1.44—2.07 (3H, m), 2.22—2.98 (8H, m), 2.75 (3H, s), 3.38—3.58 (2H, m), 3.79 (3H, s), 3.85—4.03 (2H, m), 6.72—6.87 (4H, m), 6.94 (1H, t, $J=7.6$ Hz), 7.13—7.31 (3H, m)
12	1.35—1.58 (1H, m), 1.81—2.04 (4H, m), 2.22—2.95 (8H, m), 2.72 (3H, s), 3.36—3.59 (2H, m), 3.79 (3H, s), 3.77—4.03 (2H, m), 6.68—6.85 (4H, m), 6.92 (1H, t, $J=7.9$ Hz), 7.11—7.30 (3H, m)
14	1.32—1.73 (7H, m), 1.77—2.06 (2H, m), 2.25—2.97 (8H, m), 2.67 (3H, s), 3.29—3.58 (2H, m), 3.79 (3H, s), 3.80—4.02 (2H, m), 6.65—6.82 (4H, m), 6.91 (1H, t, $J=7.6$ Hz), 7.10—7.25 (3H, m)
15	1.23—1.75 (9H, m), 1.83—2.05 (2H, m), 2.21—2.97 (4H, m), 2.57 (4H, t, $J=7.6$ Hz), 2.72 (3H, s), 3.38—3.60 (2H, m), 3.79 (3H, s), 3.82—4.04 (2H, m), 6.68—6.85 (4H, m), 6.91 (1H, t, $J=6.9$ Hz), 7.10—7.26 (3H, m)
16	1.22—2.40 (7H, m), 2.44—2.65 (2H, m), 2.74 (3H, s), 2.81—3.20 (5H, m), 3.22—3.59 (1H, m), 3.96—4.20 (2H, m), 6.84 (1H, d, $J=7.9$ Hz), 6.92 (1H, t, $J=7.3$ Hz), 7.10—7.33 (7H, m)
18	1.88—2.13 (2H, m), 2.15—2.37 (2H, m), 2.39—2.62 (2H, m), 2.68—2.98 (5H, m), 2.75 (3H, s), 3.19—3.37 (1H, m), 3.82—4.03 (2H, m), 4.16—4.28 (1H, m), 6.85 (1H, d, $J=7.9$ Hz), 6.93 (1H, t, $J=7.6$ Hz), 7.11—7.37 (7H, m)
20	1.40—2.21 (4H, m), 2.45—2.62 (1H, m), 2.72—2.98 (6H, m), 3.40—3.59 (2H, m), 3.76 (3H, s), 3.86 (2H, d, $J=4.6$ Hz), 6.64—6.83 (4H, m), 6.89 (1H, t, $J=7.3$ Hz), 7.07—7.29 (3H, m)
21	1.27—2.15 (5H, m), 2.18—2.42 (2H, m), 2.45—2.72 (2H, m), 2.75 (3H, s), 2.77—3.13 (5H, m), 3.40—3.55 (1H, m), 3.78 (3H, s), 3.96—4.19 (2H, m), 6.66—6.80 (3H, m), 6.84 (1H, d, $J=7.9$ Hz), 6.93 (1H, t, $J=7.3$ Hz), 7.12—7.33 (3H, m)
22	1.27—2.08 (6H, m), 2.10—2.32 (1H, m), 2.47—2.69 (1H, m), 2.70—2.96 (5H, m), 3.15—3.34 (1H, m), 3.40—3.53 (1H, d, $J=13$ Hz), 3.77 (3H, s), 4.02—4.24 (2H, m), 6.68—6.95 (5H, m), 7.07—7.32 (3H, m)
23	2.02—2.25 (2H, m), 2.48—2.78 (2H, m), 2.73 (3H, s), 2.81—3.09 (6H, m), 3.17—3.40 (2H, m), 3.76 (3H, s), 4.60—4.79 (1H, m), 6.65—6.85 (4H, m), 6.95 (1H, t, $J=7.3$ Hz), 7.16—7.30 (3H, m)
24	2.05—2.21 (2H, m), 2.24—2.42 (2H, m), 2.80—2.99 (4H, m), 3.21—3.38 (4H, m), 3.76 (3H, s), 4.56—4.68 (1H, m), 6.60—6.81 (4H, m), 6.92 (1H, t, $J=7.3$ Hz), 7.11—7.27 (3H, m)
25	2.77 (3H, s), 2.68—3.06 (6H, m), 3.40 (2H, t, $J=12$ Hz), 3.79 (3H, s), 4.01—4.20 (3H, m), 4.32—4.47 (1H, m), 4.51—4.64 (1H, m), 6.72—6.88 (4H, m), 6.95 (1H, t, $J=7.6$ Hz), 7.15—7.32 (3H, m)
26	2.78—2.97 (4H, m), 3.02—3.18 (2H, m), 3.36 (1H, d, $J=13$ Hz), 3.48 (1H, d, $J=13$ Hz), 3.76 (3H, s), 3.98—4.15 (4H, m), 4.24—4.37 (1H, m), 6.68—6.96 (5H, m), 7.08—7.31 (3H, m)
27	1.89—2.14 (2H, m), 2.16—2.35 (2H, m), 2.37—2.63 (2H, m), 2.77 (3H, s), 2.69—3.00 (5H, m), 3.21—3.40 (1H, m), 3.78 (3H, s), 3.80—4.09 (2H, m), 4.15—4.29 (1H, m), 6.65—6.98 (5H, m), 7.11—7.30 (3H, m)
28	1.72—2.13 (3H, m), 2.16—2.32 (2H, m), 2.42—2.59 (1H, m), 2.75—2.98 (4H, m), 3.18—3.42 (2H, m), 3.65—3.82 (1H, m), 3.76 (3H, s), 3.98—4.17 (2H, m), 6.65—6.92 (5H, m), 7.06—7.25 (3H, m)
29	1.75—2.14 (7H, m), 2.56 (2H, t, $J=11$ Hz), 2.70 (3H, s), 2.78—2.97 (4H, m), 3.47 (2H, d, $J=11$ Hz), 3.79 (3H, s), 4.02 (2H, t, $J=5.9$ Hz), 6.71—6.96 (5H, m), 7.10—7.30 (3H, m)
30	1.42—1.65 (1H, m), 1.93—2.12 (1H, m), 2.23—2.57 (3H, m), 2.59—2.79 (1H, m), 2.81—2.98 (4H, m), 2.82 (3H, s), 3.38—3.70 (2H, m), 3.78 (3H, s), 4.93—5.17 (1H, m), 6.68—6.82 (3H, m), 6.94 (1H, t, $J=7.3$ Hz), 7.00—7.29 (4H, m)
31	1.85—2.63 (6H, m), 2.77—2.94 (5H, m), 2.74 (3H, s), 3.25—3.41 (1H, m), 3.75—3.89 (1H, m), 3.80 (3H, s), 3.91—4.05 (1H, m), 4.17—4.28 (1H, m), 6.80—6.97 (4H, m), 7.05—7.27 (4H, m)
32 ^{b)}	1.90—2.14 (2H, m), 2.16—2.37 (2H, m), 2.40—2.63 (2H, m), 2.70—2.95 (5H, m), 2.78 (3H, s), 3.19—3.37 (1H, m), 3.79 (3H, s), 3.82—4.08 (2H, m), 4.15—4.29 (1H, m), 6.77—6.88 (3H, m), 6.92 (1H, t, $J=7.6$ Hz), 7.01—7.24 (4H, m)
33	1.40 (3H, t, $J=7.3$ Hz), 1.86—2.13 (2H, m), 2.15—2.36 (2H, m), 2.39—2.62 (2H, m), 2.65—2.99 (5H, m), 2.71 (3H, s), 3.21—3.40 (1H, m), 3.79—4.10 (2H, m), 4.02 (2H, q, $J=7.3$ Hz), 4.15—4.32 (1H, m), 6.78—6.98 (4H, m), 7.04—7.25 (4H, m)
34	1.39 (3H, t, $J=7.3$ Hz), 1.90—2.14 (2H, m), 2.17—2.38 (2H, m), 2.40—2.64 (2H, m), 2.68—2.97 (5H, m), 2.78 (3H, s), 3.22—3.41 (1H, m), 3.80—4.08 (2H, m), 4.00 (2H, q, $J=7.3$ Hz), 4.16—4.30 (1H, m), 6.65—6.79 (3H, m), 6.84 (1H, d, $J=7.9$ Hz), 6.93 (1H, t, $J=7.9$ Hz), 7.11—7.28 (3H, m)
35	1.40 (3H, t, $J=7.2$ Hz), 1.89—2.14 (2H, m), 2.17—2.38 (2H, m), 2.41—2.65 (2H, m), 2.70—2.99 (5H, m), 2.76 (3H, s), 3.18—3.37 (1H, m), 3.82—4.09 (2H, m), 4.01 (2H, q, $J=7.2$ Hz), 4.15—4.31 (1H, m), 6.76—6.88 (3H, m), 6.92 (1H, t, $J=7.3$ Hz), 7.04 (2H, d, $J=8.6$ Hz), 7.10—7.25 (2H, m)
36	1.91—2.13 (2H, m), 2.17—2.35 (2H, m), 2.38—2.60 (2H, m), 2.72—3.07 (5H, m), 2.78 (3H, s), 3.29—3.48 (1H, m), 3.82—4.03 (2H, m), 4.10—4.22 (1H, m), 6.82 (1H, d, $J=7.9$ Hz), 6.94 (1H, t, $J=7.6$ Hz), 7.04—7.25 (5H, m), 7.31—7.40 (1H, m)
37	1.93—2.15 (2H, m), 2.19—2.38 (2H, m), 2.41—2.63 (2H, m), 2.72—2.97 (5H, m), 2.79 (3H, s), 3.18—3.37 (1H, m), 3.81—4.06 (2H, m), 4.15—4.29 (1H, m), 6.84 (1H, d, $J=7.9$ Hz), 6.93 (1H, t, $J=7.9$ Hz), 6.95—7.05 (1H, m), 7.10—7.28 (5H, m)
38	1.92—2.14 (2H, m), 2.17—2.37 (2H, m), 2.41—2.65 (2H, m), 2.71—2.95 (1H, m), 2.77 (3H, s), 2.86 (4H, s), 3.13—3.31 (1H, m), 3.82—4.07 (2H, m), 4.12—4.28 (1H, m), 6.82 (1H, d, $J=8.6$ Hz), 6.92 (1H, t, $J=7.6$ Hz), 7.00—7.13 (3H, m), 7.16—7.31 (3H, m)
39	1.91—2.15 (2H, m), 2.19—2.38 (2H, m), 2.41—2.63 (2H, m), 2.70—2.98 (1H, m), 2.78 (3H, s), 2.88 (4H, s), 3.20—3.39 (1H, m), 3.82—4.06 (2H, m), 4.13—4.29 (1H, m), 6.77—6.98 (5H, m), 7.08—7.30 (3H, m)
40	1.92—2.16 (2H, m), 2.19—2.40 (2H, m), 2.44—2.68 (2H, m), 2.74—3.10 (5H, m), 2.79 (3H, s), 3.19—3.43 (1H, m), 3.82—4.10 (2H, m), 4.15—4.33 (1H, m), 6.85 (1H, d, $J=7.9$ Hz), 6.93 (1H, t, $J=7.3$ Hz), 7.05 (1H, t, $J=7.3$ Hz), 7.11—7.42 (5H, m)
41	1.96—2.19 (3H, m), 2.21—2.42 (2H, m), 2.47—2.65 (2H, m), 2.77—2.99 (1H, m), 2.83 (3H, s), 2.90 (4H, s), 3.20—3.38 (1H, m), 3.85—4.09 (2H, m), 4.14—4.28 (1H, m), 6.85 (1H, d, $J=7.9$ Hz), 6.91 (1H, t, $J=7.3$ Hz), 7.06 (1H, d, $J=7.3$ Hz), 7.21 (1H, t, $J=7.9$ Hz), 7.30—7.44 (3H, m), 7.50 (1H, d, $J=6.9$ Hz)
42	1.88—2.14 (2H, m), 2.15—2.39 (2H, m), 2.33 (3H, s), 2.41—2.65 (2H, m), 2.68—2.97 (5H, m), 2.75 (3H, s), 3.20—3.41 (1H, m), 3.78—4.09 (2H, m), 4.18—4.30 (1H, m), 6.82—7.09 (5H, m), 7.13—7.32 (3H, m)
43	1.92—2.58 (6H, m), 2.65—3.10 (5H, m), 2.83 (3H, s), 3.16—3.43 (1H, m), 3.60—4.09 (3H, m), 6.57 (1H, d, $J=7.3$ Hz), 6.68—6.81 (2H, m), 6.92 (1H, t, $J=7.3$ Hz), 7.00 (1H, s), 7.05 (1H, t, $J=7.9$ Hz), 7.12—7.25 (2H, m)
48	0.84—1.02 (2H, m), 1.10—1.35 (4H, m), 1.40—1.50 (2H, m), 1.60—1.84 (5H, m), 2.02—2.68 (8H, m), 2.78—3.01 (1H, m), 2.86 (3H, s), 3.32—3.52 (1H, m), 3.83—4.07 (2H, m), 4.19—4.30 (1H, m), 6.83 (1H, d, $J=8.3$ Hz), 6.92 (1H, t, $J=7.4$ Hz), 7.13—7.22 (2H, m)
(S)-27	1.91—2.12 (2H, m), 2.15—2.36 (2H, m), 2.40—2.61 (2H, m), 2.67—2.99 (5H, m), 2.76 (3H, s), 3.20—3.37 (1H, m), 3.78 (3H, s), 3.79—4.04 (2H, m), 4.15—4.30 (1H, m), 6.65—6.78 (3H, m), 6.84 (1H, d, $J=7.9$ Hz), 6.93 (1H, t, $J=7.9$ Hz), 7.13—7.30 (3H, m)
(R)-27	1.89—2.14 (2H, m), 2.16—2.37 (2H, m), 2.40—2.63 (2H, m), 2.70—2.98 (5H, m), 2.77 (3H, s), 3.21—3.40 (1H, m), 3.77 (3H, s), 3.79—4.06 (2H, m), 4.15—4.30 (1H, m), 6.65—6.80 (3H, m), 6.84 (1H, d, $J=7.9$ Hz), 6.93 (1H, t, $J=7.3$ Hz), 7.13—7.31 (3H, m)
(S)-62 ^{c)}	1.75—2.12 (2H, m), 2.20—2.40 (1H, m), 2.74—3.01 (4H, m), 2.95 (3H, s), 3.03—3.22 (1H, m), 3.49—3.68 (1H, m), 3.72 (3H, s), 3.75—3.95 (1H, m), 4.23—4.46 (2H, m), 6.70—6.85 (3H, m), 6.91 (1H, t, $J=7.3$ Hz), 7.00 (1H, d, $J=7.9$ Hz), 7.13—7.28 (3H, m)
(S)-63	1.74—2.39 (8H, m), 2.58—3.20 (13H, m), 3.76 (3H, s), 3.67—4.11 (3H, m), 6.67—6.95 (5H, m), 7.06—7.25 (3H, m)

a) Compounds 13, 17, and 19 were reported in reference 17. b) In CDCl₃+D₂O. c) In DMSO-*d*₆.

orless oil. This oil was dissolved in EtOAc (5 ml) and was treated with 4 N HCl in dioxane (0.63 ml, 2.52 mmol). The resulting solution was concentrated. The oily residue was dissolved in EtOAc (10 ml), and the solution was allowed to stand at room temperature. The precipitate formed was collected by filtration to give **18** (130 mg, 0.38 mmol, 24%) as colorless crystals.

Other pyrrolidine derivatives (**19**, **31**–**43**) were similarly prepared with the exceptions of **27** which was prepared by method D, and **28** which was prepared by method A.

2-[2-[2-(3-Methoxyphenyl)ethyl]phenoxy]ethyl]-1-methylpyrrolidine Hydrochloride (27) (Method D) DEAD (10.2 ml, 65 mmol) was added to a solution of 2-[2-(3-methoxyphenyl)ethyl]phenol **4a** ($R^1=3\text{-OMe}$) (10.6 g, 46.4 mmol), 1-methyl-2-pyrrolidineethanol (8.4 g, 65 mmol) and triphenylphosphine (17 g, 65 mmol) in CH_2Cl_2 (200 ml) and the mixture was stirred overnight at room temperature. The resulting solution was concentrated. The resulting residue was chromatographed on a silica gel column ($\text{CH}_2\text{Cl}_2/\text{MeOH}=10/1$) to give 2-[2-[2-(3-methoxyphenyl)ethyl]phenoxy]ethyl]-1-methylpyrrolidine (5.7 g, 16.8 mmol, 36%) as a yellow oil. This oil was dissolved in EtOAc (100 ml) and was treated with 4 N HCl in dioxane (5.0 ml, 20 mmol). The resulting solution was concentrated. The oily residue was dissolved in EtOAc (150 ml), and the solution was allowed to stand at room temperature. The precipitate formed was collected by filtration to give **27** (4.88 g, 13.0 mmol, 77%) as colorless crystals.

2-[2-[2-(3-Methoxyphenyl)ethyl]phenoxy]ethyl]pyrrolidine Hydrochloride (28) (Method A) To a solution of 2-[2-(3-methoxyphenyl)ethyl]phenol **4a** ($R^1=3\text{-OMe}$) (680 mg, 2.98 mmol) in DMA (5 ml) was added *tert*-BuOK (340 mg, 3.03 mmol) and the mixture was stirred at 0 °C for 10 min. Then 1-*tert*-butoxycarbonyl-2-[2-(*p*-toluenesulfonyl)oxyethyl]-pyrrolidine (1.20 g, 3.25 mmol) was added and the whole was stirred at 50 °C for 1 h. The resulting suspension was diluted with EtOAc and washed with H_2O and brine. The organic layer was dried and concentrated. The resulting residue was chromatographed on a silica gel column (benzene/EtOAc=10/1) to give 1-*tert*-butoxycarbonyl-2-[2-[2-(3-methoxyphenyl)ethyl]phenoxy]ethyl]pyrrolidine (910 mg, 2.14 mmol, 72%) as a colorless oil. This oil was dissolved in dioxane (5 ml) and treated with 4 N HCl in dioxane (5 ml). The mixture was stirred at room temperature for 3 h and the resulting solution was concentrated. The resulting residue was chromatographed on a silica gel column ($\text{CH}_2\text{Cl}_2/\text{EtOAc}=10/1$) to give 2-[2-[2-(3-methoxyphenyl)ethyl]phenoxy]ethyl]pyrrolidine (510 mg, 1.57 mmol, 73%) as a colorless oil. This oil was dissolved in dioxane (5 ml) and treated with 4 N HCl in dioxane (0.50 ml, 2.0 mmol). The resulting solution was concentrated. The oily residue was dissolved in EtOAc (10 ml), and the solution was allowed to stand at room temperature. The precipitate formed was collected by filtration to give **28** (344 mg, 0.95 mmol, 61%) as colorless crystals.

2-(2-Benzyloxybenzyl)-1-cyclohexylethane-1-ol (45) A solution of 2-benzyloxybenzylchloride **44** (41.5 g, 178 mmol) in THF (50 ml) was added to a suspension of Mg (4.33 g, 178 mmol) and I_2 (trace) in THF (300 ml). The mixture was stirred under reflux for 2 h, and cooled to room temperature. Then cyclohexanecarboxaldehyde (10 g, 89 mmol) was added, and the mixture was stirred overnight at room temperature. The reaction mixture was poured into water and extracted with EtOAc. The organic layer was washed with brine, dried and evaporated. The resulting residue was chromatographed on a silica gel column (EtOAc/hexane=1/19–3/17) to give **45** (17.9 g, 57.7 mmol, 65%) as a colorless oil. $^1\text{H-NMR}$ (CDCl_3) δ : 0.97–1.32 (5H, m), 1.35–1.48 (1H, m), 1.56–1.93 (6H, m), 2.64 (1H, dd, $J=9.2$, 14 Hz), 3.01 (1H, dd, $J=3.0$, 14 Hz), 3.58–3.70 (1H, m), 5.09 (2H, s), 6.89–6.98 (2H, m), 7.16–7.47 (7H, m).

1-Benzyloxy-2-(2-cyclohexylethyl)benzene (46) Triethylamine (4.36 ml, 31.3 mmol) was added to a solution of 2-(2-benzyloxybenzyl)-1-cyclohexylethane-1-ol **45** (8.10 g, 26.1 mmol) in THF (200 ml) and the mixture was stirred at room temperature for 15 min. Then thionyl chloride (2.23 ml, 31.3 mmol) was added, the reaction mixture was stirred overnight at room temperature, and was poured in water and extracted with EtOAc. The organic layer was washed with brine, dried and evaporated. The resulting residue was chromatographed on a silica gel column (EtOAc/hexane=3/97) to give 2-(2-benzyloxyphenyl)-1-chloro-1-cyclohexylethane (5.93 g, 18.0 mmol, 69%) as a colorless oil. To a solution of this compound (5.60 g, 17.0 mmol) and 2,2'-azobisisobutyronitrile (AIBN) (140 mg, 0.85 mmol) in toluene (50 ml) was added dropwise a solution of tributyltin hydride (5.95 g, 20.4 mmol) in toluene (10 ml). The reaction mixture was stirred under reflux for 1 h, and then the solvent was removed. The resulting residue was chromatographed on a silica gel column (hexane) to give **46** (4.51 g, 15.3 mmol, 90%) as a colorless oil. $^1\text{H-NMR}$ (CDCl_3) δ : 0.81–0.99 (2H, m), 1.05–

1.36 (4H, m), 1.40–1.82 (7H, m), 2.61–2.74 (2H, m), 5.08 (2H, s), 6.85–6.95 (2H, m), 7.14 (2H, t, $J=7.6$ Hz), 7.26–7.49 (5H, m).

2-(2-Cyclohexylethyl)phenol (47) A solution of 1-benzyloxy-2-(2-cyclohexylethyl)benzene **46** (4.51 g, 15.3 mmol) in EtOH (50 ml) was hydrogenated over 5% Pd-C (450 mg) at 60 °C for 4 h with stirring. The catalyst was filtered away, and the filtrate was concentrated. The resulting residue was chromatographed on a silica gel column (hexane/EtOAc=19/1–9/1) to give **47** (2.92 g, 14.3 mmol, 93%) as a colorless solid. $^1\text{H-NMR}$ (CDCl_3) δ : 0.83–1.05 (2H, m), 1.09–1.39 (4H, m), 1.43–1.56 (2H, m), 1.60–1.87 (5H, m), 2.54–2.66 (2H, m), 4.69 (1H, s), 6.75 (1H, d, $J=7.9$ Hz), 6.86 (1H, t, $J=7.9$ Hz), 7.01–7.14 (2H, m).

2-[2-[2-(2-Cyclohexylethyl)phenoxy]ethyl]-1-methylpyrrolidine Hydrochloride (48) To a solution of 2-(2-cyclohexylethyl)phenol **47** (500 mg, 2.45 mmol) in DMA (10 ml) was added *tert*-BuOK (549 mg, 4.89 mmol) and the mixture was stirred at room temperature for 30 min. 2-(2-Chloroethyl)-1-methylpyrrolidine hydrochloride (450 mg, 2.44 mmol) was added, and the mixture was stirred at 60 °C for 5 h. 2-(2-Chloroethyl)-1-methylpyrrolidine hydrochloride (80 mg, 0.43 mmol) was then added, and the mixture was stirred overnight at room temperature. The resulting solution was diluted with EtOAc and washed with H_2O and brine. The organic layer was dried and concentrated. The resulting residue was chromatographed on a silica gel column ($\text{CH}_2\text{Cl}_2/\text{MeOH}=97/3$) to give 2-[2-[2-(2-cyclohexylethyl)phenoxy]ethyl]-1-methylpyrrolidine (350 mg, 1.11 mmol, 45%) as a colorless oil. This oil was dissolved in dioxane (4 ml) and was treated with 4 N HCl in dioxane (0.83 ml, 3.32 mmol). The resulting solution was concentrated. The oily residue was dissolved in EtOAc (10 ml), and the solution was allowed to stand at room temperature. The precipitate formed was collected by filtration to give **48** (243 mg, 0.69 mmol, 62%) as colorless crystals.

(S)-1-Ethoxycarbonyl-2-hydroxymethylpyrrolidine ((S)-50) To a solution of (S)-2-pyrrolidinemethanol (S)-**49** (13.86 g, 137 mmol) in acetone (80 ml) and H_2O (80 ml) was added triethylamine (19.10 ml, 137 mmol) and the mixture was stirred at 0 °C for 15 min. Then ethyl chloroformate (14.35 ml, 151 mmol) was added and the whole was stirred at room temperature for 6 h. The resulting mixture was concentrated and extracted with EtOAc and washed with brine. The organic layer was dried and concentrated. The resulting residue was chromatographed on a silica gel column (hexane/EtOAc=3/7) to give (S)-**50** (20.31 g, 117 mmol, 86%) as a colorless oil. $^1\text{H-NMR}$ (CDCl_3) δ : 1.28 (3H, t, $J=7.3$ Hz), 1.48–1.67 (1H, m), 1.71–2.12 (3H, m), 3.27–3.43 (1H, m), 3.46–3.74 (3H, m), 3.86–4.07 (1H, m), 4.16 (2H, q, $J=7.0$ Hz), 4.46–4.65 (1H, m). $[\alpha]_D^{25} -53^\circ$ ($c=1.60$, CHCl_3).

(S)-1-Ethoxycarbonyl-2-(p-toluenesulfonyloxymethyl)pyrrolidine ((S)-51) To a solution of (S)-1-ethoxycarbonyl-2-hydroxymethylpyrrolidine (S)-**50** (20.84 g, 120 mmol) and *p*-toluenesulfonic anhydride (Ts_2O) (49.58 g, 152 mmol) in CH_2Cl_2 (160 ml) was added triethylamine (21.17 ml, 152 mmol) and the mixture was stirred at room temperature for 2.5 h. The resulting mixture was diluted with CH_2Cl_2 and washed with H_2O and brine. The organic layer was dried and concentrated. The resulting residue was chromatographed on a silica gel column (hexane/EtOAc=13/7) to give (S)-**51** (34.51 g, 105 mmol, 90%) as a colorless oil. $^1\text{H-NMR}$ (CDCl_3) δ : 1.05–1.32 (3H, m), 1.70–2.09 (4H, m), 2.45 (3H, s), 3.23–3.48 (2H, m), 3.82–4.24 (5H, m), 7.27–7.42 (2H, m), 7.77 (2H, d, $J=8.6$ Hz). $[\alpha]_D^{25} -48^\circ$ ($c=1.45$, MeOH).

(S)-2-(Cyanomethyl)-1-ethoxycarbonylpyrrolidine ((S)-52) To a solution of (S)-1-ethoxycarbonyl-2-(*p*-toluenesulfonyloxymethyl)pyrrolidine (S)-**51** (33.96 g, 104 mmol) in DMF (200 ml) was added NaCN (5.08 g, 104 mmol) and the mixture was stirred at 80 °C for 4.5 h. The resulting mixture was diluted with EtOAc and washed with H_2O and brine. The organic layer was dried and concentrated. The resulting residue was chromatographed on a silica gel column (hexane/EtOAc=3/1–13/7) to give (S)-**52** (16.87 g, 92.6 mmol, 89%) as a yellow oil. $^1\text{H-NMR}$ (CDCl_3) δ : 1.28 (3H, t, $J=7.3$ Hz), 1.76–2.30 (4H, m), 2.48–2.94 (2H, m), 3.35–3.61 (2H, m), 3.97–4.28 (3H, m). $[\alpha]_D^{25} -103^\circ$ ($c=1.54$, MeOH).

(S)-1-Ethoxycarbonyl-2-(ethoxycarbonylmethyl)pyrrolidine ((S)-53) To a solution of (S)-2-(cyanomethyl)-1-ethoxycarbonylpyrrolidine (S)-**52** (16.84 g, 92.4 mmol) in EtOH (20 ml) was added conc. H_2SO_4 (7.78 ml, 139 mmol) and the mixture was stirred at 80 °C for 8 h. The resulting mixture was diluted with EtOAc and washed with H_2O , NaHCO_3 solution, and brine. The organic layer was dried and concentrated. The resulting residue was chromatographed on a silica gel column (hexane/EtOAc=3/1) to give (S)-**53** (11.19 g, 48.8 mmol, 53%) as a colorless oil. $^1\text{H-NMR}$ (CDCl_3) δ : 1.26 (6H, t, $J=7.3$ Hz), 1.70–1.96 (3H, m), 2.00–2.16 (1H, m), 2.31 (1H, dd, $J=9.9$, 15 Hz), 2.74–3.03 (1H, m), 3.32–3.51 (2H, m), 4.05–4.26 (1H, m), 4.13 (4H, q, $J=7.3$ Hz). $[\alpha]_D^{25} -49^\circ$ ($c=1.47$, MeOH).

(S)-1-Ethoxycarbonyl-2-(2-hydroxyethyl)pyrrolidine ((S)-54) A solution of (S)-1-ethoxycarbonyl-2-(ethoxycarbonylmethyl)pyrrolidine (S)-53 (11.15 g, 48.6 mmol) in THF (20 ml) was added dropwise to a suspension of LiAlH_4 (1.85 g, 48.7 mmol) in THF (30 ml) at -10°C . The mixture was stirred at -10°C for 1 h. To the resulting suspension was slowly added Na_2SO_4 decahydrate and the slurry was then stirred for 30 min. The insoluble material was filtered away and the filtrate was concentrated. The resulting residue was chromatographed on a silica gel column (hexane/EtOAc=3/7) to give (S)-54 (7.07 g, 37.8 mmol, 78%) as a colorless oil. $^1\text{H-NMR}$ (CDCl_3) δ : 1.28 (3H, t, $J=7.3$ Hz), 1.40–1.57 (1H, m), 1.59–1.80 (2H, m), 1.83–2.08 (3H, m), 3.29–3.44 (2H, m), 3.51–3.70 (2H, m), 4.06–4.27 (4H, m). $[\alpha]_D^{25} -41^\circ$ ($c=1.64$, MeOH).

(S)-1-Ethoxycarbonyl-2-[2-(*p*-toluenesulfonyloxy)ethyl]pyrrolidine ((S)-55) To a solution of (S)-1-ethoxycarbonyl-2-(2-hydroxyethyl)pyrrolidine (S)-54 (7.05 g, 37.7 mmol) and Ts_2O (15.98 g, 49.0 mmol) in CH_2Cl_2 (60 ml) was added triethylamine (6.82 ml, 48.9 mmol) and the mixture was stirred at room temperature for 2 h. It was then diluted with CH_2Cl_2 and washed with H_2O and brine. The organic layer was dried and concentrated. The resulting residue was chromatographed on a silica gel column (hexane/EtOAc=3/2) to give (S)-55 (10.08 g, 29.5 mmol, 78%) as a colorless oil. $^1\text{H-NMR}$ (CDCl_3) δ : 1.22 (3H, t, $J=6.9$ Hz), 1.55–2.23 (6H, m), 2.45 (3H, s), 3.24–3.50 (2H, m), 3.78–3.92 (1H, m), 3.97–4.18 (4H, m), 7.35 (2H, d, $J=8.6$ Hz), 7.79 (2H, d, $J=7.9$ Hz). $[\alpha]_D^{25} -18^\circ$ ($c=0.97$, MeOH).

(S)-1-Ethoxycarbonyl-2-[2-[2-(3-methoxyphenyl)ethyl]phenoxy]ethylpyrrolidine ((S)-61) (*n*=2) To a solution of 2-[2-(3-methoxyphenyl)ethyl]phenol **4a** ($R^1=3\text{-OMe}$) (4.86 g, 21.3 mmol) in DMA (30 ml) was added *tert*-BuOK (2.63 g, 23.4 mmol) and the mixture was stirred at 0°C for 15 min. Then a solution of (S)-1-ethoxycarbonyl-2-[2-(*p*-toluenesulfonyloxy)ethyl]pyrrolidine (S)-55 (8.0 g, 23.4 mmol) in DMA (20 ml) was added and the whole was stirred at room temperature for 4 h. The resulting suspension was diluted with EtOAc and washed with H_2O and brine. The organic layer was dried and concentrated. The resulting residue was chromatographed on a silica gel column (hexane/EtOAc=3/1–13/7) to give (S)-61 (*n*=2) (7.56 g, 19.0 mmol, 89%) as a colorless oil. $^1\text{H-NMR}$ (CDCl_3) δ : 1.08–1.33 (3H, m), 1.75–2.09 (5H, m), 2.15–2.40 (1H, m), 2.80–2.98 (4H, m), 3.30–3.57 (2H, m), 3.78 (3H, s), 3.93–4.21 (5H, m), 6.69–6.92 (5H, m), 7.06–7.25 (3H, m). $[\alpha]_D^{25} +4.4^\circ$ ($c=1.33$, MeOH).

(S)-2-[2-[2-(3-Methoxyphenyl)ethyl]phenoxy]ethyl]-1-methylpyrrolidine Hydrochloride ((S)-27) A solution of (S)-1-ethoxycarbonyl-2-[2-[2-(3-methoxyphenyl)ethyl]phenoxy]ethylpyrrolidine (S)-61 (*n*=2) (9.10 g, 22.9 mmol) in THF (50 ml) was added dropwise to a suspension of LiAlH_4 (2.61 g, 48.7 mmol) in THF (50 ml). The mixture was refluxed for 1 h and then cooled. To the resulting suspension was slowly added Na_2SO_4 decahydrate and the slurry was then stirred for 1 h. The insoluble material was filtered away and the filtrate was concentrated. The resulting residue was chromatographed on a silica gel column ($\text{CH}_2\text{Cl}_2/\text{MeOH}=9/1$) to give 2-[2-[2-(3-methoxyphenyl)ethyl]phenoxy]ethyl]-1-methylpyrrolidine (7.35 g, 21.7 mmol, 95%) as a colorless oil. This oil (7.19 g, 21.2 mmol) was dissolved in dioxane (35 ml) and was treated with 4N HCl in dioxane (15.9 ml, 63.6 mmol). The mixture was stirred at room temperature for 10 min, then concentrated. The oily residue was dissolved in EtOAc, and the solution was allowed to stand at room temperature. The precipitate formed was collected by filtration to give colorless crystals (7.11 g, 18.9 mmol, 89%). $[\alpha]_D^{25} -41^\circ$ ($c=1.64$, MeOH).

(S)-1-Ethoxycarbonyl-2-formylpyrrolidine ((S)-56) To a solution of DMSO (6.85 ml, 96.5 mmol) in CH_2Cl_2 (120 ml) was added oxalyl chloride (8.42 ml, 97 mmol) and the mixture was stirred at -60°C for 5 min. (S)-1-Ethoxycarbonyl-2-hydroxymethylpyrrolidine (S)-50 (11.14 g, 64.3 mmol) in CH_2Cl_2 (30 ml) was then added and the mixture was stirred at -60°C for 1 h. To the resulting solution was added triethylamine (26.89 ml, 193 mmol) and the mixture was stirred at -60°C for 1 h. The resulting solution was diluted with CH_2Cl_2 and washed with H_2O and brine. The organic layer was dried and concentrated, and the resulting residue was chromatographed on a silica gel column (hexane/EtOAc=13/7) to give (S)-56 (8.67 g, 50.6 mmol, 79%) as a colorless oil. $^1\text{H-NMR}$ (CDCl_3) δ : 1.22, 1.29 (each 3H, t, $J=6.9$ Hz), 1.72–2.23 (4H, m), 3.41–3.67 (2H, m), 4.05–4.32 (3H, m), 9.51, 9.59 (each 1H, s). $[\alpha]_D^{25} -80^\circ$ ($c=1.46$, MeOH).

(S)-1-Ethoxycarbonyl-2-(2-ethoxycarbonyl-1-ethenyl)pyrrolidine ((S)-57) A solution of (S)-1-ethoxycarbonyl-2-formylpyrrolidine (S)-56 (4.00 g, 23.4 mmol) and (carbethoxymethylene)triphenylphosphorane (8.95 g, 25.7 mmol) in CH_3CN (60 ml) was refluxed for 1 h. The resulting mixture was cooled and then concentrated. The resulting residue was chromatographed on a silica gel column (hexane/EtOAc=3/1–7/3) to give (S)-57 (5.51 g, 22.8 mmol, 98%) as a colorless oil. $^1\text{H-NMR}$ (CDCl_3) δ : 1.12–

1.38 (6H, m), 1.70–1.95 (3H, m), 1.97–2.20 (1H, m), 3.33–3.59 (2H, m), 4.01–4.26 (4H, m), 4.38–4.61 (1H, m), 5.74–5.95 (1H, m), 6.73–6.93 (1H, m). $[\alpha]_D^{25} -96^\circ$ ($c=1.57$, MeOH).

(S)-1-Ethoxycarbonyl-2-(2-ethoxycarbonylethyl)pyrrolidine ((S)-58) A solution of (S)-1-ethoxycarbonyl-2-(2-ethoxycarbonyl-1-ethenyl)pyrrolidine (S)-57 (5.48 g, 22.7 mmol) in EtOH (35 ml) was hydrogenated over 5% Pd-C (550 mg) at 60°C for 5 h with stirring. The catalyst was filtered away, and the filtrate was concentrated. The resulting residue was chromatographed on a silica gel column (hexane/EtOAc=3/1) to give (S)-58 (5.09 g, 20.9 mmol, 92%) as a colorless oil. $^1\text{H-NMR}$ (CDCl_3) δ : 1.26 (6H, t, $J=7.3$ Hz), 1.29–1.39 (1H, m), 1.43–2.12 (5H, m), 2.23–2.44 (2H, m), 3.07–3.55 (2H, m), 3.70–3.96, 4.55–4.71 (each 1H, m), 4.13 (4H, q, $J=7.3$ Hz). $[\alpha]_D^{25} -33^\circ$ ($c=1.39$, MeOH).

(S)-1-Ethoxycarbonyl-2-(3-hydroxypropyl)pyrrolidine ((S)-59) A solution of (S)-1-ethoxycarbonyl-2-(2-ethoxycarbonylethyl)pyrrolidine (S)-58 (5.06 g, 20.8 mmol) in THF (20 ml) was added dropwise to a suspension of LiAlH_4 (789 mg, 20.8 mmol) in THF (40 ml) at -10°C . The mixture was stirred at -10°C for 1 h. To the resulting suspension was slowly added Na_2SO_4 decahydrate and the slurry was then stirred for 2 h. The insoluble material was filtered off and the filtrate was concentrated. The resulting residue was chromatographed on a silica gel column (hexane/EtOAc=1/1) to give (S)-59 (2.85 g, 14.2 mmol, 68%) as a colorless oil. $^1\text{H-NMR}$ ($\text{CDCl}_3 + \text{D}_2\text{O}$) δ : 1.26 (3H, t, $J=7.3$ Hz), 1.33–2.05 (8H, m), 3.29–3.54 (2H, m), 3.58–4.01 (3H, m), 4.04–4.27 (2H, m). $[\alpha]_D^{25} -57^\circ$ ($c=1.01$, MeOH).

(S)-1-Ethoxycarbonyl-2-[3-(*p*-toluenesulfonyloxy)propyl]pyrrolidine ((S)-60) To a solution of (S)-1-ethoxycarbonyl-2-(3-hydroxypropyl)pyrrolidine (S)-59 (2.83 g, 14.1 mmol) and Ts_2O (5.96 g, 18.3 mmol) in CH_2Cl_2 (35 ml) was added triethylamine (2.55 ml, 18.3 mmol) and the mixture was stirred at room temperature for 2.5 h. The resulting mixture was diluted with CH_2Cl_2 and washed with brine. The organic layer was dried and concentrated. The resulting residue was chromatographed on a silica gel column (hexane/EtOAc=13/7) to give (S)-60 (4.81 g, 13.5 mmol, 96%) as a colorless oil. $^1\text{H-NMR}$ (CDCl_3) δ : 1.23 (3H, t, $J=7.3$ Hz), 1.30–1.48 (1H, m), 1.52–2.01 (7H, m), 2.45 (3H, s), 3.23–3.54 (2H, m), 3.66–3.89 (1H, m), 3.94–4.22 (4H, m), 7.35 (2H, d, $J=7.9$ Hz), 7.79 (2H, d, $J=8.6$ Hz). $[\alpha]_D^{25} -35^\circ$ ($c=1.35$, MeOH).

(S)-1-Ethoxycarbonyl-2-[3-[2-[2-(3-methoxyphenyl)ethyl]phenoxy]propyl]pyrrolidine ((S)-61) (*n*=3) To a solution of 2-[2-(3-methoxyphenyl)ethyl]phenol **4a** ($R^1=3\text{-OMe}$) (800 mg, 3.50 mmol) in DMA (15 ml) was added *tert*-BuOK (433 mg, 3.86 mmol) and the mixture was stirred at 0°C for 15 min. A solution of (S)-1-ethoxycarbonyl-2-[3-(*p*-toluenesulfonyloxy)propyl]pyrrolidine (S)-60 (1.37 g, 3.85 mmol) in DMA (7 ml) was then added and the whole was stirred at room temperature for 3.5 h. The resulting suspension was diluted with EtOAc and washed with H_2O and brine. The organic layer was dried and concentrated. The resulting residue was chromatographed on a silica gel column (hexane/EtOAc=4/1) to give (S)-61 (*n*=3) (1.30 g, 3.16 mmol, 90%) as a colorless oil. $^1\text{H-NMR}$ (CDCl_3) δ : 1.11–1.32 (3H, m), 1.47–2.07 (8H, m), 2.79–2.96 (4H, m), 3.26–3.56 (2H, m), 3.78 (3H, s), 3.84–4.17 (5H, m), 6.70–6.92 (5H, m), 7.06–7.25 (3H, m). $[\alpha]_D^{25} -31^\circ$ ($c=1.09$, MeOH).

(S)-2-[3-[2-[2-(3-Methoxyphenyl)ethyl]phenoxy]propyl]-1-methylpyrrolidine Citrate ((S)-63) A solution of (S)-1-ethoxycarbonyl-2-[3-[2-[2-(3-methoxyphenyl)ethyl]phenoxy]propyl]pyrrolidine (S)-61 (*n*=3) (1.27 g, 3.09 mmol) in THF (20 ml) was added dropwise to a suspension of LiAlH_4 (350 mg, 9.22 mmol) in THF (15 ml). The mixture was refluxed for 1 h and then cooled. To the resulting suspension was slowly added Na_2SO_4 decahydrate and the slurry was then stirred for 2 h. The insoluble material was filtered away and the filtrate was concentrated. The resulting residue was chromatographed on a silica gel column ($\text{CH}_2\text{Cl}_2/\text{MeOH}=9/1$) to give 2-[3-[2-[2-(3-methoxyphenyl)ethyl]phenoxy]propyl]-1-methylpyrrolidine (996 mg, 2.82 mmol, 91%) as a colorless oil. To a solution of this oil (880 mg, 2.49 mmol) in EtOH (5 ml) was added citric acid (523 mg, 2.49 mmol) and the mixture was stirred at room temperature for 2 h, then concentrated. The oily residue was dissolved in EtOAc, and the solution was allowed to stand at room temperature. The precipitate formed was collected by filtration to give colorless crystals (1.30 g, 2.38 mmol, 96%). $[\alpha]_D^{25} -12^\circ$ ($c=1.30$, MeOH).

5-HT₂ Receptor Binding Assay The 5-HT₂ receptor binding assay of Leysen *et al.*²¹⁾ was employed with some modifications. It was performed using the 5-HT₂ antagonist, [³H]ketanserin, as the ³H-ligand and the cortex as reported in ref 17.

D₂ Receptor Binding Assay The D₂ receptor binding assay of Köhler *et al.*²²⁾ was employed with some modifications. It was performed using the D₂ antagonist, [³H]raclopride, as the ³H-ligand and the striatum as reported in

ref 17.

α_1 Receptor Binding Assay The α_1 receptor binding assay of Greengrass and Bremner²³⁾ was employed with modifications. It was performed in a similar manner to the 5-HT₂ receptor binding assay, except for the use of the α_1 antagonist, [³H]prazosin, as the ³H-ligand.

β Receptor Binding Assay The β receptor binding assay of U'Prichard *et al.*²⁴⁾ was employed with modifications. It was performed in a similar manner to the 5-HT₂ receptor binding assay, except for the use of the β antagonist, [³H]dihydroalprenolol (DHA), as the ³H-ligand.

5-HT₁ Receptor Binding Assay The 5-HT₁ receptor binding assay of Middlemiss²⁵⁾ was employed with modifications. It was performed in a similar manner to the 5-HT₂ receptor binding assay, except for the use of the [³H] 5-HT as the ³H-ligand.

5-HT₃ Receptor Binding Assay The 5-HT₃ receptor binding assay of Kilpatrick *et al.*²⁶⁾ was employed with modifications. It was performed in a similar manner to the 5-HT₂ receptor binding assay, except for the use of the 5-HT₃ antagonist, [³H]GR65630, as the ³H-ligand.

5-HT-Induced Vasoconstriction Experiment Contractions of the rat caudal arteries of Van Nueten *et al.*²⁷⁾ were employed with some modifications as reported in ref 17.

5-HT-Induced PRP Aggregation Preparation of Platelets: For *in vitro* experiments, human blood was withdrawn by venepuncture from normal volunteers, who had not taken any medication for a period of at least 10 d. For *ex vivo* experiments, blood was withdrawn from the left carotid artery of pentobarbital (40 mg/kg, i.p.)-anesthetized male cats (American Shorthair, Kasha, 2.5–3.6 kg) before and 0.5, 1, 2, 4 and 6 h after intravenous administration of test compounds. Blood samples were collected into plastic syringes containing 3.8% trisodium citrate (1:9, v/v). The blood was centrifuged, to obtain PRP, at 150×g (human) and 120×g (cat) for 15 min at room temperature. Platelet-poor plasma (PPP) was obtained by centrifugation of the remaining blood at 2000×g for 10 min. Platelet counts in PRP were adjusted to 3×10⁸/ml (human) and 2.5×10⁸/ml (cat) by adding PPP.

Measurements of Platelet Aggregation: All aggregation studies were performed in a 6-channel aggregometer (NKK, Tokyo, Japan). The PRP was incubated at 37 °C for 1.5 min in the aggregometer, with stirring (1000 rpm), followed by stimulation with 5-HT (10 μM) combined with collagen (0.125 μg/ml) for human platelets and 5-HT alone (4–8 μM) for cat platelets. Changes in light transmission were recorded for 10 min after the stimulation. The extent of aggregation was estimated by the percent of maximum increase in light transmission, with the PPP representing 100% transmittance. In human platelet studies, test compounds dissolved in saline were added to the PRP before agonist stimulation, and results were expressed as IC₅₀ values (μM), the concentration produced a 50% inhibition.

Acknowledgments We wish to thank Miss Takako Nagasawa²⁸⁾ for the biological data, and Mrs. Megumi Akamatsu for the syntheses.

References and Notes

- 1) Present address: Patent Department, Sankyo Co., Ltd.
- 2) Villalón C. M., De Vries P., Saxena P. R., *Drug Discovery Today*, **2**, 294–300 (1997).
- 3) Martin G. R., Humphrey P. P. A., *Neuropharmacology*, **33**, 261–273 (1994).
- 4) Leysen J. E., Gommeren W., Van Gompel P., Wynants J., Janssen P. F. M., Laduron P. M., *Mol. Pharmacol.*, **27**, 600–611 (1985).
- 5) Kennis L. E. J., Vandenberg J., Boey J. M., Mertens J. C., Van Heertum A. H. M., Janssen M., Awouters F., *Drug. Dev. Res.*, **8**, 133–140 (1986).
- 6) Blackburn T. P., Thornber C. W., Pearce R. J., Cox B., *FASEB J.*, **2**, A1404 (1988).
- 7) Shannon M., Battaglia G., Glennon R. A., Titeler M., *Eur. J. Pharmacol.*, **102**, 23–29 (1984).
- 8) De Clerck F., David J.-L., Janssen P. A. J., *Agents Actions*, **12**, 388–397 (1982).
- 9) Van Nueten J. M., *Fed. Proc.*, **42**, 223–227 (1983).
- 10) De Clerck F., Herman A. G., *Fed. Proc.*, **42**, 228–232 (1983).
- 11) De Clerck F., Van Nueten J. M., Reneman R. S., *Agents Actions*, **15**, 612–626 (1984).
- 12) De Cree J., Leempoels J., Demon B., Roels V., Verhaegen H., *Agents Actions*, **16**, 313–317 (1985).
- 13) Fozard J. R., *J. Cardiovasc. Pharmacol.*, **4**, 829–838 (1982).
- 14) Cohen M. L., Fuller R. W., Kurz K. D., *Hypertension*, **5**, 676–681 (1983).
- 15) Hara H., Osakabe M., Kitajima A., Tamao Y., Kikumoto R., *Thromb. Haemost.*, **65**, 415–420 (1991).
- 16) Kikumoto R., Hara H., Ninomiya K., Osakabe M., Sugano M., Fukami H., Tamao Y., *J. Med. Chem.*, **33**, 1818–1823 (1990).
- 17) Tanaka N., Goto R., Ito R., Hayakawa M., Ogawa T., Fujimoto K., *Chem. Pharm. Bull.*, **46**, 639–646 (1998).
- 18) Mitsunobu O., *Synthesis*, **1981**, 1–28.
- 19) Mancuso A. J., Huang S. L., Swern D., *J. Org. Chem.*, **43**, 2480–2482 (1978).
- 20) Fujimoto K., Tanaka N., Asai F., Ito T., Koike H., *Eur. Pat.* EP600717 (1994) [*Chem. Abstr.*, **123**, 169510k (1995)].
- 21) Leysen J. E., Niemegeers C. J. E., Van Nueten J. M., Laduron P. M., *Mol. Pharmacology*, **21**, 301–314 (1982).
- 22) Köhler C., Hall H., Ögren S., Gawell L., *Biochem. Pharmacol.*, **34**, 2251–2259 (1985).
- 23) Greengrass P., Bremner R., *Eur. J. Pharmacol.*, **55**, 323–326 (1979).
- 24) U'Prichard D. C., Bylund D. B., Snyder S. H., *J. Biol. Chem.*, **253**, 5090–5102 (1978).
- 25) Middlemiss D. N., *Eur. J. Pharmacol.*, **101**, 289–293 (1984).
- 26) Kilpatrick G. J., Jones B. J., Tyers M. B., *Nature (London)*, **330**, 746–748 (1987).
- 27) Van Nueten J. M., Janssen P. A. J., Van Beck J., Xhonneux R., Verbeuren T. J., Vanhoutte P. M., *J. Pharmacol. Exp. Ther.*, **218**, 217–230 (1981).
- 28) Present address: Research Institute, Sankyo Co., Ltd.

Structural Features for Fluorescing Present in Methoxycoumarin Derivatives

Akira TAKADATE,^{*,a} Toshinobu MASUDA,^a Chiyomi MURATA,^a Miki SHIBUYA,^a and Akihiko ISOBE^b

Daiichi College of Pharmaceutical Sciences,^a Minami, Fukuoka 815–8511, Japan and Laboratory of Chemistry, Gunma Prefectural Women's College,^b Tamamura, Sawagun, Gunma 370–1100, Japan.

Received August 24, 1999; accepted October 22, 1999

Structural features of fluorescent methoxycoumarins were examined from the viewpoint of substituent effect and ring structure in connection with intramolecular charge-transfer (ICT). The fluorescence of methoxycoumarins depended primarily upon the ICT from a C₆-electron-donating group to the substituents at the C₃-position of the coumarin ring. Furthermore, the presence of a lactone ring itself, including a carbonyl group, cyclic ether oxygen and ethylenic bond as partial ring structures, was found to be essential for fluorescing in methoxycoumarins according to the fluorescent behaviors of chemically deformed model compounds.

Key words methoxycoumarin; fluorophore; fluorescence emission mechanism; intramolecular charge-transfer

Fluorometric analysis is one of the most sensitive methods for detecting organic and/or inorganic compounds, and therefore it has been widely used in many scientific fields with improving analytical instruments such as high-performance liquid chromatography (HPLC), capillary electrophoresis (CE), and the like. However, as most compounds in nature are not fluorescent, it is necessary to give them fluorescence by reacting them chemically with fluorescent or fluorogenic molecules. For this purpose, a great deal of effort has gone into the development of fluorescence derivatization reagents using various fluorophores. At the stage of molecular design, having sufficient information on the relationship between the chemical structures and fluorescence characteristics of fluorophores should facilitate the development of the reagents.

Recently, Imai and co-workers established a method of predicting the fluorescent behaviour of benzofurazane compounds, some of which are commonly purchased as fluorescence derivatization reagents, from a standpoint of the Hammett's substituent effects¹⁾ and by semi-empirical molecular orbital calculations.²⁾

In a previous paper,³⁾ we have also reported the fluorescence characteristics of methoxycoumarins, some of which have been utilized as the fluorophores of the analytical reagents,⁴⁾ as well as benzofurazanes. Next, the structural features of strongly fluorescing methoxycoumarins were discussed in connection with their spectroscopic properties based on intramolecular charge-transfer (ICT) from the substituents to a coumarin ring.

Now, this paper describes the fluorescence characteristics of methoxycoumarins in further detail by means of additional substituent effects, and the conclusive and reductive chemical conversion of coumarins, because an adequate understanding of fluorophores is essential for the development of excellent fluorescence reagents, as described above.

Experimental

Materials All chemicals were of reagent grade, unless noted otherwise. The solvents (Luminasol) used for the fluorescence measurement were purchased from Dojindo Laboratories (Kumamoto, Japan). Compounds **1a–k** were prepared by means of Knoevenagel condensation of 4,5-dimethoxysalicylaldehyde with the corresponding active methylene compounds, according to the methods described in the literature.^{5–10)}

Typical synthetic procedures, as well as physical and spectral data of unknown compounds, were as follows:

1f: Yield 45%, mp 216–217 °C. ¹H-NMR (CDCl₃) δ: 3.93, 3.96 (3H, s,

C₆-, C₇-OCH₃), 6.88 (1H, s, C₅-H), 6.98 (1H, s, C₈-H), 8.37 (1H, s, C₄-H), 10.22 (1H, s, C₃-CHO). MS *m/z*: 234 (M⁺).

1h: Yield 26%, mp 167–168 °C. ¹H-NMR (CDCl₃) δ: 3.94, 3.98 (3H, s, C₆-, C₇-OCH₃), 6.89 (1H, s, C₅-H), 6.90 (1H, s, C₈-H), 7.68 (1H, s, C₄-H). MS *m/z*: 354 (M⁺).

1j: Yield 69%, mp 293–294 °C. ¹H-NMR (CDCl₃) δ: 3.97, 4.01 (3H, s, C₆-, C₇-OCH₃), 6.87 (1H, s, C₅-H), 6.89 (1H, s, C₈-H), 8.15 (1H, s, C₄-H). MS *m/z*: 231 (M⁺).

2a: A mixture of 2,5-dihydroxy-4-methoxybenzaldehyde¹¹⁾ (10 mmol) and ethyl acetoacetate (10 mmol) in absolute ethanol was refluxed in the presence of a few drops of piperidine for 10 min. After cooling, the resulting precipitates were recrystallized from ethanol to give 3-acetyl-6-hydroxy-7-methoxycoumarin as yellow needles [mp 215–216 °C. ¹H-NMR (CDCl₃) δ: 2.71 (3H, s, C₃-COCH₃), 4.02 (3H, s, C₇-OCH₃), 5.63 (1H, s, C₆-OH), 6.86 (1H, s, C₅-H), 7.11 (1H, s, C₈-H), 8.46 (1H, s, C₄-H). MS *m/z*: 234 (M⁺)]. Acetylation of this compound with acetic anhydride in pyridine by the usual method gave **2a** as pale yellow needles. Yield 75%, mp 178–179 °C. ¹H-NMR (CDCl₃) δ: 2.35 (3H, s, C₆-OCOCH₃), 2.71 (3H, s, C₃-COCH₃), 3.94 (3H, s, C₇-OCH₃), 6.91 (1H, s, C₅-H), 7.31 (1H, s, C₈-H), 8.45 (1H, s, C₄-H), 8.45 (1H, s, C₄-H). MS *m/z*: 276 (M⁺).

Compound **2b** was obtained in the same manner as that of **2a**, other than employing 3-acetyl-7-hydroxy-6-methoxycoumarin [mp 237–238 °C. ¹H-NMR (CDCl₃) δ: 2.71 (3H, s, C₃-COCH₃), 3.98 (3H, s, C₆-OCH₃), 6.42 (1H, s, C₇-OH), 6.94 (1H, s, C₈-H), 6.97 (1H, s, C₅-H), 8.48 (1H, s, C₄-H). MS *m/z*: 234 (M⁺)] derived from 2,4-dihydroxy-5-methoxybenzaldehyde.¹²⁾ Yield 83%, mp 213–215 °C. ¹H-NMR (CDCl₃) δ: 2.37 (3H, s, C₇-OCOCH₃), 2.73 (3H, s, C₃-COCH₃), 3.90 (3H, s, C₆-OCH₃), 6.91 (1H, s, C₅-H), 7.31 (1H, s, C₈-H), 8.45 (1H, s, C₄-H). MS *m/z*: 276 (M⁺).

2c: A mixture of 2,5-dihydroxy-4-methoxybenzaldehyde (5 mmol) and 2-(tosyloxymethyl)-15-crown-5-ether¹³⁾ (5 mmol) in anhydrous acetone (50 ml) was refluxed in the presence of K₂CO₃ (5 mmol) for 72 h, filtered and evaporated to dryness under reduced pressure. The residue was extracted with dichloromethane and then washed successively with water and saturated sodium chloride solution. Evaporation of the solvent left an oil, 2-hydroxy-4-methoxy-5-[2'-(15-crown-5)-methyleneoxy]benzaldehyde, which was refluxed with ethyl acetoacetate (5 mmol) and a catalytic amount of piperidine in absolute ethanol (20 ml) for 10 min without purification. The resulting precipitates were recrystallized from ethanol to give yellow-green needles of **2c**. Yield 35%, mp 148–150 °C. ¹H-NMR (CDCl₃) δ: 2.71 (3H, s, C₃-COCH₃), 3.64–4.20 (21H, m, C₆-OCH₂-15-crown-5), 3.89 (3H, s, C₆-OCH₃), 6.91 (1H, s, C₅-H), 6.94 (1H, s, C₈-H), 8.48 (1H, s, C₄-H). MS *m/z*: 466 (M⁺).

Compound **2d** was prepared in the same manner as that of **2c**, other than employing 2,4-dihydroxy-5-methoxybenzaldehyde. Yield 26%, mp 138–140 °C. ¹H-NMR (CDCl₃) δ: 2.71 (3H, s, C₃-COCH₃), 3.64–4.20 (21H, m, C₆-OCH₂-15-crown-5), 3.89 (3H, s, C₆-OCH₃), 6.91 (1H, s, C₅-H), 6.94 (1H, s, C₈-H), 8.48 (1H, s, C₄-H). MS *m/z*: 466 (M⁺).

Compound **3** was obtained by cyclic condensation of 4,5-dimethoxy-salicylaldehyde with methylvinylketone in the presence of K₂CO₃ in dioxane, according to the methods of Rene and Vincenzo.¹⁴⁾ Yield 15%, mp 115–116 °C. ¹H-NMR (CDCl₃) δ: 2.38 (3H, s, C₃-COCH₃), 3.86, 3.88 (3H, s, C₆, C₇-OCH₃), 4.97 (2H, s, C₂-H₂), 6.47 (1H, s, C₈-H), 6.68 (1H, s, C₅-H), 6.84

* To whom correspondence should be addressed.

(1H, s, C₄-H). MS *m/z*: 234 (M⁺).

Compound **4** was prepared by acetylation of 1,2-dihydro-6,7-dimethoxynaphthalene¹⁵ with acetic anhydride in the presence of aluminum chloride. Yield 56%, mp 131–133 °C. ¹H-NMR (CDCl₃) δ: 2.43 (3H, s, COCH₃), 2.57 (2H, t, C₁-CH₂), 2.78 (2H, t, C₂-CH₂), 3.90 (3H, s, OCH₃), 3.92 (3H, s, OCH₃), 6.73 (1H, s, C₅-H), 6.78 (1H, s, C₈-H). MS *m/z*: 232 (M⁺).

Compound **5** was prepared by the reaction of commercially available 3,4-dimethoxybenzaldehyde with acetone according to the text.¹⁶ Yield 65%, mp 71–74 °C. ¹H-NMR (CDCl₃) δ: 2.37 (3H, s, COCH₃), 3.94 (6H, s, OCH₃), 6.56 (1H, d, olefinic-H), 6.88 (1H, d, C₅-H), 7.08 (1H, s, C₂-H), 7.11 (1H, d, C₆-H), 7.46 (1H, d, olefinic-H). MS *m/z*: 206 (M⁺).

Apparatus and Measurements The melting points were measured on a Yanagimoto micro-melting point apparatus, and are uncorrected. ¹H-NMR were obtained with a JEOL JNM-GSX 500FT-NMR spectrometer using tetramethylsilane as an internal standard. The following abbreviations are used: s, singlet; d, doublet; t, triplet; and m, multiplet. The mass spectra (MS) were taken with a JEOL JMS-DX303 spectrometer, using the electron impact ionization (EI) mode at 70 eV. The fluorescence spectra were taken with a Hitachi F-4000 fluorescence spectrophotometer. Fluorescence quantum yields were determined according to the method of Parker and Rees,¹⁷ and the value (0.55) for quinine sulfate in 0.5 M H₂SO₄ was used as the standard.

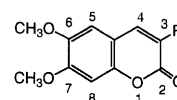
Fluorescence Quenching Efficiencies (FQE): These values were calculated by means of the following equation: FQE (%) = $(I_0 - I_M)/I_0 \times 100$, where *I*₀ and *I*_M are the fluorescence intensities (Ex 387 nm, Em 477 nm) of **2c** or **2d** (5.0 × 10⁻⁶ M) in the absence and the presence of sodium acetate (5.0 × 10⁻⁴ M), respectively, in methanol solution.

Stability Constants¹⁸: Measurements for the stability constants (*K*_s) were made on a methanol solution of **2c** or **2d** (5.0 × 10⁻⁶ M) and sodium acetate (5.0 × 10⁻⁶–5.0 × 10⁻³ M). The *K*_s were estimated by the usual treatment of Benesi–Hildebrand plots obtained from the changes in fluorescence intensities (Ex 387 nm, Em 477 nm).

Results and Discussion

Effects of Substituents at the C₃-Position In a recent publication,³ we described that i) the arrangements of an electron-donating group at the C₆-position and an electron-withdrawing group at the C₃-position on the coumarin ring contribute predominantly to the fluorescence enhancement of methoxycoumarins, ii) this enhancement can be appreciated by approximating the relationship of two substituents at the C₆- and the C₃-positions to the *para*-position in the disubstituted benzene model, and also iii) additional structural features of coumarins required for intense fluorescence include diether bonds at both the C₆- and C₇-positions, and an electron-withdrawing group at the C₃-position, as shown in 3-acetyl-6,7-dimethoxycoumarin with a quantum yield of 0.52. On the basis of these structural requirements, 3-substituted-6,7-dimethoxycoumarins, **1a–k**, with two fixed methoxy groups at the C₆- and C₇-positions were prepared to examine the effects of the substituents at C₃-position in this study. In order to understand the contribution of these substituent groups to the fluorescence characteristics, a suitable, easily available parameter was searched for. As is distinct from the condensed-ring compounds, such as pyrene and anthracene, fluorescence characteristics of the heterocyclic compounds such as coumarin and benzofurazane were attributed to the electronic effects of substituents in the molecule. The Hammett substituent constants (σ_p or σ_m)¹⁹ are practical parameters used to estimate the electronic effect in the chemical reactions. Although these constants represent gross values, including the polar effect, the resonance effect, and the solvent effect, they seemed suitable for representing total electronic effects. Thus, we tried to understand the fluorescence characteristics of 3-substituted-6,7-dimethoxycoumarins using Hammett σ_p -values as suitable parameters. Fluorescence

Table 1. Fluorescence Properties of 6,7-Dimethoxy-3-substituted Coumarins in Methanol



Compound No.	R	$F\lambda_{\max}/\text{nm}$ (Ex λ/nm)	RFI	$\sigma_p^{b)}$
1a	OH	487 (389)	91	-0.37
1b	OCH ₃	437 (338)	32	-0.27
1c	CH ₃	423 (339)	176	-0.17
1d	H ^{a)}	432 (344)	100	0
1e	OCOCH ₃	435 (344)	317	0.31
1f	CHO	433 (345)	175	0.44
1g	COOC ₂ H ₅	458 (374)	458	0.45
1h	OSO ₂ CF ₃	448 (355)	219	0.47
1i	COCH ₃ ^{a)}	482 (382)	295	0.50
1j	CN	465 (377)	530	0.66
1k	NO ₂	443 (390)	6	0.78

a) Ref. 3. b) Ref. 19.

spectral data of **1a–k**, together with Hammett σ_p -values¹⁹ are summarized in Table 1, where the relative fluorescence intensities (RFI) are relative values against the fluorescence intensity (100) of the standard compound, **1d**. As shown in Table 1, an increase in fluorescence intensities was observed for **1e–j**, substituted with electron-withdrawing groups (σ_p =0.31–0.66), compared with that of **1d**. However, non-fluorescence was observed for **1k**, with the stronger electron-withdrawing nitro group (σ_p =0.78). On the other hand, compounds **1a** and **b**, which were introduced electron-donating groups such as hydroxy- and methoxy groups at the C₃-position, showed a tendency to decrease in fluorescence intensity. The fluorescence wavelengths of these compounds were also shifted to longer wavelength regions, with increases in the electron-withdrawing ability of substituents, except for **1a**. It was suggested from these results that the fluorescence of such coumarins are subject to the ICT effect through a push–pull system between C₆- and C₇-electron-donating groups and electron-withdrawing groups on the lactone ring. As can be seen in Hammett's plots (Fig. 1) obtained from the data in Table 1, the fluorescence intensities in general increased with an increase in the electron-withdrawing ability of substituents, but a nonlinear relationship was observed. The fluorescence intensity of **1k** was particularly low. This drastic fall-off in fluorescence intensity may be ascribed to the conversion of the planar ICT state to a conformer displaying full charge separation, a twisted ICT state,²⁰ which is non-emissive in a polar solvent such as methanol, and by the acceleration of ICT between the electron-donating methoxy groups and the stronger electron-withdrawing C₃-nitro group. This is also supported by the fact that the fluorescence of **1k** is restored in less polar solvents such as benzene and chloroform. Furthermore, ¹H-NMR spectroscopic study²¹ gave additional information on the substituent effect from the standpoint of the polarization of molecules in the ground state. The plot of ¹H-NMR chemical shifts of C₄-H on the coumarin ring in deuterated chloroform, and σ_p -values, gave a positive correlation similar to that in Fig. 1, namely, the δ values of C₄-H increased with an increase in the electron-withdrawing ability of substituents at the C₃-position (Fig. 2).

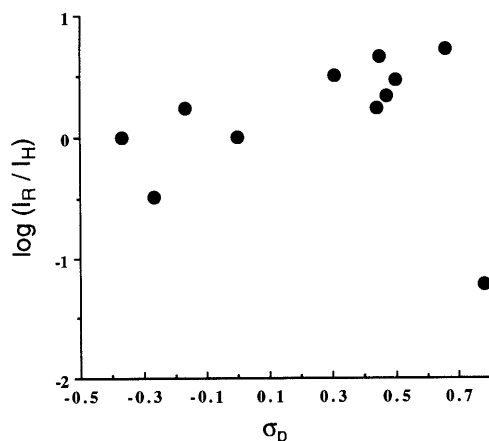
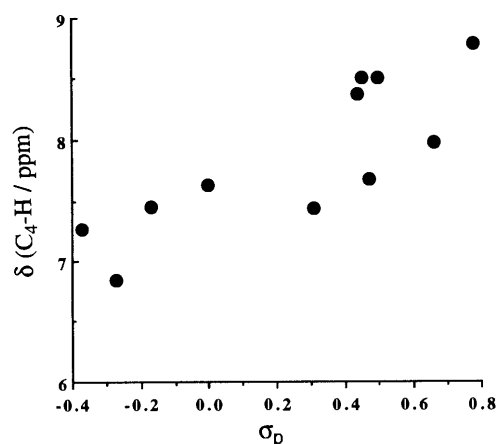
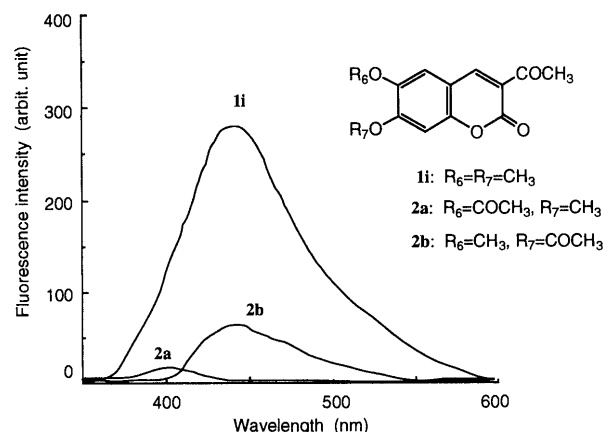


Fig. 1. Plot of RFI and Hammett Constants

Fig. 2. Plot of C₄-H Chemical Shift and Hammett Constants

Such downfield shifts apparently suggest an electron deficiency at the C₄-position caused by electron-withdrawing substituents at the adjoined C₃-position in the ground state. From these results, the fluorescence of such coumarins was found to be strongly dependent upon ICT between the electron-donating methoxy groups and the C₃-substituents. However, the virtual fluorescence mechanism is apparently not so simple.

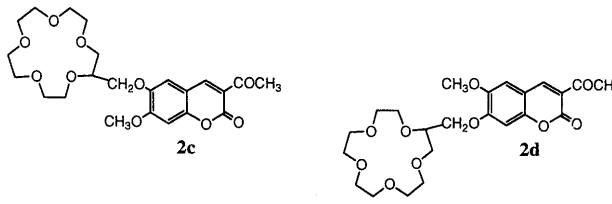
Effects of Substituents at C₆- or C₇-position To specify the contribution of the position of the C₆- or C₇-electron-donating groups to the fluorescence, 3-acetylcoumarin derivatives, **2a**—**d**, were prepared. Figure 3 shows the fluorescence spectra of **2a**, **b**, together with **1i** for comparison. The fluorescence of **2a**, a derivative of **1i** whose C₆-methoxy group was replaced with an electron-withdrawing acetoxy group, was quenched, and its blue-shifted spectrum resembled that of 7-methoxy-3-acetylcoumarin ($F\lambda_{\max}$ 428 nm).³⁾ In contrast with **2a**, a 7-acetoxy-compound, **2b**, still held about 20% of the fluorescence of **1i**. This fact suggests that the strong fluorescence of **1i** is predominantly attributable to the ICT from the C₆-methoxy group to the C₃-acetyl group on the lactone ring. This estimate was examined in further detail by employing the newly prepared crowned-coumarins, **2c**, **d**. The 15-crown-5 ether moieties introduced into C₆- or C₇-positions of **2c**, **d** have been well known to form complexes with Na⁺ or K⁺ by the electrostatic interaction of their electron-donating oxygens with metal cations.²²⁾ Therefore, this com-

Fig. 3. Fluorescence Spectra of **1i** and **2a**, **b** in Methanol at 25 °C

The concentration of coumarins; 1.0×10^{-6} M. Excitation wavelength: 382 nm for **1i**, 375 nm for **2a**, and 447 nm for **2b**.

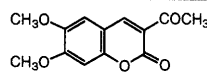
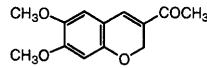
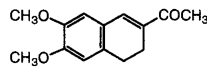
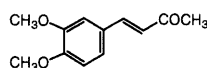
plexation event may prove the contribution of both electron-donating groups at the C₆- and C₇-positions in the fluorescence of **1i**, the same as the above substituent effect. In a recent study concerning fluorescent sensors for metal ions, photoinduced electron transfer (PET) has attracted attention as a novel operating principle.²³⁾ A number of excellent fluorescence signaling systems based on the PET mechanism have been proposed. Among them, de Silva's group has reported a unique PET sensory system²⁴⁾ in which the benzocrown unit can act not only as a receptor for metal ions but also as an efficient fluorescence quencher for fluorophores such as anthracene. More recently, Nishizawa *et al.* reported a similar fluorescent PET sensor for metal ions using pyrene as a fluorophore and benzo-15-crown-5 as a receptor for metal ions and an electron donor (a fluorescence quencher of pyrene monomer) for exciplex formation at the same time.²⁵⁾ However, aliphatic crown ether, the 15-crown-5 ether moieties introduced into the C₆- or C₇-positions of **2c**, **d** scarcely quenched their fluorescence, suggesting no PET interaction between the 15-crown-5 ether moieties and the coumarin fluorophore, as shown in Table 2. Thus, the effect of metal ions on the fluorescence spectra of **2c**, **d** was examined in methanol. The fluorescence intensities of **2c**, **d** in methanol were, in fact, decreased with the addition of sodium or potassium acetates. On the other hand, a corresponding derivative **1i**, without a 15-crown-5 ether moiety, showed no change in the fluorescence spectrum by adding these metal ions. This indicates the formation of complexes of **2c** and **2d** with metal ions. The fluorescence quenching of **2c**, **d** is considered to lower the electron-donating ability of C₆- or C₇-substituents because of the electrostatic interaction²²⁾ of electron-donating oxygens on the crown ether with metal ions. FQE and stability constants (log *K*s) for **2c**, **d** are shown in Table 2. It was noteworthy from the results that the stability constants of **2c**, **d** were almost comparable; nevertheless, a remarkable difference in FQEs of **2c** (16.9%) and **2d** (10.3%) was observed. This supports the foregoing estimate, that is, the fluorescence in methoxycoumarins depends predominantly on ICT from the C₆-electron-donating group to C₃-electron-withdrawing substituents on the lactone ring.

Effects of Lactone Ring Structure In addition to the above substituents effects, the contribution of ring structures to the fluorescence of this type of coumarin was examined

Table 2. Fluorescence Spectral Properties of **1i**, **2c**, and **2d** in Methanol at 25 °C in the Absence and Presence of Na⁺


Compound No.	$F\lambda_{\max}/\text{nm}$ ($Ex \lambda/\text{nm}$)	Φ_F (rel)	FQE (%)	$\log K_s$ (Na ⁺)
1i	479 (383)	100	—	—
2c	480 (383)	99	16.9	3.03
2d	479 (385)	103	10.3	3.11

Table 3. Fluorescence Spectral Data of **1i**, **3**, **4**, and **5** in Methanol

Compound No.	Structural formula	$F\lambda_{\max}/\text{nm}$ ($Ex \lambda/\text{nm}$)	Φ_F
1i		482 (385)	0.52
3		543 (375)	0.02
4		491 (369)	0.01
5		n.d.	n.d.

n.d.: not detected.

from the viewpoint of the necessity of a carbonyl group and ether oxygen on the lactone ring, and also on the ring itself. For this purpose, compounds **3** (chromene type), **4** (dihydronaphthalene type) and **5** (styrene type) were prepared. Their fluorescence spectral data are listed in Table 3.

First, the contribution of a lactone carbonyl group to the strong fluorescence of **1i** was estimated from the fluorescence behaviors of **3** lacking a carbonyl group. As shown in Table 3, the fluorescence quantum yield of **3** ($\Phi_F=0.02$) was remarkably low in comparison with that of **1i** ($\Phi_F=0.52$).³⁾ However, the $F\lambda_{\max}$ (543 nm) of **3** shifted to a much longer wavelength region than that (482 nm) of **1i**, and also, the emission color in the solution was distinct yellow in contrast to the whitish blue of **1i**. Thus, the presence of a lactone carbonyl group on **1i** from these results is suggested to contribute primarily to the fluorescence intensity. The remarkable red shift in $F\lambda_{\max}$ of **3** may be attributed to the enhanced ICT effect from the C₆-methoxy group to the C₃-acetyl group, due to the lack of a carbonyl group. This is also supported by the difference in $F\lambda_{\max}$ ³⁾ of 6-methoxy-3-acetylcoumarin (506 nm) and 7-methoxy-3-acetylcoumarin (428 nm). The strong fluorescence of **1i**, therefore, is presumed to result from two different ICT routes, from the C₆- and C₇-electron-donating groups to either a lactone carbonyl or a C₃-

electron-withdrawing group. The former route may contribute to the fluorescence intensity and the later to the fluorescence wavelength. Further investigation, however, is required to elucidate these mechanisms.

Subsequently, compound **4**, which converted a lactone moiety into a cyclic ethylene structure, showed a lowered quantum yield and slight red shift in $F\lambda_{\max}$ compared with **1i**, and an additional lowering in quantum yield together with a blue shift compared with the cases of **3**. The fluorescence behaviors of **4** are considered to be due to the effect of a slightly distorted cyclohexene ring. The fluorescence of **5** in the absence of a lactone ring structure was no longer detectable under the same conditions as the other compounds. These results indicate the requirement of at least a ring structure, as can be seen in **3**, as a part of the coumarin ring for fluorescing. This chromene-type compound, **3**, may also be promising for use as a novel fluorophore for fluorescent imaging because of emitting a distinct yellow.

Thus, such an approach to determining fluorescence characteristics by chemical tools was found to be practically effective for establishing reagent design structural requirements for various purposes.

References

- 1) Uchiyama S., Santa T., Fukushima T., Homma H., Imai K., *J. Chem. Soc., Perkin Trans. 2*, **1998**, 2165—2173.
- 2) Uchiyama S., Santa T., Imai K., *J. Chem. Soc., Perkin Trans. 2*, **1999**, 569—576.
- 3) Takadate A., Masuda T., Murata C., Tanaka T., Irikura M., Goya S., *Anal. Sci.*, **11**, 97—101 (1995).
- 4) Takadate A., Masuda T., Murata C., Tanaka T., Irikura M., Goya S., *Anal. Sci.*, **8**, 663—668 (1992); Takadate A., Masuda T., Murata C., Haratake C., Isobe A., Irikura M., Goya S., *ibid.*, **8**, 695—697 (1992); Takadate A., Masuda T., Murata C., Tanaka T., Miyahara H., Goya S., *Chem. Lett.*, **1993**, 811—814; Takadate A., Masuda T., Murata C., Tanaka T., Goya S., *Bull. Chem. Soc. Jpn.*, **68**, 3105—3110 (1995).
- 5) Jackson Y. A., *Heterocycles*, **41**, 1979—1986 (1995).
- 6) Shaw K. N., McMillan A., Armstrong M. D., *J. Org. Chem.*, **21**, 601—604 (1956).
- 7) Horning E. C., Horning M. G., *J. Am. Chem. Soc.*, **69**, 968—969 (1947).
- 8) Jackson A. H., Martin J. A., *J. Chem. Soc. (C)*, **1966**, 2222—2229.
- 9) Mali R. S., Yeola S. N., Kulkarni B. K., *Indian J. Chem.*, **22B**, 352—354 (1983).
- 10) Ito K., Nakajima K., *J. Heterocyclic Chem.*, **25**, 511—515 (1988).
- 11) Head F. S. H., Robertson A., *J. Chem. Soc.*, **1930**, 2434.
- 12) Mali R. S., Yadav V. J., Zaware R. N., *Indian J. Chem.*, **21B**, 759—760 (1982).
- 13) Dishong D. M., Diamond C. J., Cinoman M. I., Gokel G. W., *J. Am. Chem. Soc.*, **105**, 586—593 (1983).
- 14) Rene L., Royer R., *Eur. J. Med. Chem.-Chimica. Therapeutica*, **10**, 72—78 (1975). Fulvio L., Antonio L., Pasquale B., Vincenzo T., *Tetrahedron: Asymmetry*, **6**, 1001—1011 (1995).
- 15) Craig J. C., Torkelson S. M., Findel P. R., Weiner R. I., *J. Med. Chem.*, **32**, 961—968 (1989).
- 16) Drake N. L., Allen P., Jr., "Organic Syntheses," Coll. Vol. I, ed. by Gilman H., John Wiley and Sons, Inc., New York, 1950, p. 77.
- 17) Parker C. A., Rees W. T., *Analyst* (London), **85**, 587—600 (1960).
- 18) Fery-Forgues S., LeBris M. T., Guett J. P., Valeur B., *J. Chem. Soc. Chem. Commun.*, **1988**, 384—385; *idem*, *J. Phys. Chem.*, **92**, 6233—6237 (1988); Bourson J., Valeur B., *ibid.*, **93**, 3871—3876 (1989).
- 19) Wells P. R., "Linear Free Energy Relationships," Academic Press, London, 1968; Lowry T. H., Richardson K. S., "Mechanism and Theory in Organic Chemistry," 2nd ed., Harper & Row, Publishers, New York, 1981, pp. 130—134; Corwin H., Leo A., Taft R. W., *Chem. Rev.*, **91**, 165 (1991).
- 20) Jones II G., Jackson W. R., Halpern A. M., *Chem. Phys. Lett.*, **72**, 391—395 (1980); Jones II G., Jackson W. R., Kanoktanaporn S., Bergmark W. R., *Photochem. Photobiol.*, **42**, 477—483 (1985); Rettig

- W., Klock A., *Can. J. Chem.*, **63**, 1649—1653 (1985).
- 21) Gottlieb H. E., de Lima R. A., delle Monache F., *J. Chem. Soc. Perkin Trans. 2*, **1979**, 435—437.
- 22) Hiraoka E., "Crown Compounds—their characteristics and applications—," Elsevier, Tokyo, 1982; Vogtle F., (ed.), "Topics in Current Chemistry 98—Host Guest Complex Chemistry I—," Springer-Verlag, Berlin, 1981; Izatt R. M., Bradshaw J., Nielsen S. A., Lamb J. D., Christensen J., *Chem. Rev.*, **85**, 271—339 (1985).
- 23) de Silva A. P., Gunaratne H. Q. N., Huxley A. J. M., McCoy C. P., Rademacher J. T., Rice T. E., *Chem. Rev.*, **97**, 1515—1566 (1997).
- 24) de Silva A. P., Sandarayake K. R. A. S., *J. Chem. Soc., Chem. Commun.*, **1989**, 1183—1185.
- 25) Nishizawa S., Watanabe M., Uchida T., Teramae N., *J. Chem. Soc., Perkin Trans. 2*, **1999**, 141—143.

Scavengers for Peroxynitrite: Inhibition of Tyrosine Nitration and Oxidation with Tryptamine Derivatives, α -Lipoic Acid and Synthetic Compounds

Hidehiko NAKAGAWA,^a Erika SUMIKI,^b Mitsuko TAKUSAGAWA,^a Nobuo IKOTA,^a Yoshikazu MATSUSHIMA,^b and Toshihiko Ozawa*,^a

Bioregulation Research Group, National Institute of Radiological Sciences,^a 4-9-1, Anagawa, Inage-ku, Chiba 263-8555 and Kyoritsu College of Pharmacy,^b 1-5-30, Shibakoen, Minato-ku, Tokyo 105-8512, Japan.

Received August 25, 1999; accepted November 2, 1999

The inhibitory effects of various endogenous and synthetic compounds on the nitration and oxidation of L-tyrosine by peroxynitrite were examined. Nitrating and oxidizing activities were monitored by the formation of 3-nitrotyrosine and dityrosine with a HPLC–UV–fluorescence detector system, respectively. Glutathione, serotonin and synthetic sulfur- and selenium-containing compounds inhibited both the nitration and oxidation reaction of L-tyrosine effectively. However, 5-methoxytryptamine, melatonin and α -lipoic acid only inhibited the nitration reaction, and enhanced the formation of an oxidation product. This is important evidence that there are different intermediates in the nitrating and oxidizing reactions of L-tyrosine by peroxynitrite. It was suggested that 5-methoxytryptamine, melatonin and α -lipoic acid reacted only with the nitrating intermediate of peroxynitrite and inhibited nitration of L-tyrosine. Actually, the DNA strand breakage, which is believed to be a typical reaction of hydroxyl radical-like species, caused by peroxynitrite was not effectively inhibited by 5-methoxytryptamine. 5-Methoxytryptamine, melatonin and α -lipoic acid were viewed as useful reagents for investigating the mechanisms of damage by peroxynitrite *in vitro*.

Key words peroxynitrite; scavenger; melatonin-related compound; 5-methoxytryptamine; nitrotyrosine; synthetic selenium compound

Reactive oxygen species are well-known and important components of oxidative stress in several diseases. Recently, nitric oxide and its oxidized species, called reactive nitrogen species, have been suggested to be involved in the damage caused by oxidative stress. Peroxynitrite (PN) is one of the reactive nitrogen species, and is formed from nitric oxide and superoxide *in vivo*.^{1,2} This compound is a highly reactive oxidant and causes nitration on the aromatic ring of free tyrosine and protein tyrosine residues.³ Since the nitration of tyrosine residues is a characteristic reaction of PN, the presence of nitrotyrosine in tissues or cell cultures is often used as a marker of the production of PN. It was reported that PN induced various oxidative damages, for example, LDL (low density lipoprotein) oxidation, lipid peroxidation, DNA strand breakage and so on.^{4–13} Additionally, the nitration of tyrosine is assumed to prevent the phosphorylation of tyrosine residues in the substrate proteins of tyrosine kinase,^{14,15} and to affect tyrosine phosphorylation in the cell signal transduction.¹⁶ This would suggest that the oxidizing and nitrating reactions of PN play pathological roles in the oxidative stress. Although Pfeiffer and Mayer¹⁷ reported 3-nitrotyrosine formation by PN produced from nitric oxide and superoxide *in vivo* was below the detection limit of the HPLC method, the scavenging of PN in assays involving tyrosine nitration and oxidation *in vitro* is a useful research tool to provide information on the antioxidant profiles.

The nitration of tyrosine and other aromatic amino acids is one typical reaction of PN, as reported by Van der Vliet *et al.*¹³ and the formation of a fluorescent product assumed to be dityrosine, as an oxidation product, was detected in the reaction of L-tyrosine with PN. Various typical antioxidants were reported to have inhibitory effects on the nitration of tyrosine.^{18,3} However, the inhibitory effects of typical antioxidants on the oxidation reaction of peroxynitrite have not

been evaluated. We have briefly communicated¹⁹ that 5-methoxytryptamine (5MT) and α -lipoic acid (LA) are selective inhibitors for tyrosine nitration by PN, but not for oxidative dityrosine formation. The details of this work and further investigations of PN and its scavengers are described in this paper. The formation of nitrotyrosine and dityrosine in the reaction of L-tyrosine and PN was analyzed simultaneously, and then the inhibitory effect of various endogenous compounds and synthesized antioxidants was examined. A selective inhibitor for the nitration was applied to inhibit the PN-caused DNA strand breakage.

Experimental

Chemicals L-Tyrosine, 3,4-dihydroxy-DL-phenylalanine (DOPA), *p*-fluoro-L-phenylalanine, glutathione (reduced form), serotonin, L-cystine and *dl*-LA were purchased from Wako Pure Chemical Ind. (Osaka, Japan). 3-Nitro-L-tyrosine, 5-MT, melatonin and 2-methyl-2-nitrosopropane (MNP) were from Aldrich (Milwaukee, WI, U.S.A.). 5,5'-Dimethyl-1-pyrroline-*N*-oxide (DMPO) was from LABOTEC Co., Ltd. (Tokyo, Japan). *N*-tert-butyl- α -phenylnitron (PBN) was from Sigma (St. Louis, MO, U.S.A.). Plasmid pBR322 was purchased from Takara Shuzo Co., Ltd. (Shiga, Japan) and Tris–Borate–EDTA (TBE) buffer was from Gibco BRL (Rockville, MD, U.S.A.). All reagents used were of analytical grade.

Synthesis of Antioxidants (2*S*,3*R*,4*S*)-*N*-ethylmercapto-3,4-dihydroxy-2-hydroxymethylpyrrolidine (NEMP) (**4**) was obtained by hydrolysis of the precursor compound synthesized as described previously.²⁰ L-*N*-dithiocarboxyproline (DTCP) (**3**) was synthesized according to Shinobu *et al.*²¹ Briefly, L-proline (1.15 g) was dissolved in 7 ml of concentrated aqueous ammonia solution in an ice bath. Carbon disulfide (1.2 eq) in a small amount of ethanol was added to the L-proline solution at 0–4 °C dropwise. After the reaction mixture had become a homogenous solution, it was lyophilized and yielded pale orange powder (97.6%). The structures and purity of synthesized NEMP and DTCP were confirmed by ¹H- and ¹³C-NMR spectroscopy. DTCP(NH₄)₂: ¹H-NMR (D₂O) δ : 1.84–1.96 (2H, m), 1.84–2.27 (2H, dm), 3.68–3.85 (2H, m), 4.69–4.73 (1H, m); ¹³C-NMR (D₂O) δ : 24.20 (t), 31.05 (t), 55.20 (t), 69.00 (d), 179.72 (s), 205.32 (s). NEMP·HCl: ¹H-NMR (D₂O) δ : 2.68–2.90 (2H, m, CH₂), 3.13–3.48 (3H, m), 3.48–3.83 (2H, m), 3.85–4.05 (2H, m), 4.35–4.55 (2H, m); ¹³C-NMR (D₂O) δ : 19.64 (t), 57.01 (t), 58.14 (t), 59.30 (t), 69.78 (d), 70.76 (d); $[\alpha]_D^{20}$ +36.5° (*c*=0.5,

* To whom correspondence should be addressed.

H₂O)

(2*R*,3*R*,4*S*)-2-amino-3,4-dihydroxy-5-phenylselenopentan-1-ol (ADPP) (**5**) and (2*S*,4*RS*)-2-amino-4-phenylseleno-5-carboxybutan-1-ol (APCB) (**6**) were also synthesized from the corresponding precursors,^{22,23} and their structures and purity were confirmed by ¹H- and ¹³C-NMR spectroscopy. ADPP·HCl: mp 137–140 °C; ¹H-NMR (D₂O) δ : 2.92–3.16 (2H, m), 3.31–3.46 (1H, m), 3.54–3.67 (1H, m), 3.67–3.82 (2H, m), 3.85–4.00 (1H, m), 7.18–7.35 (3H, m), 7.44–7.59 (2H, m); ¹³C-NMR (D₂O) δ : 31.18 (t), 56.28 (d), 58.85 (t), 69.72 (d), 70.78 (d), 128.50 (d), 129.50 (s), 130.38 (d), 133.64 (d); [α]_D²⁰ +19.4° (*c*=0.3, H₂O). APCB·HCl (1:1 mixture): mp 167–170 °C (dec.); ¹H-NMR (D₂O) δ : 1.85–2.14 (2H, m), 3.34–3.59 (2H, m), 3.61–3.86 (2H, m), 7.22–7.42 (3H, m), 7.43–7.62 (2H, m); ¹³C-NMR (D₂O) δ : 31.15 and 31.29 (t), 39.08 and 39.22 (d), 52.15 and 52.42 (d), 61.11 and 61.48 (t), 125.72 (s), 130.35 and 130.40 (d), 130.63 and 130.70 (d), 137.40 and 137.62 (d), 176.26 (s); [α]_D²⁰ –14.7° (*c*=0.4, H₂O).

PN Preparation PN was synthesized as an alkaline solution according to Whiteman and Halliwell.¹⁸ Briefly, 1 ml of 1 M H₂O₂ was mixed with 1 ml of 1 M NaNO₂ in a glass tube under acidic conditions in an ice bath, and then rapidly quenched with 2 ml of 1.5 M NaOH. The resulting solution was slowly frozen with dry-ice/acetone and the top layer of the frozen solution was collected. A concentrated peroxyxynitrite solution (25 to 126 mM) was obtained. The concentration of the PN solution was determined photometrically from the absorbance at 302 nm (ϵ =1670 M^{–1} cm^{–1}), and the prepared PN solution was stored at –20 °C until used. The stock solution was diluted to the desired concentration with 0.01 N NaOH after determining concentration of the solution photometrically, and used for experiments mentioned below. Although unreacted hydrogen peroxide and sodium nitrite were assumed to be present in the prepared PN solution, neither of these residual reagents gave any oxidized or nitrated products in this system.

ESR Spin Trapping of Tyrosyl Radical The production of free radical intermediates during the reaction of PN with L-tyrosine was measured by the ESR-spin trapping method using MNP as a spin trapping reagent. Briefly, to 0.1 M phosphate buffer solution (pH 9.5) containing 1 mM L-tyrosine, 80 mM MNP and 0.2 mM diethylenetriaminepentaacetic acid (DTPA), 100 μ l of 20 mM PN solution (2 mM as final concentration) was added. Immediately, ESR spectra of the aliquot were measured at room temperature using a 9.5 GHz ESR spectrometer (FE-2X, JEOL Co., Ltd., Tokyo, Japan). Measurement conditions were as follows: microwave power: 10 mW, microwave frequency: 9.45 GHz, modulation frequency and width: 100 kHz and 0.8 G, response and sweep time: 1.0 s and 16 min/100 G, amp. gain: 2 \times 1000.

Reaction of PN with L-Tyrosine To the L-tyrosine (final 0 to 2 mM) solution in 0.1 M sodium phosphate buffer (pH 7.4), PN (final 0 to 8 mM) was added at 37 °C. After 10 min incubation at 37 °C, *p*-fluorotyrosine (final 0.91 mM) was added to the reaction mixture as an internal standard, then an aliquot of the mixture was analyzed with a HPLC–UV–fluorescence detector system (TOSOH Corp., Tokyo). The HPLC conditions were as follows: column: TSK-GEL ODS 80-Ts 4.6 \times 150 mm (TOSOH Corp.), mobile phase: 0.1 M potassium phosphate (pH 3.5), flow rate: 1.0 ml/min. The produced 3-nitro-L-tyrosine and 2,2'-dityrosine were detected by monitoring the absorbance at 274 nm and the fluorescence at 410 nm (ex. 295 nm), respectively. The detected 3-nitro-L-tyrosine was quantified using a standard curve. The formation of dityrosine was confirmed by comparing the retention time and the excitation/fluorescence spectra of a detected peak with the enzymatically synthesized authentic sample, as described previously.¹⁹ Percent changes of the produced dityrosine were calculated from the fluorescence peak area.

For the detection of dopa, the reaction mixture was analyzed by HPLC with an electrochemical detector (TOSOH Corp.). The formation of dopa was detected by monitoring the detector current at 550 mV of electrode potential. The other HPLC conditions were the same as for the detection of 3-nitrotyrosine and 2,2'-dityrosine.

Effects of Various Compounds on Nitrotyrosine and Dityrosine Formation In the presence of various concentrations of testing compounds, L-tyrosine (1 mM) was incubated with PN (0.2 mM) at 37 °C for 10 min in neutral buffer solution (pH 7.4). After the addition of fluorotyrosine as an internal standard, the formation of 3-nitro-L-tyrosine and 2,2'-dityrosine were estimated. When a testing compound showed inhibitory activity, its IC₅₀ value was determined for 3-nitro-L-tyrosine and for 2,2'-dityrosine formation.

Effects of 5-MT on PN-Induced Plasmid DNA Strand Scission DNA strand scission of pBR322 plasmid by PN was detected in the presence and absence of 5-MT with agarose gel electrophoresis and ethidium bromide staining. Plasmid pBR322 (2.5 μ l of 0.2 μ g/ml solution, final 0.05 μ g/ μ l) and PN (2.5 μ l of 0.2 mM to 10 mM alkaline solution, final 0.05–2.5 mM) were added to PBS (phosphate buffered saline solution) (5 μ l) in this order,

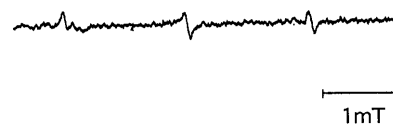


Fig. 1. ESR Spectrum of Spin Adduct of MNP with Tyrosyl Radical

PN was added to the mixture of L-tyrosine and MNP in 0.1 M sodium phosphate buffer (pH7.4).

and the solution was vortexed for 60 s. For the inhibitory experiment on 5-MT, 0.05 μ g/ μ l of pBR322 and 1 mM PN were used. An aliquot of this reaction mixture was loaded on 2% agarose gel with loading buffer (containing bromophenol blue and sucrose). Electrophoresis was performed in TBE buffer at 50 V for 50 min using a Mupid electrophoresis system (Advance Co., Ltd., Tokyo, Japan). After the electrophoresis, the gel was stained with ethidium bromide (1 μ g/ml) for 30 min and washed for 30 min, and then three forms of pBR322 plasmid DNA, supercoiled (SC), open-circular (OC) and linear (LN), were detected using a UV luminometer.

Results

Synthesized PN was mixed with L-tyrosine in sodium phosphate buffer at neutral pH, and the products of the reaction of L-tyrosine with PN were analyzed by HPLC with a UV and fluorescence detector system. It was confirmed that 3-nitrotyrosine was formed as a major product in the reaction mixture of PN and L-tyrosine, as reported.¹³ The formation of 3-nitro-L-tyrosine was dependent on the concentration of PN and L-tyrosine. The formation of a fluorescent product,¹³ which was identified as 2,2'-dityrosine by comparing its retention time and fluorescence spectra with the authentic sample prepared as described in Experimental, was also confirmed.¹⁹

To investigate the possibility of the formation of radical species during the reaction of PN, the ESR-spin trapping method was used. MNP was used for spin trapping of radical species during the reaction of PN with tyrosine. In the case of 1 mM L-tyrosine, 2 mM PN and *ca.* 80 mM MNP at pH 9.5, a triplet ESR signal (a^N =15.8 G) was observed (Fig. 1), while only a trace of the same ESR signal was detected at pH 7.4. From its hyperfine splitting constant, it was identified as a MNP-tyrosyl radical adduct.²⁴ This result showed that tyrosyl radical could be involved in the reaction of L-tyrosine with PN. In the reaction of PN with tyrosine at pH 9.5, the products were the same as those at pH 7.4 by HPLC analysis. The same intermediates could be involved in the reaction both at pH 7.4 and 9.5.

The inhibitory effects of the test compounds (Fig. 2), including glutathione, synthetic selenium- and sulfur-containing compounds, and endogenous compounds, on the reaction of PN with L-tyrosine were examined (Figs. 3, 4, Table 1). The formation of 3-nitrotyrosine and 2,2'-dityrosine was detected with UV absorption at 270 nm and fluorescence at 410 nm excited with 295 nm light, respectively. All tested compounds were water-soluble at the concentration tested except melatonin, which was used after being well dispersed in water by sonication. Glutathione, serotonin and synthetic compounds, DTCP (**3**) and NEMP (**4**) effectively inhibited both the formation of 3-nitrotyrosine and 2,2'-dityrosine, and L-cystine had a very weak inhibitory effect on the 3-nitrotyrosine formation.¹⁹ Synthetic compounds, ADPP (**5**) and APCB (**6**), also inhibited the formation of 3-nitro-L-tyrosine and 2,2'-dityrosine. In the case of 5-MT, melatonin and *dl*-LA, the formation of 2,2'-dityrosine was not inhibited, but

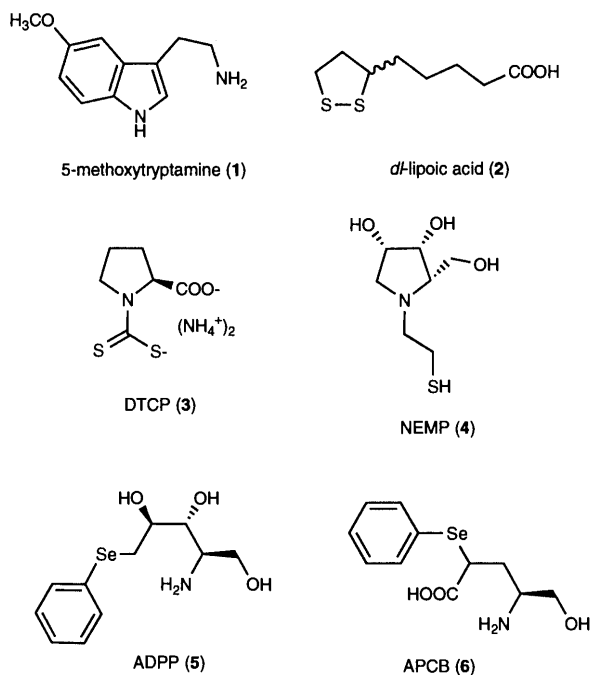


Fig. 2. Structures of Tested Compounds

The structures of endogenous and synthetic compounds used here are shown, except melatonin, serotonin, glutathione and L-cystine.

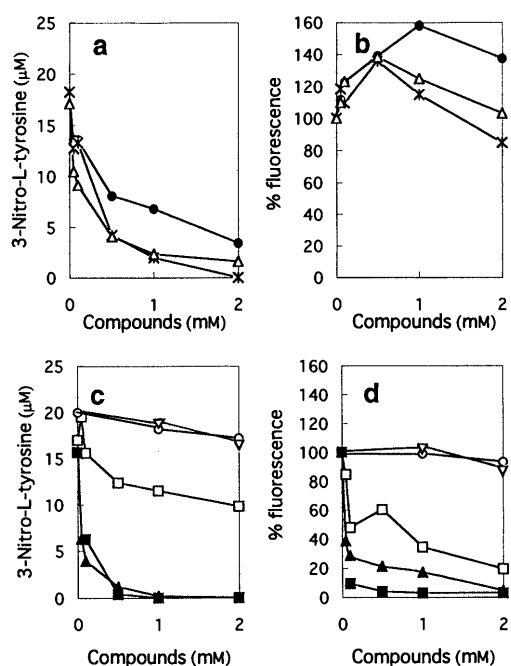


Fig. 3. Inhibitory Effects of Endogenous Compounds and DMPO on the Formation of 3-Nitro-L-tyrosine and 2,2'-Dityrosine by PN

PN and L-tyrosine were mixed in sodium phosphate buffer at pH 7.4 in the presence of various concentrations of test compounds. The formation of 3-nitro-L-tyrosine and 2,2'-dityrosine in the reaction mixture was detected. panel a and c: formation of 3-nitro-L-tyrosine, panel b and d: percent change of 2,2'-dityrosine fluorescence at 410 nm (ex. 295 nm). closed circles: 5-MT, asterisks: melatonin, open triangles: *dl*-LA, open squares: L-cystine, closed triangles: glutathione, closed squares: serotonin, open circles: DMPO, inverted triangles: PBN.

rather enhanced, although 3-nitrotyrosine was significantly inhibited.¹⁹⁾ Melatonin also inhibited the formation of 3-nitrotyrosine without inhibiting the formation of 2,2'-dityrosine (Fig. 3). Thus, these three reagents are thought to be a new type of inhibitor for the PN reaction because of their selective inhibitory activity for the nitration. Although some

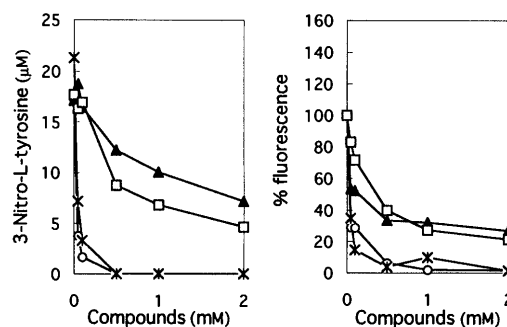


Fig. 4. Inhibitory Effects of Synthetic Compounds on the Formation of 3-Nitro-L-tyrosine and 2,2'-Dityrosine by PN

PN and L-tyrosine were mixed in sodium phosphate buffer at pH 7.4 in the presence of various concentrations of test compounds. The formation of 3-nitro-L-tyrosine and 2,2'-dityrosine in the reaction mixture was detected. panel a: formation of 3-nitro-L-tyrosine, panel b: percent change of 2,2'-dityrosine fluorescence at 410 nm (ex. 295 nm). open circles: DTCP, asterisks: NEMP, open squares: APCB, closed triangles: ADPP.

Table 1. Inhibitory Effects of Endogenous and Synthetic Compounds on 3-Nitro-L-Tyrosine and 2,2'-Dityrosine Formation

Compound	IC ₅₀ value (mM)	
	3-Nitro-L-tyrosine	2,2'-Dityrosine
Glutathione	0.04	0.042
Serotonin	0.08	0.055
L-Cystine	— ^{a)}	— ^{b)}
5-MT (1)	0.44	— ^{c)}
Melatonin	0.29	— ^{c)}
<i>dl</i> -LA (2)	0.15	— ^{c)}
DTCP (3)	0.032	0.035
NEMP (4)	0.038	0.038
ADPP (5)	1.53	0.15
APCB (6)	0.50	0.37

a) The compound did not inhibit the formation more than 50%. b) The IC₅₀ value was not calculated. c) The formation of 2,2'-dityrosine was enhanced.

radical species may be involved in this reaction based on the results obtained from the ESR experiment, the formation of both 3-nitrotyrosine and 2,2'-dityrosine was little affected by DMPO and PBN even at high concentration (>5 mM).

Without antioxidant compounds, a small amount of DOPA, another oxidized product of L-tyrosine by PN, was also detected in the reaction mixture using HPLC with an electrochemical detector. When glutathione or DTCP was used as the test compound, the amount of dopa detected first increased and then decreased with increase in the concentration of the test compound (Fig. 5). The initial increase of DOPA formation at a low concentration of test compound was assumed to be due to inhibition of further DOPA oxidation. When DOPA was treated with PN, a new product was detected by HPLC, which was considered to be the oxidized and polymerized product of DOPA. This dopa-derived product was also detected in the reaction mixture of PN and L-tyrosine. In the presence of 5-MT and LA, however, the formation of dopa was not affected. This result also supports that 5-MT and LA are selective inhibitors for the formation of 3-nitrotyrosine.

When the SC plasmid DNA was treated with 1 mM PN, DNA strand scission was observed as reported,²⁵⁾ but in this concentration range, the SC form of DNA did not completely disappear. The OC (single strand scission) and LN (double

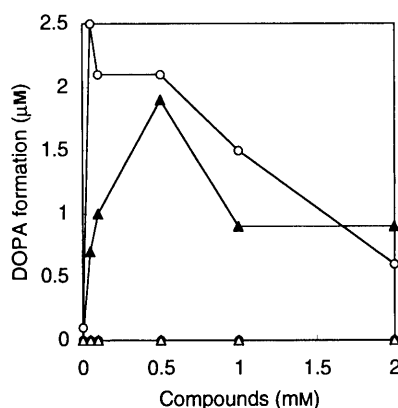


Fig. 5. The Formation of DOPA from L-Tyrosine with PN in the Presence of Test Compounds

PN and L-tyrosine were mixed in sodium phosphate buffer at pH 7.4 in the presence of various concentrations of test compounds. The formation of dopa in the reaction mixture was detected using a HPLC-electrochemical detector. open circles: DTCP, closed triangles: glutathione, closed circles: 5-MT, open triangles, dl-LA.

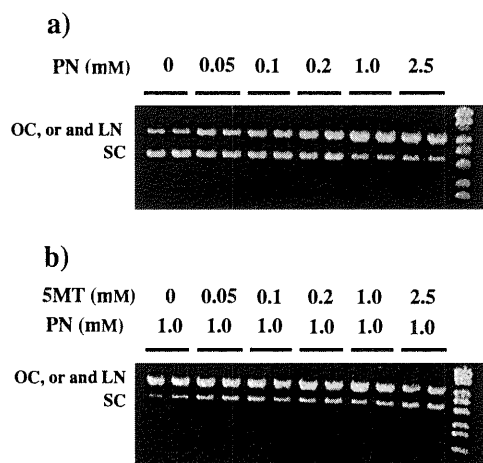


Fig. 6. Effect of 5-MT on the Plasmid DNA Scission by PN

Plasmid DNA pBR322 treated with PN was analyzed in the presence (a) and absence (b) of 5-MT by agarose gel electrophoresis and ethidium bromide staining. Three forms of pBR322 plasmid DNA, SC, OC and LN, were detected using a UV luminometer.

strand scission) form of DNA was increased in a dose dependent manner. This result showed that the DNA strands were broken by PN although its effect was less strong. In the presence of 5-MT, DNA strand breakage by 1 mM PN was not inhibited at less than 2 mM, and was only partly inhibited even at 5 mM of 5-MT (Fig. 6), although the tyrosine nitration by PN was effectively inhibited by 5-MT (IC_{50} value of 5-MT for 0.2 mM peroxynitrite = 0.48 mM).

Discussion

From the HPLC analysis, 3-nitro-L-tyrosine and 2,2'-dityrosine were confirmed to be produced from the reaction of PN with L-tyrosine, indicating they are nitration and oxidation products, respectively. The amount of 3-nitrotyrosine formed was dependent on the concentration of PN and L-tyrosine. In the reaction of decomposed PN (dilution of PN in phosphate buffer at pH 7.4 resulted in rapid decomposition and this solution was used for the reaction with tyrosine instead of PN) or nitrite anion with L-tyrosine, 3-nitrotyrosine and 2,2'-dityrosine were not detected. In the case of hydrogen peroxide treatment, 3-nitrotyrosine was not detected, but

a trace amount of dityrosine was formed. These results showed that the formation of 3-nitrotyrosine and 2,2'-dityrosine was the result of the reaction with PN, not with residual hydrogen peroxide, nitrate anion, or a decomposed product of PN.

Although there was a report on the inhibitory effects of glutathione and LA on tyrosine nitration,³⁾ the effects of antioxidants on the formation of dityrosine have not been investigated. Therefore, we studied the inhibitory effects of endogenous and newly synthetic potential antioxidants on the nitration and oxidation reaction by PN simultaneously. The formation of 3-nitrotyrosine by PN was effectively inhibited by glutathione, serotonin, the tested synthetic dithiocarbamate, thiol and selenium-containing compounds. The formation of 2,2'-dityrosine was also inhibited at a low concentration of glutathione and tested synthetic compounds. Thus, our synthetic compounds containing sulfur or selenium, DTCP, NEMP, ADPP and APCB, were as effective for the inhibition of PN reaction as was glutathione.

In the case of 5-MT, melatonin and LA, the formation of 3-nitrotyrosine was inhibited depending on the concentration. However the 2,2'-dityrosine formation was not inhibited, but rather increased at a lower dose. This result suggests that 5-MT, melatonin and LA selectively inhibited the nitration reaction of PN, and that the nitration and oxidation by PN proceeded, at least partly, via different intermediates. These endogenous compounds were selective scavengers for the nitrating intermediate of PN.

From the spin trapping study, tyrosyl radicals were shown to be formed in this reaction. This result supports the reaction pathway whereby PN is converted to a radical intermediate, and then a tyrosyl radical intermediate produced. However, the radical pathway in this reaction was not assumed to contribute much to the formation of nitrotyrosine and dityrosine, because DMPO and PBN, typical spin trapping reagents, did not affect their formation even at higher concentrations. Since dityrosine was thought to be formed by the dimerization of tyrosyl radicals, it was assumed that PN might react with tyrosine as a caged radical form such as $[ONO \cdots OH]$ without releasing free hydroxyl radicals.²⁶⁾ As described above, 5-MT, melatonin and LA inhibited only the nitration reaction. If the nitration of L-tyrosine and the dityrosine formation were carried out with the caged radical species, the tyrosyl radical formation by $\cdot OH$ -equivalent species and the addition of the $NO_2 \cdot$ -equivalent species should occur simultaneously for the nitrotyrosine formation. In this case, it is unlikely that 5-MT, melatonin or LA is able to inhibit the nitration of tyrosine selectively, because it is impossible for these reagents to react only with the nitrating $NO_2 \cdot$ -equivalent species in the caged radical pairs without interacting with the $\cdot OH$ -equivalent species. Moreover, $NO_2 \cdot$ also has the potential to subtract hydrogen atom from tyrosine to yield tyrosyl radicals. So, if 5-MT, melatonin or LA scavenges $NO_2 \cdot$ -equivalent species selectively, they have to inhibit the formation of both nitrotyrosine and dityrosine. From the results of the experiments with 5-MT, melatonin and LA, it was suggested that there are at least partly independent pathways to form 3-nitrotyrosine and 2,2'-dityrosine. It was assumed that 2,2'-dityrosine was formed from the dimerization of tyrosyl radicals derived by a caged radical like $[ONO \cdots OH]$, and that 3-nitrotyrosine was formed

via a non-radical pathway, that is, electrophilic addition of nitronium cation, which may exist in a caged dipolar form such as $[\text{ONO}^+ \dots ^-\text{OH}]$.²⁶⁾ For the selective inhibition of the nitration, 5-MT, melatonin and LA may scavenge only the caged dipolar intermediate.

In the reaction of plasmid DNA and PN, a SC form of DNA was changed to an OC and LN form by PN treatment, showing that PN caused DNA strand breakage, and suggesting that PN could produce a $\cdot\text{OH}$ -equivalent intermediate. However, the extent of the cleavage appeared to be weaker than the effect of $\text{Cu}(\text{en})_2\text{-H}_2\text{O}_2$ system, which was established to produce hydroxyl radicals,²⁷⁾ so PN may not produce a large amount of free hydroxyl radicals. In the presence of 5-MT, the extent of the OC and LN DNA formation by PN was only slightly inhibited. This means that 5-MT had little effect on the DNA cleavage by the $\cdot\text{OH}$ -equivalent intermediate of PN. This result suggested that 5-MT had no scavenging effect on the $\cdot\text{OH}$ -equivalent intermediate of PN, as in the case of the reaction of PN with L-tyrosine.

In this study, the inhibitory effects of synthetic and endogenous compounds on the formation of 3-nitrotyrosine and 2,2'-dityrosine were investigated simultaneously. The synthetic compounds tested efficiently inhibited both 3-nitro-L-tyrosine and 2,2'-dityrosine formation, and 5-MT, melatonin and LA were found to have a selective inhibitory activity for the nitration reaction of PN. These results suggest that the nitration and the oxidation by PN proceed at least in part separately, and nitration-selective inhibitors, 5-MT, melatonin and LA, should be very useful compounds to investigate reactive nitrogen species (RNS). Further investigation of the functional damage and modifications of protein tyrosine residues by PN and the protective effects of the compounds found in this study are in progress.

Acknowledgments Partial financial support by Grant-in-Aids for Scientific Research (No. 10357021, 11771475) from the Ministry of Education, Science, Sports and Culture, Japan, and a grant from the Cosmetology Research Foundation are gratefully acknowledged. This study was performed through Special Coordination Funds of the Science and Technology Agency of the Japanese Government.

References

- 1) Beckman J. S., Beckman T. W., Chen J., Marshall P. A., Freeman B. A., *Proc. Natl. Acad. Sci. U.S.A.*, **87**, 1620—1624 (1990).
- 2) Huie R. E., Padmaja S., *Free Radic. Res. Commun.*, **18**, 195—199 (1993).
- 3) Whiteman M., Tritschler H., Halliwell B., *FEBS Lett.*, **379**, 74—76 (1996).
- 4) Darley-Usmar V. M., Wiseman H., Halliwell B., *FEBS Lett.*, **369**, 131—135 (1995).
- 5) Darley-Usmar V. M., Hogg N. O., Leary V. J., Wilson M. T., Moncada S., *Free Radic. Res. Commun.*, **17**, 9—20 (1992).
- 6) White C. R., Brock T. A., Chang L. Y., Crapo J., Briscoe P., Ku D., Bradley W. A., Gianturco S. H., Gore J., Freeman B. A., Tarpey M. M., *Proc. Natl. Acad. Sci. U.S.A.*, **91**, 1044—1048 (1994).
- 7) Salgo M. G., Bermudez E., Squadrito G. L., Pryor W. A., *Arch. Biochem. Biophys.*, **322**, 500—505 (1995).
- 8) Squadrito G. L., Jin X., Pryor W. A., *Arch. Biochem. Biophys.*, **322**, 53—59 (1995).
- 9) Radi R., Beckman J. S., Bush K. M., Freeman B. A., *Arch. Biochem. Biophys.*, **288**, 481—487 (1991).
- 10) Radi R., Beckman J. S., Bush K. M., Freeman B. A., *J. Biol. Chem.*, **266**, 4244—4250 (1991).
- 11) King P. A., Anderson V. E., Edwards J. O., Gustafson G., Plumb R. C., Suggs J. W., *J. Am. Chem. Soc.*, **114**, 5430—5432 (1992).
- 12) Pryor W. A., Jin X., Squadrito G. L., *Proc. Natl. Acad. Sci. U.S.A.*, **91**, 11173—11177 (1994).
- 13) Van der Vliet A. O., Neill C. A., Halliwell B., Cross C. E., Kaur H., *FEBS Lett.*, **339**, 89—92 (1994).
- 14) Kong S. K., Yim M. B., Stadtman E. R., Chock P. B., *Proc. Natl. Acad. Sci. U.S.A.*, **93**, 3377—3382 (1996).
- 15) Gow A. J., Duran D., Malcolm S., Ischiropoulos H., *FEBS Lett.*, **385**, 63—66 (1996).
- 16) Li X., DeSarno P., Song L., Beckman J. S., Jope R. S., *Biochem. J.*, **331**, 599—606 (1998).
- 17) Pfeiffer S., Mayer B., *J. Biol. Chem.*, **273**, 27280—27285 (1998).
- 18) Whiteman M., Halliwell B., *Free Radic. Res.*, **25**, 275—283 (1996).
- 19) Nakagawa H., Sumiki E., Ikota N., Matsushima, Y., Ozawa T., *Antioxi. Redox Signaling*, **1**, 239—244 (1999).
- 20) Ikota N., Hama-Inaba H., *Chem. Pharm. Bull.*, **44**, 587—589 (1996).
- 21) Shinobu L. A., Jones S. G., Jones M. M., *Acta Pharmacol. Toxicol.*, **54**, 189—194 (1984).
- 22) Ikota N., *Heterocycles*, **29**, 1469—1472 (1989).
- 23) Ikota N., Hanaki A., *Chem. Pharm. Bull.*, **38**, 2712—2718 (1990).
- 24) Barr D. D., Gunther M. R., Deterding L. J., Tomer K. B., Mason R. P., *J. Biol. Chem.*, **271**, 15498—15503 (1996).
- 25) Salgo M. G., Stone K., Squadrito G. L., Battista J. R., Pryor W. A., *Biochem. Biophys. Res. Commun.*, **210**, 1025—10330 (1995).
- 26) Richeson C. E., Mulder P., Bowry V. W., Ingold K. U., *J. Am. Chem. Soc.*, **120**, 7211—7219 (1998).
- 27) Ozawa T., Hanaki A., *J. Chem. Soc., Chem. Commun.*, **1991**, 330—332.

Synthesis and Structure Studies of Complexes of Some Second Row Transition Metals with 1-(Phenylacetyl and Phenoxyacetyl)-4-phenyl-3-thiosemicarbazide

Sahar I. MOSTAFA* and Magdy M. BEKHEIT

Chemistry Department, Faculty of Science, Mansoura University, Mansoura, Egypt.

Received August 27, 1999; accepted October 18, 1999

The synthesis of the new complexes of 1-phenylacetyl-4-phenyl-3-thiosemicarbazide (H_2paps) and 1-phenoxyacetyl-4-phenyl-3-thiosemicarbazide (H_2p_oxaps); $[Ru(HL)_2(H_2O)_2]$, $[Rh(HL)_3]$, $[Ag(H_2L)(H_2O)_2](NO_3)$, *trans*- $[UO_2(HL)(bipy)(AcO)(H_2O)_2]$ ($H_2L=H_2paps$, H_2p_oxaps ; $bipy=2,2'$ -bipyridyl), $[Ag(H_2paps)(bipy)]^+$ and $[Pd(Hpaps)(bipy)]^+$ is described. Characterization of these complexes by IR, electronic and 1H -NMR spectra, conductometric titrations and thermal analysis is included. The complexes $[Ru(HL)_2(H_2O)_2]$ were found to be efficient catalysts for the oxidation of primary alcohols to aldehydes and acids, secondary alcohols to ketones and aryl halides to aldehydes and acids in the presence of $NaIO_4$ as co-oxidant.

Key words 1-(phenylacetyl or phenoxyacetyl)-4-phenyl-3-thiosemicarbazide; complexes; oxidation; spectra

Complexes of thiosemicarbazide and 1,4-substituted thiosemicarbazides are of general interest as models for bioinorganic processes.^{1–3} In our laboratory, many studies on transition metal complexes with thiosemicarbazide derivatives have been reported.^{4–9} As a part of continuing work on O, N¹⁰ and O, N, S^{4,9,11} donor ligands, complexes of 1-phenylacetyl-4-phenyl-3-thiosemicarbazide (H_2paps ; Fig. 1a) and 1-phenoxyacetyl-4-phenyl-3-thiosemicarbazide (H_2p_oxaps ; Fig. 1b) with some second row transition elements are now reported.

We have earlier reported first row transition metal complexes of H_2paps ⁹ and H_2p_oxaps ¹¹ in which they behave as neutral or mononegative bidentate and binegative tetradentate ligands. Here we report the synthesis of the new complexes of H_2paps and H_2p_oxaps with a number of second row transition elements. We also report their vibrational, electronic, 1H -NMR spectral data, conductometric titrations and thermal analysis. The catalytic oxidation of alcohols and aryl halides by ruthenium complexes, $[Ru(HL)_2(H_2O)_2]$ ($HL=Hpaps$, Hp_oxaps), in the presence of $NaIO_4$ as co-oxidant is also discussed.

Experimental

H_2paps and H_2p_oxaps were prepared by the reported methods.^{9,11}

Instrumentation IR spectra were measured using KBr discs on a Mattson 5000 FT-IR spectrometer. The electronic spectra were measured on Unicam UV2-100 UV-VIS spectrophotometer. Microanalyses were carried out by the Microanalytical Unit, Cairo University, Egypt. 1H -NMR spectra were measured on a Varian Gemini (200 MHz) spectrometer in National Research Centre, Cairo. Thermogravimetry (TG) measurements were made in a nitrogen atmosphere between 20 and 800 °C with a rate of 10 °C min⁻¹ using α - Al_2O_3 as a reference on a Shimadzu thermogravimetric analyzer TGA-50 by The Analytical Unit, Mansoura University. Conductometric measurements were carried out at room temperature on YSI Model 32 conductance meter.

Preparation of Complexes $[Ru(HL)_2(H_2O)_2] \cdot nH_2O$ ($HL=Hpaps$, $n=0$; $HL=Hp_oxaps$, $n=1$): Hydrated ruthenium trichloride (0.065 g, 0.25 mmol) in EtOH (25 ml) was added with stirring to H_2paps (0.285 g, 1 mmol) or H_2p_oxaps (0.301 g, 1 mmol). The reaction mixture was boiled under reflux for 2 h and 1 M AcONa (5 ml) was added. The fine brown (H_2paps) or pale brown (H_2p_oxaps) complexes were filtered off, washed with H_2O , EtOH, Et₂O and air-dried.

$[Rh(HL)_3] \cdot 2H_2O$ ($HL=Hpaps$, Hp_oxaps): Hydrated rhodium trichloride (0.105 g, 0.4 mmol) in EtOH (10 ml) was added to H_2paps (0.43 g, 1.5 mmol) or H_2p_oxaps (0.452 g, 1.5 mmol) in EtOH (20 ml). The mixture was boiled under reflux for 2 h to produce the yellow (H_2paps) or orange

(H_2p_oxaps) precipitates. These were filtered off, washed with EtOH, Et₂O and dried *in vacuo*.

$[Ag(H_2L)(H_2O)_2](NO_3) \cdot H_2O$ ($H_2L=H_2paps$, H_2p_oxaps): Silver nitrate (0.087 g, 0.5 mmol) in H_2O (1 ml) was added to H_2paps (0.143 g, 0.5 mmol) or H_2p_oxaps (0.151 g, 0.5 mmol) in EtOH (10 ml) to give yellow (H_2paps) or orange-brown (H_2p_oxaps) solids. These were left in the dark for 3 h, filtered off, washed with little H_2O , EtOH, Et₂O and dried in the dark *in vacuo*.

Trans- $[UO_2(HL)(bipy)(AcO)(H_2O)_2] \cdot nH_2O$ ($HL=Hpaps$, $n=3$; $HL=Hp_oxaps$, $n=0$; $bipy=2,2'$ -bipyridyl): Hydrated uranyl acetate (0.21 g, 0.5 mmol) in MeOH (10 ml) was added to a MeOH solution of 2,2'-bipyridyl (0.078 g, 0.5 mmol) and H_2paps (0.143 g, 0.5 mmol) or H_2p_oxaps (0.151 g, 0.5 mmol). The resulting solution was boiled under reflux for 3 h in a steam bath. The red-orange (H_2paps) or yellow (H_2p_oxaps) solutions were reduced in volume until the precipitates separated out. These were filtered off, washed with little MeOH and dried in a desiccator over silica gel.

$[Ag(H_2paps)(bipy)]BPh_4$: $AgNO_3$ (0.087 g, 0.5 mmol) in H_2O (0.5 ml) was added to 2,2'-bipyridyl (0.078 g, 0.5 mmol) in MeOH (25 ml) to form a colorless solution, to which H_2paps (0.143 g, 0.5 mmol) in MeOH (10 ml) was added to produce a red-brown solution. $NaBPh_4$ (0.17 g, 0.5 mmol) in MeOH (5 ml) was added and the precipitate was separated out. This was filtered off, washed with a little H_2O , MeOH, Et₂O and dried in the dark *in vacuo*.

$[Pd(Hpaps)(bipy)]BPh_4$: The complex $[Pd(bipy)Cl_2]$ was prepared by the literature method.¹² To a stirred suspension of $[Pd(bipy)Cl_2]$ (0.17 g, 0.5 mmol) in acetone (10 ml), H_2paps (0.143 g, 0.5 mmol) and KOH (0.056 g, 1 mmol) in MeOH (10 ml) was added. The mixture was stirred overnight. $NaBPh_4$ (0.17 g, 0.5 mmol) in MeOH (5 ml) was added to the resulting brown solution. The complex was filtered off, washed with MeOH, Et₂O and dried *in vacuo*.

Catalytic Oxidation For the catalytic oxidation by $[Ru(HL)_2(H_2O)_2]$ ($HL=Hpaps$, Hp_oxaps) complexes, the organic substrate (1.0 mmol) was added to $NaIO_4$ (2.5 mmol) in CCl_4 - CH_3CN - H_2O (1 : 1 : 2; 20 ml) and the catalyst (0.02 mmol). The reaction mixture was stirred under reflux at 70 °C, then cooled and extracted with diethyl ether (3 × 20 ml). The ethereal layer was then dried with anhydrous Na_2SO_4 and the aldehyde or ketone content quantified as its 2,4-dinitrophenylhydrazone derivatives. The aqueous layer

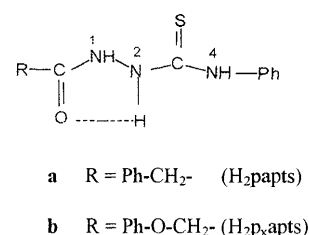


Fig. 1. Structure of 1-(Phenylacetyl and Phenoxyacetyl)-4-phenyl-3-thiosemicarbazide

* To whom correspondence should be addressed.

Table 1. Analytical and Spectroscopic Data of H₂papts, H₂p_xapts and their complexes

Compound	Found (Calcd) %				IR data (cm ⁻¹)	
	C	H	N	S	$\nu(\text{C}=\text{O})$	$\nu(\text{C}=\text{S})+\nu(\text{C}-\text{N})$ & $\nu(\text{C}=\text{S})$
H ₂ papts					1687	1230, 760
[Ru(Hpapts) ₂ (H ₂ O) ₂]	51.03 (51.06)	4.66 (4.54)	11.63 (11.91)	8.93 (9.08)	—	2125, 730
[Rh(Hpapts) ₃] · 2H ₂ O	55.00 (54.54)	4.50 (5.65)	12.61 (12.73)	9.56 (9.70)	—	1230, 760
[Ag(H ₂ papts)(H ₂ O) ₂](NO ₃) · H ₂ O	36.59 (36.66)	3.78 (3.87)	11.30 (11.41)	6.30 (6.52)	1649	1240, 745
[UO ₂ (Hpapts)(bipy)(AcO)(H ₂ O) ₂] · 3H ₂ O	37.53 (37.72)	3.95 (4.07)	8.06 (8.15)	3.80 (3.70)	—	1230, 750
[Ag(H ₂ papts)(bipy)]BPh ₄	67.71 (67.74)	4.78 (4.95)	8.00 (8.06)	3.71 (3.69)	1650	1235, 750
[Pd(Hpapts)(bipy)]BPh ₄	67.90 (67.95)	4.79 (4.85)	8.01 (8.09)	3.73 (3.70)	—	1215, 750
H ₂ p _x apts					1670	1225, 747
[Ru(Hp _x apts) ₂ (H ₂ O) ₂] · 2H ₂ O	47.63 (47.68)	4.51 (4.50)	11.10 (11.13)	8.50 (8.48)	—	1230, 745
[Rh(Hp _x apts) ₃] · 2H ₂ O	51.54 (51.98)	4.47 (4.43)	12.05 (12.13)	9.34 (9.24)	—	1225, 740
[Ag(H ₂ p _x apts)(H ₂ O) ₂](NO ₃) · H ₂ O	35.50 (35.50)	3.75 (3.75)	10.81 (11.04)	6.08 (6.31)	1650	1235, 748
[UO ₂ (Hp _x apts)(bipy)(AcO)(H ₂ O) ₂]	39.42 (39.46)	3.86 (3.76)	8.59 (8.53)	3.85 (3.90)	—	1230, 760

Compound	¹ H-NMR data (δ /ppm) ^{a)}									
	$\nu(\text{C}=\text{N})$	$\nu(\text{C}-\text{O})$	$\nu(\text{N}-\text{N})$	$\nu(\text{M}-\text{O})$	$\nu(\text{M}-\text{N})$	CH ₂ (s)	Ph-ring (m)	N ¹ H (s)	N ² H (s)	N ⁴ H (s)
H ₂ papts	—	—	990	—	—	3.55	7.1—7.5	10.15	9.85	9.75
[Ru(Hpapts) ₂ (H ₂ O) ₂]	1610	1080	1000	530	400	3.60	7.1—7.5	—	10.0	9.85
[Rh(Hpapts) ₃] · 2H ₂ O	1600	1080	1010	520	340	3.55	7.15—7.6	—	9.95	9.85
[Ag(H ₂ papts)(H ₂ O) ₂](NO ₃) · H ₂ O	—	1380 ^{b)}	1020	490	410	3.80	7.2—7.6	10.60	10.2	10.0
[UO ₂ (Hpapts)(bipy)(AcO)(H ₂ O) ₂] · 3H ₂ O	1600	1065	1015	910 ^{c)}	330	—	—	—	—	—
[Ag(H ₂ papts)(bipy)]BPh ₄	—	—	1020	495	415	3.74	d	10.40	10.2	10.05
[Pd(Hpapts)(bipy)]BPh ₄	1610	1067	1020	515	350	3.63	d	—	10.0	9.9
H ₂ p _x apts	—	—	970	—	—	3.50	6.9—7.4	10.25	9.7	9.6
[Ru(Hp _x apts) ₂ (H ₂ O) ₂] · 2H ₂ O	1605	1070	1020	500	—	3.55	7.1—7.5	—	9.9	9.65
[Rh(Hp _x apts) ₃] · 2H ₂ O	1610	1075	1020	500	415	3.68	7.1—7.6	—	9.9	9.7
[Ag(H ₂ p _x apts)(H ₂ O) ₂](NO ₃) · H ₂ O	—	1383 ^{b)}	1020	495	—	3.72	7.0—7.4	10.43	10.1	9.8
[UO ₂ (Hp _x apts)(bipy)(AcO)(H ₂ O) ₂]	1260	1060	1005	900 ^{c)}	400	—	—	—	—	—

a) ¹H-NMR spectra in CDCl₃ solution. b) $\nu(\text{NO}_3)$. c) $\nu^{\text{as}}(\text{UO}_2)$ and d) ¹H-NMR band interferes with the tetraphenyl protons (complicated multiplet).

was acidified with 5 M H₂SO₄ to pH 2, extracted with diethyl ether (3×20 ml), dried and evaporated to give the acid.

Conductometric Titration To determine the stoichiometric ratios of some of the studied complexes, conductometric titrations were carried out at room temperature. 25 cm³ of 10⁻³ M RuCl₃ or RhCl₃ in EtOH, AgNO₃ or AgNO₃-bipy (1:1) in 99% EtOH, and K₂PdCl₄-bipy (1:1) in 80% EtOH were titrated against 10⁻² M H₂papts or H₂p_xapts in EtOH. The titrations were carried out twice to test the reproducibility.

Results and Discussion

Preparations The ruthenium complexes [Ru(HL)₂(H₂O)₂] (HL=Hpapts, Hp_xapts) were prepared from hydrated ruthenium trichloride and the corresponding ligand in EtOH under basic conditions while the rhodium complexes [Rh(HL)₃] (HL=Hpapts, Hp_xapts) were obtained from the reaction of hydrated rhodium trichloride and H₂L in EtOH. The complexes [Ag(H₂L)(H₂O)₂](NO₃) (H₂L=H₂papts, H₂p_xapts) were produced from very concentrated aqueous solution of AgNO₃ and H₂L in EtOH while the *trans*-[UO₂(HL)(bipy)(AcO)(H₂O)₂] complexes were prepared from the reaction of uranyl acetate, bipy and H₂L in MeOH. The [Ag(H₂papts)(bipy)]⁺ complex was made from AgNO₃,

bipy and H₂papts in aqueous-EtOH solution while [Pd(Hpapts)(bipy)]⁺ was isolated from the reaction of [Pd(bipy)Cl₂] and H₂papts in acetone-MeOH solution in the presence of KOH.

Vibrational Spectra The IR spectral data of H₂papts and H₂p_xapts and a number of their complexes have been reported.^{9,11)} In Table 1, the IR spectra of H₂papts, H₂p_xapts and their complexes are listed with provisional assignments of selected vibrations. As expected, the free ligands exhibit broad absorption bands near 2200 and 1950 cm⁻¹ assigned to the stretching and bending vibrations of intramolecular hydrogen bonding $\nu(\text{N}(2)\text{H}\cdots\text{O})$;¹³⁾ these are not observed in the spectra of any of the complexes, indicating the involvement of the N(2) center in coordination.^{4,9,11)} This view is further supported by the slight shift of the bands at *ca.* 3300—3150 cm⁻¹ region and 990 cm⁻¹ in the free ligands and complexes owing to $\nu(\text{NH})$ and $\nu(\text{N}-\text{N})$ vibrations, respectively.⁵⁾

In the case of Ag(I) complexes, [Ag(H₂L)(H₂O)₂]⁺ (H₂L=H₂papts, H₂p_xapts) and [Ag(H₂papts)(bipy)]⁺, the strong bands near 1680 cm⁻¹ in the free ligands arising from

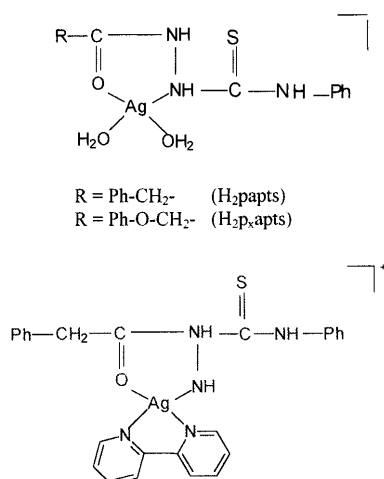


Fig. 2. Structure of $[\text{Ag}(\text{H}_2\text{L})(\text{H}_2\text{O})_2]^+$ ($\text{H}_2\text{L}=\text{H}_2\text{paps}$, $\text{H}_2\text{p}_x\text{paps}$) and $[\text{Ag}(\text{H}_2\text{paps})(\text{bipy})]^+$ Complexes

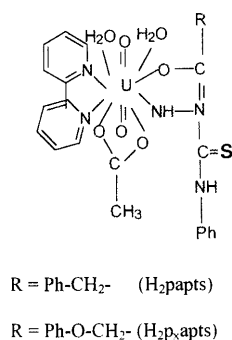


Fig. 3. Structure of $[\text{UO}_2(\text{HL})(\text{bipy})(\text{AcO})(\text{H}_2\text{O})_2]$ ($\text{HL}=\text{Hpaps}$, Hp_xpaps) Complexes

$\nu(\text{C}=\text{O})$ are affected upon coordination and shifted to lower wave number, as expected since the carbonyl oxygen centers are involved in coordination.^{14,15} This means that both H_2paps and $\text{H}_2\text{p}_x\text{paps}$ behave as neutral bidentate ligands as shown in Fig. 2. In the other reported complexes, the stretching vibrations $\nu(\text{C}=\text{O})$ of the free ligands are missing in the complexes indicating the participation of the deprotonated enolic carbonyl oxygen ($=\text{C}-\text{O}^-$) in coordination. This feature is further supported by the observation of new bands near 1600 and 1075 cm^{-1} due to $\nu(\text{C}=\text{N})$ ¹⁶ and $\nu(\text{C}-\text{O})$ ¹⁷ vibrations, respectively. In the uranyl complexes, *trans*- $[\text{UO}_2(\text{HL})(\text{bipy})(\text{AcO})(\text{H}_2\text{O})_2]$ ($\text{HL}=\text{Hpaps}$, Hp_xpaps), (Fig. 3) two extra bands are observed near 1540 and 1400 cm^{-1} attributed to $\nu^{\text{as}}(\text{OCO})$ and $\nu^{\text{s}}(\text{OCO})$ of the acetato group, respectively, indicating asymmetric bidentate coordination of the acetato group¹⁸ ($\Delta(\text{OCO})$ between $\nu^{\text{as}}(\text{OCO})$ and $\nu^{\text{s}}(\text{OCO})$ is in the 140 cm^{-1} region¹⁸). Also, the uranyl complexes show strong IR bands near 900 cm^{-1} assigned to $\nu^{\text{as}}(\text{UO}_2)$ of the *trans*- $\text{O}=\text{U}=\text{O}$ group.^{14,19} When the hydro complexes, $[\text{Ru}(\text{HL})_2(\text{H}_2\text{O})_2]$, $[\text{Ag}(\text{H}_2\text{L})(\text{H}_2\text{O})_2]^+$ and *trans*- $[\text{UO}_2(\text{HL})(\text{bipy})(\text{AcO})(\text{H}_2\text{O})_2]$ ($\text{HL}=\text{Hpaps}$, Hp_xpaps) were heated up to 120 °C, no water molecules were removed indicating their presence in the coordination sphere.⁹ The IR band near 750 cm^{-1} in the free ligands arising from $\nu(\text{C}=\text{S})$ vibrations remain more or less in the same position in the complexes indicating that the thione group is not taking part in complexation.⁹

Table 2. Electronic Spectral Data for H_2paps and $\text{H}_2\text{p}_x\text{paps}$ Complexes

Compound	Electronic spectra ^{a)} ($\lambda_{\text{max}}/\text{nm}$ ($\epsilon_0 \text{ dm}^3 \text{ mol}^{-1} \text{ cm}^{-1}$))
H_2paps	
$[\text{Ru}(\text{Hpaps})_2(\text{H}_2\text{O})_2]$	518 (532), 430 (885), 305 (7075)
$[\text{Rh}(\text{Hpaps})_3] \cdot 2\text{H}_2\text{O}$	610 (490), 520 (5636), 410 (15760)
$[\text{Ag}(\text{H}_2\text{paps})(\text{H}_2\text{O})_2]\text{NO}_3$	520 (661), 315 (18352)
$[\text{Ag}(\text{H}_2\text{paps})(\text{bipy})]^+$	515 (338), 308 (6916)
$[\text{Pd}(\text{Hpaps})(\text{bipy})]^+$	480 (225), 330 (20067)
$\text{H}_2\text{p}_x\text{paps}$	
$[\text{Ru}(\text{Hp}_x\text{paps})_2(\text{H}_2\text{O})_2] \cdot \text{H}_2\text{O}$	525 (437), 428 (1195), 310 (6877)
$[\text{Rh}(\text{Hp}_x\text{paps})_3] \cdot 2\text{H}_2\text{O}$	595 (65), 490 (250), 400 (1755)
$[\text{Ag}(\text{H}_2\text{p}_x\text{paps})(\text{H}_2\text{O})_2]\text{NO}_3$	534 (207), 300 (14010)

a) Spectra in DMSO solutions.

Most of the reported complexes show new bands near 510 and 380 cm^{-1} which may arise from $\nu(\text{M}-\text{O})$ ^{14,20,21} and $\nu(\text{M}-\text{N})$ ^{10,22,23} stretching, respectively. The complexes, $[\text{Ag}(\text{H}_2\text{L})(\text{H}_2\text{O})_2](\text{NO}_3)$ ($\text{H}_2\text{L}=\text{H}_2\text{paps}$, $\text{H}_2\text{p}_x\text{paps}$) show new strong band at 1385 cm^{-1} , which may be assigned to $\nu(\text{NO}_3^-)$ proving the presence of NO_3^- as a free ion in these complexes.²⁴

Electronic Spectra The electronic spectra in dimethyl sulphoxide for some complexes are given in Table 2. The electronic spectra of $[\text{Ru}(\text{HL})_2(\text{H}_2\text{O})_2]$ ($\text{HL}=\text{Hpaps}$, Hp_xpaps) show three bands near 520, 430 and 300 nm which may arise from $^1\text{A}_{1g} \rightarrow ^1\text{T}_{1g}$, $^1\text{A}_{1g} \rightarrow ^1\text{T}_{2g}$ and ligand ($\pi \rightarrow \pi^*$) to metal transitions, respectively, this indicates a low-spin octahedral arrangement around the diamagnetic $\text{Ru}(\text{II})$.^{23,25} The electronic spectra of $[\text{Rh}(\text{HL})_3]$ ($\text{HL}=\text{Hpaps}$, Hp_xpaps) exhibit three bands observed in the regions 610—595, 520—490 and 410—400 nm which may be assigned to $^1\text{A}_{1g} \rightarrow ^3\text{T}_{1g}$, $^1\text{A}_{1g} \rightarrow ^1\text{T}_{1g}$ and $^1\text{A}_{1g} \rightarrow ^1\text{T}_{2g}$ transitions, respectively, due to the octahedral geometry around $\text{Rh}(\text{III})$.^{14,26,27} The electronic spectra of $[\text{Pd}(\text{Hpaps})(\text{bipy})]^+$ shows two bands at 480 and 330 nm due to $^1\text{A}_{1g} \rightarrow ^1\text{B}_{1g}$ and $^1\text{A}_{1g} \rightarrow ^1\text{E}_g$ transitions, respectively, in a square planar configuration.^{9,25,28} The electronic spectra of silver(I) complexes show bands in the 540—510 and 330—300 nm regions, which may be attributed to square planar stereochemistry.²⁹

¹H-NMR Spectra The ¹H-NMR spectroscopic data of H_2paps and $\text{H}_2\text{p}_x\text{paps}$ and some of their complexes in CDCl_3 are given in Table 1, and are in close agreement with the reported data.^{9,11} In the free ligands, the aromatic protons appear in the δ 7.1—7.5 ppm region.^{25,30} The CH_2 protons give a singlet at δ 3.55 ppm while the N(1)H, N(2)H and N(4)H protons appear as singlets in the regions δ 10.40—10.15, 10.2—9.85 and 10.05—9.75 ppm, respectively; similar features have been observed for the 1-morpholineacetyl-4-phenyl-3-thiosemicarbazide (MPTSC).³¹

In the complexes, the resonance arising from the N(1)H proton disappears, whereas that arising from the N(2)H proton shifts to downfield⁹ values indicating the chelation of the ligands through the deprotonated enolic carbonyl oxygen ($=\text{C}-\text{O}^-$) and the N(2) centers to the metal ion. The ¹H-NMR of $[\text{Ag}(\text{H}_2\text{L})(\text{H}_2\text{O})_2](\text{NO}_3)$ ($\text{H}_2\text{L}=\text{H}_2\text{paps}$, $\text{H}_2\text{p}_x\text{paps}$) and $[\text{Ag}(\text{H}_2\text{paps})(\text{bipy})]^+$ are of particular interest since the N(1)H and N(2)H protons are shifted downfield indicating a decrease in the electron density caused by the withdrawing of electrons by $\text{Ag}(\text{I})$ from the coordinating centers.¹⁹

Conductometric Titrations The conductance of a solu-

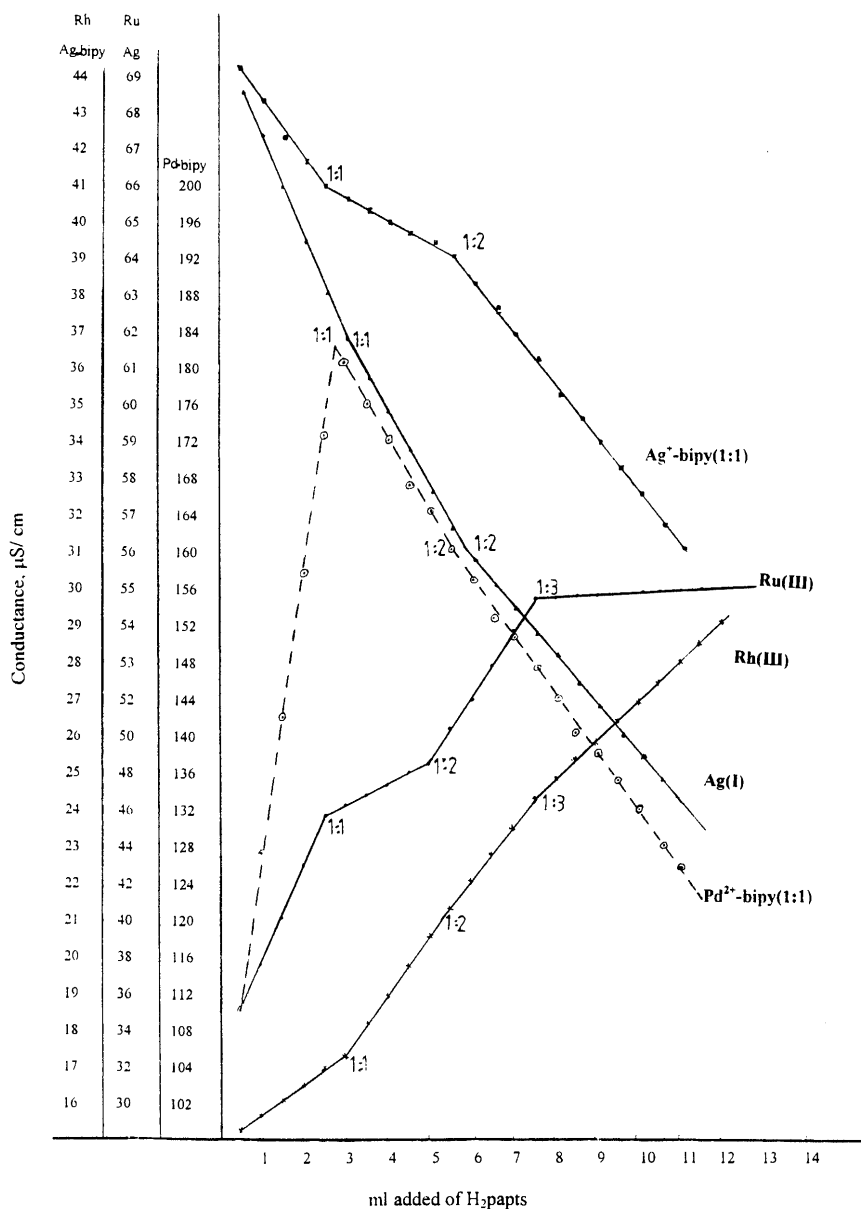


Fig. 4. Conductograms of the Metal Salts with H_2papts

tion, at a certain temperature, is affected by the mobility of the ions present. Thus, the formation of a complex in a solution can be characterized by using conductometric titrations.³²⁾ The composition of the complexes can be determined by studying the relation between the conductance measured and the volume of ligand added to the metal ion solution. The plots consist of some lines with different slopes, each intersection gives a certain molar ratio of complex formation.³³⁾

Figures 4 and 5 show the relation between the conductance of $Ru(III)$, $Rh(III)$, $Ag(I)$, $Ag(I)$ -bipy (1 : 1) and $Pd(II)$ -bipy (1 : 1) and the added volumes of H_2papts and H_2p_xapts , respectively. It is clear that, the molar ratios $M:L$, $M:2L$ are formed in all cases as well as $M:3L$ in the case of $Rh(III)$ with both ligands and $Ru(III)$ with H_2papts . The continuous increase in the conductance of the solution in successive additions of the ligand may be owing to the liberation of highly conducting hydrogen ions from the enolised hydroxyl center during complex formation^{34,35)} as supported from the IR spectral data. The decrease in the conductance of metal ions

solutions with the ligand additions may be attributed to the replacement of hydrogen ions of high conductivity by another species with low conductivity.

Thermal Studies The thermal decompositions of the complexes, $[Ru(Hpaps)_2(H_2O)_2]$, $[Rh(Hp_xapts)_3] \cdot 2H_2O$ and *trans*- $[UO_2(Hp_xapts)(bipy)(AcO)(H_2O)_2]$ were studied using the TG technique. The thermogram of the $[Ru(Hpaps)_2(H_2O)_2]$ complex shows firstly a weight loss endothermic step between 170 and 312 °C, which may be corresponding to the release of the coordinated water molecules and a phenylthiourido ($C_7H_7N_2S$) fragment^{9,36)} (Found: 27.26; Calcd: 26.52%). The second weight loss step (Found: 22.93; Calcd: 21.42%) between 321 and 410 °C may be attributed to elimination of the phenylthiourido fragment from the second ligand species while between 410 and 451 °C, a weight loss (Found: 16.88; Calcd: 16.59%) may arise from the elimination of the phenylethylimio (C_8H_7N) fragment¹¹⁾ from one ligand species. The last decomposition step at 521 °C may consist of the formation of mixed carbide- RuO_2 residue (Found: 28.34%). The TG curve of $[Rh$

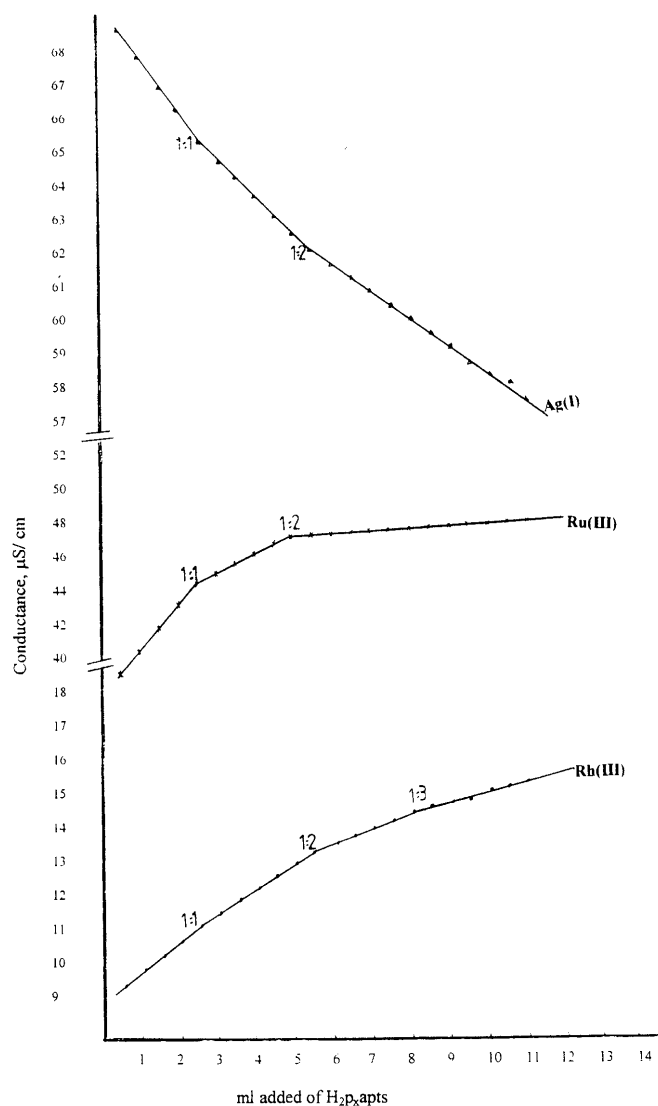


Fig. 5. Conductograms of the Metal Salts with H_2P_xapts

$(Hp_xapts)_3 \cdot 2H_2O$ shows the first weight loss between 80 and 170 °C, which may be due to the release of water molecules (Found: 3.38; Calcd: 3.47%) while the endothermic weight loss between 170 and 308 °C, which may be due to the release of two phenylthiourido fragments^{9,36} (Found: 29.63; Calcd: 29.07%). There are two other TG inflections in the ranges 308–332 and 351–404 °C, the first weight loss in these inflections may arise from the release of the third phenylthiourido (Found: 14.95; Calcd: 14.53%). The last decomposition step may consist of the elimination of two phenoxyethylimio fragments¹¹ (Found: 25.63; Calcd: 25.60%), leaving Rh_2O_3 representing (Found: 22.79; Calcd: 24.43%).²⁶ The thermogram of $trans-[UO_2(Hp_xapts)(bipy)(AcO)(H_2O)_2]$ shows three TG inflections in the ranges 161–345, 345–406 and 406–497 °C. The first weight loss may arise from the release of the coordinated water molecules and the phenylthiourido fragment^{11,36} (Found: 22.46; Calcd: 22.77%) while the second step is attributed to the removal of the acetate species^{37,38} (Found: 6.98; Calcd: 7.18%). The last TG inflection may be corresponding to the release of a half of the bipy molecule³⁹ (Found: 9.08; Calcd: 9.50%) followed by mixed carbide- U_3O_8 residue formation at 505 °C (Found: 63.70%) of the initial weight of the complex.

Table 3. Catalytic Oxidations by $[Ru(HL)_2(H_2O)_2]$ (HL = $Hpaps$, Hp_xaps) Complexes^{a)}

Substrate	$[Ru(Hpaps)_2(H_2O)_2]$ Yield %	Turn Over	$[Ru(Hp_xaps)_2(H_2O)_2]$ Yield %	Turn Over
Benzyl alcohol	60 ^{ald} , 14 ^{ac}	40.5	82 ^{ald} , 19 ^{ac}	52
3,4-Dimethoxybenzyl alcohol	68 ^{ald} , 12 ^{ac}	40	73 ^{ald} , 14 ^{ac}	51
α -Tetralol	90 ^k	45.5	93 ^k	47
Benzohedrol	64 ^k	33	70 ^k	36
Benzylchloride	42 ^{ald} , 14 ^{ac}	29	46 ^{ald} , 10 ^{ac}	29
<i>p</i> -Methoxybenzylchloride	80 ^{ald} , 16 ^{ac}	49	84 ^{ald} , 16 ^{ac}	51

a) Oxidation of alcohols were carried out for 3 h, those of aryl halides for 4 h, all at 70 °C by using 0.02 mmol of catalyst, 2.5 mmol of $NaIO_4$ (co-oxidant) in $CCl_4-CH_3CN-H_2O$ (1 : 1 : 2, 20 cm³), ^{ald}corresponding aldehyde, ^{ac}corresponding acid, ^kcorresponding ketone

Catalytic Oxidations We reported that the $[Fe^{III}(paps)Cl(H_2O)]$ complex could oxidize primary alcohols to aldehydes and secondary alcohols to ketones stoichiometrically in dichloromethane at room temperature.⁹⁾ The catalytic oxidation of alcohols by $[Ru^{III}Cl_2(NQ)(EPH_3)_2]$ ($E = P, As$)⁴⁰⁾ and $[Ru^{III}Cl_2(acac)(PPh_3)_2]$ ⁴¹⁾ using *N*-methylmorpholine-*N*-oxide (NMO) as co-oxidant in dichloromethane have been reported. Furthermore, the catalytic oxidation of lower valent ruthenium complexes in the presence of NMO⁴²⁾ or hydroquinones- $Co(salophen)(PPh_3)$ ($H_2salophen = N, N'$ -bis(salicylidene-*o*-phenylenediamine)⁴³⁾ as co-oxidants towards the oxidation of primary and secondary alcohols has been investigated. It was found that primary and secondary alcohols were oxidised to the corresponding carbonyl compounds. We tested the reported ruthenium complexes $[Ru(HL)_2(H_2O)_2]$ (HL = $Hpaps$, Hp_xaps) for possible organic catalytic oxidations by taking 0.02 mmol of the catalyst in $CCl_4-CH_3CN-H_2O$ (1 : 1 : 2) solution with $NaIO_4$ (2.5 mmol) as co-oxidant with 1.0 mmol of substrate, the reactions being carried out for 3 h in the case of alcohols and 4 h in the case of aryl halides, all at 70 °C. Aldehydes and ketones were detected and quantified as 2,4-dinitrophenylhydrazones derivatives and acids isolated and weighed as such, as shown in Table 3. Blank experiments were conducted under similar conditions, but in the absence of complexes; in all cases very small amounts of oxidation products were found.

References

- West D. X., Carlson C. S., Galloway C. P., Liberta A. E., Daniel C. R., *Transition Met. Chem.*, **15**, 91–95 (1991).
- Williams D. R., *Chem. Rev.*, **72**, 203–213 (1972).
- West D. X., Carlson C. S., Liberta A. E., Daniel C. R., *Transition Met. Chem.*, **15**, 341–344 (1990).
- Bekheit M. M., Elewady Y. A., Taha F. I., Mostafa S. I., *Bull. Soc. Chim. Fr.*, **128**, 178–183 (1991).
- Bekheit M. M., *Synth. React. Inorg. Met.-Org. Chem.*, **20**, 1273–1284 (1990).
- Bekheit M. M., Ibrahim K. M., Abu El-Reash G. M., *Bull. Soc. Chim. Fr.*, **1988**, 631–634.
- Khalifa M. E., Rakha T. H., Bekheit M. M., *Synth. React. Inorg. Met.-Org. Chem.*, **26**, 1149–1161 (1996).
- Abu El-Reash G. M., Bekheit M. M., Ibrahim K. M., *Transition Met. Chem.*, **15**, 357–360 (1990).
- Mostafa S. I., Bekheit M. M., El-Agez M. M., *Synth. React. Inorg. Met.-Org. Chem.*, to be submitted.
- Mostafa S. I., Abd El-Maksoud S. A., *Monatsh. Chem.*, **129**, 455–466 (1998).
- Rakha T. H., Mostafa S. I., El-Agez M. M., 5th International Conference on Chemistry and its Role in Development, Chem. Dept., Man-

- soura University, April (1999).
- 12) Griffith W. P., Mostafa S. I., *Polyhedron*, **11**, 871—877 (1992).
 - 13) Abu El-Reash G. M., Ibrahim K. M., Bekheit M. M., *Bull. Soc. Chim. Fr.*, **128**, 149—154 (1991).
 - 14) Mostafa S. I., *Transition Met. Chem.*, **23**, 397—401 (1998).
 - 15) Jha N. K., Joshi D. M., *Polyhedron*, **4**, 2083—2087 (1985).
 - 16) Aggarwal R. C., Singh N. K., Prasad L., *Indian J. Chem.*, **14A**, 325—327 (1976).
 - 17) Biradar N. S., Patil B. R., Kulkarni V. H., *J. Inorg. Nucl. Chem.*, **37**, 1901—1904 (1975).
 - 18) Lal R. A., Singh M. N., Das S., *Synth. React. Inorg. Met.-Org. Chem.*, **16**, 513—525 (1986).
 - 19) Griffith W. P., Mostafa S. I., *Polyhedron*, **11**, 2997—3005 (1992).
 - 20) Hingorani S., Singh K., Agarwala B. V., *J. Ind. Chem. Soc.*, **71**, 183—186 (1994).
 - 21) Leovac V. M., Jovanovic L. S., Bjelica L. J., Ceslijevec V. I., *Polyhedron*, **8**, 135—141 (1989).
 - 22) El-Hendawy A. M., *Polyhedron*, **10**, 2137—2143 (1991).
 - 23) Siddiqi Z. A., Qidwai S. N., Mathew V. J., *Synth. React. Inorg. Met.-Org. Chem.*, **23**, 709—722 (1993).
 - 24) Gutierrez M. D., Lopez R., Romero M. A., Salas J. M., *Cand. J. Chem.*, **66**, 249—255 (1988).
 - 25) Prabhakar B., Reddy K. L., Lingaiah P., *Indian J. Chem.*, **27A**, 217—221 (1988).
 - 26) Franchini G. C., Giusti A., Preti C., Tassi L., Zannini P., *Polyhedron*, **4**, 1553—1558 (1985).
 - 27) Sengupta S. K., Sahni S. K., Kapoor R. N., *Indian J. Chem.*, **19A**, 810—812 (1980).
 - 28) Lever A. B. P., "Inorganic Electronic Spectroscopy," Elsevier, New York, 1984.
 - 29) Dengel A. C., El-Hendawy A. M., Griffith W. P., Mostafa S. I., Williams D. J., *J. Chem. Soc. Dalton Trans.*, **1992**, 3489—3495.
 - 30) Mookerjee M. N., Singh R. N., Tandon J. P., *Indian J. Chem.*, **21A**, 388—390 (1982).
 - 31) Dhumwad S. D., Gudasi K. B., Goudar T. R., *Indian J. Chem.*, **33A**, 320—324 (1994).
 - 32) Pungor E., "A Practical Guide to Instrumental Analysis," CRC Press, Boca Raton, 1995.
 - 33) Srivastava A. K., Jain P. C., "Chemical Analysis"; An Instrumental Approach, S. Chand and Company Ltd., New Delhi, 1986.
 - 34) Abd El-Wahed M. G., El-Metwally S. M., Manakhly K. M. A., *Mat. Chem. Phys.*, **47**, 62—67 (1997).
 - 35) Abd El-Wahed M. G., Manakhly K. A., El-Metwally S. M., Hammad H. A., *Mat. Lett.*, **23**, 325—330 (1995).
 - 36) Zayed M. A., Nour El-Dein F. A., *Thermochim. Acta*, **114**, 359—371 (1987).
 - 37) Rakha T. H., Ibrahim K. M., Khalifa M. I., *Thermochim. Acta*, **144**, 53—63 (1989).
 - 38) Abu El-Reash G. M., Ibrahim K. M., Rakha T. H., *Transition Met. Chem.*, **14**, 209—212 (1989).
 - 39) Perlepes S. P., Garoufis A., Sletten J., Bakalbassis E. G., Plakatouras G., Katsarou E., Hadjiliadis N., *Inorg. Chim. Acta*, **261**, 93—102 (1997).
 - 40) El-Hendawy A. M., *Polyhedron*, **10**, 2511—2518 (1991).
 - 41) El-Hendawy A. M., El-Shahawy M. S., *Polyhedron*, **8**, 2813—2816 (1989).
 - 42) Sharpless K. B., Akashi K., Oshima K., *Tetrahedron Lett.*, **9**, 2503—2506 (1976).
 - 43) Backvall J. E., Chowdhury R. L., Karlsson U., *J. Chem. Soc., Chem. Commun.*, **1991**, 473—475.

Enantioselective Synthesis of (2*R*,4'*R*,8'*R*)- α -Tocopherol (Vitamin E) Based on Enzymatic Function¹⁾

Masako NOZAWA, Keiko TAKAHASHI, Keisuke KATO, and Hiroyuki AKITA*

School of Pharmaceutical Sciences, Toho University, 2-2-1 Miyama, Funabashi, Chiba 274-8510, Japan.

Received September 13, 1999; accepted November 7, 1999

Syntheses of (*S*)-chroman-2-carboxaldehyde congener **1** and (*S*)-chiral isoprene unit **3** were achieved based on the enzymatic acetylation of (\pm)-chroman-2-methanol **6** and (\pm)-(2,3)-*anti*-2-methyl-3-(*p*-methoxyphenyl)-1,3-propane diol **12**, respectively. Synthesis of the side-chain part corresponding to (3*R*,7*R*)-3,7,11-trimethyldodecan-1-ol **27** was achieved by the coupling reaction of (*S*)-**3** and (*R*)-3,7-dimethyloctyl iodide **4**. The Wittig reaction of (3*R*,7*R*)-phosphonium salt **2** derived from (3*R*,7*R*)-**27** and (*S*)-**1** gave the olefin **28** which was subjected to catalytic hydrogenation to afford (2*R*,4'*R*,8'*R*)- α -tocopherol.

Key words enantioselective acetylation; lipase; total synthesis; Vitamin E; (2*R*,4'*R*,8'*R*)- α -tocopherol

α -Tocopherol, a potent antioxidant and radical scavenger in chemical and biological systems, has increasingly been receiving attention in clinical and nutritional applications in human health. Therefore, attempts have been made to develop an efficient and stereocontrolled synthesis of the natural form of α -Tocopherol.²⁾ In terms of synthetic strategy, we considered the final carbon–carbon bond formation stage of our approach as involving a Wittig coupling of the chiral chroman-2-carboxaldehyde congener (*S*)-**1** with the 15-carbon phosphonium salt (3*R*,7*R*)-**2**. The chiral chroman part would be obtained based on the enantioselective acetylation of the racemic chroman diol (\pm)-**6**. The synthetic strategy for the side-chain moiety corresponding to the phosphonium salt (3*R*,7*R*)-**2** was based on the use of the chiral isoprene unit (*S*)-**3** in which the phenylsulfonyl group represents a reactive function capable of coupling with a ten-carbon synthon such as (3*R*)-3,7-dimethyloctyl iodide **4**.³⁾ In this paper, we wish to describe the syntheses of the chiral chroman aldehyde (*S*)-**1** and chiral isoprene unit (*S*)-**3** based on enzymatic acetylation and their application to the total synthesis of (2*R*,4'*R*,8'*R*)- α -tocopherol.

1) Synthesis of the Chiral Chroman Aldehyde (*S*)-1****
Reduction of the commercially available (\pm)-chroman-2-carboxylic acid **5** with LiAlH₄ was reported to give the (\pm)-chroman-2-methanol **6** in 42% yield.¹⁾ In order to improve the yield of (\pm)-**6**, the following four synthetic steps were undertaken to afford (\pm)-**6** in 81% overall yield from (\pm)-**5**.

Esterification of (\pm)-**5** with CH₂N₂ provided the corresponding methyl ester (\pm)-**7** (98% yield), which was treated with benzyl bromide (BnBr) and K₂CO₃ in acetone to give the benzyl ether (\pm)-**8** (93% yield). Reduction of (\pm)-**8** afforded an alcohol (\pm)-**9** (99% yield) which was subjected to catalytic hydrogenation to provide the desired (\pm)-**6** in 90% yield.

From a screening experiment for (\pm)-**6** using several kinds of commercially available lipases, lipase PL-266 from *Alcaligenes* sp. was found to be effective and the result is shown in Table 1. When vinyl acetate was employed as the acylating reagent (entry 1), (*S*)-acetate **10** (67% ee) and (*R*)-unchanged **6** (>99% ee) were obtained in 58% and 39% yields, respectively. Deprotection of (*S*)-**10** (67% ee) with LiAlH₄ gave the (*S*)-**6** (67% ee), which was repeatedly subjected to enzymatic acetylation to provide (*S*)-**10** (77% yield, >99% ee) and (*R*)-**6** (18% yield, 74% ee). The enantiomeric excess (ee) of the

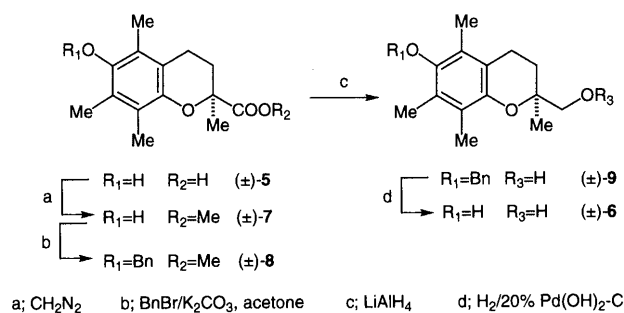


Chart 2

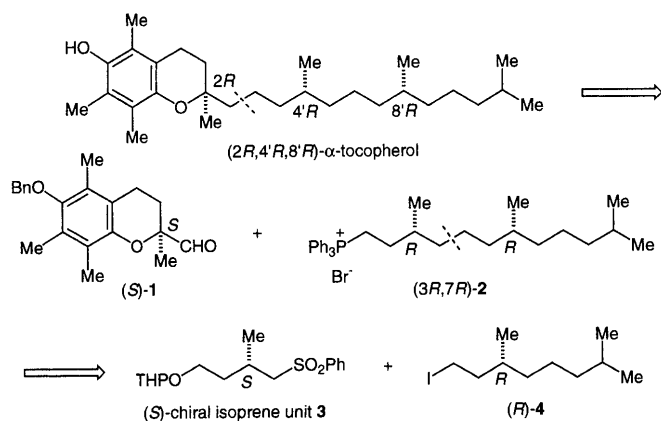
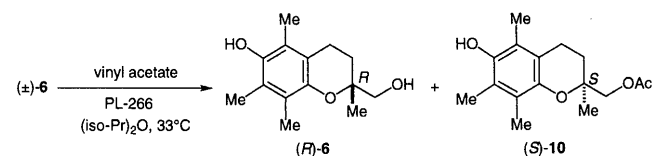


Chart 1

Table 1



Entry	Substrate (mg)	Time (h)	Products (% , % ee)
1	(\pm)- 6 (788)	6	(<i>R</i>)- 6 (39, >99) (<i>S</i>)- 10 (58, 67)
2	(<i>S</i>)- 6 (67% ee, 422) ^{a)}	4	(<i>R</i>)- 6 (18, 74) (<i>S</i>)- 10 (77, >99)

a) (*S*)-**6** (67% ee) was obtained by the reduction of (*S*)-**10** (67% ee) with LiAlH₄.

* To whom correspondence should be addressed.

(*R*)-unchanged **6** was determined by HPLC analysis on a Chiralcell OD column (250 mm×4.6 mm), while that of (*S*)-acetate **10** was confirmed by HPLC analysis of the corresponding diol (*S*)-**6** derived from the enzymatic product (*S*)-**10**. The absolute stereochemistry of the unchanged **6** was determined to be *R*-configuration by the fact that spectral data of the unchanged **6** ($[\alpha]_D +2.0$ ($c=1.0$, CH_2Cl_2) corresponding to >99% ee) were identical with those of the authentic (*S*)-**6**⁴) ($[\alpha]_D -2.36$ ($c=1.49$, CH_2Cl_2) corresponding to 98% ee) except for the sign of $[\alpha]_D$. Thus, the absolute configuration of (+)-**6** was determined to be *R* and that of the acetate **10** was confirmed to be *S*. Thus obtained (*S*)-**10** was subjected to benzylation with benzyl bromide in the presence of CsF to afford the corresponding benzyl ether (*S*)-**11** (87% yield), which was reduced with LiAlH_4 to provide the alcohol (*S*)-**9** (94% yield). Swern oxidation of (*S*)-**9** yielded the corresponding aldehyde (*S*)-**1** ($[\alpha]_D +12.6$ ($c=0.99$, CHCl_3)) in 95% yield.

2) Synthesis of the Chiral Isoprene Unit (*S*)-3**** The optically active (2,3)-*anti*-2-methyl-3-(*p*-methoxyphenyl)-1,3-propane diol **12** involving two stereogenic centers was selected as the target molecule corresponding to the chiral isoprene unit (*S*)-**3** because the *p*-methoxyphenyl group is convertible into a carboxylic acid or its congeners and the benzylic oxygen functional group can be reduced to give a useful chiral synthon possessing one stereogenic center. The Reformatsky reaction of *p*-anisaldehyde and methyl 2-bromopropionate was reported to afford (\pm)-*syn*-**13** (56% yield) and (\pm)-*anti*-**14** (42% yield).⁵ Treatment of (\pm)-*syn*-**13** with methane sulfonic acid (MeSO_3H) afforded the α,β -unsaturated ester **15** in 95% yield, which was subjected to LiAlH_4 reduction to provide the allyl alcohol **16** (90% yield). The stereochemistry of **16** was confirmed by the nuclear Over-

hauser effect (NOE) observed as shown in Fig 1. Hydroboration reaction of **16** gave the (\pm)-*anti*-1,3-diol **12** with high *anti*-diastereoselectivity (*anti/syn*=61:1) and subsequent crystallization provided a single isomer (\pm)-**12** in 89% overall yield. The ratio of *anti/syn* was determined by Chiralcel OD column (250 mm×4.6 mm, eluent, *n*-hexane/EtOH/*iso*-PrOH=300:10:5; detection, UV at 254 nm; flow rate, 1 ml/min, (\pm)-*anti*-**12**; 21.1 and 21.9 min, (\pm)-*syn*-**12**; 24.6 and 25.9 min). LiAlH_4 reduction of (\pm)-*anti*-**14** also yielded (\pm)-**12** in 96% yield.

Initially, (\pm)-**12** was subjected to a screening experiment using several kinds of commercially available lipases. Among them, lipase Amano P from *Pseudomonas* sp. was found to give the monoacetates (2*R*,3*R*)-**17** (57% yield, 65% ee) and (2*R*,3*R*)-**18** (3% yield, 80% ee), and the unchanged (2*S*,3*S*)-**12** (39% yield, ($[\alpha]_D -39.8$ ($c=1.05$, CHCl_3) corresponding to >99% ee) in the presence of vinyl acetate as an acyl donor as shown in Table 2.

Deprotection of (2*R*,3*R*)-**17** (65% ee) with K_2CO_3 in MeOH gave the (2*R*,3*R*)-**12** (65% ee), which was repeatedly subjected to enzymatic acetylation to afford the monoacetates (2*R*,3*R*)-**17** (76% yield, ($[\alpha]_D +20.9$ ($c=1.23$, CHCl_3) corresponding to 97% ee) and (2*R*,3*R*)-**18** (3% yield, ($[\alpha]_D +77.6$ ($c=1.08$, CHCl_3) corresponding to 94% ee) and the unchanged (2*S*,3*S*)-**12** (17% yield, 85% ee). The ee of the enzymatic reaction products was determined by HPLC analysis on a Chiralcell AD or OJ column (250 mm×4.6 mm). Acetylation of (2*R*,3*R*)-**17** (97% ee) followed by recrystallization gave the optically pure diacetate (2*R*,3*R*)-**19** ($[\alpha]_D +67.6$ ($c=1.06$, CHCl_3)) in 83% overall yield. In order to confirm the absolute structure of the present (+)-**19**, (+)-**19** was successfully converted to the mono alcohol **21**. Catalytic hydrogenolysis of (+)-**19** provided a monoacetate (+)-**20** (77% yield, ($[\alpha]_D +11.3$ ($c=1.08$, CHCl_3)), which was treated with K_2CO_3 in MeOH to afford the alcohol (–)-**21** in 96% overall yield. The spectral data ($[\alpha]_D -11.9$ ($c=1.02$, CHCl_3)) of **21** were identical with those ($[\alpha]_D -8.1$ ($c=0.64$,

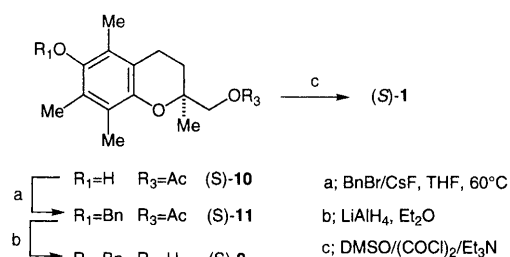


Chart 3

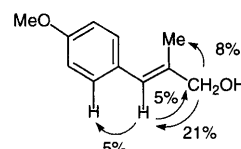


Fig. 1

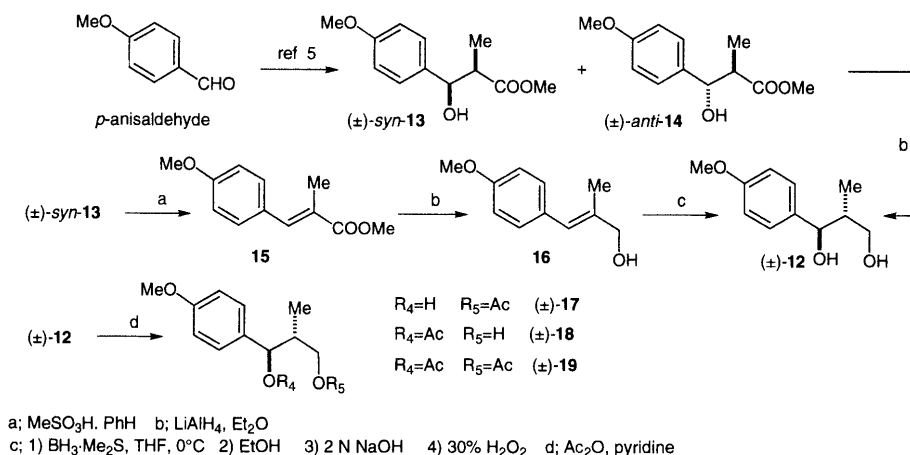
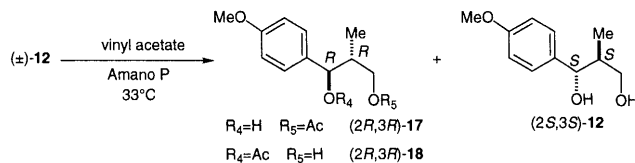


Chart 4

Table 2



Entry	Substrate (g)	Time (h)	Products (% ee)	Products (% ee)
1	(±)- 12 (12, 38)	1	(2 <i>R</i> ,3 <i>R</i>)- 17 (57, 65)	(2 <i>R</i> ,3 <i>R</i>)- 18 (3, 80)
2	(2 <i>R</i> ,3 <i>R</i>)- 12 (65% ee, 6.19) ^{a)}	0.5	(2 <i>R</i> ,3 <i>R</i>)- 17 (76, 97)	(2 <i>R</i> ,3 <i>R</i>)- 18 (3, 94)

a) (2*R*,3*R*)-**12** (65% ee) was obtained by treatment of (2*R*,3*R*)-**17** (65% ee) with K₂CO₃ in MeOH.

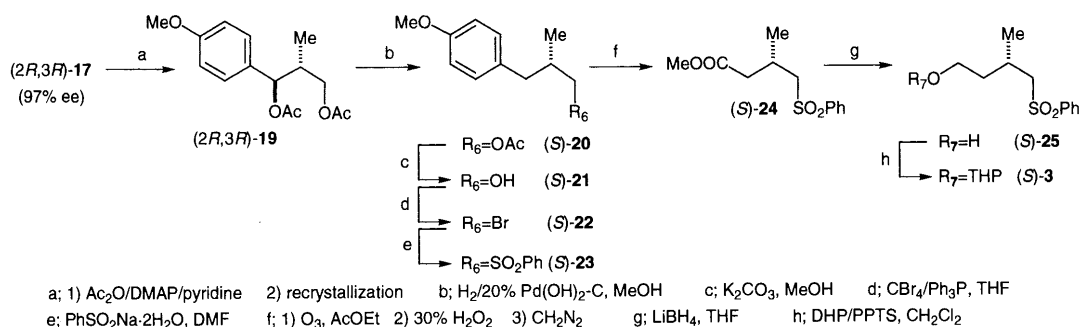


Chart 5

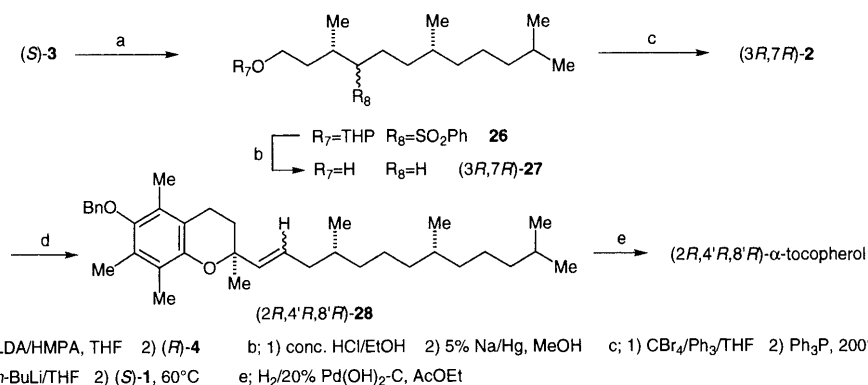


Chart 6

CHCl₃) of the reported for (*S*)-alcohol **21**.³⁾ Thus, the absolute configurations of (+)-**17** (97% ee) were determined to be 2*R*, 3*R* and those of (–)-**12** (>99% ee) were confirmed to be 2*S*, 3*S*. The absolute configurations of (+)-**18** were determined to be 2*R*, 3*R* by the fact that HPLC analysis pattern of the diol **12** derived from (+)-**18** was found to be opposite in comparison with that of (2*S*,3*S*)-**12** (97% ee). By applying the reported procedure,³⁾ thus obtained (*S*)-**21** was converted into the desired tetrahydropyranyl (THP) ether (*S*)-**3** in 53% overall yield (5 steps) as shown in Chart 5 and the overall yield (53%) was improved in comparison with the reported one (39%).³⁾

3) Total Synthesis of (2*R*,4'*R*,8'*R*)-α-Tocopherol The anion of (*S*)-**3** generated by treatment with lithium diisopropylamide (LDA) in the presence of hexamethylphosphoramide (HMPA) was subjected to alkylation with the iodide (*R*)-**4**³⁾ to give the coupling product **26** in 42% yield. Deprotection of the THP group in **26** with acid followed by reduction with Na/Hg in MeOH provided (3*S*,7*S*)-phytol **27** ([α]_D

+3.4 (*c*=1.49, CHCl₃)) in 88% overall yield. Bromination of (3*S*,7*S*)-**27** followed by treatment with triphenylphosphine (Ph₃P) gave the phosphonium salt (3*R*,7*R*)-**2**, which was subjected to the Wittig reaction with the (*S*)-chroman aldehyde **1** to afford a mixture of *Z*- and *E*-olefin **28** (*Z/E*=14:1) in 35% overall yield. Catalytic hydrogenation of **28** provided (2*R*,4'*R*,8'*R*)-α-Tocopherol ([α]_D –2.7 (*c*=0.59, benzene)) in 86% yield, whose spectral data were identical with those ([α]_D –3.0 (benzene))⁶⁾ of natural α-tocopherol.

In conclusion, chiral introductions at the 2*R* and 4'*R* positions in the synthesis of (2*R*,4'*R*,8'*R*)-α-tocopherol (vitamin E) were achieved based on the enzymatic acetylation of (±)-chroman-2-methanol **6** and (±)-(2,3)-anti-2-methyl-3-(*p*-methoxyphenyl)-1,3-propane diol **12**, respectively.

Experimental

All melting points were measured on a Yanaco MP-3S micro melting point apparatus and are uncorrected. ¹H-NMR spectra were recorded on a JEOL EX 400 spectrometer. Spectra were taken with 5–10% (w/v) solution in CDCl₃ with Me₄Si as an internal reference. The mass spectra, FAB and

El, were obtained with a JEOL JMS-600 and a JEOL JMS-AM II 50 spectrometer, respectively. IR spectra were recorded on a JASCO FT/IR-300 spectrometer. Optical rotations were measured with a JASCO DIP-370 digital polarimeter. All evaporations were performed under reduced pressure. For column chromatography, silica gel (Kieselgel 60) was employed.

Methyl 6-Hydroxy-2,5,7,8-tetramethylchroman-2-carboxylate (\pm)-7 A solution of (\pm)-5 (2.004 g, 8 mmol) in Et₂O (50 ml) was treated with a solution of CH₂N₂ in Et₂O to give a crude product, which was chromatographed on silica gel (70 g, *n*-hexane:AcOEt=10:1) to afford colorless powder (\pm)-7 (2.082 g, 98% yield). Recrystallization of (\pm)-7 from *n*-hexane-AcOEt provided colorless prism (\pm)-7. (\pm)-7: mp 74 °C. MS (EI) *m/z*: 264 (M⁺). IR (KBr): 3527, 1737 cm⁻¹. ¹H-NMR (CDCl₃) δ : 1.60 (3H, s), 1.86 (1H, ddd, *J*=6, 10.5, 13 Hz), 2.06 (3H, s), 2.15 (3H, s), 2.18 (3H, s), 2.42 (1H, ddd, *J*=3.5, 6.6, 13 Hz), 2.50 (1H, ddd, *J*=6, 10.5, 17 Hz), 2.64 (1H, ddd, *J*=3.5, 6.5, 17 Hz), 3.67 (3H, s), 4.29 (1H, s).

Methyl 6-Benzoyloxy-2,5,7,8-tetramethylchroman-2-carboxylate (\pm)-8 A mixture of (\pm)-7 (1.903 g, 7.2 mmol), benzyl bromide (2.6 ml, 21.9 mmol) and K₂CO₃ (1.49 g, 10.8 mmol) in acetone (50 ml) was refluxed for 12 h with stirring and the reaction mixture was filtered. The filtrate was evaporated, diluted with saturated brine and extracted with Et₂O. The organic layer was dried over MgSO₄ and evaporated to give a crude oil, which was chromatographed on silica gel (70 g, *n*-hexane:AcOEt=20:1) to provide colorless powder (\pm)-8 (2.371 g, 93% yield). Recrystallization of (\pm)-8 from *n*-hexane-AcOEt afforded colorless needles (\pm)-8. (\pm)-8: mp 86.5–87 °C. *Anal.* Calcd for C₂₂H₂₆O₄: C, 74.55; H, 7.39. Found C, 74.42; H, 7.49. MS (EI) *m/z*: 354 (M⁺). IR (KBr): 1745 cm⁻¹. ¹H-NMR (CDCl₃) δ : 1.63 (3H, s), 1.86–1.94 (1H, m), 2.14 (3H, s), 2.19 (3H, s), 2.24 (3H, s), 2.42–2.56 (2H, m), 2.61–2.69 (2H, m), 4.70 (2H, s), 7.35 (1H, d, *J*=7 Hz), 7.41 (2H, t, *J*=7 Hz), 7.50 (2H, d, *J*=7 Hz).

6-Benzoyloxy-2,5,7,8-tetramethylchroman-2-methanol (\pm)-9 A solution of (\pm)-8 (2.246 g, 6.34 mmol) in dry Et₂O (30 ml) was added to a suspension of LiAlH₄ (0.36 g, 9.49 mmol) in dry Et₂O (10 ml) at 0 °C and the whole mixture was stirred for 30 min. It was diluted with aqueous 2 M HCl and extracted with Et₂O. The organic layer was washed with saturated brine and dried over MgSO₄. Removal of organic solvent gave a crude product which was chromatographed on silica gel (40 g, *n*-hexane:AcOEt=5:1) to afford colorless powder (\pm)-9 (2.056 g, 99% yield). Recrystallization of (\pm)-9 from *n*-hexane gave colorless prism (\pm)-9. (\pm)-9: mp 62 °C. *Anal.* Calcd for C₂₁H₂₆O₃: C, 77.27; H, 8.03. Found C, 77.10; H, 8.15. MS (EI) *m/z*: 326 (M⁺). IR (KBr): 3260 cm⁻¹. ¹H-NMR (CDCl₃) δ : 1.23 (3H, s), 1.73–1.77 (1H, m), 1.94–2.06 (2H, m), 2.10 (3H, s), 2.17 (3H, s), 2.22 (3H, s), 2.61–2.72 (1H, m), 3.58–3.67 (2H, m), 4.70 (2H, s), 7.34 (1H, t, *J*=7 Hz), 7.40 (2H, t, *J*=7 Hz), 7.50 (2H, d, *J*=7 Hz).

6-Hydroxy-2,5,7,8-tetramethylchroman-2-methanol (\pm)-6 A solution of (\pm)-9 (235 mg, 0.72 mmol) in AcOEt (10 ml) was hydrogenated at ordinary temperature and pressure in the presence of 20% Pd(OH)₂-C (0.1 g). After hydrogen absorption had ceased, the catalyst was filtered off with the aid of Celite and the filtrate was evaporated. The residue was chromatographed on silica gel (10 g, *n*-hexane:AcOEt=4:1) to afford colorless powder (\pm)-6 (153 mg, 90% yield). Recrystallization of (\pm)-6 from AcOEt provided colorless powder (\pm)-6. (\pm)-6: mp 106.5 °C. *Anal.* Calcd for C₁₄H₂₀O₃: C, 71.16; H, 8.53. Found C, 70.95; H, 8.61. MS (EI) *m/z*: 236 (M⁺). IR (KBr): 3421 cm⁻¹. ¹H-NMR (CDCl₃) δ : 1.22 (3H, s), 1.73 (1H, ddd, *J*=4.5, 7, 14 Hz), 1.99 (1H, ddd, *J*=7, 9.5, 17 Hz), 2.11 (3H, s), 2.12 (3H, s), 2.16 (3H, s), 2.59–2.73 (2H, m), 3.59 (1H, d, *J*=11 Hz), 3.64 (1H, d, *J*=11 Hz). The racemate (\pm)-6 was analyzed to provide well separated peaks (44.9, 57.0 min) corresponding to the enantiomers using Chiralcel OD (4.6 mm×250 mm) under the following analytical conditions (eluent, *n*-hexane/EtOH=40:1; detection, UV at 254 nm; flow rate, 1 ml/min). On the other hand, the retention time (*t*_R) of authentic (*S*)-6 was found to be 57.0 min under the same analytical conditions as (\pm)-6.

Enantioselective Acetylation of (\pm)-6 with Lipase PL-266 1) A suspension of (\pm)-6 (788 mg, 3.34 mmol), lipase (0.79 g) and vinyl acetate (0.79 g) in iso-Pr₂O (200 ml) was incubated at 33 °C for 6 h. After the reaction mixture was filtered, the precipitate was washed with AcOEt. The combined organic layer was dried over MgSO₄ and evaporated. The residue was chromatographed on silica gel (30 g) to give acetate (*S*)-10 (538 mg, 58% yield, 67% ee) from *n*-hexane:AcOEt (10:1) eluent and alcohol (*R*)-6 (307 mg, 39% yield, >99% ee) from *n*-hexane:AcOEt (5:1) eluent, respectively. A part of (*R*)-6 was recrystallized from AcOEt to give colorless prism (*R*)-6. (*R*)-6: mp 89–89.5 °C. [α]_D²⁴ +2.0 (*c*=1.0, CH₂Cl₂). Spectral data (IR and ¹H-NMR) were identical with those of (\pm)-6. (*S*)-10: MS (EI) *m/z*: 278 (M⁺). IR (KBr): 3512, 1715 cm⁻¹. ¹H-NMR (CDCl₃) δ : 1.28 (3H, s), 1.79 (1H, dt, *J*=7, 12.5 Hz), 1.93 (1H, dt, *J*=7, 12.5 Hz), 2.09 (3H, s), 2.11

(3H, s), 2.15 (3H, s), 2.63 (2H, t, *J*=7 Hz), 4.08 (1H, d, *J*=11 Hz), 4.14 (1H, d, *J*=11 Hz). 2) A suspension of (*S*)-10 (67% ee, 499 mg, 1.79 mmol) and LiAlH₄ (102 mg, 2.69 mmol) in dry Et₂O (20 ml) was stirred at 0 °C for 1.5 h. The reaction mixture was worked up in the same way as for the preparations of (\pm)-9 and (\pm)-6 to give (*S*)-6 (67% ee, 423 mg, *t*_R=44.9 min (16.5%), *t*_R=57.0 min (83.5%)). A suspension of (*S*)-6 (422 mg, 67% ee, 1.79 mmol), lipase (0.42 g) and vinyl acetate (0.42 g) in iso-Pr₂O (60 ml) was incubated at 33 °C for 4 h. After the reaction mixture was filtered, the precipitate was washed with AcOEt. The combined organic layer was dried over MgSO₄ and evaporated. The residue was chromatographed on silica gel (30 g) to give acetate (*S*)-10 (383 mg, 77% yield, >99% ee) from *n*-hexane:AcOEt (10:1) eluent and alcohol (*R*)-6 (76 mg, 18% yield, 74% ee) from *n*-hexane:AcOEt (5:1) eluent, respectively. A part of (*S*)-10 was recrystallized from *n*-hexane-AcOEt to give colorless plates (*S*)-10. (*S*)-10: mp 89 °C. *Anal.* Calcd for C₁₂H₂₂O₄: C, 69.04; H, 7.97. Found C, 68.77; H, 7.99. [α]_D²² +1.9 (*c*=1.03, CHCl₃).

(*S*)-2-Acetoxyethyl-6-benzoyloxy-2,5,7,8-tetramethylchromane 11 A mixture of (*S*)-10 (303 mg, 1.09 mmol), benzyl bromide (0.57 ml, 4.8 mmol) and CsF (743 mg, 4.89 mmol) in tetrahydrofuran (THF) (5 ml) was stirred for 12 h at 60 °C. The reaction mixture was diluted with saturated brine and extracted with Et₂O. The organic layer was dried over MgSO₄ and evaporated to provide a crude oil which was chromatographed on silica gel (30 g, *n*-hexane:AcOEt=20:1) to afford homogeneous oil (*S*)-11 (371 mg, 87% yield). Crystallization of (*S*)-11 from *n*-hexane provided colorless plates (*S*)-11. (*S*)-11: mp 39 °C. *Anal.* Calcd for C₂₃H₂₈O₄: C, 74.97; H, 7.66. Found C, 74.99; H, 7.75. [α]_D²² +4.0 (*c*=0.94, CHCl₃). MS (EI) *m/z*: 368 (M⁺). IR (KBr): 1729 cm⁻¹. ¹H-NMR (CDCl₃) δ : 1.30 (3H, s), 1.81 (1H, dt, *J*=7, 12.5 Hz), 1.95 (1H, dt, *J*=7, 12.5 Hz), 2.09 (6H, s), 2.16 (3H, s), 2.22 (3H, s), 2.62 (2H, t, *J*=7 Hz), 4.09 (1H, d, *J*=11 Hz), 4.15 (1H, d, *J*=11 Hz), 4.69 (2H, s), 7.33 (1H, t, *J*=7 Hz), 7.40 (2H, t, *J*=7 Hz), 7.49 (2H, t, *J*=7 Hz).

(*S*)-6-Benzoyloxy-2,5,7,8-tetramethylchroman-2-methanol 9 A solution of (*S*)-11 (370 mg, 1.01 mmol) in dry Et₂O (3 ml) was added to a suspension of LiAlH₄ (60 mg, 1.56 mmol) in dry Et₂O (2 ml) at 0 °C and the whole mixture was stirred for 30 min at room temperature. It was diluted with aqueous 2 M HCl and extracted with Et₂O. The organic layer was washed with saturated brine and dried over MgSO₄. Removal of organic solvent gave a crude product which was chromatographed on silica gel (12 g, *n*-hexane:AcOEt=5:1) to afford (*S*)-9 (310 mg, 94% yield). (*S*)-9: [α]_D²³ +12.6 (*c*=0.99, CHCl₃). Spectral data (IR and ¹H-NMR) were identical with those of (\pm)-9.

(*S*)-6-Benzoyloxy-2,5,7,8-tetramethylchroman-2-carboxaldehyde 1 To a solution of dimethyl sulfoxide (DMSO, 198 mg, 2.54 mmol) in CH₂Cl₂ (2 ml) was added oxalyl chloride (0.11 ml, 1.32 mmol) at –78 °C and the reaction mixture was stirred for 30 min. A solution of (*S*)-9 (100 mg, 0.31 mmol) in CH₂Cl₂ (2 ml) was added to the above reaction mixture and the whole was stirred for 30 min. Et₃N (0.7 ml) was added to the above reaction mixture and the whole was stirred at –78 °C for 30 min and at 0 °C for 30 min. The reaction mixture was diluted with saturated brine and extracted with Et₂O. The organic layer was dried over MgSO₄ and evaporated to provide a crude oil which was chromatographed on silica gel (10 g, *n*-hexane:AcOEt=10:1) to afford a homogeneous oil (*S*)-1 (95 mg, 95% yield). Crystallization of (*S*)-1 from *n*-hexane provided colorless plates (*S*)-1. (*S*)-1: mp 56 °C. *Anal.* Calcd for C₂₁H₂₄O₃: C, 77.45; H, 7.46. Found C, 77.42; H, 7.54. [α]_D²³ +12.6 (*c*=0.99, CHCl₃). MS (EI) *m/z*: 324 (M⁺). IR (KBr): 1735 cm⁻¹. ¹H-NMR (CDCl₃) δ : 1.40 (3H, s), 1.79–1.87 (1H, m), 2.12 (3H, s), 2.20 (3H, s), 2.24 (3H, s), 2.25–2.30 (1H, m), 2.49–2.64 (2H, m), 4.66 (1H, d, *J*=10 Hz), 4.70 (1H, d, *J*=10 Hz), 7.34 (1H, t, *J*=7 Hz), 7.39 (2H, t, *J*=7 Hz), 7.48 (2H, d, *J*=7 Hz), 9.63 (1H, s).

Methyl 2-Methyl-3-(*p*-methoxyphenyl)-(2*E*)-propenoate 16 A mixture of (\pm)-*syn*-13 (269 mg, 1.20 mmol) and methanesulfonic acid (141 mg, 1.47 mmol) in CHCl₃ (4 ml) was stirred for 12 h at room temperature. The reaction mixture was diluted with saturated aqueous NaHCO₃ and extracted with Et₂O. The organic layer was washed with saturated brine, dried over MgSO₄ and evaporated to provide a crude oil which was chromatographed on silica gel (10 g, *n*-hexane:AcOEt=20:1) to afford homogeneous oil 15 (237 mg, 95% yield). 15: *Anal.* Calcd for C₁₂H₁₄O₃: C, 69.89; H, 6.84. Found C, 69.75; H, 7.00. MS (EI) *m/z*: 206 (M⁺). IR (neat): 1708 cm⁻¹. ¹H-NMR (CDCl₃) δ : 2.13 (3H, d, *J*=1.5 Hz), 3.81 (3H, s), 3.83 (3H, s), 6.92 (2H, d, *J*=9 Hz), 7.38 (2H, d, *J*=9 Hz), 7.60 (1H, br s).

2-Methyl-3-(*p*-methoxyphenyl)-(2*E*)-propenol 16 A solution of 15 (3.566 g, 1.20 mmol) in THF (11 ml) was added to a suspension of LiAlH₄ (0.8 g, 21.1 mmol) in THF (10 ml) at 0 °C. The whole mixture was stirred for 10 min at room temperature. The reaction mixture was diluted with H₂O and

extracted with Et₂O. The organic layer was washed with saturated brine, dried over MgSO₄ and evaporated to provide a crude oil which was chromatographed on silica gel (105 g, *n*-hexane:AcOEt=4:1) to afford homogeneous oil **16** (2.792 g, 90% yield). Crystallization of **16** from *n*-hexane gave a colorless plate **16**. **16**: mp 62 °C. *Anal.* Calcd for C₁₁H₁₄O₂: C, 74.13; H, 7.92. Found C, 74.04; H, 7.88. FAB-MS *m/z*: 178 (M⁺). IR (KBr): 3349 cm⁻¹. ¹H-NMR (CDCl₃) δ: 1.89 (3H, d, *J*=1.5 Hz), 3.80 (3H, s), 4.16 (2H, s), 6.45 (1H, br s), 6.87 (2H, d, *J*=8.5 Hz), 7.21 (2H, d, *J*=8.5 Hz).

(±)-(2,3)-anti-2-Methyl-3-(*p*-methoxyphenyl)-1,3-propane Diol 12 Borane-methyl sulfide complex (2 M solution in THF, 10 ml, 20 mmol) was added to a solution of **16** (1.028 g, 5.77 mmol) in THF (3 ml) at 0 °C and the whole was stirred for 2 h at room temperature. EtOH (3 ml), 2 M aqueous NaOH (1 ml) and 30% aqueous H₂O₂ (1.5 ml) were gradually added to the above reaction mixture and the whole was diluted with H₂O and extracted with Et₂O. The organic layer was washed with saturated brine, dried over MgSO₄ and evaporated to provide a crude oil which was chromatographed on silica gel (35 g, *n*-hexane:AcOEt=1:1) to afford 61:1 mixture of (±)-(2,3)-anti-diol **12** (1.008 g, 89% yield). The ratio of *syn/anti* was determined by Chiracel OD column (250 mm×4.6 mm) under the following analytical conditions (eluent, *n*-hexane/EtOH/iso-PrOH=300:10:5; detection, UV at 254 nm; flow rate, 1 ml/min, (±)-*anti*-**12**: 21.1 and 21.9 min, (±)-*syn*-**12**: 24.6 and 25.9 min). Crystallization of **12** from *n*-hexane-AcOEt gave a colorless plate *anti*-**12**. *anti*-**12**: mp 110 °C. *Anal.* Calcd for C₁₁H₁₆O₃: C, 67.32; H, 8.22. Found C, 67.06; H, 8.22. MS (EI) *m/z*: 196 (M⁺). IR (KBr): 3328 cm⁻¹. ¹H-NMR (CDCl₃) δ: 0.65 (3H, d, *J*=7 Hz), 1.97–2.07 (1H, m), 3.17 (1H, br s), 3.28 (1H, br s), 3.66–3.74 (2H, m), 3.81 (3H, s), 4.46 (1H, d, *J*=8.5 Hz), 6.88 (2H, d, *J*=8.5 Hz), 7.24 (2H, d, *J*=8.5 Hz).

(±)-(2,3)-anti-2-Methyl-3-(*p*-methoxyphenyl)-1,3-propane Diol 12 A solution of **14** (6.261 g, 27.9 mmol) in Et₂O (20 ml) was added to a suspension of LiAlH₄ (1.6 g, 42.2 mmol) in Et₂O (130 ml) at 0 °C. The whole mixture was stirred for 10 min at room temperature. The reaction mixture was diluted with 2 M aqueous HCl and extracted with Et₂O. The organic layer was washed with saturated brine, dried over MgSO₄ and evaporated to provide a crude oil which was chromatographed on silica gel (100 g, *n*-hexane:AcOEt=1:1) to afford (±)-(2,3)-anti-diol **12** (5.252 g, 95% yield). Crystallization of **12** from *n*-hexane-AcOEt gave a colorless plate *anti*-**12**.

Acetylation of (±)-(2,3)-anti-2-Methyl-3-(*p*-methoxyphenyl)-1,3-propane Diol 12 A solution of (±)-**12** (331 mg, 1.69 mmol) and Ac₂O (177 mg, 1.73 mmol) in pyridine (5 ml) was stirred for 2 h at room temperature. The reaction mixture was diluted with H₂O and extracted with Et₂O. The organic layer was washed with aqueous 2 M HCl, saturated aqueous NaHCO₃, saturated brine and dried over MgSO₄. Evaporation of organic solvent gave a crude oil which was chromatographed on silica gel (20 g) to afford (±)-**19** (67 mg, 15% yield) from *n*-hexane:AcOEt=10:1 eluent, (±)-**17** as a homogeneous oil (208 mg, 52% yield) and (±)-**18** (10 mg, 2% yield) from *n*-hexane:AcOEt=5:1 eluent in elution order, and (±)-**12** (67 mg, 20% recovery) from *n*-hexane:AcOEt=2:1 eluent. Crystallization of (±)-**18** from *n*-hexane gave a colorless powder (±)-**18**. Crystallization of (±)-**19** from *n*-hexane provided colorless needles (±)-**19**. (±)-**17**: MS (EI) *m/z* 238 (M⁺). IR (neat) 3460, 1730 cm⁻¹. ¹H-NMR (CDCl₃) δ: 0.77 (3H, d, *J*=7 Hz), 2.08 (3H, s), 2.11–2.19 (1H, m), 3.80 (3H, s), 4.07 (1H, dd, *J*=4.5, 11 Hz), 4.16 (1H, dd, *J*=5.5, 11 Hz), 4.44 (1H, dd, *J*=3, 8 Hz), 6.88 (2H, d, *J*=8.5 Hz), 7.23 (2H, d, *J*=8.5 Hz). The racemate (±)-**17** was analyzed to provide well separated peaks (28 and 31 min) corresponding to the enantiomers using Chiralcel AD (250 mm×4.6 mm) under the following analytical conditions (eluent, *n*-hexane/EtOH=20:1; detection, UV at 254 nm; flow rate, 1 ml/min). (±)-**18**: mp 72 °C. MS (EI) *m/z* 238 (M⁺). IR (KBr) 3427, 1728 cm⁻¹. ¹H-NMR (CDCl₃) δ: 0.80 (3H, d, *J*=6.5 Hz), 2.06 (3H, s), 2.08–2.17 (1H, m), 3.58 (1H, dd, *J*=4.5, 11 Hz), 3.62 (1H, dd, *J*=4.5, 11 Hz), 3.80 (3H, s), 5.63 (1H, d, *J*=9 Hz), 6.87 (2H, d, *J*=9 Hz), 7.25 (2H, d, *J*=9 Hz). (±)-**19**: mp 66 °C. *Anal.* Calcd for C₁₅H₂₀O₅: C, 64.27; H, 7.19. Found C, 64.17; H, 7.32. FAB-MS *m/z* 280 (M⁺). IR (KBr) 1730 cm⁻¹. ¹H-NMR (CDCl₃) δ: 0.82 (3H, d, *J*=7 Hz), 2.04 (3H, s), 2.07 (3H, s), 2.29–2.37 (1H, m), 3.79 (3H, s), 4.04 (1H, dd, *J*=5, 11 Hz), 4.12 (1H, dd, *J*=6, 11 Hz), 5.60 (1H, d, *J*=8.5 Hz), 6.87 (2H, d, *J*=9 Hz), 7.23 (2H, d, *J*=9 Hz). The racemate (±)-**20** was analyzed to provide well separated peaks (11 and 13 min) corresponding to the enantiomers using Chiralcel AD (4.6 mm×250 mm) under the following analytical conditions (eluent, *n*-hexane/EtOH=50:1; detection, UV at 254 nm; flow rate, 1 ml/min).

Enantioselective Acetylation of (±)-12** with Lipase Amano P** 1) A suspension of (±)-**12** (ca. 6 g), lipase (3 g) and vinyl acetate (225 ml) was incubated at 33 °C for 1 h. This scale experiment was carried out two times (total amount (12.38 g) of (±)-**12**). After the reaction mixture was filtered, the precipitate was washed with AcOEt. The combined organic layer was

dried over MgSO₄ and evaporated. The residue was chromatographed on silica gel (300 g) to give (2*R*,3*R*)-**17** (7.882 g, 57% yield) as a colorless oil from *n*-hexane:AcOEt=4:1 eluent, (2*R*,3*R*)-**18** (405 mg, 3% yield, 80% ee) from *n*-hexane:AcOEt=2:1 eluent and (2*S*,3*S*)-**12** (4.412 g, 39% yield) from *n*-hexane:AcOEt=1:1 eluent. (2*R*,3*R*)-**17**: *Anal.* Calcd for C₁₃H₁₈O₄: C, 65.53; H, 7.61. Found C, 65.27; H, 7.65. 65% ee, *t*_R=31 min (82.5%) and *t*_R=28 min (17.5%). (2*R*,3*R*)-**18**: 80% ee. [α]_D²⁵+66.3 (*c*=1.04, CHCl₃). (2*S*,3*S*)-**12**: >99% ee, *t*_R=36 min (>99%) and *t*_R=32 min (<0%). [α]_D²⁵−39.8 (*c*=1.05, CHCl₃). 2) A suspension of (2*R*,3*R*)-**17** (65% ee, 7.882 g, 33.1 mmol) and K₂CO₃ (5.5 g, 39.9 mmol) in MeOH (100 ml) was stirred for 1.5 h at room temperature. The reaction mixture was evaporated, diluted with saturated brine and extracted with AcOEt. The organic layer was dried over MgSO₄ and evaporated to afford a crude product which was chromatographed on silica gel (100 g) to give (2*R*,3*R*)-**12** (6.19 g, 95% yield) from *n*-hexane:AcOEt=1:1 eluent. A suspension of (2*R*,3*R*)-**12** (6.19 g, 31.5 mmol), lipase (3.8 g) and vinyl acetate (250 ml) was incubated at 33 °C for 30 min. After the reaction mixture was filtered, the precipitate was washed with AcOEt. The combined organic layer was dried over MgSO₄ and evaporated. The residue was chromatographed on silica gel (150 g) to give (2*R*,3*R*)-**17** (5.743 g, 76% yield), (2*R*,3*R*)-**18** (257 mg, 3% yield) from *n*-hexane:AcOEt=4:1 eluent in elution order and (2*S*,3*S*)-**12** (1.020 g, 17% yield) from *n*-hexane:AcOEt=1:1 eluent. (2*R*,3*R*)-**18**: 94% ee. [α]_D²⁵+77.6 (*c*=1.08, CHCl₃). (2*R*,3*R*)-**18**: 97% ee. (2*S*,3*S*)-**12**: 85% ee. 3) A suspension of (2*R*,3*R*)-**18** (80% ee, 60 mg, Table 2, entry 1) and K₂CO₃ (46 mg) in MeOH (2 ml) was stirred for 3 h at room temperature. The reaction mixture was diluted with saturated brine and extracted with Et₂O. The organic layer was dried over MgSO₄ and evaporated to afford a crude product which was chromatographed on silica gel (10 g) to give (2*R*,3*R*)-**12** (40 mg) from *n*-hexane:AcOEt=1:1 eluent. The ee of the present (2*R*,3*R*)-**12** was estimated by HPLC analysis. 4) A suspension of (2*R*,3*R*)-**18** (94% ee, 61 mg, Table 2, entry 2) and K₂CO₃ (46 mg) in MeOH (2 ml) was stirred for 3 h at room temperature. The reaction mixture was worked up in the same way as for 3) to give (2*R*,3*R*)-**12** (41 mg) from *n*-hexane:AcOEt=1:1 eluent. The ee of the present (2*R*,3*R*)-**12** was estimated by HPLC analysis.

(2*R*,3*R*)-(1,3)-Diaceoxy-2-methyl-3-*p*-methoxyphenylpropane 19 A solution of (2*R*,3*R*)-**17** (97% ee, 5.194 g, 21.8 mmol), Ac₂O (12.66 g, 124 mmol) and 4-dimethylaminopyridine (DMAP, 133 mg, 1.1 mmol) in pyridine (20 ml) was stirred for 30 min at room temperature. The reaction mixture was diluted with H₂O and extracted with Et₂O. The organic layer was washed with aqueous 2 M HCl, saturated aqueous NaHCO₃, saturated brine and dried over MgSO₄. Evaporation of the organic solvent gave crude crystal which was recrystallized from *n*-hexane-AcOEt to give optically pure (2*R*,3*R*)-**19** (5.27 g, 83% yield). (2*R*,3*R*)-**19**: mp 66 °C. [α]_D³⁰+67.6 (*c*=1.06, CHCl₃).

(2*S*)-1-Acetoxy-2-methyl-3-*p*-methoxyphenylpropane 20 A solution of (2*R*,3*R*)-**19** (1.006 g, 3.59 mmol) in MeOH (10 ml) was hydrogenated at ordinary temperature and pressure in the presence of 20% Pd(OH)₂-C (0.2 g). After hydrogen absorption had ceased, the catalyst was filtered off with the aid of Celite and the filtrate was evaporated. The residue was chromatographed on silica gel (20 g, *n*-hexane:AcOEt=5:1) to afford a colorless oil (2*S*)-**20** (612 mg, 77% yield). (2*S*)-**20**: *Anal.* Calcd for C₁₃H₁₈O₅: C, 70.25; H, 8.16. Found C, 69.87; H, 8.38. MS (EI) *m/z*: 222 (M⁺). [α]_D²⁴+11.3 (*c*=1.08, CHCl₃). IR (neat): 1738 cm⁻¹. ¹H-NMR (CDCl₃) δ: 0.91 (3H, d, *J*=7 Hz), 2.06 (3H, s), 2.02–2.08 (1H, m), 2.39 (1H, dd, *J*=8, 13.5 Hz), 2.66 (1H, dd, *J*=6, 13.5 Hz), 3.78 (3H, s), 3.88 (1H, dd, *J*=6.5, 11 Hz), 3.95 (1H, dd, *J*=6, 11 Hz), 6.82 (2H, d, *J*=8.5 Hz), 7.06 (2H, d, *J*=8.5 Hz).

(2*S*)-2-Methyl-3-*p*-methoxyphenylpropanol 21 A suspension of (2*S*)-**20** (233 mg, 1.05 mmol) and K₂CO₃ (210 mg, 1.5 mmol) in MeOH (5 ml) was stirred for 2 h at room temperature. The reaction mixture was diluted with saturated brine and extracted with Et₂O. The organic layer was dried over MgSO₄ and evaporated to afford a crude product which was chromatographed on silica gel (10 g) to give (2*S*)-**21** as a homogeneous oil (182 mg, 96% yield) from *n*-hexane:AcOEt=5:1 eluent. (2*S*)-**21**: [α]_D²⁵−11.9 (*c*=1.02, CHCl₃). *Anal.* Calcd for C₁₁H₁₆O₂: C, 73.30; H, 8.95. Found C, 73.10; H, 9.13. Spectral data (IR and ¹H-NMR) were identical with those of reported (2*S*)-**21**.³¹

(2*S*)-1-Bromo-2-methyl-3-*p*-methoxyphenylpropanol 22 Triphenylphosphine (Ph₃P, 295 mg, 1.12 mmol) and CBr₄ (372 mg, 1.12 mmol) were added to a solution of (2*S*)-**21** (126 mg, 0.7 mmol) in THF (2 ml) and the resulting solution was stirred for 15 min at room temperature. The reaction mixture was diluted with saturated brine and extracted with Et₂O. The organic layer was dried over MgSO₄ and evaporated to afford a crude product which was chromatographed on silica gel (15 g) to give (2*S*)-**22** as a homogeneous oil (168 mg, 98% yield) from *n*-hexane:AcOEt=5:1 eluent. (2*S*)-

22: $[\alpha]_D^{23} +28.3$ ($c=1.21$, CHCl_3). Spectral data (IR and $^1\text{H-NMR}$) were identical with those of reported (2S)-22.³⁾

(2S)-2-Methyl-3-(*p*-methoxyphenyl)-1-phenylsulfonylpropane 23 A mixture of (2S)-22 (1.543 g, 6.34 mmol) and sodium benzenesulfinate ($\text{PhSO}_2\text{Na} \cdot 2\text{H}_2\text{O}$, 5.03 g, 25.1 mmol) in dimethylformamide (DMF, 30 ml) was heated at 100 °C for 1 h with stirring, then diluted with H_2O and extracted with Et_2O . The organic layer was washed with saturated brine, dried over MgSO_4 and evaporated to afford a crude product which was chromatographed on silica gel (30 g) to give (2S)-23 as a homogeneous oil (1.548 g, 80% yield) from *n*-hexane : $\text{AcOEt}=5:1$ eluent. Spectral data (IR, $^1\text{H-NMR}$) were identical with those of reported (2S)-23.³⁾

Methyl (3S)-3-Methyl-4-phenylsulfonylbutanoate 24 Ozone was passed through a solution of (2S)-23 (1.517 g, 4.98 mmol) in AcOEt (20 ml) at -78°C for 2.5 h, then 30% aqueous H_2O_2 (10 ml) was added to the ozonolyzed product. The reaction mixture was stirred for 10 min at room temperature, then diluted with H_2O and extracted with Et_2O . The organic layer was washed with saturated brine, dried over MgSO_4 and evaporated to afford a crude product which was treated with CH_2N_2 in Et_2O to provide an oily product. This was subjected to chromatographic separation on silica gel (50 g) to give (2S)-24 as a homogeneous oil (1.063 g, 83% overall yield) from *n*-hexane : $\text{AcOEt}=5:1$ eluent. Spectral data (IR, $^1\text{H-NMR}$) were identical with those of reported (3S)-24.³⁾

(3S)-3-Methyl-4-phenylsulfonylbutanol 25 LiBH_4 (157 mg, 7.21 mmol) was added to a solution of (2S)-24 (1.063 g, 4.15 mmol) in THF (20 ml) at 0 °C and the whole was stirred for 12 h at 60 °C. The reaction mixture was diluted with H_2O and extracted with Et_2O . The organic layer was washed with saturated brine, dried over MgSO_4 and evaporated to afford a crude product which was chromatographed on silica gel (30 g) to give (3S)-26 as a homogeneous oil (812 mg, 86% yield) from *n*-hexane : $\text{AcOEt}=1:2$ eluent. Spectral data (IR, $^1\text{H-NMR}$) were identical with those of reported (3S)-25.³⁾

(3S)-3-Methyl-4-phenylsulfonylbutyltetrahydropyranyl Ether 3 A mixture of (2S)-25 (109 mg, 0.47 mmol), 3,4-dihydropyran (DHP) (108 mg, 1.28 mmol) and pyridinium *p*-toluenesulfonate (PPTS, 11 mg, 0.043 mmol) in CH_2Cl_2 (2 ml) was stirred for 12 h at room temperature. The reaction mixture was washed with aqueous NaHCO_3 and saturated brine, and dried over MgSO_4 . The organic layer was evaporated to afford a crude product which was chromatographed on silica gel (15 g) to give (3S)-3 as a homogeneous oil (142 mg, 95% yield) from *n*-hexane : $\text{AcOEt}=4:1$ eluent. Spectral data (IR, $^1\text{H-NMR}$) were identical with those of reported (3S)-3.³⁾

(3R,7R)-3,7,11-Trimethyldodecan-1-ol 27 1) *n*-Butyllithium (*n*-BuLi, 1.6 M in hexane, 10 ml, 16 mmol) was added to a stirred solution of diisopropylamine (2 ml) in THF (7 ml) at -78°C under an argon atmosphere and the mixture was stirred for 30 min at the same temperature. The resulting LDA-THF solution was added to a solution of (3S)-3 (820 mg, 2.63 mmol) in THF (2 ml) at -78°C and then HMPA (2 ml) was added. The whole was stirred for 30 min at -78°C , then a solution of (3R)-3,7-dimethyloctyl iodide **4** (523 mg, 1.95 mmol) in THF (3 ml) was added at the same temperature. The reaction mixture was stirred for 30 min at -20°C and for 30 min at room temperature, then diluted with H_2O and extracted with Et_2O . The organic layer was washed with saturated brine and dried over MgSO_4 . Removal of the organic solvent gave an oily product, which was chromatographed on silica gel (50 g, *n*-hexane : $\text{AcOEt}=10:1$) to afford **26** as a homogeneous oil (374 mg, 42% overall yield). 2) A mixture of **26** (374 mg) and concentrated HCl (4 drops) in EtOH (10 ml) was stirred for 12 h at room temperature. The reaction mixture was condensed and diluted with H_2O and extracted with Et_2O . The organic layer was washed with saturated brine and dried over MgSO_4 . Removal of the organic solvent gave an oily product, which was chromatographed on silica gel (15 g, *n*-hexane : $\text{AcOEt}=3:1$) to afford a homogeneous oil (292 mg, 95% yield). 3) 5% Na/Hg (1.688 g, 0.377 mmol) was added to a solution of the above mentioned oil (125 mg, 0.34 mmol) described in 2) in MeOH (5 ml) and the mixture was refluxed for 2.5 h with stirring, then diluted with H_2O and extracted with Et_2O . The organic layer was washed with saturated brine and dried over MgSO_4 . Removal of the organic solvent gave an oily product, which was chromatographed on silica gel (10 g, *n*-hexane : $\text{AcOEt}=10:1$) to afford (3R,7R)-27 as a homogeneous oil (72 mg, 93% yield). Spectral data (IR, $^1\text{H-NMR}$)

were identical with those of reported (3R,7R)-27.³⁾

(2R,4'R,8'R)-1',2'-Dehydro- α -tocopheryl Benzyl Ether 28 1) Triphenylphosphine (Ph_3P , 352 mg, 1.35 mmol) and CBr_4 (445 mg, 1.34 mmol) were added to a solution of (3R,7R)-27 (100 mg, 0.44 mmol) in THF (2 ml) and the resulting solution was stirred for 15 min at room temperature. The reaction mixture was diluted with saturated brine and extracted with Et_2O . The organic layer was dried over MgSO_4 and evaporated to afford a crude product which was chromatographed on silica gel (10 g) to give (3R,7R)-3,7,11-trimethyldodecanyl bromide ($[\alpha]_D^{22} -3.1$ ($c=1.62$, *n*-hexane)) as a homogeneous oil (129 mg, quantitative yield) from *n*-hexane eluent. 2) A mixture of (3R,7R)-3,7,11-trimethyldodecanyl bromide (72 mg, 0.25 mmol) and Ph_3P (72 mg, 0.27 mmol) was heated at 200 °C for 6 h with stirring and the generated phosphonium salt **2** was dissolved in THF (2 ml) after cooling. *n*-BuLi (1.6 M in hexane, 0.14 ml, 0.22 mmol) was added to the above THF-solution at -78°C under an argon atmosphere and the whole was stirred for 30 min at the same temperature. A solution of chroman aldehyde (S)-1 (81 mg, 0.25 mmol) in THF (2 ml) was added to the above phosphine-ylide at -78°C . The whole was stirred at -78°C for 30 min, at 0 °C for 30 min and heated at 60 °C for 2.5 h. The reaction mixture was diluted with saturated brine and extracted with Et_2O . The organic layer was dried over MgSO_4 and evaporated to afford a crude product which was chromatographed on silica gel (10 g) to give a mixture of *Z*- and *E*-(2R,4'R,8'R)-28 (*Z/E*=14:1) as a homogeneous oil (45 mg, 35% yield based on (3R,7R)-27)) from *n*-hexane : $\text{AcOEt}=100:1$ eluent. (2R,4'R,8'R)-28: MS (EI) m/z 518 (M^+). *Z*-28: $^1\text{H-NMR}$ (CDCl_3) δ : 5.32–5.48 (2H, m, olefinic H). *E*-28: $^1\text{H-NMR}$ (CDCl_3) δ : 5.00 (1H, ddd, $J=1.4, 10.7, 17.3$ Hz), 5.79 (1H, dd, $J=10.7, 17.3$ Hz).

(2R,4'R,8'R)- α -Tocopherol A solution of (2R,4'R,8'R)-28 (43 mg, 0.08 mmol) in AcOEt (2 ml) was hydrogenated at ordinary temperature and pressure in the presence of 20% $\text{Pd}(\text{OH})_2\text{-C}$ (16 mg). After hydrogen absorption had ceased, the catalyst was filtered off with the aid of Celite and the filtrate was evaporated. The residue was chromatographed on silica gel (10 g, *n*-hexane : $\text{AcOEt}=50:1$) to afford (2R,4'R,8'R)- α -Tocopherol as a homogeneous oil (31 mg, 86% yield). (2R,4'R,8'R)- α -tocopherol: *Anal.* Calcd for $\text{C}_{55}\text{H}_{100}\text{O}_2$: C, 80.87; H, 11.70. Found C, 80.77; H, 11.93. $[\alpha]_D^{27} -2.7$ ($c=0.59$, benzene). MS (EI) m/z : 430 (M^+). IR (neat): 3460 cm^{-1} . $^1\text{H-NMR}$ (CDCl_3) δ : 0.83–0.87 (12H, m), 1.01–1.63 (24H, m), 1.71–1.84 (2H, m), 2.11 (6H, s), 2.15 (3H, s), 2.59 (2H, t, $J=7$ Hz), 4.20 (1H, br s). $^{13}\text{C-NMR}$ (CDCl_3) δ : 11.7 (q), 12.3 (q), 12.7 (q), 20.1 (q), 20.2 (q), 21.2 (t), 21.5 (t), 23.1 (q), 23.2 (q), 23.4 (q), 24.9 (t), 25.3 (t), 28.4 (d), 32.0 (t), 33.1 (d), 33.2 (d), 37.7 (t), 37.8 (t), 37.9 (t), 38.0 (t), 39.8 (t), 40.2 (t), 74.8 (s), 117.6 (s), 118.7 (s), 121.2 (s), 122.8 (s), 144.7 (s), 145.7 (s). Spectral data (IR, MS (EI), $^1\text{H-NMR}$ and $^{13}\text{C-NMR}$) were identical with those of (\pm)- α -Tocopherol.

Acknowledgements This work was supported by a grant for the Bio-design Research Program from The Institute of Physical and Chemical (RIKEN) to H. A.

References and Notes

- 1) A part of this work was published as a preliminary communication: Akita H., Nozawa M., Umezawa I., Nagumo S., *Biocatalysis*, **9**, 79–87 (1994).
- 2) a) Recent asymmetric synthesis of α -tocopherol; Hübscher J., Barner R., *Helv. Chim. Acta*, **73**, 1068–1086 (1990); b) Recent asymmetric approach to vitamin E; Trost B. M., Toste F. D., *J. Am. Chem. Soc.*, **120**, 9074–9075 (1998) and references cited therein.
- 3) Chen C. Y., Nagumo S., Akita H., *Chem. Pharm. Bull.*, **44**, 2153–2156 (1996).
- 4) Sugai T., Watanabe N., Ohta H., *Tetrahedron: Asymmetry*, **2**, 371–376 (1991).
- 5) Akita H., Chen C. Y., Nagumo S., *J. Chem. Soc. Perkin Trans. 1*, **1995**, 2159–2164.
- 6) The MERCK INDEX, Eleventh Ed., Merck and Company, Inc., Whitehouse Station, N. J., **1996**, 1712.

Synthesis and Pharmacological Activity of *O*-(5-Isioxazolyl)-L-serine

Fumio IKEGAMI,^{*,a} Akemi YAMAMOTO,^a Toshikazu SEKINE,^a Tsutomu ISHIKAWA,^a
Kuniko KUSAMAE-EGUCHI,^b Tadashi KUSAMA,^b and Kazuko WATANABE^b

Faculty of Pharmaceutical Sciences, Chiba University,^a Yayoi-cho 1-33, Inage-ku, Chiba 263-8522, Japan and Nihon University College of Pharmacy,^b Narashinodai 7-7-1, Funabashi 274-8555, Japan.

Received September 24, 1999; accepted October 25, 1999

A novel isoxazole derivative, *O*-(5-isioxazolyl)-L-serine (OIS, 1), was synthesized by a Mitsunobu reaction of isoxazolin-5-one (4) with *N*-Boc-L-serine *tert*-butyl ester (5) and subsequent deprotection of the coupling product. Its structure was elucidated by spectroscopic analyses. The pharmacological activity of 1 was also examined with cloned glutamate receptors and transporters using a *Xenopus* oocyte-expressing system showing substrate activity on an excitatory amino acid carrier 1 (EAAC 1) as a glutamate transporter.

Key words synthesis; *O*-(5-isioxazolyl)-L-serine; pharmacological activity; excitatory amino acid carrier 1; *Xenopus* oocyte

O-(5-Isioxazolyl)-L-serine (OIS, 1) is thought to be a structural isomer of naturally occurring isoxazolinone derivatives, β -(isoxazolin-5-on-2-yl)-L-alanine (BIA, 2) and β -(isoxazolin-5-on-4-yl)-L-alanine (TAN, 3), but it has not yet been found in nature. BIA (2) was identified in the leguminous genus *Lathyrus*, *Lens* and *Pisum*, was confirmed to be the biosynthetic precursor of the neurotoxin 3-*N*-oxalyl-L-2,3-diaminopropionic acid (β -ODAP) in grass pea (*Lathyrus sativus* L.),^{1–5} and was also found to have antimycotic activity.⁶ BIA was synthesized from *N*-Boc-L-serine (9) by Baldwin *et al.*⁷ TAN (3) was isolated from *Streptomyces platensis* as an antifungal antibiotic,⁸ and was also synthesized by Tsubotani *et al.*⁹ However, OIS (1) has not yet been synthesized, in spite of its stable structure.

During the pharmacological study of isoxazolinone derivatives and such related compounds as neurotoxins, which cause crippling human neurolathyrism, we reported that TAN was a potential agonist for glutamate receptors (Glu R) and glutamate transporters (Glu T) as well as β -ODAP, a major causative agent of neurolathyrism, which is caused by eating the grass pea seeds, whereas BIA had almost no activity.^{10–12}

Therefore, we have focused on the synthesis of an isomer, OIS (1), to clarify the structure–activity relationship of isoxazolinone compounds. We now report the synthesis and pharmacological activity of 1 in comparison with its two isomers and other related compounds.

Results and Discussion

Synthesis of OIS (1) OIS (1) was synthesized by a Mitsunobu reaction¹³ of isoxazolin-5-one (4) with *N*-Boc-L-serine *tert*-butyl ester (5) and subsequent deprotection of the coupling product (6), as shown in Chart 1. Its structure was elucidated by spectroscopic analyses. The IR spectrum of 1 showed an absorption band for carbonyl functionality (1689 cm^{–1}) of an amino acid. The ¹H-NMR spectrum revealed two doublet signals of aromatic protons of the isoxazole ring at δ 5.46 (d, 1H, *J*=2.2 Hz, C₄H) and 8.17 (d, 1H, *J*=2.2 Hz, C₃H), and two multiplet signals of one methine group at the α -position of an amino acid at δ 4.10 (m, 1H) and the adjacent oxymethylene group at δ 4.56 (m, 2H). The ¹³C-NMR spectrum also showed three signals (δ 79.3, 154.8, 173.2) due to an isoxazole skeleton, together with three signals (δ 54.5, 71.2, 171.7) of serine moiety. A downfield shifted carbon signal at δ 71.2, which does not appear in the spectrum

of BIA (2) or TAN (3), clearly indicated that this carbon is bonded to the isoxazole ring through an oxygen atom (Fig. 1). Information concerning the coupling position was obtained from the heteronuclear multiple bond correlation (HMBC) spectrum of protected OIS (6), in which a cross-peak was observed between the oxymethylene proton (δ 4.54) and quaternary carbon (δ 172.9) of the isoxazole nucleus, indicating that a serine moiety is attached to the C-5 position of the isoxazole ring. This structure was reinforced by comparison of the previously observed NMR data for 2 and 3.^{7,9} Finally, the structure of newly synthesized 1 was concluded to be a positional isomer of 2 and 3, and is represented by the structure formula in Chart 1.

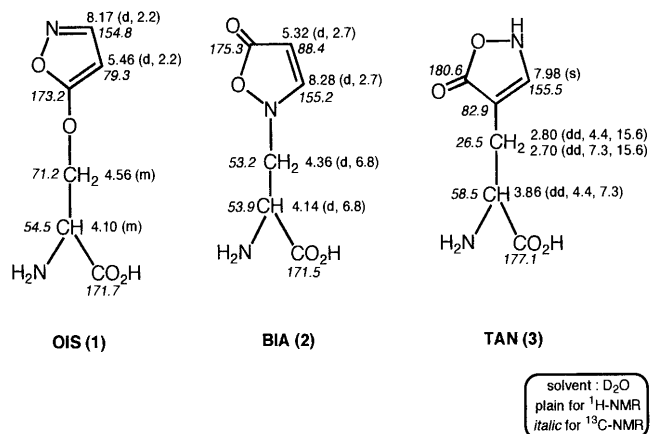


Fig. 1. ¹H- and ¹³C-NMR Spectral Data of OIS (1), BIA (2) and TAN (3)

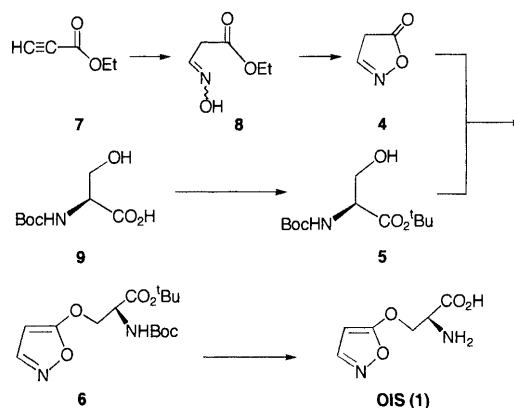


Chart 1. Synthetic Routes of OIS (1)

* To whom correspondence should be addressed.

Table 1. Effects of OIS (**1**) and Related Compounds on the Cloned Glu R and Glu T Expressed in *Xenopus* Oocytes

	NMDA ^{a)}		AMPA ^{b)}	GLAST ^{b)}	EAAC 1 ^{b)}	GLT 1 ^{b)}
	Glu site ^{c)}	Gly site ^{d)}				
OIS (1)	0.4±0.1	9.3±2.1	1.0±0.7	0.4±0.3	7.7±2.0	2.8±1.7
BIA (2)	1.5±0.9	3.9±1.0	2.0±0.4	0.5±0.4	4.3±2.5	2.3±1.9
TAN (3)	17.3±0.5	15.9±5.3	57.0±3.4	31.6±0.3	18.1±4.0	0.8±0.5
β-ODAP	1.1±0.6	0.9±0.5	81.0±7.6	2.0±0.5	0.8±0.6	0.5±0.5

Inward currents evoked by 0.1 mM **1** and related compounds are expressed as percentage responses of *a*) those with 0.1 mM L-glutamate (Glu) and 0.1 mM glycine (Gly), and of *b*) 0.1 mM Glu. *c*) Glu site agonist activities induced by 0.1 mM compounds and Gly. *d*) Gly site agonist activities induced by 0.1 mM compounds and Glu. Slight responses are observed for each site without an appropriate agonist: *c*) 0.5±0.2, *d*) 0.3±0.05. Data are means±S.E.M. (*n*=3–7).

Pharmacological Activity of OIS (1**)** The pharmacological activity of **1** was examined for its activity on Glu R and Glu T by using a *Xenopus* oocyte-expressing system in comparison with its two isomers, **2** and **3**, and the results are summarized in Table 1. Macroscopic currents were recorded using a two-electrode voltage-clamp method as described previously.^{11,12)} In the voltage-clamp experiments using cloned rat Glu R and Glu T expressed in *Xenopus* oocytes, **1** at 0.1 mM showed weak substrate activity on an excitatory amino acid carrier 1 (EAAC 1), a neuron-type Glu T, while **2** had no activity. OIS (**1**) also had slight agonistic activity on the glycine site of a *N*-methyl-D-aspartic acid (NMDA)-subtype of Glu R composed of 1_A and 2B subunits. However, **1** showed almost no activity on the α-amino-3-hydroxy-5-methyl-4-isoxazole propanoic acid (AMPA)-subtype of Glu R composed of α1 and α2 subunits, nor on glutamate/aspartate transporter (GLAST) or glutamate transporter 1 (GLT 1) of Glu T, both being glia-type transporters. As we reported before,^{11,12)} **3** had a potential activity against all Glu R and Glu T examined, and β-ODAP also showed agonistic activity on the AMPA receptor, while **2** showed no activity toward Glu R or Glu T (Table 1). In summary, **1** had moderate activity toward the glycine site of the NMDA receptor as well as toward the EAAC 1-type Glu T in sharp contrast to its isomer, **3**.

Amino Acid Analysis of Some *Lathyrus* and *Pisum* Species Detection of the newly synthesized **1** in the seedlings and seeds of grass pea (*Lathyrus sativus* L.), sweet pea (*L. odoratus* L.), perennial sweet pea (*L. latifolius* L.) and pea (*Pisum sativum* L.) was attempted using an automatic amino acid analyzer equipped with a UV detector as described previously,¹⁴⁾ since **2** was identified in these plants^{1,2)} and **1** had not yet been found. However, **1** could not be detected in these plants examined, under standard operating conditions.

In conclusion, a novel isoxazole compound **1** was synthesized from isoxazolin-5-one (**4**) and *N*-Boc-L-serine *tert*-butyl ester (**5**) for the first time, and was found to have substrate activity on EAAC 1 as a Glu T, while **1** could not be found in the *Lathyrus* or *Pisum* species examined. This suggests that it may be a potential lead compound for the development of new Glu T drugs.

Experimental

Melting points were measured on a Yanagimoto apparatus and are uncorrected. IR spectra were recorded on a JASCO FT/IR-300E spectrometer by the diffuse reflection measurement method. NMR spectra were measured on a JEOL GSX-500α (500 MHz for ¹H and 125 MHz for ¹³C) in CDCl₃ solution and on a JEOL GSX-400α (400 MHz for ¹H and 100 MHz for ¹³C) in D₂O solution, and chemical shifts were reported in δ (ppm) from tetra-

methylsilane (TMS) as an internal standard. FAB-MS were recorded on a JEOL JMS-HX-110A spectrometer in an *m*-nitrobenzylalcohol (NBA) matrix in the positive ion mode. The electrospray ionization-mass spectra (ESI-MS) were obtained on a JEOL JMS-700T spectrometer in H₂O:CH₃CN:CH₃OH:AcOH=33:33:33:1. TLC: Kieselgel 60 F₂₅₄ 0.25 mm (Merck), Column chromatography (CC): Kieselgel 60 (70–230 mesh) or Kieselgel 60 (230–400 mesh) (Merck).

BIA (**2**) was obtained from plants as described previously.¹⁾ TAN (**3**) and β-ODAP were purchased from Takeda Chemical Ind., Ltd., and from Tocris Cookson, Ltd., respectively. All chemicals used in the pharmacological study were dissolved in glass-distilled water.

Isoxazolin-5-one (4**)** **4** was synthesized from ethyl propiolate (**7**) via ethyl malonaldehyde oxime (**8**, 400.5 mg, 3.07 mm) as colorless prisms (180.5 mg, 69.2%) in accordance with the method of Sarlo.¹⁵⁾

***N*-Boc-L-serine *tert*-Butyl Ester (**5**)¹⁶⁾** A mixed solution of *N*-Boc-L-serine (**9**, 1.003 g, 4.89 mm) and *N,N*-dimethylformamide di-*tert*-butylacetal (DFBA, 6.21 ml, *d*=0.848, 25.9 mm) in dry benzene (8.0 ml) was refluxed for 19 h under Ar. To the mixture, 5% aq. NaHCO₃ was added and stirred for 30 min, then an adequate amount of CH₃OH was added to give one layer. After extraction with AcOEt, its fraction was rinsed 3 times with H₂O and once with sat. NaCl aq., which was dried over MgSO₄ and filtered. The AcOEt solution was concentrated *in vacuo* to give a yellow oil (1.427 g), which was purified by CC [SiO₂, Kieselgel Art. 7734, *n*-hexane:AcOEt=2:1 (v/v)] to give **5** and its formyl ester (**5'**) as a by-product.

N-Boc-L-serine *tert*-Butyl Ester (**5**): Colorless prisms (837.2 mg, 65.8%): mp 79.0–83.5°C. IR (CHCl₃) ν_{\max} cm⁻¹: 3432, 1709. ¹H-NMR (500 MHz): δ 1.38 (s, 9H, *tert*-Bu), 1.41 (s, 9H, *tert*-Bu), 2.62 (s, 1H, OH), 3.82 (d, 2H, *J*=3.4 Hz, CH₂), 4.18 (br s, 1H, CH), 5.41 (d, 1H, *J*=1.0 Hz, NH). ¹³C-NMR (125 MHz): δ 27.9 (3CH₃), 28.3 (3CH₃), 56.3 (CH), 63.9 (CH₂), 80.1 (O–C), 82.6 (O–C), 156.0 (C=O), 170.0 (C=O). FAB-MS *m/z*: 262 (MH⁺), 206 (MH⁺–*tert*-Bu), 150 (MH⁺–2-*tert*-Bu).

N-Boc-O-formyl-L-serine *tert*-Butyl Ester (**5'**): Colorless prisms (23.0 mg): IR (CHCl₃) ν_{\max} cm⁻¹: 3438, 1730. ¹H-NMR (500 MHz): δ 1.38 (s, 9H, *tert*-Bu), 1.40 (s, 9H, *tert*-Bu), 4.35 (dd, 1H, *J*=3.0, 11.0 Hz, CH₂), 4.40 (m, 1H, CH), 4.46 (dd, 1H, *J*=3.0, 11.0 Hz, CH₂), 5.23 (d, 1H, *J*=7.1 Hz, NH), 7.98 (s, 1H, CHO). ¹³C-NMR (125 MHz): δ 27.9 (3CH₃), 28.3 (3CH₃), 53.2 (CH), 64.1 (CH₂), 80.2 (O–C), 83.0 (O–C), 155.1 (C=O), 160.3 (HC=O), 168.4 (C=O). FAB-MS *m/z*: 290 (MH⁺), 234 (MH⁺–*tert*-Bu), 178 (MH⁺–2-*tert*-Bu).

Protected OIS (6**)** Isoxazolin-5-one (**4**, 25.8 mg, 0.30 mm), *N*-Boc-L-serine *tert*-butyl ester (**5**, 79.2 mg, 0.30 mm) and PPh₃ (95.5 mg, 0.36 mm) were dissolved in 1.0 ml of tetrahydrofuran (THF) at 0°C under Ar, then diisopropyl azodicarboxylate (DIAD, 0.045 ml, *d*=1.027, 0.36 mm) was added dropwise in accordance with the Mitsunobu reaction.¹³⁾ The resulting mixture was stirred at room temperature for 6 h. To the reaction mixture, water was added and extracted with AcOEt. The AcOEt solution was rinsed 3 times with water and once with sat. NaCl aq. After drying over MgSO₄, the filtrated solvent was removed *in vacuo* to give a yellow oil (283.5 mg). This was purified by CC [SiO₂, Kieselgel Art. 7734, *n*-hexane:AcOEt=2:1 (v/v)] followed by prep. TLC [*n*-hexane:ether=2:1 (v/v)] to give a colorless powder (26.1 mg, 26.2%): mp 58.5–62.0°C. IR (CHCl₃) ν_{\max} cm⁻¹: 1707. ¹H-NMR (500 MHz): δ 1.43 (s, 9H, *tert*-Bu), 1.44 (s, 9H, *tert*-Bu), 4.42 (m, 1H, CH), 4.54 (m, 2H, CH₂), 4.63 (m, 1H, NH), 5.20 (d, 1H, *J*=2.0 Hz, C₄-H), 8.05 (d, 1H, *J*=2.0 Hz, C₃-H). ¹³C-NMR (125 MHz): δ 27.7 (3CH₃), 28.3 (3CH₃), 53.7 (C₈H), 66.7 (CH₂), 76.7 (C₄H), 80.4 (O–C), 83.4 (O–C), 152.8 (C₃H), 155.2 (C=O), 167.8 (C₉=O), 172.9 (C₅). FAB-MS *m/z*: 329 (MH⁺).

OIS (1**)** Protected OIS (**6**, 12.0 mg, 0.04 mm) and CF₃COOH (10.0 ml) were stirred for 30 min as with the synthetic method of **3** by Tsubotani *et*

al.,⁹⁾ then rinsed 2–3 times with ether after removing the solvent. The resulting yellow oil was applied to CC [SiO₂, Kieselgel, ethanol:H₂O=4:1 (v/v)], and **1** was obtained as a colorless powder (7.5 mg, quant.): mp 109.5–112.0 °C. IR (nujol) ν_{\max} cm⁻¹: 3377, 1689, 1596, 1459. ¹H-NMR (400 MHz): δ 4.10 (m, 1H, CH), 4.56 (m, 2H, CH₂), 5.46 (d, 1H, $J=2.2$ Hz, C₄H), 8.17 (d, 1H, $J=2.2$ Hz, C₃H). ¹³C-NMR (100 MHz): δ 54.5 (C₈H), 71.2 (CH₂), 79.3 (C₄H), 154.8 (C₃H), 171.7 (C₉=O), 173.2 (C₅-O). ESI-MS m/z : 173 (MH⁺).

Pharmacological Activity Assay This assay of newly synthesized **1** and related compounds was performed using a *Xenopus* oocyte-expressing system as previously described.^{11,12)}

Amino Acid Analysis Selected *Lathyrus* and *Pisum* seeds were germinated in the dark at 25–26 °C. After 6 or 7 d, the seedlings were collected and extracted in 75% EtOH. Detection of **1** in the seedlings and seeds was attempted using an automatic amino acid analyzer (Hitachi 835-10) equipped with a UV detector (265 nm) under standard operating conditions as described previously:¹⁴⁾ **1** was eluted at about 31 min from the column, and **2** and **3** were eluted at about 23 and 37 min, respectively, at a flow rate of 0.275 ml per min.

References

- 1) Lambein F., Kuo Y.-H., Van Parijs R., *Heterocycles*, **4**, 567–593 (1976).
- 2) Lambein F., De Bruyn A., Ikegami F., Kuo Y.-H., "Lathyrus and Lathyrism," ed. by Kaul A. K., Combes D., Third World Medical Research Foundation, New York, 1986, pp. 246–256.
- 3) Lambein F., Ongena G., Kuo Y.-H., *Phytochemistry*, **29**, 3793–3796 (1990).
- 4) Kuo Y.-H., Ikegami F., Lambein F., *Phytochemistry*, **49**, 43–48 (1998).
- 5) Ikegami F., Yamamoto A., Kuo Y.-H., Lambein F., *Biol. Pharm. Bull.*, **22**, 770–771 (1999).
- 6) Schenk S. U., Werner D., *Phytochemistry*, **30**, 467–470 (1991).
- 7) Baldwin J. E., Adlington R. M., Birch D. J., *Tetrahedron Lett.*, **26**, 5931–5934 (1985).
- 8) Hakoda S., Tsubotani S., Iwasa T., Suzuki M., Kondo M., Harada S., *J. Antibiotics*, **45**, 854–860 (1992).
- 9) Tsubotani S., Funabashi Y., Takamoto M., Hakoda S., Harada S., *Tetrahedron*, **47**, 8079–8090 (1991).
- 10) Ikegami F., Kusama-Eguchi K., Sugiyama E., Watanabe K., Lambein F., Murakoshi I., *Biol. Pharm. Bull.*, **18**, 360–362 (1995).
- 11) Kusama-Eguchi K., Ikegami F., Kusama T., Lambein F., Watanabe K., *Environ. Toxicol. Pharmacol.*, **2**, 339–342 (1996).
- 12) Kusama-Eguchi K., Kusama T., Ikegami F., Lambein F., Watanabe K., *Mol. Brain Res.*, **52**, 166–169 (1997).
- 13) Mitsunobu O., Wada M., Sano T., *J. Am. Chem. Soc.*, **94**, 679–680 (1972).
- 14) Ikegami F., Ongena G., Sakai R., Itagaki S., Kobori M., Ishikawa T., Kuo Y.-H., Lambein F., Murakoshi I., *Phytochemistry*, **33**, 93–98 (1993).
- 15) Sarlo F. D., Dini G., Lacrimini P., *J. Chem. Soc. (C)*, **1971**, 86–89.
- 16) Widmer U., *Synthesis*, **1983**, 135–136.

Acetylated and Non-acetylated Flavonol Triglycosides from *Galega officinalis*

Yves CHAMPAVIER,^a Daovy P. ALLAIS,^a Albert J. CHULIA,^{*,a} and Mourad KAOUADJI^b

UPRES-EA 1085, Laboratoire de Pharmacognosie et de Phytochimie, UFR Pharmacie, Université de Limoges,^a 2, rue Docteur Marcland, F-87025 Limoges Cedex, France and Département de Chimie, UFR Sciences, Université de Limoges,^b 123, avenue A. Thomas, F-87060 Limoges Cedex, France. Received June 28, 1999; accepted September 29, 1999

Three flavonol triglycosides kaempferol 3-[2^{Gal}-(4-acetylramnosyl)robinobioside], kaempferol 3-(2^{Gal}-rhamnosylrobinobioside) and quercetin 3-(2^G-rhamnosylrutinoside) have been isolated from a methanolic extract of *Galega officinalis* aerial parts. They are reported for the first time in the genus *Galega*; moreover, the acetylated triglycoside is a new natural product.

Key words *Galega officinalis*; Fabaceae; acylated flavonol triglycoside; kaempferol 3-[2^{Gal}-(4-acetylramnosyl)robinobioside]

Goat's rue (*Galega officinalis* L.) has been used in traditional medicine for treatment of diabetes mellitus.¹⁾ The plant has been previously investigated and the rare nortriterpenoid glucoside dearabinosyl pneumonanthiside was isolated.²⁾ We carried out a chemical investigation of *G. officinalis* and isolated a new acetylated flavonol triglycoside along with two known flavonol triglycosides. This paper describes the isolation and structural elucidation of these components.

The methanolic extract of the aerial parts²⁾ was suspended in H₂O and partitioned by CH₂Cl₂ and EtOAc successively. Compounds 1–3 were present in the EtOAc soluble part. Compounds 2 and 3 were identified as mauritanin³⁾ and quercetin 3-(2^G-rhamnosylrutinoside),^{4,5)} respectively, by comparing their ¹H- and ¹³C-NMR spectral data with reported values. Compound 1 is new, while 2 and 3 were isolated for the first time from this plant.

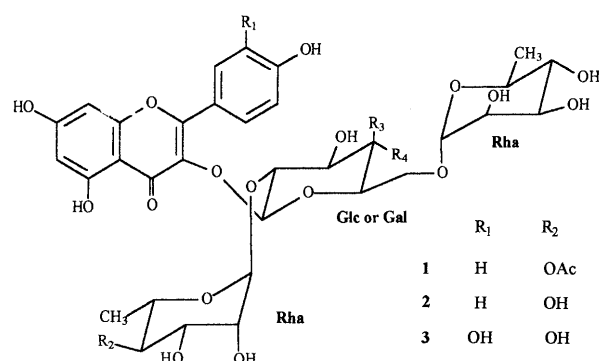
Among the three isolated triglycosides, component 1 was the least polar on silica gel and BAW-cellulose TLC systems (see Experimental). Its UV spectra in the usual shift reagents indicated a kaempferol 3-conjugated structure⁶⁾ as for 2. Furthermore, the positive FAB mass spectrum exhibited a signal at *m/z* 783 (M+H)⁺ consistent with a molecular formula C₃₅H₄₂O₂₀ for the glycoside. Other significant peaks visible at *m/z* 637 [(M+H)–146]⁺, *m/z* 595 [(M+H)–146–42]⁺, *m/z* 449 [(M+H)–146–42–146]⁺ and finally *m/z* 287 [(M+H)–146–42–146–162]⁺ indicated the successive loss of two branched rhamnose units of which one was acetylated as was as an inner hexose, the base signal at *m/z* 287 corresponding to kaempferol. The two branched α-L-rhamnosyl moieties were confirmed by the ¹H broad doublets at δ 4.52 (*J*=1.4 Hz) and δ 5.23 ppm (*J*=1.3 Hz) for anomeric protons

and the doublets (*J*=6.2 Hz) at δ 1.17 and 0.88 ppm for the methyls, as well as the ¹³C-NMR peaks at δ 101.9 and 102.6 ppm for both anomeric carbons and δ 18.0 and 17.4 for CH₃ groups. The inner hexose exhibited ¹H- and ¹³C-NMR values characteristic of β-D-galactose at δ 5.52, d (*J*=7.7 Hz) and δ 101.2 for the anomeric CH as well as those at δ 3.77, brd (*J*=3.3 Hz) and δ 70.7 for CH-4 as recorded for component 2 (Tables 1 and 2). Finally, a substituted robinobiose structure was evidenced in this compound as for 2 by all the ¹H- and ¹³C-NMR shifts and multiplicities relative to the osidic part, thus locating the second rhamnosyl unit at C-2 of the galactose as indicated by δ 3.92 and δ 77.9 (Tables 1 and 2). However, the supplementary rhamnosyl group was different from that of 2 by an acetyl function located at C-4, and was

Table 1. ¹H-NMR Data of Compounds 1–3 (400 MHz, CD₃OD/TMS)^{a)}

No.	1	2	3
Kaempferol or quercetin			
6	6.20 d (2.0)	6.18 d (1.6)	6.18 d (2.0)
8	6.39 d (2.0)	6.38 d (1.6)	6.37 d (2.0)
2'	8.05 d (8.9)	8.06 d (8.8)	7.59 br s
3'	6.89 d (8.9)	6.89 d (8.8)	—
5'	6.89 d (8.9)	6.89 d (8.8)	6.87 d (8.1)
6'	8.05 d (8.9)	8.06 d (8.8)	7.60 dd (8.1, 2.2)
Robinobiose or rutinoside ^{b)}			
1	5.52 d (7.7)	5.60 d (7.8)	5.59 d (7.7)
2	3.92 dd (9.5, 7.7)	3.93 dd (9.5, 7.8)	3.64 dd (9.0, 7.7)
3	3.70 dd (9.5, 3.2)	3.70 dd (9.5, 3.4)	3.54 br t (9.0, 8.7)
4	3.77 br d (3.3)	3.77 br d (3.3)	3.27 br t (9.5, 8.9)
5	3.63 br t (6.1)	3.63 br t (6.3)	3.32 m
6 _A	3.45 dd (10.3, 6.7)	3.44 dd (10.2, 6.6)	3.40 br d (11.6)
6 _B	3.71 dd (10.2, 5.4)	3.72 dd (10.3, 5.7)	3.82 br d (11.6)
1	4.52 br d (1.4)	4.52 br d (1.2)	4.50 br d (1.3)
2	3.57 dd (3.4, 1.6)	3.56 dd (3.3, 1.6)	3.58 dd (3.3, 1.6)
3	3.50 dd (9.3, 3.4)	3.50 dd (9.3, 3.3)	3.49 dd (9.5, 3.4)
4	3.27 t (9.5)	3.26 t (9.5)	3.23 t (9.5)
5	3.52 dq (9.5, 6.2)	3.52 dq (9.5, 6.2)	3.41 dq (9.5, 6.2)
6	1.17 d (6.2)	1.17 d (6.2)	1.08 d (6.2)
Rhamnose			
1	5.23 br d (1.3)	5.21 br d (1.0)	5.22 br d (1.2)
2	4.04 dd (3.3, 1.6)	4.00 br dd (3.0, 1.4)	4.00 dd (3.3, 1.6)
3	4.00 dd (9.8, 3.3)	3.80 dd (9.8, 3.3)	3.80 dd (9.8, 3.4)
4	4.89 t (9.8)	3.34 br t (9.5)	3.35 br t (9.8)
5	4.26 dq (9.8, 6.2)	4.06 dq (9.6, 6.2)	4.08 dq (9.6, 6.2)
6	0.88 d (6.2)	0.98 d (6.2)	1.00 d (6.2)
Acetyl			
CH ₃	2.00 s	—	—

a) δ ppm (*J* Hz). b) Robinobiose: Gal⁶→¹ Rha; rutinoside: Glc⁶→¹ Rha.



* To whom correspondence should be addressed.

Table 2. ^{13}C -NMR Data of Compounds 1–3 (100 MHz, $\text{CD}_3\text{OD}/\text{TMS}$, δ ppm)

No.	1	2	3
Kaempferol or quercetin			
2	158.9	158.7	159.0
3	134.6	134.5	134.5
4	179.4	179.5	179.3
5	163.2	163.2	163.2
6	99.8	99.8	99.8
7	165.7	165.7	165.7
8	94.8	94.7	94.7
9	158.5	158.5	158.5
10	105.9	105.9	106.0
1'	123.0	123.1	123.6
2'	132.2	132.3	117.5
3'	116.2	116.2	146.0
4'	161.4	161.3	149.6
5'	116.2	116.2	116.1
6'	132.2	132.3	123.5
Robinoside or rutinose			
1	101.2	100.9	100.5
2	77.9	77.6	80.1
3	75.7	75.8	79.0
4	70.7	70.8	71.9
5	75.3	75.4	77.1
6	67.3	67.2	68.3
1	101.9	101.9	102.3
2	72.1	72.1	72.2
3	72.3	72.3	72.3
4	73.9	73.9	73.9
5	69.7	69.7	69.8
6	18.0	18.0	17.9
Rhamnose			
1	102.6	102.7	102.7
2	72.5	72.5	72.5
3	70.4	72.4	72.4
4	75.8	74.1	74.1
5	67.7	69.9	70.0
6	17.4	17.6	17.6
Acetyl			
CO	172.9	—	—
CH_3	21.1	—	—

responsible for the large ^1H and ^{13}C deshielding of CH-4 at δ 4.89 and δ 75.8 in comparison with δ 3.34 and δ 74.1 for 2. This group also induced downfield shifts to vicinal protons H-3 (δ 4.00, $\Delta\delta$ +0.20 ppm) and H-5 (δ 4.26, $\Delta\delta$ +0.20 ppm) by decreasing, as expected, the electron density caused by the conjugated 4-oxygen with the carbonyl. Inversely, upfield shifts were recorded for the corresponding carbons C-3 (δ 70.4, $\Delta\delta$ -2.0 ppm) and C-5 (δ 67.7, $\Delta\delta$ -2.2 ppm) following both the anisotropic effect involving the carbonyl and steric hindrance of the substituent.⁷⁾ These results which were completely confirmed by both 2D-NMR including ^1H - ^1H and ^1H - ^{13}C COSY correlation spectroscopy experiments as well as by acid hydrolysis resulted in assignation of the new structure kaempferol 3-*O*-[4-*O*-acetyl- α -L-rhamnopyranosyl-(1 \rightarrow 2)- α -L-rhamnopyranosyl-(1 \rightarrow 6)]- β -D-galactopyranoside or kaempferol 3-[2^{Gal}-(4-acetylramnosyl)robinobioside] to compound 1.

Experimental

General CC was achieved on polyamide SC-6 (Macherey-Nagel) and Sephadex LH20 (Pharmacia). Chromatographic mobilities were recorded in three systems: system 1 (Silica gel F₂₅₄, EtOAc-H₂O-HCO₂H-HOAc, 20:2:1:1), system 2 (Cellulose F₂₅₄, *n*-BuOH-HOAc-H₂O, 4:1:5, upper

phase), system 3 (Cellulose F₂₅₄, H₂O-HOAc, 9:1). Prep. HPLC was performed on a Merck model (Prep Septeck) with Lichrospher 100 DIOL (10 μm , 250 \times 10 mm). UV spectra were recorded on a Jasco V-560 spectrophotometer. ^1H -NMR and ^{13}C -NMR spectra were measured in CD_3OD at 400 MHz for ^1H -NMR and 100 MHz for ^{13}C -NMR on a Bruker DPX Avance spectrometer using tetramethylsilane as internal standard. The complete proton and carbon assignments were based on 1D (^1H standard, ^{13}C *J* mod and ^{13}C distortionless enhancement by polarization transfer (DEPT)), 2D (^1H - ^1H correlation spectroscopy (COSY), ^1H - ^{13}C heteronuclear multiple quantum coherence (HMQC) and ^1H - ^{13}C heteronuclear multiple bond correlation (HMBC)) NMR experiments. Fast atom bombardment (FAB) mass spectra were obtained on a Nermag Sidar V 3.1 spectrometer (70 eV) in the positive ion mode using glycerol matrix. Acid hydrolysis was performed at 110 °C for 2 h with 9 mg for 1, 5 mg for 2 and 3 in 4 ml of 2 N HCl. After neutralization with NaOH, the aqueous residue was extracted twice with Et₂O. Aglycones were detected in the organic layer whilst sugars were identified in the aqueous phase. Glucose, galactose and rhamnose were visualized by TLC (20 cm) on silica gel (EtOAc-H₂O-MeOH-HOAc 13:3:3:4) after spraying *p*-anisidine phthalate reagent.

Plant Material *G. officinalis* was harvested during flowering by Pharmet Plantes (Valanjou, France), and the aerial parts in powder form were deposited at Laboratoire de Pharmacognosie et de Phytochimie (Université de Limoges) along with a control certificate.

Extraction and Isolation *G. officinalis* powdered aerial parts (9 kg) were percolated at room temperature with successive solvents of increasing polarity: 57 l *n*-hexane (110 g), 200 l CH_2Cl_2 (120 g), 140 l EtOAc (52 g) and 100 l MeOH (500 g). A part of the MeOH extract (150 g) was suspended in 1.2 l of water and then divided into 5 portions and added with 150 ml of petrol ether, CH_2Cl_2 , EtOAc, and *n*-BuOH. After concentration, residues were 2.3 g for the petrol ether part, 6.4 g for the CH_2Cl_2 part, 13.9 g for the EtOAc part, 61.3 g for the *n*-BuOH part and, finally, 59.4 g for the aqueous residue. The last mentioned EtOAc extract (13.9 g) was then fractionated on a Sephadex LH20 CC (800 \times 45 mm, MeOH) to give nine fractions (A–I). Compounds 1–3 issued from fraction C were separated by a Lichroprep C18 MPLC (15–25 μm , 460 \times 15 mm, MeOH gradient in H₂O) to give four fractions (I, II, III, IV). Fraction II (542 mg) eluted with H₂O-MeOH (1:1) was passed through two polyamide MPLC (230 \times 15 mm, MeOH gradient in toluene) to afford compound 2 in the toluene-MeOH (4:1) mixture and compound 3 in toluene-MeOH (13:7) fractions. The final purification of 2 was carried out by centrifugal thin layer chromatography [Chromatotron, Silica gel 60 F₂₅₄, 1 mm thickness, *n*-hexane-EtOAc-MeOH (5:2:3)] affording 17 mg. Finally, compound 3 was subjected to a Sephadex LH20 CC (550 \times 15 mm, MeOH) to give 17 mg. Fraction III (430 mg) eluted with H₂O-MeOH (2:3) was submitted to three successive polyamide MPLC (230 \times 15 mm, MeOH gradient in toluene) and finally to a Lichrospher 100 DIOL HPLC [10 μm , 250 \times 10 mm, *n*-hexane-isoPrOH-MeOH (12:3:10)] to yield 127 mg of pure 1.

Kaempferol 3-[2^{Gal}-(4-acetylramnosyl)robinobioside] (1): A yellow amorphous powder, C₃₅H₄₂O₂₀. ^1H - and ^{13}C -NMR: see Tables 1 and 2. UV $\lambda_{\text{max}}^{\text{MeOH}}$ nm: 266, 298 sh, 351; (+NaOH): 274, 329, 394; (+AlCl₃): 275, 306, 353, 401; (+AlCl₃+HCl): 275, 305, 351, 398; (+NaOAc): 270, 303, 356; (+NaOAc+H₃BO₃): 267, 301 sh, 350. Positive FAB-MS (glycerol): *m/z* 783 (M+H)⁺; 637 (M+H-Rha)⁺; 595 (M+H-AcRha)⁺; 449 (M+H-Rha-AcRha)⁺; 287 (M+H-Rha-AcRha-Gal)⁺. Chromatographic mobilities: *Rf* 0.20 (system 1), *Rf* 0.44 (system 2), *Rf* 0.88 (system 3).

Acknowledgements The authors are grateful to Mrs C. Hemmerlin (Service commun de RMN, UFR de Pharmacie, Université de Limoges) for performing the NMR experiments and to la Région Limousin for financial assistance.

References

- Müller A., Diemann E., Sassenberg P., *Naturwissenschaften*, **75**, 155–156 (1988).
- Champavier Y., Comte G., Vercauteren J., Allais D. P., Chulia A. J., *Phytochemistry*, **50**, 1219–1223 (1999).
- Yasukawa K., Takido M., *Phytochemistry*, **26**, 1224–1226 (1987).
- Vidal-Ollivier E., Elias R., Faure F., Babadjamian A., Crespin F., Balansard G., Boudon G., *Planta Medica*, **55**, 73–74 (1989).
- Haribal M., Renwick J. A. A., *Phytochemistry*, **41**, 139–144 (1996).
- Mabry T. J., Markham K. R., Thomas M. B., "The Systematic Identification of Flavonoids," Springer-Verlag, Berlin, 1970, p. 121.
- Agrawal P. K. (ed.), "Studies in Organic Chemistry," Vol. 39, "Carbon-13 of Flavonoids," Elsevier, Amsterdam, 1989, pp. 78–80.

Effect of Polymer Excipients on the Enzyme Activity of Lyophilized Bilirubin Oxidase and β -Galactosidase Formulations

Sumie YOSHIOKA,* Yukio ASO, Shigeo KOJIMA, and Tsuyoshi TANIMOTO

National Institute of Health Sciences, 1-18-1 Kamiyoga, Setagaya-ku, Tokyo 158-8501, Japan.

Received July 28, 1999; accepted October 29, 1999

The effects of excipients on the protein stability during lyophilization as well as the storage stability of lyophilized bilirubin oxidase (BO) and β -galactosidase (GA) formulations were studied using four polymer excipients: dextran, polyvinylalcohol (PVA), poly(acrylic acid) (PAA), and α , β -poly(*N*-hydroxyethyl)-L-aspartamide (PHEA). Denaturation of BO and GA during lyophilization largely depended on the excipient used. Dextran appeared to cause severe damage to proteins, whereas PHEA protected proteins effectively from denaturation. Storage stability of BO and GA formulations also depended on the excipients, such that the formulations containing dextran and PAA were relatively unstable. Storage stability was improved by absorption of a small amount of water for all the formulations studied. Absorption of a larger amount of water, however, decreased the storage stability of the formulations containing PVA, PAA or PHEA. In contrast, the storage stability of formulations containing dextran did not decrease noticeably with increasing water. This may be because formulations containing dextran have a higher glass transition temperature than formulations containing PVA, PAA or PHEA when a large amount of water is absorbed.

Key words lyophilization; enzyme activity; bilirubin oxidase; β -galactosidase; protein stability

Lyophilization is considered to be a very promising formulation for proteins susceptible to chemical and physical degradation.¹⁾ Protein stability during lyophilization is largely affected by the excipients used in the formulations. Excipients that hydrogen bond to proteins can inhibit protein degradation during dehydration. Furthermore, excipients that produce amorphous phase having a high collapse temperature can also prevent proteins from degradation.¹⁾ On the other hand, excipients that induce phase separation during lyophilization generally enhance protein degradation.²⁾ Thus, the choice of optimal excipients plays an important role in improving protein stability during lyophilization.

The choice of excipients is also important for the storage stability of lyophilized protein formulations. Excipients that have a higher glass transition temperature (T_g) in the dry state can provide lyophilized formulations of higher T_g , which exhibit lower molecular mobility, and consequently tend to offer better storage stability.^{3–5)} Excipients that lower the T_g of lyophilized formulations to a temperature close to ordinary operating temperature upon moisture absorption, on the other hand, may decrease storage stability.⁶⁾

In the present study, the effects of excipients on the protein stability during lyophilization, as well as the storage stability of lyophilized bilirubin oxidase (BO) and β -galactosidase (GA) formulations were studied using four polymer excipients: dextran, polyvinylalcohol (PVA), poly(acrylic acid) (PAA), and α , β -poly(*N*-hydroxyethyl)-L-aspartamide (PHEA).

Experimental

Materials GA from *Aspergillus oryzae* was purchased from Toyobo Co. (Osaka) and used without further purification. Bovine serum γ -globulin (BGG, G5009) and bovine serum albumin (BSA, fraction V) was provided by Sigma Chemical Co., Inc. (St. Louis, MO). Lyophilized BO (*Myrothecium verrucaria*) powder containing 25% sucrose and 25% ammonium sulfate was kindly provided by Amano Pharmaceutical Co. (Nagoya). BO was purified by dialysis and lyophilized as described previously.⁷⁾

Dextran (D-4133, average molecular weight of 42000) was obtained from Sigma Chemical Co., Inc. PVA (average molecular weight of 31000–50000) and PAA (32366-7, average molecular weight of 2000) were pur-

chased from Aldrich Chemical Co., Inc. (Milwaukee, WI). PAA was dissolved in water (80 mg/ml), titrated to pH 7.0 with 2.5 N NaOH solution, and lyophilized. PHEA was prepared *via* polysuccinimide by polycondensation of aspartic acid as reported.⁸⁾ All other chemicals were of reagent grade and purchased from Wako Pure Chemical Industries Ltd. (Osaka).

Preparation of Lyophilized BO and GA Formulations Protein (BO, GA) was dissolved in distilled water (0.8 mg/g), and mixed with an equivalent weight of aqueous solutions of polymer excipients (PVA, PHEA, dextran, PAA) (80 mg/g). The weight ratio of protein to excipient was 1 : 100. Three hundred microliters of the solution was frozen in a polypropylene sample tube (10 mm diameter) by immersion in liquid nitrogen for 10 min, and then dried in a vacuum below 5 Pa for 23.5 h in a lyophilizer (Freezevac C-1, Tozai Tsusho Co., Tokyo), as previously described.⁹⁾ The shelf temperature was between -35 and -30°C for the first 1 h, 20°C for the subsequent 19 h, and 30°C for the last 3.5 h.

Solid-State Rehydration and Storage Testing For solid-state rehydration, lyophilized samples were stored at 15°C for 24 h in a desiccator with a saturated solution of potassium acetate (23.4% relative humidity (RH)), $\text{CaCl}_2 \cdot 6\text{H}_2\text{O}$ (35.7%RH), $\text{K}_2\text{CO}_3 \cdot 2\text{H}_2\text{O}$ (43%RH), or $\text{NaBr} \cdot 2\text{H}_2\text{O}$ (60.2%RH). Then, water content was determined by the Karl Fisher method (684 KF Coulometer, Switzerland) (Table 1). The lyophilized samples before and after solid-state rehydration were stored at 70°C for 5 h.

Determination of Enzyme Activity of Lyophilized BO and GA Formulations Enzyme activity of BO was determined as described previously.⁷⁾ Briefly, lyophilized BO formulation was reconstituted with pH 7.0 phosphate buffer to make a $3.2 \mu\text{g/ml}$ BO solution. The solution was added to a preincubated (37°C) buffer containing BSA, bilirubin and sodium cholate, and the decrease in absorbance at 460 nm was monitored. BO activity was determined within 30 min of reconstitution.

Enzyme activity of GA was measured as described previously.¹⁰⁾ Lyophilized GA formulations were dissolved in distilled water to make $1 \mu\text{g/ml}$ GA solution. The activity was determined using 2-nitrophenyl- β -D-galactopyranoside as a substrate.

Results

Inactivation during Lyophilization Figure 1 shows the enzyme activity of BO and GA remaining after lyophilization with various polymer excipients. This value is expressed as a percentage of the enzyme activity of the solutions prior to lyophilization. When dextran was used as the excipient, marked inactivation during lyophilization was observed in both BO and GA formulations. When lyophilized with PVA, BO exhibited a marked decrease in activity, whereas GA

* To whom correspondence should be addressed.

Table 1. Water Content of Lyophilized BO and GA Formulations before and after Solid-State Rehydration under Various Humidity Conditions (g/g of Solid)

Humidity (%RH)	BO				GA			
	Dextran	PVA	PAA	PHEA	Dextran	PVA	PAA	PHEA
None	0.012	0.003	0.012	0.003	0.010	0.010	0.018	0.007
23.4	0.054	0.020	0.101	0.035	0.056	0.020	0.105	0.037
35.7	0.085	0.042	0.172	0.061	0.082	0.038	0.166	0.059
43.0	0.124	0.075	0.282	0.091	0.124	0.070	0.273	0.092
60.2	0.168	0.101	0.413	0.136	0.165	0.101	0.409	0.140

$n=3$; standard error: less than 5%.

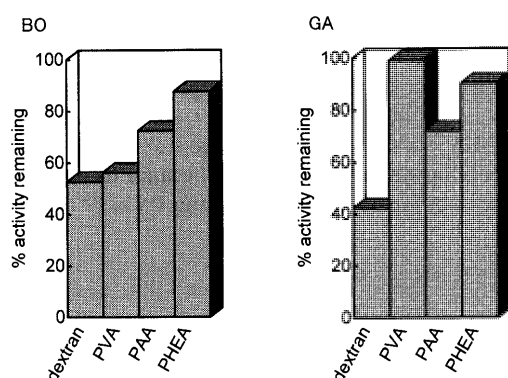


Fig. 1. Enzyme Activity of BO and GA Remaining after Lyophilization with Various Polymer Excipients

Expressed as a percentage of the enzyme activity of solutions prior to lyophilization ($n=3$, standard error: less than 4% for BO and less than 3% for GA).

showed no significant decrease. Lyophilization with PAA yielded BO and GA formulations with a relatively high remaining activity. BO and GA formulations with the highest remaining activity of more than 90% were obtained when PHEA was used as the excipient.

Figure 2 shows the effect of solid-state rehydration and subsequent storage on the enzyme activity of lyophilized BO and GA formulations. The rear columns represent the enzyme activity remaining after solid-state rehydration under various humidity conditions. For the BO formulations (upper figures), the remaining activity decreased with increasing humidity for the formulations lyophilized with dextran, whereas an increase in remaining activity with increasing humidity was observed for the formulations lyophilized with PVA. The effect of humidity conditions on the remaining activity was not significant for the formulations lyophilized with PAA and PHEA. In contrast, the GA formulations (lower figures) exhibited an increase in remaining activity with increasing humidity for any formulations lyophilized with dextran, PAA or PHEA.

Inactivation during Storage The front columns in Fig. 2 represent the enzyme activity remaining after storage (at 70°C for 5 h) of the lyophilized BO and GA formulations with water absorbed at various humidities. The remaining activity of the lyophilized formulation without solid-state rehydration is also shown. This figure shows that the formulations containing dextran and PAA were relatively unstable. All the formulations studied exhibited lower storage stability without solid-state rehydration compared to the samples rehydrated at 23.4%RH. On the other hand, solid-state rehydration under higher humidity decreased the storage stability of

formulations lyophilized with PVA, PAA and PHEA, except the GA formulation containing PHEA in which the stability was very high. Storage stability did not decrease remarkably with increasing humidity in the formulations lyophilized with dextran.

Discussion

Denaturation of BO and GA during lyophilization largely depended on the excipient used. Dextran appeared to induce severe damage in proteins, whereas PHEA protected proteins effectively from denaturation, as shown in Fig. 1. The enzyme activity of the BO formulation lyophilized with PHEA, which was determined after rehydration in buffer, was more than 90% of the solutions prior to lyophilization. This is higher than the activity reported for BO formulations lyophilized with trehalose,⁷⁾ which is an effective stabilizer against protein denaturation during dehydration. It is well known that excipients with ability to hydrogen bond to the protein can inhibit protein denaturation during lyophilization.¹⁾ The stabilizing effect of PHEA may be due to its flexible hydrophilic groups that can interact with protein. Dextran, which is considered to be too bulky to hydrogen bond to protein,¹⁾ may cause substantial denaturation of BO and GA during lyophilization.

The effect of excipients on protein denaturation during lyophilization naturally varies with the properties of the proteins. PVA inhibited GA almost completely from denaturation during lyophilization, but its stabilizing effect was not as effective for BO, as shown in Fig. 1. GA generally appears to be more stable than BO. When dextran was used as the excipient, marked inactivation during lyophilization was observed in both BO and GA formulations. Some of the activity loss in the GA formulations was recovered by solid-state rehydration, whereas solid-state rehydration caused further denaturation rather than activity recovery in the BO formulations, as shown in Fig. 2. These findings suggest that GA undergoes partially reversible structural damage during lyophilization, indicating a lower degree of damage than that which occurs in BO formulations.

The storage stability of BO and GA formulations was improved by absorption of a small amount of water (Fig. 2), suggesting that protein structure damage during lyophilization can be repaired to provide a more stable structure by appropriate solid-state rehydration. However, absorption of a larger amount of water decreased storage stability for most formulations. The decrease in storage stability with increasing absorption of water can be ascribed to an increase in molecular mobility with the absorption. This effect appeared

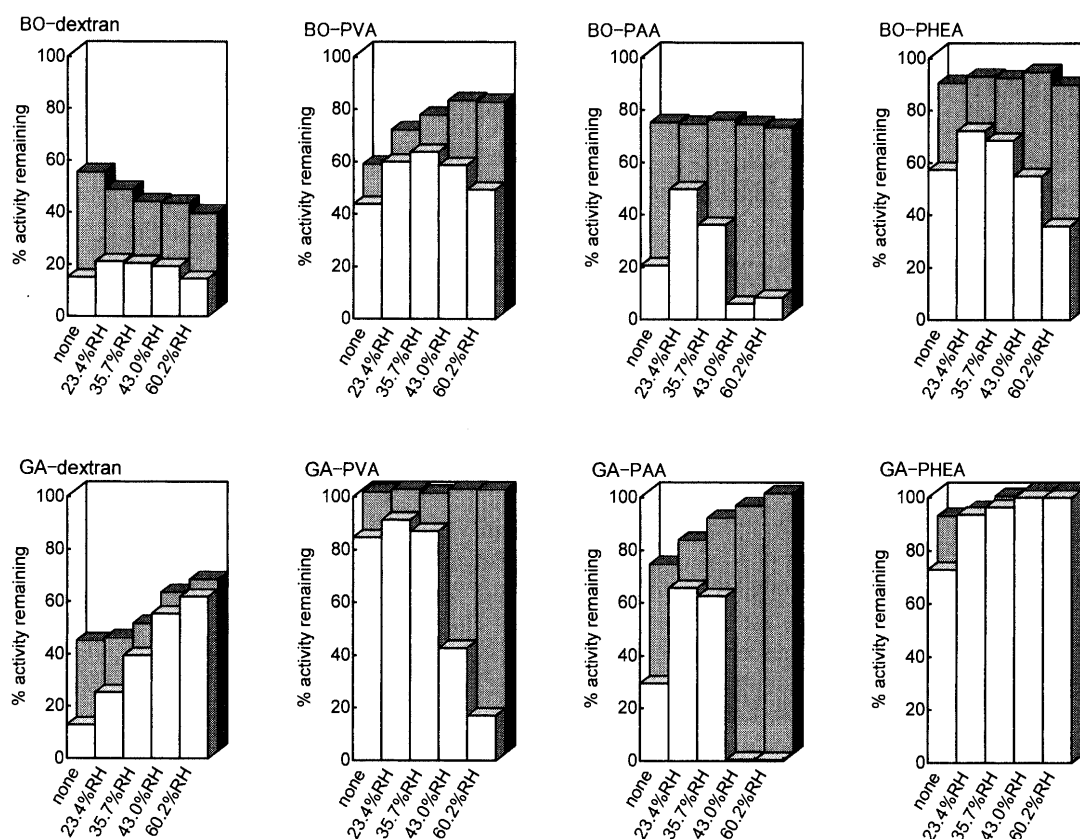


Fig. 2. Enzyme Activity of Lyophilized BO and GA Formulations Containing Various Polymer Excipients

Remaining after solid-state rehydration under various humidity conditions (rear column) and after subsequent storage at 70 °C for 5 h (front column), expressed as a percentage of the enzyme activity of solutions prior to lyophilization ($n=3$, standard error: less than 4% for BO and less than 3% for GA).

to vary according to the excipient used, such that formulations containing dextran did not exhibit as clear a decrease as formulations containing PVA, PAA or PHEA. This may be because formulations containing dextran have a higher glass transition temperature than formulations containing PVA, PAA or PHEA when a large amount of water absorption occurs. Although a decrease in storage stability with increasing water was also not observed in GA formulations containing PHEA, this may be due to the stabilizing effect of PHEA which inhibits protein unfolding/denaturation during lyophilization due to protein–excipient interaction.

References and Notes

- 1) Carpenter J. F., Pikal M. J., Chang B. S., Randolph T. W., *Pharm. Res.*, **14**, 969–975 (1997).
- 2) Randolph T. W., *J. Pharm. Sci.*, **86**, 1198–1203 (1997).
- 3) Roy M. L., Pikal M. J., Rickard E. C., Maloney A. M., *Develop. Biol. Standard.*, **74**, 323–340 (1991).
- 4) Duddu S. P., Dal Monte P. R., *Pharm. Res.*, **14**, 591–595 (1997).
- 5) Duddu S. P., Zhang G., Dal Monte P. R., *Pharm. Res.*, **14**, 596–600 (1997).
- 6) Yoshioka S., Aso Y., Kojima S., *Pharm. Res.*, **16**, 135–140 (1999).
- 7) Nakai Y., Yoshioka S., Aso Y., Kojima S., *Chem. Pharm. Bull.*, **46**, 1031–1033 (1998).
- 8) Giammona G., Carlisi B., Palazzo S., *J. Polym. Sci. Polym. Chem. Ed.*, **25**, 2813–2818 (1987).
- 9) Yoshioka S., Aso Y., Kojima S., *Pharm. Res.*, **14**, 736–741 (1997).
- 10) Izutsu S., Yoshioka S., Takeda Y., *Chem. Pharm. Bull.*, **38**, 800–803 (1990).

A New Oleanene Glucuronide Obtained from the Aerial Parts of *Melilotus officinalis*¹⁾

Tomoki HIRAKAWA, Masafumi OKAWA, Junei KINJO,* and Toshihiro NOHARA

Faculty of Pharmaceutical Sciences, Kumamoto University, 5-1 Oe-honmachi, Kumamoto 862-0973, Japan.

Received August 5, 1999; accepted October 20, 1999

A new oleanene glucuronide called melilotus-saponin O₂ (**1**) was isolated together with three known ones (soyasaponin I, astragaloside VIII, wistariasaponin D) from the aerial parts of *Melilotus officinalis* (L.) PALLAS (Leguminosae). The structure of **1** was determined to be 3-*O*- α -L-rhamnopyranosyl-(1 \rightarrow 2)- β -D-xylopyranosyl-(1 \rightarrow 2)- β -D-glucuronopyranosyl melilotigenin by spectroscopic and chemical methods.

Key words *Melilotus officinalis*; Leguminosae; triterpene saponin; oleanene glucuronide; melilotus-saponin; melilotigenin

Melilotus officinalis (L.) PALLAS is distributed worldwide and is known as common yellow melilot or medicinal sweet clover in English.²⁾ This plant is used not only as food and forage but also as a medicine. The preventive effect of its extract of whole plant on experimental atherosclerosis in rabbits was reported.³⁾ The effect of a medical preparation (Esberiven) using its extract was also evaluated on dermatological disease.⁴⁾ Earlier researchers found that an extract of the aerial parts showed potent inhibitory activity on the migration of leucocytes, and one of the constituents responsible for the action was azukisaponin V.⁵⁾ During our course of studies on leguminous plants,¹⁾ we also investigated the oleanene-type triterpene glucuronides (oleanene glucuronides) of the roots of *Melilotus officinalis* collected in Hokkaido, Japan.⁶⁾ Herein, we describe the structural elucidation of oleanene glucuronides obtained from the aerial parts of the titled plant.

The aerial parts of *M. officinalis* were collected in the medicinal garden of Kumamoto University. A methanolic extract of the aerial parts of the titled plant afforded saponins (**1**–**4**) after various chromatographic purifications. Saponins **2**–**4** were identified as soyasaponin I (**2**),⁷⁾ wistariasaponin D (**3**),⁸⁾ and astragaloside VIII (**4**)⁹⁾ by comparison with various data.

Melilotus-saponin O₂ (**1**) was obtained as a white amorphous powder, $[\alpha]_D^{25} -45.7^\circ$ (pyridine). In the negative FAB-MS, **1** showed an $[M-H]^-$ ion at m/z 939. Fragment ion peaks at m/z 793 $[M-\text{methylpentose}]^-$ and 661 $[M-\text{methylpentose}-\text{pentose}]^-$ were also observed. The exact measurement under high resolution (HR) conditions showed that the composition is C₄₇H₇₂NaO₁₉ at m/z 963.4564 $[M+Na]^+$ in the HR/positive FAB-MS. The sapogenol obtained by enzymatic hydrolysis was identified with meliloti-

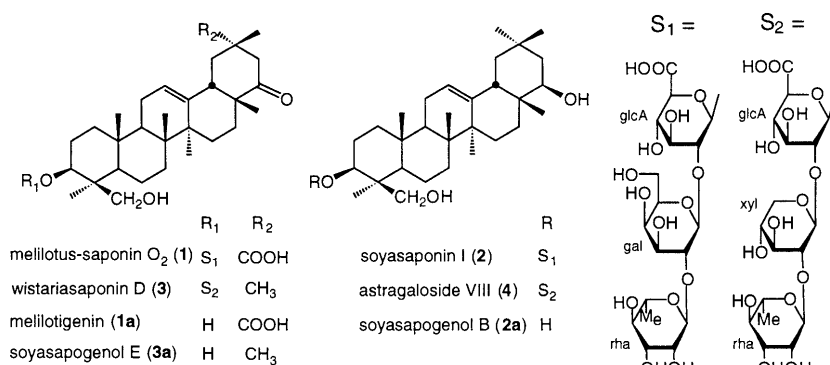
genin (**1a**).^{5c,10)} The monosaccharide mixture obtained by acid hydrolysis of **1** revealed the presence of glucuronic acid, xylose and rhamnose by TLC. Their absolute configurations were determined to be the D-form (glucuronic acid, xylose) and the L-form (rhamnose), according to the procedure developed by Hara *et al.*¹¹⁾ In the sugar region of the ¹³C-NMR spectrum for **1**, signals due to a sugar moiety were identical with those of **3** and **4**. Since the signal at C-3 of **1** was shifted to a lower field by glycosylation,¹²⁾ the structure of **1** was deduced to be 3-*O*- α -L-rhamnopyranosyl-(1 \rightarrow 2)- β -D-xylopyranosyl-(1 \rightarrow 2)- β -D-glucuronopyranosyl melilotigenin. Although melilotigenin glycosides were already obtained from *Trifolium repens*,¹³⁾ melilotus-saponin O₂ is the first example of a tri-glycosidic saponin having the same aglycone.

Experimental

The instruments and reagents used in this study were the same as those previously described.^{6,10)}

Extraction and Isolation The dried aerial parts (356 g) of *Melilotus officinalis* collected in the medicinal garden of Kumamoto University were extracted with MeOH. The extract (40 g) was partitioned with *n*-hexane and 80% MeOH. Removal of the solvent from the latter phase under reduced pressure gave an aqueous extract (35 g). The aqueous extract was subjected to Diaion HP-20 column (6 \times 30 cm) chromatography using H₂O and MeOH. A part (5.2 g) of the MeOH eluate (10 g) was subjected to Sephadex LH-20 column (5 \times 35 cm) chromatography using MeOH to give a total saponin fraction (0.73%). After silica gel column chromatography using CHCl₃:MeOH:H₂O=7:3:0.5–6:4:1, the saponin fractions were separated by silica gel (1-BuOH:AcOH:H₂O=8:1:0.1–4:1:2) to provide compounds **1** (0.032%), **2** (0.019%), **3** (0.020%) and **4** (0.19%), respectively. Soyasaponin I⁷⁾ (**2**) and Astragaloside VIII⁹⁾ (**4**) were identified by comparison of their t_R (HPLC)^{7c,14)} and R_f (TLC) values with the authentic samples.

Compound 1 (Melilotus-Saponin O₂) A white amorphous powder, $[\alpha]_D^{25} -45.7^\circ$ ($c=0.50$, pyridine). HR positive ion FAB-MS m/z : 963.4564 (C₄₇H₇₂NaO₁₉, Calcd for 963.4566). Negative ion FAB-MS m/z : 939



* To whom correspondence should be addressed.

[M-H]⁻, 793 [M-H-rha]⁻, 661 [M-H-rha-xy]⁻, 485 [M-H-rha-xy]-glcA]⁻. ¹H-NMR (in pyridine-*d*₅): 0.69, 0.85, 1.19, 1.28, 1.45, 1.46 (each 3H, s, *tert*-Me×6), 1.82 (3H, d, *J*=6.1 Hz, rha H₃-6), 4.08 (1H, t, *J*=8.4 Hz, xyl H-3), 4.71 (1H, dd, *J*=3.1, 9.2 Hz, rha H-3), 4.93 (1H, d, *J*=7.9 Hz, glcA H-1), 5.27 (1H, s, H-12), 6.23 (1H, s, rha H-1). ¹³C-NMR (in pyridine-*d*₅): 38.8, 26.3, 90.9, 44.0, 56.3, 18.5, 33.0, 39.7, 47.5, 36.4, 23.9, 123.2, 141.6, 42.0, 25.4, 27.4, 48.2, 47.4, 42.0, 45.2, 47.1, 216.8, 22.7, 62.8, 15.5, 16.7, 25.4, 20.9, 181.0, 21.9 (C-1—30), 104.9, 78.2, 76.4, 73.8, 77.8, 175.7 (glcA C-1—6), 102.4, 78.9, 78.0, 70.6, 66.5 (xyl C-1—5), 101.7, 72.0, 72.0, 73.9, 69.2, 18.6 (rha C-1—6).

Characterization of Sapogenol for 1 To a solution of **1** (4 mg) in acetate buffer (pH 5.0, 6 ml) was added glycyrrhizin hydrolase,¹⁵⁾ and the mixture was incubated at 37°C for 40 h. When the hydrolysis was completed, the hydrolysate was evaporated and suspended in MeOH. After filtration of the suspension, the filtrate was methylated in ethereal CH₂N₂. The methylated sample was identified to be a methylester of melilotigenin^{5c,10)} by TLC. *R*_fs: 0.54 [CHCl₃:MeOH (19:1)], 0.83 [*n*-hexane:acetone (1:1)].

Characterization of Sugars for 1 A small amount of **1** (2 mg) was dissolved in 2 M HCl/H₂O (1 ml) and heated at 80°C for 2 h. After neutralization of 2 M NaOH/H₂O, the sugar mixture was subjected to TLC analysis [TLC, Kieselgel 60 F₂₅₄ (Merck Art. 5554), CHCl₃:MeOH:H₂O=6:4:1, *R*_fs: 0.09 (glucuronic acid), 0.45 (xylose), 0.61 (rhamnose)].

D, L Determination of Sugars for 1 The absolute configuration of glucuronic acid was determined after NaBH₄ reduction, according to Tanaka *et al.*¹⁶⁾ A small amount of **1** (3 mg) in MeOH (0.5 ml) was methylated with ethereal CH₂N₂. To a solution of the methylated sample of **1** was added NaBH₄, and the mixture was kept at room temperature for 30 min. The reaction mixture was worked up with MCI gel CHP 20P. The MeOH eluate was evaporated and heated in 2 M HCl/H₂O at 90°C for 3 h. The hydrolysate was subjected to MCI gel CHP 20P and Amberlite IRA-400 to give a sugar fraction. This fraction was dissolved in pyridine (0.1 ml), then the solution was added to a pyridine solution (0.2 ml) of L-cysteine methyl ester hydrochloride (0.1 mol/l) and heated at 80°C for 1 h. The solvent was evaporated under a N₂ stream and dried *in vacuo* with heating. The remaining syrup was trimethylsilylated with trimethylsilylimidazole (0.1 ml) at 60°C for 1 h. After the addition of *n*-hexane and H₂O, the *n*-hexane layer was taken out and checked by GC. The retention times of the peaks coincided with those of D-glucose (*t*_R 11.6 min), D-xylose (*t*_R 6.6 min) and L-rhamnose (*t*_R 8.0 min).

Wistariasaponin D (3)⁸⁾ A white amorphous powder, [α]_D¹⁴ -29.5° (*c*=0.46, pyridine). Negative ion FAB-MS *m/z*: 910 [M-H]⁻, 764 [M-H-rha]⁻, 632 [M-H-rha-xy]⁻. ¹H-NMR (in pyridine-*d*₅): 0.76, 0.85, 0.88, 0.96, 1.16, 1.31, 1.53 (each 3H, s, *tert*-Me×7), 1.81 (3H, d, *J*=6.1 Hz, rha H₃-6), 4.11 (1H, t, *J*=8.4 Hz, xyl H-3), 4.69 (1H, dd, *J*=3.1, 9.2 Hz, rha H-3), 5.02 (1H, d, *J*=7.9 Hz, glcA H-1), 5.25 (1H, s, H-12), 5.68 (1H, d, *J*=7.3 Hz, xyl H-1), 6.34 (1H, s, rha H-1). ¹³C-NMR (in pyridine-*d*₅): 38.7, 26.6, 90.9, 44.2, 56.2, 18.5, 33.0, 39.7, 47.8, 36.4, 23.9, 123.9, 141.7, 42.0, 25.3, 27.2, 47.7, 47.5, 46.6, 34.0, 50.8, 215.6, 22.9, 62.8, 15.4, 16.7, 25.1, 20.9, 32.0, 25.4 (C-1—30), 105.4, 78.6, 77.4, 73.8, 77.7, 172.4 (glcA C-1—6), 102.5, 79.4, 78.3, 70.8, 66.7 (xyl C-1—5), 102.3, 72.3, 72.7, 74.3

69.4, 18.8 (rha C-1—6).

Acknowledgements We are grateful to Prof. H. Okabe, Dr. T. Nagao and Mr. H. Hanazono of the Faculty of Pharmaceutical Sciences, Fukuoka University, for measurement of the HR-MS. We appreciate Dr. K. Mizutani of Maruzen Pharm. Co., Ltd., for supplying glycyrrhizin hydrolase.

References and Notes

- 1) Part 63 in a series of studies on leguminous plants.
- 2) Bisby F. A., Buckingham J., Harborne J. B. (eds.), "Phytochemical Dictionary of the Leguminosae," Chapman & Hall, London, 1994, pp. 472—474.
- 3) Sakamoto W., Ohashi K., Nishikaze O., *Oyo Yakuri*, **15**, 1—14 (1978).
- 4) Okuma M., *Yakuri To Chiryō*, **10**, 581—584 (1978); Higo S., Nakamura Y., Kawasaki M., *Oyo Yakuri*, **15**, 231—240 (1978).
- 5) a) Kang S. S., Lim C.-H., Lee S. Y., *Arch. Pharm. Res.*, **10**, 9—13 (1987); b) Kang S. S., Lee Y. S., Lee E. B., *Kor. J. Pharmacognosy*, **18**, 89—93 (1987); c) Kang S. S., Woo W. S., *J. Nat. Prod.*, **51**, 335—338 (1988); d) Kang S. S., Lee Y. S., Lee E. B., *Arch. Pharm. Res.*, **11**, 197—202 (1988).
- 6) Udayama M., Kinjo J., Yoshida N., Nohara T., *Chem. Pharm. Bull.*, **46**, 526—527 (1998).
- 7) a) Kitagawa I., Yosikawa M., Yosioka I., *Chem. Pharm. Bull.*, **24**, 121—129 (1976); b) Kitagawa I., Wang H. K., Taniyama T., Yoshikawa M., *ibid.*, **36**, 153—161 (1988); c) Kinjo J., Kishida F., Watanabe K., Hashimoto F., Nohara T., *ibid.*, **42**, 1874—1878 (1994).
- 8) Konoshima T., Kozuka M., Haruna M., Ito K., *J. Nat. Prod.*, **54**, 830—836 (1991).
- 9) a) Kitagawa I., Wang H. K., Yoshikawa M., *Chem. Pharm. Bull.*, **31**, 716—722 (1983); b) Kinjo J., Fujishima Y., Saino K., Tian R., Nohara T., *ibid.*, **43**, 636—640 (1995).
- 10) Takeshita T., Yokoyama K., Yi D., Kinjo J., Nohara T., *Chem. Pharm. Bull.*, **39**, 1908—1910 (1991).
- 11) Hara S., Okabe H., Mihashi K., *Chem. Pharm. Bull.*, **35**, 501—506 (1987).
- 12) Kasai R., Suzuo M., Asakawa J., Tanaka O., *Tetrahedron Lett.*, **1977**, 175—178; Tori K., Seo S., Yoshimura Y., Arita H., Tomita Y., *ibid.*, **1977**, 179—182.
- 13) Sakamoto S., Kofuji S., Kuroyanagi M., Ueno A., Sekita S., *Phytochemistry*, **31**, 1773—1777 (1992).
- 14) Kinjo J., Hatakeyama M., Udayama M., Tsutanaga Y., Yamashita M., Nohara T., Yoshiki Y., Okubo K., *Biosci. Biotechnol. Biochem.*, **62**, 429—433 (1998); Kinjo J., Aoki K., Okawa M., Shii Y., Hirakawa T., Nohara T., Nakajima Y., Yamazaki T., Hosono T., Someya M., Niiho Y., Kurashige T., *Chem. Pharm. Bull.*, **47**, 708—710 (1999).
- 15) Sakai Y., Morita T., Kuramoto T., Mizutani K., Ikeda R., Tanaka O., *Agric. Biol. Chem.*, **52**, 207—210.
- 16) Tanaka R., Nagao T., Okabe H., Yamauchi T., *Chem. Pharm. Bull.*, **38**, 1153—1157 (1990).

An Efficient One-Pot Method for the Large-Quantitative Production of Radiopharmaceutical Ligand : Diazadioximes

Hueisch-Jy DING,^{*,a} Ying-Fong HUANG,^a Cherng-Chyi TZENG,^b Si-Jung YEH,^c and Li-Lan WEI^d

Department of Nuclear Medicine, School of Technology for Medical Sciences,^a Department of Chemistry,^b Kaohsiung Medical University, Kaohsiung City 807, Taiwan, R.O.C., Institute of Nuclear Science, Tsing Hua University,^c Hsinchu, Taiwan, R.O.C., and Department of Applied Chemistry, Fooyin Institute of Technology,^d Kaohsiung City 831, Taiwan, R.O.C. Received August 6, 1999; accepted September 26, 1999

An efficient one-pot procedure for the preparation of diazadioxime was described. Treatment of ketooximes with alkyldiamine followed by NaBH₄ in dry ethanol afforded the corresponding *d,l*-diazadioximes in 56–74% yield without isolation of the intermediates.

Key words brain radiopharmaceutical ligand; one-pot method; diazadioxime; large-quantitative production

Single photon emission computerized tomography (SPECT) used as a measure of regional cerebral blood flow has received much attention in the development of technetium-99m complexes for imaging the brain.^{1–3} During recent years, numerous brain imaging radiopharmaceuticals have been synthesized including *N*-isopropyl-*p*-I-123-iodoamphetamine (IMP),⁴ *N,N,N'*-trimethyl-*N'*-2-hydroxy-3-methyl-5-I-123-iodobenzyl-1,3-propane-diamine (I-123-HIPDM),⁵ TI-201-dimethyl-dithiocarbamate (TI-201-DDC),⁶ Tc-99m-*d,l*-hexamethylpropylene amine (Tc-99m-HMPAO),^{7–8} and Tc-99m-*l,l*-ethylcystinatedimer (Tc-99m-*l,l*-ECD).⁹ Ligands are very important as an excellent brain imaging agent. Although there are several synthetic methods of preparing these ligands exist, most of them suffer from tedious synthetic procedures and low chemical yields. For instance, the method reported by Murmann^{10–12} involves the reaction of nitrosyl chloride with the corresponding alkenes, followed by the reaction of the chlorides with diamines. The method results in low yields. Herein we wish to report a new, simple and efficient one-pot preparation of diazadioxime with NaBH₄ in dry ethanol.

The one-pot synthesis of diazadioxime is achieved by treatment of ketooximes (**1**) with alkyldiamines, followed by reduction of diimine-dioximes with NaBH₄ without isolation of the intermediates. Various solvents, including benzene, methanol, and tetrahydrofuran (THF), were examined in order to achieve higher yield, but dry ethanol had the most acceptable results. The *d,l*-diazadioximes were separated from meso-isomers by fractional recrystallization. The results are summarized in Table 1. Using this method, the over-

all yield of dioxime (HMPAO) is 74% which is higher than the 28% reported by Neirinx and his colleagues.^{8,13} The yield of *d,l*-HMPAO is 70% which is also higher than the 33% by the same authors.

General Procedure To a stirred solution of ketooximes (**1**) (0.23 mol) in dry ethanol (300 ml) was added diamines (0.098 mol). The reaction mixture was heated to reflux and stirred at this temperature for 6 h. After cooling to room temperature, the reaction mixture was chilled in an ice bath, then NaBH₄ (0.2 mol) was added slowly in portions into the reaction mixture and it was stirred until the solution turned an ivory color. Ethanol was then removed *in vacuo*, and water (100 ml) was added. The solution was kept at 4 °C for 2 d. Solids were filtered, washed with ice water and recrystallized with EtOAc. All diazadioximes were found to be in accord with known compounds by comparing their spectral data, such as mass, ¹H-NMR and ¹³C-NMR.

In conclusion, this method provides an efficient one-pot synthesis of diazadioxime without isolation of intermediates and good chemical yields. The procedure is easy to perform and does not require tedious purification procedures. All reagents are commercially available and inexpensive. This method is useful for commercial mass production.

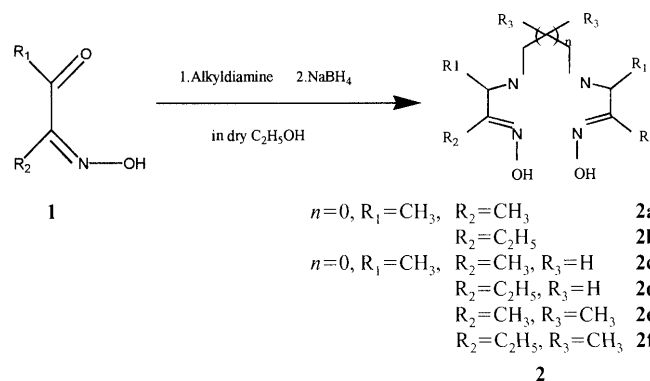
Spectroscopic Data 3,8-Dimethyl-4,7-diazadecane-2,9-dione dioxime (**2a**)^{14–16}: Yield, 67%; white solid; mp 119–120 °C. IR (KBr) 3330 cm^{–1} (OH), 3210–3090 cm^{–1} (OH, NH), 1685 cm^{–1} (–C=N–). ¹H-NMR (CD₃OD) δ: 1.198 (6H, d, *J*=6.78 Hz, Me), δ: 1.787 (6H, s, Me), δ: 2.682 (4H, q, *J*=10.7 Hz, CH₂N), δ: 3.346 (2H, q, *J*=6.78 Hz, CHMe). Anal. Calcd for C₁₀H₂₂N₄O₂: C, 52.17; H, 9.57; N, 24.38. Found: C, 52.29; H, 9.81; N, 24.16.

Table 1. Reagents and Yields of Diazadioxime

Entry	R ₁	R ₂	Diamine	Diazadioxime	Yield ^{a,b} (%)
1a	CH ₃	CH ₃	1,2-Ethanediamine	2a	67
1b	CH ₃	C ₂ H ₅	1,2-Ethanediamine	2b	56
1c	CH ₃	CH ₃	1,3-Propanediamine	2c	70
1d	CH ₃	C ₂ H ₅	1,3-Propanediamine	2d	71
1e	CH ₃	CH ₃	2,2-Dimethyl-1,3-propanediamine	2e	74
1f	CH ₃	C ₂ H ₅	2,2-Dimethyl-1,3-propanediamine	2f	63

a) All products were identified by comparison of their physical and spectral data with those of authentic samples. b) Recrystallized yield.

* To whom correspondence should be addressed.



4,9-Dimethyl-5,8-diazadodecane-3,10-dione dioxime (**2b**)¹⁴⁻¹⁶: Yield, 56%; white solid; mp 126–128 °C. IR (KBr) 3310 cm⁻¹ (OH), 3220–3050 cm⁻¹ (OH, NH), 1670 cm⁻¹ (–C=N–). ¹H-NMR (CD₃OD) δ: 0.934 (6H, t, *J*=6.77 Hz, Me), δ: 1.199 (6H, d, *J*=6.80 Hz, Me), δ: 1.678 (4H, q, *J*=6.78 Hz, CH₂Me), δ: 2.682 (4H, q, *J*=10.8 Hz, CH₂N), δ: 3.361 (2H, q, *J*=6.80 Hz, CHMe). *Anal.* Calcd for C₁₂H₂₆N₄O₂: C, 55.77; H, 10.15; N, 21.68. Found: C, 55.79; H, 10.09; N, 21.62.

3,9-Dimethyl-4,8-diazaundecane-2,10-dione dioxime (**2c**)^{14,17}: Yield, 70%; white solid; mp 123–125 °C. *Anal.* Calcd for C₁₁H₂₄N₄O₂: C, 54.10; H, 9.84; N, 22.95. Found: C, 53.92; H, 9.80; N, 23.01.

4,10-Dimethyl-5,9-diazatridecane-3,11-dione dioxime (**2d**)¹⁴⁻¹⁶: Yield, 71%; white solid; mp 133–135 °C. IR (KBr) 3295 cm⁻¹ (OH), 3210–3030 cm⁻¹ (OH, NH), 1695 cm⁻¹ (–C=N–). ¹H-NMR (CD₃OD) δ: 0.932 (6H, t, *J*=6.80 Hz, Me), δ: 1.201 (6H, d, *J*=7.20 Hz, Me), δ: 1.32–1.39 (2H, m), δ: 1.67–1.79 (4H, m), δ: 2.382 (4H, q, *J*=10.6 Hz, CH₂N), δ: 3.269 (2H, q, *J*=6.67 Hz, CHMe). *Anal.* Calcd for C₁₃H₂₈N₄O₂: C, 57.35; H, 10.29; N, 20.58. Found: C, 57.39; H, 10.53; N, 20.56.

3,6,6,9-Tetramethyl-4,8-diazaundecane-2,10-dione dioxime (**2e**): Yield, 74%; white solid; mp (mixture of *d,l*- and *meso*-) 137–138 °C. Recrystallization from EtOAc gave *d,l*-isomer in 70%, mp (*d,l*-) 128–130 °C (Lit.^{13,8}) mp (*d,l*-) 128–130 °C) and *meso*-isomer in 30%, mp (*meso*-) 147–149 °C.

4,7,7,10-Tetramethyl-5,9-diazatridecane-3,11-dione dioxime (**2f**): Yield, 63%; white solid; mp 141–142 °C. IR (KBr) 3313 cm⁻¹ (OH), 3210–3080 cm⁻¹ (OH, NH), 1675 cm⁻¹ (–C=N–). ¹H-NMR (CD₃OD) δ: 0.879 (6H, s, Me), δ: 0.943 (6H, t, *J*=7.08 Hz, Me), δ: 1.187 (6H, d, *J*=7.60 Hz, Me), δ: 1.675 (4H, q, *J*=7.06 Hz, CH₂Me), δ: 2.678 (4H, q, *J*=10.2 Hz, CH₂N), δ: 3.296 (2H, q, *J*=6.78 Hz, CHMe).

Anal. Calcd for C₁₅H₃₂N₄O₂: C, 60.00; H, 10.67; N, 18.67. Found: C, 60.33; H, 10.72; N, 18.62.

Acknowledgements The authors wish to express their sincere thanks to the National Science Council of R.O.C. for its financial support of this work. They would also like to thank Professor M. J. Wu and Dr. C. F. Lin for their valuable assistance.

References

- 1) Oldendorf W. H., *J. Nucl. Med.*, **19**, 1182–1187 (1978).
- 2) Loberg M. D., *J. Nucl. Med.*, **21**, 183–186 (1980).
- 3) Kung H. F., Molnar M., Billing J., Wicks R., Blau M., *J. Nucl. Med.*, **25**, 326–332 (1984).
- 4) Winchell H. S., Baldwin R. M., Lin J. H., *J. Nucl. Med.*, **21**, 940–946 (1980).
- 5) Kung H. F., Tramposch K. M., Blau M., *J. Nucl. Med.*, **24**, 66–72 (1983).
- 6) Bruine J. F., Royen E. A., Vyth J. M. B. V., Shoot J. B., *J. Nucl. Med.*, **26**, 925–930 (1985).
- 7) Holmes R. A., Chaplin S. B., Royston K. G., Hoffman T. J., Volkert W. A., Nowotnik D. P., Canning L. R., Cumming S. A., Harrison R. C., Higley B., Nechvatal G., Pickett R. D., Piper I. M., Neirinck R. D., *Nucl. Med. Commun.*, **6**, 443–447 (1985).
- 8) Neirinckx R. D., Canning L. R., Piper I. M., Nowotnik D. P., Pickett R. D., Holmes R. A., Volkert W. A., Forster A. M., Weisner P. S., Marriott J. A., Chaplin S. B., *J. Nucl. Med.*, **28**, 191–202 (1987).
- 9) Vallabhajosula S., Zimmerman R. E., Picard M., Stritzke P., Mena I., Hellman R. S., Tikofsky R. S., Stsbin M. G., Morgan R. A., Goldsmith S. J., *J. Nucl. Med.*, **30**, 599–604 (1989).
- 10) Murmann J. R., *J. Am. Chem. Soc.*, **79**, 521–526 (1957).
- 11) Murmann J. R., *J. Am. Chem. Soc.*, **80**, 4174–4179 (1958).
- 12) Morton J. R., Wilcox H. W., "Inorganic Synthesis," Vol. IX, ed. by McGraw-Hill Book Co., New York, 1953, pp. 48–53.
- 13) Ding H. J., Yeh S. J., *Appl. Radiat. Isot.*, **43**, 1013–1017 (1992).
- 14) Costa G., Mestroni G., Mestroni E. L., *Inorg. Chim. Acta.*, **3**, 323–331 (1969).
- 15) Schrauzer G. N., Sibert J. W., Windgassen R. J., *J. Am. Chem. Soc.*, **90**, 6681–6687 (1968).
- 16) Ramanujam V. V., Alexander V., *J. Inorg. Chem.*, **26**, 3124–3129 (1987).
- 17) Costa G., Mestroni G., *Tetrahedron Lett.*, **41**, 4005–4011 (1968).

Cardiac Glycosides from *Erysimum cheiranthoides*

Zhen-Huan LEI,^{*,a} Shoji YAHARA,^b Toshihiro NOHARA,^{*,b} Bao-Shan TAI,^a Jin-Zhe XIONG,^a and Ying-Li MA^b

Department of Traditional Chinese Medicine,^a Heilongjiang Institute of Commerce, 138 Tongda St., Daoli, Harbin, China and Faculty of Pharmaceutical Sciences, Kumamoto University,^b 5-1 Oe-honmachi, Kumamoto 862-0973, Japan. Received August 12, 1999; accepted November 2, 1999

Two new cardiac glycosides called cheiranthosides VI (2) and VII (3) were isolated together with a known one, glucoerysimoside (1) from the seeds of *Erysimum cheiranthoides*. Based on spectroscopic data, the structures of 2 and 3 were characterized as periplogenin 3-*O*- β -D-glucopyranosyl(1 \rightarrow 4)- β -D-fucopyranoside and periplogenin 3-*O*- β -D-glucopyranosyl(1 \rightarrow 4)- β -D-antiaropyranoside, respectively.

Key words *Erysimum cheiranthoides*; Cruciferae; cardiac glycoside; cheiranthoside; antiarose

Erysimum cheiranthoides L. (Cruciferae) is a Chinese crude drug used for treating cardiac diseases, weak cardiopalmus, edema, dyspepsia, etc.¹⁾ In previous papers,^{2,3)} we reported five new cadenolides. As a continuing study on the constituents in the seeds, additional two new cardiac glycosides, called cheiranthosides VI (2) and VII (3), respectively, were isolated along with a known cardiac glycoside, glucoerysimoside (1)⁴⁾ and their chemical structures are here described.

Glucoerysimoside (1) obtained as a colorless powder, $[\alpha]_D^{25} +11.5^\circ$ (MeOH), showed a quasimolecular ion at m/z 857 $[M-H]^-$ in the negative FAB-MS. Its ¹H-NMR spectrum displayed signals due to 18-Me (3H, s) at δ 1.00, 17-H (1H, br d, $J=8.5$ Hz) at δ 2.78, 21-H₂ (each 1H, d, $J=18.3$ Hz) at δ 5.02, 5.28, 22-H (1H, s) at δ 6.10, 19-CHO at δ 10.39 on the cardiac steroidal framework and three anomeric protons at δ 4.95 (1H, d, $J=8.0$ Hz), 5.21 (1H, d, $J=7.3$ Hz) and 5.36 (1H, br d, $J=9.8$ Hz), and 6-Me of one 6-deoxy-sugar at δ 1.63 (d, $J=6.1$ Hz) in the sugar moiety. The ¹³C-NMR spectrum showed signals due to total forty one carbons, among which the chemical shifts of twenty three carbons originating from steroidal aglycone part and six carbons due to a sugar moiety were coincident with those of strophanthidin³⁾ and a terminal glucopyranosyl moiety,^{2,3)} respectively; the remaining twelve carbon signals were shown to be composed of a 4-*O*-substituted- β -D-glucopyranosyl moiety (δ 105.7, 74.7, 76.6, 80.9, 76.3, 61.9) and a 4-*O*-substituted- β -D-digitopyranosyl moiety (δ 97.5, 38.9, 67.6, 83.4, 69.0, 18.5) by comparing with those of erysimoside.^{2,5)} Therefore, 1 was characterized as 3-*O*- β -D-glucopyranosyl(1 \rightarrow 4)- β -D-glucopyranosyl(1 \rightarrow 4)- β -D-digitoxopyranosyl strophanthidin as shown in Chart 1. This compound was regarded as an identical one with glucoerysimoside,⁴⁾ which appeared in the Russian report,⁵⁾ however, with no available detailed NMR data for comparison.

Cheiranthoside VI (2) obtained as a colorless powder, $[\alpha]_D^{25} +4.6^\circ$ (MeOH), exhibited a quasimolecular ion peak at m/z 697 $[M-H]^-$ in the negative FAB-MS. The ¹H-NMR spectrum showed signals due to 18-Me at δ 1.04, 19-Me at δ 1.09, 17-H (1H, br d, $J=8.3$ Hz) at δ 2.80, 21-H₂ (each 1H, dd, $J=1.5$, 17.7 Hz) at δ 5.05, 5.32, 22-H (1H, s) at δ 6.15 in the aglycone part and two anomeric protons at δ 4.82 (1H, d, $J=8.0$ Hz) and 5.20 (1H, d, $J=8.0$ Hz) and a methyl group at δ 1.62 (3H, d, $J=6.1$ Hz) of a 6-deoxyhexosyl moiety in the sugar part. Among the sugar signals, the ¹H-¹H chemical

shift correlation spectroscopy (COSY) revealed the sequential connectivities of H-1—H-6 in an β -D-fucopyranosyl moiety at δ 4.82 (1H, d, $J=8.0$ Hz), 4.34 (1H, t-like, $J=7.9$ Hz), 4.11 (1H, dd, $J=3.7$, 8.6 Hz), 4.12 (1H, s), 3.80 (1H, br q, $J=6.1$ Hz), 1.62 (3H, d, $J=6.1$ Hz), and of H-1—H-5, H₂-6 in an β -D-glucopyranosyl moiety at δ 5.20 (1H, d, $J=8.0$ Hz), 4.05 (1H, t-like, $J=8.0$ Hz), 4.21 (2H, overlapped), 3.92 (1H, m), 4.37 (1H, dd, $J=5.5$, 11.7 Hz), 4.51 (1H, dd, $J=2.4$, 11.7 Hz). The ¹³C-NMR spectrum of 2 showed a total of thirty-five carbon signals, twenty-three of which were assigned to an aglycone, periplogenin,⁶⁾ six to a terminal glucopyranosyl moiety, and the remaining six (δ 101.8, 72.8, 75.7, 83.3, 70.8, 17.6) to a 4-*O*-substituted-fucopyranosyl moiety, by comparing with those of cheiranthoside IV. Therefore, the chemical structure of 2 was characterized as 3-*O*- β -D-glucopyranosyl(1 \rightarrow 4)- β -D-fucopyranosyl periplogenin as shown in Chart 1.

Cheiranthoside VII (3) obtained as a colorless powder, $[\alpha]_D^{25} -23.3^\circ$ (MeOH), showed a quasimolecular ion peak at m/z 697 $[M-H]^-$ in the negative FAB-MS. The ¹H-NMR spectrum showed signals due to 18-Me at δ 1.06, 19-Me at δ 1.09, 17-H (1H, br d, $J=8.5$ Hz) at δ 2.83, 21-H₂ (each 1H, dd, $J=1.8$, 16.0 Hz) at δ 5.07, 5.34, and 22-H (1H, s) at δ 6.12, two anomeric protons at δ 5.02 (1H, d, $J=7.9$ Hz) and 5.42 (1H, d, $J=7.9$ Hz). Moreover, the respective proton signals at δ 5.42 (1H, d, $J=7.9$ Hz), 4.60 (1H, dd, $J=3.0$, 7.9 Hz), 5.00 (1H, t-like, $J=3.0$ Hz), 4.36 (1H, br s), 4.60 (1H, br q, $J=6.1$ Hz), 1.55 (3H, d, $J=6.1$ Hz), 5.02 (1H, d, $J=7.9$ Hz), 4.03 (1H, dd, $J=7.9$, 9.2 Hz), 4.23 (1H, t-like, $J=9.2$ Hz), 4.21 (1H, t-like, $J=9.2$ Hz), 3.89 (1H, m), 4.37 (1H, dd, $J=6.1$, 11.6 Hz), 4.55 (1H, dd, $J=2.4$, 11.6 Hz) could be assigned to the H-1—H-5 and H₃-6 of an β -D-antiaropyranosyl and the H-1—H-5 and H₂-6 of an β -D-glucopyranosyl residue. The ¹H-NMR spectrum of the acetate derivatized by methanolysis of 3 also supported the existence of antiarose in the sugar linkage. The ¹³C-NMR spectrum of 2 showed thirty-five carbon signals, twenty-three of which were assigned to the aglycone, periplogenin, six to a terminal glucopyranosyl moiety, and the remaining six (δ 99.4, 69.5, 70.0, 79.0, 69.1, 17.1) to a 4-*O*-substituted- β -D-antiaropyranosyl moiety.^{7,8)} Therefore, the chemical structure of 3 was characterized as 3-*O*- β -D-glucopyranosyl(1 \rightarrow 4)- β -D-antiaropyranosyl periplogenin as shown in Chart 1.

It is worthy of note that these cardiac glycosides were isolated from the Cluciferae plant and have sugar linkages in-

* To whom correspondence should be addressed.

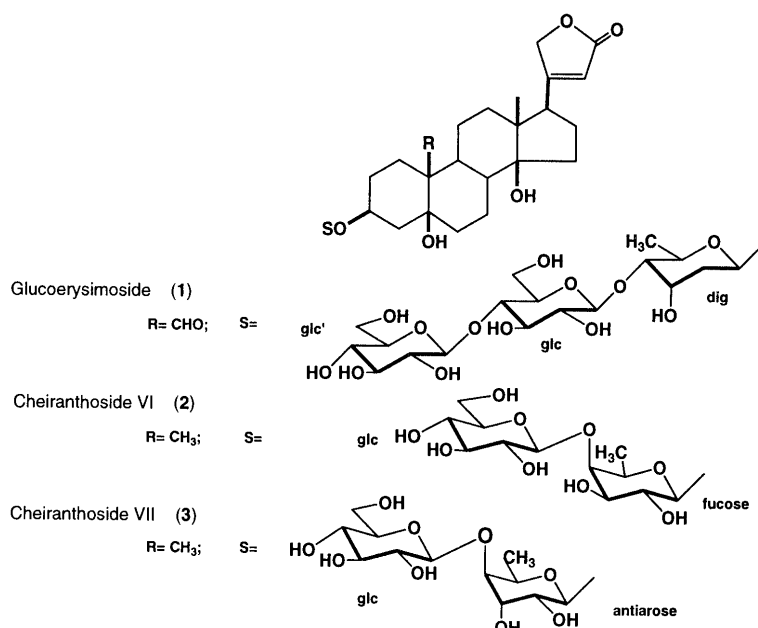


Chart 1

cluding fucose or antiarose in **2** and **3**.

Experimental

Optical rotations were determined on a JASCO DIP-1000 digital polarimeter. FAB-MS were obtained in a glycerol matrix in the negative ion mode using JEOL JMS-DX 300 and JMS-DX 303 HF instruments. NMR spectra were measured in pyridine-*d*₅ on a JEOL α -500 spectrometer and chemical shifts were relative to tetramethylsilane (TMS). TLC was performed on precoated Silica gel 60F₂₅₄ (0.2 mm, Merck) and detection was achieved by spraying 10% H₂SO₄ following by heating. Column chromatography was carried out on polystyrene gel (75–150 μ m, Mitsubishi Kasei), Sephadex LH-20 (25–100 μ m, Pharmacia Fine Chemicals), octadecyl silica gel (ODS) (30–50 μ m, Fuji Silysia Chemical, Ltd.) and Silica gel 60 (230–400 mesh, Merck).

Plant Material The seeds of *E. cheiranthoides* L. were harvested at Harbin, Heilongjiang Province, in China.

Extraction and Separation These seeds (2.5 kg) were extracted with MeOH and the extract (189 g) was partitioned between hexane and water. The aqueous layer (123 g) was subjected to MCI gel CHP 20P column chromatography eluted with water, 40% MeOH, 60% MeOH, 80% MeOH and MeOH, gradually increasing MeOH. The 40% eluate (10 g) was subjected to Sephadex LH-20, Chromatorex ODS and Silica gel column chromatographies to provide glucoerysimoside (**1**, 23 mg), cheiranthoside VI (**2**, 10 mg) and cheiranthoside VII (**3**, 21 mg).

Glucoerysimoside (1): A colorless powder, $[\alpha]_D^{15} +11.5^\circ$ (*c*=0.99, MeOH). Anal. Calcd for C₄₁H₆₂O₁₉·2H₂O: C, 55.02; H, 7.43. Found: C, 54.98; H, 7.24. Neg. FAB-MS (*m/z*): 857 [M–H][–], 531 [M–2×hexose–H][–]. ¹H-NMR (pyridine-*d*₅) δ : 1.00 (3H, s, 18-Me), 1.63 (3H, d, *J*=6.1 Hz, dig 6-Me), 1.90, 2.25 (each 1H, m, dig 2-H₂), 2.78 (1H, br d, *J*=8.5 Hz, 17-H), 3.62 (1H, br d, *J*=9.8 Hz, dig 4-H), 3.92 (each 1H, overlapped, glc 2-H, 4-H), 4.01 (1H, m, glc' 5-H), 4.10 (1H, br t, *J*=8.3 Hz, glc' 2-H), 4.19 (1H, overlapped, glc' 3-H), 4.21 (1H, overlapped, glc' 4-H), 4.25 (1H, t-like, *J*=8.3 Hz, glc 3-H), 4.30 (1H, m, glc' 6-H), 4.34 (1H, m, dig 5-H), 4.41, 4.53 (each 1H, br d, *J*=9.8 Hz, glc H₂-6), 4.53 (1H, br d, *J*=9.8 Hz, glc' 6-H'), 4.65 (1H, br s, dig 3-H), 4.95 (1H, d, *J*=8.0 Hz, glc 1-H), 5.21 (1H, d, *J*=7.3 Hz, glc' 1-H), 5.02, 5.28 (each 1H, d, *J*=18.3 Hz, 21-H₂), 5.36 (1H, br d, *J*=9.8 Hz, dig 1-H), 6.10 (1H, s, 22-H), 10.39 (1H, s, 19-H). ¹³C-NMR (pyridine-*d*₅) δ : 18.4, 25.5, 74.9, 36.2, 73.9, 36.9, 24.7, 41.9, 39.5, 55.3, 22.6, 39.5, 49.8, 84.4, 32.1, 27.2, 51.0, 15.8, 208.5, 175.7, 73.7, 117.7, 174.5 (C-1–23), 97.5, 38.9, 67.6, 83.4, 69.0, 18.5 (dig C-1–6), 105.7, 74.7, 76.6, 80.9, 76.3, 61.9 (inner glc C-1–6), 104.9, 74.6, 78.2, 71.5, 78.4, 62.4 (terminal glc C-1–6).

Cheiranthoside VI (2): A colorless powder, $[\alpha]_D^{18} +4.60^\circ$ (*c*=0.59, MeOH). Anal. Calcd for C₃₅H₅₄O₁₄·H₂O: C, 58.63; H, 7.88. Found: C, 58.71; H, 7.89. Neg. FAB-MS (*m/z*): 697 [M–H][–]. ¹H-NMR (pyridine-*d*₅) δ : 1.04 (3H, s, 18-Me), 1.09 (3H, s, 19-Me), 1.62 (3H, d, *J*=6.1 Hz, fuc 6-Me),

2.80 (1H, br d, *J*=8.3 Hz, 17-H), 3.80 (1H, br q, *J*=6.1 Hz, fuc 5-H), 3.92 (1H, m, glc 5-H), 4.05 (1H, t-like, *J*=8.0 Hz, glc 2-H), 4.11 (1H, dd, *J*=3.7, 8.6 Hz, fuc 3-H), 4.12 (1H, s, fuc 4-H), 4.21 (2H, overlapped, glc H-3, H-4), 4.34 (1H, t-like, *J*=7.9 Hz, fuc 2-H), 4.37 (1H, dd, *J*=5.5, 11.7 Hz, glc 6-H), 4.51 (1H, dd, *J*=2.4, 11.7 Hz, glc 6-H'), 4.82 (1H, d, *J*=8.0 Hz, fuc 1-H), 5.20 (1H, d, *J*=8.0 Hz, glc 1-H), 5.05, 5.32 (each 1H, dd, *J*=1.5, 17.7 Hz, 21-H₂), 6.15 (1H, s, 22-H). ¹³C-NMR (pyridine-*d*₅) δ : 26.1, 27.3, 74.2, 34.1, 73.2, 36.4, 24.6, 40.9, 39.2, 41.2, 21.9, 39.9, 50.0, 84.7, 33.2, 26.7, 51.3, 16.1, 17.2, 176.0, 73.7, 117.2, 174.5 (C-1–23), 101.8, 72.8, 75.7, 83.3, 70.8, 17.6 (fuc C-1–6), 106.9, 76.1, 78.6, 71.6, 78.6, 62.8 (glc C-1–6).

Cheiranthoside VII (3): A colorless powder, $[\alpha]_D^{18} -23.30^\circ$ (*c*=0.78, MeOH). Anal. Calcd. for C₃₅H₅₄O₁₄·H₂O: C, 58.63; H, 7.88. Found: C, 58.58; H, 7.79. Neg. FAB-MS (*m/z*): 697 [M–H][–]. ¹H-NMR (pyridine-*d*₅) δ : 1.06 (3H, s, 18-Me), 1.09 (3H, s, 19-Me), 1.55 (3H, d, *J*=6.1 Hz, ant 6-Me), 2.83 (1H, br d, *J*=8.5 Hz, 17-H), 3.89 (1H, m, glc 5-H), 4.03 (1H, dd, *J*=7.9, 9.2 Hz, glc 2-H), 4.21 (1H, t-like, *J*=9.2 Hz, glc 4-H), 4.23 (1H, t-like, *J*=9.2 Hz, glc 3-H), 4.36 (1H, br s, ant 4-H), 4.37 (1H, dd, *J*=6.1, 11.6 Hz, glc 6-H), 4.55 (1H, dd, *J*=2.4, 11.6 Hz, glc 6-H'), 4.60 (1H, dd, *J*=3.0, 7.9 Hz, ant 2-H), 4.60 (1H, br q, *J*=6.1 Hz, ant 5-H), 5.00 (1H, t-like, *J*=3.0 Hz, ant 3-H), 5.02 (1H, d, *J*=7.9 Hz, glc 1-H), 5.07, 5.34 (each 1H, dd, *J*=1.8, 16.0 Hz, 21-H₂), 5.42 (1H, d, *J*=7.9 Hz, ant 1-H), 6.12 (1H, s, 22-H). ¹³C-NMR (pyridine-*d*₅) δ : 26.1, 27.3, 74.0, 34.2, 73.3, 36.2, 24.6, 40.9, 39.2, 41.2, 21.9, 39.9, 49.9, 84.7, 33.1, 26.8, 51.3, 16.1, 17.2, 176.0, 73.7, 117.7, 174.5 (C-1–23), 99.4, 69.5, 70.0, 79.0, 69.1, 17.1 (ant C-1–6), 103.2, 74.8, 78.5, 71.9, 78.65, 63.0 (glc C-1–6).

Methanolysis of 3 Compound **3** (15 mg) was hydrolyzed with 2 mol/l HCl in MeOH for 2 h at 80 °C. The reaction mixture was neutralized with 2 mol/l NaOH–MeOH, and was evaporated to dryness; acetone was then added and the mixture was filtered. The filtrate was evaporated to dryness, dissolved in methanol, and this solution was passed through a Sephadex LH-20 column. The obtained sugar fraction was further purified by silica gel column chromatography (CH₃Cl:MeOH:H₂O=9:2:0.1) to give methyl β -D-antiaropyranoside (1.6 mg) and a mixture (3.2 mg) of α - and β -D-glucopyranosides, the former of which was acetylated with acetic anhydride and pyridine to give the acetate (1.6 mg).

Methyl 2,3,4-Tri-O-acetyl β -D-Antiaropyranoside: Colorless resin, $[\alpha]_D^{24} -52.90^\circ$ (*c*=0.16, MeOH). ¹H-NMR (CDCl₃) δ : 1.22 (3H, d, *J*=6.1 Hz, 6-Me), 2.12, 2.13, 2.16 (each 3H, s, 3×OAc), 3.52 (3H, s, OMe), 4.13 (1H, m, 5-H), 4.67 (1H, d, *J*=8.6 Hz, 1-H), 4.85 (1H, dd, *J*=1.2, 3.7 Hz, 4-H), 4.98 (1H, dd, *J*=3.7, 8.6 Hz, 2-H), 5.36 (1H, dd, *J*=3.7, 3.7 Hz, 3-H).

References and Notes

- Zhu Y. C. (ed.), "Plantae Medicinales Chinae Boreali-Orientalis," Heilongjiang Science and Technology Publishing House, 1989, p. 463.
- Lei Z. H., Yahara S., Nohara T., Tai B. S., Xiong J. Z., *Phytochemistry*, **41**, 1187–1189 (1996).

- 3) Lei Z. H., Xiong J. Z., Ma Y. L., Tai B. S., Kong Q., Yahara S., Nohara T., *Phytochemistry*, **49**, 1801—1803 (1998).
- 4) Makarevich I. F., *Khim. Prir. Soedin.*, **6**, 566—571 (1970).
- 5) Makarevich I. F., Kolesnikov D. G., *Khim. Prir. Soedin.*, **5**, 363—367 (1965).
- 6) Kawaguchi K., Hirotani M., Furuya T., *Phytochemistry*, **28**, 1093—1098 (1989).
- 7) Mahato S. B., Sahu N. P., Roy S. K., *J. Chem. Soc., Perkin Trans. I*, **1989**, 2065—2068.
- 8) Carter C. A., Gray E. A., Schneider T. L., *Tetrahedron*, **53**, 16959—16968 (1997).

Design, Synthesis, Conformational Analysis and Biological Activities of Purine-Based 1,2-Di-substituted Carbocyclic Nucleosides

Carmen TERAN,^a Lourdes SANTANA,^b Marta TEIJEIRA,^b Eugenio URIARTE,^{*,b} and Erik DE CLERCQ^c

Departamento de Química Física y Química Orgánica, Universidad de Vigo,^a 36200-Vigo, Spain, Laboratorio de Química Farmacéutica, Facultad de Farmacia, Universidad de Santiago de Compostela,^b 15706-Santiago de Compostela, Spain, and Rega Institute for Medical Research, Katholieke Universiteit Leuven,^c Minderbroedersstraat 10, B-3000 Leuven, Belgium. Received August 16, 1999; accepted October 22, 1999

New 1,2-di-substituted carbocyclic nucleosides with 6-chloropurine, adenine and hypoxanthine bases were synthesized by construction of purine on the primary amino group of (\pm)-*trans*-2-aminocyclopentylmethanol. AM1 calculations showed close correspondence between the positions of the heteroatoms in the adenine derivative and dideoxyadenosine. The most active of the new compounds in antiviral assays and antitumoral assays against L1210/0, MOLT4/C8 and CEM/0 cells was the 6-chloropurine derivative.

Key words carbonucleosides; purine derivative; AM1 semiempirical method; antiviral agent; antitumor agent

In the past decade, a large number of nucleoside analogues with antiviral and/or antitumoral properties have been successfully designed and synthesized.^{1–3)} Some 2',3'-dideoxynucleosides are currently the drugs of choice for the treatment of certain viral infections (including human immunodeficiency virus (HIV) infection), these work by blocking viral reproduction, thus inhibiting reverse transcriptase.⁴⁾ Another successful modification has been the replacement of the endocyclic oxygen atom of the nucleoside sugar ring with a methylene group,⁵⁾ which reduces phosphorylase- and hydrolase-catalyzed reactivity (thereby increasing the *in vivo* half life)⁶⁾ and increases lipophilicity (thus favoring absorption and penetration of the cell membrane). The potent HIV-1 inhibitor carbovir combines both these structural modifications.⁷⁾

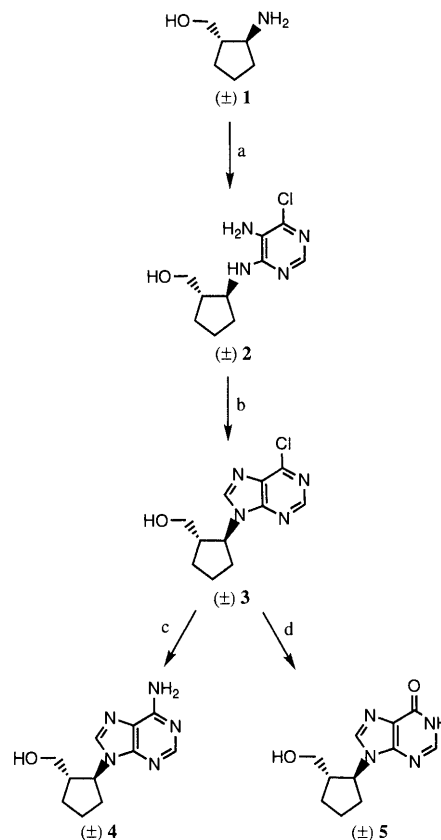
We have recently investigated the properties of 1,2-disubstituted carbocyclic nucleosides (OTCs), in which the hydroxymethyl group of a carbocyclic sugar analogue is substituted at a position adjacent to the nitrogenated base.⁸⁾ Molecular modeling of the *cis* isomers of cyclopentane-based OTCs has shown that in the most stable conformers the glycoside linkage is *anti* ($\chi = -90^\circ$, where for purine aglycons $\chi = C4-N9-C1'-C2'$) and γ ($C1'-C2'-C1''-O2''$) can, as in most active nucleosides,^{9,10)} be -60° (*gg*), $+60^\circ$ (*gt*) or 180° (*tg*).¹¹⁾

In this paper we report the synthesis, theoretical conformational analysis and preliminary antiviral and antitumoral activities of a new series of cyclopentane-based OTCs in which the hydroxymethyl group is *trans* to a purine base (adenine, 6-chloropurine or hypoxanthine).

Results and Discussion

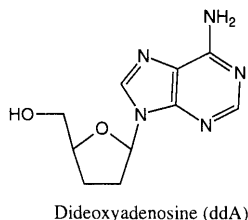
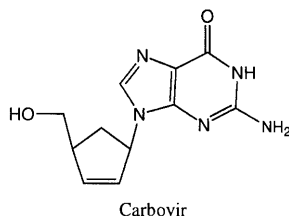
As shown in Chart 1, racemic compounds **3**, **4** and **5** were synthesized starting from (\pm)-*trans*-2-aminocyclopentyl-

methanol (**1**), which was separated from a mixture of *cis* and *trans* isomers obtained in two steps from commercially available ethyl 2-oxocyclopentylcarboxylate (overall yield 84%).¹²⁾ The amine **1** was condensed with 5-amino-4,6-dichloropyrimidine in refluxing *n*-butanol containing triethylamine, affording compound **2** in 71% yield. Ring closure with triethyl orthoformate in an acidic medium then gave an 80% yield of the 6-chloropurine **3**, the *trans* stereochemistry of which was shown by a proton nuclear Overhauser effect (NOE) experiment.¹³⁾ Compound **3** was treated with a solution of ammonia in methanol to obtain the adenine derivative



Reagents: a) 5-Amino-4,6-dichloropyrimidine, *n*-BuOH, Et₃N, reflux; b) CH(OEt)₃, HCl, r.t.; c) NH₃, MeOH, reflux; d) 0.5 M NaOH, reflux.

Chart 1



* To whom correspondence should be addressed.

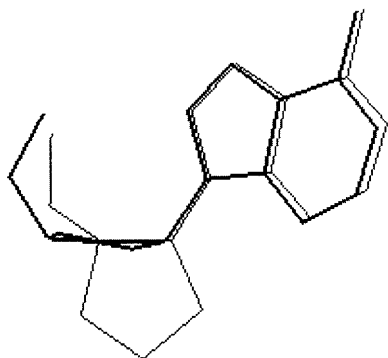


Fig. 1. Superimposition of the Stable Conformers of Compound **4** (non bold) and ddA (bold)

4 in 98% yield, and with hot sodium hydroxide to obtain the hypoxanthine derivative **5** in 94% yield.

Conformational analysis of compounds **3**–**5** was performed by means of AM1 calculations in which the parameters varied were those with the most influence on the relative positions of the base and the hydroxyl group on C1': the dihedral angles χ and γ , and the pucker of the cyclopentane ring. Great conformational freedom was shown by the finding that the conformers detected for any given compound differed in energy by no more than about 4 kcal/mol. However, in keeping with published data for similar compounds,^{9,10} the most stable had *anti* glycoside linkages ($\chi = -90^\circ$ or -115°) and hydroxymethyl side chains with *gg*, *gt* or *tg* conformations ($\gamma = -60^\circ$, $+60^\circ$ or 180°). In the conformer with $\chi = -90^\circ$ and $\gamma = +60^\circ$, the cyclopentane ring adopted an N conformation and the distances of the OH group from the nitrogen atoms of the base were almost identical to those found in ddA (2',3'-dideoxyadenosine) and in most other active nucleosides. This similarity is illustrated by the root mean square (RMS) distances between corresponding heteroatoms being just 0.2–0.35 Å when this conformer was superimposed on the active conformer of ddA ($\chi = -90^\circ$, $\gamma = -60^\circ$) in such a way as to minimize this RMS, although the attainment of this minimum requires the cyclopentane ring to lie perpendicular to the ddA sugar ring; see Fig. 1.

Compounds **3**–**5** achieved no significant inhibition of replication of the following viruses in assays carried out in the following cell cultures: HIV-1 and HIV-2 in human T-lymphocyte (CEM) cells; Vesicular stomatitis, Coxsackie B4 and Polio-1 in human epithelial (HeLa) cells; HSV-1 (KOS), HSV-2 (G), HSV-1 TK⁻ (B2006), HSV-2 TK⁻ (VMW1837), Vaccinia and Vesicular stomatitis in human embryonic skin–muscle fibroblast (E6SM) cells, or Parainfluenza-3, Reovirus-1, Sindbis, Coxsackie B4 and Semliki forest in African green monkey kidney (Vero) cells. Assays comparing compounds **3**–**5** with Ara A showed compound **3** to cause a 50% reduction in cell proliferation at concentrations of $56.1 \pm 3.0 \mu\text{M}$ for murine leukemia cells L1210 (Ara A: $14.2 \pm 6.4 \mu\text{M}$), $39.2 \pm 8.0 \mu\text{M}$ for Molt4/C8 human T-lymphocytes (Ara A: $11.9 \pm 7.3 \mu\text{M}$) and $19.0 \pm 4.2 \mu\text{M}$ for CEM/0 T cells (Ara A: $24.8 \pm 1.9 \mu\text{M}$).

Experimental

Chemistry Melting points were determined in a Reichert Kofler thermopan apparatus and are uncorrected. IR spectra (KBr discs) were recorded on a Perkin-Elmer 1640FT spectrometer (ν in cm^{-1}). ¹H- and ¹³C-NMR spectra were recorded on a Bruker AMX 300 NMR spectrometer, using

tetramethylsilane (TMS) as an internal standard (δ in ppm, J in Hz). Mass spectrometry was carried out in a Hewlett Packard 5988A spectrometer. Elemental analyses were performed by a Perkin-Elmer 240B microanalyzer. Flash chromatography (FC) was performed on silica gel (Merck 60, 230–400 mesh).

(±)-trans-5-Amino-6-chloro-4-[2-(hydroxymethyl)cyclopentylamino]pyrimidine (2) A mixture of the aminoalcohol **1**¹² (1 g, 8.70 mmol), 5-amino-4,6-dichloropyrimidine (1.48 g, 9.02 mmol), Et₃N (5 ml) and *n*-BuOH (30 ml) was refluxed for 1 h under Ar. The solvent was then evaporated under a vacuum, and the solid residue was redissolved in ethyl acetate by stirring with IRA-420 (OH) until all turbidity had disappeared. The resin was filtered out, the solvent was evaporated under a vacuum, and the residue was purified by FC using 98 : 2 CH₂Cl₂/MeOH as an eluent, which gave pure **2** (1.5 g, 71%). IR (KBr) cm^{-1} : 3250, 2923, 1650, 1581, 1484, 1475, 1444, 1012. ¹H-NMR (DMSO-*d*₆) δ : 1.32–1.98 (m, 7H, (–CH₂)₃, –CH–C–O), 3.42 (m, 2H, –CH₂–O), 4.07 (q, $J = 6.76$, 1H, –CH–N), 4.59 (t, $J = 5.14$, 1H, aliphatic –OH), 5.07 (br s, 2H, –NH₂), 6.63 (d, $J = 6.86$, 1H, NH–), 7.69 (s, 1H, H-2). ¹³C-NMR (DMSO-*d*₆) δ : 22.5 (4'), 27.7 (3'), 32.3 (5'), 45.1 (2'), 54.5 (1'), 61.6 (6'), 124.0, 137.4, 146.3, 152.3. MS m/z (%): 244 ([M+2]⁺, 11), 242 (M⁺, 32), 221 (37), 169 (15), 146 ([M+2]⁺–C₆H₁₀O, 29), 144 (M⁺–C₆H₁₀O, 100), 117 (13), 67 (12). Anal. Calcd for C₁₀H₁₅ClN₄O: C, 49.49; H, 6.23; N, 23.08. Found: C, 49.56; H, 6.30; N, 23.28.

(±)-trans-6-Chloro-9-[2-(hydroxymethyl)cyclopentyl]-9H-purine (3) A mixture of compound **2** (150 mg; 0.62 mmol), CH(OEt)₃ (3.4 ml; 0.02 mol) and conc. HCl (0.04 ml) was stirred for 12 h at room temperature. The solvent was then evaporated under a vacuum and the solid residue was redissolved in tetrahydrofuran (THF) (10 ml) and 0.5 M HCl (13 ml). After 2 h of stirring at room temperature, the mixture was neutralized with 0.5 M NaOH, the solvent was evaporated under vacuum (forming an azeotropic mixture with ethanol–toluene) and the solid residue was purified by FC using 99 : 1 CH₂Cl₂/CH₃OH as an eluent, which gave pure **3** (125 mg, 80%), mp 108–110°C. IR (KBr) cm^{-1} : 3292, 3065, 2953, 1593, 1565, 1394, 1337, 1220, 1063, 952, 634. ¹H-NMR (CDCl₃) δ : 1.64–2.51 (m, 7H, (–CH₂)₃, –CH–C–O), 2.77 (m, 1H, aliphatic –OH), 3.62 (m, 2H, –CH₂–O), 4.85 (q, $J = 8.18$, 1H, –CH–N), 8.21 (s, 1H, H-8), 8.73 (s, 1H, H-2). ¹³C-NMR (CDCl₃) δ : 23.4 (4'), 27.6 (3'), 32.4 (5'), 48.7 (2'), 59.1 (1'), 63.5 (6'), 132.4 (5), 144.4 (8), 151.5 (4), 151.9 (2), 152.1 (6). MS m/z (%): 254 ([M+2]⁺, 4), 252 (M⁺, 11), 181 (12), 157 ([M+2]⁺–C₆H₉O, 33), 155 (M⁺–C₆H₉O, 100), 119 (12), 80 (6), 67 (11). Anal. Calcd for C₁₁H₁₃ClN₄O: C, 52.28; H, 5.19; N, 22.17. Found: C, 52.31; H, 5.17; N, 22.09.

(±)-trans-9-[2-(Hydroxymethyl)cyclopentyl]adenine (4) Gaseous ammonia was bubbled for 1 h through a solution of **3** (100 mg, 0.39 mmol) in CH₃OH (20 ml) in a steel reactor at –80°C. The reactor was closed and heated for 20 h in an oven at 60°C, the solvent was evaporated under a vacuum, and the solid residue was purified by FC using 98 : 2 CH₂Cl₂/CH₃OH as an eluent, which gave pure **4** (90 mg, 98%), mp 153–155°C; IR (KBr) cm^{-1} : 3300, 2950, 2871, 1687, 1610, 1567, 1477, 1419, 1303, 651. ¹H-NMR (CDCl₃) δ : 1.48–2.13 (m, 6H, (–CH₂)₃), 2.50 (m, 1H, –CH–C–O), 3.36 (m, 2H, –CH₂–O), 4.58 (m, 2H, –CH–N, aliphatic –OH), 7.14 (br s, 2H, –NH₂), 8.11, 8.17 (each s, each 1H, H-2, H-8). ¹³C-NMR (CDCl₃) δ : 23.0 (4'), 27.7 (3'), 32.5 (5'), 47.1 (2'), 57.9 (1'), 62.6 (6'), 119.6 (5), 140.3 (8), 149.8 (4), 152.4 (2), 156.3 (6). MS m/z (%): 233 (M⁺, 23), 216 (M⁺–NH₃, 24), 162 (27), 136 (70), 135 (M⁺–C₆H₁₀O, 100), 108 (31), 81 (6), 67 (9). Anal. Calcd for C₁₁H₁₅N₅O: C, 56.64; H, 6.48; N, 30.02. Found: C, 56.49; H, 6.60; N, 29.68.

(±)-trans-9-[2-(Hydroxymethyl)cyclopentyl]hypoxanthine (5) A mixture of **3** (100 mg, 0.39 mmol) and 0.5 M NaOH (5 ml) was refluxed for 5 h. The solvent was then evaporated under a vacuum and the solid residue was purified by FC using 95 : 5 CH₂Cl₂/CH₃OH as an eluent, which gave pure **5** (87 mg, 94%), mp 237–238°C. IR (KBr) cm^{-1} : 3350, 3337, 2863, 1702, 1593, 1545, 1414, 1132, 643. ¹H-NMR (DMSO-*d*₆) δ : 1.46–2.17 (m, 6H, (–CH₂)₃), 2.47 (m, 1H, –CH–C–O), 3.33 (m, 2H, CH₂–O), 4.59 (q, $J = 8.10$, 2H, –CH–N), 8.01, 8.15 (each s, each 1H, H-2, H-8), 12.26 (br s, 1H, aromatic –OH). ¹³C-NMR (DMSO-*d*₆) δ : 23.0 (4'), 27.7 (3'), 32.9 (5'), 47.5 (2'), 58.1 (1'), 62.5 (6'), 124.7 (5), 139.6 (8), 145.5 (4), 148.6 (2), 157.1 (6). MS m/z (%): 234 (M⁺, 25), 204 (M⁺–CH₂, 9), 164 (13), 163 (12), 137 (M⁺–C₆H₉O, 100), 136 (M⁺–C₆H₁₀O, 60), 109 (22), 81 (14), 67 (14). Anal. Calcd for C₁₁H₁₄N₄O₂: C, 56.40; H, 6.02; N, 23.92. Found: C, 56.45; H, 5.83; N, 23.84.

Computational Methods Optimization of theoretical molecular geometries was carried by the AM1 semiempirical quantum mechanical method¹⁴ using the program AMPAC,¹⁵ which was run on an SGI work station. The geometry was optimized by varying the torsion angles χ [C4–N9–C1'–C2'] and γ [C1'–C2'–C10'–O2'] between 0° and 360° in 10° increments.

Biological Activity Assays Assays of antiviral activity and cytotoxicity were carried out in accordance with established procedures.¹⁶⁾

Acknowledgments We thank the Spanish Ministry of Education and Science (APC1998-0151) for partial financial support.

References

- 1) Hobbs J. B., "Purine and Pyrimidine Targets," in *Comprehensive Medicinal Chemistry*, Vol. 2, ed. by Hansch C., Pergamon Press, Ch., 1990, pp. 299—332.
- 2) De Clercq E., *J. Med. Virol.*, **5**, 149—164 (1995).
- 3) Mansour T. S., Storer R., *Current Pharmaceutical Design*, **3**, 227—264 (1997).
- 4) a) De Clercq E., *Clinical Microbiology Reviews*, **10**, 674—693 (1997);
b) *Idem*, *The Medical Letter*, **1998**, 5—10.
- 5) Marquez V. E., *Advances in Antiviral Drug Design*, **2**, 89—146 (1996).
- 6) Shealy Y. F., Clayton J. D., *J. Am. Chem. Soc.*, **88**, 3885—3887 (1966).
- 7) Vince R., Hua M., *J. Med. Chem.*, **33**, 17—21, (1990).
- 8) Santana L., Teijeira M., Uriarte E., De Clercq E., Balzarini J., *Nucleosides & Nucleotides*, **14**, 521—523, (1995); Santana L., Teijeira M., Uriarte E., Fadda A., Podda G., Catinella S., Traldi P., *Rapid Commun. Mass Spectrom.*, **1996**, 1316—1319.
- 9) Saenger W., "Principles of Nucleic Acid Structure," Springer-Verlag, New York, Inc., New York, 1984.
- 10) Herdewyn P., Balzarini J., De Clercq E., "Advances in Antiviral Drug Design," Vol. 1, ed. by De Clercq E., JAI Press, Inc., Greenwich, CT, 1993, pp. 233—318.
- 11) Santana L., Teijeira M., Terán C., Uriarte E., Casselato U., Graziani R., *Nucleosides & Nucleotides*, **15**, 1179—1187 (1996).
- 12) Teijeira M., Doctoral Thesis, University of Santiago de Compostela, Spain, 1996.
- 13) Teijeira M., Santana L., Uriarte E., *Magn. Reson. Chem.*, **35**, 806—807 (1997).
- 14) Dewar M. J. S., Zebisch E. G., Healy E. F., Stewart J. J. P., *J. Am. Chem. Soc.*, **107**, 3902—3909 (1985).
- 15) BIOSYM Technologies, Inc., 10065 Barnes Canyon Road, San Diego, CA 92121.
- 16) De Clercq E., "In vitro and ex vivo test systems to rationalize drug design and delivery," ed. by Crommelin D., Couvreur P., Duchene D., Editions de Santé, Paris, 1994, pp. 108—125.

Synthesis of Peptides with α,β -Dehydroamino Acids. XIII

Photoisomerization of Ac-(Z)- Δ Phe-NHMe: Ac-(E)- Δ Phe-NHMe^{1,2)}

Zbigniew KUBICA,^a Tomasz KOZŁECKI,^b and Barbara RZESZOTARSKA^{*,a}

Department of Organic Chemistry, University of Opole,^a 48 Oleska St., 45–052 Opole, Poland and Faculty of Chemistry, University of Wrocław,^b 14 Joliot-Curie St., 50–383 Wrocław, Poland.

Received August 17, 1999; accepted October 2, 1999

Easily accessible Ac-(Z)- Δ Phe-NHMe was photoisomerized to so far unknown Ac-(E)- Δ Phe-NHMe. Some parameters of the process leading to a diastereomeric mixture of ratio 90(Z):10(E) have been tested and the photoisomerization has been carried out on a preparative milligram scale. The isomers were separated *via* crystallization followed by preparative HPLC.

Key words Ac-(E)- Δ Phe-NHMe; (E)-dehydrophenylalanine; α,β -dehydroamino acid; photoisomerization; (Z)/(E)-diastereoisomer separation; HPLC

One of the natural variants of common amino acids is α,β -dehydroamino acids, which have a double bond between the C $^{\alpha}$ and C $^{\beta}$ atoms. Thus, the chirality gets lost and (Z)/(E) isomerism appears. Both (Z)- and (E)-forms occur in nature.^{3,4)}

The introduction of the double bond into a peptide chain leads to a cross-conjugated system,^{5,6)} which may influence the conformation of the peptide backbone and the orientation of the amino acid side-chain. These special features have made α,β -dehydroamino acids valuable modifiers of peptides and consequently, α,β -dehydropeptides became attractive targets for conformational studies.^{7,8)} To these ends (Z)-dehydrophenylalanine is used most often, mainly perhaps because of its convenient chemical synthesis and the fact that all synthetic routes give exclusively the (Z)-isomer. On the other hand, receptor proteins discriminate quite precisely between the (Z) and (E)-disposition of the double bond in their α,β -dehydropeptide bioligands, as can be observed for the few available (Z)/(E)- Δ Phe couples of peptide analogs.^{9–11)} In contrast to the stability of dehydrophenylalanine in the (Z)-configuration, the (E)-configuration is quite unstable to the usual chemical conditions of peptide synthesis, converting always into the (Z)-configuration.^{12,13)} This synthetic limitation requires a procedure to invert the configuration of the dehydro unit from (Z) to (E) in the final stage of the synthesis. An appropriate method turned out to be photoisomerization.^{9,10,14)}

The significance of (E)-dehydrophenylalanine in the peptide modification generates a need for a deeper understanding of this amino acid conformational profile. Investigated was Ac-(E)- Δ Phe-NHMe, the simple model system, which mimics well the (E)- Δ Phe residue incorporated in a peptide chain. However, only theoretical structural study has been undertaken,¹⁰⁾ as the corresponding compound was unknown. Therefore, we provide here a synthesis of Ac-(E)- Δ Phe-NHMe. This was achieved *via* photoisomerization of easily accessible Ac-(Z)- Δ Phe-NHMe¹⁵⁾ (Table 1). With Ac-(E)- Δ Phe-NHMe in hand we were able to explore its conformational preferences experimentally.¹⁶⁾

The photoisomerization of Ac-(Z)- Δ Phe-NHMe was performed in an ethanol solution. On an introductory testing by HPLC of some parameters of the process (Table 1), we selected for the final preparation of Ac-(E)- Δ Phe-NHMe the irradiation of 10^{-3} M solution of Ac-(Z)- Δ Phe-NHMe (Fig.

1a) with a 313-nm light over 16 h. As expected, the post-reaction mixture contained both isomers in a ratio of 90(Z):10(E) (Fig. 1b). Their separation and isolation require long-lasting operations, whereas (E)-2-phenyl-4-benzylidene-5(4H)-oxazolone was reported to isomerize to a 40(Z):60(E) equilibrium point, when left in an acetonitrile solution at room temperature in light for a few days.¹⁷⁾ Hence, the preparation of an (E)-dehydrophenylalanine peptide was carried out in the absence of direct light.⁹⁾ We therefore checked the stability of Ac-(E)- Δ Phe-NHMe under conditions of work-up at every stage of our procedure: concentration, crystallization and preparative HPLC separation.

A sample of the irradiated solution was left standing in direct light over 12 h and then condensed to about $5 \cdot 10^{-2}$ M concentration. The (Z):(E)-isomer ratio did not change. The separation from this concentrated solution, of the majority of (Z)-isomer by crystallization affords a new mixture, enriched significantly in the (E)-isomer, in a ratio of 20(Z):80(E) (Fig. 1c). This is also stable to direct light (when irradiated with 313-nm light over 16 h, however, it passes to a ratio of 40(Z):60(E)). Preparative HPLC of this enriched mixture

Table 1. Photoisomerization of Ac-(Z)- Δ Phe-NHMe: the Content of Ac-(E)- Δ Phe-NHMe (by HPLC) as a Function of Wavelength, Irradiation Time and Solution Concentration

The reaction scheme shows the photoisomerization of the Z isomer to the E isomer of Ac-ΔPhe-NHMe. The Z isomer is on the left, and the E isomer is on the right. An arrow with 'hv' above it indicates the photochemical process. Both molecules consist of an acetamido group (H₃C-C(=O)-NH-) and a methylamino group (-NH-CH₃) connected by a conjugated system that includes a phenyl ring. In the Z isomer, the phenyl ring is in a cis configuration relative to the conjugated system, while in the E isomer, it is in a trans configuration.

Time: 16 h; concentration: 10^{-5} M			
λ (nm)	293 ^{a)}	313 ^{b)}	365 ^{b)}
E (%)	8.1	10.8	5.2

Wavelength: 313 nm; concentration: 10^{-5} M							
Time (h)	0.7	5.5	6.5	10.5	12.0	16.0	22.0
E (%)	0.2	5.9	7.6	8.4	10.5	10.8	11.9

Time: 16 h; wavelength: 313 nm			
Conc. (M)	10^{-5}	10^{-3}	$4 \cdot 10^{-3}$ ^{c)}
E (%)	10.8	10.1	3.5

a) Wavelength 293 nm resulted from the UV spectrum of Ac-(Z)- Δ Phe-NHMe. b) (Z)-Phenylalanine peptides^{9,10)} and (Z)-2-phenyl-4-benzylidene-5(4H)-oxazolone¹⁴⁾ were isomerized with 313-nm and 365-nm light, respectively. c) Presumably, this concentrated solution was poorly transmittable for 313-nm light and the isomerization proceeded only near the reactor wall. On dilution to 10^{-3} M, the process took a normal course.

* To whom correspondence should be addressed.

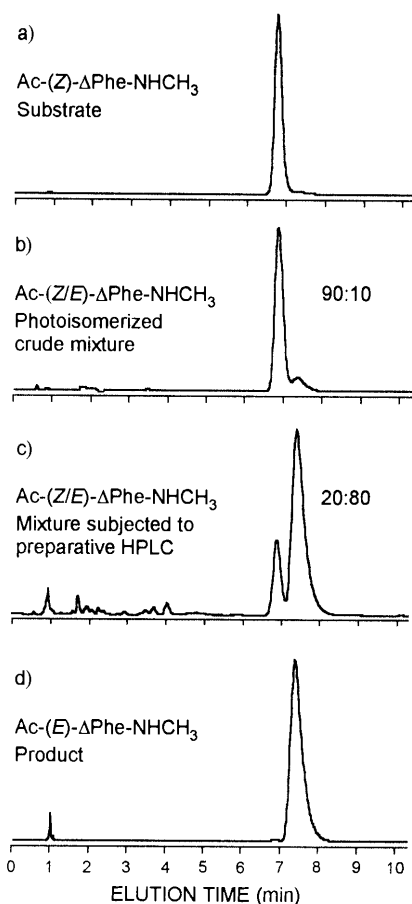


Fig. 1. HPLC Separation Profile of Ac-(Z/E)-ΔPhe-NHMe

Alltech Alltima, C_{18} , 5 μ m, 150 \times 4.6 mm column; acetonitrile: water (15 : 85); flow rate 1 ml/min. t_R of Ac-(Z)-ΔPhe-NHMe 6.85 min; t_R of Ac-(E)-ΔPhe-NHMe 7.35 min.

provides Ac-(E)-ΔPhe-NHMe of 99.8% purity (Fig. 1d). The compound was stored several months in a refrigerator with neither stereomutation nor other change. Its ^1H -NMR spectrum is consistent with expectations as compared with the (Z)-isomer spectrum. For (Z)/(E) configuration assignment of an α,β -dehydroamino acid residue, resonances $C^\beta\text{-H}$ and NH-C^α can be of diagnostic value. We observed in the spectra of a few (Z)/(E) couples of constitutionally identical compounds that the vinyl and enamide protons of the (Z)-isomers resonate at lower and higher field, respectively, compared with the corresponding protons of the (E)-isomers.^{1,13,18} In spectra of mixtures Ac-(Z/E)-ΔPhe-NHMe (taken in DMSO- d_6 due to the (Z)-compound solubility), the signal $C^\beta\text{-H(E)}$ appears at 6.79 ppm while that of (Z)-isomer is at 7.04 ppm; in turn, the signal $\text{NH-C}^\alpha(\text{E})$ appears at 9.58 ppm and that of (Z)-isomer is at 9.36 ppm.

Experimental

General Experimental Procedures Ac-(Z)-ΔPhe-NHMe, obtained according to the reported method,¹⁵ was crystallized from ethanol to be of 100% purity by HPLC. Ethanol was distilled over NaOH and then through a Hempel column. The solvents from reaction mixtures and from column chromatographic separations were removed *in vacuo* on a rotary evaporator at a bath temperature not exceeding 30 °C. Analytical and preparative HPLC was performed on a Beckman "System Gold" chromatograph for Methods Development consisting of a Model 126 programmable module, a Model 168 diode array detector (working at 210 nm), a Model 210A injection valve and a PC386SX (Wearnes) with "System Gold" version 5.1 software for data collection and controller function. For analytical runs the following were used: an Alltech Alltima, C_{18} , 5 μ m, 150 \times 4.6 mm column, a 5 μ l loop,

acetonitrile: water (15 : 85) as a mobile phase and a flow rate of 1 ml/min; t_R of Ac-(Z)-ΔPhe-NHMe 6.85 min, t_R of Ac-(E)-ΔPhe-NHMe 7.35 min.

Irradiations Irradiations were performed at constant temperature of 22 °C, in 250 and 1500 ml bottles made of PET and equipped with a magnetic stirrer. Prior to the process, the solutions were bubbled with nitrogen for 5 min and thereafter space above the surface of the liquid was filled up with argon. The source of 293-nm and 313-nm light was a Photochemical Reactors, Ltd. 400-W medium-pressure mercury lamp fitted with appropriate filters. The source of 365-nm light was an 80-W lamp.

Ac-(E)-ΔPhe-NHMe Two solutions each Ac-(Z)-ΔPhe-NHMe (270 mg) in ethanol (1.2 l) were irradiated with 313-nm light over 16 h, then combined and concentrated to about 50 ml. A mixture of ethyl ether: hexane (1 : 1) (250 ml) was added and the whole left for crystallization. The resulting Ac-(Z)-ΔPhe-NHMe was filtered off (400 mg) and the filtrate concentrated. Precipitation and filtration were repeated once more to furnish the second crop of (Z)-isomer (60 mg), both of 99.8% purity by HPLC. The filtrate was evaporated to dryness to give a mixture of Ac-(Z/E)-ΔPhe-NHMe (20 : 80) (65 mg). This was dissolved in methanol (850 μ l) and water (2550 μ l) was added. The solution in 850 μ l portions was applied with an 850 μ l loop to an Alltech Alltima, C_{18} , 10 μ m, 250 \times 22 mm column. The column was eluted with water: methanol (80 : 20) at a flow rate of 20 ml/min and fractions were collected using a fraction collector Gilson 202. The fractions appropriate by analytical HPLC were combined and evaporated to dryness to afford Ac-(E)-ΔPhe-NHMe (15 mg) of 99.8% purity by HPLC.

^1H NMR (Tesla BS 567 100 MHz; a saturated solution in CDCl_3 with TMS as an internal standard) δ (ppm): 2.10 (s, 3H, CH_3CO), 2.67 (d, 3H, NHCH_3), 6.62 (s, 1H $C^\beta\text{-H}$), 7.32 (m, 5H, Ph), 7.36 (q, 1H, NHCH_3), 8.01 (s, 1H, NH-C^α).

Acknowledgment The authors acknowledge financial support for this work from a grant-in-aid from the Polish State Committee for Scientific Research (KBN).

References and Notes

- Part XII: Smelka L., Rzeszotarska B., Broda M. A., Kubica Z., *Org. Prep. Proced. Int.*, **29**, 696—701 (1997).
- Abbreviations: Ac=acetyl, (Z)-ΔPhe=(Z)-dehydrophenylalanine, (E)-ΔPhe=(E)-dehydrophenylalanine.
- Noda K., Shimohigashi Y., Izumiya N., "The Peptides. Analysis, Synthesis, Biology," Vol. 5, ed. by Gross E., Meienhofer J., Academic Press, New York-London, 1983, pp. 285—339.
- Schmidt U., Lieberknecht A., Wild J., *Synthesis*, **1988**, 159—172.
- Broda M. A., Rzeszotarska B., "Peptides. Proc. 25th Eur. Pept. Symp., Budapest 1998," ed. by Bajusz S., Hudecz F., Akadémiai Kiadó, Budapest, 1999, pp. 452—453.
- Thormann M., Hofmann H.-J., *J. Mol. Struct. (Theochem)*, **431**, 79—96 (1998).
- Pietrzyński G., Rzeszotarska B., *Polish J. Chem.*, **69**, 1595—1614 (1995).
- Jain R., Chauhan V. S., *Biopolymers*, **40**, 105—119 (1996).
- Nitz T. J., Shimohigashi Y., Costa T., Chen H.-Ch., Stammer Ch. H., *Int. J. Peptide Protein Res.*, **27**, 522—529 (1986).
- Mosberg H. I., Dua R. K., Pogozheva I. D., Lomize A. L., *Biopolymers*, **39**, 287—296 (1996).
- Edwards J. W., Fanger B. O., Cashman E. A., Eaton S. R., McLean L. R., "Peptides: Chemistry and Biology, Proc. 12th Am. Pept. Symp.," ed. by Smith J. A., Rivier J. E., Escom-Leiden, 1991, pp. 52—53; Edwards J. W., Fanger B. O., Patent No. 16105 (1993).
- Nitz T. J., Holt E. M., Rubin R., Stammer Ch. H., *J. Org. Chem.*, **46**, 2667—2671 (1981).
- Makowski M., Rzeszotarska B., Kubica Z., Pietrzyński G., Hetper J., *Liebigs Ann. Chem.*, **1986**, 980—991.
- Ullman E. F., Baumann N., *J. Am. Chem. Soc.*, **92**, 5892—5899 (1970).
- Aubry A., Allier F., Boussard G., Marraud M., *Biopolymers*, **24**, 639—646 (1985).
- Broda M. A., Rzeszotarska B., Kubica Z., in preparation.
- Brocklehurst K., Williamson K., *Tetrahedron*, **30**, 351—354 (1974).
- Makowski M., Rzeszotarska B., Kubica Z., Wiczorek P., *Liebigs Ann. Chem.*, **1984**, 920—928; Makowski M., Rzeszotarska B., Kubica Z., Pietrzyński G., *ibid.*, **1985**, 893—900; Makowski M., Rzeszotarska B., Smelka L., Kubica Z., *ibid.*, **1985**, 1457—1464; Kubica Z., Rzeszotarska B., Makowski M., Głowska M. L., Gałdecki Z., *Polish J. Chem.*, **62**, 107—113 (1988).

Surface Active Properties of Simple Cyclic and Heterocyclic Amines in Water

Yoshihiro FUJINO and Shoko YOKOYAMA*

Kyoritsu College of Pharmacy, 1–5–30, Shibakoen, Minato-ku, Tokyo 105–8512, Japan.

Received August 20, 1999; accepted October 9, 1999

The surface tension of aqueous solutions of simple cyclic, heterocyclic and aromatic amines was measured with a Du Nöuy tensiometer at 25°C and the results discussed in terms of structure–aggregation relationships. The simple compounds used in this study were piperazine, piperidine, morpholine, 3-methylpyridine, cyclohexylamine and benzylamine, with carbon numbers ranging from four to seven.

Piperazine, piperidine and morpholine did not form micellar associations but cyclohexylamine, benzylamine and 3-methylpyridine did, indicating that more than six carbons are necessary to form micellar associations, at least for compounds having a six-membered ring.

Key words surface tension; self-association; simple ring compound; cyclic amine; heterocyclic compound; aqueous solution

It is generally known that compounds without any distinct hydrophobic and hydrophilic moieties do not easily form micelles. In contrast to a large number of studies on the surface activity of aliphatic compounds,¹⁾ only a few^{2–4)} have been published on the surface activity of aromatic and/or cyclic compounds (especially simple compounds with a ring-structure). In 1995, we reported the self-association of cyclohexylamine in water.²⁾ In the same year, Glinski *et al.* reported³⁾ the surface tension of dilute aqueous solutions of cyclohexylamine and benzylamine, however the self-association of those compounds was not apparent because very dilute solutions were used.

On the other hand, the surface tension of some common surfactants in methylpyridine have been measured,^{5–7)} although the surface active properties of methylpyridine were not discussed.

It would be interesting to know the degree of hydrophobicity necessary to form micelles, and it would also be of interest to investigate the surface activity of simple cyclic, heterocyclic and aromatic compounds in terms of structure–aggregation relationships. For systematic study of the surface activity of simple compounds with a ring-structure, we chose piperazine, piperidine, morpholine, 3-methylpyridine, cyclohexylamine and benzylamine, compounds with four to seven carbon atoms.

Experimental

Materials Piperazine (hexahydropyrazine), piperidine (hexahydropyridine), morpholine (tetrahydro-2H-1,4-oxazine), cyclohexylamine, 3-methylpyridine and benzylamine purchased from Wako Pure Chemical Industries, Ltd. were of guaranteed reagent grade and were used without further purification. The structural formulas of those compounds are shown in Chart 1. Deionized and twice-distilled water were used throughout this study.

The pK_b values of piperazine,⁸⁾ piperidine,⁸⁾ morpholine,⁸⁾ cyclohexylamine,⁹⁾ 3-methylpyridine⁹⁾ and benzylamine⁹⁾ are 4.2, 2.8, 5.6, 3.34, 8.0 and 4.65, respectively. 3-Methylpyridine is a weak base and exists as ionic and non-ionic forms in water, while the other five amines are strong bases and exist almost entirely in ionic form in water. The solubility of piperazine in water is about 3 M, while the other five amines are freely soluble in water.⁸⁾

Measurement of Surface Tension The surface tension was measured with a Du Nöuy tensiometer. A platinum ring with a diameter of 19 mm was heated in an oxidizing flame before use. The thermostat temperature was maintained at 25±0.1°C. To calculate the surface tension of aqueous solutions, the value of 71.96 mN m^{−1} was used as the surface tension of pure water at 25°C. The experimental determination of the surface tension was precise to ±0.1 mN m^{−1}.

Results and Discussion

Surface Tension of Aqueous Solutions of Simple Amines with a Ring-Structure The surface tension (γ) of aqueous solutions of piperazine, piperidine, cyclohexylamine, morpholine, 3-methylpyridine and benzylamine are presented in Figs. 1 and 2.

The surface tension of an aqueous solution of morpholine fell continuously with increasing concentration of morpholine, and no inflection point in the surface tension curve was found, even above 10 M. Morpholine is unlikely to exhibit self-association. The surface tension of an aqueous solution of piperazine is higher than that of morpholine at the same concentration and so piperazine is also unlikely to exhibit self-association, although the surface tension of aqueous solutions of piperazine at concentrations above 4 M could not be measured because of the low solubility⁸⁾ of piperazine. The surface activity of morpholine is slightly greater than that of piperazine, and so the substitution of –O– for –NH– seems to increase the surface activity of heterocyclic compounds.

In the case of cyclohexylamine, benzylamine and 3-methylpyridine, a marked decrease in γ and inflection points in the γ vs. $\log C$ curves were found, suggesting that these compounds undergo self-association like micelles. If the critical micelle concentration (cmc) is estimated from the inflection point in the γ vs. $\log C$ curve, cmcs are obtained as 0.54, 0.77 and 1.8 M for cyclohexylamine, benzylamine and 3-methylpyridine, respectively. In addition, the surface tension

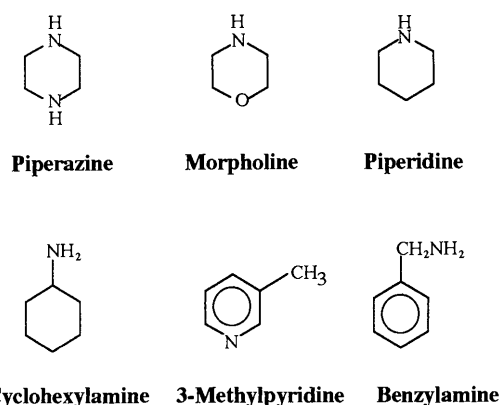


Chart 1. Structural Formulas of Simple Cyclic and Heterocyclic Compounds

* To whom correspondence should be addressed.

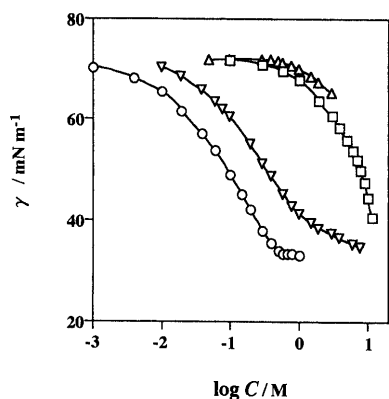


Fig. 1. Surface Tension of Simple Cyclic and Heterocyclic Amines in Water at 25 °C

○, cyclohexylamine; ▽, piperidine; □, morpholine; △, piperazine.

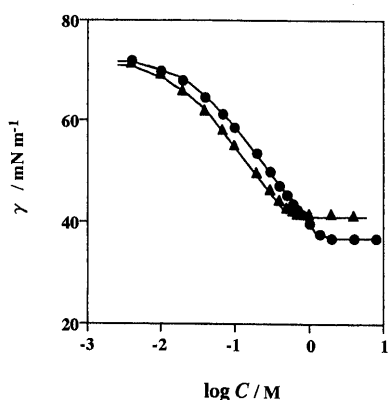


Fig. 2. Surface Tension of Benzylamine and 3-Methylpyridine in Water at 25 °C

▲, benzylamine; ●, 3-methylpyridine.

at the cmc (γ_{cmc}) is 33.5, 41.5 and 36.7 mN m⁻¹ for cyclohexylamine, benzylamine, and 3-methylpyridine, respectively.

The change in surface tension just below the cmc is gradual. This is considered to be due to the fact⁽¹⁰⁾ that surface active compounds with aromatic hydrophobic groups are generally thought to undergo association by a process in which aggregate growth occurs by the continuous stepwise addition of monomers. We have obtained similar results for piperidolate hydrochloride,⁽¹¹⁾ [*N*-ethyl-3-piperidyl diphenylacetate hydrochloride] (an anti-cholinergic drug) and dibucaine hydrochloride,⁽¹²⁾ [2-butoxy-*N*-[2-(diethylamine)ethyl]-4-quinolinecarboxamide] (a local anesthetic).

The aggregation numbers of 3-methylpyridine, benzylamine and cyclohexylamine are thought to be relatively small because of the six-membered ring-structure of those compounds and the large cmc value. In general, the micellar aggregation number of aromatic compounds is low: about equal to the micellar aggregation numbers of dibucaine hydrochloride⁽¹³⁾ and piperidolate hydrochloride⁽¹⁴⁾ which are 9 and 12, respectively.

The surface tension of aqueous solutions of piperidine decreased with increasing concentration of piperidine but a clear inflection point, as shown in the case of cyclohexylamine, benzylamine and 3-methylpyridine, was not found although the decrease in γ was gradual above 2 M. Therefore,

piperidine is unlikely to form a micellar association. Even if piperidine forms such associations, the aggregation number of the self-association would be much smaller than that of cyclohexylamine, benzylamine or 3-methylpyridine. The self-association of piperidine in water may result in a dimer or further dimerization of the dimer at the most. For a more detailed discussion, it is necessary to know the aggregation numbers of the self-associations of these cyclic and heterocyclic amines. Further measurement by light scattering or fluorescence quenching methods will be required to obtain the aggregation numbers of these compounds.

Piperidine has five methylene units, while cyclohexylamine and 3-methylpyridine have six carbons which suggests that more than six carbons are necessary to form micellar associations.

Regarding the surface activity of *ortho*-, *meta*- and *para*-isomers, it has been reported⁽⁴⁾ that *meta*-chlorobenzamide shows greater surface activity than *ortho*-chlorobenzamide under the same conditions and that the effect is related to the dipole moment of the molecule. So, the surface activity of 3-methylpyridine may differ from that of 2-methylpyridine and 4-methylpyridine. We intend to examine the surface active properties of 2-methylpyridine and 4-methylpyridine in the subsequent study.

The surface activity of cyclohexylamine with 6 carbons is greater than that of benzylamine with 7 carbons. This is because of the presence of unsaturated bonds in benzylamine. Regarding the effect of double-bonds, it has been reported^(15,16) that incorporation of a double-bond near the center of the hydrocarbon chain in long-chain surfactants has an effect on the cmc, equivalent to the removal of 1 to 1.5 CH₂ groups from a saturated chain. We have reported that the cmc of icosapolyenoic acid increased twofold on increasing the number of double-bonds.⁽¹⁷⁾ In the case of benzylamine, which has a benzene-ring, the surface activity of benzylamine is nearly equal to that of saturated cyclic compounds with a carbon number of 5.5.

In conclusion, piperidine did not form micellar associations but cyclohexylamine, benzylamine and 3-methylpyridine did (although the aggregation numbers of those associations are still unknown), indicating that more than six carbons in a molecule are needed to form micellar associations of compounds with a six-membered ring. Further measurement by light scattering or fluorescence quenching methods is necessary to obtain the aggregation numbers of these compounds. Nevertheless, the concentration of 3-methylpyridine, cyclohexylamine and benzylamine, when these compounds are used as a medium for synthesis or as a solvent, may be important.

References

- 1) Fendler J. H., Fendler E. J., "Catalysis in Micellar and Macromolecular Systems," Academic Press, New York, 1975.
- 2) Yokoyama S., Fujino Y., Kondo M., Fujie T., *Chem. Pharm. Bull.*, **43**, 1055–1056 (1995).
- 3) Glinski J., Chavepeyer G., Platten J. K., *New J. Chem.*, **19**, 1165–1170 (1995).
- 4) Kamiński B., Młodnicka T., *Bull. Acad. Polon. Sci., Ser. Sci. Chim.*, **14**, 389–394 (1966).
- 5) Sharma V. K., Singh J., Yadav O. P., *Indian J. Chem., Sect. A*, **37A**, 498–506 (1998).
- 6) Sharma V. K., Singh J., Yadav O. P., *Indian J. Chem., Sect. A*, **35A**, 1056–1061 (1996).

- 7) Sharma V. K., Yadav O. P., Singh J., *Colloid Surf., A*, **110**, 23—35 (1996).
- 8) "The Merck Index X," Merck and Co., Inc., U.S.A., pp. 899, 1076, 1077 (1983).
- 9) "Kagaku Binran," 4th ed., Nippon Kagakukai, Maruzen, Tokyo, p. II-321 (1993).
- 10) Mukerjee P., *J. Pharm. Sci.*, **63**, 972—975 (1974).
- 11) Yokoyama S., Fujino Y., Kawamoto Y., Kaneko A., Fujie T., *Chem. Pharm. Bull.*, **42**, 1351—1353 (1994).
- 12) Yokoyama S., Fujino Y., Fujie T., *Prog. Anesthetic Mechanism*, **3**, 392—397 (1995).
- 13) Attwood D., Fletcher P., *J. Pharm. Pharmacol.*, **38**, 494—497 (1986).
- 14) Attwood D., *J. Pharm. Pharmacol.*, **28**, 407—409 (1976).
- 15) Tanford C., "The Hydrophobic Effect," 2nd ed., John Wiley and Sons, Inc., New York, pp. 8—9, 16, 71, 97 (1980).
- 16) Klevens H. B., *J. Am. Oil Chem. Soc.*, **30**, 74—76 (1953).
- 17) Yokoyama S., Nakagaki M., *Colloid Polym. Sci.*, **271**, 512—518 (1993).

Two New Meliacarpinins from the Roots of *Melia azedarach*

Yoshiyasu FUKUYAMA,* Mari OGAWA, Hironobu TAKAHASHI, and Hiroyuki MINAMI

Institute of Pharmacognosy, Faculty of Pharmaceutical Sciences, Tokushima Bunri University, Yamashiro-cho, Tokushima 770-8514, Japan. Received September 27, 1999; accepted October 21, 1999

Two new azadirachtin-type limonoids, 1-methacrylyl-3-acetyl-11-methoxymeliacarpinin (1) and 1-(2-methylpropanoyl)-3-acetyl-11-methoxymeliacarpinin (2), together with the known compounds, meliacarpinin D (3), melianin B (4) and 2 β ,3 β -dihydroxy-5 α -pregn-17(20)-(Z)-en-16-one (5), were isolated from the roots of *Melia azedarach*. The structures of 1 and 2 were elucidated by analysis of spectroscopic data and comparison of their NMR data with those of 3. Compounds 1 and 5 exhibited significant activity in the brine shrimp lethality test (BST).

Key words *Melia azedarach*; limonoid; meliacarpinin; azadirachtin; brine shrimp lethality; brine shrimp test

J. L. McLaughlin and colleagues¹⁾ have developed “the brine shrimp (*Artemia salina*) lethality test (BST)” as a convenient bioassay for screening and fractionation in the discovery and monitoring of biologically active natural products. Particularly, it attracts our attention that brine shrimp lethality has often a positive correlation to 9 KB cytotoxicity and pesticidal activity.^{2,3)} Hence, BST has the advantage of being rapid, inexpensive, and simple enough to carry out screening a number of plant extracts. During our preliminary screening of plant extracts by using the BST, the methanol extract of the roots of *Melia azedarach*^{4,5)} exhibited significant lethal activity. The bioassay-guided fractionation of the methanol extract has resulted in the isolation of the two new meliacarpinins 1 and 2 along with the previously reported meliacarpinin D (3),^{5,6)} melianin B (4)^{7,8)} and a pregnane (5).⁹⁾

In this paper, we describe the structural elucidation of the two new meliacarpinins 1 and 2 isolated from an active fraction of the root of *M. azedarach*.

The methanol extract of the root of *M. azedarach* was fractionated by silica gel chromatography. One of the active fractions eluted with CH₂Cl₂–AcOEt (2:3) was subjected to re-

peated silica gel and octadecyl silica gel (ODS) column chromatography, and finally purified by HPLC using an ODS column to yield the new compounds 1, 2 along with the known compounds, meliacarpinin D (3), melianin B (4) and 2 β ,3 β -dihydroxy-5 α -pregn-17(20)-(Z)-en-16-one (5). Identification of 3–5 was performed by spectral comparison with those reported in the literatures.^{7,9)}

Compound 1, with the molecular formula C₃₄H₄₄O₁₄ determined by its high-resolution (HR) FAB-MS at m/z 699 [M+Na]⁺, showed IR absorption at 3409, 1739 and 1626 cm⁻¹ attributable to a hydroxyl, ester and ketone groups, respectively. The ¹H-NMR and ¹³C-NMR data (Table 1) of 1 indicated the presence of the meliacarpinin skeleton with three singlet methyls (δ_H 1.01, 1.56, 1.61), one methoxyl (δ_H 3.38; δ_C 52.5), one methyl ester (δ_H 3.74; δ_C 169.3, 53.2), one acetyl (δ_H 2.00; δ_C 170.1, 21.0) and one methacrylyl group [δ_H 1.95 (3H, br s), 5.63 (1H, m), 6.15 (1H, m); δ_C 166.0, 136.1, 126.1, 11.9] and were similar to those of meliacarpinin D (3)^{5,6)} (1-tigloyl-3-acetyl-11-methoxymeliacarpinin). All the structural units obtained from the ¹H–¹H correlation spectroscopy (COSY) and ¹H detected multiple quantum coherence (HMQC) spectra, as shown by the bold lines in Fig. 1, and seven quaternary carbons resonated at δ_C 106.9 (C-11), 94.9 (C-13), 93.3 (C-14), 86.2 (C-20), 51.2 (C-8), 49.6 (C-10) and 42.6 (C-4) corresponded well to those existing in the known meliacarpinin D (3). Additionally, the heteronuclear multi-bond correlation (HMBC) experiment, as summarized in Fig. 1, could assemble the partial units and seven quaternary carbons into the assumed meliacarpinin

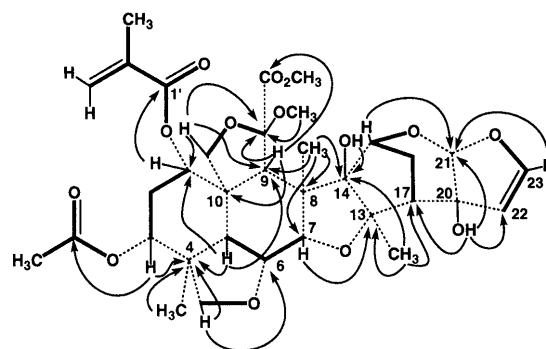
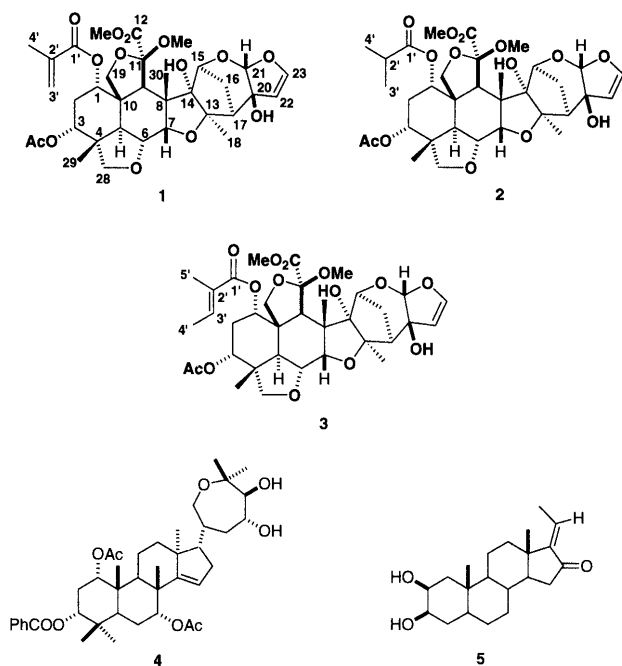


Fig. 1. HMBC Correlations of 1

Bold lines indicate the partial structures inferred from COSY and HMQC, and arrows denote the correlation between protons (tail) and carbons (head) in the HMBC.

* To whom correspondence should be addressed.

structure. The HMBC correlation of H-1 resonated at δ_{H} 4.98 with the C-1' ester carbonyl at δ_{C} 166.0 placed the methacrylyl group on the C-1 position. The HMBC correlation between H-3 at δ_{H} 4.60 and CH_3COO at δ_{C} 170.1 proved the sole acetyl group to be linked at the C-3 position. Having the same stereochemistry with **1** as that of **3** was also supported by phase-sensitive nuclear Overhauser and exchange

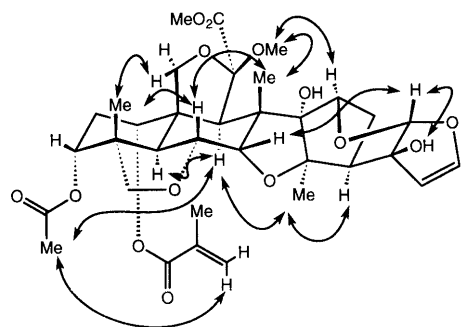


Fig. 2. Relative Configuration of **1** Based on NOEs Indicated by Arrows

spectroscopy (NOESY) spectrum as shown in Fig. 2 as well as by small J values for H-1 and H-3 (Table 1). Thus compound **1** was assigned as 1-methacrylyl-3-acetyl-11-methoxymeliacarpinin.

Compound **2** had the molecular formula $\text{C}_{34}\text{H}_{46}\text{H}_{14}$ determined from HR-FAB-MS at m/z 701.2925 $[\text{M}+\text{Na}]^+$. Its ^1H - and ^{13}C -NMR spectra (Table 1) were similar to those of **1** except for the presence of a newly appeared 2-methylpropanoyl group [δ_{H} 1.16 (3H, d, $J=6.7$ Hz), 1.20 (3H, d, $J=6.7$ Hz), 2.51 (1H, qq, $J=6.7$, 6.7 Hz; δ_{C} 18.1, 18.6, 34.2, 175.8) instead of the methacrylyl group existing in **1**. The HMBC of **2** showed a cross peak between H-1 (δ_{H} 4.91) and the ester carbonyl (δ_{C} 175.8) involved in the 2-methylpropanoyl group, thereby confirming that the 2-methylpropanoyl group was located at the C-1 position. The relative stereochemistry for **2** was identical with that of **1** from the analysis of its NOESY. Thus the structure of compound **2** was determined as 1-(2-methylpropanoyl)-3-acetyl-11-methoxymeliacarpinin.

Compound **1** exhibited significant lethal activity ($\text{LC}_{50}=19 \mu\text{g/ml}$) in the BST. The other meliacarpinins **2** and **3**,

Table 1. ^1H - (600 MHz) and ^{13}C - (150 MHz) NMR (in CDCl_3) Data for Compounds **1**—**3**

	1		2		3	
	H	C	H	C	H	C
1	4.98 (dd, 2.7, 2.7)	70.7	4.91 (dd, 2.7, 2.7)	70.3	4.98 (dd, 2.7, 2.7)	70.3
2 α	2.07 (dt, 16.7, 2.7)	27.9	2.27 (dt, 17.0, 2.7)	27.8	2.34 (dt, 16.7, 2.7)	27.9
2 β	2.37 (dt, 16.7, 2.7)		2.07 (dt, 17.0, 2.7)		2.06 (dt, 16.7, 2.7)	
3	4.60 (dd, 2.7, 2.7)	71.0	4.57 (dd, 2.7, 2.7)	71.0	4.54 (dd, 2.7, 2.7)	71.07
4		42.6		42.5		42.6
5	3.08 (d, 12.9)	35.1	2.99 (d, 12.9)	34.9	3.07 (d, 12.6)	35.1
6	3.97 (dd, 12.9, 3.0)	71.1	3.94 (dd, 12.9, 2.7)	71.01	3.96 (dd, 12.6, 3.0)	71.05
7	4.53 (d, 3.0)	83.8	4.52 (d, 2.7)	83.7	4.89 (d, 3.0)	83.8
8		51.2		51.2		51.2
9	3.67 (3H, s)	47.9	3.67 (3H, s)	47.8	3.67 (3H, s)	47.9
10		49.6		49.6		49.6
11		106.9		106.91		106.9
12		169.3		169.4		169.4
13		94.9		94.9		94.8
14		93.3		93.2		93.3
15	4.14 (d, 2.5)	81.1	4.13 (d, 2.5)	81.1	4.14 (d, s)	81.1
16 β	2.22 (ddd, 13.4, 6.3, 2.5)	29.7	2.24 (ddd, 13.4, 6.0, 2.5)	29.7	2.24 (ddd, 13.4, 6.3, 2.5)	29.7
16 α	1.87 (dd, 13.4, 1.4)		1.86 (dd, 13.4, 1.4)		1.87 (dd, 13.4, 1.4)	
17	2.17 (dd, 6.3, 1.4)	50.8	2.17 (dd, 6.0, 1.4)	50.7	2.17 (dd, 6.3, 1.4)	50.8
18	1.61 (3H, s)	25.9	1.61 (3H, s)	25.9	1.59 (3H, s)	25.9
19 α	3.86 (d, 9.3)	70.6	3.85 (d, 9.3)	70.5	3.86 (d, 9.3)	70.6
19 β	4.16 (d, 9.3)		4.15 (d, 9.3)		4.16 (d, 9.3)	
20		86.2		86.2		86.2
21	5.64 (s)	109.3	5.64 (s)	109.3	5.64 (s)	109.3
22	4.89 (d, 3.0)	107.9	4.89 (d, 3.0)	107.9	4.59 (d, 3.0)	107.9
23	6.39 (d, 3.0)	145.8	6.38 (d, 3.0)	145.8	6.39 (d, 3.0)	145.8
28 α	3.62 (3H, s)	76.5	3.46 (d, 7.7)	76.5	3.55 (d, 8.0)	76.4
28 β	3.57 (d, 8.6)		3.56 (d, 7.7)		3.59 (d, 8.0)	
29	1.01 (3H, s)	18.0	0.98 (3H, s)	18.1	0.99 (3H, s)	18.0
30	1.56 (3H, s)	17.8	1.58 (3H, s)	17.7	1.56 (3H, s)	17.8
20-OH	6.14 (s)		6.16 (s)			
11-OMe	3.38 (3H, s)	52.5	3.39 (3H, s)	52.5	3.39 (s)	52.5
12-OMe	3.74 (3H, s)	53.2	3.75 (3H, s)	53.2	3.74 (3H, s)	53.2
3-AcO	2.00 (3H, s)	170.1	2.08 (3H, s)	170.2	1.99 (3H, s)	170.1
		21.0		21.2		21.1
1'		166.0		175.8		166.6
2'		136.1	2.51 (qq, 6.7, 6.7)	34.2		128.3
3'	5.63 (m)	126.1	1.20 (d, 6.7)	18.1	6.99 (qq, 7.0, 1.3)	138.2
	6.15 (m)					
4'	1.95 (3H, s)	11.9	1.16 (d, 6.7)	18.6	1.82 (dq, 7.0, 1.3)	11.9
5'					1.83 (dq, 1.3, 1.0)	14.5

however, had no lethal activity at 100 $\mu\text{g/ml}$. This result presumes that the methacrylyl group attached to the C-1 position would play an important role in having toxicity against the brine shrimp. Of all the compounds isolated from one of the active fractions the pregnane **5** was most active ($\text{LC}_{50} = 2.1 \mu\text{g/ml}$) in the BST. A number of the potent antifeedants and cytotoxic active compounds, however, have been isolated from *M. azedarach* L.¹⁰⁾ Most of the active principles belong to the azadirachtin-type tetranortriterpenoids and the sendanin-type limonoids. Therefore, our further search for other BST-active substances in the root of *M. azedarach* is in progress.

Experimental

Optical rotations were measured with a Jasco DIP-1000 digital polarimeter. IR spectra were recorded on a Jasco FT-IR 5300 IR spectrophotometer. One dimensional (1D) and two dimensional (2D)-NMR spectra were recorded on a Varian Unity 600 instrument in CDCl_3 . Chemical shifts were given as δ (ppm) with tetramethylsilane (TMS) as an internal standard. MS were recorded on a JEOL AX-500 instrument.

Plant Materials The roots of *Melia azedarach* Linn. var. *Japonica* MAKINO were collected in Tokushima, Japan and a voucher specimen (1428RT) has been deposited in this institute of Tokushima Bunri University.

Extraction and Purification The MeOH extract (91 g) of the dried powdered root of *M. azedarach* was chromatographed on silica gel (Merck, 70–230 mesh) eluting with a CH_2Cl_2 –EtOAc gradient and eluant were separated into 1–6 fractions. The BST-active (100% death at 200 $\mu\text{g/ml}$) fraction 2 (3.8 g) was fractionated into 7–12 fractions by Sephadex LH-20 chromatography with MeOH. The BST-active fraction 9 (3.2 g) was subjected to a reverse phase column chromatography on Cosmosil 40C₁₈-OPN eluting with MeOH–H₂O (9:1) to give 13–19 fractions. The BST-active fraction 17 (11.6 mg) was purified by HPLC [Cosmosil 5C₁₈-AR ($\phi 10 \times 250$ mm); MeOH–H₂O (7:3; 2.0 ml min⁻¹); UV 220 nm] to give compounds **1** (4.6 mg) and **2** (5.2 mg), and meliacarpinin D (**3**) (6.2 mg). The BST-active fraction 14 (127 mg) was purified by silica gel chromatography [CHCl_3 –MeOH (97:3)] and finally by HPLC [Cosmosil 5C₁₈-AR ($\phi 10 \times 250$ mm); MeOH–H₂O (8:2; 2.0 ml min⁻¹); UV 220 nm] to give melianin B (**4**) (9 mg) and 2 β ,3 β -dihydroxy-5 α -pregn-17(20)-(Z)-en-16-one (**5**) (3 mg).

1-Methacrylyl-3-acetyl-11-methoxymeliacarpinin (**1**): Amorphous powder. $[\alpha]_D^{25} + 2.5^\circ$ ($c = 0.19$, CHCl_3). IR cm^{-1} : 3409 (OH), 1739 (C=O), 1626 (C=O). FAB-MS m/z : 699 [M+Na]⁺, 659 [M+H–18]⁺, 617 [M+H–60]⁺. HR-FAB-MS m/z : 699.2673 [M+Na]⁺ (Calcd for C₃₄H₄₄O₁₄Na: 699.2629). ¹H-NMR and ¹³C-NMR: Table 1.

1-(2-Methylpropanoyl-3-acetyl-11-methoxymeliacarpinin (**2**): Amorphous

powder. $[\alpha]_D^{25} - 169.8^\circ$ ($c = 0.21$, CHCl_3). IR cm^{-1} : 3402 (OH), 1738 (C=O), 1624 (C=O). FAB-MS m/z : 701 [M+Na]⁺, 661 [M+H–18]⁺, 619 [M+H–60]⁺. HR-FAB-MS m/z : 701.2925 [M+Na]⁺ (Calcd for C₃₄H₄₆O₁₄Na: 701.2911). ¹H-NMR and ¹³C-NMR: Table 1.

Brine Shrimp Bioassay The bioassay was carried out according to essentially the same literature procedure.¹¹⁾ A half spoon of brine shrimp eggs (Nihon Animal Pharmaceutical Inc., Tokyo, Japan) were hatched in a container filled with air-bubbled artificial sea water which was prepared with 10 g of a commercial salt mixture (GEX Inc., Osaka, Japan) and 500 ml of distilled water. After 48 h, the phototropic shrimps were collected by pipette for bioassay. Ten shrimps were transferred to each vial, and artificial water was added to make 5 ml. To this vial each sample which was dissolved in 0.025 ml of dimethyl sulfoxide (DMSO), whereas the vial containing 0.025 ml of DMSO was regarded as a control. The surviving shrimps were counted microscopically in the stem of the pipette against a lightened background after 24 h. The percent deaths at each dose was counted as the following formula: % deaths = (the number of death shrimps – the number of half death shrimps $\times 0.7$) / 10 $\times 100$.

Acknowledgements We are indebted to Dr Masami Tanaka and Miss Yasuko Okamoto for measuring 600 MHz NMR and MS spectra, respectively. This work was partially supported by the Science Research Promotion Fund from the Promotion and Mutual Aid Corporation for Private Schools of Japan.

References

- 1) Meyer B. N., Ferrigni N. R., Putnam J. E., Jacobsen L. B., Nichols D. E., McLaughlin J. L., *Planta Med.*, **45**, 31–34 (1982).
- 2) McLaughlin J. L., Rogers L. L., *Drug Information J.*, **32**, 513–524 (1998).
- 3) Johnson H. A., Rogers L. L., Alkire M. L., McCloud T. G., McLaughlin J. L., *Natural Product Letters*, **11**, 241–250 (1998).
- 4) Takeya K., Qiao Z.-S., Hirobe C., Itokawa H., *Phytochemistry*, **42**, 709–712 (1996).
- 5) Itokawa H., Qiao Z.-S., Hirobe C., Takeya K., *Chem. Pharm. Bull.*, **43**, 1171–1175 (1995).
- 6) Zhou J.-B., Minami Y., Yagi F., Tadera K., Nakatani M., *Heterocycles*, **45**, 1781–1786 (1997).
- 7) Rogers L. L., Zeng L., Kozlowski J. F., Shimada H., Alali F. Q., Johnson H. A., McLaughlin J. L., *J. Nat. Prod.*, **61**, 64–70 (1998).
- 8) Okogum J. I., Fakunle C. O., Ekong D. E. U., *J. Chem. Soc. Perkin Trans. 1*, **1975**, 1352–1356.
- 9) Inada A., Murata H., Inatomi Y., Nakanishi T., Darnaedi D., *Phytochemistry*, **45**, 1225–1228 (1997).
- 10) Ley S. V., Denholm A. A., Wood A., *Nat. Prod. Rep.*, **10**, 109–159 (1993).

Facile Synthesis of Optically Active γ -Lactones via Lipase-catalyzed Reaction of 4-Substituted 4-Hydroxybutyramides

Yasufumi MATSUMURA,^{*,a} Teruko ENDO,^a Mitsuo CHIBA,^a Hidemichi FUKAWA,^a and Yoshiyasu TERAOKA^b

Research Center, Toyotama Koryo Co., Ltd.,^a 65 Numata Minami-ashigara, Kanagawa 250-0115, Japan and Graduate School of Nutritional & Environmental Sciences, University of Shizuoka,^b 52-1 Yada, Shizuoka 422-8526, Japan.

Received October 5, 1999; accepted December 3, 1999

Lipase-catalyzed transesterification of racemic 4-substituted 4-hydroxybutyramides with succinic anhydride proceeded enantioselectively to afford (*S*)-succinic acid monoester and unreacted (*R*)-4-hydroxybutyramide derivative, which were separated easily by treatment with an alkaline solution. Both enantiomers were converted easily to optically active γ -substituted γ -butyrolactones.

Key words γ -butyrolactone; lipase; resolution; succinic anhydride

γ -Butyrolactones are widespread in nature; some are flavor compounds existing in plants¹⁾ and others are significant in insect behavior.²⁾ Many naturally occurring γ -butyrolactones are optically active compounds. It is well established that chiral discrimination is an important principle in odor perception and insect sex pheromones. Therefore development of a convenient synthetic method for chiral γ -butyrolactones has attracted the attention of synthetic chemists.

Recently, several chemists have reported the syntheses of chiral γ -butyrolactones with sufficient optical purity by lipase-catalyzed resolution of 4-substituted 4-hydroxybutyric acid esters.³⁾ In these cases, however, a mixture of the reaction product and unreacted substrate was separated by a chromatographic method, which is a barrier to industrial-scale preparation. Previously, racemic alcohols were found to be enantioselectively acylated with succinic anhydride using a lipase catalyst in organic solvents, leading to the formation of succinic acid monoester which was easily separable by treatment with an alkaline solution.⁴⁾ For the application of this method to the synthesis of chiral γ -lactones via lipase-catalyzed resolution, ordinary esters did not appear to be the best substrate because of their lability to alkaline treatment. Our strategy includes the choice of a substrate stable in an alkaline solution, as well as appropriately enantioselective lipases.

We employed 4-substituted 4-hydroxybutyramides as substrates for lipase-catalyzed transesterification with succinic anhydride in organic solvents. A variety of 4-substituted 4-hydroxy-*N*-benzylbutyramides were prepared by aminolysis of racemic γ -lactone derivatives.⁵⁾ Several preliminary experiments using various types of lipase indicated that lipase PL (*Alcaligenes* sp.) and lipase PS-C (*Pseudomonas* sp.)⁶⁾ were well suited for enantioselective transesterification. Therefore we mainly used those two lipases for resolution of 4-substituted 4-hydroxy-*N*-benzylbutyramides.

The general procedure is as follows: A mixture of 4-substituted 4-hydroxy-*N*-benzylbutyramide 2 mmol, succinic an-

hydride 2 mmol, and lipase 50 mg in *tert*-butyl methyl ether (MTBE) 25 ml was stirred at 25°C. After consumption of half the substrate had been confirmed by HPLC analysis, the lipase was removed by filtration and washed with MTBE. The combined organic layer was shaken with sodium carbonate 0.2 M (100 ml \times 2). The reacted enantiomer passed over into an aqueous layer as a succinic acid monoester, and the unreacted enantiomer remained in the organic layer. The aqueous layer was treated with 10% sodium hydroxide and extracted with MTBE. Both enantiomers isolated were converted into optically active γ -lactones in almost quantitative yields without racemization (Chart 1).

Table 1 shows the results of reactions of six 4-substituted 4-hydroxybutyramides. The results in entries 1–10 demonstrate that these lipases react preferentially with the *S*-enantiomer, and that the chain length of the substrate has little influence on the reaction rate and enantioselectivity. On the other hand, the reaction with lipase PS-C is faster than that with lipase PL, regardless of the alkyl chain length. It is of interest that an unsaturated alkyl group of the substrate is more effective on the enantioselectivity than a saturated one (compare entries 11 and 12 with 5 and 6, respectively). In general, these reactions proceed faster, especially with lipase PS-C, than the reported lactonization or acylation of the 4-hydroxybutyric acid esters with lipases,³⁾ although the optical yields are comparable.

We successfully converted the resultant chiral 4-hydroxybutyramides to the corresponding γ -butyrolactones, all of which are used as flavors (**R-1a–f**) or a naturally occurring pheromone (**R-1e**),⁷⁾ by hydrolysis with diluted hydrochloric acid without racemization.⁸⁾ In addition, the inversion of an enantiomer to a γ -lactone with the opposite configuration was also examined. As shown in Chart 2, the γ -lactonization of mesylated **S-2c** and **S-2f**, which were prepared from **S-3c** and **S-3f** purified by recrystallization, gave the corresponding (*R*)- γ -butyrolactones with high optical purity in moderate yields.⁹⁾ Optimal conditions for this reaction are under investigation.

Thus the present procedure provides a facile method for the conversion of racemic γ -lactones to only the required enantiomer via lipase-catalyzed resolution of 4-hydroxybutyramide derivatives and inversion of the enantiomer not required.

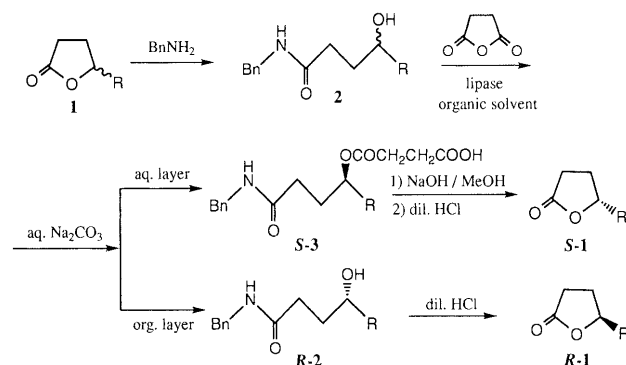


Chart 1

* To whom correspondence should be addressed.

Table 1. Lipase-Catalyzed Transesterification of 4-Substituted 4-Hydroxy-*N*-benzylbutyramides

2 $\xrightarrow[\text{in } t\text{-butyl methyl ether}]{\text{lipase}}$ S-3 + R-2

Entry	Substrate		Lipase	Time (h)	Product S-3		Unreacted R-2	
	No.	R			C.Y. (%) ^{a)}	O.Y. (%ee) ^{b,c)}	C.Y. (%) ^{a)}	O.Y. (%ee) ^{b,c)}
1	2a	<i>n</i> -C ₄ H ₉	PS-C	5	50	89.7	43	92.2
2	2a	<i>n</i> -C ₄ H ₉	PL	24	49	91.7	46	86.4
3	2b	<i>n</i> -C ₅ H ₁₁	PS-C	4.5	47	88.9	47	90.5
4	2b	<i>n</i> -C ₅ H ₁₁	PL	28.5	46	82.6	44	79.3
5	2c	<i>n</i> -C ₆ H ₁₃	PS-C	3	44	85.5	44	86.7
6	2c	<i>n</i> -C ₆ H ₁₃	PL	17	46	84.5	46	86.0
7	2d	<i>n</i> -C ₇ H ₁₅	PS-C	3.5	47	87.5	43	86.7
8	2d	<i>n</i> -C ₇ H ₁₅	PL	17.5	46	88.2	46	88.7
9	2e	<i>n</i> -C ₈ H ₁₇	PS-C	5.5	49	80.7	44	85.5
10	2e	<i>n</i> -C ₈ H ₁₇	PL	23	46	88.6	46	85.9
11	2f		PS-C	9	47	96.9	48	95.1
12	2f		PL	29	47	91.2	47	90.0

a) Isolated yield. b) Optical yields were determined by HPLC analyses (using Chiralcel OD in entries 1—10, and Chiralcel OD-R in entries 11 and 12) after the hydrolysis. c) Absolute configurations were determined by comparison of the optical rotations with those reported, after the lactonization.

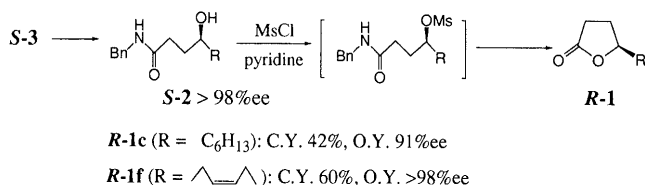


Chart 2

References and Notes

- 1) a) Mosandl A., Gunther C., *J. Agric. Food Chem.*, **37**, 413—418 (1989); b) Guichard E. *ACS Symp. Ser.*, **596**, 258—267 (1995); c) Guichard E., Kustermann A., Mosandl A., *J. Chromatogr.*, **498**, 396—401 (1990).
- 2) a) Tumlinson J. H., Klein M. G., Doolittle R. E., Ladd T. L., Proveaux A. T., *Science*, **197**, 789—792 (1977); b) Naoshima Y., Hasegawa H., Saeki T., *Agric. Biol. Chem.*, **51**, 3417—3419 (1987).
- 3) a) Gutman A. L., Bravdo T., *J. Org. Chem.*, **54**, 4263—4265 (1989); b) Gutman A. L., Zuobi K., Bravdo T., *J. Org. Chem.*, **55**, 3546—3552 (1990); c) Sugai T., Ohsawa S., Yamada H., Ohta H., *Synthesis*, **1990**, 1112—1114; d) Fukusaki E., Senda S., Nakazono Y., Omata T., *Tetrahedron*, **47**, 6223—6230 (1991).
- 4) Terao Y., Tsuji K., Murata M., Achiwa K., Nishio T., Watanabe N., Seto K., *Chem. Pharm. Bull.*, **37**, 1653—1655 (1989).
- 5) Preparation of 4-substituted 4-hydroxy-*N*-benzylamides: Racemic γ -substituted γ -lactone **1** 10 mmol and benzylamine 11 mmol were placed in an autoclave, and stirred at 80—90° for 4—12 h to afford the product in 85—95% yield. The structures of products were determined by ¹H-NMR, IR, and MS spectral analyses.
- 6) Lipase PL and lipase PS-C were supplied by Meito Sangyo Co., Ltd., and Amano Pharmaceutical Co., Ltd., respectively.
- 7) The ¹H-NMR spectra of all of chiral γ -alkyl γ -lactones (**1a—g**) agreed with those of the starting racemates. The specific rotations of chiral γ -alkyl γ -lactones (**1a—g**) were reported previously.^{1a)} **1f** was determined after conversion to **1c** by catalytic reduction.
- 8) Recently, a few chiral γ -lactones have been obtained in kilogram amounts using this method in our company.
- 9) Mesityl chloride 2 mmol was added dropwise to a solution of **S-2c** or **S-2f** 1.8 mmol in pyridine 5 ml at 0 °C with stirring. The mixture was stirred overnight at room temperature and poured into ice water. The mixture was extracted with hexane. The organic layer was washed with diluted HCl and brine, and dried over MgSO₄. Removal of the solvent gave an oily residue, which was chromatographed on a silica gel column using an AcOEt-hexane system to afford an oily product. The optical purity was determined by comparison of the specific rotation of the product with that described in Reference 1a).

One-pot Enantioselective Synthesis of Optically Active Homoallylic Alcohols from Allyl Halides

Makoto NAKAJIMA,* Makoto SAITO, and Shunichi HASHIMOTO

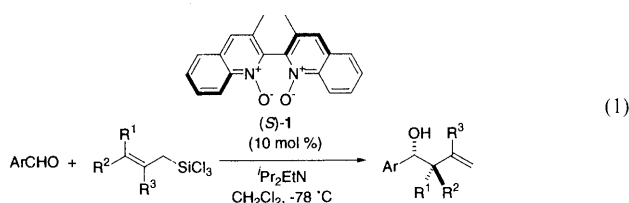
Graduate School of Pharmaceutical Sciences, Hokkaido University, Kita-12 Nishi-6, Kita-ku, Sapporo 060-0812, Japan.

Received October 12, 1999; accepted December 4, 1999

A one-pot, convenient method for the preparation of optically active homoallylic alcohols from allyl halides was developed. Allyltrichlorosilanes were generated *in situ* from allyl halides and trichlorosilane in the presence of cuprous chloride and tertiary amine. Without isolation of the allyltrichlorosilanes, benzaldehyde and chiral biquinoline *N,N'*-dioxide were introduced into the same flask, producing the corresponding homoallylic alcohols with good to high enantioselectivities.

Key words one-pot synthesis; homoallylic alcohol; *N*-oxide; enantioselective allylation; chiral catalyst

The asymmetric allylation of aldehydes to generate two successive stereogenic centers has been the subject of investigation in recent years.¹⁾ While high enantioselectivities have been achieved with allyltin or allylsilane reagents in the presence of chiral Lewis acids as catalysts,²⁾ these processes afford preferentially *syn* homoallylic alcohols from both stereoisomers of allyl metals *via* an acyclic transition state. On the other hand, Lewis base-catalyzed allylations with allyltrichlorosilanes as allylating reagents developed recently by Kobayashi³⁾ are presumed to proceed *via* chair-like transition states involving hypervalent silicates,^{4,5)} in which the stereochemical information present in the allyltrichlorosilanes is transmitted to an *anti* (from *E*-alkene precursors) or a *syn* (from *Z*-alkene precursors) relationship about the new C–C bond of the product. Asymmetric versions of the Lewis base-catalyzed allylations using chiral HMPA or DMF derivatives as catalysts reported by Denmark⁶⁾ and Iseki⁷⁾ afforded the homoallylic alcohols with moderate to good enantioselectivities with rather modest catalytic activities. Recently, we have developed an amine *N*-oxide-catalyzed allylation, which has been extended to enantioselective allylation with high chemical and optical yield using a chiral bipyridine *N,N'*-dioxide derivative ((*S*)-**1**) (Eq. 1).^{8,9)}



The most common procedure for the preparation of allyltrichlorosilanes which are often utilized in the Lewis base-catalyzed allylation involves the silylation of the corresponding allyl chloride with trichlorosilane followed by distillation.¹⁰⁾ Although the silylation in the presence of cuprous chloride and tertiary amine proceeds almost quantitatively, the distillation of the product often proves to be troublesome. Since allyltrichlorosilanes are easily hydrolyzed to produce

polymeric gum and hydrogen chloride, special care is required throughout the distillation, especially when labile substrates are employed. From a synthetic point of view, Kobayashi has developed a one-pot process for the preparation of homoallylic alcohols from allyl halides and aldehydes wherein aldehyde and excess DMF as a Lewis base were added to a solution of the allyltrichlorosilane generated *in situ* from allyl halide and trichlorosilane in ether.^{3b)} However, no one-pot process employing a catalytic amount of Lewis base has been reported to date. Herein we describe the first one-pot synthesis of optically active homoallylic alcohols from allyl halides exploiting a catalytic amount of chiral *N*-oxide as a Lewis base.

The major problem in one-pot synthesis is the reduction of the Lewis base by excess trichlorosilane. To avoid the reduction of *N*-oxide, we removed the trichlorosilane from the reaction mixture with a rotary evaporator before adding aldehyde and *N*-oxide to the same flask. As expected, the allylation proceeded smoothly without the reduction of *N*-oxide, affording the homoallylic alcohol in good chemical and optical yields (95%, 87%ee), comparable to those obtained by our original allylation procedure employing the isolated allyltrichlorosilane (89%, 88%ee).⁸⁾

Some representative results under optimized conditions are summarized in Table 1. Not only allyl chloride but allyl bromide (entry 2) or allyl tosylate (entry 3) could be used as precursors of allylating reagents without any loss of chemical and optical yields. *E*-Crotlyl- (66%, 86%ee vs. 68%, 86%ee in the original allylation) and methallyl chloride (62%, 52%ee vs. 70%, 49%ee in the original allylation) also gave almost the same results as in our original allylation procedure (entries 4, 5). More noteworthy is that halides (entries 6–9), of which trichlorosilane derivatives are prone to isomerize or decompose during distillation, produce the corresponding homoallylic alcohols in good yields. As expected, *anti*- and *syn*-homoallylic alcohols were obtained from *E*- and *Z*-cinnamyl chlorides (entries 6, 7), respectively, which shows that the one-pot allylation in the presence of copper salt proceeds *via* the same mechanism as the allylation in the original method. Modest enantioselectivity with α -bromomethylstyrene (entry 8) as well as methallyl chloride (entry 5) can be explained by the 1,3-diaxial-type steric repulsion between the β -substituents (R^3) of the allyltrichlorosilanes and the wall of the biaryl unit in the proposed transition state involving hypervalent silicate (Fig. 1).⁸⁾

The representative procedure for one-pot enantioselective allylation is as follows: To a solution of *E*-cinnamyl chloride (80 mg, 0.52 mmol), diisopropylethylamine (0.30 ml, 1.7 mmol) and cuprous chloride (6.0 mg, 0.061 mmol) in ether (5 ml) was added trichlorosilane (0.1 ml, 0.99 mmol) at room temperature and the mixture was stirred for 1 h under an Ar atmosphere. Disappearance of the chloride was checked by ¹H-NMR of an aliquot of the reaction mixture. Excess trichlorosilane and ether were evaporated *in vacuo* with a rotary evaporator and the residue was dissolved in dichloromethane (2 ml). The solution of benzaldehyde (50 mg, 0.46 mmol) and (*S*)-**1** (15 mg, 0.046 mmol) in dichloromethane (1 ml) was added to the mixture at –78 °C and the whole was stirred at the same temperature for 6 h. Aqueous work-up followed by silica gel column chromatog-

* To whom correspondence should be addressed.

Table 1. One-pot Enantioselective Synthesis of Homoallylic Alcohols from Benzaldehyde and Allyl Halides Catalyzed by (S)-1

Entry	Allyl halide	Yield, % ^{a)}	ee, % (Confgn) ^{b)}	Entry	Allyl halide	Yield, % ^{a)}	ee, % (Confgn) ^{b)}
1		95	87 (S)	6 ^{e)}		76 ^{f)}	91 (1R,2S)
2		92	87 (S)	7 ^{g)}		70 ^{h)}	77 — ⁱ⁾
3		90	86 (S)	8		52	43 (S)
4 ^{c)}		66 ^{d)}	86 (1R,2S)	9 ^{j)}		68 ^{k)}	86 — ^{l)}
5		62	52 (S)				

a) Isolated yield. b) Determined by HPLC analysis employing a Daicel Chiralcel OD, OJ, or Chiralpak AD. Configuration assignment by comparison with the values of optical rotations in Reference 8, 11, 12. c) *E*:*Z*=97:3. d) *syn*:*anti*=3:97. e) *E*:*Z*=>99:<1. f) *syn*:*anti*=<1:>99. g) *E*:*Z*=5:95. Reference 13. h) *syn*:*anti*=95:5. Relative stereochemical assignment by comparison with chemical shift values of NMR in Reference 14. i) $[\alpha]_D^{25} -18.4$ (c 1.3 CHCl₃). j) *E*:*Z*=<1:>99. k) *syn*:*anti*=>99:<1. Relative stereochemical assignment by comparison with chemical shift values of NMR in Reference 15. l) $[\alpha]_D^{25} -14.9$ (c 1.1 C₆H₆).

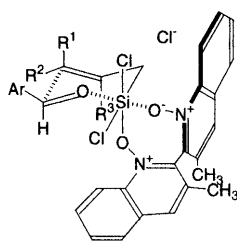


Fig. 1

raphy gave the homoallylic alcohol (76 mg, 76%) of 91%ee on the basis of chiral HPLC analysis. Stereochemistry of the alcohol was assigned by comparison with data in the literature.¹¹⁾

The present modification of the *N*-oxide-catalyzed enantioselective allylation provides a simple and versatile method for the preparation of optically active homoallylic alcohols. Further studies for the application of the present protocol to the enantioselective synthesis of biologically active compounds are under investigation in our laboratory.

Acknowledgments This work was partly supported by a Grant-in-Aid for Scientific Research from the Ministry of Education, Science, Sports, and Culture of Japan and the Otsuka Chemical Award in Synthetic Organic Chemistry, Japan. The authors thank the Japan Society for the Promotion of Science for Research Fellowships for Young Scientists (to M.S.).

References and Notes

- For reviews on asymmetric allylation of carbonyl compounds, see: a) Hoffmann R. W., *Angew. Chem. Int. Ed. Engl.*, **26**, 489—594 (1987); b) Yamamoto Y., Asao N., *Chem. Rev.*, **93**, 2207—2293 (1993); c) Marshall J. A., *Chem. Rev.*, **96**, 31—47 (1997).
- For a review on chiral Lewis acid-catalyzed allylation of aldehydes, see: Cozzi P. G., Tagliavini E., Umani-Ronchi A., *Gazz. Chim. Ital.*, **127**, 247—254 (1997).
- a) Kobayashi S., Nishio K., *Tetrahedron Lett.*, **34**, 3453—3456 (1993); *Idem*, *J. Org. Chem.*, **59**, 6620—6628 (1994); c) *Idem*, *J. Am. Chem. Soc.*, **117**, 6392—6393 (1995); d) Kobayashi S., Hirabayashi R., *ibid.*, **121**, 6942—6943 (1999).
- For recent reviews on hypervalent silicates, see: a) Sakurai H., *Synlett*, **1989**, 1—8; b) Chuit C., Corriu R. J. P., Reye C., Young J. C., *Chem. Rev.*, **93**, 1371—1448 (1993).
- For Lewis base-promoted enantioselective reactions based on hypervalent silicates other than allylation, see: a) Kohra S., Hayashida H., Tominaga Y., Hosomi A., *Tetrahedron Lett.*, **29**, 89—92 (1988); b) Schiffrs R., Kagan H. B., *Synlett*, **1997**, 1175—1178; c) Denmark S. E., Winter S. B. D., Su X., Wong K.-T., *J. Am. Chem. Soc.*, **118**, 7404—7405 (1996); d) Denmark S. E., Stavenger R. A., Su X., Wong K.-T., Nishigaichi Y., *Pure Appl. Chem.*, **70**, 1469—1476 (1998); e) Denmark S. E., Barsanti P. A., Wong K.-T., Stavenger R. A., *J. Org. Chem.*, **63**, 2428—2429 (1998).
- Denmark S. E., Coe D. M., Pratt N. E., Griedel B. D., *J. Org. Chem.*, **59**, 6161—6163 (1994).
- a) Iseki K., Kuroki Y., Takahashi M., Kobayashi Y., *Tetrahedron Lett.*, **37**, 5149—5150 (1996); b) Iseki K., Kuroki Y., Takahashi M., Kishimoto S., Kobayashi Y., *Tetrahedron*, **53**, 3513—3526 (1997); c) Iseki K., Mizuno S., Kuroki Y., Kobayashi Y., *Tetrahedron Lett.*, **39**, 2767—2770 (1998); d) Iseki K., Kuroki Y., Kobayashi Y., *Tetrahedron: Asymmetry*, **9**, 2889—2894 (1998); e) Iseki K., Mizuno S., Kuroki Y., Kobayashi Y., *Tetrahedron*, **55**, 977—988 (1999).
- Nakajima M., Saito M., Shiro M., Hashimoto S., *J. Am. Chem. Soc.*, **120**, 6419—6420 (1998).
- Studies on bipyridine *N,N'*-dioxide derivatives by our group: a) Nakajima M., Sasaki Y., Shiro M., Hashimoto S., *Tetrahedron: Asymmetry*, **8**, 341—344 (1997); b) Nakajima M., Sasaki Y., Iwamoto H., Hashimoto S., *Tetrahedron Lett.*, **39**, 87—88 (1998).
- Furuya N., Sukawa T., *J. Organomet. Chem.*, **96**, C1—C3 (1975).
- a) Basaiaiah D., Rao P. D., *Tetrahedron: Asymmetry*, **6**, 789—800 (1995); b) Coxon J. M., Simpson G. W., Steel P. J., Trenerry V. C., *Tetrahedron Lett.*, **24**, 1427—1428 (1983).
- Fouquey C., Jacques J., *Bull. Soc. Chim. Fr.*, **1973**, 618—621.
- Rideout J. L., Krenitsky T. A., Chao E. Y., Elion G. B., Williams R. B., Latter V. S., *J. Med. Chem.*, **26**, 1489—1494 (1983).
- Sidduri A., Rozema M. J., Knochel P., *J. Org. Chem.*, **58**, 2694—2713 (1993).
- Takahara J. P., Masuyama Y., Kurusu Y., *J. Am. Chem. Soc.*, **114**, 2577—2586 (1992).

Synthesis of Peptides Mimicking Chemokine Receptor CCR5 and Their Inhibitory Effects against HIV-1 Infection

Koji KONISHI,^a Kiyoshi IKEDA,^{*,a} Kazuo ACHIWA,^a
Hiroo HOSHINO,^b and Kiyoshi TANAKA^{*,a}

School of Pharmaceutical Sciences, University of Shizuoka,^a 52-1 Yada, Shizuoka 422-8526, Japan and Department of Hygiene and Virology, Gunma University School of Medicine,^b Showa-machi, Maebashi, Gunma 371-8511, Japan.

Received October 14, 1999; accepted December 2, 1999

Peptides mimicking chemokine receptor CCR5 were synthesized and their anti-HIV-1 activities evaluated. Prepared compounds, especially a sulfated derivatives, showed significant anti-HIV-1 activities. Furthermore, a hybrid molecule linked to an *N*-carboxymethoxycarbonyl-prolyl-phenylalanine (CPF) moiety had a greater effect.

Key words mimicking peptide; anti-HIV-1 activity; CPF; sulfation; chemokine receptor; hybrid molecule

CD4 is the primary cellular receptor for human immunodeficiency virus type 1 (HIV-1), but CD4 alone is not sufficient to allow the entry of HIV-1 into cells. In 1996, the cellular coreceptors that HIV-1 requires in conjunction with CD4 were identified as members of the chemokine receptor family of seven-transmembrane G protein-coupled receptors.¹⁾ This discovery of distinct chemokine receptors explains the differences in cell tropism between viral strains. Thus CXCR4 supports entry of T cell (T)-tropic HIV-1 strains, whereas CCR5 supports macrophage (M)-tropic HIV-1 strains. Recently, these chemokine receptors have received much attention as attractive targets for new antiviral therapies.²⁾ The mechanism of entry of HIV-1 into cells is thought to be: first, gp120-CD4 conjugation induces conformational changes in the gp120 subunit, including exposure of the V3 loop, and then conjugation with the coreceptor occurs.³⁾ It is known that these coreceptors are rich in tyrosines and acidic amino acids at their *N*-terminal region, and this contributes to the ability of HIV-1 to fuse with and enter into target cells.⁴⁾ A strongly positive region of the V3 loop has

been shown to be important for the association with CCR5. Consequently, it can be considered that some of these positively charged residues may directly and complementarily interact with a sequence of highly negatively charged acidic amino acids. It is known that *N*-carboxymethoxycarbonyl-prolyl-phenylalanine (CPF)⁵⁾ mimics CD4 and binds selectively to gp120. We previously reported the synthesis of the hybrid compounds linked to the CPF moiety as HIV protease inhibitors⁶⁾ and showed that these compounds bind selectively to infected cells, probably based on an interaction between CPF and gp120. Therefore we focused on the synthesis of peptides mimicking CCR5 with a CPF moiety. As a part of a program aimed at the development of new HIV-1 inhibitors, we would like to report the design and synthesis of peptides mimicking CCR5 for prevention of HIV-1 infection based on a strategy of binding to gp120.

Results and Discussion

In the amino acid sequences of the *N*-terminal domain of CCR5, we first chose the region of Tyr¹⁰-Glu¹⁸ including tyrosines, glutamic acid, and aspartic acid as a target peptide moiety. The peptide of natural type **2a** from **1** and its mimicking peptides **2b–e** consisting of acidic amino acids as well as unnatural-type amino acids as the spacer unit were prepared (Chart 1).⁷⁾ Resistance to the action of protease was expected from the latter compounds.

Compounds **2a–e** had no expected anti-HIV-1 activities⁸⁾ against M-tropic strains of HIV-1; on the other hand, these compounds showed significant anti-HIV-1 activities against T-tropic strains. Thus the percentage of HIV-1 antigen-positive cells with **2a–e** was 23.3–28.3%, whereas that with CPF was 27.7%. Furthermore, the anti-HIV-1 activities of **2a–e** were increased by the addition of CPF as an additive (11.0–26.7%).

To enhance the selectivity of binding to HIV-1 and hence the anti-HIV-1 activity, a hybrid compound **3**⁹⁾ of **2a** and CPF was designed and prepared (Chart 2). The synthesis of the hybrid molecule was straightforward and the construction of the covalent linkage between the CPF moiety and the peptide moiety was carried out using spacers derived from *o*-aminophenol. However, compound **3** prepared in this way exhibited the same level of anti-HIV-1 activity as that of **2a**.

Recently, it was suggested that the hydroxyl groups of ty-

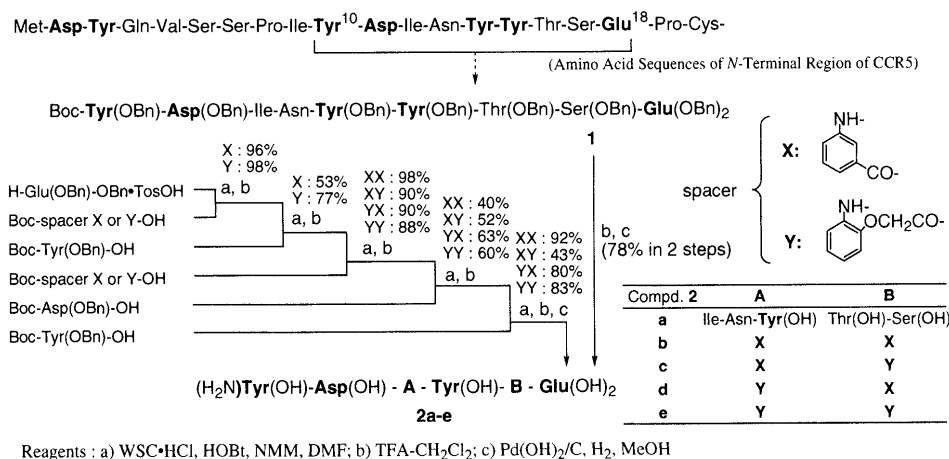


Chart 1

* To whom correspondence should be addressed.

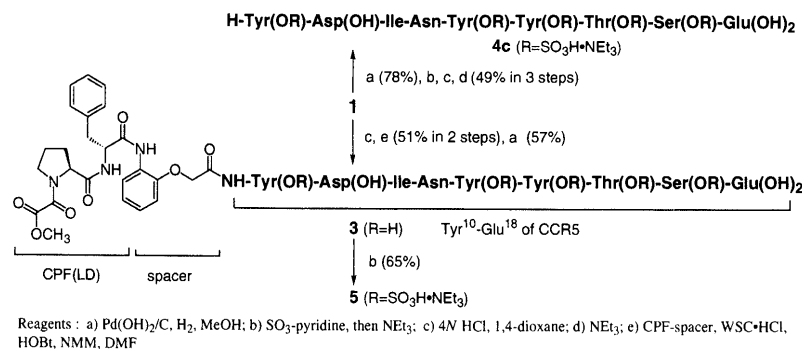


Chart 2

Table 1. The Anti-HIV-1 Activities of **4a–c** and **5**^{a)}

Compd.	-SO ₃ X	Drug concentration (μg/ml)			
		1000 ^{b)}	200	50	0
4a	H	232	258	225	219
4b	Na	207	236	255	251
4c	NEt ₃	57	138	245	n.t. ^{c)}
5	NEt ₃	2	40	223	n.t.

a) C8166/GUN1WT syncytium assay. b) No significant cytotoxicity of the compounds at 1000 μg/ml was observed. c) Not tested.

rosines in the *N*-terminal region of CCR5 are modified in the form of sulfates.¹⁰⁾ For the purpose of achieving increased anti-HIV-1 activity, some sulfated analogues were prepared. The sulfates¹¹⁾ **4a–c** and **5** were derived from **1** and **3**, respectively, and these transformations are also shown in Chart 2.¹²⁾ The results of biological assay for sulfated compounds **4a–c** and **5** are listed in Table 1. As can be seen from the table, in spite of the low activity of **4a** and **b**, compounds **4c** and **5**, especially **5**, showed significantly higher anti-HIV-1 activity.

Conclusions

In this study, it was confirmed that enhancement of anti-HIV-1 activities with mimicking peptides was achieved by the addition of CPF. Additionally, the sulfation of the parent peptide, and more effectively, the conjugation of the sulfated peptide with CPF, caused an increase in anti-HIV-1 activity. These results suggest that highly negatively charged sulfated groups interact strongly with a positively charged region of the V3 loop. The observations in this study will be helpful for a better understanding of the mechanism of HIV-1 infec-

tion, and hence development of new types of drugs against AIDS.

References and Notes

- Feng Y., Broder C. C., Kennedy P. E., Berger E. A., *Science*, **272**, 872–877 (1996).
- a) Nishiyama Y., Murakami T., Kurita K., Yamamoto N., *Chem. Pharm. Bull.*, **45**, 2125–2127 (1997); b) Tamamura H., Waki M., Imai M., Otaka A., Ibuka T., Waki K., Miyamoto K., Matsumoto A., Murakami T., Nakashima H., Yamamoto N., Fujii N., *Bioorg. Med. Chem.*, **6**, 473–479 (1998).
- Doms R. W., Peiper S. C., *Virology*, **235**, 179–190 (1997).
- a) Efremov R. G., Legret F., Vergoten G., Capron A., Bahr G. M., Arseniev A. S., *J. Biomol. Struct. Dyn.*, **16**, 77–90 (1998); b) Wu L., LaRosa G., Kassam N., Gordon C. J., Heath H., Ruffing N., Chen H., Humblas J., Samson M., Parmentier M., Moore J. P., Mackay C. R., *J. Exp. Med.*, **186**, 1373–1381 (1997).
- Finberg R. W., Diamond D. C., Mitchell D. B., Rosenstein Y., Soman G., Norman T. C., Schreiber S. L., Burakoff S. J., *Science*, **249**, 287–291 (1990).
- a) Asagarsu A., Takayanagi N., Achiwa K., *Chem. Pharm. Bull.*, **46**, 867–870 (1998); b) Asagarsu A., Uchiyama T., Achiwa K., *ibid.*, **46**, 697–703 (1998); c) Shimizu N. S., Handa A., Shimizu N. G., Ikeda R., Uchiyama T., Achiwa K., Hoshino H., *Antivir. Chem. Chemother.*, **6**, 17–24 (1995).
- 2a**: FAB-MS *m/z* 1167 (M+1)⁺, **2b**: FAB-MS *m/z* 827 (M+1)⁺, **2c**: FAB-MS *m/z* 857 (M+1)⁺, **2d**: FAB-MS *m/z* 857 (M+1)⁺, **2e**: FAB-MS *m/z* 887 (M+1)⁺.
- a) Handa A., Hoshino H., Nakajima K., Adachi M., Ikeda K., Achiwa K., Itoh T., Suzuki Y., *Biochem. Biophys. Res. Comm.*, **175**, 1–9 (1991); b) Shimizu N., Haraguchi Y., Takeuchi Y., Soda Y., Kanbe K., Hoshino H., *Virology*, **259**, 324–333 (1999).
- 3**: FAB-MS *m/z* 1669 (M+Na)⁺.
- Farzan M., Mirzabekov T., Kolchinsky P., Wyatt R., Cayabyab M., Gerard N. P., Gerard C., Sodroski J., Choe H., *Cell*, **96**, 667–676 (1999).
- Meyer B., Stuike-Prill R., *J. Org. Chem.*, **55**, 902–906 (1990).
- 4c**: FAB-MS *m/z* 1567 M⁺, **5**: FAB-MS *m/z* 1849 (M–3SO₃H+2Na–2H)⁺.

Synthesis of J-111,347, a Novel 1 β -Methylcarbapenem with Broad-spectrum Antibacterial Activity

Hideaki IMAMURA,* Norikazu OHTAKE,
Shunji SAKURABA, Aya SHIMIZU, Koji YAMADA, and
Hajime MORISHIMA

Banyu Tsukuba Research Institute, 3 Okubo, Tsukuba 300-2611,
Ibaraki, Japan.

Received October 26, 1999; accepted November 27, 1999

Synthesis of J-111,347 (1),¹⁾ a new 1 β -methylcarbapenem with broad-spectrum antibacterial activity including that against methicillin-resistant *Staphylococcus aureus* (MRSA) and *Pseudomonas aeruginosa*, was achieved via diastereoselective preparation of a side-chain thiol 3 from an optically active (R)-3,4-dihydroxybutanal 4.

Key words J-111,347; carbapenem; MRSA; *P. aeruginosa*; diastereoselective preparation

Several 1 β -methylcarbapenems possessing antibacterial activities against MRSA have been reported, although these did not show any appreciable anti-pseudomonal activity.²⁾ Carbapenems with activity against MRSA and *P. aeruginosa* would be useful for monotherapy in immunocompromised patients with a high risk of polymicrobial infections and would also offer cost-benefit advantages considering the relatively high costs of combination therapy that includes broad-spectrum antibiotics plus vancomycin.

Recently, we identified J-111,347 (1) as a new class of 1 β -methylcarbapenems since 1 exhibited a broad antibacterial spectrum against MRSA and *P. aeruginosa*.¹⁾ 1 and vancomycin had MIC ($\mu\text{g/ml}$) values of 0.78 and 0.78 against *S. aureus* pMS/Smith (an MRSA strain), respectively. Also 1 and imipenem had MIC ($\mu\text{g/ml}$) values of 0.39 and 1.56 against *P. aeruginosa* AK109, respectively. The *trans*-(3*S*,5*R*) pyrrolidinylthio structure of the C-2 side chain of 1 is unique, since the known pyrrolidinylthio-1 β -methylcarbapenems such as meropenem, BO-2727, and S-4661 possess *cis*-(3*S*,5*S*) pyrrolidinylthio side chains, which were thought to be indispensable for potent antibacterial activity.^{3,4)} An aminomethylphenyl group directly attached to the pyrrolidine ring in the *trans*-configuration might play an important role in the remarkable antibacterial activities of 1 against both MRSA and *P. aeruginosa*. In this paper, we describe diastereoselective synthesis of the side-chain thiol 3, followed by conversion to 1 (Fig. 1).

Aldol reaction of optically active (R)-3,4-dihydroxybutanal 4⁵⁾ with substituted phenyllithium yielded an insepara-

ble diastereomeric mixture of alcohols (5(*S*):5(*R*))=4:3) in 88% yield. To obtain the desired isomer 5(*S*), we performed diastereoselective reduction of ketone 6 which was formed by the oxidation of 5 with tetrapropylammonium perruthenate (TPAP)-4-methylmorpholine *N*-oxide (NMO) combination in good yield. It is well known that hydride reduction of β -hydroxy- or β -alkoxy-ketones proceeds diastereoselectively in the presence of Lewis acid to provide a 1,3-*syn*-diol system via chelating intermediates.⁶⁾ Based on this information, ketone 6 was reduced under various conditions with or without Lewis acids, as shown in Table 1. Reduction with NaBH₄ did not provide acceptable diastereoselectivity, regardless of the temperature and the presence of Lewis acids such as LiI, CeCl₃, MgCl₂, and SmCl₃. Reduction with Zn(BH₄)₂ at low temperature (−78 °C) resulted in good selectivity with moderate yield (entry 2, 76%de, 60% yield). Under the conditions of the LiAlH₄–LiI system,⁷⁾ good selectivity and acceptable yield (entry 5, 90%de, 76% yield) were obtained by using 10 mol of LiI at −78 °C. When less LiI was used, both selectivity and yield were decreased (entry 3, 4). Subsequently, the optically active alcohol 5(*S*) was converted to a carbapenem 1, as shown in Chart 2. The secondary hydroxyl group of 5(*S*) was substituted with sodium azide via its mesylate. Subsequent phosphine reduction of azide and protection of the resulting amino group with allyloxycarbonyl (Alloc) chloride afforded an Alloc-amine 7. Removal of the *tert*-butyldimethylsilyl (TBS) group of 7 with tetra-*n*-butylammonium fluoride (TBAF) and subsequent introduction of the azide group gave 8 in 91% yield. The azide 8 was transformed to a diol 9 in 78% yield by reduction of the azide, Alloc-protection of the resulting primary amine, and deprotection of the acetonide group under acidic conditions (*p*-TsOH, MeOH).¹⁰⁾ Selective tosylation of the primary hydroxyl group of the 1,2-diol 9 proceeded in good yield (TsCl, triethylamine [TEA], 4-[dimethylamino]pyridine [DMAP], [80%]) to give a tosylate 10. When 10 was treated under basic conditions, pyrrolidine ring formation did not

Table 1. Diastereoselective Reduction of 6

Entry	Reagent	Additive (equiv.)	Solvent	Temp. (°C)	Yield ^{a)} (%)	Ratio of 5(<i>S</i>) and 5(<i>R</i>) ^{b)}
1	NaBH ₄	None	MeOH	0	47	48:52
2	Zn(BH ₄) ₂	None	Et ₂ O	−78	60	88:12
3	LiAlH ₄	LiI (2)	Et ₂ O	−78	44	76:24
4	LiAlH ₄	LiI (5)	Et ₂ O	−78	51	90:10
5	LiAlH ₄	LiI (10)	Et ₂ O	−78	76	95:5

a) Isolated yield as a mixture of 5(*R*) and 5(*S*). b) Determined by HPLC (DAI-CEL CHIRALPAK AS).⁸⁾

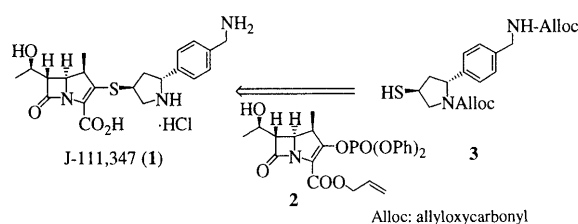
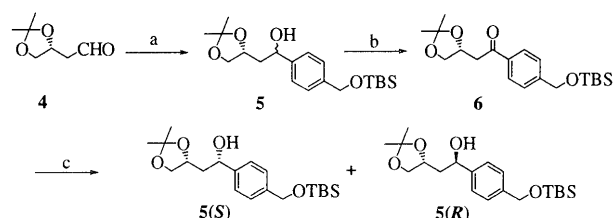


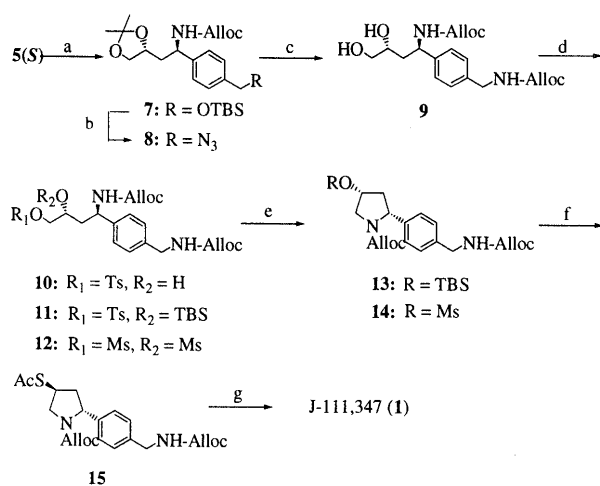
Fig. 1



a) 4-(*tert*-butyldimethylsilyloxymethyl)bromobenzene, *n*-BuLi, THF, −70°C, 88%; b) TPAP, NMO, CH₂Cl₂, 88%; c) Reducing agents (see Table 1).

Chart 1

* To whom correspondence should be addressed.



a) i) TEA, MsCl, CH₂Cl₂, 0°C; ii) NaN₃, DMF, 50°C; iii) PPh₃, THF-H₂O, room temperature; vi) TEA, Alloc-Cl, THF, 0°C, 61%; b) i) *n*-Bu₄NF, THF, 0°C; ii) TEA, MsCl, CH₂Cl₂, 0°C; iii) NaN₃, DMF, room temperature, 91%; c) i) PPh₃, THF-H₂O, room temperature; ii) TEA, Alloc-Cl, THF, 0°C; iii) *p*-TsOH, MeOH, room temperature, 78%; d) TEA, MsCl, CH₂Cl₂, 0°C; e) *t*-BuOK, THF, -20°C, 97%; f) AcSK, DMF, 65°C, 87%; g) i) NaOH, MeOH, 0°C; ii) *i*-Pr₂NEt, 2, CH₃CN, 0°C, 65%; iii) (PPh₃)₂PdCl₂, *n*-Bu₃SnH, H₂O, CH₂Cl₂, 72%.

Chart 2

take place to recover **10**, probably due to inactivation of the carbamate group by intramolecular hydrogen bonding. Therefore the secondary hydroxyl group of **10** was protected with a TBS group (TBS-Cl, imidazole, room temperature, 60%), giving **11** prior to the cyclization reaction. The desired pyrrolidine **13** was obtained in quantitative yield by treatment of **11** with *tert*-BuOK at -20 °C. Next, pyrrolidine ring formation was carried out using a dimesylate of the diol **9**. As expected, the dimesylate **12** was easily cyclized under the same conditions to afford 4-mesyloxy-pyrrolidine **14** (97% yield), which was then treated with potassium thioacetate in DMF at 70 °C to produce the thioacetate **15** (87% yield). Coupling reaction of the carbapenem enolphosphate **2**¹¹⁾ and the thiol **3** derived by alkaline hydrolysis of the thioacetate **15** followed by deprotection of the coupling product¹²⁾ in the usual manner¹³⁾ afforded the carbapenem **1** in 72% yield.

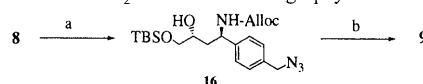
In summary, an efficient method for the synthesis of J-111,347 (**1**), a new carbapenem showing broad-spectrum antimicrobial activity, was established *via* diastereoselective reduction of the ketone **6** and intramolecular cyclization of the dimesylate **12**.

Acknowledgment We are grateful to Ms. A. Dobbins, Merck & Co., for her critical reading of this manuscript.

References and Notes

- Shimizu A., Sugimoto Y., Sakuraba S., Imamura H., Sato H., Ohtake

- N., Ushijima R., Nakagawa S., Suzuki C., Hashizume T., Morishima H., Program and Abstracts of the 38th Intersci. Conf. on Antimicrob. Agents Chemother., F052, P246, San Diego, Sept. 25, 1998.
- a) Sumita Y., Nouda H., Kanazawa K., Fukasawa M., *Antimicrob. Agents Chemother.*, **39**, 910—916 (1995); b) Rylander M., Roloff J., Jacobsson K., Norrby S. R., *ibid.*, **39**, 1178—1181 (1995); c) Nagano R., Shibata K., Naito T., Fuse A., Asano K., Hashizume T., Nakagawa S., *ibid.*, **41**, 2278—2281 (1997).
- a) Sunagawa M., Matsumura H., Inoue T., Fukasawa M., Kato M., *J. Antibiot.*, **43**, 519—532 (1990); b) Iso Y., Irie T., Nishino Y., Motokawa K., Nishitani Y., *ibid.*, **49**, 199—209 (1996); c) Ohtake N., Okamoto O., Mitomo R., Kato Y., Yamamoto K., Haga Y., Fukatsu H., Nakagawa S., *ibid.*, **50**, 598—613 (1997).
- Iso Y., Irie T., Iwaki T., Kii M., Sendo Y., Motokawa K., Nishitani Y., *J. Antibiot.*, **49**, 478—484 (1996).
- Mori K., Takigawa T., Matsuo T., *Tetrahedron*, **35**, 933—940 (1979).
- a) Narasaka K., Pai F.-C., *Tetrahedron*, **40**, 2233—2238 (1984); b) Nakata T., Tani Y., Hatozaki M., Oishi T., *Chem. Pharm. Bull.*, **32**, 1411—1415 (1984); c) Bonadies F., Di Fabio R., Gubbiotti A., Mecozzi S., Bonini C., *Tetrahedron Lett.*, **28**, 703—706 (1987).
- Mori Y., Takeuchi A., Kageyama H., Suzuki M., *Tetrahedron Lett.*, **29**, 5423—5426 (1988).
- HPLC analysis: column, DAICEL CHIRALPAK AS (250×4.6 mm); detection, 254 nm; eluent, *n*-hexane/isopropanol=90:10; flow rate, 0.5 ml/min; *t*_R of **5(S)**, 9.1 min; *t*_R of **5(R)**, 8.6 min. The stereochemical structure of **5(R)** was determined by the advanced Mosher method with the corresponding MTPA ester.⁹⁾
- Ohtani I., Kusumi T., Kashman Y., Kakisawa H., *J. Am. Chem. Soc.*, **113**, 4092—4096 (1991).
- The diol **9** with high purity (>99%de) was obtained *via* separation of compound **16** on SiO₂ column chromatography.



a) i) *p*-TsOH, MeOH, room temperature; ii) TBS-Cl, imidazole, CH₂Cl₂, room temperature, 75%; iii) SiO₂ column chromatography; b) i) PPh₃, THF-H₂O, room temperature; ii) TEA, Alloc-Cl, 0°C; iii) HCl-MeOH, 92%.

- a) Berks A. H., *Tetrahedron*, **52**, 331—375 (1996); b) Deziel R., Endo M., *Tetrahedron Lett.*, **29**, 61—64 (1988); c) Shih D. H., Baker F., Cama L., Christensen B. G., *Heterocycles*, **21**, 29—40 (1984).
- The coupling product derived from the diol **9** (90%de) could be purified by separation of its diastereomer on SiO₂ column chromatography.
- Dangles O., Guibe F., Balavoine G., Lavielle S., Marquet A., *J. Org. Chem.*, **52**, 4984—4993 (1987).
- Spectral data were obtained for new compounds.
5(S): [α]_D²⁵ -27.4 (*c* 1.0, CHCl₃); IR λ_{max} (Nujol) 3461, 1257 cm⁻¹; ¹H-NMR (300 MHz, CDCl₃) δ 0.08 (6H, s), 0.92 (9H, s), 1.36 (3H, s), 1.44 (3H, s), 1.86 (1H, m), 1.97 (1H, m), 3.53 (1H, t, *J*=8.1 Hz), 4.03 (1H, dd, *J*=8.1, 5.9 Hz), 4.23 (1H, m), 4.70 (2H, s), 4.89 (1H, dd, *J*=8.5, 4.2 Hz), 7.27 (2H, d, *J*=8.5 Hz), 7.32 (2H, d, *J*=8.5 Hz); FAB-HRMS *m/z* Calcd for C₂₀H₃₄O₄SiNa (M+Na)⁺: 389.2124, Found: 389.2112.
1: IR ν_{max} (KBr) 3421, 1749, 1646, 1558 cm⁻¹; ¹H-NMR (300 MHz, D₂O) δ 1.22 (3H, d, *J*=7.0 Hz), 1.27 (3H, d, *J*=6.5 Hz), 2.51 (1H, m), 2.73 (1H, m), 3.40 (3H, m), 3.86 (1H, dd, *J*=12.5, 6.0 Hz), 4.25 (5H, m), 5.03 (1H, dd, *J*=10.5, 7.0 Hz), 7.20 (4H, m); FAB-HRMS *m/z* Calcd for C₂₁H₂₈N₃O₄S (M+H)⁺: 418.1801, Found: 418.1800; UV λ_{max} 298 (ε 9520).

New Estrogenic Antagonists Bearing Dicarba-*closo*-dodecaborane as a Hydrophobic Pharmacophore

Yasuyuki ENDO,* Tomohiro YOSHIMI, and
Yuko YAMAKOSHI

Graduate School of Pharmaceutical Sciences, The University of
Tokyo, 7-3-1, Hongo, Bunkyo-ku, Tokyo 113-0033, Japan.

Received October 27, 1999; accepted December 18, 1999

We have designed and synthesized estrogen antagonists bearing dicarba-*closo*-dodecaborane (carborane) as a hydrophobic pharmacophore based on the structure of 1-(4-hydroxyphenyl)-1,12-dicarba-*closo*-dodecaborane, a potent estrogen agonist that we reported previously. Compounds with a long alkyl chain bearing an amide moiety on the carborane skeleton (6, 7) showed estrogen antagonistic activity in a luciferase reporter gene assay using COS-1 cells transfected with a rat ER α -expression plasmid and as an appropriate reporter plasmid.

Key words carborane; dicarba-*closo*-dodecaborane; estrogen; antagonist; hydrophobic moiety

The carborane (dicarba-*closo*-dodecaborane)¹⁾ skeleton is stabilized by 26 delocalized skeletal electrons and exhibits remarkable thermal and chemical stability. The icosahedral geometry, in which the carbon and boron atoms are hexacoordinated, accounts for these unusual properties, which make such molecules uniquely suitable for several specialized applications, including materials chemistry²⁾ and medicinal chemistry.³⁾ We have focused on the possibility of using carboranes as a hydrophobic component in biologically active molecules which interact hydrophobically with receptors. We reasoned that the remarkable thermal and chemical stability, the exceptionally hydrophobic character and the spherical geometry of carboranes made them interesting candidates for use as a hydrophobic pharmacophore. Recently, we have reported a potent estrogen agonist bearing a carborane, 1-hydroxymethyl-12-(4-hydroxyphenyl)-1,12-dicarba-*closo*-dodecaborane (Chart 1, 1),⁴⁾ which exhibits greater activity than that of 17 β -estradiol (3). We also designed and synthesized novel estrogen antagonists based on the structure of tamoxifen.⁵⁾ In the present article, we describe the synthesis and biological evaluation of new estrogen antagonists based on the phenylcarborane skeleton.

Since the discovery of the estrogen antagonist tamoxifen,⁶⁾

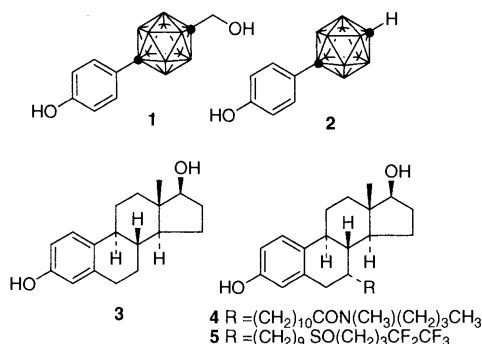


Chart 1. Structures of Potent Estrogen Agonists Bearing a Carborane Skeleton, and Conventional Steroidal Estrogen Agonist and Antagonists

many stilbene derivatives and triarylethylenes have been synthesized and shown to possess activity, and some have been developed for clinical use.⁷⁾ Steroidal estrogen antagonists have also been developed, and although substitutions at various carbon atoms of estradiol have been tried, one of the most potent classes of antagonists consists of compounds that are 7 α -substituted with an alkyl chain bearing an amide (ICI 164,384, 4)⁸⁾ or sulfoxide moiety (ICI 182,780, 5).⁹⁾

The high agonistic activity of compound 1 suggested that the carborane cage works as a hydrophobic group binding to the hydrophobic cavity of the estrogen receptor (ER), and the hydrophobic and van der Waals contacts along the spherical carborane cage produce a stronger interaction than that in the case of 17 β -estradiol. Further, 1-(4-hydroxyphenyl)-1,12-dicarba-*closo*-dodecaborane (2), which lacks a hydroxymethyl group on the carborane cage, also exhibits potent estrogenic activity. Therefore, we set out to design new estrogen antagonists based on the carborane skeleton. Substitution of an alkyl group at the 2-position of the carborane cage might correspond to substitution at the 7-position of the steroidal skeleton. Therefore, we synthesized and biologically evaluated compounds having an *o*- or *m*-carborane skeleton with an alkyl chain bearing an amide and a hydroxyl group at the *para*-position of the aromatic nucleus (6–9), as shown in Chart 2. In icosahedral cage structures throughout this paper, closed circles (●) represent carbon atoms and other vertices represent BH units.

The syntheses of the designed molecules are summarized in Chart 3. Compounds 6 and 7 were prepared from 1-(4-methoxyphenyl)-1,2-dicarba-*closo*-dodecaborane (10), which was prepared by construction of the *o*-carborane cage from 4-ethynylanisole and *nido*-decaborane. Compound 10 was converted to 11 by reaction of the lithiate of 10 with 2-(11-bromoundecyloxy)tetrahydro-2H-pyran (50%). Deprotection of the THP group of 11 with *p*-toluenesulfonic acid gave the alcohol 12 (92%). Oxidation of 12 with chromium trioxide gave the acid 13 (15%) and the ester 14 (48%). The ester 14 was hydrolyzed with sulfuric acid-1,4-dioxane to give the acid 13 (70%). Demethylation of the methoxy group of 13 with boron tribromide followed by coupling with *n*-butylamine or *N*-*n*-butyl-*N*-methylamine afforded 6 (38%) or 7 (26%), respectively. Compounds 8 and 9 were prepared from 1-(4-methoxyphenyl)-1,7-dicarba-*closo*-dodecaborane¹⁰⁾ by means of the same procedures as used in the synthesis of 6 and 7. The structures of the carborane-containing molecules (6–9) were confirmed by spectroscopic data including ¹H-NMR and HRMS.¹¹⁾

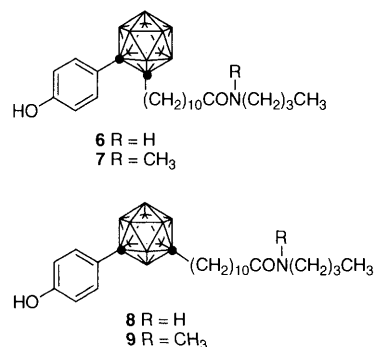


Chart 2. The Designed Carborane-containing Molecules (6–9)

* To whom correspondence should be addressed.

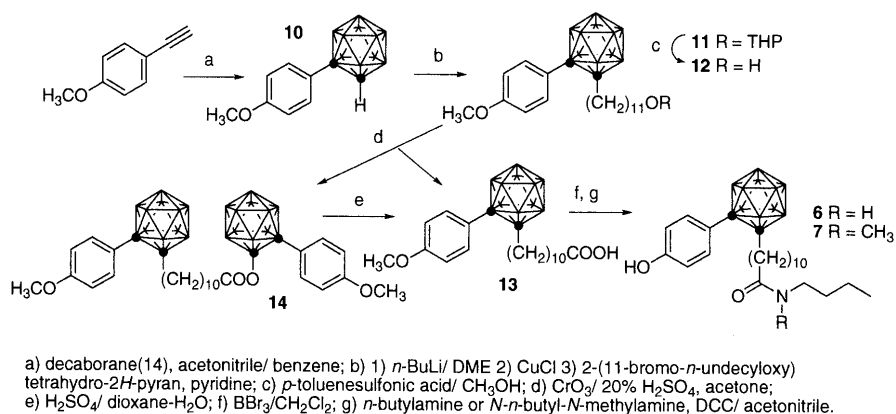


Chart 3

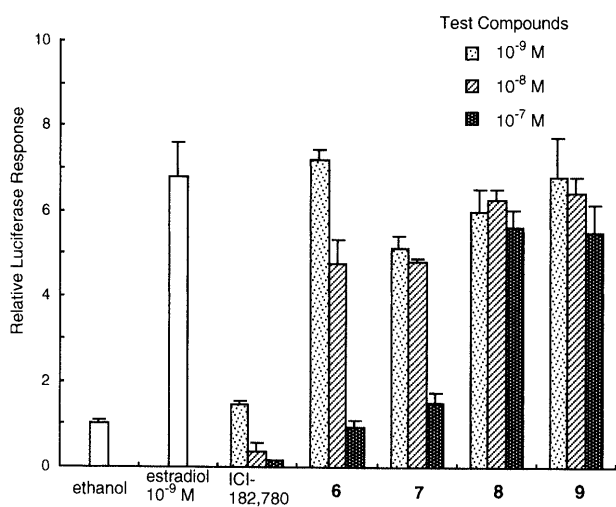


Fig. 1. Inhibition of Transcriptional Activation of 17 β -Estradiol by the Test Compounds

COS-1 cells were transfected with ERE \times 5-pGL-TK and pCI-rER α (see text) and incubated with no agonist (ethanol), with 17 β -estradiol (10⁻⁹ M) or with a test compound (10⁻⁹–10⁻⁷ M) plus 17 β -estradiol (10⁻⁹ M). Results are shown as means \pm S.D. for triplicate transfections.

The estrogenic activities of the synthesized compounds were examined by luciferase reporter gene assay,¹²⁾ in which a rat ER α -expression plasmid¹³⁾ and a reporter plasmid, which contains 5 copies of an estrogen response element, are transiently transfected into COS-1 cells. 17 β -Estradiol at 1 \times 10⁻¹⁰–1 \times 10⁻⁸ M induced the expression of luciferase in a dose-dependent manner. The results of inhibition of transcriptional activity of 17 β -estradiol at a concentration of 10⁻⁹ M by our carborane-containing molecules (6–9) are summarized in Fig. 1. Compounds based on *ortho*-carborane (6 and 7) inhibited the activity of 17 β -estradiol in the concentration range of 1 \times 10⁻⁸–10⁻⁷ M. The potency of 6 is less than that of ICI 182,780, which is the most potent full estrogen agonist currently known. However, compound 6 at 1 \times 10⁻⁷ M inhibited 85% of the transcriptional response to 10⁻⁹ M 17 β -estradiol. Compounds based on *meta*-carborane (8 and 9) did not exhibit antagonistic activity.

Recently, studies on the three-dimensional structures of the complexes formed by raloxifene and the human estrogen receptor- α ligand binding domain (hER α LBD),¹⁴⁾ and by 4-hydroxytamoxifen and hER α LBD have been reported.¹⁵⁾ The structural studies suggest that an agonist-induced conforma-

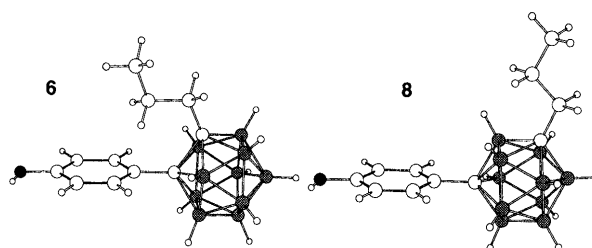


Chart 4. Core Structures of 6 and 8

tional change involving helix 12, the most C-terminal helix of LBD, is essential for activation function (AF-2) activity and the appearance of estrogenic action.¹⁴⁾ Although the binding mode of 7-substituted steroidal antagonists to ER has not been clarified, the role of a linear alkyl substituent seems to be similar to that in the case of 4-hydroxytamoxifen. The alkyl group is considered to fit in a narrow corridor in the receptor cavity. Although the linear alkyl substituents of these antagonists are flexible, the direction of the substituents plays a critical role in the antagonistic activity. Chart 4 shows the core structures of compounds bearing an *o*- or *m*-carborane skeleton. The great difference in activity between 6 and 8 may be interpreted in terms of the direction of the alkyl substituent. The antagonistic activity of these carborane-containing molecules is moderate, but optimization of the structure may afford more potent and selective antagonists.

In summary, we have developed novel carborane-containing molecules with antagonistic activity for estrogen. These carborane-containing estrogen antagonists, having a new skeletal structure and unique characteristics, should provide a basis for the design of further compounds as potential therapeutic agents.

References and Notes

- For a recent review see: Bregardze V. I., *Chem. Rev.*, **92**, 209–223 (1992).
- For a recent review see: Plesek J., *Chem. Rev.*, **92**, 269–286 (1992).
- For recent reviews see: Hawthorne M. F., *Angew. Chem. Int. Ed. Engl.*, **32**, 950–984 (1993); Soloway A. H., Tjarks W., Barnum B. A., Rong F.-G., Barth R. F., Codogni I. M., Wilson J. G., *Chem. Rev.*, **98**, 1515–1562 (1998).
- Endo Y., Iijima T., Yamakoshi Y., Yamaguchi M., Fukasawa H., Shudo K., *J. Med. Chem.*, **42**, 1501–1504 (1999).
- Endo Y., Yoshimi T., Iijima T., Yamakoshi Y., *BioMed. Chem. Lett.*, **9**, 3387–3392 (1999).

- 6) Bedford G. R., Richardson D. N. *Nature*, **212**, 733—734 (1966); Harper M. J. K., Walpole A. L., *Nature*, **212**, 87 (1966).
- 7) Ray S., Dwivedy I., "Advances in Drug Research," Vol. 29, ed. by Testa B., Meyer U. A., Academic Press, San Diego, 1997; pp. 171—270.
- 8) Bowler J., Lilley T. J., Pittam J. D., Wakeling A. E., *Steroids*, **54**, 71—99 (1989).
- 9) Wakeling A. E., Bowler J. J., *Steroid Biochem. Molec. Res.*, **43**, 173—177 (1992).
- 10) Coult R., Fox M. A., Gill W. R., Herbertson P. L., MacBride J. A. H., Wade K., *J. Organometal. Chem.*, **462**, 19—29 (1993). Fox M. A., MacBride J. A. H., Peace R. J., Wade K., *J. Chem. Soc., Dalton Trans.*, 401—411 (1998).
- 11) Compound 6: Colorless viscous liquid, $^1\text{H-NMR}$ (CDCl_3) 0.85—1.40 (m, 18H), 0.95 (t, $J=7.3$ Hz, 3H), 1.50—1.60 (m, 2H), 1.5—3.2 (br m, 10H), 1.80 (m, 2H), 2.22 (t, $J=7.3$ Hz, 2H), 3.31 (dt, $J=5.8, 7.1$ Hz, 2H), 5.60 (br s, 1H), 6.86 (d, $J=8.8$ Hz, 2H), 7.44 (d, $J=8.8$ Hz, 2H), 9.50 (br s, 1H). HRMS: Calcd for $\text{C}_{23}\text{H}_{45}^{10}\text{B}_2^{11}\text{B}_8\text{NO}_2$, 475.4453; Found, 475.4450. Compound 7: Colorless viscous liquid, $^1\text{H-NMR}$ (CDCl_3) 0.85—1.40 (m, 18H), 0.94, 0.97 (t \times 2, $J=7.3$ Hz, 3H), 1.50—1.65 (m, 2H), 1.5—3.2 (br m, 10H), 1.79 (m, 2H), 2.35, 2.36 (t \times 2, $J=7.3$ Hz, 3H), 2.98, 3.02 (s \times 2, 3H), 3.30, 3.42 (t \times 2, $J=7.5$ Hz, 3H), 6.87, 6.88 (d \times 2, $J=8.8$ Hz, 2H), 7.43 (d, $J=8.8$ Hz, 2H), 9.79, 9.82 (br s \times 2, 1H) (conformational mixture of *cis*- and *trans*-amide (1 : 1) in CDCl_3). HRMS: Calcd for $\text{C}_{24}\text{H}_{47}^{10}\text{B}_2^{11}\text{B}_8\text{NO}_2$, 489.4610; Found, 489.4607. Compound 8: Colorless viscous liquid, $^1\text{H-NMR}$ (CDCl_3) 0.92 (t, $J=7.3$ Hz, 3H), 1.05—1.42 (m, 18H), 1.48 (quint, $J=7.6$ Hz, 2H), 1.6—3.1 (br m, 10H), 1.95 (m, 2H), 2.16 (t, $J=7.6$ Hz, 2H), 3.25 (dt, $J=5.9, 7.0$ Hz, 2H), 5.44 (br s, 1H), 6.30 (br s, 1H), 6.71 (d, $J=8.8$ Hz, 2H), 7.26 (d, $J=8.8$ Hz, 2H). HRMS: Calcd for $\text{C}_{23}\text{H}_{45}^{10}\text{B}_2^{11}\text{B}_8\text{NO}_2$, 475.4453; Found, 475.4460. Compound 9: Colorless viscous liquid, $^1\text{H-NMR}$ (CDCl_3) 0.91, 0.95 (t \times 2, $J=7.3$ Hz, 3H), 1.05—1.42 (m, 18H), 1.45—1.60 (m, 2H), 1.6—3.1 (br m, 10H), 1.95 (m, 2H), 2.29, 2.31 (t \times 2, $J=7.4$ Hz, 3H), 2.92, 2.98 (s \times 2, 3H), 3.26, 3.36 (t \times 2, $J=7.5$ Hz, 3H), 6.72 (d, $J=8.8$ Hz, 2H), 7.25 (d, $J=8.8$ Hz, 2H). (conformational mixture of *cis*- and *trans*-amide (1 : 1) in CDCl_3). HRMS: Calcd for $\text{C}_{24}\text{H}_{47}^{10}\text{B}_2^{11}\text{B}_8\text{NO}_2$, 489.4610; Found, 489.4613.
- 12) Meyer T., Koop R., von Angerer E., Schonenberger H., Holler E. A., *J. Cancer Res. Clin. Oncol.*, **120**, 359—64 (1994).
- 13) Koike S., Sakai M., Muramatsu M., *Nucleic Acids Res.*, **15**, 2499—2513 (1987).
- 14) Brzozowski A. M., Pike A. C. W., Dauter Z., Hubbard R. E., Bonn T., Engstrom O., Ohman L., Greene G. L., Gustafsson J., Carlquist M., *Nature*, **389**, 753—758 (1997).
- 15) Shiau A. K., Barstad D., Loria P. M., Cheng L., Kushner P. J., Agard D. A., Greene G. L., *Cell*, **95**, 927—937 (1998).